

**METALLOGENY OF THE FAIRBANKS  
MINING DISTRICT, ALASKA AND  
ADJACENT AREAS**

**PAUL ANTHONY METZ**

A thesis in two volumes submitted for the degree of Doctor of Philosophy of the University of London

**VOLUME I  
TEXT (Chapters 1 - 9)**

**VOLUME II  
TEXT (Chapters 10 - 13),  
APPENDICES, AND PLATES**

**Department of Geology  
Royal School of Mines  
Imperial College of Science, Technology, and Medicine  
London**

**May 1991**

*Library of Congress Cataloging in Publication Data*

Library of Congress Catalog Card Number 91-67232  
ISBN 0-911043-13-6

Published by

Mineral Industry Research Laboratory  
212 O'Neill Building  
University of Alaska Fairbanks  
Fairbanks, Alaska 99775-1180

## ABSTRACT

The Fairbanks mining district encompasses an area of 1500 km<sup>2</sup> (600 miles<sup>2</sup>) centred just north of the City of Fairbanks, Alaska. The district is one of six mining areas located in or near the northwestern margin of the Yukon-Tanana Uplands of east-central Alaska and the Yukon Territory, Canada. The six mining districts in Alaska (Fairbanks, Circle, Steese, Richardson, Tolovana and Kantishna) and the Klondike district nearby in the Yukon Territory, have an aggregate placer gold production of 25 million troy ounces. This production establishes the region as one of the largest gold producing areas of North America. The aim of the present investigation is to define, classify and explain the genesis of the several primary sources from which the placer gold deposits of the region were derived.

Through geological mapping and sampling of the districts, the 350 identified primary mineral occurrences are classified into eight categories as follows: (1) metamorphosed volcanic-exhalative and associated low-sulfide Au-quartz veins, (2) Cu-Mo-Au porphyries, (3) precious metal enriched massive sulfides, (4) epithermal veins in plutonic rocks, (5) Au-bearing tungsten skarns, (6) Sn greisen-gold-quartz veins, (7) Sediment-hosted gold of the Carlin type, and (8) palaeoplacer gold deposits. Geological mapping and sampling has also established that recent faulting and regional uplift are responsible for stream capture, stream drainage reversal, resorting of stream sediments, and modern alluvial placer formation.

The volcanic-exhalative mineralization is hosted in metamorphosed low-K tholeiitic basalts, Ca-poor rhyolitic tuffs, and cherts. In the Fairbanks district the rocks are informally referred to as the Cleary sequence. Detrital zircons from the sequence yield U-Pb ages in the ranges 1.2, 1.3-1.4, 1.8-1.9, 2.5, and 3.4 Ga. The bimodal volcanic rocks are enriched in Au, Ag, As, Sb, and W. Average gold contents of the rocks exceed average crustal abundances by two orders of magnitude. Locally the metavolcanic rocks contain base metal massive sulfide mineralization with grades up to 20% combined Pb-Zn, 3 g/tonne Au, and 500 g/tonne Ag.

These metavolcanic rocks are correlated with those occurring in the Kantishna district (Spruce Creek sequence) and in the Circle district (Bonanza Creek sequence). The mineralized bimodal metavolcanic suite is thus shown to extend along strike for 350 km (210 miles) through the Yukon-Tanana Terrane.

In the Fairbanks district the Cleary sequence rocks are thrust over Type C eclogites. These eclogites trend northeasterly along the regional strike to the Circle quadrangle and are correlated with the eclogites of the central Yukon Territory. Lead 206/204 and 207/204 ratios from galena from the metavolcanic sequences and from the vein deposits are similar with average values of 19.10 and 15.69 respectively. The eclogitic rocks are less radiogenic with 206/204 and 207/204 ratios of 18.80 and 15.65 respectively.

Low sulfide Au-quartz veins within the metavolcanic sequences are shown to be the product of multiple thermal and deformational events in the terrane taking place at 160-185, 140-145, and 90-125 Ma, K-Ar. Studies of the fluid inclusions in the metamorphic and vein quartz demonstrate that fluid compositions (1-20 mole % CO<sub>2</sub>; 3-5 wt % NaCl equiv.) and homogenization temperatures (275-375°C) are closely similar. Gold contents of the vein systems range from 5 to 18 g/tonne.

Calc-alkaline plutons of Cretaceous (85-110 Ma) and Tertiary (50-70 Ma) age K-Ar host epithermal veins, Sn-greisen, and W-skarn mineralization, all of which are demonstrably gold-bearing. Rb-Sr initial ratios for the mineralized composite plutons are greater than 0.711 indicating that anatexis of the lower crust was the source of the granitic magma. The Cu-Mo-Au porphyry mineralization is hosted in the Tertiary plutons that intrude lower Palaeozoic and Mesozoic sediments of the North American Continental Margin (NACM) in the Tolovana district. The NACM rocks are separated from the metavolcanic sequence by the eclogitic rocks and by major thrust faults.

Paleoplacer Au deposits hosted in continental clastic rocks of Eocene to Pliocene age are described. These have formed in small grabens adjacent to major strike-slip faults bounding the Yukon-Tanana Terrane on the northeast and southwest respectively. These structures, the Tinina and Denali Faults, controlled sedimentation and placer formation in these grabens.

Using compilations of tonnage/grade data from examples of primary deposits analogous to those identified in the Yukon-Tanana Terrane, it is shown that a single large-scale deposit of any of these types could have supplied all the gold contained in the placer deposits of the region.

# TABLE OF CONTENTS

	Page
ABSTRACT .....	i
TABLE OF CONTENTS .....	iii
ACKNOWLEDGMENTS .....	xxiii
CHAPTER 1 INTRODUCTION AND PREVIOUS INVESTIGATIONS .....	1
1.1 OBJECTIVE AND SCOPE OF THE INVESTIGATION .....	1
1.2 LOCATION .....	1
1.3 PREVIOUS INVESTIGATIONS .....	1
1.4 PERIOD OF INVESTIGATION .....	2
CHAPTER 2 REGIONAL GEOLOGY .....	2
2.1 YUKON-TANANA TERRANE .....	2
2.1.1 Introduction .....	2
2.1.2 Major Rock Units .....	2
2.1.2.1 Southern Yukon Territory, Canada .....	2
2.1.2.2 East-Central Alaska .....	3
2.2 REGIONAL GEOCHRONOLOGY .....	4
2.3 REGIONAL STRUCTURES .....	4
2.3.1 Major Mapped Structures .....	5
2.3.2 Linear Trends from Landsat Imagery .....	6
2.4 MINING DISTRICTS AND DISTRIBUTION OF MINERAL OCCURRENCES .....	6
2.4.1 Regional Distribution of Lode and Placer Deposits. ....	6
2.4.2 Regional Variation in Elemental Associations and Elemental Distribution .....	14
2.5 SUMMARY .....	14
CHAPTER 3 GENERAL GEOLOGY OF THE FAIRBANKS MINING DISTRICT .....	15
3.1 LOCATION AND GEOLOGICAL SETTING .....	15
3.2 MAJOR ROCK UNITS .....	15
3.2.1 Metamorphic Terranes/Sequences .....	15
3.2.1.1 Chatanika Terrane .....	15
3.2.1.2 Cleary Sequence .....	16
3.2.2 Intrusive Rock Units .....	17
3.2.2.1 Pedro Dome Area .....	17
3.2.2.2 Gilmore Dome Area .....	17
3.2.2.3 Treasure Creek Area .....	18
3.2.2.4 Ester Dome Area .....	18
3.2.3 Tertiary Sedimentary and Volcanic Sequences .....	18

## TABLE OF CONTENTS (Continued)

	<u>Page</u>
3.3 STRUCTURAL GEOLOGY .....	18
3.3.1 Folding Events .....	19
3.3.2 Joint Systems .....	19
3.3.3 Fault Systems .....	20
3.3.4 Linear Trends .....	21
3.3.5 Mineralized Shear Zones .....	21
CHAPTER 4 LODE MINERAL DEPOSIT DESCRIPTIONS AND ORE PETROLOGY OF THE FAIRBANKS MINING DISTRICT .....	21
4.1 INTRODUCTION .....	21
4.2 FIELD CLASSIFICATION OF MINERAL DEPOSITS .....	22
4.2.1 Type I Mineralization .....	22
4.2.2 Type II Mineralization .....	23
4.2.3 Type III Mineralization .....	23
4.2.4 Type VI Mineralization .....	23
4.2.5 Type V Mineralization .....	23
4.3 MINERAL DEPOSIT DESCRIPTIONS .....	23
4.3.1 Type IA Stratabound Copper-Lead-Zinc .....	24
4.3.1.1 Steese eclogite Sulphide Occurrence .....	24
4.3.2 Type IB Stratabound Arsenopyrite-Scheelite .....	24
4.3.2.1 Ryan lode Footwall .....	24
4.3.3 Type IC Stratabound Galena-Sphalerite-Tetrahedrite .....	24
4.3.3.1 Nordale Adit .....	24
4.3.4 Type ID Stratabound Arsenopyrite-Jamesonite-Gold .....	25
4.3.4.1 Wackwitz Prospect .....	25
4.3.4.2 Tolovana Mine .....	26
4.3.5 Type IE Stratabound Lead-Zinc .....	26
4.3.5.1 Cheechako Prospect .....	26
4.3.6 Type IIA Intrusive Related Gold .....	27
4.3.6.1 Fort Knox Prospect .....	27
4.3.7 Type IIB Intrusive Related Lead-Silver .....	28
4.3.7.1 Silver Fox Mine .....	28
4.3.8 Type III Tungsten Skarn .....	29
4.3.8.1 Tungsten Hill Prospect .....	29
4.3.9 Type IV Metamorphic Hosted Gold-Quartz Veins .....	30

## TABLE OF CONTENTS (Continued)

	Page
4.3.9.1 Vetter Prospect .....	30
4.3.10 Type V Monomineralic Stibnite .....	32
4.3.10.1 Scrafford Mine .....	32
4.4 QUANTITATIVE ORE MINERALOGY .....	33
4.4.1 Electron Microprobe Determinations .....	33
4.4.2 Arsenopyrite and Gold Association .....	33
4.4.2.1 Arsenopyrite Textures and Gold Content .....	33
4.4.2.2 Arsenopyrite Compositions and Geobarometry .....	39
4.5 MINERAL PARAGENESIS .....	39
4.6 APPLICATIONS OF ORE MINERALOGY AND PETROLOGY .....	46
4.6.1 Applications to Exploration .....	46
4.6.2 Applications to Evaluation .....	46
4.6.3 Applications to Recovery .....	47
CHAPTER 5 PLACER GOLD DEPOSITS OF THE FAIRBANKS MINING DISTRICT .....	50
5.1 INTRODUCTION .....	50
5.2 PREVIOUS INVESTIGATIONS AND PLACER STRATIGRAPHY .....	50
5.3 BEDROCK SOURCES OF PLACER GOLD .....	54
5.4 MECHANISMS OF ALLUVIAL PLACER FORMATION .....	54
5.4.1 Stream Longitudinal Profiles .....	54
5.4.2 Periods of High Discharge and Placer Formation .....	55
5.4.3 Alteration of Stream Drainage Patterns and Stream Capture .....	58
5.5 PLACER GOLD FINENESS VALUES .....	60
5.6 SUMMARY AND CONCLUSIONS .....	63
CHAPTER 6 TRACE ELEMENT GEOCHEMISTRY OF THE FAIRBANKS MINING DISTRICT .....	63
6.1 INTRODUCTION .....	63
6.2 SAMPLING .....	64
6.3 STREAM SEDIMENT DATA .....	64
6.3.1 Sample Analysis .....	64
6.3.2 Data and Data Reduction .....	64
6.4 PAN CONCENTRATE DATA .....	64
6.4.1 Sample Analysis .....	64
6.4.2 Data and Data Reduction .....	65
6.5 MINERALIZED ROCK DATA .....	65
6.5.1 Sample Analysis .....	65
6.5.2 Data and Data Reduction .....	65
6.6 MAPPABLE ROCK UNIT DATA .....	65

## TABLE OF CONTENTS (Continued)

	<u>Page</u>
6.6.1 Sample Analysis . . . . .	65
6.6.2 Data and Data Reduction . . . . .	66
6.7 DISCUSSION . . . . .	66
6.8 CONCLUSIONS . . . . .	70
<b>CHAPTER 7 FLUID INCLUSION AND STABLE ISOTOPE GEOCHEMISTRY OF THE FAIRBANKS MINING DISTRICT . . . . .</b>	<b>70</b>
7.1 INTRODUCTION . . . . .	70
7.2 SAMPLE COLLECTION . . . . .	71
7.2.1 Sampling of Metamorphic Rocks . . . . .	71
7.2.2 Sampling of Plutonic Rocks . . . . .	71
7.2.3 Sampling of Mineral Deposit Types . . . . .	71
7.2.4 Sampling within Mineral Deposit Types . . . . .	72
7.3 FLUID INCLUSION CLASSIFICATION BY MAJOR COMPONENTS . . . . .	72
7.4 ESTIMATION OF FLUID INCLUSION ABUNDANCE . . . . .	72
7.5 FLUID INCLUSION MICROTHERMOMETRY . . . . .	72
7.5.1 Data Summary . . . . .	73
7.5.1.1 Fluids in Metamorphic Quartz . . . . .	73
7.5.1.2 Fluids in Plutonic Quartz . . . . .	73
7.5.1.3 Fluids in Type I Mineral Occurrences . . . . .	73
7.5.1.4 Fluids in Type II Mineral Occurrences . . . . .	73
7.5.1.5 Fluids in Type III Mineral Occurrences . . . . .	73
7.5.1.6 Fluids in Type IV Mineral Occurrences . . . . .	80
7.5.1.7 Fluids in Type V Mineral Occurrences . . . . .	80
7.5.1.8 Discussion . . . . .	80
7.6 FLUID INCLUSION ANALYSES BY MASS SPECTROMETRY . . . . .	91
7.6.1 Methodology . . . . .	91
7.6.2 Results . . . . .	91
7.6.3 Discussion . . . . .	91
7.7 SULPHUR ISOTOPE INVESTIGATIONS . . . . .	93
7.7.1 Methodology . . . . .	93
7.7.2 Results . . . . .	93
7.7.3 Discussion . . . . .	93
7.9 SUMMARY AND CONCLUSIONS . . . . .	101
<b>CHAPTER 8 GENERAL GEOLOGY AND TRACE ELEMENT GEOCHEMISTRY OF THE CIRCLE, STEESE, RICHARDSON, TOLOVANA AND KANTISHNA MINING DISTRICTS . . . . .</b>	<b>101</b>
8.1 INTRODUCTION . . . . .	101

## TABLE OF CONTENTS (Continued)

	<u>Page</u>
8.2 CIRCLE MINING DISTRICT .....	101
8.2.1 Location and Previous Investigations .....	101
8.2.2 Bedrock Geology .....	101
8.2.2.1 Regionally Metamorphosed Rocks .....	103
8.2.2.1.1 Quartzite and Pelitic Schist .....	103
8.2.2.1.2 Mafic Schist .....	103
8.2.2.1.3 Bonanza Creek Sequences .....	103
8.2.2.1.4 Grit and Quartzite .....	103
8.2.2.2 Tertiary Gravels .....	104
8.2.2.3 Intrusive Rocks .....	104
8.2.2.3.1 Circle Hot Springs Pluton .....	104
8.2.2.3.2 Two-Bit Pluton .....	105
8.2.2.4 Contact Metamorphic Rocks .....	105
8.2.2.5 Regional Structure .....	105
8.2.3 Lode Mineral Occurrences .....	106
8.2.3.1 Porcupine Dome .....	106
8.2.3.2 Miller House .....	106
8.2.3.3 Bedrock Creek .....	106
8.2.3.4 Deadwood Creek .....	107
8.2.3.5 Portage Creek .....	107
8.2.3.6 Ketchem Dome .....	107
8.2.3.7 Switch Creek and Discovery Gulch .....	107
8.2.3.8 Butte Creek .....	107
8.2.3.9 Gold Dust Creek .....	107
8.2.3.10 Eagle Summit .....	107
8.2.3.11 Porcupine Dome .....	107
8.2.3.12 Bonanza Creek .....	108
8.2.3.13 Independence Creek .....	108
8.2.4 Placer Deposits .....	108
8.2.5 Trace Element Geochemistry .....	110
8.2.6 Discussion .....	110
8.3 STEESE MINING DISTRICT .....	111
8.3.1 Location and Previous Investigations .....	111
8.3.2 Bedrock Geology .....	111
8.3.2.1 Regionally Metamorphosed Rocks .....	111
8.3.2.1.1 Lower Fairbanks Schist .....	111

## TABLE OF CONTENTS (Continued)

	<u>Page</u>
8.3.2.1.2 Cleary Sequence .....	113
8.3.2.1.3 Upper Fairbanks Schist .....	113
8.3.2.1.4 Meta-grit Sequence .....	113
8.3.2.1.5 Maroon and Green Grit .....	114
8.3.2.1.6 Fossil Creek Volcanics .....	114
8.3.2.2 Intrusive Rocks .....	115
8.3.2.2.1 Lime Peak Pluton .....	115
8.3.2.2.2 Quartz Creek Pluton .....	115
8.3.2.2.3 Mt. Prindle Pluton .....	115
8.3.2.2.4 Minor Intrusive Rocks .....	116
8.3.2.3 Contact Metamorphic Rocks .....	116
8.3.2.4 Regional Structure .....	116
8.3.3 Lode Mineral Occurrences .....	117
8.3.3.1 Faith-Charity Creeks Stratiform Au .....	118
8.3.3.2 Bachelor Creek Stratiform Au .....	118
8.3.3.3 Pinnell Trail Sb Anomaly .....	118
8.3.3.4 Table Mountain Au Occurrences .....	118
8.3.3.5 Lower Hope Creek Au Anomaly .....	119
8.3.3.6 Bedrock Creek Sn-Ag Occurrence .....	119
8.3.3.7 Cliff Sn-Ag Occurrence .....	119
8.3.3.8 Tin-Ridge Sn-Ag Occurrence .....	119
8.3.3.9 North Fork Sn-Ag Prospect .....	120
8.3.3.10 Mascot Creek Sn-Ag Occurrence .....	120
8.3.3.11 South Lime Peak Sn-Ag .....	120
8.3.3.12 Upper Preacher Creek .....	120
8.3.3.13 Mt. Prindle Sn-Ag and U-REE Occurrences .....	120
8.3.3.14 Hope Creek Sn-Ag Occurrence .....	121
8.3.3.15 Fluorite Creek Sn-Ag .....	121
8.3.4 Placer Deposits .....	121
8.3.5 Trace Element Geochemistry .....	121
8.3.6 Discussion .....	122
8.4 RICHARDSON MINING DISTRICT .....	122
8.4.1 Location and Previous Investigations .....	122
8.4.2 Bedrock Geology .....	122
8.4.2.1 Regionally Metamorphosed Rocks .....	122
8.4.2.1.1 Schistose Rocks .....	124

## TABLE OF CONTENTS (Continued)

	<u>Page</u>
8.4.2.1.2 Gneissic Rocks . . . . .	124
8.4.2.1.3 Granofels . . . . .	125
8.4.2.2 Igneous Rocks . . . . .	125
8.4.2.2.1 Plutonic Rocks . . . . .	125
8.4.3 Lode Mineral Occurrences . . . . .	126
8.4.4 Placer Deposits. . . . .	126
8.4.5 Trace Element Geochemistry . . . . .	127
8.4.6 Discussion . . . . .	127
8.5 TOLOVANA MINING DISTRICT . . . . .	128
8.5.1 Location and Previous Investigations . . . . .	128
8.5.2 Bedrock Geology. . . . .	128
8.5.2.1 Grit Unit . . . . .	128
8.5.2.2 Paleozoic Sedimentary, Igneous, and Low Grade Metamorphic Rocks. . . . .	128
8.5.2.3 Chert Terrane . . . . .	130
8.5.2.4 Paleozoic Clastics and Chert Unit . . . . .	130
8.5.2.5 Tolovana Limestone . . . . .	130
8.5.2.6 Devonian Clastics and Mafic Complex . . . . .	130
8.5.2.7 Rampart Group . . . . .	130
8.5.2.8 Mesozoic Flysch . . . . .	130
8.5.2.9 Granitic Rocks . . . . .	131
8.5.2.10 Regional Structure . . . . .	131
8.5.3 Lode Mineral Occurrences . . . . .	131
8.5.4 Placer Deposits . . . . .	132
8.5.5 Trace Element Geochemistry . . . . .	132
8.5.6 Discussion . . . . .	132
8.6 KANTISHNA MINING DISTRICT . . . . .	134
8.6.1 Location and Previous Investigations . . . . .	134
8.6.2 Bedrock Geology . . . . .	135
8.6.2.1 Birch Creek Schist . . . . .	135
8.6.2.2 Spruce Creek Sequence . . . . .	135
8.6.2.3 Keevy Peak Formation . . . . .	137
8.6.2.4 Tertiary Intrusive Rocks . . . . .	137
8.6.2.5 Tertiary Sedimentary Rocks . . . . .	138
8.6.2.6 Regional Structure . . . . .	138
8.6.3 Lode Mineral Occurrences . . . . .	138
8.6.3.1 Precious Metal Vein Mineralization . . . . .	139

## TABLE OF CONTENTS (Continued)

	<u>Page</u>
8.6.3.2 Antimony Lodes .....	139
8.6.3.3 Stratabound Massive Sulphide Mineralization .....	139
8.6.3.3.1 Lloyd Prospect .....	139
8.6.3.3.2 Red Dirt Occurrence .....	139
8.6.3.3.3 Moonlight Creek Occurrence .....	139
8.6.3.3.4 Spruce Creek Occurrences .....	140
8.6.4 Placer Deposits .....	140
8.6.5 Trace Element Geochemistry .....	140
8.6.6 Discussion .....	141
8.7 SUMMARY AND CONCLUSIONS .....	142
CHAPTER 9 MAJOR OXIDE AND RARE EARTH ELEMENT GEOCHEMISTRY OF THE FAIRBANKS MINING DISTRICT AND ADJACENT AREAS .....	145
9.1 INTRODUCTION .....	145
9.2 SAMPLING .....	145
9.3 GEOCHEMISTRY OF THE ROCK TYPES .....	146
9.3.1 Fairbanks District Metamorphic Terranes/ Sequences .....	146
9.3.1.1 Chatanika Terrane .....	146
9.3.1.2 Cleary Sequence .....	146
9.3.1.3 Goldstream Sequence .....	164
9.3.1.4 Birch Hill Sequence .....	164
9.3.1.5 Major Oxide and Rare Earth Element Variation .....	164
9.3.1.6 Discussion .....	164
9.3.2 Granitic Rock Types .....	174
9.3.2.1 Fairbanks Mining District .....	175
9.3.2.2 Circle Mining District .....	177
9.3.2.3 Richardson Mining District .....	177
9.3.2.4 Major Oxide and Trace Element Variation .....	177
9.3.2.5 Discussion .....	180
9.4 CONCLUSIONS .....	180
CHAPTER 10 RADIOGENIC ISOTOPIC GEOCHEMISTRY OF THE FAIRBANKS MINING DISTRICT AND ADJACENT AREAS .....	183
10.1 INTRODUCTION .....	183
10.2 RUBIDIUM-STRONTIUM AGE DETERMINATIONS .....	183
10.2.1 Metamorphic Rock Sequences .....	183
10.2.2 Intrusive Rocks .....	183
10.2.2.1 Gilmore and Pedro Dome Plutons .....	183

## TABLE OF CONTENTS (Continued)

	<u>Page</u>
10.2.2.2 Circle Intrusive Complex . . . . .	183
10.2.2.3 Birch Lake Pluton . . . . .	184
10.2.2.4 Summary of Initial Ratios and Crystallization Histories . . . . .	184
10.3 POTASSIUM-ARGON AGE DETERMINATIONS . . . . .	186
10.3.1 Metamorphic Rock Sequences . . . . .	186
10.3.2 Intrusive Rocks . . . . .	186
10.3.2.1 Gilmore and Pedro Dome Plutons . . . . .	186
10.3.2.2 Circle Intrusive Complex . . . . .	186
10.3.2.3 Birch Lake Pluton . . . . .	186
10.3.2.4 Summary of K-Ar Evidence for Thermal Events in the Yukon-Tanana Terrane . . . . .	186
10.4 URANIUM-LEAD (U-Pb) DETERMINATIONS . . . . .	187
10.4.1 Data from Southeastern Yukon-Tanana Terrane . . . . .	187
10.4.2 Data from Northwestern Yukon-Tanana Terrane . . . . .	187
10.4.3 Zircons from the Fairbanks Mining District . . . . .	187
10.4.4 U-Pb evidence for Evolution of the Yukon-Tanana Terrane . . . . .	188
10.5 LEAD-LEAD ISOTOPIC DETERMINATION . . . . .	188
10.5.1 Determinations from Southeastern Yukon-Tanana Terrane . . . . .	188
10.5.2 Determinations from the Fairbanks Mining District . . . . .	188
10.5.2.1 Sample Collection . . . . .	188
10.5.2.2 Sample Preparation, Analysis and Data Reduction . . . . .	188
10.5.3 Discussion . . . . .	190
10.5.4 Summary of Pb-Pb Isotopic Evidence for the Evolution of the Rock Sequences and Mineral Occurrences . . . . .	190
10.6 SUMMARY AND CONCLUSIONS . . . . .	191
CHAPTER 11 MINERAL DEPOSIT MODELS FOR THE FAIRBANKS MINING DISTRICT AND ADJACENT AREAS . . . . .	191
11.1 INTRODUCTION . . . . .	191
11.2 PARAMETERS INCLUDED IN THE MINERAL DEPOSIT MODELS . . . . .	191
11.3 EXAMPLES OF THE MINERAL DEPOSIT TYPES . . . . .	192
11.3.1 Metamorphosed Volcanic-Exhalative Gold and Associated Low Sulphide Gold- Quartz Veins . . . . .	192
11.3.2 Copper-Molybdenum-Gold Porphyry . . . . .	192
11.3.3 Precious Metal Enriched Massive Sulphides . . . . .	192
11.3.4 Epithermal Veins in Volcanic and Plutonic Rocks . . . . .	192
11.3.5 Precious Metal Skarns . . . . .	192
11.3.6 Tin Greisen-Gold-Veins . . . . .	199

## TABLE OF CONTENTS (Continued)

	<u>Page</u>
11.3.7 Carlin-Type Sediment-Hosted Gold .....	199
11.3.8 Paleoplacers .....	199
11.4 SUMMARY BY MINING DISTRICT .....	199
11.4.1 Circle Mining District .....	199
11.4.2 Steese Mining District .....	199
11.4.3 Richardson Mining District .....	199
11.4.4 Tolovana Mining District .....	199
11.4.5 Kantishna Mining District .....	199
11.4.6 Fairbanks Mining District .....	199
11.5 SUMMARY AND CONCLUSIONS .....	199
CHAPTER 12 ECONOMIC ANALYSIS OF MAJOR MINERAL DEPOSIT TYPES IN THE FAIRBANKS MINING DISTRICT .....	200
12.1 INTRODUCTION .....	200
12.2 DISSEMINATED GOLD DEPOSITS .....	200
12.2.1 Mining and Milling Cost Analysis .....	201
12.2.2 Cash Flow Analysis .....	201
12.2.3 Discussion .....	201
12.3 VEIN TYPE GOLD DEPOSITS .....	203
12.3.1 Mining and Milling Cost Analysis .....	203
12.3.2 Cash Flow Analysis .....	203
12.3.3 Discussion .....	203
12.4 CONCLUSIONS .....	204
CHAPTER 13 SUMMARY, CONCLUSIONS, AND RECOMMENDATIONS .....	204
13.1 SUMMARY .....	204
13.2 CONCLUSIONS .....	205
13.3 RECOMMENDATIONS FOR FUTURE INVESTIGATIONS .....	206
REFERENCES CITED .....	207
APPENDICES .....	229

## APPENDICES

		<u>Page</u>
Appendix A	Classification and structural data for lode mines and prospects in the Fairbanks mining district . . . . .	229
Appendix B	Summary of thin section and polished section petrographic reports for the Fairbanks mining district . . . . .	245
Appendix B1	Summary of thin section petrographic reports for the Fairbanks mining district . . . . .	245
Appendix B2	Summary of polished section petrographic reports for the Fairbanks mining district . . . . .	254
Appendix C	Geochemical data . . . . .	262
Appendix C1	Histograms and log concentration-probability plots of stream sediment, pan concentrate, and rock geochemical data from the Fairbanks mining district, Alaska . . . . .	262
Appendix C2	Histograms and log concentration-probability plots of stream sediment data from the Circle mining district, Alaska . . . . .	282
Appendix C3	Histograms and log concentration-probability plots of stream sediment and pan concentrate data from the Richardson mining district . . . . .	288
Appendix C4	Histograms and log concentration-probability plots of stream sediment, pan concentrate, and rock geochemical data from the Tolovana mining district, Alaska . . . . .	303
Appendix D	Placer mine, lode mine, and prospect summaries . . . . .	322
Appendix D1	Placer mines and prospects in the Fairbanks mining district, Alaska . . . . .	322
Appendix D2	Placer mines and prospects in the Circle mining district, Alaska . . . . .	333
Appendix D3	Placer mines and prospects in the Steese mining district, Alaska . . . . .	344
Appendix D4	Placer mines and prospects in the Richardson mining district, Alaska . . . . .	348
Appendix D5	Placer mines and prospects in the Tolovana mining district, Alaska . . . . .	351
Appendix D6	Classification of and structural data for lode mines and prospects in the Kantishna mining district, Alaska . . . . .	355
Appendix D7	Placer mines and prospects in the Kantishna mining district, Alaska . . . . .	366

## LIST OF PLATES (In Pocket)

- Ch. 2, Plate I      General geologic map and mineral occurrences in the Yukon-Tanana Terrane.
- Ch. 3, Plate I      Bedrock geology of the Fairbanks mining district, Alaska.
- Ch. 3, Plate II     Supplemental data for bedrock geology of the Fairbanks mining district, Alaska.
- Ch. 3, Plate III    Structural geologic map of the Fairbanks mining district, Alaska.
- Ch. 3, Plate IV    Vein map of Cleary Summit area, Fairbanks mining district, Alaska.
- Ch. 4, Plate I      Stream sediment sample locations for the Fairbanks mining district, Alaska.
- Ch. 4, Plate II     Rock geochemical and pan concentrate sample locations for the Fairbanks mining district, Alaska.
- Ch. 4, Plate III    Copper mineral occurrences and anomalous sample locations for the Fairbanks mining district, Alaska.
- Ch. 4, Plate IV    Lead mineral occurrences and anomalous sample locations for the Fairbanks mining district, Alaska.
- Ch. 4, Plate V     Zinc mineral occurrences and anomalous sample locations for the Fairbanks mining district, Alaska.
- Ch. 4, Plate VI    Antimony mineral occurrences and anomalous sample locations for the Fairbanks mining district, Alaska.
- Ch. 4, Plate VII   Arsenic mineral occurrences and anomalous sample locations for the Fairbanks mining district, Alaska.
- Ch. 4, Plate VIII   Gold mineral occurrences and anomalous sample locations for the Fairbanks mining district, Alaska.
- Ch. 4, Plate IX    Silver mineral occurrences and anomalous sample locations for the Fairbanks mining district, Alaska.
- Ch. 4, Plate X     Tungsten-Tin mineral occurrences and anomalous sample locations for the Fairbanks mining district, Alaska.
- Ch. 4, Plate XI    Mercury mineral occurrences and anomalous sample locations for the Fairbanks mining district, Alaska.
- Ch. 4, Plate XII   Geologic map of the Nordale adit, Kawalita shaft, and Christina Adit, Christina vein system, Fairbanks mining district, Alaska.
- Ch. 5, Plate I      Placer mining districts and Tertiary basins of Alaska.
- Ch. 5, Plate II     Stream drainage patterns and placer gold locations of the Fairbanks mining district, Alaska.
- Ch. 8, Plate I      Locations of stream sediment and other geochemical samples from the Circle B-2 quadrangle, Circle mining district, Alaska.
- Ch. 8, Plate II     Locations of stream sediment and other geochemical samples from the Circle B-3 quadrangle, Circle mining district, Alaska.
- Ch. 8, Plate III    Locations of stream sediment and other geochemical samples from the Circle B-4 quadrangle, Circle mining district, Alaska.
- Ch. 8, Plate IV    Locations of stream sediment and other geochemical samples from the Circle C-2 quadrangle, Circle mining district, Alaska.

## LIST OF PLATES (Continued)

- Ch. 8, Plate V      Locations of stream sediment and other geochemical samples from the Circle C-3 quadrangle, Circle mining district, Alaska.
- Ch. 8, Plate VI     Locations of stream sediment and other geochemical samples from the Circle C-4 quadrangle, Circle mining district, Alaska.
- Ch. 8, Plate VII    Locations of placer mines, lode mineral occurrences, and anomalous geochemical samples in the Circle B-2 quadrangle, Circle mining district, Alaska.
- Ch. 8, Plate VIII   Locations of placer mines, lode mineral occurrences, and anomalous geochemical samples in the Circle B-3 quadrangle, Circle mining district, Alaska.
- Ch. 8, Plate IX     Locations of placer mines, lode mineral occurrences, and anomalous geochemical samples in the Circle B-4 quadrangle, Circle mining district, Alaska.
- Ch. 8, Plate X      Locations of placer mines, lode mineral occurrences, and anomalous geochemical samples in the Circle C-2 quadrangle, Circle mining district, Alaska.
- Ch. 8, Plate XI     Locations of placer mines, lode mineral occurrences, and anomalous geochemical samples in the Circle C-3 quadrangle, Circle mining district, Alaska.
- Ch. 8, Plate XII    Locations of placer mines, lode mineral occurrences, and anomalous geochemical samples in the Circle C-4 quadrangle, Circle mining district, Alaska.
- Ch. 8, Plate XIII   Locations of placer mines, lode mineral occurrences and geochemical anomalous areas in the Steese mining district, Alaska.
- Ch. 8, Plate XIV    Locations of placer mines, lode mineral occurrences and geochemical samples from the Big Delta B-5 quadrangle, Richardson mining district, Alaska.
- Ch. 8, Plate XV     Locations of placer mines, lode mineral occurrences and geochemical samples from the Big Delta B-6 quadrangle, Richardson mining district, Alaska.
- Ch. 8, Plate XVI    Locations of anomalous geochemical samples and aeromagnetic data, Big Delta B-5 quadrangle, Richardson mining district, Alaska.
- Ch. 8, Plate XVII   Locations of anomalous geochemical samples and aeromagnetic data, Big Delta B-6 quadrangle, Richardson mining district, Alaska.
- Ch. 8, Plate XVIII   Locations of placer mines, lode mineral occurrences, and geochemical samples, Livengood B-3, B-4, C-3, C-4 quadrangles, Tolovana mining district, Alaska.
- Ch. 8, Plate XIX    Locations of anomalous stream sediment, pan concentrate, and rock geochemical samples from the Livengood B-3, B-4, C-3, C-4 quadrangles, Tolovana mining district, Alaska.
- Ch. 8, Plate XX     Locations of placer mines, lode mineral occurrences, and geochemically anomalous areas in the Kantishna mining district, Alaska.

## LIST OF FIGURES

		<u>Page</u>
Figure 4.1a	The maximum As/S variation within arsenopyrite grains in various Type I mineral occurrences .....	40
Figure 4.1b	The maximum As/S variation within arsenopyrite grains in Type II mineral occurrences .....	40
Figure 4.1c	The maximum As/S variation within arsenopyrite grains in Type IV mineral occurrences .....	41
Figure 4.1d	The maximum As/S variation within arsenopyrite grains in Type V mineral occurrences .....	41
Figure 4.2	Paragenetic diagram for Type I stratabound Au-Ag-As-Sb-W mineralization .....	42
Figure 4.3	Paragenetic diagram for Type IV gold-quartz vein and Type V monomineralic stibnite mineralization .....	42
Figure 4.4a	Photomicrograph of isoclinally folded arsenopyrite layer in muscovite-quartz schist, field of view 1.5 mm .....	43
Figure 4.4b	Photomicrograph of arsenopyrite grain in 4.4a with inclusion of gold, field of view 0.15 mm .....	43
Figure 4.4c	Rhythmically layered sulphides (sphalerite, medium grey; jamesonite/tetrahedrite, light grey; and euhedral arsenopyrite and pyrite, white) in metachert (dark grey, Type I mineralization, field of view 40.0 mm .....	44
Figure 4.4d	Photomicrograph of stage two gold in arsenopyrite, Type IV mineralization, field of view 0.15 mm .....	44
Figure 4.4e	Photomicrograph of stage three gold in arsenopyrite, Type IV mineralization, field of view 0.15 mm .....	45
Figure 4.4f	Photomicrograph of gold and arsenopyrite at quartz grain boundary, Type IV mineralization, field of view 0.15 mm .....	45
Figure 4.5	Gold leach rate profiles for Christina shear zone samples .....	49
Figure 5.1	Schematic section of surficial stratigraphy of the Yukon-Tanana Terrane .....	53
Figure 5.2	Longitudinal profile for Fairbanks Creek, Fairbanks mining district, Alaska .....	56
Figure 5.3	Longitudinal profile for Cleary Creek, Fairbanks mining district, Alaska .....	56
Figure 5.4	Longitudinal profile for Dome Creek, Fairbanks mining district, Alaska .....	57
Figure 5.5	Longitudinal profile for the Pedro-Goldstream drainage system, Fairbanks mining district, Alaska .....	57
Figure 5.6	Stream flow directions in (a) hypothetical tectonically stable schist terrane, (b) tectonically active schist terrane before stream capture, and (c) tectonically active terrane after stream capture .....	59
Figure 5.7	Placer-gold fineness versus distance plot for the Pedro-Goldstream drainage system, Fairbanks mining district, Alaska .....	61
Figure 5.8	Placer-gold fineness versus distance plot for Dome Creek, Fairbanks mining district, Alaska .....	61

## LIST OF FIGURES (Continued)

		<u>Page</u>
Figure 5.9	Placer-gold fineness versus distance plot for Cleary Creek, Fairbanks mining district, Alaska .....	62
Figure 5.10	Placer-gold fineness versus distance plot for Fairbanks Creek, Fairbanks mining district, Alaska .....	62
Figure 7.1	Histogram of homogenization temperatures of fluid inclusions in metamorphic quartz, sample 3809 .....	74
Figure 7.2	Histogram of homogenization temperatures of fluid inclusions in metamorphic quartz, sample 20505 .....	74
Figure 7.3	Histogram of homogenization temperatures of fluid inclusions in metamorphic quartz, sample 21152 .....	75
Figure 7.4	Histogram of homogenization temperatures of fluid inclusions in metamorphic quartz, sample 21320 .....	75
Figure 7.5	Histogram of homogenization temperatures of fluid inclusions in metamorphic quartz, sample 21346 .....	76
Figure 7.6	Histogram of homogenization temperatures of fluid inclusions in plutonic quartz, sample 81JB137 .....	76
Figure 7.7	Histogram of homogenization temperatures of fluid inclusions in plutonic quartz, sample 81JB162 .....	77
Figure 7.8	Histogram of homogenization temperatures of fluid inclusions in plutonic quartz, sample 81JB211 .....	77
Figure 7.9	Histogram of homogenization temperatures of fluid inclusions in plutonic quartz, sample 81JB213 .....	78
Figure 7.10	Histogram of homogenization temperatures of fluid inclusions in quartz from the Wackwitz prospect, sample 81MIRL22A .....	78
Figure 7.11	Histogram of homogenization temperatures of fluid inclusions in quartz from the Tolovana prospect, sample 81MIRL19A .....	79
Figure 7.12	Histogram of homogenization temperatures of fluid inclusions in vein quartz from the Silver Fox Mine, sample 81MIRL17A .....	79
Figure 7.13	Histogram of homogenization temperatures of fluid inclusions in vein quartz from the Gil prospect, sample 81MIRL06 .....	81
Figure 7.14	Histogram of homogenization temperatures of fluid inclusions in scheelite from the Stepovich prospect, sample 82STEP SCH .....	81
Figure 7.15	Histogram of homogenization temperatures of fluid inclusions in quartz from the skarn mineralization at the Yellow Pup prospect, sample 82YP01 .....	82
Figure 7.16	Histogram of homogenization temperatures of fluid inclusions in quartz from the skarn mineralization at the Tungsten Hill prospect, sample 81PM202 .....	82
Figure 7.17	Histogram of homogenization temperatures of fluid inclusions in vein quartz from Hi-Yu Mine, sample 81MIRL08 .....	83

## LIST OF FIGURES (Continued)

		<u>Page</u>
Figure 7.18	Histogram of homogenization temperatures of fluid inclusions in vein quartz from the Christina vein, sample 82NA01 . . . . .	83
Figure 7.19	Histogram of homogenization temperatures of fluid inclusions in vein quartz from the Christina vein, sample 82CA03 . . . . .	84
Figure 7.20	Histogram of homogenization temperatures of fluid inclusions in vein quartz from the Christina vein, sample 81MIRL21A . . . . .	84
Figure 7.21	Histogram of homogenization temperatures of fluid inclusions in vein quartz from the Christina vein, sample 81MIRL21B . . . . .	85
Figure 7.22	Histogram of homogenization temperatures of fluid inclusions in vein quartz from the Cleary Hill Mine, sample 82CH02 . . . . .	85
Figure 7.23	Histogram of homogenization temperatures of fluid inclusions in vein quartz from the Wyoming Mine, sample 81MIRL25 . . . . .	86
Figure 7.24	Histogram of homogenization temperatures of fluid inclusions in vein quartz from the Tolovana Mine, sample 82TV05 . . . . .	86
Figure 7.25	Histogram of homogenization temperatures of fluid inclusions in vein quartz from the Newsboy Mine, sample 82NB01 . . . . .	87
Figure 7.26	Histogram of homogenization temperatures of fluid inclusions in vein quartz from the Clipper Mine, sample 81MIRL03 . . . . .	87
Figure 7.27	Histogram of homogenization temperatures of fluid inclusions in vein quartz from the Grant Mine, sample 81MIRL07 . . . . .	88
Figure 7.28	Histogram of homogenization temperatures of fluid inclusions in vein quartz from the Ryan Lode, sample 81MIRL15A . . . . .	88
Figure 7.29	Histogram of homogenization temperatures of fluid inclusions in vein quartz from the Rogasch prospect, sample 81MIRL13A . . . . .	89
Figure 7.30	Histogram of homogenization temperatures of fluid inclusions in scheelite from the Johnson prospect, sample 81MIRL09 . . . . .	89
Figure 7.31	Histogram of homogenization temperatures of fluid inclusions in quartz from the Scrafford Mine, sample 81MIRL16 . . . . .	90
Figure 7.32	Histogram of homogenization temperatures of fluid inclusions in quartz from the Farmer prospect, sample 81MIRL05 . . . . .	90
Figure 7.33	Summary of sulphur isotope and fluid inclusion data for the Fairbanks mining district, Alaska . . . . .	99
Figure 8.1	Generalized geologic map of the Circle mining district, Alaska . . . . .	102
Figure 8.2	Generalized geologic map of the Steese mining district, Alaska . . . . .	112
Figure 8.3	Generalized geologic map of the Richardson mining district, Alaska . . . . .	124
Figure 8.4	Generalized geologic map of the Tolovana mining district, Alaska . . . . .	129
Figure 8.5	Generalized geologic map and mineral deposits of the Kantishna mining district, Alaska . . . . .	136

## LIST OF FIGURES (Continued)

		<u>Page</u>
Figure 8.6	Composite stratigraphic section for the Kantishna-Fairbanks-Circle metallogenic province . . . . .	143
Figure 9.1	Plot of Chatanika terrane samples on an AFM diagram . . . . .	161
Figure 9.2	Plot of Chatanika terrane samples on an Na-Ca-K diagram . . . . .	161
Figure 9.3	Plot of samples from the Chatanika terrane on a Al-Si-Fe diagram . . . . .	162
Figure 9.4	Plot of metavolcanic samples from the Cleary sequence on an AFM diagram . . . . .	162
Figure 9.5	Plot of metavolcanic samples from the Cleary sequence on an Na-Ca-K diagram . . . . .	163
Figure 9.6	Plot of metavolcanic samples from the Cleary sequence on a Al-Si-Fe diagram . . . . .	163
Figure 9.7	Plot of metasedimentary samples from the Fairbanks Schist and Cleary, Goldstream, and Birch Hill sequences on an AFM diagram . . . . .	165
Figure 9.8	Plot of metasedimentary samples from the Fairbanks Schist and Cleary, Goldstream, and Birch Hill sequences on a Na-Ca-K diagram . . . . .	165
Figure 9.9a	Plot of metasedimentary samples from the Cleary sequence, Chopawamsic rocks (Pavlides, 1982) and London-Virginia Mine rocks (Mangan, et al., 1984) on a Al-Si-Fe diagram . . . . .	166
Figure 9.9b	Plot of metasedimentary samples from the Fairbanks Schist, and Goldstream and Birch Hill sequence on a Al-Si-Fe diagram . . . . .	166
Figure 9.10a	Chondrite-normalized rare earth element patterns for samples of metamorphic rocks from the Chatanika Terrane and for an average of North American shales (NAS) and for an average of continental tholeiitic basalts (CTB) . . . . .	167
Figure 9.10b	Chondrite-normalized rare earth element patterns for samples of metamorphic rocks from the Chatanika Terrane . . . . .	167
Figure 9.10c	Chondrite-normalized rare earth element patterns for samples of metavolcanic rocks from the Cleary sequence . . . . .	168
Figure 9.10d	Chondrite-normalized rare earth element patterns for samples of metavolcanic rocks from the Cleary sequence . . . . .	168
Figure 9.10e	Chondrite-normalized rare earth element patterns for samples of metavolcanic rocks from the Cleary sequence . . . . .	169
Figure 9.10f	Chondrite-normalized rare earth element patterns for samples of metavolcanic rocks from the Cleary sequence . . . . .	169
Figure 9.10g	Chondrite-normalized rare earth element patterns for samples of metasedimentary rocks from the Cleary sequence . . . . .	170
Figure 9.10h	Chondrite-normalized rare earth element patterns for samples of metasedimentary rocks from the Cleary sequence . . . . .	170
Figure 9.10i	Chondrite-normalized rare earth element patterns for samples of metasedimentary rocks from the Cleary sequence . . . . .	171
Figure 9.10j	Chondrite-normalized rare earth element patterns for samples of metamorphic rocks from the Fairbanks Schist . . . . .	171

## LIST OF FIGURES (Continued)

		<u>Page</u>
Figure 9.10k	Chondrite-normalized rare earth element patterns for samples of metamorphic rocks from the Goldstream sequence . . . . .	172
Figure 9.10l	Chondrite-normalized rare earth element patterns for samples of metamorphic rocks from the Goldstream sequence . . . . .	172
Figure 9.10m	Chondrite-normalized rare earth element patterns for samples of metamorphic rocks from the Birch Hill sequence . . . . .	173
Figure 9.10n	Chondrite-normalized rare earth element patterns for samples of metasomatic skarns . . . . .	173
Figure 9.10o	Chondrite-normalized rare earth element patterns for samples of metasomatic skarns . . . . .	174
Figure 9.11a	Samples of mafic metaigneous rocks from the Chatanika terrane (closed circles) and Cleary sequence (open circles) on a Harker variation diagram . . . . .	175
Figure 9.11b	Samples of felsic metaigneous rocks from the Chatanika terrane (closed circles) and Cleary sequence (open circles) on a Harker variation diagram . . . . .	175
Figure 9.12	Plot of samples of igneous rocks from the Fairbanks mining district on a AFM diagram . . . . .	176
Figure 9.13	Plot of samples of igneous rocks from the Fairbanks mining district on a Na-Ca-K diagram . . . . .	176
Figure 9.14	Major oxide data for samples of igneous rocks from the Fairbanks mining district plotted on a Harker variation diagram . . . . .	177
Figure 9.15	Plot of samples from the Circle Intrusive Complex and the Birch Lake Pluton on an AFM diagram . . . . .	178
Figure 9.16	Plot of samples from the Circle Intrusive Complex and Birch Lake Pluton on a Na-Ca-K diagram . . . . .	178
Figure 9.17a	Major oxide data for samples of igneous rocks from the Circle mining district plotted on a Harker variation diagram . . . . .	179
Figure 9.17b	Major oxide data for samples of igneous rocks from the Richardson mining district plotted on a Harker variation diagram . . . . .	179
Figure 9.18	Line plots showing ratios of whole rock a) Ba/Rb, b) K/Rb, and c) Rb/Sr for tin granites, barren granites, average granites, of Govet (1983) and the granites in the Fairbanks, Circle, Steese (Newberry and Burns, 1987) and Richardson mining districts . . . . .	181
Figure 10.1a	Rubidium-strontium variation diagram for igneous rocks from the Fairbanks district (after Blum, 1983), the Circle district, and the Richardson mining district . . . . .	185
Figure 10.1b	Whole Rock $^{87}\text{Rb}/^{86}\text{Sr}$ versus $^{87}\text{Sr}/^{86}\text{Sr}$ for the plutonic rocks from the Fairbanks (F), Circle (C), and Richardson (R) mining districts . . . . .	185
Figure 10.2	Plot of lead-lead isotopic data for the Fairbanks district and adjacent areas versus various mineral deposit types . . . . .	190
Figure 10.3	Detailed plot of lead-lead isotopic data for the Fairbanks district and adjacent areas of the Yukon-Tanana Terrane . . . . .	191
Figure 12.1	Tonnage-grade curve for underground and open pit mine models with a 20 percent internal rate of return on investment . . . . .	202

## LIST OF TABLES

		<u>Page</u>
Table 2.1	Major lode and placer deposits in the Yukon-Tanana Terrane and adjacent areas between the Denali and Tintina Faults .....	7
Table 4.1	Assay data for the Truck Sulphide System .....	25
Table 4.2	Channel sample assay data for the Wackwitz Prospect .....	26
Table 4.3	Analytical results for the surface trenches at the Tolovana Mine, Fairbanks district, Alaska .....	27
Table 4.4	Atomic-absorption analyses of samples from the under-ground quartz-molybdenite stockwork, Silver Fox Mine, Fairbanks mining district, Alaska .....	28
Table 4.5	Atomic-absorption analyses of grab and chip samples from sulphide veins in the granodiorite, Silver Fox Mine, Fairbanks mining district, Alaska .....	29
Table 4.6	Atomic-absorption analyses of channel samples from the Trench No. 1, Silver Fox Mine, Fairbanks mining district, Alaska .....	29
Table 4.7	Assay results of chip and channel samples from the Scrafford Mine, Fairbanks mining district, Alaska .....	32
Table 4.8	Electron microprobe analyses of select sulphide minerals from the Fairbanks mining district, Alaska .....	34
Table 4.9	Comparison of grade estimates from channel sampling and diamond drill hole data versus bulk sample, Christina vein system, Fairbanks mining district, Alaska .....	47
Table 4.10	Sieve analysis of gold from bulk sample, Christina vein, Fairbanks mining district, Alaska .....	47
Table 4.11	Cyanide leaching and froth flotation results from Type I (Orange Free Zone) and Type IV (Christina quartz vein) mineralization, Fairbanks mining district, Alaska .....	48
Table 4.12	Overall metallurgical results, bottle roll tests, cuttings samples, 80 percent minus 3/8 inch feed size, Christina vein, Fairbanks mining district, Alaska .....	48
Table 5.1	Historic gold production .....	51
Table 5.2	Screen analysis of gold from lower Goldstream Creek .....	54
Table 6.1	Statistical parameters for analyses of stream sediment samples from the Fairbanks mining district, Alaska .....	64
Table 6.2	Statistical parameters for analyses of pan concentrate samples from the Fairbanks mining district, Alaska .....	65
Table 6.3	Statistical parameters for analyses of mineralized rock samples from the Fairbanks mining district, Alaska .....	65
Table 6.4	Trace element content of major rock units of the Fairbanks mining district, Alaska .....	67
Table 6.5	Comparison of average trace element abundances for the Fairbanks mining district with average crustal abundances for all rock types .....	66

## LIST OF TABLES (Continued)

		<u>Page</u>
Table 7.1	Mass spectrographic analyses of fluid inclusions from various lode mineral occurrences in the Fairbanks mining district, Alaska .....	92
Table 7.2	Sulphur isotopic compositions of sulphides from the Fairbanks district, Alaska .....	94
Table 7.3	Calculated temperatures from sulphur isotopic compositions of sulphide mineral pairs and fluid inclusion homogenization temperature ranges from the Fairbanks mining district, Alaska .....	100
Table 8.1	Criteria used for textural classification and grain size of the granitic rocks of the Yukon-Tanana Terrane .....	104
Table 8.2	Statistical parameters for stream sediment samples from the Circle mining district, Alaska .....	110
Table 8.3	Statistical parameters for stream sediment samples from the Steese mining district, Alaska .....	123
Table 8.4	Statistical parameters for pan concentrate samples from the Steese mining district, Alaska .....	123
Table 8.5	Statistical parameters for stream sediment samples from the Richardson mining district, Alaska .....	127
Table 8.6	Statistical parameters for stream and pan concentrate samples from the Richardson mining district, Alaska .....	127
Table 8.7	Statistical parameters for stream sediment samples from the Tolovana mining district, Alaska .....	133
Table 8.8	Statistical parameters for pan concentrate samples from the Tolovana mining district, Alaska .....	133
Table 8.9	Statistical parameters for rock samples from the Tolovana mining district, Alaska .....	133
Table 8.10	Statistical parameters for stream sediment samples from the Kantishna mining district, Alaska .....	141
Table 8.11	Statistical parameters for pan concentrate samples from the Kantishna mining district, Alaska .....	141
Table 8.12	Number of mineral occurrences by probable deposit type in the Fairbanks, Circle, Steese, Richardson, Tolovana, and Kantishna mining districts, Alaska .....	144
Table 9.1a	Major oxide analysis of the major rock units of the Fairbanks mining district .....	147
Table 9.1b	Normative mineralogies of the major rock units of the Fairbanks mining district .....	153
Table 9.2a	Major oxide analyses of granitic rocks from the Circle mining district, Alaska .....	157
Table 9.2b	CIPW normative analyses of granitic rocks from the Circle mining district, Alaska .....	158

## LIST OF TABLES (Continued)

		<u>Page</u>
Table 9.3a	Major oxide analyses of granitic rocks from the Richardson mining district, Alaska . . . . .	159
Table 9.3b	Table 9.3b CIPW normative analyses of granitic rocks from the Richardson mining district, Alaska . . . . .	160
Table 10.1	$^{87}\text{Sr}/^{86}\text{Sr}$ and $^{87}\text{Rb}/^{86}\text{Sr}$ ratios for the intrusive rocks of the Fairbanks, Circle, and Richardson mining districts . . . . .	184
Table 10.2	Lead-lead isotopic data for the Fairbanks district and adjacent areas of the Yukon-Tanana Terrane . . . . .	188
Table 11.1	Major gold deposit types with analogues in east-central Alaska . . . . .	193
Table 12.1	Surface mining and mineral beneficiation capital and operating costs for disseminated gold mineralization in the Fairbanks mining district, Alaska . . . . .	201
Table 12.2	Calculation of annual positive cash flow for open pit gold mining operation in the Fairbanks district, Alaska . . . . .	201
Table 12.3	Underground mining and mineral beneficiation capital and operating costs for gold-quartz vein mineralization in the Fairbanks mining district, Alaska . . . . .	203
Table 12.4	Calculation of annual positive cash flow for underground gold mining operation in the Fairbanks district, Alaska . . . . .	203

## ACKNOWLEDGEMENTS

Initial funding for this research was provided by a grant from the State of Alaska. This was supplemented by a grant from the National Environmental Research Council of the United Kingdom for the use of the Isotope Laboratory of the British Geological Survey for the fluid inclusion, sulphur isotopic and Pb-isotopic analyses. A grant from Geochron Laboratories Division of Krueger Enterprises was received for the rubidium-strontium isotopic analyses.

Access to mining properties and company data was essential in completing the investigation. The most notable assistance was received from: BP Minerals America, Inc (Kennecott Copper Corp.), St. Joe Minerals, Inc. (Bond Gold), Silverado Mines, Inc., Citigold, Inc., Fairbanks Gold, Inc., Fairbanks Exploration, Inc., AMAX, Inc., and Asarco, Inc. Numerous individuals in the placer mining industry provided access to their properties and operational data. These discussions were essential in the modelling of the processes of placer formation.

Advice and critical comments from Dr. Christopher Halls on all aspects of the project were greatly appreciated. Drs. E.N. Wolff and Barry Donnellan provided editorial comments and critical review of the text.

The secretarial staff of the University of Alaska, Mineral Industry Research Laboratory, and in particular Mrs. Cathy Farmer exercised great skill and patience in the typing and reproduction of the text. Finally, I would like to thank my family for the support and understanding during the extensive periods of remote field and laboratory work.



---

---

## CHAPTER 1 INTRODUCTION AND PREVIOUS INVESTIGATIONS

### 1.1 OBJECTIVE AND SCOPE OF THE INVESTIGATIONS

This research was conducted as part of a project to investigate the mineral resource potential of the Fairbanks mining district and adjacent areas of east-central Alaska. In 1980 the State of Alaska funded a research grant proposal to conduct a mineral resource appraisal of the Fairbanks, Tolovana, Circle and Richardson mining districts. The project was referred to as the "Interior Mining Project" and was conducted as a cooperative research program between the University of Alaska and the Alaska Department of Natural Resources. The co-principal investigators on the project were Paul A. Metz, Economic Geologist, Mineral Industry Research Laboratory (MIRL), School of Mineral Engineering, University of Alaska, and Wyatt Gilbert, Deputy State Geologist, Alaska Division of Geological and Geophysical Surveys (ADGGS), Alaska Department of Natural Resources.

The objective of the project is to estimate the mineral potential of the four mining districts for future mineral discoveries and mineral production. The procedure to realize the objective of the project as outlined in the proposal is as follows:

1. Map the geology of the four mining districts at a scale of 1:24,000 or larger;
2. Examine each of the known mineral occurrences in these districts;
3. Map selected mineral occurrences at a scale of 1:1,000 or larger;
4. Sample bedrock and mineralized lithologies;
5. Collect stream sediment samples;
6. Conduct geochemical analyses of ore, bedrock, and stream sediment samples;
7. Conduct petrographic examinations of ore and bedrock samples;
8. Complete stable isotopic studies of ore samples;
9. Complete radiometric age dating of ore and related host rock samples;
10. Conduct fluid inclusion studies of ore and related host rocks;
11. Examine major structural controls of the mineralization through interpretation of aerial photography and Landsat imagery;
12. Examine the distribution and morphology of gold placer deposits;
13. Construct ore deposit models for the mineralization;
14. Estimate the mineral potential of the region by comparing the ore deposit models with similar deposit types producing in other parts of the world; and
15. Publish a geologic map and report on each district.

The 1980 appropriation was for approximately one half of the original proposal. In 1982, the balance of the funds requested in the original proposal were appropriated, however, due to changes in indirect cost accounting only 60 percent of the original funding request was actually available for the research.

The "Interior Mining Project" was supplemented by additional state appropriations to the ADGGS for the Tolovana and Steese districts. However, the majority of the funding for the ADGGS investigation in the Steese district came in the form of a grant from the U.S. Geological Survey (USGS).

A grant from the National Environmental Research Council of Great Britain provided the Author with access to the facilities and staff of the Isotope Laboratory of the British Geological Survey (BGS). These facilities made the stable isotope, lead/lead isotope and quantitative fluid inclusion analyses possible. A grant to the Author from Geochron Laboratory Inc. facilitated the completion of the Rb/Sr isotope study.

### 1.2 LOCATION

The Fairbanks mining district is located in east-central Alaska and includes an area of approximately 1,500 square kilometers (600 sq. miles). The major placer gold production is from two areas that are centred approximately 16 and 40 kilometers (10 and 25 miles) west and northeast respectively of the City of Fairbanks. The district extends for approximately 48 kilometers (30 miles) in a northeast-southwest direction and is 16 kilometers (10 miles) wide.

The district is in the northwestern extremity of the Yukon-Tanana Terrane (YTT). The terrane is a 750 kilometer (450 mile) long by 350 kilometer (210 mile) wide metamorphic belt and metallogenic province that includes most of east-central Alaska and southwestern Yukon Territory, Canada. The Kantishna district is located 180 kilometers (108 miles) southwest of Fairbanks. The Richardson district is located 80 kilometers (50 miles) southeast of Fairbanks. The Tolovana district is centred at the village of Livengood approximately 100 kilometers (60 miles) north of Fairbanks and is at the northern boundary of the terrane. The Steese and Circle districts are located 80 and 165 kilometers (48 and 100 miles) respectively northeast of Fairbanks and are within the northeastern limit of the terrane.

### 1.3 PREVIOUS INVESTIGATIONS

Prior to the "Interior Mining Project" there were several publications on the geology and mineral deposits of the Fairbanks district but none were considered definitive studies. These general overview investigations included: Prindle and Katz (1913), Hill (1933), Mertie (1937), Sandvik (1964), and Chapman and Foster (1969). Also, prior to the "Interior Mining Project," there was considerable unpublished information both in the public and private sectors relating to the placer and lode mining activity in the district. The available data was compiled by the Author under three grants from the U.S. Bureau of Mines (USBM) entitled "Compilation of the

data on the gold and silver resources of Alaska"; "Mineral resources of the Fairbanks and Livengood quadrangles, Alaska"; and "Mercury-antimony-tungsten metal provinces of Alaska" all of which were completed in the period 1975-1980. These unpublished data compilations became part of the USBM Minerals Availability System data base. The data are available on request from the USBM. Three additional regional resource evaluations were completed under grants to the Author from the USBM during the 1979-1980 time period (Robinson and Metz, 1979; Metz et al., 1979; and Metz and Wolff, 1980). These investigations included portions of the Fairbanks, Livengood, and Richardson mining districts.

## 1.4 PERIOD OF INVESTIGATION

Geologic mapping and geochemical sampling in the Fairbanks district began in 1980 and continued through the 1981 field season. The work was completed jointly by ADGGS and MIRL. Detailed mineral deposit and topical studies were funded through 1983. Unfunded research has been on-going through 1989.

Geologic mapping and geochemical sampling were conducted in the Tokovana district by ADGGS in 1982. Geochemical data reduction was completed by MIRL in 1984. Unfunded mineral deposit studies have been on-going since 1984.

Geologic mapping and geochemical sampling in the Richardson district were undertaken by MIRL in 1982 and data reduction was completed by 1984. Unfunded mineral deposit investigations have been conducted since 1984.

Geologic mapping and geochemical sampling were conducted in the Circle district by MIRL in 1983. Geochemical data reduction was completed in 1984 and unfunded mineral deposit studies have been in progress since 1984.

ADGGS conducted the field investigations of the Steese district in 1986 and completed topical studies of the area in 1987. The USBM also conducted field investigations in the Steese area during the period 1986-87.

Prior to the "Interior Mining Project" ADGGS conducted geologic mapping in the Kantishna district (Bundtzen, 1981) and MIRL compiled the extensive unpublished and published data on the lode and placer deposits of the district. These investigations were conducted during the period 1975 through 1976. These investigations in part provided the outline of the "Interior Mining Project" proposal.

---

---

## CHAPTER 2 REGIONAL GEOLOGY

### 2.1 YUKON-TANANA TERRANE

#### 2.1.1 Introduction

The Yukon-Tanana Terrane (YTT) includes an area of approximately 240,000 square kilometers in southern Yukon Territory, Canada and in east-central Alaska, USA (Ch. 2, Plate I). The terrane is bounded on the northeast by the Tintina Fault and on the southwest by the Denali Fault.

### 2.1.2 Major Rock Units

#### 2.1.2.1 Southern Yukon Territory, Canada

In the southeastern portion of the terrane in the Yukon Territory, the rocks are referred to as the Yukon Crystalline Terrane (Tempelman-Kluit, 1976). The terrane contains several distinctly different metamorphic assemblages. In west-central Yukon, the terrane is composed of cataclastic rocks including: Late Proterozoic (Windemere) biotite schist; Ordovician, Silurian and/or Devonian Nazina quartzite; Upper Devonian and Mississippian Klondike schist and Pelly gneiss; and Pennsylvanian and Permian amphibolites, marbles, and serpentinites.

The rocks in west-central Yukon are primarily metamorphosed to upper greenschist facies however locally they attain amphibolite facies. The characteristic mineral assemblages of the lower grade rocks are quartz-chlorite-muscovite  $\pm$  albite-epidote and actinolite. In the amphibolite facies rocks, the assemblage is quartz-plagioclase-biotite-garnet  $\pm$  hornblende-K-feldspar-kyanite or sillimanite. Stratigraphic evidence brackets the metamorphism to early or middle Triassic time. Limited potassium-argon (K-Ar) data support this estimate with a maximum age date of 202 m.y. and younger dates ranging between 137 and 187 m.y. (Tempelman-Kluit, 1976).

In the south-central Yukon, the terrane is composed of: Late Proterozoic (Windemere) biotite schist; Ordovician, Silurian and/or Devonian age Nazina quartzite; and Upper Jurassic and Cretaceous Kluane schist. The biotite schist and Nazina quartzite are similar to the rocks in west-central Yukon Territory. The Kluane schist is a rather homogeneous coarsely crystalline regionally metamorphosed rock composed of quartz-biotite-muscovite  $\pm$  cordierite and staurolite. Metamorphism in the south-central area is primarily upper greenschist facies; however the Kluane schist is metamorphosed to amphibolite facies. The schist contains mineral assemblages indicative of the lower pressure Buchan series while the biotite schist and Nazina quartzite have typical Barrovian assemblages.

Mortensen and Jilson (1985) describe the geology of the southern portion of the YTT in southeastern Yukon Territory between the Tintina Fault and the Finlayson Lake Fault Zone (see Plate I). The area contains the following six major lithologic packages: a) a sequence of layered metasedimentary and metavolcanic rocks; b) Paleozoic metaplutonic rocks; c) Late Paleozoic mafic and ultramafic rocks and chert along major shear zones; d) Early Mesozoic clastic rocks; e) Mesozoic plutonic rocks; and f) Late Cretaceous and/or Early Tertiary volcanic rocks.

The layered metamorphic sequence is estimated to include an aggregate thickness of 3 kilometers (10,000 feet) of pre-Late Devonian quartz-mica  $\pm$  garnet schist, micaceous feldspathic quartzite, and in the upper part of the sequence calcareous schist, marble, and black siliceous and calcareous phyllite. The carbonaceous rocks are interlayered with major mafic and minor felsic metavolcanic rocks. The felsic metavolcanics have Rb-Sr and U-Pb zircon ages of Late Devonian to mid-Mississippian (Mortensen, 1982; 1983).

The top of the sequence includes chlorite-quartz grits and white quartzites and carbonates that contain Early Pennsylvanian to Early Permian conodonts (Mortensen and Jilson, 1985). This sequence includes the Nisutlin Allochthon of Tempelman-Kluit (1979) which is correlated with the cataclastic rocks of west-central Yukon.

The Paleozoic metaplutonic rocks are divided into the following compositional suites: Simpson Range Pluton (quartz monzonite to quartz diorite; 349-359 m.y., U-Pb zircon); augen orthogneisses (leucogranite, 342 m.y., Rb-Sr whole rock and U-Pb zircon); and monzonitic orthogneisses (quartz monzonite, 340-345 m.y., U-Pb zircon). This Late Devonian thru Lower Mississippian differentiated plutonic suite probably represents the intermediate magma chamber for the bimodal metavolcanic rocks described previously.

The Late Paleozoic mafic and ultramafic rocks include sheared greenstone, gabbro, serpentinized peridotite and dunite. Minor chert and shale occur with the greenstones. The rocks are highly sheared and are in fault contact; thus the suite probably represents a transported ophiolite sequence. It is referred to as the Anvil Allochthon (Tempelman-Kluit, 1979).

The early Mesozoic clastic rocks are predominantly siltstones and shales with minor conglomerate and sandstones of Norian age. The basal conglomerate and sandstones occur northwest of Faro; however, the inferred unconformity has not been mapped to date. The clastic assemblage includes fragments of mylonite, volcanics, gabbro, peridotite limestone, quartz, feldspar, chert, mica, and granitic rocks. Tempelman-Kluit (1979) interprets the sequence as representing a fanglomerate and turbidite depositional environment.

The Mesozoic plutonic rocks include unmetamorphosed early Jurassic (189 m.y., U-Pb zircon) mafic and intermediate composition plutons and Late Cretaceous (91 m.y., U-Pb zircon) quartz monzonitic plutons. The mafic and intermediate plutonic rocks of the southern portion of the terrane are the approximate compositional and time equivalent of the Klotassin Suite and Ruby Range Granodiorite (Tempelman-Kluit, 1976) of west-central and south-central Yukon Territory. The Klotassin Suite forms large, elongate northwest trending batholiths in the central YTT. K-Ar ages of these rocks range from 174 m.y. to 199 m.y. The Ruby Range Granodiorite also forms a major northwest trending batholith north and sub-parallel to the Shakwak (Denali) Fault. K-Ar dates of these rocks average approximately 176 m.y. The Late Cretaceous quartz monzonitic plutons are compositional and time equivalent of the Coffee Creek Quartz Monzonite of Tempelman-Kluit (1976). The Coffee Creek Quartz Monzonite rocks give K-Ar ages of 90 to 100 m.y.

The Klotassin Suite is composed primarily of coarse grained hornblende-quartz diorite which contains subhedral andesine, quartz, perthite, and about 15 percent euhedral hornblende. The Ruby Range Granodiorite is composed primarily of medium grained hornblende-biotite granodiorite and is modally equivalent to the Klotassin Suite except for the addition of biotite.

The Coffee Creek Suite is more heterogeneous than the old plutonic rocks, and ranges in composition from granite to granodiorite. The predominant rock type in the Coffee Creek Batholith is a coarse-grained biotite quartz monzonite with equal quantities of quartz, perthite and albite and minor biotite.

The Late Cretaceous and Early Tertiary subvolcanic and volcanic rocks are not metamorphosed but are locally faulted and tilted. The subvolcanic rocks include the Nisling Range alaskite of Muller (1967). The alaskite occurs as dike swarms and is comprised of equal quantities of subhedral perthite in an aphanitic groundmass of quartz and albite. Locally the alaskite grades into a medium to coarse-grained equigranular biotite granite. The dike swarms and discordant circular stocks may be overlain by or intrude into felsic to intermediate tuff breccias, tuffs, and volcanic flows of equivalent composition. The volcanic equivalents are the Mt. Nansen Group of Bostock (1936) and the Skukum Group of Wheeler (1961). The Nisling Range alaskite yields K-Ar ages between 50 and 60 m.y.

Two assemblages of subaerial basaltic rocks occur sporadically throughout the terrane. The older assemblage, the Carmacks Group of Bostock (1936) may be as old as Late Cretaceous or as young as Pliocene. The assemblage includes a basal conglomerate and an immature channel-fill sandstone unit with minor tuff breccia and sandy tuff that is overlain by at least 1,000 meters (3,000 feet) of tholeiitic basalt. Locally the lower portions of the basalt sequence contains rhyolitic flow and volcanoclastic rocks. Depositional dips of the Carmacks Group rocks range up to 15 degrees.

The youngest assemblage of basaltic rocks found in the terrane is the Selkirk Volcanics. The rocks occur as columnar-jointed flows, pillow basalts and minor breccias and tuffs. The Selkirk Volcanics overlie unconsolidated sediments of Pleistocene or Holocene age. Radiocarbon dates indicate the rocks are older than 38,000 yr B.P. (Bostock, 1966). The volcanics are the product of local fissure eruptions.

#### 2.1.2.2 East-Central Alaska

In the northwestern portion of the Yukon-Tanana Terrane in east-central Alaska, the terrane is composed of regionally metamorphosed sedimentary and volcanic rocks which are intruded by Mesozoic and Tertiary plutons and dikes. Prior to Mertie (1937), the metamorphic rocks had several formational names for various locations in Alaska and the Yukon Territory. Mertie (1937) applied the name "Birch Creek" Schist to all metasedimentary rocks in the region. No type section was defined, however Spurr (1898) used the term Birch Creek "series" for the metamorphic rocks at the headwaters of Birch Creek in the Circle mining district. Mertie (1937) excluded the metavolcanic rocks from his description of the "unit" (more appropriately super group) however he included metavolcanic rocks as Birch Creek Schist in regional mapping programs.

Foster et al. (1973) recommended the abandonment of the term Birch Creek Schist. As an alternative the metamor-

phic rocks were divided into two geographic groups based on metamorphic facies.

The Fairbanks-Big Delta region is described as containing polydeformational greenschist, amphibolite, and eclogite facies rocks that form several northeast-trending belts. The most southerly belt at Fairbanks is exposed along the Tanana River and includes calc-phyllite and phlogopite calc-schist. North of this belt is an amphibolite facies sequence that includes biotite-muscovite-garnet schist, amphibolite and minor gneiss. North of this belt is a sequence of eclogitic rocks first described by Prindle (1913) and later by Swainbank and Forbes (1975).

The northeast trending rocks of the Fairbanks-Big Delta region cannot be traced eastward to the Fortymile-Eagle region. The two regions are separated by large granitic batholiths and major faults. In the Fortymile-Eagle area the regional strike is northwesterly which is sub-parallel to the Tintina Fault zone.

The rocks in this region range from lower greenschist to upper-amphibolite facies. Characteristic rock types in the southern part of the region include biotite-quartz schist and augen gneiss with a noted absence of marble. In the northern part of the region quartzite and marble are abundant along with lesser quantities of biotite quartz schist and biotite quartz gneiss, but augen gneiss is absent. In the extreme northern portion of the region, just south of the Tintina Fault, slate and phyllite are present and massive greenstone is ubiquitous. As in the Fairbanks-Big Delta region the rocks are polymetamorphic and have undergone retrograde metamorphism.

Poorly preserved crinoid columnals and bryozoans have been recovered from marbles in the Fortymile-Eagle region. The evidence suggests that at least part of the terrane is Lower Paleozoic. Radiometric data for the metamorphic rocks is discussed in section 2.2 of this Chapter.

In the northwestern portion of the terrane in the Livengood and Circle quadrangles, slightly metamorphosed Late Precambrian and or Lower Paleozoic rocks are underthrust by a sequence of grits, quartzites, and mica schists (Churkin et al., 1980). The unmetamorphosed or slightly metamorphosed sequence includes quartzite, phyllite, grit, chert, distinctive maroon and green slate and dark limestone. The Cambrian trace fossil *Oldhamia* is reported in the green slate by Churkin and Brabb (1965). Ordovician, Silurian, and Devonian sections are present and are discussed in detail in Chapter 8.

Plutonic rocks occur throughout the terrane with the following bulk compositions; granite, quartz monzonite, granodiorite, quartz diorite, syenite, and gabbro. The largest intrusives are of batholithic dimensions and are generally granodioritic.

Volcanic rocks were deposited as both flows and volcanoclastics during the Paleozoic, Mesozoic, Tertiary, and Holocene (Foster et al., 1973).

Ultramafic rocks occur throughout the terrane and are generally serpentized peridotites. The ultramafics are spatially associated with major strike slip or thrust faults.

## 2.2 REGIONAL GEOCHRONOLOGY

The geochronology of the southeastern portion of the terrane is discussed by Tempelman-Kluit and Wanless (1975), Le Couteur and Tempelman-Kluit (1976), Tempelman-Kluit (1976, 1979), Mortensen (1983), and Mortensen and Jilson (1985). A review of radiometric data for the terrane is provided by Wilson et al. (1985).

The earliest radiometric data for the terrane was the result of the Pb-alpha work of Matzko et al. (1958), Jaffe et al. (1959), and Gottfried et al. (1959). The amount of Pb-isotope data for Alaska in general and the YTT in particular has been increased dramatically since the early work (see Church et al., 1987).

K-Ar and Rb-Sr age determinations for the terrane were begun by Wasserburg et al. (1963). Major additional contributions to the K-Ar data base were made by Foster et al. (1979), Wilson and Shew (1981), and Wilson et al. (1985). Mortensen (1983a, 1983b and 1986), Mortensen (1988), and Aleinikoff et al. (1981a, 1981b, 1983a, 1983b) have made significant contributions to the U-Th-Pb data base for the terrane.

The geochronologic investigations for the terrane prior to the present study indicate that at least six plutonic and thermal metamorphic events have occurred in the region. The plutonic events are as follows:

1. Late Cretaceous (75-50 m.y.)
2. Mid Cretaceous (105-85 m.y.)
3. Early Jurassic (180 m.y.)
4. Mississippian (350 m.y.)

A metamorphic event during the Early Cretaceous (125-105 m.y.) in the western part of the terrane is distinctive from the mid-Cretaceous (105-85 m.y.) plutonic event. Early Jurassic (180 m.y.) and Mississippian (350 m.y.) metamorphic events are also postulated by Wilson et al. (1985).

Previous U-Th-Pb investigations and this present study indicate several thermal events occurred in the Precambrian in or adjacent to the terrane. The above radiometric data confirms the suggestions of polymetamorphism for the terrane which were based on multiple foliations and mineral-facies associations.

The radiometric data also suggests that the terrane can be divided into five thermal event domains by the following major structures or lineaments:

1. Tok Lineament
2. Sixtymile Lineament
3. Mt. Harper Lineament
4. Shaw Creek Fault

These domains are also reflected in the differing lithologies as well as mineral deposit types that occur in the terrane.

## 2.3 REGIONAL STRUCTURES

The Tintina and Denali Faults that bound the terrane on the northeast and southwest respectively are first order regional right lateral strike slip systems. Second order shears formed at about 70° to the parallel first order systems. These second order shears include the Shaw Creek Fault and the Mt.

Harper, Sixtymile, and Tok Lineaments (See Ch. 2, Plate I). As noted above, these second order structures divide the terrane into chronologic as well as petrologic domains. The first order structures will be discussed in detail. The second order structures have not been vigorously examined and discussed in the literature.

Metz and Wolff (1980) identified major linear trends on Landsat imagery of Alaska that parallel the first and second order structures. Less prominent Landsat lineations probably reflect regional joint and fold directions.

### 2.3.1 Major Mapped Structures

Roddick (1967) provides a definitive discussion on the form, timing, and offset of the Tintina Trench. The structure can be traced from the northern part of the Laird Plain of northern British Columbia thru the Yukon Territory to the Yukon Flats in east-central Alaska, a distance of over 960 kilometers (600 miles). The Tintina Trench has a slightly different orientation (15 degrees) than the Rocky Mountain Trench which extends from the southern part of the Laird Plain thru British Columbia into Montana a distance of 1,440 kilometers (900 miles). Roddick (1967) suggests that the structures if not one and the same are intimately related. The total strike length of the systems is about 2,400 kilometers (1,500 miles) with a right lateral offset.

The Tintina Fault juxtaposes the crystalline rocks of the YTT with Proterozoic thru Triassic unmetamorphosed miogeoclinal strata of the North American Continental Margin (NACM). From Circle, Alaska to just northeast of Faro, Yukon Territory, the NACM rocks are found northeast of the fault while the YTT is to the southwest. From the Faro area to Watson Lake and on to the Laird Plain the YTT rocks are found in the northeast side of the Tintina Trench and are bounded on the northeast by the Finlayson Lake Fault Zone. Within this same portion of the fault zone the NACM rocks are found to the southwest of the Tintina Fault. Tempelman-Kluit (1976) interprets the Finlayson Lake Fault Zone as a major thrust zone in which YTT rocks are overthrust onto the NACM rocks prior to major right-lateral motion on the Tintina Fault.

Within the Tintina Trench in the Yukon Territory, there are poorly consolidated conglomerate, sandstone, shale, and coal deposits which yield Paleocene plant fossils (Kindle, 1946). At several localities the Paleocene sediments dip at angles up to 45°. Locally Tertiary basalts overlie the Paleocene sediments. In the Woodchopper and Coal Creek areas of Alaska, plant fossils which correlate with the Eocene or Miocene plant fossils of the Nenana Coal Field are observed.

As noted above, the Tintina Trench is a fault zone that juxtaposes the YTT and NACM rocks. Offsets are estimated by the major terrane sequences rather than individual rock units. The fault zone is marked by intense shearing and high angle dips. Fault gouge is measured in excess of a hundred meters (325 feet) in width. The total strike slip movement is estimated at over 350 kilometers (220 miles).

Roddick (1967) notes that movement along the fault began as early as the Carboniferous. The Carboniferous

displacement is estimated at about 65 kilometers (40 miles) with the major transverse motion taking place in the Upper Cretaceous. As noted previously, Paleocene sediments are found in the trench and are relatively undisturbed. Thus the minimum age of fault movement is lower Tertiary. However, Lowdon (1961) estimates a minimum age of motion of 66 million years based on K-Ar dating of biotite from an unshaped granodiorite stock within the trench.

The time of onset of the major transverse motion is equivocal. Early Cretaceous sediments appear to be terminated at the trench at Dawson, Yukon Territory and in the Woodchopper Creek and Coal Creek area of Alaska. Lowdon (1963) determines K-Ar ages of 100 and 117 million years for the Carmacks volcanics which are offset by the fault. From the above evidence the major transverse motion is estimated to have begun as early as the Late Jurassic and to have continued to Paleocene time. Thus the 350 plus kilometer (220 mile) motion is estimated to have taken place over an interval of about 75 million years at a average rate of approximately 0.5 centimeters (0.2 inches) per year.

Tempelman-Kluit (1976, 1979) interprets the Tintina Fault as a Carboniferous rift system. The YTT is inferred to have then collided at an oblique angle along the older suture zone and the oblique collision subsequently resulted in transverse motion from the Late Jurassic to the Tertiary.

The Denali Fault system is located approximately parallel to and 400 kilometers (250 miles) southwest of the Tintina Fault. The Denali system juxtaposes the YTT with Late Paleozoic and Mesozoic metasediments and metavolcanics. The latter rocks are divided into the following tectonostratigraphic terranes: Wrangellia, Maclaren, Clearwater and an unnamed terrane of ultramafic rocks (Nokleberg et al., 1985). The Late Paleozoic sediments include limestone and argillite while the volcanics are andesitic to dacitic. The Mesozoic rocks include mafic volcanics, andesitic tuffs and flows, chert, and greywacke.

The Denali Fault system extends for about 2,000 kilometers (1,200 miles) from southeastern Alaska thru northern British Columbia and the Yukon Territory to central Alaska. Based on the offset of major metamorphic sequences Forbes et al. (1973, 1974), Turner and Smith (1974), Turner et al. (1974), Hickman et al. (1977), and Wahrhaftig et al. (1975) estimate that the total right lateral displacement is 400 kilometers (240 miles). Lanphere (1977) notes that 350 kilometers (210 miles) of motion took place between 55 and 38 m.y. ago. Less than 40 kilometers (24 miles) of motion is estimated to have occurred since 38 m.y. ago.

The terranes south of the Denali Fault are interpreted by Richter and Jones (1973) as accreted island arc and subduction complexes. Thus the Denali system represents an earlier subduction zone that has also experienced back arc rifting and an oblique collisional event.

During the Pennsylvanian and Permian, volcanic, volcanoclastic, and sedimentary rocks were deposited in an island arc environment. In the Middle and Late Triassic, rifting occurred with the initial submarine extrusion of the Nikolai Greenstone and later its compositional subaerial

equivalents in various parts of Wrangellia.

In the Jurassic and Cretaceous, Wrangellia moved northwestward accompanied by deposition of the flysch sediments and andesitic volcanics of the Gravina-Nutzotin belt. This island arc formation was superceded by a granitic plutonic event with minimum ages of 120 to 149 m.y.

The Alexander terrane of southeastern Alaska has undergone contemporaneous sedimentation and volcanism of similar character to Wrangellia. Thus the two terranes combined with the Peninsular terrane and coalesced into a single terrane in the Middle or Late Jurassic.

Wrangellia was subsequently obducted onto the accretionary margin of North America as the ocean basin closed. During obduction the East Susitna Batholith was emplaced at 100 to 110 m.y. The collisional event and batholith emplacement resulted in a regional Barrovian-type metamorphism to form the Maclaren Glacier metamorphic belt over the East Susitna batholith.

After the oblique obduction of Wrangellia, the suture zone developed a transverse sense of motion and the Denali Fault system was developed during the early Tertiary. This first order structure was active from Lower Tertiary time to the present.

Of the above second order structures, only the Shaw Creek Fault is mapped in detail (Foster et al., 1979). The fault is traced in a northeasterly direction from the confluence of Shaw Creek with the Tanana River to within a few kilometers of the Tintina Fault, a distance of approximately 200 kilometers (120 miles).

The Mt. Harper, Sixtymile, and Tok Lineaments parallel the Shaw Creek Fault and are interpreted to extend over about the same strike length as the Shaw Creek structure. Sections of each of the lineaments are mapped as fault structures. The structures locally exhibit left-lateral offsets of a few kilometers.

The relative motions of the first and second order structures indicate alternating zones of tension and compression at the fault intersections. Along the Tintina Fault system, the zones of tension are on the northwest of the second order structures while the zones of compression are on the southeast. The opposite is true near the intersection of the second order structures with the Denali Fault.

### 2.3.2 Linear Trends from Landsat Imagery

Metz and Wolff (1980) provide an interpretation of Landsat data for all of Alaska to delineate major linear trends associated with major mineral occurrences. Major mapped faults and linear trend directions are displayed along with major mineral occurrences. Linear trend directions are plotted as rose diagrams for each Landsat image. No attempt is made to subdivide the frames via the major mapped structures, thus peak directions reflect linear data on both sides of major structures. Examination of linears on individual frames suggests that locally there may be significant changes in the direction of domains across major transverse faults. However, the limited regional and detailed mapping of these structures precludes subdivision of frames into structural domains at this time.

Within the YTT in Alaska, two major linear trends are noted and these trends are parallel to the first order (N50-60W) and second order structures (N40-45E). A less well developed trend is north-south. Third order structures and thrust faults, joints, and folds may be represented in the circular histograms however such a detailed interpretation is not attempted.

Major mining districts are located along the second order structures or at the intersections of the first and second order structures (see Ch. 2, Plate I). The Richardson district and Woodchopper and Coal Creeks east of the Circle district are adjacent to the Shaw Creek Fault. The Circle district is near the intersection of the Shaw Creek Fault and Tintina Fault.

The Koroko type massive sulphides of the eastern end of the Bonfield district and the Eagle/Fortymile district are located near the Mt. Harper Lineament. The Delta massive sulphides and the Sixtymile district are proximal to the Sixtymile Butte Lineament. The major copper porphyry prospects of the Nabesna and Tanacross quadrangles are localized near the Tok Lineament while the Klondike district is at the intersection of this lineament and the Tintina Fault. This spatial relationship of mining districts and major prospects to the first and second order structures and the definition of these structures from Landsat images suggests that more detailed Landsat interpretations thru image enhancement may lead to additional mineral discoveries.

No comparable Landsat data interpretations exist for the YTT in the Yukon Territory. It is expected that major linear trends would parallel the first order structures (transform faults) in the Yukon Territory as they do in Alaska. Second and third order structures may be less obvious as Landsat linear trends due to the more extensive thrust faulting in the Yukon Territory relative to that in Alaska.

## 2.4 MINING DISTRICTS AND DISTRIBUTION OF MINERAL OCCURRENCES

Plate I gives the location of the mining districts and major mineral occurrences in the YTT. Brief descriptions of the districts and the major mineral occurrences are given in Table 2.1. In addition to the seventy-two occurrences listed in Table 2.1, there are at least an order of magnitude more minor mineral occurrences in the YTT. The abundance of mineral occurrences, the historic production, and the rate of new discoveries indicates that the terrane is a major metallogenic province.

### 2.4.1 Regional Distribution of Lode and Placer Deposits

Of the twenty-five major lode and placer deposits in the Yukon Territory between the Tintina and Denali Faults, only eight are actually in the YTT. The most significant deposits in the YTT in the Yukon Territory include the lead-zinc-silver volcanogenic massive sulphide deposits in the Anvil district, the copper-molybdenum porphyry deposits including Cash, Casino, and Lucky Joe and the placer gold deposits of the Klondike district. The past production and current reserves of the Anvil district have a gross value of approximately \$8 billion at current market prices. Similarly the past

Table 2.1 Major lode and placer deposits in the Yukon-Tanana Terrane and adjacent areas between the Denali and Tintina Faults (Data source: Staff, DIAND, 1984-1989; Nokleberg, et al., 1987).

Location Number	Name	Commodity(ies)	Host Rock Type	Host Rock Age	Deposit Type	Comments
1.	Midway	Pb, Zn, Ag	Limestone	Devonian	Pb-Zn Skarn	6.0 million tonnes @ 18% Pb + Zn, 400 g/t Ag
2.	Logtung	W, Mo	Monzogranite	Cretaceous	Sheeted veins	162 million tonnes @ 0.13% WO <sub>3</sub>
3a.	Venus	Au, Ag	Andesites/ Dacite	Cretaceous	Polymetallic Vein	108,000 tonnes @ 7.6 g/t Au, 226 g/t Ag.
3b.	Arctic Caribou	Au	Granodiorite	Cretaceous	Au Quartz Vein	5,700 tonnes @ 13.0 g/t Au, 744 g/t Ag
4.	Whitehorse Copper Belt	Cu, Au, Ag	Quartz diorite	Cretaceous	Cu Skarn	9.4 million tonnes @ 1.4% Cu, 0.8 g/t Au, 7.9 g/t Ag
5.	Rex	Fe	Iron formation Chert	Proterozoic	Banded Iron Formation	5.6 billion tonnes @ 47% Fe
6.	Wellgreen	Cu, Ni, Co Pt, Pd	Gabbro	Triassic	Alpine Ultramafic	0.6 million tonnes 1.4% Cu, 2.0% Ni, 0.07% Co
7.	Nordenskiold	Coal	Sandstone/ Conglomerate	Tertiary	Terrestrial Coal	Bituminous 3.7 million tonnes
8.	Red Mountain	Mo	Quartz Monzonite	Cretaceous	Mo Porphyry	72 million tonnes @ 0.22% MoS <sub>2</sub>
9.	Laple River	Coal	Sandstone/ Conglomerate	Tertiary	Terrestrial Coal	High volatile bituminous B, 1 million tonnes
10a.	Anvil District	Pb, Zn, Ag	Chlorite Schist/ Quartzite	Proterozoic/ Cambrian	Volcanogenic Massive Sulfide	100 million tonnes @ 3.0% Pb, 4.8% Zn, 37 g/t Ag

Table 2.1 (Continued)

Location Number	Name	Commodity(ies)	Host Rock Type	Host Rock Age	Deposit Type	Comments
10b.	Grew Creek	Au	Felsic Tuffs	Eocene	Au-Quartz Vein	852,100 tonnes @ 9 g/t Au
10c.	Ketza River	Au	Limestone	Cambrian	Mantos	495,800 tonnes @ 18 g/t Au
11.	Tantalus Butte	Coal	Sandstone/ Conglomerate	Tertiary	Terrestrial Coal	High volatile Bituminous B
12a.	Mount Nansen	Au, Ag	Quartz Monzonite	Cretaceous	Polymetallic Vein	180,000 tonnes @ 11.3 g/t Au, 446 g/t Ag
12b.	Brown-McDade	Au	Quartz Monzonite	Jurassic	Au Quartz Vein	50,000 tonnes @ 15 g/t Au, 202 g/t Ag
13.	Tinta Hill	Zn, Pb, Ag, Au	Granodiorite	Jurassic	Polymetallic Veins	0.8 million tonnes @ 6.0% Zn, 4.7% Pb, 183 g/t Ag, 2.6 g/t Au
14.	Laforma	Au	Granodiorite	Jurassic	Au Quartz Vein	130,000 tonnes @ 15 g/t Au
15.	Williams Creek	Cu	Granodiorite	Jurassic	Cu Skarn	14 million tonnes @ 1.0% Cu
16.	Cash	Cu, Mo	Granite/ Granodiorite	Tertiary	Cu-Mo porphyry	40 million tonnes @ 0.2% Cu, 0.02% MoS <sub>2</sub>
17.	Minto	Cu, Ag, Au	Granodiorite	Jurassic	Cu Skarn	6.6 million tonnes @ 1.9% Cu, 6.8 g/t Ag, 0.5 g/t Au
18.	Casino	Cu, Mo	Granite/ Granodiorite	Cretaceous	Cu-Mo porphyry	162 million tonnes @ 0.37% Cu, 0.04% MoS <sub>2</sub>
19.	Lucky Joe	Cu	Mica Schist	Lower Paleozoic	Sedimentary Cu	0.3% Cu
20.	Lone Star	Au	Mica Schist	Devonian/	Stratabound	4-5 g/t Au

Table 2.1 (Continued)

Location Number	Name	Commodity(ies)	Host Rock Type	Host Rock Age	Deposit Type	Comments
21.	Dawson/Klondike	Placer Au	Alluvial Gravel	Tertiary/ Pleistocene	Alluvial Placer	Past gold production 16 million ounces
22.	Caley	Asbestos	Pyroxenite	Late Paleozoic	Alpine ultramafic	1 million tonnes
23.	Clinton Creek	Asbestos	Pyroxenite	Late Paleozoic	Alpine ultramafic	Past Production 930,623 tonnes asbestos
24.	Eagle	Placer Au	Alluvial Gravel	Pleistocene	Alluvial Placer	Past Production 40,000 ounces
25.	Fortymile	Placer Au	Alluvial Gravel	Pleistocene	Alluvial Placer	Past Production 430,000 ounces
26.	Eagle C3	PGE	Pyroxenite	Late Paleozoic	Alpine Ultramafic	3-4 g/t Pt + Pd
27.	Slate Creek	Asbestos	Harzburgite	Late Paleozoic	Alpine Ultramafic	55 million tonnes @ 6.3% asbestos
28.	Purdy	Au	Mica Schist	Proterozoic/ Paleozoic	Au Quartz Vein	Minor Production
29.	Taurus	Cu, Mo	Granite	Tertiary	Cu-Mo Porphyry	700 million tonnes @ 0.5% Cu, 0.03% Mo
30.	Bluff	Cu, Mo	Granodiorite	Cretaceous/ Tertiary	Cu-Mo Porphyry	No Data
31.	ASARCO	Cu, Mo	Quartz Porphyry	Tertiary	Cu-Mo Porphyry	No Data

Table 2.1 (Continued)

Location Number	Name	Commodity(ies)	Host Rock Type	Host Rock Age	Deposit Type	Comments
32.	Mosquito	Cu, Mo	Quartz Monzonite	Cretaceous/ Tertiary	Cu-Mo Porphyry	No Data
33.	Tibbs Creek	Au, Ag, Sb	Mica Schist	Proterozoic/ Paleozoic	Polymetallic Vein	6-7 g/t Au
34.	Delta Massive Sulfides	Pb, Zn, Cu, Ag, Au	Rhyolite	Devonian	Kuroko	18 million tonnes @ 3-7% combined.
35.	McGinnis Glacier	Zn, Cu, Pb, Ag	Rhyolite	Devonian	Kuroko	No Data
36.	Hayes Glacier	Cu, Pb, Zn, Au, Ag	Rhyolite	Devonian	Kuroko	No Data
37.	Red Mt.	Cu, Pb, Zn, Ag	Rhyolite	Devonian	Kuroko	1.1 million tonnes @ 10% combined Pb + Zn, 270 g/t Ag
38.	Anderson Mt.	Cu, Pb, Zn, Ag	Rhyolite	Devonian	Kuroko	1-20% Cu, 0-5% Pb, 0.28% Zn
39.	Sheep Creek	Zn, Pb, Sn	Rhyolite	Devonian	Kuroko	10-11% combined Pb + Zn
40.	Liberty Bell	As, Cu, Bi, Au	Rhyolite	Devonian	Kuroko	91,000 tonnes @ 2% Cu, 34 g/t Au
41.	Bonnifield	Placer Au	Alluvial Gravel	Pleistocene	Alluvial Placer	Past Production 45,000 ounces
42.	Nanana Coal Field	Coal	Sandstone and Conglomerate	Tertiary	Terrestrial Coal	250 million tonnes drill indicated and 1 billion tonnes inferred

Table 2.1 (Continued)

Location Number	Name	Commodity(ies)	Host Rock Type	Host Rock Age	Deposit Type	Comments
43.	Stampede	Sb	Mica Schist	Proterozoic/ Paleozoic	Sb Vein	400,000 tonnes @ 10% Sb
44.	Spruce Creek	Au, Ag, Pb, Zn, Sb	Mica Schist	Proterozoic/ Paleozoic	Stratabound Massive sulfide	77,000 tonnes @ 2.4 g/t Au, 276 g/t Ag
45.	Kantishna	Placer Au	-	-	Alluvial Placer	Past Production 55,000 ounces
46.	Banjo	Au, Ag, Pb, Zn, Sb	Mica Schist	Proterozoic/ Paleozoic	Polymetallic Vein	160,000 tonnes @ 18.4 g/t Au, 123 g/t Ag
47.	Quigley Ridge	Ag, Au, Pb, Zn	Mica Schist	Proterozoic/ Paleozoic	Polymetallic Vein	380,000 tonnes, 1300 g/t Ag, 4.8 g/t Au, 6.4% Pb, 2.3% Zn
48.	Slate Creek	Sb-Au	Mica Schist	Proterozoic/ Paleozoic	Polymetallic Vein	64,000 tonnes @ 12% Sb
49.	Salcha River	W	Granodiorite	Cretaceous	W Skarn	No Data
50.	Ketchum Dome	Sn	Granodiorite	Cretaceous	Sn Vein	No Data
51.	Miller House	Au	Mica Schist	Proterozoic/ Paleozoic	Au-Quartz Vein	4.0 g/t Au
52.	Bedrock Creek	Au, Sn, W	Mica Schist	Proterozoic/ Paleozoic	Au-Quartz Vein	No Data
53.	Table Mt.	Au, Sn, W	Mica Schist	Proterozoic/ Paleozoic	Au-Quartz Vein	140 g/t Au

Table 2.1 (Continued)

Location Number	Name	Commodity(ies)	Host Rock Type	Host Rock Age	Deposit Type	Comments
54.	Dempsey Pup	Sb	Mica Schist	Proterozoic/ Paleozoic	Sb Vein	No Data
55.	Circle	Placer Au	Alluvial Gravel	Tertiary/ Pleistocene	Alluvial Placer	Past Production 1 million ounces
56.	Democrat	Au	Rhyolite	Cretaceous	Au Porphyry	No Data
57.	Gilmore Dome	Au	Granodiorite	Cretaceous	Au Porphyry	80 million tonnes @ 1-2 g/t Au
58.	Cleary Summit	Au, Ag, As, Sb, Pb, Zn	Mica Schist	Proterozoic/ Paleozoic	Stratabound Massive sulfides and Au-Quartz Veins	Past Production 280,000 ounces
59.	Scrafford	Sb	Mica Schist	Proterozoic/ Paleozoic	Sb Vein	Past Production 944,500 kg Sb
60.	Ester Dome	Au	Mica Schist	Proterozoic/ Paleozoic	Polymetallic Vein	Past Production 100,000 ounce
61.	Fairbanks	Placer Au	Alluvial Gravel	Pleistocene	Alluvial Placer	Past Production 7,500,000 ounces
62.	Lime Peak	Sn, Ag	Granodiorite	Cretaceous	Sn Vein	0.16% Sn
63.	Roy Creek	U, Th, REE	Rhyolite	Cretaceous	Intrusive U	5 to 10% REE
64.	Hudson	Hg	Granite	Cretaceous/ Tertiary	Hg Quartz Vein	No Data
65.	Griffen	Au, Ag, Sb	Calc-schist and Quartz Monzonite	Paleozoic/ Cretaceous	Sb Vein	15% Sb, 3.9 g/t Au

Table 2.1 (Continued)

Location Number	Name	Commodity(ies)	Host Rock Type	Host Rock Age	Deposit Type	Comments
66.	Sawtooth	Sb, Au, Ag	Monzonite/ Syenite	Cretaceous	Sb Vein	No Data
67.	Livengood	Placer Au	Alluvial Gravel	Tertiary/ Pleistocene	Alluvial Placer	Past production and drill indicated reserves total 1 million ounces
68.	Shorty Creek	Au, Ag	Granodiorite	Cretaceous	Au Porphyry	No Data

production of the Klondike has a gross value of \$6 billion. The Keno Hill district north of the Tintina Fault, not included in Table 2.1 is credited with a total production of 250 million ounces of silver with a gross value of \$1.3 billion at present market prices. The Whitehorse copper belt, also outside the YTT but between the Denali and Tintina Faults, has an aggregate gross metal product value of about \$0.4 billion. Thus developed deposits within or proximal to YTT account for or have the productive capacity to produce approximately \$16 billion worth of metal at current market prices.

The major lead-zinc-silver mineralization in and adjacent to the YTT is localized along the Tintina Fault. In the Yukon Territory the mineralization occurs in both the schist terrane and in the miogeoclinal rocks of the North American craton. In Alaska, the lead-zinc-silver mineralization also occurs in both geologic settings. In the Kantishna, Fairbanks, Steese, and Circle districts the mineralization occurs in the schist rocks of the YTT and the elemental association also includes gold. In the Livengood district and in the areas north of the Steese and Circle districts, the association does not include gold and the host rocks are the carbonates and clastic sediments of the North American craton.

The Cretaceous and Tertiary copper-molybdenum porphyries are restricted to west-central Yukon Territory and east-central Alaska. They are spatially associated with the orthogneissic dome complexes. Intrusive related gold mineralization occurs in the Fairbanks, Richardson, and Circle districts. The host rocks in these areas are Cretaceous age granitic to granodioritic plutons of probable S-type affinities. These plutons show minor tin-tungsten type mineralization and low copper contents. In the Livengood area, a major copper-molybdenum porphyry contains high gold, arsenic, antimony and silver values. This intrusive complex is not unlike the copper-molybdenum porphyries of the central YTT, however the arsenic and antimony content appears to be greater.

Stratabound gold-quartz veins of the Kantishna, Fairbanks, Steese, and Circle districts are localized within arsenic-antimony-lead-zinc  $\pm$  copper  $\pm$  gold  $\pm$  silver bearing massive sulphide sections of the schist sequences. This association is restricted to the northwest margin of the terrane within the major thrust fault belt that juxtaposes the terrane with the North American cratonic rocks south and west of the Tintina Fault. The schists and associated massive sulphide mineralization are late Proterozoic or Paleozoic in age. A belt of copper-lead-zinc-arsenic-antimony  $\pm$  gold  $\pm$  silver bearing volcanogenic massive sulphides extends on the north side of the Denali Fault from Tok to the Kantishna district. The rhyolitic host rocks are of probable Devonian age and thus are time equivalent to the Greens Creek orebody in southeastern Alaska.

All the major placer production from the terrane has occurred from the Klondike district westward to the Kantishna district. The Klondike district has had the greatest production, with an estimated output of 16 million ounces while Fairbanks, Circle, and Fortymile have produced 7.5 million, 1.0 million and 430 thousand ounces respectively. The placer

production has come from areas with bedrock ranging in composition from greenschist to lower amphibolite facies metavolcanics and metasediments.

#### 2.4.2 Regional Variation in Elemental Associations and Elemental Distribution

The regional variation in elemental associations is reflected in the above discussion on the regional distribution of the various mineral deposit types. The lead-zinc-silver association occurs in volcanic massive sulphides along the Tintina Fault or in the platform sediments of the North American craton.

Copper-molybdenum association occurs only in the central portion of the terrane and to a minor extent in the Livengood district. The copper grades of the porphyry deposits are low, generally less than 0.5 percent, thus reflecting the lack of major supergene enrichment zones.

The arsenic-antimony-lead-zinc  $\pm$  copper  $\pm$  gold  $\pm$  silver association is restricted to the Kantishna, Fairbanks, Steese, and Circle districts. The arsenic content of the stratiform and stratabound mineralization is extremely high while the copper content is moderate. In the Fairbanks district they are much lower, below the Clarke.

In contrast, the Devonian massive sulphides of the north flank of the Alaska Range have a higher copper content and a lower gold content than the massive sulphides of the Kantishna, Fairbanks, Steese, and Circle districts. The copper rich association is localized on the south and southwestern margin of the YTT.

The intrusive related gold mineralization in the Fairbanks, Richardson, and Circle districts is associated with arsenic, and minor tungsten and tin mineralization. Alteration of these intrusives is restricted to silicification and minor greissenization. This association is limited to the northwestern margin of the terrane.

The relative abundance of the elements in the YTT has been estimated from published grade data for major mineral occurrences. No systematic sampling of the various deposit types has been undertaken for the terrain as a whole. Similarly regional stream sediment geochemical sampling has been limited to the historic mining districts. In most cases, these district-wide geochemical programs were not designed to be compatible either in sampling techniques or elemental analysis.

## 2.5 SUMMARY

The Yukon-Tanana Terrane is a heterogeneous accumulation of rocks with both continental and oceanic affinities. The oldest rocks in the terrane are probably of late Proterozoic age while the youngest are Tertiary in age.

There is evidence that the terrane was rifted from the North American continental margin at least once in the mid-Paleozoic. The subsequent collision of the terrane with North America is manifested by thrust faulting, regional metamorphism, strike-slip faulting, plutonism, and regional uplift.

These events are responsible for a complex history of

diverse and widespread mineralization. The major past placer gold production of 25 million troy ounces is an indication of the lode gold potential of the terrane. Lead-zinc-silver, copper-molybdenum, and tin-tungsten mineralization as well as gold is noted at numerous locations. The total estimated value of past metal production and measured reserves at current market prices is \$16 billion. Thus the terrane is a major metallogenic province that warrants more detailed exploration and evaluation.

---

## CHAPTER 3 GENERAL GEOLOGY OF THE FAIRBANKS MINING DISTRICT

### 3.1 LOCATION AND GEOLOGICAL SETTING

The Fairbanks mining district is located just north of Fairbanks, Alaska (see Ch. 1, Plate I). It extends approximately 48 kilometers (30 miles) northeast-southwest by 16 kilometers (10 miles) northwest-southeast with its centre about 24 kilometers (15 miles) north of the city. It extends from Ester Dome on the southwest to Gilmore Dome and Pedro Dome on the northeast with the Goldstream Valley forming the approximate northeast-southwest axis of the district. The domal areas have been the locale of major gold placer operations as well as small hardrock mines and prospects. The Chatanika, Chena, and Goldstream Valleys and their tributary drainages have been the sites of extensive placer operations.

The first placer location was made in 1902 in the north-central part of the district. The greatest production occurred between 1923 and 1962 when the Fairbanks Exploration Company operated seven dredges in the drainages between Chatanika and Ester. During this period the production for the district was over 7,500,000 troy ounces of placer gold. This average grade of the placer production was 2 gm per cubic meter (0.05 troy ounces per cubic yard).

The lode mines developed in the areas of Ester, Pedro and Gilmore Domes and were found as prospectors attempted to trace the source of the placers. Ester Dome is a structural feature while Pedro Dome and Gilmore Dome are the topographic expressions of Mesozoic granitic intrusives which intrude the surrounding metavolcanic terrane. Lode mining activity has resulted in the production of about 325,000 troy ounces of gold and several thousand short tons of antimony and tungsten. The average grade for the lode gold production was 1.08 troy ounces per ton (OPT).

### 3.2 MAJOR ROCK UNITS

#### 3.2.1 Metamorphic Terranes/Sequences

The first general description of the bedrock and surficial geology of the Fairbanks mining district was provided by Prindle and Katz (1913). Subsequent investigators have retained many of the original names for the rock units defined by Prindle and Katz. The major contribution by Prindle and

Katz was their detailed description of the gold placer deposits which they related to the gold-quartz-sulphide veins, the formation of which, in turn, was attributed to the intrusion of the granitic rocks of Pedro Dome and Gilmore Dome. Smith (1913) gave detailed descriptions of several lode deposits which support the earlier observations of Prindle and Katz (1913). Prindle and Katz (1913) also described the lode deposits of the district and noted the close spatial relationship between the placer deposits and the lode occurrences. These investigators considered the gold-quartz veins to be the sole lode source and the veins were thought to be genetically related to the granitic intrusive rocks. Chapman and Foster (1969) also related the gold-quartz vein deposits of the district to the Cretaceous-age granitoid intrusions and concluded that the quartz veins were the sole source of the placer gold. Mineralization in the area of Ester Dome was thought to be related to a complex of aplite dikes which may be offshoots of an as-yet unrecognized larger underlying intrusive body.

Metz (1977) and Metz and Robinson (1980) suggest that the antimony-tungsten and associated lode gold mineralization of the Fairbanks district is related to previously unrecognized metavolcanic rocks in the Yukon-Tanana Terrane (YTT). Subsequent 1:24,000 scale geologic mapping by Metz (1982), Bundtzen (1982), and Robinson (1982) delineates the extent of these metavolcanic rocks, named the Cleary sequence by Metz (1982). A compilation of this mapping is provided by Robinson et al. (1990). Two non-mineralized pelitic schist sequences, the Goldstream sequence and the Chatanika sequence, make up most of the exposed bedrock of the Fairbanks district. A majority of the 236 known lode mineral occurrences in the district are found within the Cleary sequence; however eight of the occurrences are in the eclogitic rocks of the structurally lower Chatanika terrane. Most of the mineral occurrences in both the Chatanika terrane and the Cleary sequence are not spatially associated with exposed intrusive rocks.

The following are descriptions of the units mapped by Metz (1982), Bundtzen (1982) and Robinson (1982). Some of these units have been combined in the compilation by Robinson et al. (1990).

#### 3.2.1.1 Chatanika Terrane

The Chatanika terrane is structurally the lowest sequence of rocks exposed in the Fairbanks district. The sequence includes eclogitic rocks, described and classified by Swainbank and Forbes (1975) as group "C" metabasite eclogite of Coleman et al. (1965). These eclogitic rocks are in fault contact with lower greenschist facies metaplates of probable late Precambrian or early Paleozoic age that occur north of the Chatanika River. The eclogites are also in thrust contact with the Cleary sequence which outcrops to the south along Cleary Creek. The thrust strikes east-west in the Cleary Creek/Cleary Summit area and dips to the south at less than 45°. The terrane can be subdivided into five mappable rock units.

Unit EC - The eclogitic rocks can be divided into at least

three distinct types including: a) garnet-clinopyroxene rocks; b) garnet-clinopyroxene-amphibole rocks; and c) garnet-amphibole rocks. The garnet-clinopyroxene variety occurs as mylonitic, layered, laminated, and massive types, and is characterized by the presence of pale-pink pyrope garnet and pale-green omphacitic pyroxene. Un-twinned albite is present in the mylonitic variant and is usually associated with garnet and chlorite. Quartz generally occurs as granoblastic aggregates with calcite and clinozoisite. The garnet-clinopyroxene-amphibole variety occurs as finely laminated and massive variants characterized by zoned garnet, light-green, poikiloblastic clinopyroxene, and pleochroic, pale-green amphibole that becomes more absorptive near garnet grains. Calcite is more abundant than quartz. The subunit locally contains disseminated pyrrhotite, pentlandite, chalcopyrite, sphalerite, and galena. The garnet-amphibole rocks occur as massive varieties with incipient foliation. Amphibole varies in composition and garnet occurs as porphyroblasts with euhedral overgrowths on subhedral cores.

Unit IM - Impure Marble is a grey to dark grey, buff weathering coarse grained massive carbonate rock with minor clinopyroxene, garnet, amphibole, phlogopite, and epidote.

Unit CS - Muscovite Calc-Schist is a light brown to red brown finely laminated rock composed of calcite, quartz, muscovite, with or without biotite, garnet, and pyrite.

Unit MQS - Garnet-Feldspar-Muscovite-Quartz-Schist is a medium to dark brown coarse grained rock with garnet porphyroblasts up to one cm in diameter. The unit contains minor biotite and chlorite and at one locality kyanite and staurolite have been reported (Brown, 1962). The feldspar is plagioclase (An<sub>15</sub>) in a granoblastic fabric.

Unit MQ - Micaceous Quartzite is a dark grey to black fine grained quartzite with fuchsite, graphite, and locally biotite, garnet, and chlorite. The protolith for the unit was probably a graphitic siltstone or chert.

The eclogitic rocks of the Chatanika terrane have been correlated by Erdmer and Helmstaedt (1983) with the type "C" eclogites of the Nisutlin Allochthon, Yukon Territory (Faro, Lost Peak, Campbell Range, and Mt. Hundere) and the Pinchi Lake area, British Columbia. These eclogite localities are evidence of a 1,000 kilometers (600 mile) long subduction zone of late Paleozoic or Mesozoic age that extended along the western margin of ancient North America.

### 3.2.1.2 Cleary Sequence

The Cleary sequence includes at least 300 meters of predominantly bimodal metavolcanic and volcanoclastic rocks with minor intercalated metasedimentary units that outcrop in a belt 10 kilometers (6 miles) wide by 50 kilometers (30 miles) along strike. The "type locality" for the Cleary sequence is a section along the Steese Highway from Skoogy Gulch over Cleary Summit to Mile 25. The Cleary sequence is thrust over the eclogitic rocks of the Chatanika terrane to the north. The basal contact is thus a thrust contact, along the Cleary Creek Thrust. This thrust strikes NE-SW in the Cleary Summit area and dips to the south. The upper contact of the

Cleary sequence is also a thrust contact (Goldstream Creek Thrust) with the Goldstream sequence. These thrusts are generally parallel to sub-parallel.

Plate I (Chapter 3) includes a stratigraphic column for the Cleary sequence. The column is compiled from bore hole data in sections 20, 21, 28, and 29 T3N, R2E, Fairbanks Meridian (F.M.).

The lower 200 meters of the Cleary sequence is composed primarily of calcareous actinolitic greenschist (CAG) and chloritic schist (CAC) with a probable metabasite protolith, while the upper 100 meters (325 feet) contains the economically significant lenses of metapyroclastic rocks (MFV and MRT) with a metafelsite association.

Unit CAG - Calcareous Actinolitic Greenschist is composed of actinolitic-hornblende and andraditic garnet with minor calcite, albite-oligoclase, clinozoisite, magnetite, pyrrhotite, pentlandite, and chalcopyrite. The protolith of the greenschist was probably a basalt.

Unit CAC - Chlorite Schist is composed of penninite, albite-oligoclase (An<sub>5</sub>-An<sub>15</sub>), epidote, calcite, and quartz. Locally the chlorite is mangiferous clinocllore. The chlorite schist is well foliated with the foliation parallel to compositional layering which ranges from a few millimeters to several centimeters thick. The chlorite schists are intercalated with dark grey to black metachert. Both the mangiferous chloritic schists and metacherts contain disseminations and bands of pyrite, arsenopyrite, sulfosalts (primarily jamesonite and boulangerite), sphalerite, and minor galena, magnetite, ilmenite, rutile, and sphene. The protolith of the chloritic schist was probably a mafic tuff.

Unit MC - Quartz Pebble Metaconglomerate consists of dark grey, cobble to boulder size rounded to subrounded clasts of quartz with minor pebble size clasts of dark grey to black shale. The matrix is silt to very coarse sand size clasts of quartz, feldspar, and carbonate. The unit has a limited areal distribution; never exceeds 10 meters (32 feet) in thickness; and locally is iron stained and contains minor pyrite.

Unit CS - Calcareous Muscovite Schist unit is a dark brown medium grained rock consisting of calcite, pale green muscovite, quartz, albite-oligoclase (An<sub>5</sub>-An<sub>15</sub>) with or without andraditic garnet and dark brown to red-brown biotite. The unit does not contain major sulphides and probably represents a metamorphosed calcareous pelitic sediment. This unit is intercalated with all the units described below of the Cleary sequence but generally increases in abundance in the upper part of the section.

Unit MFV - K-Feldspar Quartz Schist is comprised of pink porphyroblasts of potassium feldspar and quartz blastophenocrysts in a foliated matrix of albite-oligoclase, and clear to yellow muscovite with minor biotite, pistacite, penninite, and zircon. Locally the unit contains disseminated arsenopyrite and pyrite. The unit has a limited areal distribution and occurs primarily as rubblecrop on upper Pedro Creek, Solo Creek, Bear Creek, and on Cleary Summit. The protolith was probably a rhyolitic flow or sill.

Unit MRT - Muscovite Quartz Schist is composed predominantly of yellow white to clear muscovite, albite and

quartz but locally it contains tourmaline, zircon, and blastopyroclasts of potassium feldspar and lithic fragments. The unit crops out as discontinuous lenses up to two meters (6.5 feet) thick and 1,000 meters (3,250 feet) along strike and may grade upward to a laminated quartzite (metachert). The unit contains lenses of massive sulphides up to 25 cm thick. The sulphides include jamesonite, boulangerite, tetrahedrite, sphalerite, arsenopyrite, pyrite, and galena. Locally the unit has gold and silver contents in excess of 3 ppm and 600 ppm, respectively. The protolith was probably a felsic pyroclastic and/or exhalite chert.

Unit GS - Graphitic Schist unit is composed of dark grey to black fine grained graphite-quartz schist with minor sulphides including arsenopyrite and pyrite. The protolith was probably a carbonaceous chert.

Unit IM - Impure Marble unit varies from a green to red, brown, or buff colored medium to coarse-grained carbonate rock with calcite in excess of dolomite and minor quartz, garnet, and chlorite. Where the unit is in contact with the Pedro Dome and Gilmore Dome intrusive rocks the mineral assemblage is altered to calcite, garnet, diopside, idocrase, and hornblende, and locally fluorite, scheelite, molybdenite, and pyrrhotite.

Unit M - Marble unit is a dark-grey, green to buff fine grained siliceous carbonate rock with calcite predominating over dolomite. Locally the unit contains sphalerite, galena, bornite, chalcopyrite, and pyrite, contained in conformable compositionally layered rock. The unit is at least 10 meters (32 feet) thick at most outcrops and exceeds 30 meters (100 feet) at two outcrops.

The extremely light oxygen isotopic values of the marble, -25 to -30 per mil, may be indicative of a volcanic hot spring origin for the carbonate while sulphur isotopic values of 0 to +5 per mil for the sulphides also suggest a volcanic origin for the copper, lead, and zinc mineralization (Metz, 1984b). The marble unit is thus designated as the uppermost unit of the volcanogenic Cleary sequence and is the only major marker horizon for the sequence.

Units MQS and MQ - Muscovite-Quartz-Schist and Micaceous Quartzite are two pelitic units that are intercalated with the volcanoclastic and volcanic sedimentary units of the Cleary sequence. Where units MQS and MQ comprise over 50 percent of the stratigraphic column the rock units have been designated the Fairbanks Schist. Unit MQW, muscovite-quartz schist, is a light brown to buff medium grained rock composed of light grey to brownish muscovite, and grey quartz with or without garnet and biotite. Unit MQ, Micaceous Quartzite, is a light brown to buff fine grained massively bedded quartzite with grey to light brown muscovite. These units occur throughout the Cleary sequence but are in greater abundance in the upper one-third of the sequence.

### 3.2.2 Intrusive Rock Units

The granitic rocks of the Pedro Dome and Gilmore Dome areas are composed of four major phases. The relative ages of the phases are based on crosscutting and textural evidence and from oldest to youngest these phases include:

fine-grained granodiorite, porphyritic granodiorite, porphyritic quartz monzonite, and aplite-pegmatite dikes. The fine-grained granodiorite is the predominant phase of the Pedro Dome stock while the Gilmore Dome stock is composed primarily of porphyritic quartz monzonite (Blum, 1983).

#### 3.2.2.1 Pedro Dome Area

The fine-grained granodiorite accounts for 90 percent of the Pedro Dome pluton while porphyritic granodiorite and porphyritic quartz monzonite each account for 5 percent of the exposed intrusive complex.

The fine-grained granodiorite is composed of equigranular grains of plagioclase (45%), quartz (22%), biotite (13%), hornblende (11%), and potassium feldspar (7%) with accessory augite, hypersthene, sphene, zircon, apatite, rutile, and opaques. Grain sizes range from 0.5 to 2.0 mm. Locally mafic xenoliths from 1 cm to 30 cm in diameter are present (Blum, 1983).

Porphyritic granodiorite and porphyritic quartz monzonite occur in a small pluton approximately 3 kilometers southeast of the main Pedro Dome intrusive. The porphyritic granodiorite is composed of plagioclase (49%), quartz (26%), potassium feldspar (16%), biotite (8%), and hornblende (1%) with accessory muscovite, sphene, apatite, zircon, rutile, and opaques. Potassium feldspar and quartz megacrysts range up to 20 mm and 10 mm in diameter, respectively, while the matrix of feldspar and quartz has an average grain size of about 2.0 mm.

Porphyritic quartz monzonite is composed of plagioclase (36%), quartz (30%), potassium feldspar (28%), and biotite (6%) with accessory muscovite, sphene, apatite, zircon, rutile, and opaques. The grain size distribution of the megacrysts in the porphyritic quartz monzonite is similar to that in the porphyritic granodiorite, however the matrix in the quartz monzonitic rocks has an average grain size of 4.0 mm.

Aplite dikes occur in and adjacent to the porphyritic phases. The aplites are composed of potassium feldspar (38%), quartz (31%), plagioclase (30%), muscovite (1%), and biotite (1%) with accessory garnet, sphene, pyrite, arsenopyrite, apatite, zircon, and rutile (Blum, 1983). The aplite dikes range from very fine-grained rocks to medium to coarse grained pegmatite rocks.

#### 3.2.2.2 Gilmore Dome Area

Porphyritic quartz monzonite accounts for 80 percent of the Gilmore Dome pluton while porphyritic granodiorite accounts for 19 percent of the outcrop/rubblecrop area. Aplite-pegmatite occurs as a large 0.5 square kilometers area in the porphyritic quartz monzonite and as numerous dikes throughout the porphyritic phases. The compositions of the porphyritic rocks are similar to the compositions in the Pedro Dome plutons. Aplite dikes are much more abundant in the Gilmore Dome plutons and the dikes in these plutons contain up to several percent sulphides, primarily as pyrite and arsenopyrite.

Potassium-argon radiometric dating of the Pedro-Gilmore Dome plutons have yielded an age of  $90.7 \pm 5.1$  m.y. (Britton,

1970). The age estimate is based on hornblende from fine-grained granodiorite. Rubidium-strontium techniques have yielded an age of  $91.0 \pm 0.7$  m.y. and initial  $^{87}\text{Sr}/^{86}\text{Sr}$  ratio of  $0.71238 \pm 0.00010$  (Blum, 1983). From the  $^{87}\text{Sr}/^{86}\text{Sr}$  initial ratios, mineralogical and textural relationships, and whole rock major oxide analyses of Blum (1983), these granitic rocks can be classified as S-Type intrusives (after Chappel and White, 1974).

#### 3.2.2.3 Treasure Creek Area

A small pluton of porphyritic quartz monzonite occurs in sections 32 and 33, T3N, R1W, F.M. The pluton is approximately 1.5 kilometers (5,000 feet) long by 750 meters (2,500 feet) wide. It is only exposed as rubble crop and in excavations along the Trans-Alaska Pipeline. No geochemical or petrologic data is available for this occurrence.

A slightly smaller size body of porphyritic granodiorite occurs in the upper reaches of Any Creek in sections 18 and 19, T2N, R2W, F.M. and sections 13 and 24, T2N, R1W, F.M. The rock is composed of plagioclase (50%), quartz (25%) and potassium feldspar (20%) with muscovite, kaolinite, and disseminated pyrite and arsenopyrite. The sulphides occur along microscale and small scale structures with or without secondary quartz. The exposure is primarily as rubble crop but a few outcrops occur in the creek bottom. Samples of slightly altered rock indicate gold contents of up to 2 ppm.

Numerous aplite dike occur between the two small plutons and on to the west near Moose Creek. There does not appear to be a preferred orientation of the dikes except near Moose Creek and O'Connor Creek there is a dominant north-south trend. The dikes occur primarily as rubble crop and are very fine-grained and altered. The exposures suggest that the dikes range from less than a meter (3.25 feet) to 60 meters (200 feet) in width. Maximum exposed strike lengths are near 800 meters (2,600 feet).

#### 3.2.2.4 Ester Dome Area

A small intrusive of porphyritic granodiorite similar to the Any Creek pluton occurs on the ridge east of Eva Creek (section 5, T1S, R2W, F.M.). The intrusive may extend as far north as the Ryan Lode (section 32, T1N, R2W, F.M.), thus the body is elongated in a north-south direction for approximately a kilometer (3,300 feet). It is at least 150 meters (500 feet) wide. The rock is highly altered and cut by small quartz sulphide veinlets. No chemical data are available for either the intrusive or the mineralized structures.

On the northwest side of Ester Dome a series of aplite dikes occur in the upper reaches of Nugget Creek (section 23, 24, 25, and 26, T1N, R3W, F.M.). The aplites form a poorly defined radial pattern and extend over an area of 10 square kilometers (4 square miles). The dikes are highly altered and contain fractures of quartz and minor arsenopyrite. No geochemical data are available for these rocks and little structural data are available since most of the occurrences are as rubble crop. The radial pattern and the visual similarity between these dikes and those associated with the Pedro

Dome and Gilmore Dome plutons suggest that the Nugget Creek aplites may indicate the presence of a larger intrusive at depth.

#### 3.2.3 Tertiary Sedimentary and Volcanic Sequences

Basaltic rocks and associated Tertiary age terrestrial clastic units crop out at several localities in the Fairbanks mining district including Fourth of July Hill and Captains Bluff in the northern part of the district and at Birch Hill, Sage Hill, Lakloey Hill, and Brown's Hill in the south. The basalts are chemically transitional between tholeiites and alkali basalts (Furst, 1968), and those exposed on Birch and Sage Hills include pillow lavas and palagonite breccias (Forbes and Weber, 1982), both of which indicate subaqueous emplacement. At several localities, the basalt flow units contain silicified *Metasequoia* remains, which suggest an early or middle Tertiary age (Péwé et al., 1976).

The Tertiary sediments are generally poorly exposed and thus little descriptive or quantitative data are available. The Tertiary clastics are probably time stratigraphic equivalents to the numerous coal bearing sequences throughout south-central and east-central Alaska. Except for the deposits in the Fairbanks area, most of the Tertiary coal bearing formations are located near large strike slip fault systems such as the Tintina and Denali Faults.

### 3.3 STRUCTURAL GEOLOGY

The structural geology of the district was first discussed by Prindle and Katz (1913). Regional structural investigations that included the Fairbanks district were conducted by Mertie (1937) and Foster et al. (1973). Detailed studies of the Pedro Dome area were undertaken by Brown (1962) and Swainbank (1971). Geologic mapping that contained structural data was done by Péwé (1958, 1975), Williams et al. (1959), Péwé and Revard (1961), Péwé et al. (1966, 1975, 1976a, 1976b, and 1976c), Bundtzen (1982), Metz (1982), Robinson (1982), and Robinson et al. (1990). Hall (1985) conducted a detailed investigation of the small-scale fold structures of the district.

The following discussions are drawn primarily from Hall (1985). The detailed description of the structural geology of the district is in part predicated on the defining of mappable rock units. Of particular importance is the delineation of marker horizons and the definition of a stratigraphic sequence. The stratigraphic column in Plate II is the result of relogging of all the diamond drill holes in the Cleary Summit area completed up to 1987.

The narrow lensoidal nature of the volcanoclastic and sedimentary units and the limited distribution of outcrops make the definition of a stratigraphic sequence tenuous. The concentration of data collected in roadcuts, mine workings, and other excavation sites may bias the data.

Finally, the analysis of the structural geology of the district should be based on the knowledge of the relative ages of the rock units. There is no evidence for the relative ages of the metamorphic sequences other than metamorphic facies. The Cretaceous age granitic rocks ( $91.0 \pm 0.7$  m.y., Rb/Sr) are

not metamorphosed. Thus, the structures associated with the emplacement of the intrusives and the post intrusive structures post date the metamorphic structures.

### 3.3.1 Folding Events

Hall (1985) recognizes four generations of mesoscopic folds. The first two events (F1 and F2) are characterized by overturned to recumbent, subisoclinal to isoclinal folds. The F1 folds have an axial plane schistosity that strikes easterly to northwesterly (85 to 175 degrees). The F2 folds have an axial plane cleavage that strikes north to northeast (10 to 75 degrees).

The third event is characterized by overturned, open to subisoclinal folds that trend from northerly to easterly. The folds are associated with major shear zones (see Ch. 3, Plate III). These shear zones are the product of both ductile and brittle deformation.

The fourth event is characterized by upright to overturned open folds that trend from north-south to east-west. These crosscut and deform F1, F2, and F3 folds and occur at scales ranging from small crenulations to broad warps in the mesoscopic fold axes.

Hall (1985) notes both geographic and lithologic variations associated with the population density, distribution, and orientation of the folds. The geographic differences may be a function of the distribution of exposure or may be due to real spatial variations in structure.

The lithologic controls of fold structures are exemplified by the long wavelength and large amplitudes of the F3 and F4 folds in the quartzose rocks and the shorter wavelengths and smaller amplitudes in the micaceous rocks. The evidence for refolding is not apparent in most outcrops. The evidence may be obscure or may occur on a larger scale than that of individual outcrops. The bimodal population of fold axis is thus the best evidence for district wide refolding.

Hall (1985) notes the difficulty in identifying F1 folds in outcrop and attributes this to extensive recrystallization. Although there is extensive recrystallization and isoclinal folding, it is possible to trace individual compositional layers for several kilometers along strike.

Compositional layering (S0) is the oldest planar fabric. The S1 planar element is a schistosity defined by parallel alignment of the platy or prismatic minerals which lie axial planar to F1 folds and parallel to subparallel to S0. The S1 fabric is best observed in quartzose rocks that exhibit the following microstructural textures: 1) equant, to coarse-grained crystal aggregates bounded by triple junctions; 2) quartz, mica, and amphibole grains with strong preferred orientation in the hinges of F1 folds; and 3) non-rotated porphyroblastic garnet grains.

The S2 planar fabric is primarily a cleavage of variable style but it also includes a schistosity in the Birch Hill sequence. The S2 fabric is parallel to the axial planes of the F2 folds and subparallel to S0 and S1. The fabric is found primarily in micaceous rocks.

The S2 fabric is characterized by a cataclastic structure. Quartz, feldspar, amphibole and garnet occur as

porphyroclasts. The quartz and feldspar exhibit undulose extinction. The feldspars are sericitized and the large lenticular quartz grains are surrounded by a fine-grained aggregate of quartz. The highly strained grain boundaries suggest that the recrystallization is incomplete and that the coarse grains and surrounding fine-grained aggregates may represent the original mineral grains. The lack of new mineral phases associated with the S2 fabric also suggests that thermal conditions did not change significantly during S2 development.

The S3 fabric is also a cleavage that is axial planar to F3 folds. Hall (1985) recognizes two subtypes. The first has a cataclastic microtexture identical to S2 and is associated with sub-isoclinal F3 folds. The second has a cataclastic microtexture and is associated with fault gouge or fault breccia.

The S2 and S3 fabrics are similar in similar rock types, indicative that the deformational history is probably comparable. Recrystallization is incomplete and the deformation is less ductile than that associated with the S1 fabric. The S3 fabric thus represents the transition from ductile to brittle deformation.

The S4 fabrics are cleavages axial planar to F4 folds. The S4 fabric crosscuts the S0, S1, and S2 fabrics at angles of 60 to 90 degrees and the S3 fabrics at 20 to 45 degrees. There are no polygonized grains as in S2 and S3 fabrics and no evidence of new mineral growth. Quartz and feldspar grains are sheared, thus the development of the S4 fabric is the result of brittle deformation.

Two large scale fold structures have been inferred from the geologic mapping. These structures trend northeast-southwest to east-west and are associated with the F2 event. The most northerly structure is an anticlinorium with a fold axis that trends east-west in the Cleary Summit area and is referred to as the Cleary Creek Anticlinorium. A more southerly fold structure is mapped on the east side of Gilmore Dome and trends northeast-southwest from the Tungsten Hill area and is referred to as the Tungsten Anticlinorium.

The Pedro Dome intrusive is elongate along the Cleary Creek Anticlinorium. Similarly the Gilmore Dome pluton is elongate along the trace of the Tungsten Anticlinorium. The Cleary sequence rocks are exposed along the structural as well as topographic highs of the two structures. A synclinorium between the anticlinoria is asymmetrical; the trace of this structure occurs along the Bear Creek drainage. These same fold structures are inferred in the Ester Dome area (see Ch. 3, Plates I and III).

### 3.3.2 Joint Systems

Hall (1985) identifies joint orientations at ten degree intervals from north-south to east-west in the district. Some of these joint sets are associated with the axial traces of major anticlinoria and synclinoria in the northeastern portion of the district. The joint sets are both parallel and orthogonal to the fold axes.

There is a definite geographic distribution of joint orientations. There is a major east-west joint set in the Cleary Summit area and a major north-south joint set on the east side

of Ester Dome.

Joint distribution is also related to major shear zones. The shears are characterized by close spaced joints parallel to the strike of the shear with joint spacing increasing with distance from the altered and mineralized zones.

Finally, unresolved joint sets may be related to the emplacement of the intrusive rocks and regional uplift. Thus the analysis of the joint systems alone cannot resolve the deformational history of the district.

### 3.3.3 Fault Systems

Thrust faults are inferred to be the contacts between the Chatanika terrane and Fairbanks schist; between the Goldstream sequence/Birch Hill sequence and the Fairbanks schist in the Goldstream Valley; and between the Goldstream sequence/Birch Hill sequence and the Fairbanks schist in the Birch Hill area (see Ch. 3, Plate III). These faults are referred to as the Cleary Creek, Goldstream Creek, and Cripple Creek Thrusts, respectively. Evidence for these thrusts is primarily the juxtaposition of radically differing metamorphic sequences. Outcrop evidence which is limited, usually consists of the presence of a meter (3 foot) or less wide zone of brecciated schist and fault gouge. None of these zones are visible for more than a few tens of meters (30 to 100 feet) along strike.

The Cleary Creek Thrust generally strikes east-west and dips to the south at less than 10 degrees, thus the Chatanika terrane occurs as a *fenster*. The Goldstream Creek Thrust strikes northeast-southwest and dips at varying low angles. The Goldstream sequence is thrust over the Fairbanks schist and occurs as a *klippe* in the Goldstream valley. The Cripple Creek Thrust strikes northeast-southwest and dips at low to high angles. The high angle portion of the structure is well exposed in a road cut on the Steese Highway at approximately mile six. At this locality the fault gouge is at least 30 meters (100 feet) wide.

Four high angle faults are mapped in the district; they are inferred from aerial photography, aeromagnetic data, and the juxtaposition of rock units. The most northerly structure is the Chatanika River Fault, which strikes northeast-southwest and appears to be nearly vertical. The structure separates the eclogitic rocks of the Chatanika terrane to the south from lower greenschist facies rocks north of the Chatanika River. The Chatanika fault is inferred to be a strike-slip structure (Forbes, 1982) based on its linear strike for over 60 kilometers (36 miles).

The Fairbanks Creek Fault extends from the headwaters of Cleary Creek to the Fairbanks Creek-Wolff Creek divide and down Fairbanks Creek to the Fourth of July Hill area. It strikes east-west and is nearly vertical. The structure is visible in only two outcrops but there is enough evidence to infer its existence for over 16 kilometers (10 miles). In the upper reaches of Fairbanks Creek below the McCarty Mine, the fault zone is exposed in placer mining excavations. The fault is a shear zone at least 30 meters (100 feet) wide. The zone is defined by closely spaced joints and clay gouge which enclose less deformed schist fragments. In the areas of

intense deformation the maximum size of the fault breccia fragments is less than a few centimeters. The slickensides in the shear are horizontal, thus indicating strike slip motion. The fault zone does not contain any readily apparent mineralization in this area. The fault zone appears as a linear feature on aerial photography and Landsat imagery. Alaska Gold Company drill records for lower Fairbanks Creek indicate a fault gouge zone that extends to the east near the Fourth of July Hill.

A vertical 10 meter (32 foot) wide shear zone is exposed in mine excavations at the Tolovana Mine. This shear zone is the inferred extension of the Fairbanks Creek Fault. In addition to fault breccia and clay gouge the shear is mineralized and is referred to as the Tolovana vein. A second mineralized shear occurs approximately 200 meters (650 feet) north of the Tolovana vein. The shear is parallel to the Tolovana vein and is host to lead and zinc sulphides in a fault breccia and clay matrix. This shear is referred to as the Willow Creek lode. These two structures are probably a bifurcation of the Fairbanks Creek Fault.

On the east side of Ester Dome a major shear zone strikes north-south and appears to be nearly vertical. The field evidence for the shear consists of boulders and cobbles of fault breccia in the placer tailings of Sheep, Eva and Ester Creeks and a major change in bedrock elevation at the confluence of Sheep and Goldstream Creeks. The linear nature of the Moose Creek drainage and the topography on the east side of Ester Dome results in an aerial photographic linear that can be traced for 20 kilometers (12 miles). The northeast-southwest aeromagnetic trends are offset along this linear feature. The aeromagnetic data indicate that the structure may extend for 50 kilometers (30 miles) north of Ester Dome. No aeromagnetic data are available south of Ester Dome, thus the southerly extent of the structure is unknown. The asymmetry of the aeromagnetic anomaly suggests that the structure dips steeply to the east. The structure is herein designated the Moose Creek Fault.

The compositional layering and trend of the major anticlinoria and synclinoria in the Ester Dome area are easterly to northeasterly. The mapped vein structures in the area trend primarily north-south and dip at high angles to the east and west. Small intrusives of aplite and granodiorite are elongate in a north-south direction near Eva Creek. The localization of these intrusives may be controlled by the Moose Creek shear.

A few shear zone hosted veins parallel the structural grain of the metamorphic rocks. These structures are in turn offset by small scale north-south faults. The north-south vein structures and the small scale north-south faults are probably a manifestation of the larger Moose Creek structure.

A regional scale north-south structure (Minto Flats fault) is mapped near Nenana 60 kilometers (36 miles) west of Ester Dome. This fault is a large normal fault that extends for at least 100 kilometers (60 miles) along strike. The topographic expression of the structure cannot be followed north of Livengood in the Tolovana district. Although not visible south of Nenana, it may extend under the Tanana valley fill

to the south. Gravity data (Barnes, 1961) indicate that the westerly dipping Minto Flats Fault may have an offset of over 600 meters (2,000 feet).

Placer drilling data and seismic investigations indicate that the bedrock in Goldstream Creek to the west of the Moose Creek Fault is approximately 8 meters (26 feet) deep and dips at a low angle to the west. East of the fault the alluvium is at least 125 meters (400 feet) thick. Thus Ester Dome and the highlands between the dome and Minto Flats appears to be a horst structure.

The prevalence of the chlorite schist unit of the lower Cleary sequences and the paucity of upper Cleary sequence lithologies in the Ester Dome area also suggests that the area is uplifted relative to the Cleary Summit area. The outcrop of the Goldstream sequence in a klippe to the east of the Moose Creek Fault, the stream drainage patterns, and the relatively thick alluvium east of the fault are all evidence of rotational offset along the Moose Creek Fault.

Just to the east of the district, a major north-south structure is mapped in the valley of the Little Chena River. This may be an extension of the Champion Creek Fault (Foster et al., 1984; and F. Weber, USGS personal comm.). The Champion Creek Fault is seismically active (Gedney and Berg, 1969). The only Tertiary sections that are visible in outcrop occur in the eastern margin of the district just to the west of the fault. This is indirect evidence that the area west of the Champion Creek Fault and east of the Moose Creek Fault is a recent graben structure with a small rotation to the west.

### 3.3.4 Linear Trends

Metz and Wolff (1980) in an examination of Landsat imagery for the Fairbanks area report linear trends of N-S, N60°W, E-W, N15°E, N45°E, N60°E, and N75°E. These are either parallel or orthogonal to the major anticlinorium or parallel to the major fault structures described above. These linear trends are similar to the joint orientations measured by Hall (1985).

### 3.3.5 Mineralized Shear Zones

The mineralized veins in the district can be divided into three major groups based on structural data. In the Cleary Summit area the predominant trend is N60-80°W with dips to the south at 45° to 65° (see Ch. 3, Plate II and IV). These structures are en echelon and are restricted primarily to the area between the Fairbanks Creek Fault and the Cleary Creek Thrust.

At flexures in the Cleary Creek Anticlinorium the veins also exhibit changes in strike and dip. East of Cleary Summit the anticlinorium trends northeasterly and the mineralized shears all strike northwesterly and dip to the south. At Cleary Summit the anticlinorium trends east-west as does the Cleary Hill vein. West of Cleary Summit near the easterly contact of the Pedro Dome pluton the anticlinorium trends to the southwest. The veins in this area including the Tolovana, Newsboy, and Robinson, trend northeast-southwest and dip to the north at 70 degrees.

The mineralized shears in the Cleary Summit area are characterized by zones of closely spaced joints and two types of alteration. The zones range from a few meters (10 feet) to 70 meters (225 feet) wide. There are two types of alteration, the results of an early sericitic event followed by a late argillic event. Both events are accompanied by the introduction of silica. The quartz can occur as a stockwork of narrow veinlets up to 2 cm wide or as discrete quartz veins from 25 cm to 4.5 meters (15 feet) wide. The larger quartz veins are usually localized near the hanging wall of the shear zone.

The shear zones are mapped up to 1.8 kilometers along strike. The individual shears occur at intervals from 50 meters (100 feet) to 300 meters (1,000 feet). The zone of intensely mineralized shears in the Cleary Summit area extends from the east contact of the Pedro Dome pluton to the Hi-Yu Mine, a distance of about 13 kilometers (8 miles).

A second group of mineralized shears is located in the Ester Dome area. This group strikes northeast-southwest and dips to the south at 60 to 70 degrees, and includes the Grant Vein and Ryan Lode.

A third group is also localized in the Ester Dome area. The dominant trend of this group is north-south with high angle dips to the east and west. These structures are parallel to sub-parallel to the Moose Creek Fault.

The alteration and mineralization of the latter two groups of shears is grossly similar to that in the Cleary Summit area. The mineralization will be discussed in more detail in Chapter 4.

---

## CHAPTER 4

### LODE MINERAL DEPOSIT DESCRIPTIONS AND ORE PETROLOGY OF THE FAIRBANKS MINING DISTRICT

#### 4.1 INTRODUCTION

The lode deposits of the Fairbanks mining district are the best exposed lode mineralization in the northwestern portion of the Yukon-Tanana Terrane (YTT). These deposits have analogues in the Kantishna, Steese, Circle, and Richardson mining districts. This chapter provides a description of 11 of the 36 known mineral occurrences in the district and provides an empirical classification system for these occurrences.

Ore deposit models for analogues of the mineralization in the Fairbanks district as well as adjacent mining districts are discussed in Chapter 11. These genetic models include tonnage and grade parameters as well as mineralogic, petrologic, and structural controls of the mineralization. This empirical classification of the deposits will facilitate the evaluation of known occurrences and enhance the chance of discovery of new deposits.

The mineral deposit classification that follows is primarily a descriptive classification that can be utilized in the field. The field observations are later supplemented with laboratory data including fluid inclusion measurements, whole rock

geochemistry, and isotopic analyses. These investigations provide the basis for a more general classification of the mineral occurrences with genetic implications.

The field examinations and sampling of the various deposits were made possible thru the cooperation of private industry. These companies have been recognized in the acknowledgements; however it is also important to note the restrictions on such sampling that may have biased the data base. The major lode occurrences in the Cleary Summit area to the east of the Steese Highway were not sampled during the initial stage of this investigation that was funded by the State of Alaska. The area was under the control of a private mining company that would not allow sampling of its holdings until 1986. All the public assay results for the "Interior Mining Project" were completed by 1984 thus little public assay data were available for the Cleary Summit area. Mineralogical, isotopic, and fluid inclusion investigations were not restricted in the same manner as the geochemical investigations.

#### 4.2 FIELD CLASSIFICATION OF MINERAL DEPOSITS

Detailed investigations of the lode mineral deposits in the Fairbanks district have resulted in the definition of the following five major types of mineralization:

- I. Volcanogenic stratabound sulphides
- II. Intrusive hosted gold and silver
- III. Tungsten skarn
- IV. Metamorphic hosted gold-quartz-sulphide veins
- V. Stibnite veins

This classification system has resulted from mineralogic and petrologic observations of approximately 400 rock and polished ore sections and from detailed mineral deposit mapping. Fluid inclusion and stable isotope investigations further contribute to the classification and will be discussed in subsequent sections.

##### 4.2.1 Type I Mineralization

Metabasites of both the Chatanika terrane and the Cleary sequence contain disseminated sulphides that predate the last metamorphic event and are probably syngenetic. The garnet-clinopyroxene-amphibole variety of eclogitic rocks of the Chatanika terrane contains disseminated pyrrhotite, pentlandite, chalcopyrite, and locally sphalerite and galena. The copper and iron sulphides occur as 0.01 mm to 0.5 mm grains within the matrix of plagioclase, calcite, and quartz, whereas the sphalerite and galena occur as porphyroblasts up to 5 mm in diameter. Total sulphide content rarely exceeds one percent of the rock and never exceeds three percent. The Chatanika terrane, and the eclogitic rocks in particular, have relatively low arsenic, antimony, and gold contents compared to the metafelsic rocks of the Cleary sequence (Metz 1984a); visible gold has not been detected in any of the ore sections from the sulphide bearing eclogitic rocks. Placer gold has been produced from several streams that drain only the Chatanika terrane. The gold/silver ratios for these deposits differ significantly from those of placer deposits of streams draining the Cleary sequence (Metz, 1983). Lead/lead iso-

topic ratios (see Chapter 10) for the Chatanika terrane are significantly different from those of the Cleary sequence and its included vein systems. These data suggest a different source of gold for the Chatanika terrane, but the source is not well delineated.

Calcareous actinolitic greenschist (CAG unit), the lowest unit of the Cleary sequence, contains disseminations and layers of pyrrhotite  $\pm$  chalcopyrite, pentlandite, and scheelite. The sulphide grains range from 0.01 to 0.10 mm, and the scheelite grains from 0.001 to 0.005 mm in diameter. Sulphide content averages approximately one percent of the rock, and tungsten contents may exceed 50 ppb (Metz, 1984a). The CAG unit generally contains less than 100 ppb Au, and gold has not been observed in polished sections or by electron microprobe methods.

Unit CAC (chlorite schist) of the Cleary sequence, which is stratigraphically above unit CAG, contains both disseminated and layered sulphides of iron, arsenic, antimony, zinc, and lead. The disseminated sulphide grains range from 0.01 to 1.0 mm. Pyrite plus arsenopyrite account for 90 percent of the total sulphides and occur parallel to the compositional banding in the schist. Arsenic concentrations in the CAC unit generally exceed 1,000 ppm and locally exceed 1.0 percent. Native gold occurs as inclusions, 0.001 to 0.010 mm in size, in arsenopyrite. The gold to silver ratio of the inclusions, as determined by electron microprobe techniques, ranges from 2.5/1 to 4/1. Limited sampling of the CAC unit that contains disseminated sulphides indicates that gold contents range from 40 ppb to 30,000 ppb. Scheelite occurs in the unit as 0.001 to 0.005 mm grains. Tungsten contents may exceed 100 ppb.

Unit MRT (muscovite-quartz schist and metachert), the upper third of the 300 meter (1,000 foot) thick Cleary sequence, also contains major sulphide and precious metal mineralization. The lenses of iron, arsenic, antimony, zinc, and lead sulphides locally contain native gold as inclusions in arsenopyrite, and silver occurs in argentiferous tetrahedrite. The sulphide grains range from 0.01 to 5.0 mm in diameter and occur in lenses up to 25 cm thick and over 800 meters (2,600 feet) in length along strike. The paragenetic sequence is pyrite-arsenopyrite (with or without gold) - sphalerite - galena - sulfosalts (including jamesonite, boulangerite, freibergite). Within the metapyroclastic rocks the sulphides are associated with muscovite and albite and are not segregated into layers. In the siliceous metachert horizons, however, the sulphides form layers up to one centimeter thick. These exhibit the same general paragenetic sequence as the non-banded sulphides. Some banded sulphides exhibit a rhythmic pattern that is repeated for four or five cycles over a 25 cm lens.

Gold contents of the MRT unit range from 40 ppb to 3 ppm over 2-meter (6 foot) intervals, with higher values restricted to the sulphide-rich portions of the unit. Silver contents range from 100 ppb to 600 ppm but are restricted to the sulphide bodies within the lenses of the MRT unit (Metz, 1984a).

In the Cleary Summit area, the MRT unit in aggregate

may account for more than 30 meters (100 feet) of the upper 100 meters (300 feet) of the Cleary sequence. In this area, at the crest of the Cleary Anticlinorium, the sulphide lenses of the MRT unit are nearly flat lying and can be traced for up to one kilometer (3,250 feet) along strike. Between lenses of the MRT, are units of muscovite quartz schist and micaceous quartzite a few centimeters to several meters thick. Thus, in the Cleary Summit area the MRT unit represents a low grade bulk mineable gold/silver target.

#### 4.2.2 Type II Mineralization

The fine-grained and porphyritic granodioritic phases of the Pedro Dome stock have been subjected to several brittle shear events. The resulting shear zones contain fracture fillings and replacement type sulphide vein and quartz-vein mineralization. The shear zones are the foci of potassic, sericitic, argillic, and propylitic alteration which extends for less than a meter into the unshered rock.

The sulphide vein paragenetic sequence is pyrite - arsenopyrite - chalcopyrite - sphalerite - galena and/or argentiferous tetrahedrite. Calcite is the principal gangue mineral, with subordinate quartz. The sulphide vein widths are usually less than 0.6 meters (2 feet) and the veins occur discontinuously over a few tens of meters along strike or down dip. The veins are notably deficient in gold but locally may contain up to 20 OPT silver.

Locally the shear zones develop into extensive quartz-vein stockworks with individual veinlets up to a centimeter wide. Locally these stockworks contain gold and traces of molybdenite, bismuthinite and scheelite (Sherman, 1983).

#### 4.2.3 Type III Mineralization

Scheelite-bearing skarns occur as discontinuous bodies along the margins of the porphyritic quartz monzonite phase of the Gilmore Dome intrusive complex. The exoskarns are hosted in the metasediments and metabasites of the Cleary sequence. The skarns can be classified into two calc-silicate types. Type A is hosted in marble units which are altered to pyroxene (Hd<sub>70</sub>) + garnet (Alm<sub>10</sub>) + scheelite which may be overprinted by quartz + hornblende ± calcite ± scheelite which may be overprinted by quartz + hornblende + calcite + scheelite ± idocrase ± fluorite ± pyrrhotite ± molybdenite. Type B is hosted in marl units which are altered to quartz + amphibole + calcite + scheelite ± chlorite ± clinozoisite ± biotite (Allegro, 1984). Minor veinlets crosscut the skarns and these structures contain quartz + scheelite + amphibole + chlorite + mica and only traces of gold.

#### 4.2.4 Type IV Mineralization

Most of the lode gold production from the district has come from discordant gold-quartz-sulphide veins in the Cleary sequence metavolcanics and metaexhalites. The district historic production of 325,000 troy ounces has come from veins that averaged or exceeded 1.0 OPT gold content. The gold-quartz structures are shear-zone and open-space filling-type veins from 10 cm to 5 meters (4 inches to 16 feet)

in width, and with strike lengths of over 1.8 kilometers (6,000 feet). Most of the structures have been developed over a vertical distance of less than 100 meters (325 feet).

The vein mineralogy is highly variable and apparently is controlled by the mineralogy of the host rocks. Gold-quartz veins hosted by sulphide-poor banded quartzite or banded-muscovite quartzite (metaexhalites) contain gold, arsenopyrite and only traces of pyrite, sphalerite, galena, hematite, magnetite, and sulfosalts. The major gangue mineral is fine to coarse grained, to massive vuggy quartz that was introduced in less than five (usually three) discrete episodes.

The quartz veins in the metarhyolites and chlorite schists contain up to 5 percent sulphides. The paragenetic sequence of these veins can be summarized as follows: early quartz - pyrite - arsenopyrite (± gold) - sphalerite - chalcopyrite - bornite - gold and/or galena, argentiferous tetrahedrite, boulangerite, jamesonite - late quartz ± ankerite. Antimony only rarely occurs as stibnite which is always associated with late quartz. High grade gold samples (greater than 1 OPT) usually contain abundant calcite or ankerite.

The grain size distribution of gold in the veins ranges from 1 micron inclusions in arsenopyrite to 5 mm diameter grains and wires that fill fractures in early sulphides and quartz. There is a positive correlation between grade and grain size in the quartz veins.

#### 4.2.5 Type V Mineralization

Monomineralic stibnite veins occur as fracture fillings and replacement structures either above known gold-quartz ore shoots or as isolated structures. The stibnite generally fills or replaces the entire structure and is not associated with major quartz or other gangue mineralogy. Traces of pyrite, arsenopyrite, kermesite, stibiconite, and gold are found in or adjacent to the stibnite. The stibiconite, can occur as fine-grained massive ore or as very coarse-grained aggregates with subhedral grains up to 5 cm in diameter.

The stibnite lodes range from several centimeters to two meters (3 inches to 6.5 feet) in width and are highly irregular with strike lengths of less than 100 meters (325 feet). Individual structures have produced from 100 to several thousand tonnes of ore. The most productive and the largest number of stibnite veins are hosted in the quartzites and metarhyolites of the Cleary sequence, however several occurrences are within the Chatanika terrane.

Most of the Type IV and V vein-type mineralization occurs in structures that strike NW-SE or NE-SW and dip to the south at 45° to 55° in the Cleary Summit area or N-S with vertical dips in the Ester Dome area. Two larger structures in the Ester Dome area strike NE-SW and dip 70°S.

### 4.3 MINERAL DEPOSIT DESCRIPTIONS

Table A1, Appendix A is a classification of the lode mines and prospects in the Fairbanks district and a summary of the structural data for each occurrence. These occurrences were previously defined by Chapman and Foster (1969) and the locations are shown on Ch. 4, Plates II through XI. This

tabulation is a very brief description of the occurrences and is supplemented by the following descriptions of "reference occurrences" for each mineral deposit type.

#### 4.3.1 Type IA Stratabound Copper-Lead-Zinc

##### 4.3.1.1 Steese Eclogite Sulphide Occurrence

The Steese eclogite sulphide occurrence is located in section 12, T3N, R1E, F.M. Swainbank and Forbes (1975) described the eclogitic rocks at this locality but did not report the occurrence of the base metal sulphides.

The mineralization consists of disseminated sphalerite, galena, chalcopyrite and pyrrhotite in garnet-clinopyroxene-amphibole rocks. The mineralization is in compositional banding in the host and is present as 0.5 mm size sulphide grains. The mineralized rock is only noted in the gold dredge tailings in the creek bottom and is not apparent in the sparse outcroppings on either side of the valley. The angular nature of the tailings indicate that the host rocks were not transported by the stream but was probably dislodged as the dredge dug into the bedrock. The eclogitic rocks of the Chatanika terrane crop out on the valley walls both upstream and downstream from the mineral occurrence thus mineralization is well within the terrane. With the exception of several Type V antimony veins, this is the only reported sulphide mineral occurrence in the eclogitic rocks of the Chatanika terrane.

The examination of polished sections 81MIRL04A, 81MIRL04B, 81MIRL27A, 81MIRL27B, and 81PM106 (see Appendix B) indicates that sphalerite and galena grains are restricted to narrow compositional bands with the two sulphides in close proximity. The pyrrhotite and chalcopyrite tend to occur throughout the rock although higher concentrations occur near the base metal sulphides. Cobaltite and gold may occur as micron size inclusions in the pyrrhotite. The sulphides constitute less than 3 percent of the rock and are in greater abundance in amphibole rich bands along with pale green white-mica.

Microfractures cut the compositional bands at high angles and occasionally these fractures contain secondary calcite. The microfractures may also offset the sulphide bands and cause local remobilization of the galena.

The classification of this occurrence is tentative due to the limited available data. Trace element data does suggest however that zinc and copper mineralization is present along the regional strike of the eclogitic rocks in the Lulu Creek and Pilot Creek area (see Ch. 4, Plates III and IV).

#### 4.3.2 Type IB Stratabound Arsenopyrite-Scheelite

##### 4.3.2.1 Ryan Lode Footwall

The Ryan Lode is a shear zone located in section 31, T1N, R2W, F.M. (see location 141, Ch. 4, Plate VIII). The Ryan Lode per se is classified as a Type IV deposit, however the host rocks contain stratabound and probably stratiform sulphide mineralization.

Diamond drilling by St. Joe Minerals indicates disseminated sulphides and scheelite in the footwall and hanging wall of the Ryan shear zone. The mineralization is at least

100 meters (325 feet) away from the known structure and occurs primarily in chlorite schist and laminated quartzite. The lateral extent of the mineralization is unknown due to the limited amount of drilling and the limited extent of the outcrop.

Examination of the drill core indicates that sulphide mineralization occurs at several horizons and over intervals of up to 10 meters (33 feet). The sulphides are primarily arsenopyrite with minor pyrite and jamesonite (polished sections 81MIRL15A, 81MIRL15B, 81RL71, 81RL73, 81RL76, 75PM009, 82RLO-3A, and 82RLO-3B, Appendix B). The sulphides occur as 0.1 to 1.5 mm size grains disseminated in host or as small lenses 1.5 cm thick and several centimeters in lateral dimensions. The lenses are parallel to the compositional layering of the host. Where the host exhibits small scale folds, the sulphides bands are thickened at the fold axis. The sulphides constitute up to 5 percent of the rock.

Scheelite grains occur intergrown with the arsenopyrite. Microprobe analyses of the scheelite indicate little or no molybdenum in the larger grains. Grain size ranges from 1 to 10 microns.

Prior to this investigation, the known tungsten mineralization in the district was restricted to skarn occurrences in the Gilmore Dome area. Rock geochemical data indicate that tungsten mineralization occurs over nearly the entire outcrop area of the Cleary sequence. At most of the localities shown on Ch. 4, Plate X, there are no major exposures of intrusive rocks as there are on Gilmore Dome. It may be fortuitous that the largest number of tungsten rock geochemical anomalies occurs near the Ryan Lode where the predominant rock type is the chlorite schist of the lower Cleary sequence. However the fact that tungsten anomalies are widespread on Ester Dome and that the chlorite schist and metachert units of the Cleary sequence are the dominant rock types on the dome can not be dismissed.

#### 4.3.3 Type IC Stratabound Galena-Sphalerite-Tetrahedrite

##### 4.3.3.1 Nordale Adit

The Nordale Adit is located in section 21, T3N, R2E, F.M. (see location 25, Ch. 4, Plate VIII). The occurrence is also known as the Homestake Mine. Ch. 4, Plate XII is a geologic map of the Nordale Adit as well as the Christina Adit and the Kawalita Shaft.

The adit is driven in the chlorite schist and the metachert units of the lower Cleary sequence. The adit cross cuts the Christina vein system approximately 1,250 meters (4,062 feet) from the portal and then continues along the vein for 100 meters (325 feet). At 1,100 meters (3,575 feet) from the portal the adit cuts a 3 meter (10 foot) thick section of stratabound sulphide mineralization. The sulphides are hosted in a chlorite-quartz schist.

The sulphide phases include sphalerite, galena, tetrahedrite, pyrrhotite, pyrite, stibnite, and jamesonite. Traces of gold occur as micron size inclusions in the arsenopyrite. The iron sulphides form grains greater than 1.5 mm in diameter

while the antimony bearing phases rarely form grains greater than 0.1 mm in diameter.

The sulphides form alternating compositional bands one to two centimeters thick. The sulphide layers are separated by slightly thicker layers of quartz and chlorite. The sulphides constitute about 40 percent of the mineralized horizon. The host rocks are nearly horizontal but are locally disrupted by high angle shears.

At the southerly limit of the adit, an underground diamond drill hole (UDDH-6-KS-83) intercepts the sulphide system (Placid Oil Company, unpublished data). This drill hole is 185 meters (600 feet) south of the adit section. Three surface drill holes (DDH-5-KS-83, DDH-6-KS-83, and DDH-7-KS-83) cut the sulphides 75 meters (245 feet) east of the underground drill hole. A fifth drill hole (DDH-1-KS-85) intercepts the sulphides 75 meters (245 feet) east and 145 meters (475 feet) south of the adit section. All the bore holes intercept a major carbonate unit below the massive sulphides. The carbonate unit contains similar mineral assemblages that are disseminated throughout a 3 meter (10 foot) thick section. The assay data for the sulphide system intercepts in these drill holes is presented in Table 4.1. This system has been called the Truck Sulphide System

The drill hole data indicate that the Truck System ranges from 2.2 to 6.6 meters (7 to 21.5 feet) thick. The three surface holes east of the underground hole indicate that grades may change radically over short distances. The relatively high silver and gold content warrants that the system receive additional examination along strike and dip.

Examination of the mine dumps at the Hi-Yu (location 7, Ch. 4, Plate VIII) and Cleary Hill (location 47, Ch. 4, Plate VIII) properties shows the presence of similar massive sulphide mineralization in chlorite schist. The Hi-Yu Mine is 4.4 kilometers (2.75 miles) east of the Nordale Adit and the Cleary Hill Mine is 3.2 kilometers (2 miles) to the west. Two high grade silver zones, the Circle Trail zone and the Too

Much Gold zone, occur along strike between the Nordale Adit and the Hi-Yu Mine (see Ch. 3, Plate I). Indicated reserves from the surface down to 15 meters (50 feet) are calculated from trenching and surface sampling to be at least 2 million tons at 0.075 OPT Au equivalent in these two zones. Between the Nordale Adit and the Cleary Hill Mine the massive sulphides and the associated carbonates are exposed by trenching in the Chatham Creek area. These exposures suggest that the Truck Sulphide System may have a strike length of nearly 8 kilometers (4.8 miles). The Truck Sulphide System should be subjected to additional exploration.

The grades and the mineralogy of the Truck Sulphide System show striking similarity to the mineralization at the Greens Creek Mine on Admiralty Island, Alaska. Greens Creek contains approximately 4.5 million tons at 0.1 OPT Au, 25 OPT Ag and 20 percent combined Pb and Zn. Arsenic and antimony sulphides are also abundant at Greens Creek.

#### 4.3.4 Type ID Stratabound Arsenopyrite-Jamesonite-Gold 4.3.4.1 Wackwitz Prospect

The Wackwitz Prospect is located in section 31, T3N, R2E, F.M. (see location 70, Ch. 4, Plate VIII). The mineralization is exposed in a road cut and in three large trenches that delineate a strike length of over 800 meters (2,500 feet).

The mineralization consists of lenses of massive arsenopyrite and jamesonite hosted in metafelsic tuffs of the upper Cleary sequence. The sulphide lenses are up to 25 cm thick and the individual metavolcaniclastic layers are about 1 meter (3.25 feet) thick. Three metavolcaniclastic horizons are exposed in the excavations. The three metafelsic lenses are separate by one to two meters of pelitic schist. The metapelites are dominantly garnet-biotite-muscovite-quartz schist. A massive greenstone lens about 1.8 meters (6 feet) thick occurs 6 meters (20 feet) up section from the uppermost metafelsite lens. The greenstone is primarily composed of

Table 4.1 Assay data for Truck Sulphide System  
(Placid Oil Company, unpublished data)

Sample	Au (OPT)	Ag (OPT)	Pb (%)	Zn (%)	Sb (%)	% Core Recovery	Intercept (Feet)
Nordale Adit	0.039	11.90	6.24	7.31	0.59	100%	10
UDDH-6KS83	0.013	0.66	0.66	1.67	0.28	60%	10
DOH 5 KS-83	0.013	0.77	0.74	7.63	0.28	95%	7
DDH 6 KS-83	0.014	0.78	1.21	3.90	0.51	95%	1
	0.015	1.71	1.30	2.93	0.78	95%	8
DDH 1 KS-85	0.054	13.78	4.18	-	2.90	68%	10
	0.071	1.52	0.75	0.07	0.36	36%	11.5
DDH 7 KS-83	0.120	10.92	8.49	-	4.65	60%	8.4
	0.276	4.30	2.40	-	1.15	60%	2.0

amphibole with minor epidote and chlorite.

The metavolcaniclastic host is composed predominantly of quartz (up to 70 percent) and white-mica (up to 25 percent). The balance includes potassium feldspar, tourmaline, garnet, and zircon (see Appendix B). The tourmaline is light green and zoned and may constitute over one percent of the rock. The metapelites above and below the metafelsites do not contain abundant tourmaline and are devoid of sulphide mineralization. It is inferred that the tourmaline, sulphide, and gold mineralization are cogenetic and syngenetic with the metavolcaniclastic host.

The occurrence is near the crest of the Cleary Anticline. The host rocks strike east-west and dip to the south at 6 degrees. East of the occurrence, the mineralized section has been removed by erosion while to the west the mineralization strikes under several tens of meters of overburden along the eastern margin of Pedro Dome.

The following mineral descriptions are based on observations from 33 polished sections listed in Appendix B. Other minor sulphide phases include bornite, boulangerite, covellite, galena, pyrite, sphalerite, stibnite, and argentiferous tetrahedrite. Native gold occurs as micron size inclusions in the arsenopyrite and as discrete 5 to 10 micron size particles formed along the sulphide grain boundaries. The sulphides range in size from 0.1 to 1.25 mm with the majority of the grains in the 0.2 to 0.4 mm. There is a noted absence of massive quartz in the sulphide bearing lenses.

Table 4.2 lists assay data for one meter (3.25 foot) long channel samples taken across the mineralized horizon. The data indicate gold grades in excess of 0.1 OPT and silver grades exceeding 6 OPT. The lead contents of 6 percent are approaching ore grade however the high arsenic and antimony contents would result in severe problems in the smelting of these ores.

#### 4.3.4.2 Tolovana Mine

The Tolovana Mine is located in section 25, T3N, R2E, F.M. (see location 54, Ch. 4, Plate VIII). The mine has produced several thousand tons of high grade gold-quartz vein ore (Hill, 1933). Recent trenching on the property has exposed a section of mineralized Cleary sequence that is at

least 50 meters (160 feet) thick and is composed of metafelsite and metachert. This section is host to the gold-quartz vein mineralization.

The metafelsites range from 25 centimeters to 2 meters (10 inches to 6.5 feet) thick and are interlayered with nearly equal sections of metachert. The metachert is a finely laminated quartz rock with 3 to 5 percent white-mica. The metachert may contain disseminated arsenopyrite but other sulphide phases are absent.

The host rocks and sulphide lenses strike east-west and dip to the north at 10 to 15 degrees. The mineralized section appears to be continuous along strike for 800 meters (2,500 feet) to Bedrock Creek.

The mineralization is similar to that at the Wackwitz Prospect except that the metafelsites are intercalated with metachert rather than with metapelites. Sulphide mineralogy includes: major arsenopyrite, jamesonite, and stibnite; and minor argentiferous tetrahedrite, boulangerite, chalcopyrite, covellite, galena, pyrrhotite, and sphalerite. Gold usually occurs as micron size inclusions in the arsenopyrite but at the eastern extremity of the property above Bedrock Creek, gold grains up to 1.0 mm are intergrown with the sulphides. The ore mineral descriptions are based on observations of the 34 polished sections listed in Appendix B.

Limited analytical data is available for the property due to initial restrictions on access. Table 4.3 is from analytical data provided by Kennecott-Alaska Exploration (A Division of Kennecott Copper Corp., Salt Lake City, Utah).

The stratabound mineralization of the Tolovana Mine is 1,600 meters (5,000 feet) north and 300 meters lower in elevation than the Wackwitz Prospect. The parallelism of the dip of the units and the slope of the hill places the two occurrences at about the same stratigraphic position. The mineralization can be traced along strike to the Cleary Hill Mine to the east and on into the drainage of Chatham Creek, a distance of over 2.5 kilometers (1.5 miles).

#### 4.3.5 Type IIE Stratabound Lead-Zinc

##### 4.3.5.1 Cheechako Prospect

The Cheechako Prospect is located in section 25, T3N, R1E, F.M. (see location 56, Ch. 4, Plate VIII). The prospect

Table 4.2 Channel sample assay data for the Wackwitz Prospect  
(base metals in ppm, precious metals in ppb,  
N/A not available).

Sample Number	Cu	Pb	Zn	Au	Ag	Sb	As
807	271	8,308	600	1,130	44,900	1,710	>1,000
808	860	N/A	N/A	3,780	N/A	N/A	<1,000
809	129	6,100	131	110	18,600	511	<1,000
1778	760	60,000	1,780	3,800	230,000	11,000	N/A

Table 4.3 Analytical results for the surface trenches at the Tolovana Mine, Fairbanks district, Alaska

Sample Number	QUANT			
	Au (ppm)	Au (ppm)	Ag (ppm)	As (ppm)
WC-1	1.42	*	1.4	1,550
WC-2	*	0.84	24.	1,900
WC-4	*	0.48	1.4	1,200
WC-5	*	0.56	0.4	2,400
WC-6	*	0.16	0.6	850
WC-7	*	0.23	0.4	1,850
WC-8	*	0.05	0.2	800
WC-9	*	0.02	0.2	450
WC-11	*	0.38	8.4	700
WC-12	*	0.17	3.4	4,200
WC-13	*	0.10	0.6	1,050
WC-14	*	0.09	0.2	400
WC-15	*	0.15	0.2	350
WC-16	9.3	*	22.	4,300
WC-17	*	0.12	0.4	550
WC-18	*	0.17	0.8	550
WC-19	*	0.63	0.4	2,000
WC-20	*	0.31	0.2	1,050
WC-21	*	0.11	0.2	650
WC-22	0.92	*	2.8	1,150
WC-23	3.2	*	8.8	3,550
WC-24	*	0.32	0.8	1,050
WC-25	*	0.18	0.8	550
WC-26	*	0.16	6.4	1,050
WC-27	*	0.94	0.2	2,050

is also known as the Westonvitch property.

The mineralization consists of major sphalerite, pyrite, and galena with minor jamesonite and stibnite hosted in marble and chlorite calc-schist. The marble is intercalated with metachert. Massive greenstone and chlorite calc-schist and graphitic schist outcrop 300 meters (1,000 feet) southeast of the exposed carbonates. These units appear to underlie the marble and sulphide mineralization.

The host rocks strike east-west and dip to the north at 10 to 15 degrees. This mineralized section is at least 10 meters (32 feet) thick and may continue to the east in the Cleary Hill Mine area. Carbonate hosted base metal sulphide mineralization is found on the lower mine dump at the Cleary Hill and in placer tailings on lower Chatham Creek. Recent placer mining activity in Chatham Creek exposes carbonate and chlorite schist-hosted mineralization upstream from the previous placer workings. These occurrences as well as the

carbonate hosted mineralization below the Truck Sulphide System suggests that the carbonate hosted mineralization may extend for over 5 kilometers (3 miles) along strike.

The sulphides occur in alternating bands of pyrite rich horizons and sphalerite rich layers. Galena, arsenopyrite, jamesonite, and tetrahedrite are associated with the sphalerite rich bands. The bands range from 5 mm to 2 cm thick and are separated by equal widths of carbonate.

Pyrite grains range up to 1.5 mm and constitute at least forty percent of the total sulphides. Sphalerite grains may exceed 1.5 mm but most grains are 0.2 to 0.4 mm in diameter. The sphalerite contains abundant inclusions of chalcopyrite. Galena forms grains up to 1.5 mm and these large grains have white and brown inclusions that are probably polybasite and jordanite respectively. The inclusions are in the micron range thus quantitative analysis is not possible by electron microprobe techniques. Jamesonite occurs as 0.05 to 0.1 mm size grains and represents up to five percent of the total sulphides. Tetrahedrite, pyrrhotite, and covellite are present only in trace amounts. No grade data is available for the stratabound mineralization.

The stratabound mineralization is cut by a high angle shear zone that strikes N80oE and dips 75oN. The shear zone ranges from 1.0 to 8.3 meters (3.25 to 27.0 feet) wide. The zone includes intense clay alteration with minor sericitic alteration. Sulphide mineralization up to a meter (3.25 feet) wide fills the fractured carbonate and schistose host rock. The same sulphide minerals as occur in the stratabound sequence are found in the shear zone but in different abundances. Argentiferous tetrahedrite, sphalerite, and galena are in greater abundance in the shear zone. Channel samples across the shear indicate grades of up to 0.09 OPT Au, 60 OPT Ag, 27% Pb, 20% Zn, and 1% Sb over meter (3.25 foot) widths. A 168 tonne (185 ton) bulk sample of the ore indicates an average grade of 0.07 OPT Au, 38 OPT Ag, 19% Pb, 2% Zn, 2.6% Sb, and 1.8% As (unpublished Placid Oil data).

#### 4.3.6 Type IIA Intrusive Related Gold

##### 4.3.6.1 Fork Knox Prospect

The Fort Knox property is located in section 16, T2N, R2E, F.M. (see location 118, Ch. 4, Plate VIII). This occurrence is listed in Chapman and Foster (1969) as the Vogt, Monte Cristo, or Melba Creek. The property is centred on the ridge between Monte Cristo and Melba Creeks.

The mineralization consists of gold in quartz veinlets in sheared and weakly altered porphyritic granodiorite. The host intrusive crops out over an area 1,500 meters (5,000 feet) long and 460 meters (1,500 feet) wide. The elevation of the outcrop area ranges from 460 meters (1,500 feet) to 580 meters (1,900 feet). Drilling indicates that the mineralization extends to a depth of at least 300 meters (1,000 feet).

Native gold occurs in the veinlets with native bismuth, bismuthinite, molybdenite, and scheelite. The mineralization is associated with relatively high tellurium concentrations although no telluride minerals have been observed.

The intrusive is hosted in Cleary sequence rocks. It is notable that this mineralized pluton is completely surrounded by Cleary sequence rocks while a more southerly porphyritic granodiorite is not in contact with Cleary sequence rocks and is not mineralized. The predominant rock types are garnet-biotite-muscovite-quartz schist and micaceous quartz. These units represent the middle pelitic section of the sequence; however limited lenses of metafelsite, and calcareous schist are present.

A major reverse circulation drilling program over the past two years has resulted in the completion of 178 drill holes totaling 22,000 meters (72,000 feet). The operator of the project, Fairbanks Gold Ltd., Vancouver, British Columbia, Canada reports a resource of 80-100 million tons at 0.036 to 0.047 OPT with a cut-off grade of 0.02 OPT.

#### 4.3.7 Type IIB Intrusive Related Lead-Silver

##### 4.3.7.1 Silver Fox Mine

The Silver Fox Mine is located in section 9, T2N, R1E, F.M. (see location 91, Ch. 4, Plate VIII). The property has also been known as the Silvertone or Busty Belle. The mineralization is exposed in trenches and road cuts and is accessed by an adit 100 meters (325 feet) long.

The mineralization in the adit consists of base metal sulphides filling a shear zone in the granodiorite host, and disseminated molybdenum mineralization in the intrusive. On the surface, trenches expose sheared and sericitically altered granodiorite that hosts narrow gold-quartz veinlets. This mineralization is similar to the Type IIA mineralization at the Fort Knox occurrence.

The property is located at the western extreme of the Pedro Dome stock. Two phases of the intrusive complex are present. The earlier phase is fine-grained granodiorite and is the predominant intrusive phase at the property. The later phase is a quartz monzonite. The quartz monzonite is present at two separate locations named the Flume and Fox Creek plutons by Britton (1970). The Flume Creek pluton includes two textural variants. One variant is a coarse-grained equigranular rock and the other is a fine-grained to porphyritic rock. The Fox Creek pluton is a coarse-grained equigranular rock.

The granodiorite exhibits potassic, sericitic, argillic, and propylitic alteration. The potassic alteration is manifested by potassium feldspar veinlets. Incipient sericitic alteration is represented by traces of sericite on plagioclase rims while pervasive alteration is marked by complete destruction of the feldspar. Argillic alteration is ubiquitous in the pluton and is manifest by at least traces of kaolinite. Propylitic alteration is best observed in the underground workings of the Silver Fox Mine where biotite is altered to chlorite and epidote and calcite veinlets are common.

The quartz monzonite plutons exhibit well developed sericitic alteration which is characteristic and pervasive. Similarly kaolinite occurs in large quantities in both the Fox Creek and Flume Creek plutons. Propylitic alteration is poorly developed and is not well manifested due to the lack of mafic minerals. Calcite veinlets are present in some

outcrops. Potassic alteration is conspicuously absent from the quartz monzonite.

An early stage of quartz molybdenum mineralization occurs in the granodiorite as a stockwork of narrow quartz veins up to 0.5 cm wide with molybdenite and minor scheelite. Potassium feldspar is present in the veins while pyrite is common in the wallrock. The veinlets generally strike northeast-southwest and dip 70 to 80°N.

Sherman (1983) reports analytical data for three samples of the quartz-molybdenite mineralization and this data is included as Table 4.4.

Table 4.4 Atomic-absorption analyses of samples from the underground quartz-molybdenite stockwork, Silver Fox Mine, Fairbanks mining district, Alaska (all values in ppm) (After Sherman, 1983).

Sample no.	Sample type	Cu	Pb	Zn	Mo	Au	Ag	W
60-3	Grab	14	146	81	11	-0.1	2	*
60-4	Grab	13	490	93	9	-0.1	1	*
107-3	Chip	9	*	*	8	*	*	35

\* No analysis requested.

The extent of the molybdenum mineralization is not well documented. It is pervasive in the Silver Fox Adit but is reported at only one locality on the surface above the adit.

Base metal sulphide mineralization occurs in shear zones in the granodiorite that strike northeast and northwest and dip 40 to 60 degrees to the south and north respectively. The sulphide mineralogy includes major arsenopyrite, pyrite, sphalerite, galena, and argentiferous tetrahedrite. Sherman (1983) reports that the galena is "argentiferous" while in fact it contains abundant white inclusions that are probably polybasite. A silver-copper-antimony mineral stytotypite may be present or the high silver content material may be an intergrowth of argentiferous tetrahedrite and polybasite or pyrrargyrite.

Sherman (1983) reports analyses of several grab samples from the sulphide veins and these data are included as Table 4.5.

The sulphide veins contain little or no quartz. The known sulphide veins are restricted to the granodiorite however the exposure in the area is very poor thus additional mineralized structures may be found in both the schist and quartz monzonites with additional exploration.

The sulphide veins range in width from a few centimeters to a meter (1.5 inches to 3.25 feet). The veins extend for at least 20 meters (65 feet) along strike and have a vertical dimension of at least 15 meters (50 feet).

Gold-quartz vein stockwork mineralization is reported by Forbes et al. (1968) and Sherman (1983). The major

Table 4.5 Atomic-absorption analyses of grab and chip samples from sulphide veins in the granodiorite, Silver Fox Mine, Fairbanks mining district, Alaska (all values in ppm) (After Sherman, 1983).

Sample no.	Sample type	Cu	Pb	Zn	Mo	Au	Ag
36-1	Grab	680	9900	1160	8	70.0	975
36-2	Grab	36	8900	2100	4	11.7	663
60-1	Chip	100	7700	19400	5	Trace	79
60-2	Chip	100	7700	19400	5	Trace	79
70-2	Grab	4000	9000	800	19	2.9	1120
107-1	Chip	149	29600	1600	35	0.8	92
107-4	Grab	760	95500	37600	6	1.4	662

mineralization is in the quartz monzonite of the Fox Creek pluton. The mineralized zone contains major sericitic and argillic alteration. Sherman reports that the mineralization is weakly developed however the data in Table 4.6 suggests that there is considerable potential for stockwork gold mineralization at the Silver Fox Mine similar to the mineralization at the Fort Knox Property. The data are for one meter (3 foot) channel samples collected across the exposed mineralization in Trench No. 1 which is located approximately 300 meters (1,000 feet) northeast of the portal of the adit. The mineralized zone averages 3 meters (10 feet) wide and is exposed in the trench for approximately 7 meters (23 feet) along strike. The average grade across the zone is 0.104 OPT.

Since the trenching in the immediate area is limited to this single excavation, and the mineralization is only exposed in the trench, the lateral and vertical extent of the mineralization is unknown. The mineralization appears to be similar to that at the Fort Knox property however additional trace element data is necessary for a definitive comparison.

#### 4.3.8 Type III Tungsten Skarn

##### 4.3.8.1 Tungsten Hill Prospect

The Tungsten Hill prospect is located in section 34, T2N, R1E, F.M. (see location 126, Ch. 4, Plate X). The occurrence is also known as the Spruce Hen and has been described in detail by Allegro (1987). The following is a synopsis of that investigation.

The occurrence is located approximately 600 meters (2,000 feet) northeast of the outcrop of the porphyritic quartz monzonite phase of the Gilmore Dome intrusive complex. Trenching on the property exposes interlayered white-mica schist, graphitic schist, laminated quartzite, amphibolite, and marble. The units strike N 40 to 50° E and dip to the northwest at 40 degrees. These are the upper units of the Cleary sequence.

The schist units exhibit the effects of contact metamorphism with the presence of secondary biotite and white-mica

Table 4.6 Atomic-absorption analyses of channel samples from the Trench No. 1, Silver Fox Mine, Fairbanks mining district, Alaska (unpub. data from Peter Rutledge, State-wide Office of Land Management, University of Alaska Fairbanks).

Sample Description	Au ppb
TC.25.C2.2	1090
TC.25.C2.3	1500
TC.25.C2.4	2440
TC.35	960
TC.35.C3.1	545
TC.35.C3.2	320
TC.35.C3.3	2090
TC.35.C3.4	95
TC.48.C4.1	380
TC.48.C4.2	635
TC.48.C4.3	2420
TC.71	8250
TC.75.C5.1	5780
TC.75.C5.2	580
TC.75.C5.3	65
TC.75.C5.4	35
TC.82	840
TC.92	3150
TC.92.C6.1	410
TC.92.C6.2	2580
TC.125	10
TC.125.C7.1	20
TC.125.C7.2	340
TC.125.C7.3	5
TC.128	5
TC.140.A	65
TC.140.B	280
TC.140.C8.1	1100
TC.140.C8.2	< 5
TC.140.C8.3	< 5
TC.140.C8.4	170
TC.151.C9.1	610

and tourmaline cross-cutting the foliation. The two marble layers, each between 1 and 2 meters (3.25 and 6.50 feet) wide, are exposed over a strike length of 90 meters (290 feet). The marbles contain calcite (80 to 90 percent) and variable amounts of idocrase, diopside, garnet, scheelite, and wolastonite.

Vertical narrow felsic dikes (3 to 8 cm wide) cut across

the foliation at low angles. The dikes are composed of potassium feldspar, plagioclase (An 30-50), and quartz. The grain size ranges from 0.5 to 1.0 mm. The felsic dikes are abundant in and adjacent to the west end of the Gilmore Dome intrusive complex (Blum, 1983).

The scheelite mineralization is in massive nonfoliated calc-silicate skarn (exoskarn) that contains a zone of non-mineralized marble. The calc-silicate assemblage of the mineralized marble suggests that silica, iron, aluminum, magnesium, manganese, fluorine, and tungsten were added by the mineralizing fluids.

The exoskarn can be divided into early and late skarns. The early skarn is characterized by pyroxene and garnet with or without idocrase, wollastonite, quartz, and scheelite. Zoning is noted with respect to the schist/marble contact thus suggesting the exchange of components between the two rock types. From the schist to the marble the assemblages are as follows:

1. Schist or idocrase layer
2. Garnet + pyroxene ± quartz
3. Pyroxene + garnet + scheelite
4. Idocrase ± wollastonite ± pyroxene ± scheelite ± quartz
5. Marble

The zoning is not always well defined nor are all zones always present.

The scheelite is disseminated throughout the garnet pyroxene skarn and appears to correlate with the abundance of pyroxene. The scheelite grains range from 0.2 to 0.4 mm in diameter, are subhedral to anhedral, and occur as isolated grains or as aggregates. Both relatively pure scheelite and scheelite with a high powellite component are found at the prospect. The high powellite scheelite is usually surrounded by low molybdenum content scheelite.

Fluorite is abundant at the prospect and may comprise 20 to 30 percent of the exoskarn. The fluorite occurs as colorless subhedral grains that range from 0.2 to 1.4 mm in diameter. The fluorite generally occurs in vugs with quartz and calcite in the skarn or occurs in veins that cut the marble.

The late skarn is a hydrous alteration product of the early pyroxene-garnet skarn. The mineral assemblages of the late skarn include: amphibole ± calcite ± quartz (after pyroxene), clinozoisite ± quartz ± calcite (after garnet and idocrase), high grade scheelite, and minor chlorite, biotite, iron oxides, and sulphides.

Scheelite in the retrograde skarn may occur in concentrations up to 8 percent. The grain size is larger than in the early skarn with crystal aggregates up to 1.5 mm in diameter. The scheelite in the retrograde skarn is associated with assemblage amphibole ± calcite + quartz. The late stage scheelite may contain inclusions of calcite, pyroxene, clinozoisite, or fluorite. The late skarn forming event is followed by the introduction of iron oxides and minor sulphides including pyrite, pyrrhotite, chalcopyrite, and arsenopyrite.

The skarn mineralization can be traced for 50 meters (160 feet) along strike. Allegro (1987) reports 52 rock geochemical analyses for the property. Tungsten concen-

trations range from trace to 1.17 percent. The higher scheelite concentrations are associated with elevated gold contents that generally range from 100 to 800 ppb. One sample of a scheelite bearing felsite dike contains 5.5 ppm Au.

#### 4.3.9 Type IV Metamorphic Hosted Gold-Quartz Veins

The metamorphic hosted gold-quartz veins account for the entire 325,000 ounces of lode gold produced from the district. The following five operations on four separate vein structures are responsible for the majority of the production prior to 1980:

1. Newsboy Mine (Newsboy vein, 40,000 troy ounces),
2. Cleary Hill Mine (Cleary vein, 100,000 troy ounces),
3. McCarty Mine (American Eagle-Kawalita-Christina vein system, 40,000 troy ounces),
4. Kawalita and Vetter-Sheldon (American Eagle-Kawalita-Christina vein system, 20,000 troy ounces),
5. Hi-Yu Mine (Hi-Yu vein, 100,000 troy ounces).

Since 1980 the Ryan Lode and the Grant Mine have produced 16,750 and 11,017 troy ounces respectively (Bundtzen and Kline, 1981).

As noted previously the quartz veins are fracture fillings in shear zones that range from less than a meter to 70 meters (3.25 to 225 feet) wide. The quartz veining is generally near or at the hanging wall contact of the shear. Not all mineralized shear zones have discrete quartz veins. Where present the quartz vein may range in width from a few centimeters to 4.5 meters (one inch to 15 feet).

On the east side of Pedro Dome and west of Cleary Summit, the Newsboy and Robinson veins strike N45°E and dip to the NW at 65-80 degrees. North of Cleary Summit the veins strike N75°W to N85°E and dip to the south at 55-60 degrees (Cleary Hill, Colorado, and Wyoming veins). East of the Cleary Hill Mine, the veins strike approximately N70°W and dip to the south at 55 to 70 degrees.

Plate IV (Chapter 3) shows the major veins in the Cleary Summit area. Adding the known strike length of the Newsboy and Robinson veins to the strike length of the veins on the plate results in a total length of 22,300 meters (72,500 feet).

##### 4.3.9.1 Vetter Prospect

The Vetter Property is a large claim holding (20,000 acres) that is centred in section 20, T3N, R2E, F.M. (see location 28, Ch. 4, Plate VIII). The major vein occurrence on the property and the best exposed Type IV mineralization in the district is the Christina-Kawalita-American Eagle system (see Ch. 3, Plate I). The vein is well exposed at the surface for 1,000 meters (3,250 feet) of the 2,000 meter (6,500 foot) known strike length. The vein is also delineated by a total of 11,470 meters (37,277 feet) of diamond drilling and 4,623 feet of reverse circulation drilling. The Christina Adit is driven 458 meters (1,489 feet) to crosscut the vein approximately 60 meters (200 feet) below the surface while the Nordale Adit is driven 1,350 meters (4,400 feet) to intercept the vein 120 meters (400 feet) below the outcrop. The deepest bore hole intercepts the vein approximately 300 meters

(1,000 feet) below the surface.

The mineralization consists of two subtypes. The first is relatively high grade gold-quartz veining at or near the hanging wall of the structure and the second is low grade disseminated gold in the shear zone and in the footwall of the structure.

The mineral assemblages in the quartz vein include argentiferous tetrahedrite, arsenopyrite, boulangerite, bornite, covellite, galena, gold, jamesonite, pyrite, sphalerite, and stibnite. The sulphide mineral content of the vein generally is less than 0.5 percent. Arsenopyrite constitutes 80 to 90 percent of the sulphides present.

The arsenopyrite forms euhedral to subhedral grains from 0.1 to 1.5 mm in diameter with an average size of 0.4 mm. Arsenopyrite occurs as the earliest sulphide phase and is replaced by all other sulphide phases and by gold and quartz. The euhedral grains usually show well developed concentric zoning. Arsenopyrite alters to scorodite which imparts a distinctive light green color to the host rock. The replaced and altered arsenopyrite may develop caries texture or the replacing phases may form in fractures or as rims around the grains.

After arsenopyrite, the various sulfosalts are the most abundant ore minerals. Boulangerite is the most common phase associated with the higher grade mineralization however jamesonite is the most abundant sulfosalt. Argentiferous tetrahedrite is spatially and genetically associated with jamesonite and these two phases are indicative of high silver contents in the more sulphide rich portions of the vein. Boulangerite forms as distinctive needles up to 5 mm long. The other sulfosalts occur as anhedral to subhedral grains 0.05 to 0.1 mm in diameter and as aggregates of such grains up to several mm in diameter.

Bornite and chalcopyrite occur in trace amounts as 0.01 to 0.05 mm grains spatially associated with the tetrahedrite. This low abundance is reflected in the low copper content of the veins and the host rocks.

Galena is rare and occurs as euhedral grains up to 2 mm in diameter and is spatially associated with subhedral sphalerite of the same grain size. These phases are not necessarily spatially associated with the gold mineralization.

Stibnite rarely occurs with the other sulphide phases but forms large masses that crosscut the sulphide and gold mineralization. The mineral grains are euhedral to subhedral and range from 0.1 mm to 3.0 cm in diameter. Most of the grains are 0.5 to 1.5 mm in diameter. Occasionally arsenopyrite and pyrite are found as small inclusions in the stibnite. Lensoidal aggregates of stibnite up to 30 cm in maximum dimension are associated with massive milky quartz. This mineralization is thus transitional to the Type V monomineralic stibnite type.

Individual ore shoots in the vein are not apparent from the drilling and surface and subsurface sampling. Quartz vein widths vary from 15 cm to 2.5 meters (6 inches to 10 feet). There is no definite correlation between quartz vein width and gold grade. The vein widths may change by an order of magnitude over a 100 meter (325 foot) strike length. Similar

changes are noted in the vertical direction.

Approximately 60,000 troy ounces of gold have been produced from about 60,000 tons of ore for an average grade of 1.0 OPT. This is comparable to other producing veins in the district. From the diamond and rotary drilling, a drill indicated reserve of 166,500 tonnes (185,000 tons) of 0.6 OPT Au over a 1.5 meter (5 foot) mining width is estimated for the west end of the vein above the Christina Adit level. An additional 166,500 tonnes (185,000 tons) of equivalent grade is estimated between the Nordale and Christina Adit levels. A few 300 meter (1,000 foot) diamond drill holes indicate similar ore grades at depth. The vertical and lateral grade continuity of the vein is typical of metamorphic hosted systems. Such grade continuity is not common in epithermal vein systems.

The disseminated mineralization in the shear zone and in the footwall of the shear is less well defined than the vein mineralization. On the surface, the shear zone consists of a highly deformed zone of fragmented schist 1.5 to 4.5 meters (5 to 15 feet) wide and a less intensely deformed zone at least 10 meters (30 feet) wide. The highly deformed zone is characterized by intense sericitic alteration overprinted by clay alteration. The rocks are fragmented and the long axis of the fragments are parallel to the shear zone. The latter (less deformed) zone exhibits sericitic alteration without clay alteration. The local trend of the foliation can be recognized as well as the compositional continuity of the schist. Hereinafter the former zone will be referred to as the clay zone and the latter the footwall zone.

Both zones indicate the major introduction of silica. In the clay zone the silica forms the above described high grade quartz veining. In the footwall zone, the silicification occurs as narrow fracture and joint fillings up to 5 mm wide. On the surface these fillings contain iron oxides, scorodite, and gold. At depths below 45 meters (150 feet) the fracture fillings contain quartz, arsenopyrite, pyrite, boulangerite, and native gold.

The Christina Adit cuts two zones of intense shearing north of the Christina shear zone, with an aggregate width of 60 meters (200 feet). The footwall zone of the Christina is at least 10 meters (30 feet) wide. These two shear zones are covered with lagging, thus sampling of the rock in situ and detailed descriptions are not possible.

The clay zone and the footwall zone were sampled on the surface at three localities across the western end of the Christina system (see sections A-A', B-B, and C-C', Ch. 3, Plate IV). The sampling did not include the high grade gold-quartz vein. The channel sample widths were 1.5 meters (5 feet) and each sample weighed approximately 10 kilograms. The total sampled width for each section was 15.4 meters (50 feet). The average grade of each sample was 0.065, 0.082, and 0.075 OPT gold respectively. The sections were resampled and the channel samples for each section were composited for metallurgical testing. The grades for the composited samples were 0.082, 0.247, and 0.058 OPT for gold sections A-A', B-B' and C-C' respectively. The resampling of section B-B' suggests that there may be a second zone of gold-quartz vein

mineralization in either the clay zone or in the footwall zone.

Disseminated shear zone mineralization similar to that in the Christina system is recognized in other structures in the district including: the Grant Mine and the Ryan Lode in the Ester Dome area; and the Saddle Zone, Circle Trail Zone, and the Too Much Gold Zone at Cleary Summit (see Ch. 3, Plate IV). It is probable that the other veins shown on Ch. 3, Plate IV will be found to contain similar mineralization.

#### 4.3.10 Type V Monomineralic Stibnite

##### 4.3.10.1 Scrafford Mine

The Scrafford Mine is located in section 16, T2N, R1W, F.M. (see location 109, Ch. 4, Plate VI). The mineralization is partially exposed in surface trenches, however none of the underground excavations are accessible. Robinson and Bundtzen (1982) provide a geologic map of the surface exposures and summary report on the property.

The property is the second largest antimony producer in Alaska with a recorded production of 944,500 kilograms (2,077,920 lbs) of metal from 2,510 tonnes (2,761 tons) of ore (Robinson and Bundtzen, 1982). This is a minimum production since official records are incomplete. The recorded production is for the years 1915-1918 and 1970-1971.

The mineralization consist of lens shaped masses of stibnite and disseminated stibnite in a shear zone that cuts various units of the Cleary sequence. The shear zone strikes N 80-85° E and dips 55-60° S. The host rocks are white-mica schist, metachert, feldspathic schist, calcareous schist and graphitic schist.

The massive mineralization consists of 2.5 mm to 5 cm

size fibrous and columnar twinned crystals of stibnite in a finer grained groundmass of stibnite. The groundmass contains traces of arsenopyrite and pyrite. The disseminated mineralization consists of 0.1 to 1.5 mm size grains of euhedral to subhedral stibnite in quartz veinlets and in compositional layers of the sheared feldspathic schist and metachert.

The massive mineralization forms en echelon lenses or pods that diverge 15-20° from the trend of the shear. The podiform ore shoots range from 10 to 25 meters (30 to 80 feet) long and up to a meter (3.25 feet) wide. The pods extend for at least 15 meters (50 feet) in the vertical direction. The host to the pods is broken feldspathic schist and metachert. The shear zone contains both sericitic and clay alteration. The zone of intense shearing and clay alteration ranges from 1.25 to 6 meters (4 to 20 feet) wide while the entire zone of sericitic and clay alteration ranges from 2 to 12 meters (6 to 38 feet) wide. The hanging wall of the shear is moderately well exposed and there is no indication that the alteration extends into it. The footwall is poorly exposed and the sericitic alteration may be wider than 12 meters (38 feet).

The massive mineralization tends to occur on the footwall of the clay alteration zone. Below this zone stockworks of scorodite-stained quartz veinlets contain elevated gold values that range up to 5 ppm. Table 4.7 after Robinson and Bundtzen (1982) includes 14 channel samples from the massive stibnite zone and the underlying disseminated zone. These data indicate that the monomineralic stibnite mineralization may be a higher level expression of underlying gold-quartz vein mineralization.

Table 4.7 Assay results of chip and channel samples from the Scrafford Mine, Fairbanks mining district, Alaska (after Robinson and Bundtzen, 1982).

Sample Number	Length of channel (ft)	Trace Element Concentrations (ppm)					
		Au	Ag	Cu	Pb	Zn	Sb
225	4	0.87	0.4	64	10	34	11,950
226	4	2.1	0.4	139	8	25	11,900
227	4	0.75	0.3	77	28	97	227
228	3	0.98	0.7	158	5	19	115,000
229	3.5	1.92	0.4	159	10	6	86,000
240	1.5	0.01	0.1	83	20	96	90
241	2	1.41	0.2	104	11	44	38
242	4	3.06	1.3	93	110	193	379
243	1.5	5.70	0.6	92	25	29	13,500
244	1	1.41	0.1	77	12	41	100
245	4	0.01	0.1	59	22	60	55
247	2	0.01	0.0	70	11	50	38
475	2.5	0.01	0.0	66	15	68	1,980
495	3	0.10	0.1	68	15	102	472

## 4.4 QUANTITATIVE ORE MINERALOGY

### 4.4.1 Electron Microprobe Determinations

Electron microprobe analyses of the various ore minerals were performed to confirm the identifications made from reflected light microscopy, and to determine elemental content of the variable component phases. The phases that contained precious metal components and those phases that would adversely affect mineral recovery were of particular interest.

Table 4.8 presents the analytical results from electron microprobe analyses of select sulphide minerals from several of the mineral occurrences in the district. The data are for energy dispersive analyses conducted on the Cambridge Instruments Geoscan instrument at Imperial College, University of London.

Bournonite is abundant only in samples collected from the Tolovana Mine. It is associated with high gold contents in the vein mineralization but is not recognized in the stratabound massive sulphides. Copper mineralization is not abundant in the district. Only the Tolovana and adjacent Cheechako and Willow Creek properties have relatively high copper contents. Other copper phases include chalcopyrite and tetrahedrite. The above three occurrences (Tolovana, Cheechako, and Willow Creek) are the only occurrences in the district that have major copper bearing phases other than tetrahedrite.

Boulangerite is ubiquitous in the high grade Type IV occurrences and in the stockwork footwall mineralization in the shear zones. It does occur in Type I mineralization such as the Cheechako, Wackwitz, and Truck Sulphide System (Nordale Adit). The presence of boulangerite in the stratabound sulphides is an indicator of elevated gold contents.

Chalcopyrite is absent in major quantities from most of the occurrences in the district except the three named above in the upper Cleary Creek area. The chalcopyrite from the Tolovana occurrence contains detectable levels of arsenic and silver but no gold.

Jamesonite is the most widespread sulfosalt in the district. It occurs in greatest abundance in the Type I mineralization and is correlated with high silver contents in the lenses. Jamesonite does occur in Type IV sulphide rich veins and is generally associated with argentiferous tetrahedrite. Silver is not detected in any of the samples listed in Table 4.8 and thus jamesonite is probably not a source of silver in either the Type I or Type IV occurrences. Detectable copper and zinc are noted in samples from the sulphide rich veins from the Cleary Hill, Hi-Yu, and Tolovana Mines.

Pyrite contains detectable arsenic at several locations however no detectable gold is present in the samples listed in Table 4.8. Observations of the polished sections containing pyrite have failed to indicate the presence of inclusions of gold in pyrite; however cogenetic arsenopyrite frequently contains micron size gold inclusions.

Pyrrhotite is relatively rare in the district compared to pyrite. Pyrrhotite occurs in the eclogitic rocks and in the actinolitic greenschists in trace amounts. It is relatively plentiful in the contact zone at the Fort Knox occurrence. At this locality, copper is detected in the microprobe analyses

and chalcopyrite inclusions are noted in the reflected light petrography. At the Wyoming prospect, there is detectable arsenic in the stratabound pyrrhotite. Visible gold also is present in the associated stratabound arsenopyrite. Actinolitic greenschists near the Newsboy Mine (see sample 82FM01) contain abundant pyrrhotite and scheelite. No detectable gold is noted in any of the pyrrhotite grains analyzed to date.

Sphalerite is common in both Type I and Type IV deposits. Detectable quantities of arsenic and copper are found in the sphalerite. The analyzed areas do not contain visible inclusions of arsenopyrite or chalcopyrite. The mole percent FeS in the samples ranges from 3.50 to 10.85. At or above 300°C the pyrite + sphalerite assemblage is stable and this is the assemblage observed in each sample.

Sübnite analyses do not detect either arsenic or gold. Sample 81MRL16 is from the Scrafford Mine (Type V occurrence) and 82NB01 is from the Newsboy Mine, a high grade Type IV occurrence.

Stylopyrite, a silver sulfosalt, may occur in the high sulphide content Type II mineralization at the Silver Fox Mine. Alternatively the material in 75Z010A may be a mixture of tetrahedrite and either pyrargyrite or polybasite. The analyzed material appears to be homogenous and a single phase. The grains analyzed exceeded 0.02 mm in diameter. The polished section contains 10 percent galena and the galena has abundant micron size white inclusions that are probably polybasite. The inclusions are too small for quantitative analysis but indicate a silver and antimony bearing phase.

Tetrahedrite occurs in both Type I and Type IV mineralization. All the tetrahedrites measured in the district are argentiferous with silver ranging from 6.97 to 18.35 weight percent. The sample with the upper limit of the range is from the Silver Fox Mine. This extreme value may also be due to the analysis of inclusions of polybasite in the tetrahedrite.

### 4.4.2 Arsenopyrite and Gold Association

Gold is always associated with high arsenic concentrations and below the oxidation zone, arsenopyrite is always present when gold concentrations exceed 100 ppb. The reverse is not true. Even very high concentrations of arsenopyrite in the stratabound sulphides and in the sulphide rich veins does not assure the presence of even anomalous gold. However arsenopyrite textural and compositional data can be used to provide an indication of favorable conditions for gold deposition.

#### 4.4.2.1 Arsenopyrite Textures and Gold Contents

Observation of arsenopyrite in reflected light indicates three prevalent textures: (1) concentric zonation, (2) presence of inclusions, and (3) carries texture if multiple ore deposition events are present. Concentric zoning may be used to constrain the classification of the mineralization. This is possible only if quantitative data is available. This topic will be discussed in the subsequent section.

The presence of gold inclusions in the arsenopyrite usually indicates gold concentrations above 1 ppm. Although

Table 4.8 Electron microprobe analyses of select sulfide minerals from the Fairbanks mining district, Alaska

Mineral Sample Number	Elements (Wt %)									
	Sample Location(1)	As	Sb	Cu	Fe	Pb	Ag	Zn	S	Total
<b>Bournonite</b>										
82TV04B										
Loc. No. 54	0.26	24.76	13.18	0.60	40.54	--	0.18	19.92	99.44	
<b>Boulangerite</b>										
81MIRL03										
Loc. No. 150	0.15	24.89	0.20	0.11	53.46	0.40	0.58	19.24	99.03	
82TV04B										
Loc. No. 54	0.18	26.92	0.34	--	53.25	--	0.28	18.93	99.82	
TPB46										
Loc. No. 56	0.08	25.79	0.15	--	53.73	--	0.48	19.32	99.55	
82NA01										
Loc. No. 25	0.31	26.05	0.83	--	53.20	--	--	19.42	99.81	
82TV05										
Loc. No. 54	--	27.17	0.13	--	53.67	0.63	--	19.25	100.85	
WACK 14B										
Loc. No. 70	--	27.12	--	--	53.71	--	--	19.31	100.14	
<b>Chalcopyrite</b>										
82TV05										
Loc. No. 54	0.34	--	33.33	30.40	--	0.28	--	34.69	99.04	

Note (1) Location number for Ch. 4, Plate III thru XI.

	As	Sb	Cu	Fe	Pb	Ag	Zn	S	Total
<b>Jamesonite</b>									
82TV04B Loc. No. 54	--	35.12	0.36	2.75	39.36	--	0.47	21.63	99.69
Hi-Yu 57 Loc. No. 7	--	34.50	0.54	2.43	42.17	--	0.28	19.79	99.71
81MIRL02D Loc. No. 47	--	33.46	0.47	2.43	43.90	--	0.36	19.76	100.38
81MIRL25G Loc. No. 48	--	32.82	0.33	2.67	45.03	--	--	19.26	100.11
<b>Pyrite</b>									
82PR01 Loc. No. --	0.99	--	--	45.96	--	--	--	53.63	100.58
81MIRL27 Loc. No. --	--	--	--	46.86	--	--	--	52.20	99.06
81MIRL11C Loc. No. 140	0.43	--	--	46.58	--	--	--	52.84	99.85
TPB46 Loc. No. 56	1.74	--	--	45.92	--	--	--	51.94	99.60
82MELO1A Loc. No. 118	--	--	--	47.17	--	--	--	52.68	99.85
81MIRL23 Loc. No. 57	1.44	--	--	46.77	--	--	--	52.27	100.48

	As	Sb	Cu	Fe	Pb	Ag	Zn	S	Total
<b>Pyrite</b>									
81MIR124B Loc. No. 96	--	--	--	46.92	--	--	--	53.19	100.11
81MIRL25B Loc. No. 48	1.76	--	--	46.46	--	--	--	51.73	99.95
21150B Loc. No. 25	0.79	--	--	46.79	--	--	--	52.09	99.67
<b>Pyrrhotite</b>									
82MEL01A Loc. No. 118	--	--	0.48	60.03	--	--	--	38.50	99.01
82MEL01A Loc. No. 118	--	--	0.86	59.63	--	--	--	38.69	99.18
81MIRL25B Loc. No. 48	2.52	--	--	59.35	--	--	--	37.74	99.61
82FM01 Loc. No. 59	--	--	--	59.57	--	--	--	39.74	99.31
<b>Sphalerite</b>									
81MIRL01 Loc. No. 43	--	--	0.13	6.89	--	--	60.78	32.48	100.28
TPB46(2) Loc. No. 56	0.93	--	0.20	6.35	--	--	59.85	32.23	100.01

Note (2) Cadmium content of 0.45 included in total.

	As	Sb	Cu	Pb	Bi	Ag	Zn	S	Total
<b>Sphalerite</b>									
Hi-Yu 57A Loc. No. 7	0.25	--	--	4.13	--	--	63.64	31.80	99.82
Hi-Yu 57B Loc. No. 7	0.32	--	1.37	2.46	--	--	62.91	32.47	99.53
Hi-Yu 58 Loc. No. 7	--	--	0.15	6.48	--	--	60.28	32.21	99.12
82TV04B Loc. No. 54	0.86	--	0.46	2.23	--	--	63.14	32.82	99.51
<b>Stibnite(3)</b>									
81MIRL16 Loc. No. 109	--	72.81	--	--	--	--	--	26.40	99.21
82NB01 Loc. No. 60	--	72.40	--	--	--	--	--	26.65	99.05
<b>Stylopyrite(?)</b>									
75Z010A Loc. No. 91	--	25.95	15.74	3.34	--	30.87	3.01	20.28	99.19
75Z010B Loc. No. 91	0.44	25.95	15.36	3.70	--	31.70	2.86	20.18	100.19
<b>Tetrahedrite</b>									
Silver Fox 13A Loc. No. 91	0.56	25.68	24.78	3.05	--	18.35	3.83	23.17	99.42

Note (3) None of the stibnite samples examined contained detectable Au.

	As	Sb	Cu	Fe	Pb	Ag	Zn	S	Total
Tetrahedrite									
Hi-Yu 54 Loc. No. 7	--	28.98	32.54	3.82	--	9.23	3.28	23.01	100.86
Hi-Yu 55 Loc. No. 7	0.59	28.56	32.73	3.56	--	8.12	3.83	23.59	100.98
Hi-Yu 57 Loc. No. 7	0.76	28.39	31.58	3.55	--	9.72	3.24	23.17	100.41
82TV04B Loc. No. 54	0.91	27.83	26.34	3.25	--	15.03	3.09	22.95	99.40
82TV05 Loc. No. 54	0.98	28.81	32.17	3.32	--	6.97	3.72	23.70	99.67

most inclusions are in the 1 to 5 micron range they are readily visible in reflected light due to the great differences in color and relief between the host and the inclusion. Gold inclusions are easily distinguished from those of chalcopyrite, pyrite, sphalerite, quartz, and rutile, which are common impurities in the arsenopyrite.

Gold inclusions are found in both stratabound and epigenetic ores. Most of the gold observed in stratabound ore is as inclusions while most of the gold in the epigenetic veins is not. Thus the absence of readily visible gold inclusions in the vein ores should not be a criterion for dismissing the gold potential of a vein. Where the host arsenopyrite is altered and replaced by gold, the inclusions provide strong evidence for multiple mineralizing events. In vein ores where inclusions are present, such as the Christina vein system, grades may well exceed 0.6 OPT gold.

Carries texture is a replacement texture due to late stage fluids removing the early stage arsenopyrite and depositing various sulphide phases as well as quartz and gold in embayments in the arsenopyrite. The texture can develop whether or not there is gold deposition associated with either the early arsenopyrite or the replacing phases. Thus the presence of the texture is not a criterion for the presence of economic gold grades. The major veins that have produced in the past all exhibit carries texture; however samples from non-productive veins also show the texture. The major productive systems do show at least two stages of gold mineralization. Thus the presence of both gold inclusions in early arsenopyrite and carries texture may indicate elevated gold grades.

#### 4.4.2.2 Arsenopyrite Compositions and Geobarometry

Barton (1969), Kretschmar and Scott (1976), and Berglund and Ekström (1980) demonstrate the method and efficiency of utilizing arsenopyrite as a geobarometer. The method is dependent on the buffering of sulphur in the hydrothermal system. The pertinent buffer for the system Fe-As-S is pyrrhotite.

Although arsenopyrite is ubiquitous in the gold mineralization of the district, cogenetic pyrrhotite is not. Not a single sampled mineral occurrence in the district was found that would allow application of the arsenopyrite geobarometer. However, the range in arsenopyrite composition as exemplified by concentric zoning does qualitatively indicate that the As/S ratio of the hydrothermal fluids changed radically over the period of ore deposition.

Samples from 23 different mineral occurrences were examined for the presence of zoned arsenopyrite. All occurrences were found to contain abundant euhedral grains and microanalyses were conducted on multiple grains from each occurrence. The analyses were made on orthogonal traverse lines across each grain. Note was made of the presence of gold inclusions in the arsenopyrite. Atomic percents of Fe, As, and S were then calculated from the weight percent data.

Arsenic contents for all measured grains show a maxi-

mum near the centre indicating a drop in temperature in the system as the grains developed. There is no definite arsenopyrite composition associated with the gold inclusions, thus no direct relationship between arsenic and gold can be demonstrated.

The maximum and minimum atomic percents of As vs. S for the mineral grain with largest range for each occurrence are plotted on Figures 4.1a thru 4.1d. Figure 4.1a includes Type I mineral occurrences. These occurrences demonstrate a wide range in As vs. S as a group. Sulphur content ranges from 33.50 to 37.25 atomic percent and As content ranges from 29.00 to 32.50 atomic percent. The individual occurrences also have wide ranges in atomic percents. The grain from the Christina Adit stratabound mineralization has ranges in As and S that are almost as wide as the group ranges.

Figure 4.1b includes data for the single sulphide rich Type II occurrence. The range is narrower than most of the Type I occurrences and is near the centre of the range of the Type I occurrences as a group.

Figure 4.1c includes the Type IV mineral occurrences. Individual occurrences in this group have very narrow ranges with some grains showing almost no changes in composition across the mineral grains. The As contents are considerably higher with most in the range of 31.0 to 32.75 atomic percent.

Figure 4.1d includes three Type V mineral occurrences. The ranges in As and S atomic percentages as a group are between the extremes of the Type I and Type IV mineralization. Samples from the Farmer and the Johnson occurrences have a wide range in atomic percentages but the Scrafford samples have a very narrow range similar to the Type IV occurrences.

These data indicate that the Type I and Type IV mineralization can be characterized by the ranges in atomic percentages of As and S in individual arsenopyrite grains. The hydrothermal fluids that produced these two types of mineralization differed markedly in pressure, temperature, and composition. The intrusive activity and subsequent vein mineralization are thought to be related to the late stages of regional metamorphism. These data suggest that the pre-metamorphic ores were at least not completely homogenized by the thermal event and in fact may have not been altered to any significant degree by the regional metamorphism.

## 4.5 MINERAL PARAGENESIS

Hill (1933) recognized four phases of silica introduction in the gold-quartz vein systems of the Fairbanks district. He developed a paragenetic diagram that related these phases of silica and sulphide mineral introduction to several deformational events. The four phases of quartz introduction according to Hill (1933) and Sandvik (1964) are:

1. Early coarsely-crystalline white quartz unaccompanied by metals. This quartz was later brecciated and crushed and followed by;
2. More finely crystalline quartz, with pyrite, arsenopyrite, and gold primarily as inclusions in arsenopyrite. Phase 2 quartz was then fractured and brecciated and cemented by;

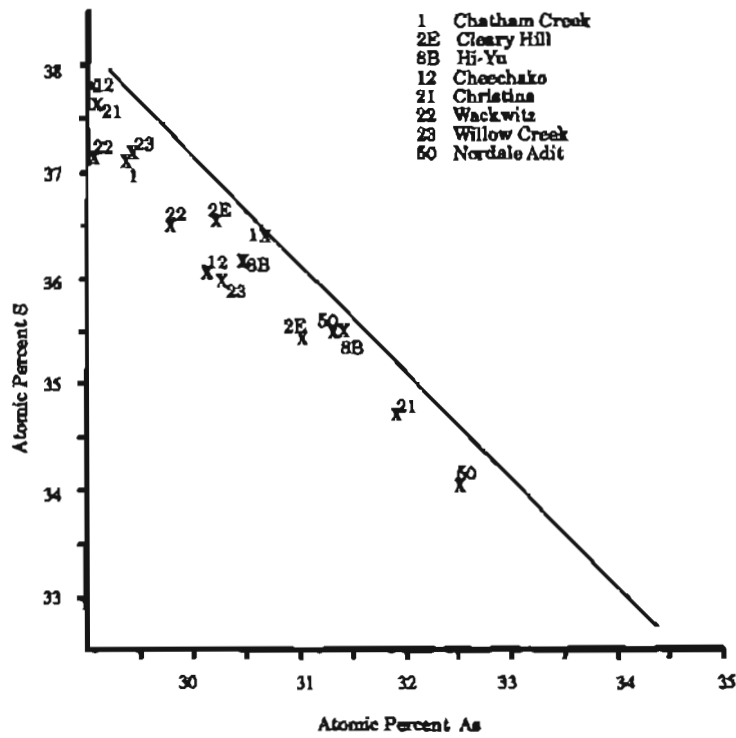


Figure 4.1a Maximan As/S variation within arsenopyrite grains from various Type I mineral occurrences.

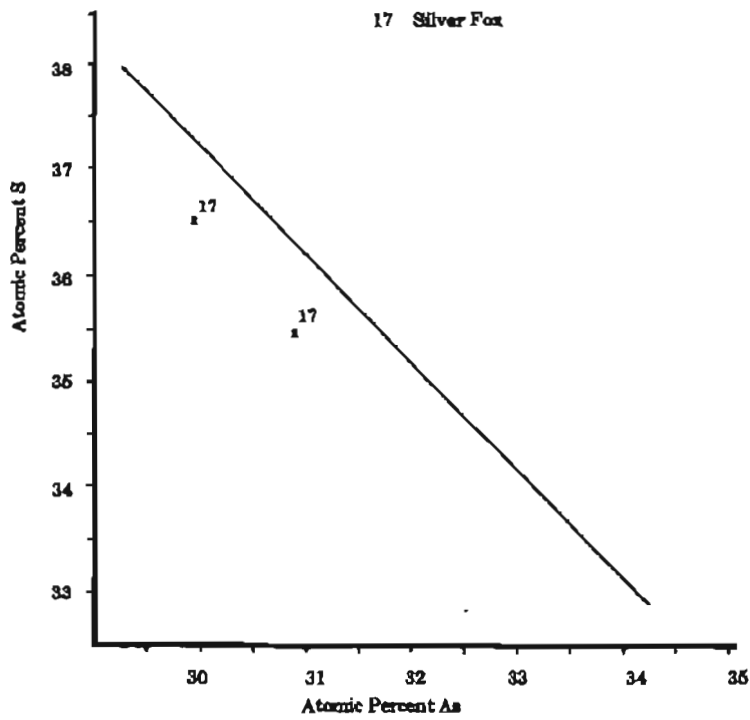


Figure 4.1b Maximan As/S variation within arsenopyrite grains from the Silver Fox Mine (Type II mineral occurrences).

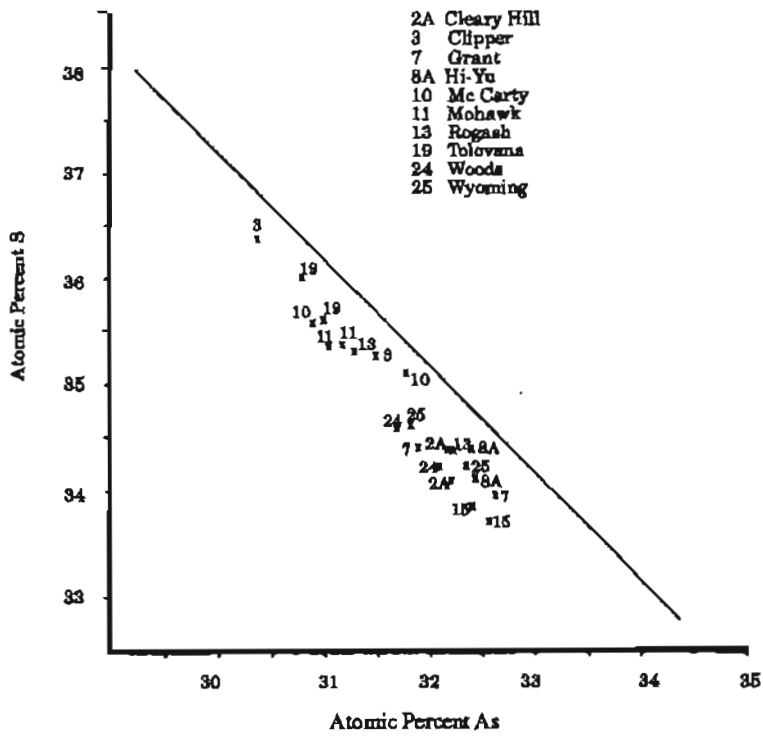


Figure 4.1c Maximan As/S variation within arsenopyrite grains from various Type IV mineral occurrences.

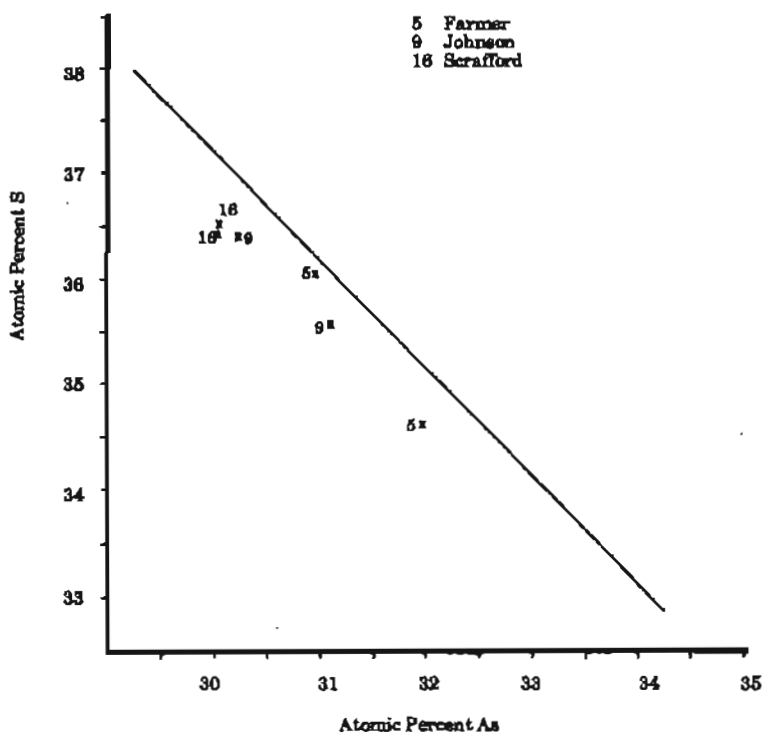


Figure 4.1d Maximan As/S variation within arsenopyrite grains from various Type V mineral occurrences.

3. Fine-grained bluish-grey quartz with sulfosalt and base metal sulphides and abundant free gold. These veins were reopened and introduced with;
4. Small dogtooth crystals of white quartz and stibnite. Minor fine-grained quartz fills small fractures in the monomineralic stibnite lodes.

Both Hill (1933) and Sandvik (1964) were unable to distinguish between the stratabound mineralization and the various types of vein occurrences. Figure 4.2 is a paragenetic diagram for Type I mineralization and Figure 4.3 is a companion diagram for Types IV and V mineralization.

Type I mineralization shows evidence of two phases of ore deposition which, however, may be a function of differences in primary host-rocks and their response to regional metamorphism. The loellingite-pyrrhotite-scheelite assemblage appears to be related to the chlorite schist units (the more mafic metavolcaniclastics) whereas the arsenopyrite-jamesonite-base metal sulphide  $\pm$  argentiferous tetrahedrite  $\pm$  gold assemblage is associated with the muscovite quartz schist (metafelsite/metaexhalite units). The gold in Type I occurrences is always in small inclusions as noted above (see Figure 4.4a and 4.4b). Silver in Type I mineralization occurs primarily in tetrahedrite although rare minute (less than 1 micron) silver sulphide inclusions occur in galena (Figure 4.4c).

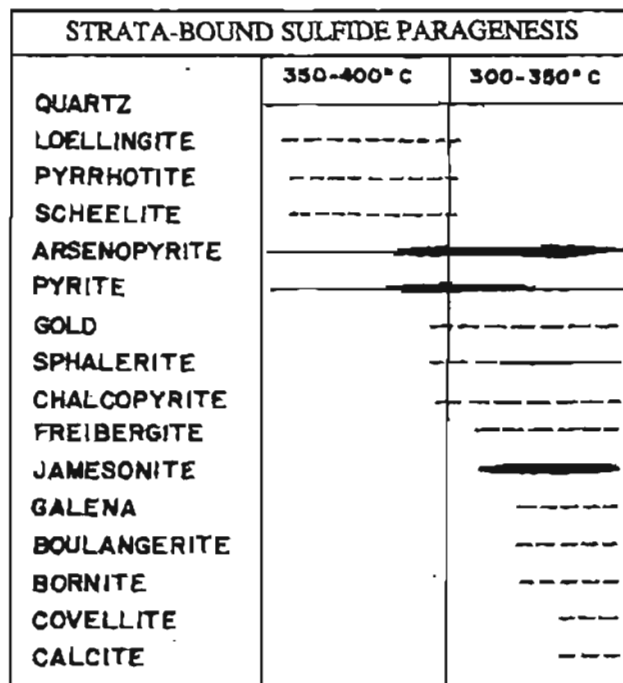


Figure 4.2 Paragenetic diagram for Type I Stratabound Au-Ag-As-Sb-W mineralization.

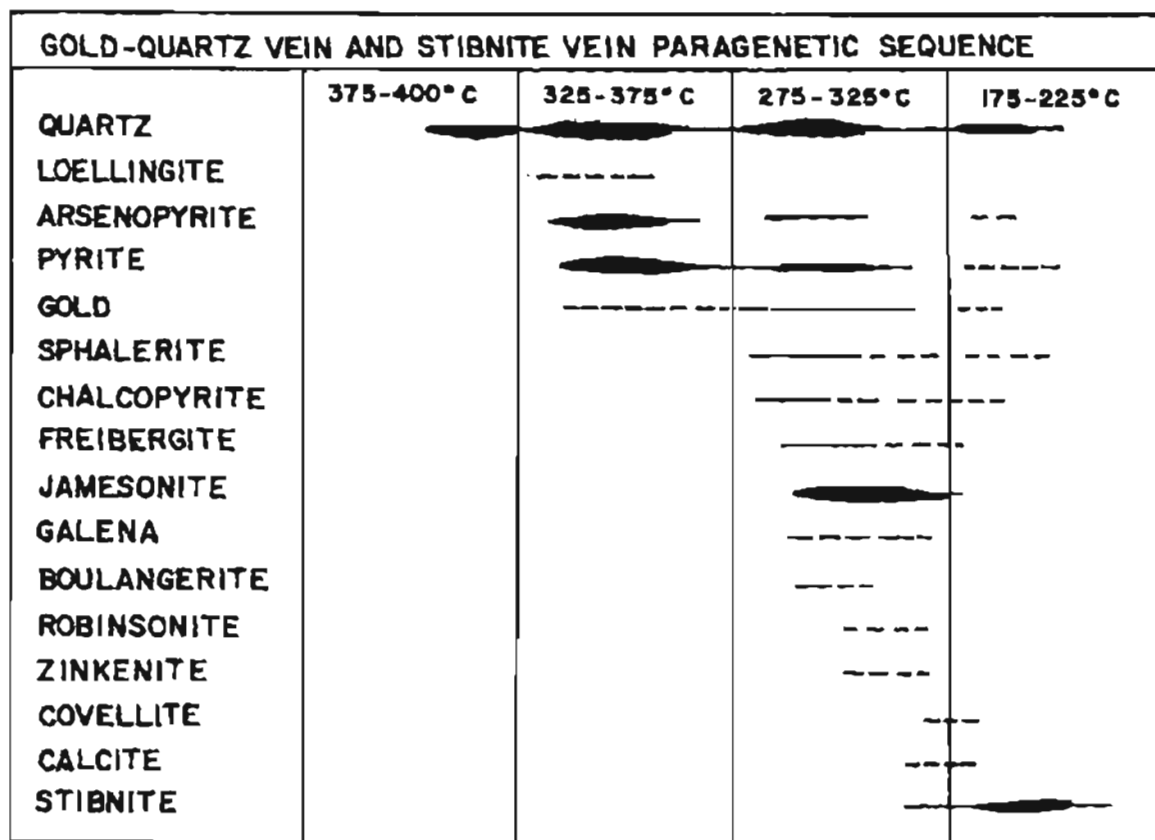


Figure 4.3 Paragenetic diagram for Type IV gold-quartz vein and type V monomineralic stibnite mineralization.

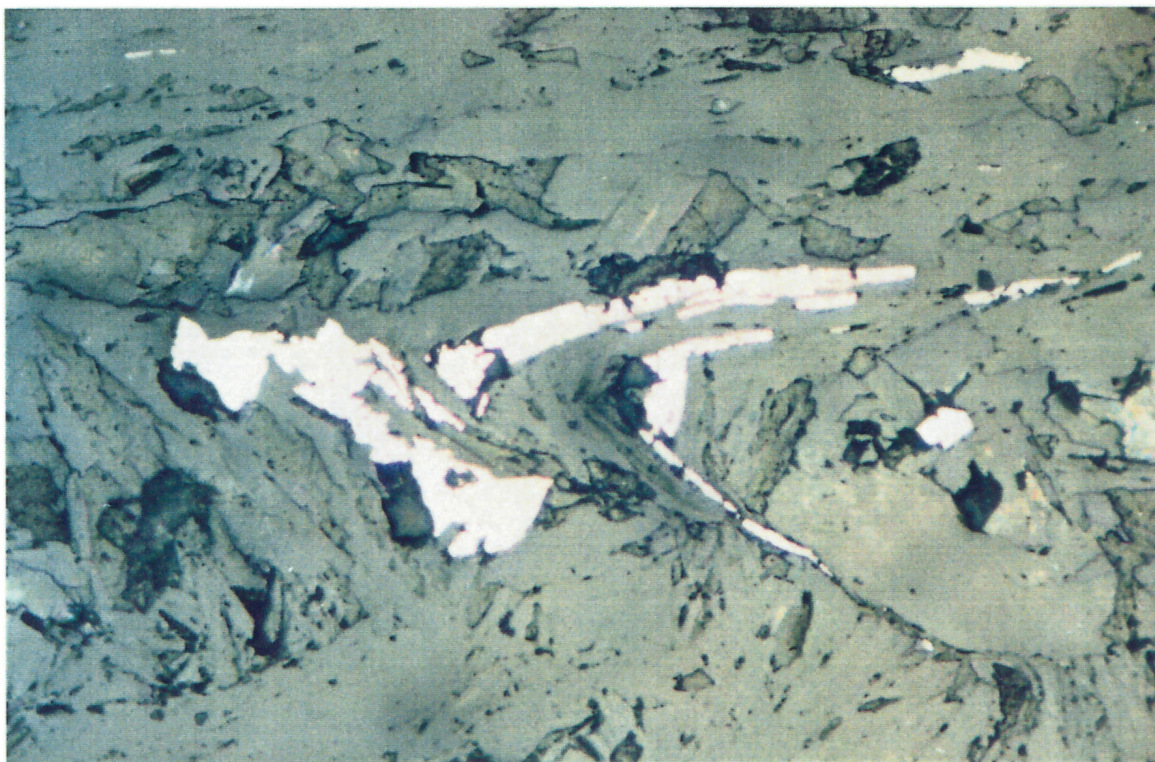


Figure 4.4a. Photomicrograph of isoclinally folded arsenopyrite layer in muscovite-quartz schist, field of view 1.5 mm.



Figure 4.4b. Photomicrograph of arsenopyrite grain in 4.4a with inclusion of gold, field of view 0.15 mm.



Figure 4.4c. Rhythmically layered sulphides (sphalerite, medium grey; jamesonite/tetrahedrite, light grey; and euhedral arsenopyrite and pyrite, white) in metachert (dark grey, Type I mineralization, field of view 40.0 mm).

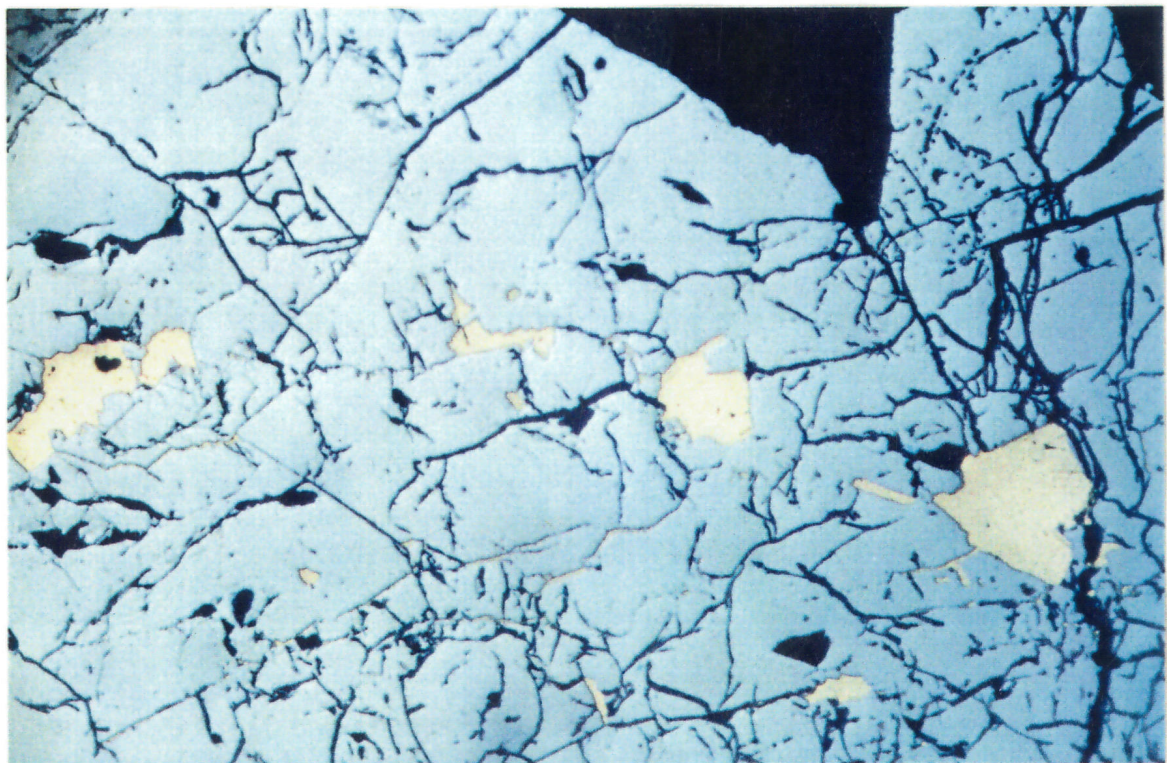


Figure 4.4d. Photomicrograph of stage two gold in arsenopyrite, Type IV mineralization, field of view 0.15 mm.

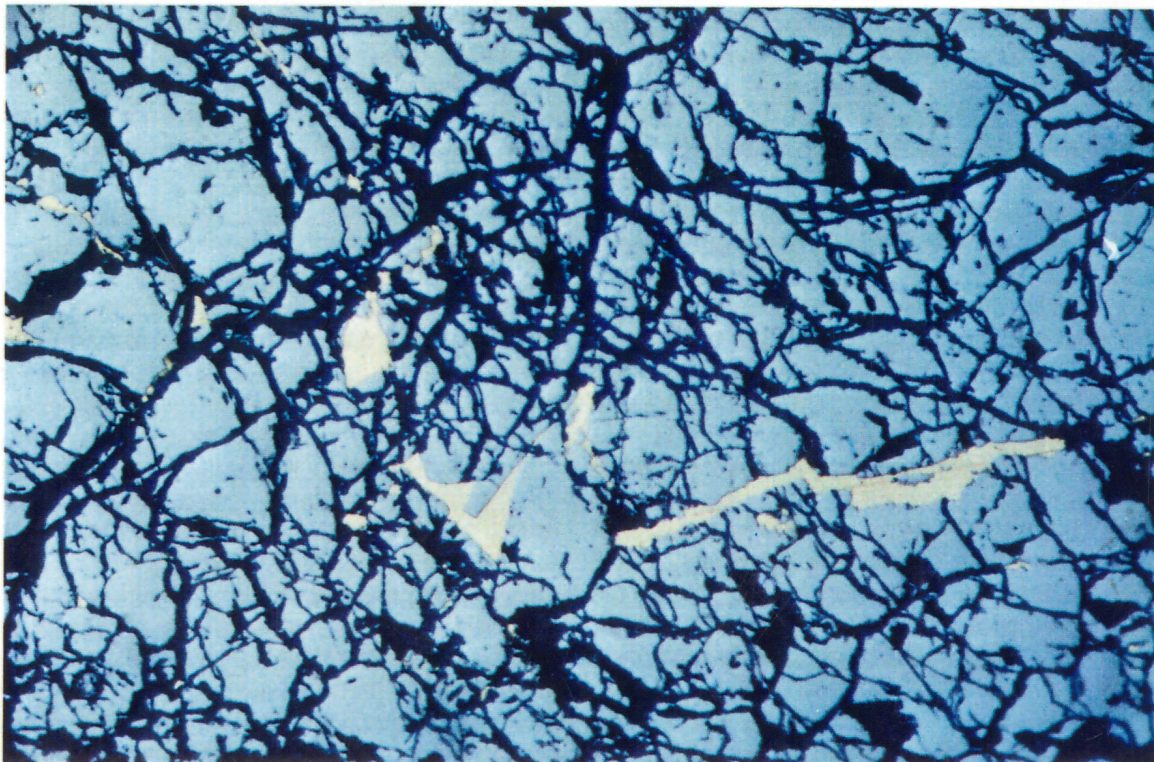


Figure 4.4e. Photomicrograph of stage three gold in arsenopyrite, Type IV mineralization, field of view 0.15 mm.

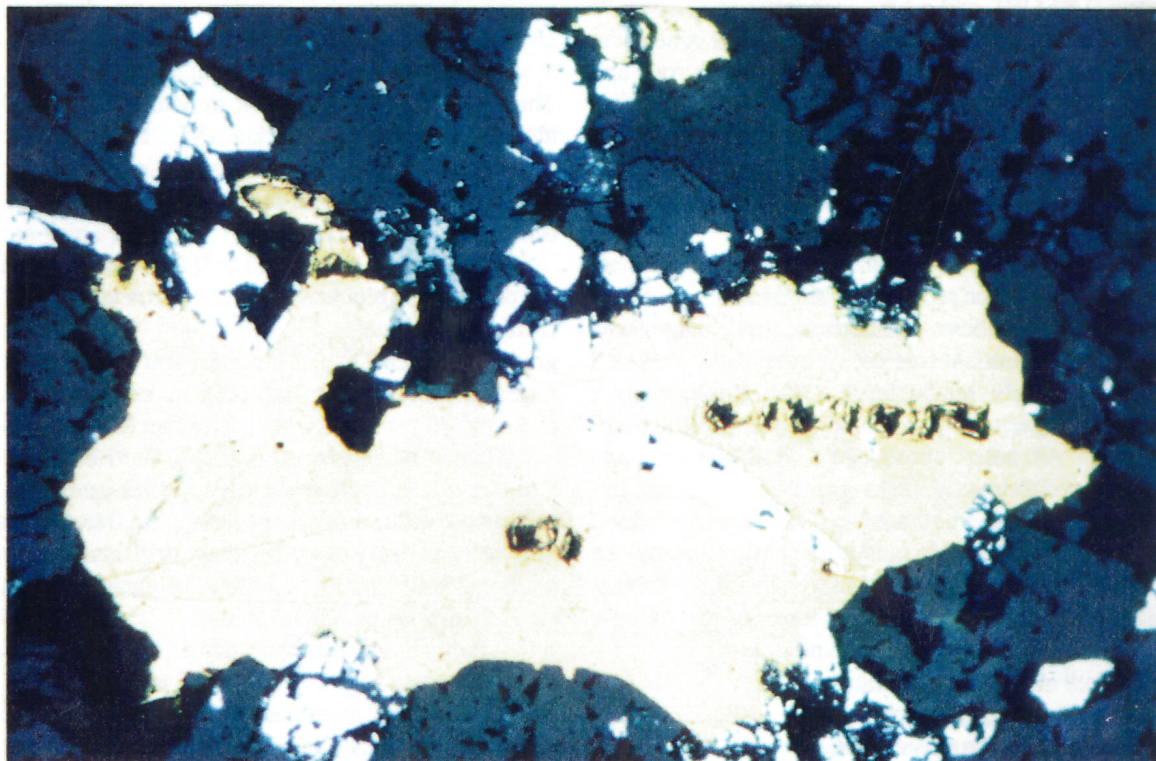


Figure 4.4f. Photomicrograph of gold and arsenopyrite at quartz grain boundary, Type IV mineralization, field of view 1.50 mm.

The multiple stages of Type IV mineralization described by Hill (1933) and Sandvik (1964) have been quantified by fluid inclusion analysis as shown in Figure 4.3. Gold occurs in both stages two and three, but in stage two it occurs primarily as inclusions in arsenopyrite (Figure 4.4d) or as 1 to 50 micron size grains along quartz grain boundaries. In the high grade phase (stage three), gold occurs as fracture fillings in early sulphides (Figure 4.4e) and as large grains up to 5 mm in diameter (Figure 4.4f). Stage three gold is always associated with the lead-rich sulfosalts: boulangerite,  $Pb_5Sb_4S_{11}$ ; zinkenite,  $Pb_6Sb_{14}S_{27}$ ; robinsonite,  $Pb_4Sb_6S_{13}$ ; and semseyite,  $Pb_9Sb_8S_{21}$ . This sulfosalt association is in marked contrast to the lower grade stage two gold assemblage and to the Type I stratabound assemblage which is usually the iron-bearing sulfosalt jamesonite,  $Pb_4FeSb_6S_{14}$  or rarely bournonite,  $PbCuSbS_3$ .

Type V monomineralic stibnite deposits were formed at much lower temperatures than either Type I or Type IV mineralization. The stibnite lodes are characteristically devoid of major gold mineralization; at several occurrences, however, the stibnite lodes can be followed down structure to both Type IV and Type I mineralization.

#### 4.6 APPLICATIONS OF ORE MINERALOGY AND PETROLOGY

##### 4.6.1 Applications to Exploration

Ore mineralogy and petrology are the key factors in the field classification of the various mineral deposit types. Metz (1982b) and Metz and Hamil (1986) demonstrate that all the metavolcaniclastic/metaexhalite lenses with gold concentrations above 0.10 OPT and silver concentrations above 10 OPT contain the characteristic mineral assemblage jamesonite and tetrahedrite. Weathering and erosion of outcrops and subcrops of Type I lenses result in stream sediment anomalies of As, Cu, Ag, Pb, and Zn with threshold values of 52, 28, 0.5, 17, and 74 ppm respectively. Although arsenic is ubiquitous the Cu, Ag, Pb, and Zn anomalies are indicative of either Type I or IV mineralization.

Within Type IV vein systems, ore mineralogy is an important indicator of the presence or absence of high-grade ore shoots. As noted above, the bonanza-grade stage three assemblage, with abundant free gold, contains the lead-rich sulfosalts, particularly boulangerite. The small acicular crystals of boulangerite impart a blue-grey tint to the high-grade quartz. As noted above, gold in the stage three assemblage is predominantly coarse-grained and free-milling.

Although monomineralic stibnite Type V mineralization contains little or no detectable gold, these gash veins may be guides to both Type I and Type IV mineralization. Type V mineralization is associated with either bright yellow (stibiconite) or red (kermesite) color anomalies.

##### 4.6.2 Applications to Evaluation

Type I mineralization may exhibit little or no visible gold or field identifiable silver minerals even though it may contain significant concentrations of both Au and Ag. Type

I mineralization also contains minor quantities of quartz and thus this type had not been the target of previous gold-quartz vein evaluation efforts. Since Type I mineralization is contained in the metavolcanic/metaexhalite units, all such units with both arsenopyrite and jamesonite are potential gold targets. Sampling for evaluation of these targets should be directed along and across the strike of the foliation and compositional layering of the host rock.

Type IV mineralization has three very important mineralogical characteristics that complicate ore evaluation. First, the gold values are somewhat irregular in the stage three ores. Second, the vein quartz is highly fractured and generally included in sheared and altered country rock. Third, there is usually an inverse correlation between vein width and gold grade.

The irregularity of gold values necessitates either closely spaced drill and channel samples or very large sample sizes for adequate estimation of ore grade. Generally these sampling requirements are cost prohibitive. The highly fractured nature of the quartz veins and the friable nature of the enclosing and highly altered country rock results in poor drill core recovery. Since gold values are expected in these friable sections of lost core, the result is lower average assay values than would be expected for 100 percent core recovery. Finally, the inverse correlation between vein width and gold grade results in under-estimation of ore grade.

In order to determine the effect of these mineralogical characteristics on ore grade estimates, a comparison was made of the grades estimated for the Christina vein system by diamond drilling, rotary drilling, and bulk sampling techniques. On surface, the Christina vein, which strikes  $N 80^\circ W$  and dips south at  $55^\circ$ , is composed of 0.3 meters of fine- to medium- grained quartz with less than 1 percent sulphides. The vein is exposed by surface trenching for over 600 meters along strike (see Ch. 3, Plate IV). From observations in underground workings and of drill core, the vein appears to grade into a quartz stockwork in sheared and banded micaceous quartzite.

Over 11,000 meters (35,000 feet) of diamond drilling has delineated a block of ore within 60 meters (200 feet) of the surface that contains 136,000 tonnes (150,000 tons) with a grade of 0.60 OPT Au. This ore reserve is diluted over a 1.8 meter (5 foot) mining width with core recovery rates that averaged 80 percent for the entire block.

Sixteen hundred meters (5,200 feet) of rotary drilling was completed in the same area. The assay results for each rotary hole were compared with those of the closest diamond drill hole. In every case, the rotary drill assays exceeded the diamond drill assays and on the average the difference was close to a factor of 2.0.

A bulk sample was then taken on the surface. The sample dimensions were approximately 0.3 meters (1 foot) wide x 1 meter (3.25 feet) down dip by 37 meters (120 feet) along strike. The total sample weight was approximately 27 tonnes (30 tons). The sample was crushed to minus 10 mesh (Tyler) and the heavy minerals were concentrated on a shaking table.

The calculations for the grade of the bulk sample are given in Table 4.9 and the size distribution of the gold is given in Table 4.10. The calculated grade of the bulk sample is 1.87 OPT which is approximately four times the average grade of the entire 136,000 tonnes (150,000 ton) block below the sample site. Although this difference may be a function of vertical variability in the vein, the grade is similar to that obtained by rotary drilling and is approximately three times that estimated from diamond drilling. The bulk sample grade is also comparable to the historic production grade of 1.07 OPT (19,549 ounces/18,166 tons).

From the above data, it can be concluded that ore reserves are being underestimated by as much as 100 percent from diamond drill hole sampling. The effects of inherent population variability and the inverse correlation of grade and vein thickness cannot be determined from the available data.

#### 4.6.3 Applications to Recovery

Several bench-scale cyanide leaching and froth flotation tests have been conducted on ores from Type I and Type IV mineralization by the Colorado School of Mines Research Institute. The results of the tests on 270 kg (600 lb) samples from the Orange Free Zone (Type I mineralization in the footwall of the Christina vein) and the Christina vein (Type IV mineralization) were reported by Metz (1987; see Table 4.11).

The leaching tests were completed on material ground to approximately 50% minus 400 mesh. Pulp densities were maintained at 60 percent. Cyanide consumption rates for the Type I sample for optimum recovery were 1.22 kg/tonne with a resident time of 24 hours. For the Type IV sample, the

values were 1.18 kg/tonne and 24 hours, respectively.

The flotation tests were completed on samples crushed to minus 10 mesh and rod milled for 30 minutes. Flotation reagents used were Aero Promoter 208, Aero 350 Xanthate, Aerofloat 33, Minflo TPE, copper sulfate and a froth mix.

The cyanide leaching of Type I mineralization gave very low silver recovery rates, and the gold recovery was also low. Prior optical examination of these ores could have indicated possible leaching problems.

All of the silver in the Type I mineralization probably occurs as argentiferous tetrahedrite that is finely intergrown with jamesonite. Typical Type I tetrahedrite analyses are given in Table 4.8. This sulphide mineralogy probably precludes higher silver recoveries from cyanide leaching without prior roasting of the ores. The moderate gold recovery rate probably results because the gold occurs as inclusions in arsenopyrite and as small grains along the arsenopyrite/gangue boundaries. Roasting of the ores would similarly increase gold recovery rates.

Gold recovery from Type IV mineralization (Christina vein) was reasonable for the leaching test and high for the flotation tests. The relatively coarse grain size of the gold (see Figure 4.4 and Table 4.10) and the low sulphide content of 0.5% can account for this high recovery rate. Optical and SEM examinations of the sulphide concentrate from the 27 tonne (30 ton) bulk sample indicate that less than 1 percent of the gold is in the minus 80 mesh fraction and occurs as inclusions in sulphides.

Silver recovery rates from Type IV mineralization must be considered with respect to the low head values. Silver recovery rates were good for the froth flotation tests but poor for the cyanide leaching. Silver occurs in Type IV mineral-

Table 4.9 Comparison of grade estimates from channel sampling and diamond drill hole data versus bulk sample, Christina vein system, Fairbanks mining district, Alaska.

Vein Width: 1-8 feet
Vein Strike Length: 6000 feet
Sample Dimensions: 1' x 3' x 120'
Sample Weight: 30 tons
Table Product Weight: 117 troy ounces
Average Grade: 3.9 OPT Au
Diluted Grade Over 1.5 meter (5 Foot) Mining Width: 0.78 OPT Au
Sulphide Concentrate Weight: 0.125 tons
Sulphide Concentrate Grade: 104 OPT Au
Tailing Grade: 0.33 OPT Au
Calculated Average Grade of Vein Diluted Over 5 Foot Mine Width: 1.87 OPT Au
Estimated Average Grade of Vein From Channel Sampling and Diamond Drilling (Average Recovery 80%): 0.45 OPT Au

Table 4.10 Sieve analysis of gold from bulk sample, Christina vein, Fairbanks mining district, Alaska.

Mesh (Tyler)	DIRECT		CUMULATIVE PASSING	
		Wt%	Mesh (Tyler)	Wt%
Head		100.0		
+10	—	—	—	—
-10 +20	20.8		10	100.0
-20 +40	32.5		20	79.2
-40 +60	18.7		40	46.7
-60 +80	10.5		60	28.0
-80	17.5		80	17.5

SAMPLE: 100+ troy ounces of gold from the Christina vein  
 PROCEDURE: 30 ton sample crushed and gravity concentrate recovered from shaking table. Dry screened (Ro-Tap 10 min)

Table 4.11 Cyanide leaching and froth flotation results from Type I (Orange Free Zone) and Type IV (Christina quartz vein) mineralization, Fairbanks mining district, Alaska

	CYANIDE LEACH				PERCENT EXTRACTION	
	FEED		TAILINGS		Au	Ag
	Au(opt)	Ag(opt)	Ag(opt)	Ag(opt)		
Orange Free Zone	0.167	15.4	0.026	10.7	84.4	30.5
Christina Vein	0.551	0.6	0.030	0.4	94.6	31.1

	FROTH FLOTATION					PERCENT RECOVERY	
	FEED		Wt%	CONCENTRATE		Au	Ag
	Au(opt)	Ag(opt)		Au(opt)	Ag(opt)		
Orange Free Zone	0.167	15.4	26.6	0.310	24.1	52.7	42.5
Christina Vein	0.551	0.6	25.3	0.949	2.0	97.0	83.1

Table 4.12 Overall metallurgical results, bottle roll tests, cuttings samples, 80 percent minus 3/8 inch feed size, Christina vein, Fairbanks mining district, Alaska

Metallurgical Results	Sample		
	89 PM001	89 PM002	89 PM003
Extraction: pct total Au			
in 2 hours	21.4	7.0	17.0
in 6 hours	25.8	12.5	26.8
in 24 hours	35.7	22.0	44.4
in 48 hours	43.1	27.3	52.6
in 72 hours	48.0	29.4	54.5
in 96 hours	50.3	31.1	57.7
in 120 hours	51.1	32.3	61.3
Extracted, oz Au/ton ore	0.067	0.105	0.057
Tail Assay, oz Au/ton	0.064	0.220	0.036
Calculated Head, oz Au/ton ore	0.131	0.325	0.093
Average Head, oz Au/ton ore*	0.082	0.247	0.058
Cyanide Consumed, lb/ton ore	0.39	0.30	0.15
Lime Added, lb/ton ore	13.3	10.0	13.5
Final Solution pH	11.0	11.0	11.0
Natural pH (40 pct. solids)	6.4	7.3	7.3

\*Average of triplicate direct head assays.

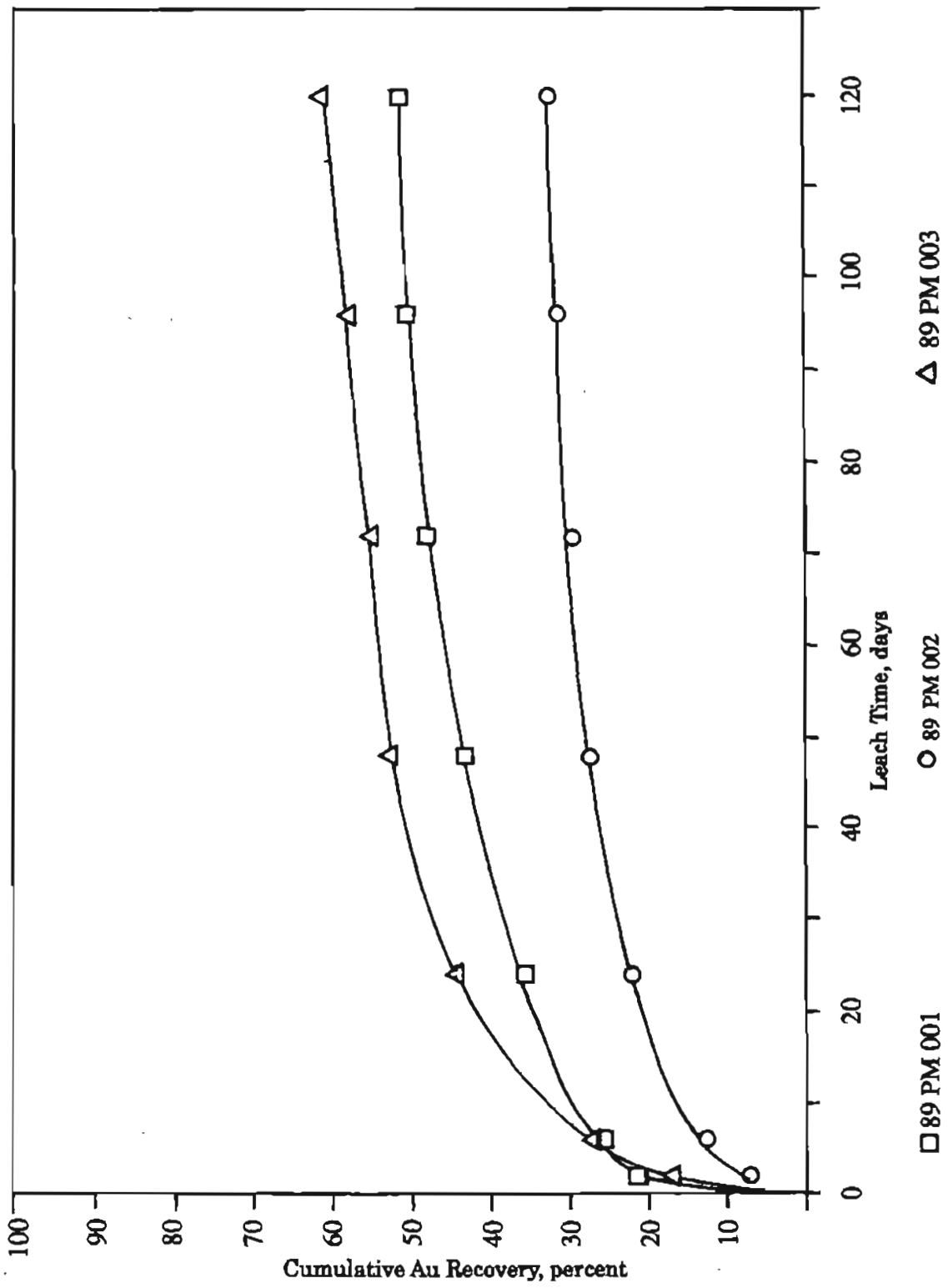


Figure 4.5 Gold leach rate profiles for Christina shear zone samples.

ization as electrum with a gold fineness of about 825, and as argentiferous tetrahedrite. Leaching of silver would be inhibited by its inclusion in the tetrahedrite, and this is probably the cause of the poor recovery rates from the leaching tests.

A 290 tonne (319 ton) bulk sample was extracted from the west end of the Christina vein (see Christina vein section A-A', B-B', and C-C' on Ch. 3, Plate IV). The sample was taken over a 3 meter (10 foot) width of the hanging wall portion of the structure that includes 15 to 60 centimeters of quartz in sheared and sericitically altered metachert.

The bulk sample was taken to a mill belonging to Tri-Con Mining Co. at Ester, Alaska and processed through jigging and the carbon-in-pulp circuit. The head grades were determined by continuous sampling and fire assays at the Tri-Con laboratory while duplicate assays were completed by Bondar-Clegg Ltd., Vancouver, British Columbia, Canada. The average of all the head grade assays was 0.342 OPT. The total recovery was 108.9 troy ounces with approximately 50 ounces recovered in the jigging and tabling portion of the circuit. The apparent recovery rate was 98.9 percent of the head grade as indicated by the assays.

During the bulk sampling of the quartz rich portion of the Christina structure, a 15 meter (50 foot) wide alteration zone in the footwall was exposed. Channel samples were taken at 1.5 meter (5 foot) intervals at each of the above three sections across the Christina shear zone. The apparent high grade quartz in the hanging wall was excluded from the sampling. The samples were composited for each section and sent to McClelland Laboratories, Inc., Sparks, Nevada for bottle roll tests.

The test results are given in Table 4.12 and the gold leach rate profiles are shown in Figure 4.5. The recovery rates and profiles for samples 89 PM 001 and 89 PM 003 are moderately good. The poor recovery rate and leach profile of sample 89 PM 002 is probably due to coarse-grained gold in the relatively high grade sample.

These data indicate that the design of recovery systems must take into account the complex mineralogy and petrology of these ores. Gold grain-size data are particularly important in the design of heap leaching operations.

---

## CHAPTER 5

### PLACER GOLD DEPOSITS OF THE FAIRBANKS MINING DISTRICT

#### 5.1 INTRODUCTION

As noted previously the Yukon-Tanana Terrane (YTT) has yielded in excess of twenty-five million troy ounces of placer gold with unequal amounts produced in Alaska and the Yukon Territory. The majority of the gold production in the YTT in Alaska has come from: the Fairbanks mining district (7,464,000 troy ounces); the Circle and Steese mining districts (730,000 troy ounces); the Fortymile mining district (415,000 troy ounces); the Tolovana mining district (375,000 troy ounces);

the Kantishma mining district (55,000 troy ounces); and the Richardson mining district (105,000 troy ounces) with minor production from the Bonifield mining district (45,000 troy ounces) and the Eagle mining district (40,000 troy ounces). Most of the placer gold production from the Yukon Territory has come from the Klondike district (16,000,000 troy ounces).

Although some of the placer gold production in Alaska has come from middle Tertiary continental clastic rocks, most of the historic production has come from Pliocene, Pleistocene and Recent alluvial and beach deposits (see Ch. 5, Plate I and Table 5.1). Of the 28.5 million ounces of gold produced in Alaska approximately 21 million was from placer deposits and of that amount 9.5 million ounces was from the YTT. Although the YTT accounts for only 6 percent of the land mass of Alaska, it has rendered 45 percent of the placer gold production of the state.

Gold was discovered in the Fairbanks mining district in 1902 and since then the area has produced approximately 7,500,000 troy ounces of placer gold and 325,000 troy ounces of lode gold. In addition, the district has produced several thousand tonnes of antimony and several thousand kilograms of tungsten. Although it has been the single most important placer district in Alaska, the critical controls of placer formation are only now being recognized. In this chapter new evidence is presented on the bedrock source of the placer gold, bedrock structural controls of stream drainage, and surficial depositional controls of placer formation. Of the major controls of placer formation, the alteration of stream drainages by reactivation of basement structures leading to stream capture, stream reversal and sediment resorting is the most important.

Plate II shows the location of the placer producing streams in the Fairbanks mining district. Appendix D1 is a summary description for each location.

#### 5.2. PREVIOUS INVESTIGATIONS AND PLACER STRATIGRAPHY

Prindle and Katz (1913) were the first to provide a general description of the bedrock and surficial geology of the Fairbanks mining district. Many of the rock units which they defined have been retained by subsequent investigators; however, the most significant contribution was their detailed descriptions of the gold placer deposits. Of particular importance are data on the thickness of overburden (including reworked loess and organic material locally known as muck) and the auriferous alluvial gravels. Prindle and Katz (1913) also recorded data on the thickness, length and width of the economic concentrations or "paystreaks" of placer gold, as well as the average depth to bedrock for most of the creeks in the district. Although their predictions of ultimate production were 50 percent lower than the total achieved to date, their estimates must be recognized as reasonable in view of the data then available.

In addition to providing fundamental geological descriptions, Prindle and Katz (1913) were the first to describe two important mechanisms of placer formation: headward migration of stream drainage and changes in base level.

Table 5.1 Historic gold production (after Robinson and Bundtzen, 1979).

No.	Camp	Production (oz.)	Discovery Date	No.	Camp	Production (oz.)	Discovery Date
1.	Nome	4,051,155	1898	32.	Tolovana	375,000	1914
2.	Solomon	251,000	1899	33.	Fairbanks	7,464,167	1902
3.	Bluff	98,560	1899	34.	Chena (included in Fairbanks production)		1902
4.	Council	705,443	1898	35.	Bonnifield	45,000	1903
5.	Koyuk	87,225	1915	36.	Richardson	95,000	1905
6.	Fairhaven (Candle)	299,890	1901	37.	Circle	730,000	1893
7.	Fairhaven (Inmachuck)	277,000	1900	38.	Woodchopper-Coal Creek (included in Circle production)		
8.	Kougarok	245,000	1900	39.	Seventymile (included in Fortymile production)		
9.	Port Clarence	45,294	1898	40.	Eagle	40,220	1895
10.	Noatak	9,000	1898	41.	Fortymile	415,000	1886
11.	Kobuk (Squirrel River)	7,000	1909	42.	Valdez Creek	37,000	1903
12.	Kobuk (Shungnak)	15,000	1898	43.	Delta	2,500	
13.	Koyukuk (Hughes)	209,000	1910	44.	Chistochina-Chisna	141,000	1898
14.	Koyukuk (Nolan)	295,000	1893	45.	Nabesna	63,300	1899
15.	Chandalar	30,708	1905	46.	Chisana	44,760	1910
16.	Marshall (Anvik)	120,000	1913	47.	Nizina	143,500	1901
17.	Goodnews Bay	29,700	1900	48.	Nelchina	2,900	1912
18.	Kuskokwim (Aniak)	230,555	1901	49.	Girdwood	125,000	1895
19.	Kuskokwim (Georgetown)	14,500	1909	50.	Hope (included in Girdwood production)		1888
20.	Kuskokwim (McKinley)	173,486	1910	51.	Kodiak	4,800	1895
21.	Iditarod	1,320,000	1908	52.	Yakataga	15,709	1898
22.	Innoko	350,000	1906	53.	Yakutat	2,500	1880
23.	Tolstoi-Cripple	87,218	1916	54.	Lituya Bay	1,200	1894
24.	Iliamna (Lake Clark)	1,500	1902	55.	Porcupine	53,250	1898
25.	Skwentna (included in Yentna production)		1905	56.	Juneau (Gold Belt)	6,883,556	1880
26.	Yentna (Cache Creek)	115,200	1905	57.	Ketchikan-Hyder	62,000	1898
27.	Kantishna	55,000	1903	58.	Sumdum	15,000	1869
28.	Ruby	389,100	1907	59.	Glacier Bay	11,000	
29.	Gold Hill	1,200	1907	60.	Chichagof	770,000	1871
30.	Hot springs	447,850	1898	61.	Willow Creek	652,000	1897
31.	Rampart	86,800	1882	62.	Prince William Sound	137,900	1894
				63.	Unga Island	107,900	1891

Headward migration of stream drainage was described only qualitatively, and no analytical study was made of stream gradients, stream profiles or the critical point between degradation and aggradation. The existence of both older terrace deposits and buried placers was noted as evidence of major changes in sea level.

Further, Prindle and Katz (1913) related the placer deposits to gold-quartz and gold-quartz-sulphide veins, the formation of which in turn was attributed to the intrusion of granitic rocks in the district. Smith (1913a) provided detailed descriptions of several lode deposits, which gave support to the observations made by Prindle and Katz (1913).

Smith (1913b) also reported gold fineness values for 167 placer and six lode occurrences. He noted that placer gold tended to have a fineness value greater than lode gold and that the fineness value increased downstream. However, he did not describe in detail how the fineness value changed nor did he relate fineness values to the mechanisms of placer formation.

Chapin (1914, 1919), Mertie (1918a) and Hill (1933) also described the lode deposits of the district, and each noted the close spatial relationship of the placer deposits to the lode occurrences. The gold-quartz veins were considered to be the sole lode source and the veins were thought to be related to the granitic intrusive rocks of Gilmore Dome and Pedro Dome. Hill (1933) included a brief description of the placer deposits and provided records of placer production from 1903 to 1931. Mertie (1937, 1940) reiterated the mechanisms of placer formation described by Prindle and Katz (1913) but also noted the importance of Pleistocene and Recent climatic variations affecting the geomorphology of the entire Yukon-Tanana region.

Tuck (1968) noted that although the alluvial and beach placer gold is usually disseminated throughout the gravel sections, the most productive zones are all on or near the contact of the gravels with the underlying bedrock. Historically, commercial operations were confined to paystreaks containing gold particles heavier than 1 mg, and gold further than a few feet from bedrock tends to be finer grained than this. Gold values tend to be distributed laterally along bedrock with major concentrations in narrow paystreaks usually less than 100 meters (325 feet) wide. Gold particles weighing more than 1 mg are usually limited to downstream transport of 3 to 5 kilometers (1 to 3 miles) however gold grains of less than 1 mg may travel much greater distances (Tuck, 1968).

Chapman and Foster (1969) also related the gold-quartz vein deposits of the district to the Cretaceous granitoid intrusions exposed at Pedro and Gilmore Domes and concluded that the quartz veins were the sole source of the placer gold.

Péwé (1975) described 15 stratigraphic units of Quaternary age in central Alaska, of which 13 type sections are in the Fairbanks mining district. Two stratigraphic units, the Cripple Gravel and the Fox Gravel, are the main gold placer units of the area (see Figure 5.1).

The Cripple Gravel is a brown auriferous gravel of late Pliocene or early Pleistocene age. The unit consists of poorly

sorted to well stratified, coarse, angular sandy gravel with lenses of silt and sand. The gravel clasts consist of quartz-mica schist, quartzite, chlorite schist, biotite-garnet schist, feldspathic schist, calc-schist, graphitic schist, phyllite, slate, quartz monzonite, grandiorite, and granite. Gravel fragments range from 2 to 15 cm (1 to 4.5 inches) in diameter with basal cobbles and boulders from 25 cm to 1 meter (10 inches to 3 feet) in diameter. A minor white facies of the gravel occurs at the mouth of Engineer Creek and is composed of well-rounded quartz and quartzite cobbles and boulders in a grey sand matrix. The white gravel facies is devoid of other metamorphic or igneous rock types. This mature facies was a major source of gold and is similar to the White Channel deposit of the Klondike district, Yukon Territory.

The Cripple Gravel ranges from 1 meter thick on terrace benches to 25 meters (80 foot) thick in the lower end of stream drainages. The Cripple Gravel is generally underlain by a 0.5- to 2 meters (2 to 6.5 foot) thick auriferous clay which overlies bedrock. Bell (1974) attributed the clay to either pre-Pleistocene weathering or to percolation of groundwater during Pleistocene interglacial times. The Cripple Gravel is in turn overlain by the Fox Gravel and either the Tanana Formation, Dawson Cut formation, Fairbanks loess, Gold Hill loess or the Goldstream formations (Péwé, 1975).

The Fox Gravel is a tan colored auriferous gravel of early or middle Pleistocene age. The unit consists of poorly to well-stratified, angular sandy gravel with lenses of sand and silt. The gravel contains a similar population of clasts as found in the Cripple Gravel; the composition varies according to the bedrock source area. Gravel size distribution is comparable to the Cripple Gravel. The Fox Gravel is restricted to valley bottoms below loess and solifluction deposits and is exposed only in mining excavations.

The Fox Gravel lies directly on bedrock or on the Cripple Gravel and is overlain in turn by the solifluction deposits of the Tanana formation, the Dawson Cut formation, Fairbanks loess, Gold Hill loess or the Goldstream formation. The Fox Gravel is the predominant source of placer gold in the YTT (Péwé, 1975).

The Fox Gravel varies in thickness from 1 meter in the upper stream drainages to over 30 meters in the lower reaches. Where the unit lies near bedrock it is usually underlain by a 0.5- to 2 meter (2 to 6.5 foot) thick yellow to blue clay layer which is thought to have the same origin as the clay layer below the Cripple Gravel (Bell, 1974).

Péwé (1975) defined four criteria for distinguishing the older Cripple Gravel from the Fox Gravel. First, the Cripple Gravel is always on bedrock benches above modern valleys that contain Fox Gravel. Second, gold in the Cripple Gravel has a higher average fineness value than Fox Gravel gold when the samples are taken from the same creek and the same distance from the probable lode source. Third, Cripple Gravel pebbles are stained by iron oxide to a dark brown color while Fox Gravel is tan and less stained. Fourth, Fox Gravel frequently contains fossil bones of Pleistocene mammals; Cripple Gravel is devoid of fossil bones.



### 5.3 BEDROCK SOURCES OF PLACER GOLD

Detailed descriptions of the lode deposits of the Fairbanks district are included in Chapter 4; however a review of the sources of placer gold is essential to the present discussion. Detailed investigations of the lode mineral deposits have resulted in the definition of five major types of lode mineralization within the district:

Two types of lodes contain free milling gold that contributed to placer formation. Sulphide lenses and disseminations in the metavolcanics contain free gold. These lenses have been deformed during metamorphism; thus, native gold within the sulphides must be of premetamorphic origin and is probably syngenetic. Gold in the sulphide lenses is always fine-grained (<1 mg) and thus probably has not contributed significantly to the gold mineralization exploited in commercial placer operations to date. This source of fine-grained gold may provide the finer grained material disseminated vertically and laterally throughout the gravels, extending for considerable distances beyond major paystreaks. This size fraction of gold would also tend to accumulate further downstream with finer grained sediment.

The gold-quartz vein deposits that have been the sole source of lode-gold production in the district contain fine- to coarse-grained gold. In order to determine the probable grain size distribution from a typical vein system a 27 tonne (30 ton) bulk sample was taken from the Christina vein. The sample was crushed and the free milling gold was recovered from a shaking table. A sieve analysis was conducted on the 100 plus troy ounces of recovered gold and the results are reported in Table 4.10. This size distribution is not atypical of the size distribution of gold from the district. Cook (1973) reported a similar size distribution for alluvial gold from lower Goldstream Creek (see Table 5.2).

Table 5.2 Screen analysis of gold from lower Goldstream Creek (after Cook, 1973).

DIRECT		CUMULATIVE PASSING	
Mesh(Tyler)	Wt %	Mesh(Tyler)	Wt %
Head	100.0		
-3+8	—	3	100.0
-8+20	0.37	8	100.0
-20+28	7.42	20	99.63
-28+35	25.47	28	92.21
-35+65	34.79	35	66.74
-65+100	25.94	65	31.95
100 —	6.01	100	6.01

### 5.4 MECHANISM OF ALLUVIAL PLACER FORMATION

Mosley and Schumm (1977) and Adams et al. (1978) conducted extensive laboratory studies to determine possible mechanisms of alluvial-placer formation; however, those

studies did not attempt to relate the flume model results to field observations in major alluvial placer-producing areas. The major alluvial gold placers of the Fairbanks district provide an opportunity to test these models, particularly the significance of the basin rejuvenation process proposed by Adams et al. (1978) as the predominant mechanism responsible for placer concentration.

The locations of the gold placer deposits of the Fairbanks district together with the present stream drainage systems are shown on Plate II. In addition to the study of the stratigraphy of the Pliocene-Pleistocene surficial deposits, the examination of the patterns of stream drainage and the longitudinal profiles of the streams provide the best evidence for the understanding of the critical mechanisms of alluvial placer formation.

#### 5.4.1 Stream Longitudinal Profiles

The significance of stream longitudinal profiles can be summarized as follows. First, the concavity of the profile reflects the relative increase in discharge in the lower reaches of the drainage system. Extreme concavity of the profile indicates increased discharge in the lower reaches, whereas a linear profile indicates constant discharge for the entire system. Convex upward profiles are possible in arid regions, where discharge decreases because of evaporation and infiltration.

Second, the stream profile is an expression of changes in the size distribution of the bed load material in a downstream direction (Shulitz, 1941). The slope-discharge relationship (Sternberg, 1875; Woodford, 1951) and the slope-grain size relationship (Shulitz, 1941) are exponential functions, the former having a positive exponent and the latter a negative exponent.

Gravels are found in the steeper upper parts of the profile, whereas finer material accumulates in the lower reaches. There is a critical point on the profile above which material of a given grain size and specific gravity is maintained in a continuous state of transport (the zone of degradation) and below which the material begins to accumulate (the zone of aggradation). Since gold has a much higher specific gravity than rock-forming minerals, the critical point for gold accumulation lies further upstream than that of other fluvial materials. Thus there is a zone in which rock material is constantly being removed relative to gold, thereby forming a placer concentration.

Third, the stream drainage develops by headward migration of the stream profile, and coarse material and gold in the zone of accumulation are gradually buried by finer grained sediments as the critical point moves headward.

Fourth, the shape of the profile is a reflection of the maturity of the stream drainage. Generally regular profiles indicate mature drainage systems involving long periods of weathering and erosion (and adequate time for major placer formation). Irregular profiles generally indicate immature drainage; for such profiles the alternating steep and gentle slopes produce marked changes in stream velocity, which may result in local minor placer accumulation.

Stream profiles for all drainages of the Fairbanks district have been plotted (note topographic maps are in nonmetric units, thus profiles and slopes are expressed in feet/mile). The locations of major placer deposits and tributary confluences are included on the profiles. After plotting, profiles were tested for fit to the function:

$$y = a^{bx}$$

in which  $y$  = elevation in feet,  $x$  = distance in feet.

The correlation coefficients ( $R^2$ ) and the values for  $a$  and  $b$  were then calculated. Figures 5.2 thru 5.5 are profiles for Fairbanks, Cleary, Dome, and Pedro Creeks and are representative examples of most profiles in the district.

A number of general observations can be made from an analysis of the profiles:

1. The profiles are very regular with  $R^2$  values greater than 0.90.
2. The maximum stream gradient at the upper limit of major placer formation is 80 meters/kilometer (440 feet/mile), a slope of 1/12.
3. The maximum elevation of major placer formation varies systematically from 402 meters (1,320 feet) on Kokomo Creek in the northeastern end of the district to 183 meters (600 feet) on Cripple Creek in the southwestern extremity. Elevations of major summits and stream divides vary in the same manner.
4. Tributary streams have little effect on the stream profiles.
5. Elevated benches are apparent on some stream profiles, notably at the 549 meters (1,800-foot) elevation on Pedro Creek.
6. The stream profile cannot be used as the sole criterion to predict the presence (or absence) of a major placer deposit. Several streams with profiles similar to those of productive streams draining areas of gold-bearing metavolcanic rocks do not contain major placer accumulation.

Evidently, the maturity of the stream drainages of the district is one of the necessary conditions for major placer accumulation. This should be an essential consideration in the assessment of the placer potential of other mining districts and should be considered when planning future exploration programs in the Fairbanks district.

The maximum elevation of major placers in the Fairbanks district is a criterion that should be used with caution in delineating additional target areas. It may be used locally within the district, but the chief factor in assessing placer potential is the gradient of the stream at the upper point of major placer formation. The reach of the stream at the upper extreme of placer formation probably marks the critical zone between degradation and aggradation on the stream. The gradient of 80 meters/kilometer (440 ft/mile) is a slope of one in twelve, which is remarkably close to the average slope adopted by placer miners for the operation of sluice boxes.

The sluice is the traditional primary gold-recovery system for Alaskan alluvial placer operations. The system is

restricted to the recovery of +65 mesh (1 mg maximum, assuming a 4-to-1 shape factor) gold particles. Particles finer than 65 mesh in the alluvial environment are transported to lower energy regimes just as they are transmitted to tailings in most sluices. Generally, overbank placer deposits on meandering stream and distal beach deposits will have gold particles in the 100 to 400 mesh range.

Tributary streams may locally affect the paystreak in the main channel by shifting it laterally, but the overall effect on the distribution of placer formation is minimal. Tributary channels do not change the stream profiles appreciably at or below the confluence with the main drainage.

The identification of elevated benches in stream profiles is important for two reasons. First, the benches may be important sites of placer formation and second, they may contribute gold to sites of secondary accumulation.

Because most stream profiles in the district are similar and because some streams that drain potential bedrock source areas do not contain known major placer accumulations, two inferences can be made. First, such streams may contain major placer accumulations that have not yet been discovered and second, there exist other factors controlling placer accumulation that are not revealed in the stream profile.

#### 5.4.2 Periods of High Discharge and Placer Formation

Without data on stream discharge rates it is not possible to quantitatively determine whether the present stream profiles formed as a result of stable climatic conditions during the whole period of stream drainage development. Such a determination would add greatly to the interpretation of the paleoclimatic conditions of the late Tertiary and Pleistocene, which has by necessity been made from the surficial stratigraphic record.

Several of the major placer producing drainages in the district are underfit streams. The best examples are Goldstream and Fish Creeks (see Plate II). The method of Drury (1965) of relating valley formative discharge to the meander wavelength-bankfill discharge equation indicates that valley formative discharge for Goldstream and Fish Creeks may have exceeded normal present discharges by 25 to 100 times. Thus, the placer deposits are probably the product of periods of much higher discharge rates.

All indications are that the Fairbanks mining district was free of glacial ice during the late Pliocene and Pleistocene, yet the placer deposits of the area are associated with the coarse, poorly sorted alluvial Cripple and Fox Gravels. These gravels are much coarser than the material in the current channels (Péwé, 1952). The transport of this coarse material would require significantly higher rates of discharge than those found in modern drainages (Tourtelot, 1968).

The Cripple and Fox Gravels contain large quantities of silt, which was transported as a suspended load. Leopold and Maddock (1953) note the importance of suspended load in the transport of the bed load during flooding, and Cheney and Patton (1967) suggest flooding as a mechanism for placer accumulation on bedrock. Although flooding is difficult to document from the stratigraphic record, Mertie (1937) and

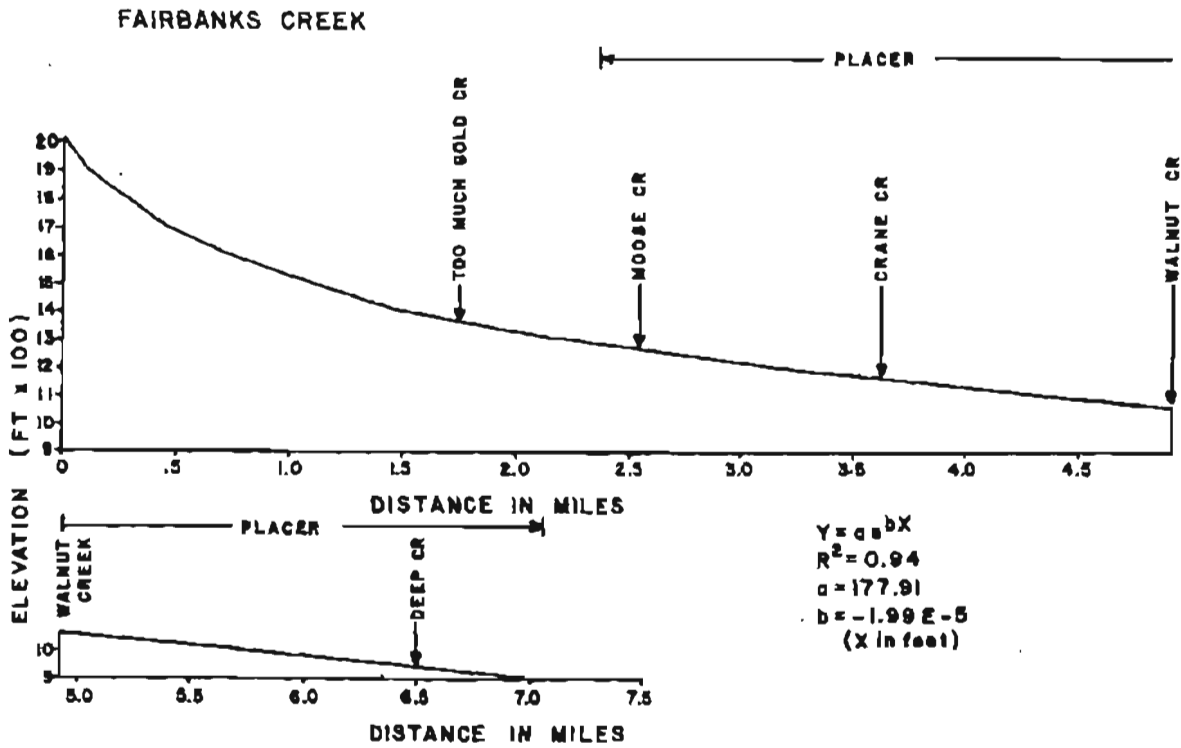


Figure 5.2 Longitudinal profile for Fairbanks Creek, Fairbanks mining district, Alaska.

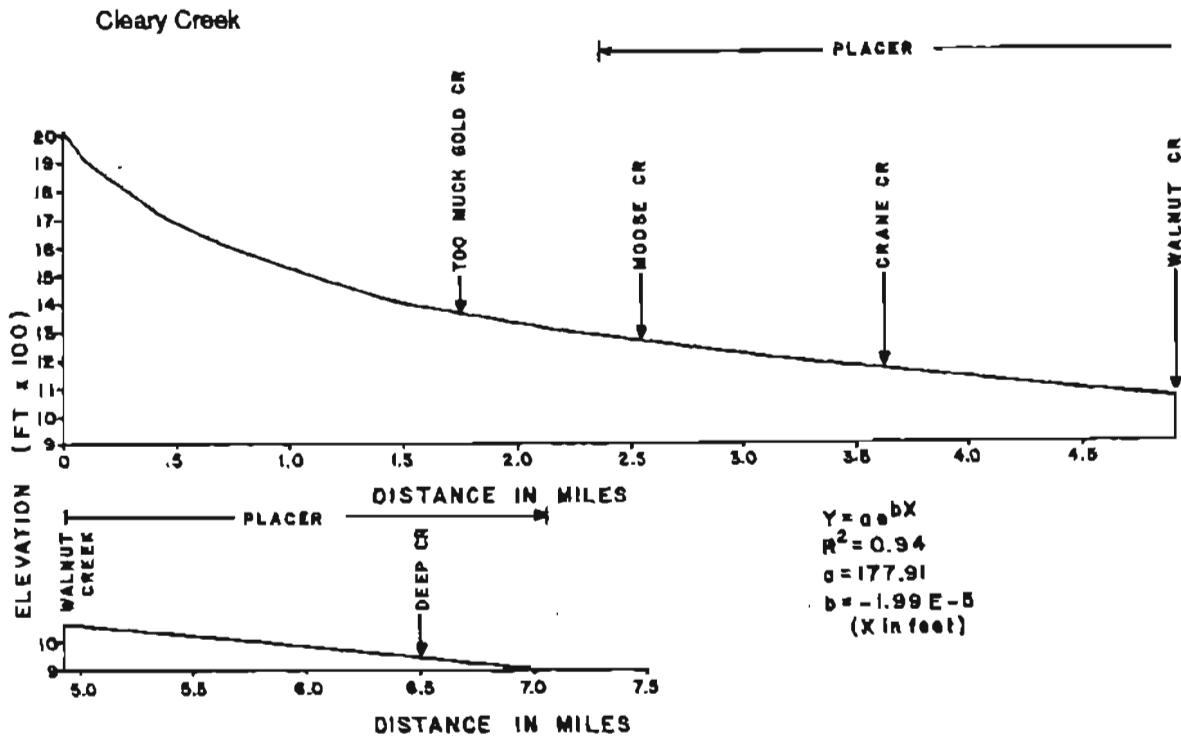


Figure 5.3 Longitudinal profile for Cleary Creek, Fairbanks mining district, Alaska.

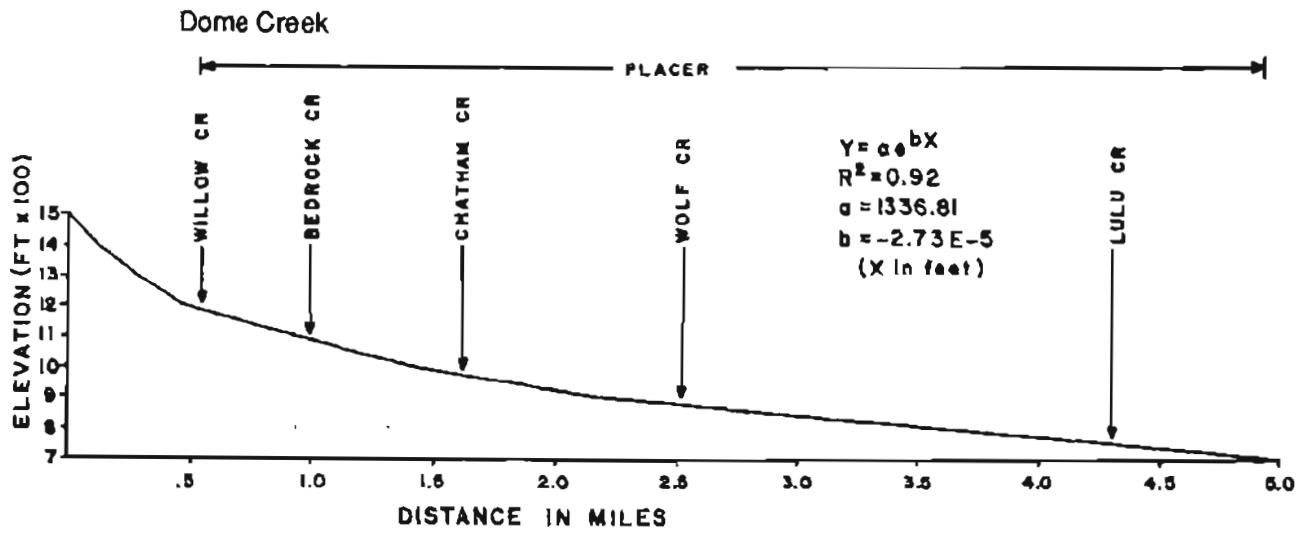


Figure 5.4 Longitudinal profile for Dome Creek, Fairbanks mining district, Alaska.

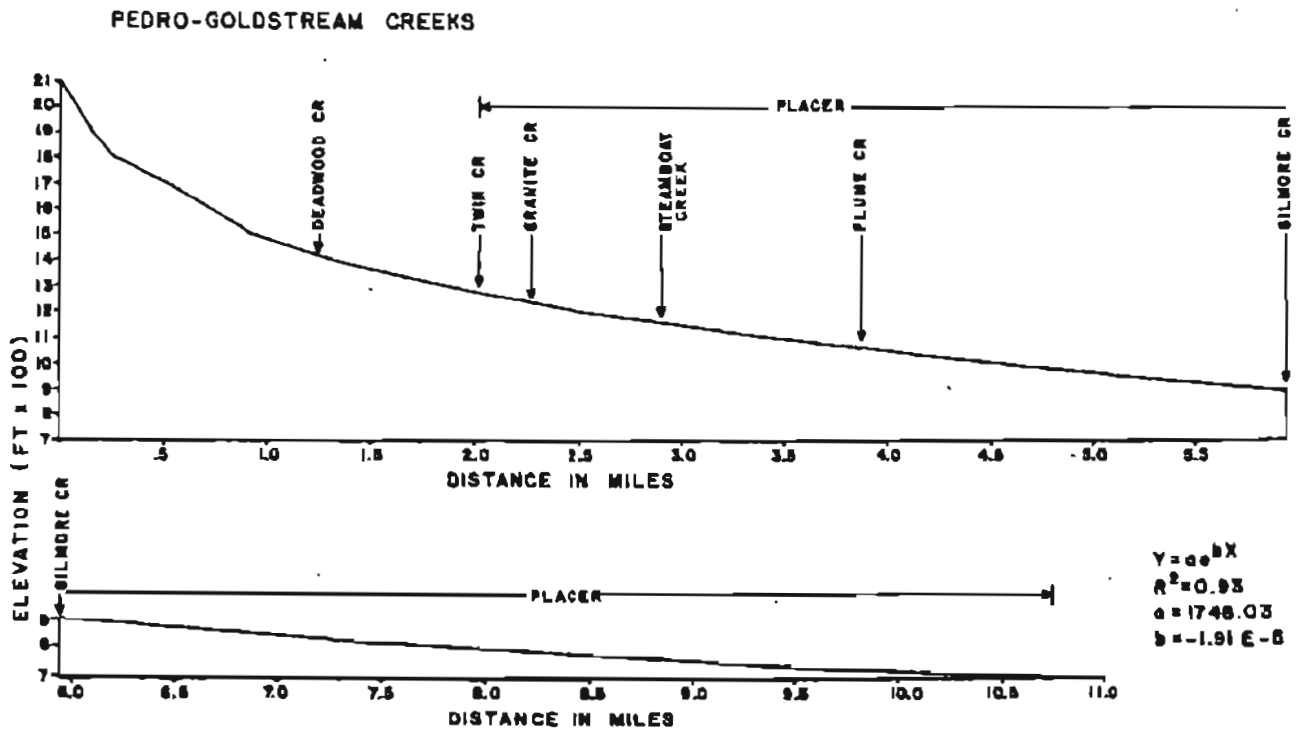


Figure 5.5 Longitudinal profile for Pedro-Goldstream Creek, Fairbanks mining district, Alaska.

Péwé (1975) note that the late Pliocene and early to middle Pleistocene were periods of rigorous and variable climate in Interior Alaska. Change in discharge rates of streams is expected to accompany this major change in climate.

Glaciers north and south of the YTT produced much silt during this time - silt that was transported by wind to the uplands and was subsequently introduced into the stream channels. The scouring of stream channels and the transport of coarse material and gold in the Fairbanks district were probably facilitated by the high discharge rates and high silt content of Pleistocene streams.

#### 5.4.3 Alternation of Stream Drainage Patterns and Stream Capture

The existence of older terrace and buried placer deposits led early workers to suggest minor changes in stream drainage due to lowering and raising of the base level. Lowering of the base level was considered to be caused by regional uplift or lowering of sea level; conversely, raising of the base level was attributed to regional subsidence or raising of sea level.

Regional changes in base level could account for widespread terrace and buried placers in the uplands; however, they could not account for the following morphological features:

1. Uniform and large local differences in elevation of summits, stream divides, and major placer deposits,
2. Asymmetry of stream-valley cross sections,
3. Pronounced linearity of some stream drainages,
4. Opposing directions of streamflow in adjacent valleys.

As noted previously, the maximum elevation of major placer formation ranges from 402 meter (1,320 feet) (Kokomo Creek) in the northeast to 183 meter (600 feet) (Cripple Creek) in the southwest, thus a difference in elevation of 219 meters (720 feet) exists over a distance of 56 kilometer (35 miles). The divides in the Kokomo and Fairbanks Creek area are at an elevation of 686 meter (2,250 feet); those in the Cripple and Ester Creek area are at 457 meter (1,500 feet), a difference of 230 meter (750 feet). Similarly, Twin Buttes in the northeast has a summit of 922 meter (3,025 feet) and the summit of Ester Dome in the southwest lies at 720 meter (2,364 feet), a difference in elevation of 201 meter (661 feet). These local differences in elevation are twice as large as the inferred changes in sea level since the Pleistocene (Hopkins, 1967).

The asymmetry of stream valleys has been attributed to several factors, including differential slope transport in arctic environments, differential stream erosion due to differences in lithology, and differential headward migration of streams due to increase in bedrock slope (caused in turn by local tectonic activity). The variation in angle of slope between north- and south-facing cross sectional profiles in areas of permafrost has been examined by Hopkins and Taber (1962), Curry (1964), Kennedy and Melton (1971), and Kennedy (1976).

Since north-facing slopes have less exposure to solar radiation, the slope should be less susceptible to thawing and

less subject to erosion by solifluction. South-facing slopes should have increased solifluction because of alternate freezing and thawing, leading to increased erosion and lower slope angle.

None of the above investigators are able to demonstrate a simple dependent relationship between slope orientation and slope angle. A simple explanation is even less plausible in the Fairbanks district because, in some major drainages such as Goldstream Creek and the Little Chena River, the south-facing slopes are actually steeper; also, other creeks display little difference in slope angles between north- and south-facing cross sectional profiles.

Differential stream erosion due to differences in lithology can also be ruled out as an explanation for valley asymmetry in the Fairbanks area. The bedrock in the area is predominantly schist and the regularity of the longitudinal stream profiles indicates the uniform resistance of the bedrock to erosion. Schist generally exhibits uniform weathering characteristics under varied climatic conditions.

Cotton (1942) and Lauder (1962) show that asymmetry of slope angles can be caused by shifting of stream divides due to local tectonic activity. In extreme cases, the weaker stream drainage is captured by the more aggressive stream and the result is a major change in direction of stream flow. Figure 5.6a shows a stream drainage pattern developed in a schist terrane in a stable craton without major tectonic activity (note the orientation of the arrows indicating stream flow). Figure 5.6b (after Lauder, 1962) shows the development of a precedent stream along the Wellington Fault, North Island, New Zealand. Tilting of the fault block to the northwest results in steepening of slopes down dip, but the gradient of the precedent stream along the strike of the fault remains constant. The result of the tectonic activity is to increase erosion up-dip, leading to imminent stream capture at P1, P2, and P3. In Figure 5.6c, stream capture is complete at C1, C2, and C3. The former southerly reaches of the precedent stream flow north, but form barbed drainages at B1 and B2 and enter channels that flow to the south (note the orientation of arrows indicating streamflow).

To determine if similar processes were active in the Fairbanks district, Ch. 5, Plate II was examined for the presence of barbed streams. From southwest to the northeast, major barbed drainages developed on Cripple, Ester, Nugget, Sheep, Our, Treasure, Cleary, Kokomo, Fairbanks, and Fish Creeks (note the orientation of arrows indicating streamflow).

Although the Fairbanks area is tectonically active (Gedney and Berg, 1969), the structural control of barbed streams is less obvious in the Fairbanks district than along the Wellington Fault in New Zealand. In the southwest part of the Fairbanks district, a major structural feature is identified on Landsat imagery and on aerial photography (Metz and Wolff, 1980). The feature extends from Cripple Creek along the north side of Chena Ridge to Isabella Creek and French Gulch and on toward Gilmore Dome (Ch. 5, Plate II). The area between Cripple Creek and Isabella Creek is a prominent topographic low. Streams crossing the feature from the north are displaced in swampy terrane and do not continue south-

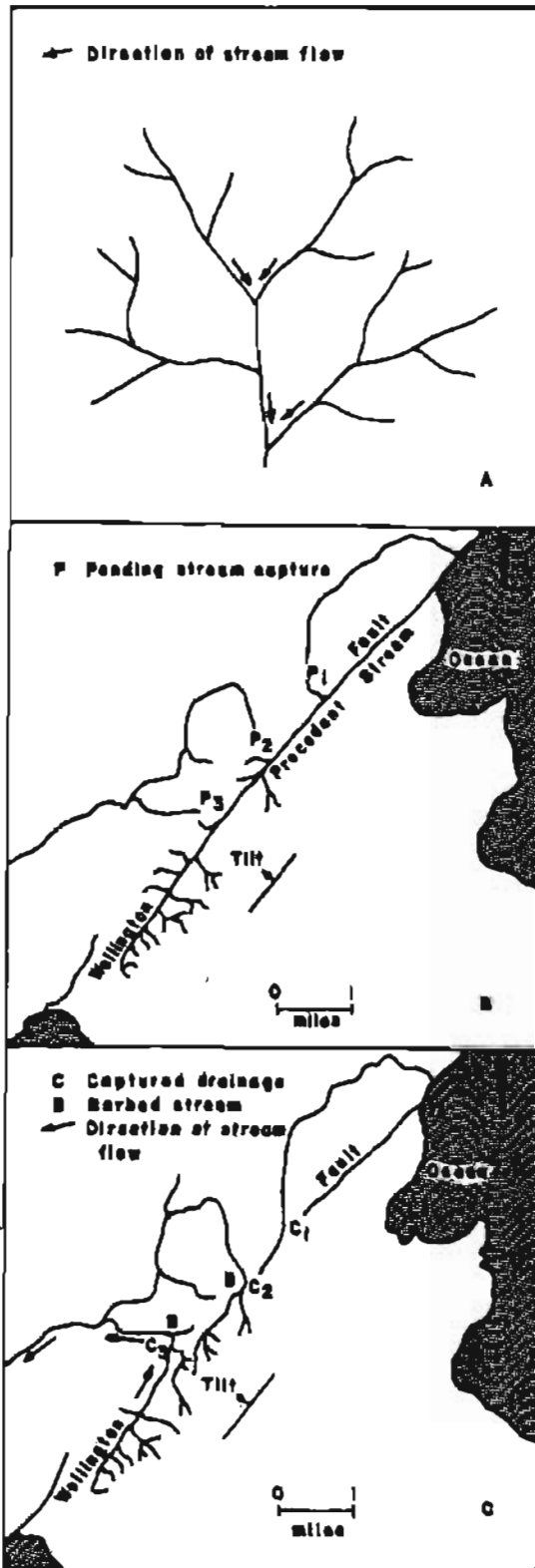


Figure 5.6 Stream flow directions in (A) hypothetically tectonically stable schist terrane, (B) tectonically active schist terrane before stream capture, (C) tectonically active schist terrane after stream capture.

ward to the Chena River.

The divides between Cripple and Rosie Creek and between Isabella Creek and French Gulch suggest wind gaps. Benches along the tributaries of Rosie Creek suggest a larger protodrainage to the west of the current drainage. This is evidence that the earlier drainage system probably included the upper reaches of Cripple Creek and flowed to the southwest, directly into the Tanana River. The valley of Isabella Creek is very wide and swampy, suggesting the presence of an earlier, larger drainage basin. Recent geological mapping defines a 400 meter (1,300 foot) wide fault zone in a road cut at the divide between French Gulch and Isabella Creek. The fault strikes northeast-southwest; is congruent with the Landsat feature; and is here designated the Cripple Creek-French Gulch Thrust. This fault is probably responsible for the capture of both Cripple Creek and Engineer Creek.

Movement along the Cripple Creek-French Gulch Thrust caused rapid headward migration of the proto-Engineer Creek, resulting in the capture of the upper reaches of Isabella Creek and reversal in the flow direction of French Gulch. The reworking of the stream sediments resulted in the formation of a very high grade placer in lower Engineer Creek as well as the deposition of the resistant quartz-rich white facies of the Cripple Gravel at the mouth of Engineer Creek.

A few miles to the west of Engineer Creek lies Ester Dome, the western end of the Fairbanks district. Ester Dome is bounded on the north by Goldstream Creek and on the east by a low area that connects Goldstream Creek and the Tanana Valley. Sheep Creek and Little Nugget Creek contains significant gold placers and drain into Goldstream Creek from the north and northeast side of Ester Dome. Happy Creek and St. Patrick Creek which drain the east side of Ester Dome flow into a poorly drained low area that discharges into the Chena River and subsequently into the Tanana River.

Metz and Wolff (1980) in examination of Landsat imagery note a major linear feature extending from the east side of Ester Dome in a northerly direction for about 48 kilometers (30 miles). This linear feature offsets the northeast-southwest trending regional structure and associated aeromagnetic anomalies.

Surface evidence for a major shear zone in the Ester Dome area includes fault breccia in placer tailings of Sheep Creek and the predominance of lower grade metamorphic rocks west of the linear feature. The lack of marker horizons in the schist sequence precludes definitive determination of fault motions. In the Grant Mine near Happy Creek, northeast-trending gold quartz veins are truncated by a north-south striking fault zone, but, the extension of the truncated veins have not been located and no offsets can be calculated. Slickensiding suggests both dip-slip and strike-slip components. This fault system is congruent with the linear feature and is designated the Moose Creek Shear Zone (Ch. 3, Plate III).

Placer drill records for the Sheep Creek and Goldstream area define a bedrock high at the confluence of the two creeks. To the east bedrock drops off rapidly, whereas the slope is less steep to the west. This bedrock high is an expression of an earlier stream divide.

Movement along the Moose Creek Shear caused increased headward migration of the proto-lower Goldstream Creek toward the divide and, ultimately, capture of proto-upper Goldstream Creek, which previously had flowed southward around the east side of Ester Dome to the Chena River. Moose, Sheep, Little Nugget, Happy, St. Patrick, and O'Conner Creeks were all previously flowing east by southeast to the Chena River via proto-upper Goldstream Creek. Stream capture not only caused resorting of the Sheep Creek placer but affected the hydraulics of the entire Goldstream drainage, resulting in the formation of the largest single placer in the region.

Twenty miles to the west of the Moose Creek Shear and parallel to it lies another major north-south striking normal fault system which includes a large depressed structure called Minto Flats. The Minto Flats fault dips to the west and has a vertical displacement of over 610 meters (2,000 feet) (Barnes, 1961). It can be traced for about 128 kilometers (80 miles), and appears to offset Pleistocene eolian deposits in the Tanana Valley.

In the northern and northeastern part of the district, two previously mapped faults (Forbes et al., 1968), the Chatanika Valley Fault and the Cleary Creek Thrust, are probably responsible for the alteration of the drainages of Treasure, Vault, Dome, Little Eldorado, Cleary and Kokomo Creeks. Cleary Creek, which produced 1,000,000 troy ounces of placer gold, provides the best example of the structural control of stream drainage in this part of the district. The upper reaches of Cleary Creek flow to the northeast while the Chatanika River, which is the main drainage system in the area, flows southwest. From the stream drainage patterns, it is inferred that Willow, Bedrock, and Chatham Creeks, all tributaries of Cleary Creek, originally drained directly into the Chatanika River. Relatively faster headward migration of the proto-lower Cleary Creek along the Cleary Creek Thrust caused capture of Willow, Bedrock, and Chatham Creeks.

Similarly, the Fairbanks Creek and Fish Creek drainage system forms a major barbed drainage to the Little Chena River. The tributary streams flow east by northeast, whereas the Little Chena River flows southwest (Ch. 5, Plate II). Recent geologic mapping in the Cleary Creek and Fairbanks Creek area defines a major east-west shear zone that appears to control the gold-quartz vein mineralization in this part of the district. The shear zone is nearly vertical and exhibits evidence of strike-slip movement. The structure is mapped at several lode deposit localities over an 8 kilometer (5 mile) strike length, however placer drilling in the Fairbanks and Deep Creek area suggests that it may extend for another 6.4 kilometer (4 miles) to the east. Fairbanks Creek follows this structure which is here designated the Fairbanks Creek Shear Zone.

A second major structure is mapped along the valley of the Little Chena River (F. Weber, USGS, personal commun.). This structure strikes northeast-southwest, controls the lower reaches of the Little Chena River Valley, and is visible on aerial photographs and Landsat imagery for at least 80 kilometers (50 miles) (Metz and Wolff, 1980).

Movement along these structures apparently gave rise to the relatively rapid headward migration of Fish Creek, which resulted in the capture of Fairbanks, Bear, and Solo Creeks. Prior to stream capture, these tributaries flowed southeast directly into the Little Chena drainage. These captures caused resorting in the tributaries and the formation of the placer deposits in upper Fish Creek and Fairbanks Creek.

The reaches of Fish Creek below the confluences of Solo, Bear, and Fairbanks Creeks are areas of potential placer accumulation. Several small, recent mining operations on lower Fish Creek below Fairbanks Creek demonstrate the existence of economic concentrations of placer gold in this area.

Previous descriptions of the relationship between placer formation and stream capture are very limited. Cox (1879) describes lode-gold occurrences in the schist terrane adjacent to the Wellington Fault in New Zealand. He also notes the occurrence of placer gold in the streams that Cotton and Lauder later describe as captured drainages; neither Cotton nor Lauder consider the possibility of a relationship between stream capture and placer-gold accumulation.

Mertie (1918b) describes the change in flow direction of Livengood Creek in central Alaska and notes that the stream system contains the most significant placer deposit in the Tolovana district. During examination of the Goodnews Bay placer platinum deposit, Mertie (1976) provides evidence for the capture of Platinum Creek but does not seem to recognize the significant part played by stream capture in the localization of the placer.

Smirnov (1976) discusses the importance of tectonic processes in placer formation; however, he does not analyze the role of individual processes in the localization of placer deposits.

Examination of Plate II indicates that most of the major placer deposits in the Fairbanks district lie in stream systems that exhibit barbed reaches. This suggests that the reworking of gravels caused by alteration of drainages and changes in stream-flow direction is a major control of placer formation in the district.

## 5.5 PLACER GOLD FINENESS VALUES

Gold fineness is defined as  $[\text{Au}/(\text{Au} + \text{Ag})] \times 1,000$ .

Metz and Hawkins (1981) discuss the regional distribution of gold fineness values from Alaskan placer deposits and review the significance of local difference in fineness values from placer and lode deposits. Desborough (1970), Hallbauer and Uter (1977), and Forbes (1980) explain local differences in placer gold fineness values by demonstrating the existence of silver depletion rinds on nuggets from alluvial deposits. The existence of such rinds is attributed to the greater solubility of silver relative to gold in the alluvial environment. The relative thickness of the rind increases as the grain size decreases downstream, thus the increased gold fineness away from the lode source.

Gold fineness values from both Smith (1913b) and this investigation are shown on Plate II. In addition, the fineness values for placers on Pedro-Goldstream Creek, Dome Creek,

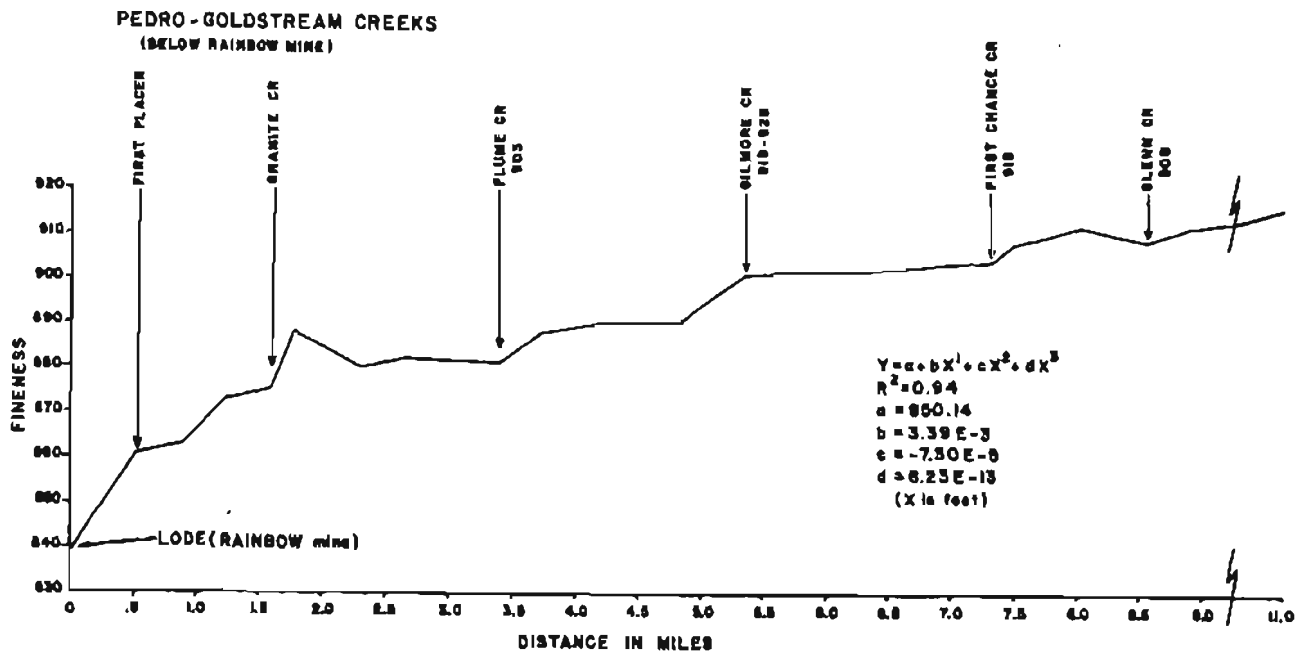


Figure 5.7 Placer-gold fineness versus distance plot for Pedro-Goldstream drainage system, Fairbanks mining district, Alaska

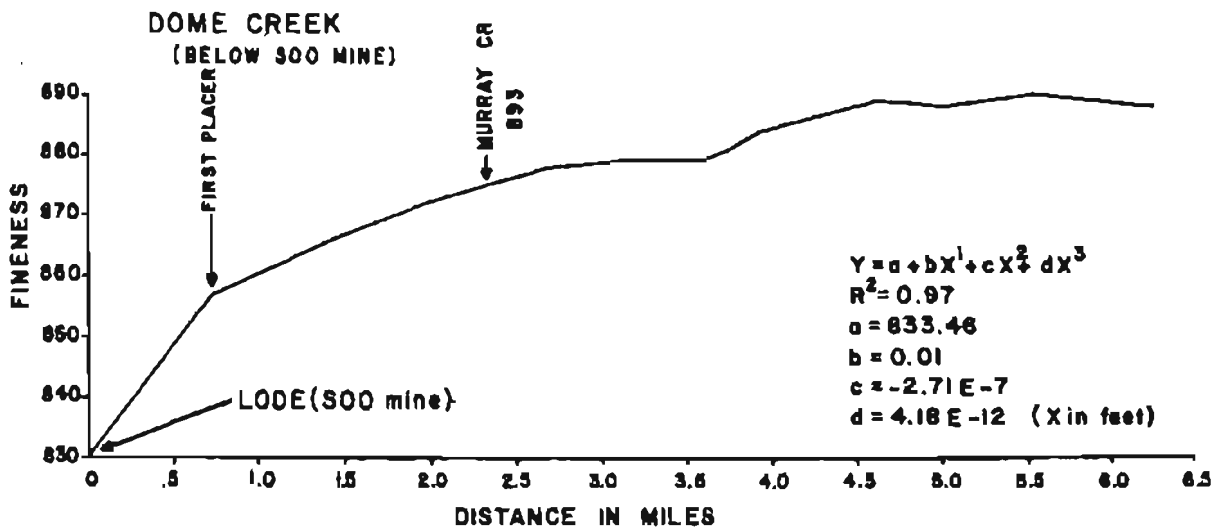


Figure 5.8 Placer-gold fineness versus distance plot for Dome Creek, Fairbanks mining district, Alaska.

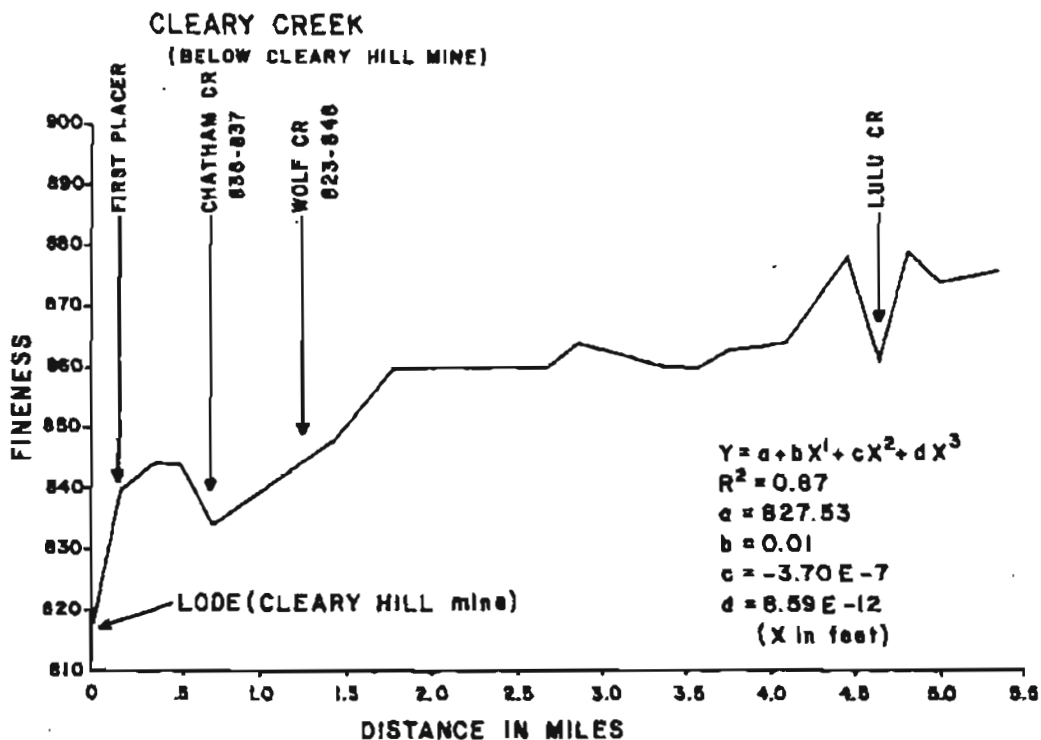


Figure 5.9 Placer-gold fineness versus distance plot for Cleary Creek, Fairbanks mining district, Alaska

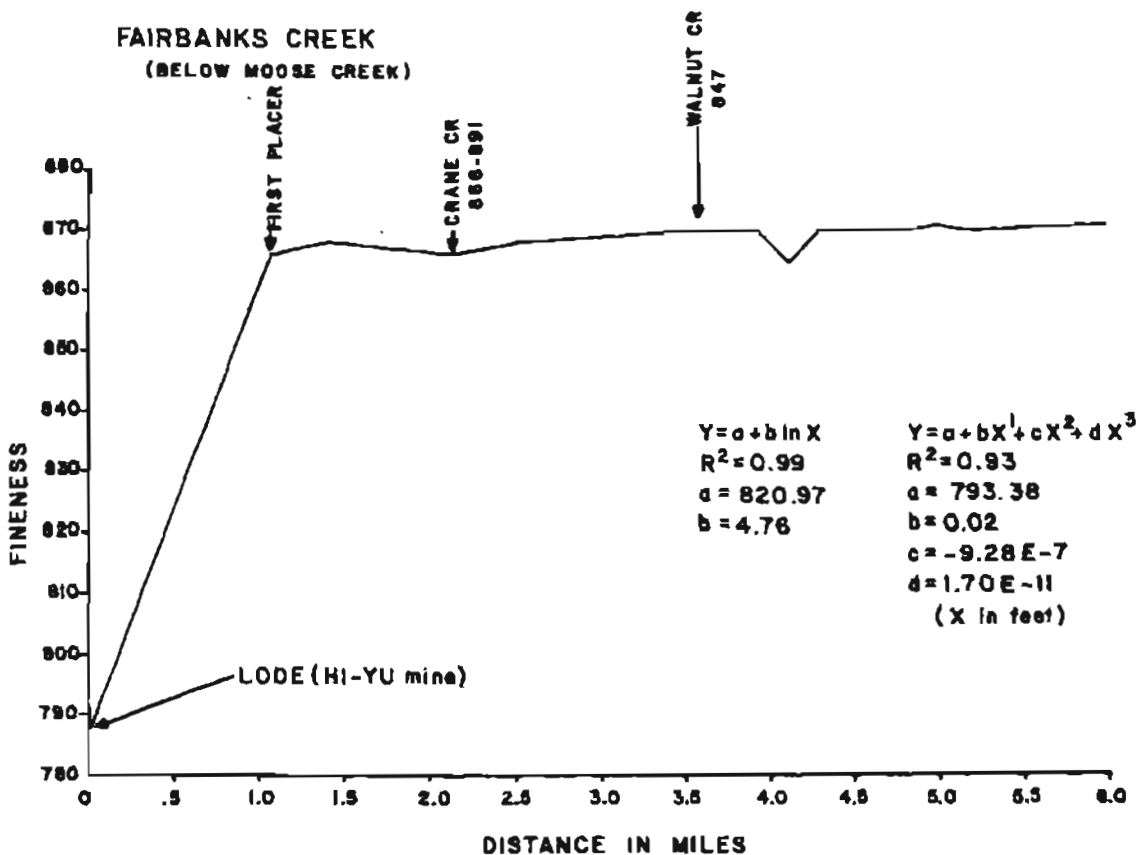


Figure 5.10 Placer-gold fineness versus distance plot for Fairbanks Creek, Fairbanks mining district, Alaska

Cleary Creek, and Fairbanks Creek were plotted as a function of distance downstream from probable lode sources (Figures 5.7-5.10). The figures include the location of the tributary streams and the fineness values of tributary placers. The fineness value-distance plots are fitted to a polynomial function, and regression coefficient ( $R^2$ ) values are calculated.

In the Pedro-Goldstream system (Figure 5.7), gold fineness increases 20 mils (unit of fineness) within the first 800 meters (1/2 mile) below the Rainbow Mine at the site of the first major alluvial workings. The fineness changes by 60 mils over the remaining 17 kilometer (10.5 mile) extent of the placer workings. The gradients are thus 25 mils per kilometer (40 mils per mile) up to the alluvial deposits and 3.5 mils per kilometer (6 mils per mile) in the placer environment. The regression coefficient for the polynomial is 0.94, indicating a relatively predictable change in fineness.

Fineness values increase below the confluences of Granite, Flume, and Gilmore Creeks with the main drainage system. These increases reflect the higher fineness of the gold from the tributary streams and give a semiquantitative value for the relative contribution of gold from the tributary to the main channel. In the case of Granite Creek, the change indicates a high probability of a significant placer in the tributary or a new lode source of higher fineness.

Fineness of gold from Dome Creek (Figure 5.8) increases 30 mils in the 1.2 kilometer (0.75 mile) distance from the Soo Mine, a change of 15 mils per kilometer (40 mils per mile). The change in fineness for the remainder of the placer deposit is 3.5 mils per kilometer (6 mils per mile) and is very uniform with  $R^2 = 0.97$ .

The placer-gold fineness values for Cleary Creek (Figure 5.9) are much less regular, with  $R^2 = 0.87$ . This is a reflection of the multiple lode source areas on the ridge between Cleary and Fairbanks Creeks (Ch. 5, Plate II). The fineness increases 23 mils in the first 400 meters (0.25 mile) below the Cleary Hill Mine, or 58 mils per kilometer (92 mils per mile), whereas in the rest of the drainage the values increase by an average of 4.4 mils per kilometer (7 mils per mile). The expected value below Lulu Creek is 879 mils, whereas the actual value is 861 mils, suggesting an alternate lode source in the drainage area.

The plot for Fairbanks Creek (Figure 5.10) shows an increase in fineness of 49 mils per kilometer (78 mils per mile) from the Hi-Yu Mine to the first major placer. The fineness increases only 5 mils over the remaining 8 kilometers (5 miles) of the placer deposit. The tributaries of lower Fairbanks Creek either have fineness values comparable to those in the main drainage or are not making a significant contribution to the total volume of placer gold. The change in fineness values from the McCarty Mine (814 fine) on upper Fairbanks Creek is 26 mils per kilometer (42 mils per mile) from the mine to the first placer workings (Ch. 5, Plate II). The change is similar to the rates of change noted for the other drainage systems.

These data suggest that the greatest change in alluvial gold fineness takes place in the weathering and erosional

environment rather than in the placer depositional environment. Because the change in gold fineness value in the alluvial environment is small, these changes may not reflect change in flow direction caused by stream capture. Gold fineness values thus must be used with caution in placer exploration and evaluation.

## 5.6 SUMMARY AND CONCLUSIONS

Placer deposits of the Fairbanks mining district occur in streams that drain areas of metavolcanic rocks of the Cleary sequence of the YTT. Two distinct types of lode sources are identified, each with different gold grain-size distributions. Premetamorphic sulphide lenses contain fine-grained gold (<1 mg), whereas postmetamorphic gold-quartz-sulphide veins contain fine- to coarse-grained gold. Commercial gold placer operations to date are limited to proximal high-grade gold accumulations. Fine-grained gold from premetamorphic bedrock sources are probably transported greater distances and thus may accumulate in distal terraces or deeply buried placer deposits.

The surficial depositional controls leading to formation of commercial placers include:

1. Deposition in streams with regular gradients reflecting stream maturity and sufficient time for placer formation,
2. Placer gold is concentrated on or near bedrock in reaches of streams with gradients less than 80 meter/kilometer (440 feet/mile),
3. Placer formation takes place under conditions of high discharge rates relative to rates found in the present stream systems,
4. Placer gold fineness values increase systematically downstream; however, rates of change are greatest in the weathering and erosional environment rather than in the depositional environment,
5. Most of the major placer deposits occur in streams with barbed drainages. Several of these barbed drainages are related to basement structures. Stream capture and the alteration of stream flow by basement structure are the most important factors in producing economic concentrations of gold in the placer deposits.

---

## CHAPTER 6

### TRACE ELEMENT GEOCHEMISTRY OF THE FAIRBANKS MINING DISTRICT

#### 6.1 INTRODUCTION

Stream sediment, pan concentrate (heavy mineral concentrate), and rock geochemical sampling were conducted in conjunction with geological mapping of the Fairbanks district in 1981 thru 1983. The purposes of the geochemical investigations were as follows: 1) to provide trace element

data for the various mappable rock units thereby enhancing the geologic mapping, 2) to provide trace element data for the various mineral deposit types that were known to occur in the district, and 3) to provide data to guide in the discovery of additional mineral occurrences in the district.

Albanese (1982a, 1982b, and 1982c) reported the analytical results and Metz (1984) provided a preliminary reduction of the data. The following is extracted from Metz (1984) with additional data compiled from unpublished company reports. The industry data were essential in determining trace element contents of a number of mineral occurrences in the district.

## 6.2 SAMPLING

Stream sediment samples were collected on 400 meter (1320 foot) intervals from all active drainages in the district except from areas disturbed by mining or other human activities. Minus 80 mesh size material was collected where possible. Generally even on streams draining thick loess sections, enough clay size material was collected to meet the two gram sample requirement. A total of 1013 stream sediment samples was collected for analysis.

Pan concentrate samples were collected at each fourth stream sediment sample site. Minus 10 mesh size material was panned in the field to produce at least 5 kilograms (10 lbs) of concentrates. The samples were then further reduced with a 30 centimeter (12 inch) sluice in the laboratory to yield at least two grams of concentrate. A total of 159 pan concentrate samples was collected for analysis.

Rock geochemical samples were collected from each outcrop and from prospects where such sampling was authorized by the property owner. Not all outcrop samples were selected for geochemical analysis. The main criterion for sample selection was either the presence of visible indications of mineralization or the representative nature of the outcrop with respect to a mappable lithology. A total of 812 mineralized rock samples was selected for analysis. A total of 78 representative lithologic samples was collected for trace element analysis. These 10 kg (20 lb) samples were selected

away from visible indications of mineralization. The sample suite included at least one sample from each map unit described in the district wide geologic mapping (Bundtzen, 1982; Metz, 1982; and Robinson, 1982).

The stream sediment, pan concentrate and mineralized rock samples were collected by 15 geologists and field assistants who participated in the geologic mapping of the district. The 78 rock unit samples were collected by the author. Locations of the stream sediment, pan concentrate, and rock samples are shown on Ch 4, Plates I and II.

## 6.3 STREAM SEDIMENT DATA

### 6.3.1 Sample Analyses

The stream sediment samples were sent to Bondar-Clegg Ltd., Vancouver, British Columbia, Canada for sample preparation and analysis for arsenic while Cu, Pb, Zn, and Ag analyses were conducted at the Alaska Division of Geological and Geophysical Surveys (ADGGS) laboratory in Fairbanks, Alaska. Arsenic determinations were by coulometry with a lower detection limit of 2 ppm. The Cu, Pb, Zn, and Ag analyses were by atomic-absorption spectrophotometry with a lower detection limit of 0.01 ppm.

### 6.3.2 Data and Data Reduction

Histograms and log concentration-probability plots of the stream sediment data are included in Appendix C. The data are reduced by the method of Lepeltier (1969). The sample statistics are summarized in Table 6.1. Threshold values are defined as those concentrations at the 97.5 probability level. The anomalous samples are plotted on Ch 4, Plates III through XI, as are the locations of the known lode mineral occurrences in the district.

## 6.4 PAN CONCENTRATE DATA

### 6.4.1 Sample Analysis

The pan concentrate samples were also sent to Bondar-Clegg for preparation and analysis for Sn and W. The W analyses were by colorimetry with a lower detection limit of 2 ppm. The Sn analyses were by x-ray fluorescence with a

Table 6.1 Statistical parameters for analyses of stream sediment samples from the Fairbanks mining district, Alaska

Element	Geometric Mean (ppm)	Geometric Deviation	Coefficient of Deviation	Coefficient of Variation (%)	Threshold (ppm)
As	18	1.67	0.22	1.2	52
Cu	18	1.22	0.09	0.5	28
Pb	10	1.40	0.15	1.5	17
Ag <sup>(1)</sup>	180	1.78	0.25	0.14	0.5
Zn	53	1.17	0.07	0.13	74

(1) Ag in ppb

lower detection limit of 5 ppm. The ADGGS laboratory completed the Au and Sb analyses by atomic-absorption spectrophotometry with lower detection limits of 0.01 ppm.

#### 6.4.2 Data and Data Reduction

Pan concentrate data are displayed and reduced in the same manner as the stream sediment data. A summary of the statistical parameters is given in Table 6.2.

### 6.5 MINERALIZED ROCK DATA

#### 6.5.1 Sample Analysis

The mineralized rock samples were also sent to Bondar-Clegg for preparation and analysis of As, Hg, Sn, and W. The Hg analyses were conducted by cold-vapor atomic-absorption spectrophotometry with a lower detection limit of 5 ppb. The As, Sn, and W analyses were completed by the same techniques that were utilized for the pan concentrate analyses. The Cu, Pb, Zn, Au, Ag, and Sb analyses were conducted at

the ADGGS laboratory by the same techniques that were utilized for the stream sediment analyses.

#### 6.5.2 Data and Data Reduction

The mineralized rock data are displayed and reduced in the same manner as the stream sediment and pan concentrate data. Table 6.3 is a summary of the statistical parameters for the mineralized rock analyses.

### 6.6 MAPPABLE ROCK UNIT DATA

#### 6.6.1 Sample Analysis

The seventy-eight 10 kilogram (20 lb) samples were sent to Bondar-Clegg for sample preparation and analysis by Instrumental Neutron Activation Analysis (INAA). The samples were analyzed for the following elements: Au, Sb, As, Ba, Cd, Cr, Co, Hf, Fe, La, Mo, Ni, Na, Ta, Th, W, U, and Zn. The lower detection limit for gold was 5 ppb and the limits for the other elements ranged from 0.1 to 200 ppm.

Table 6.2 Statistical parameters for analyses of pan concentrate samples from the Fairbanks mining district, Alaska.

Element	Geometric Mean (ppm)	Geometric Deviation	Coefficient of Deviation	Coefficient of Variation (%)	Threshold (ppm)
Sb	6	1.27	0.10	1.7	10
Au <sup>(1)</sup>	330	1.15	0.06	0.02	450
Sn	3.2	1.88	0.27	8.5	12
W	12	1.25	0.10	0.8	19

(1) Au in ppb

Table 6.3 Statistical parameters for analyses of mineralized rock samples from the Fairbanks mining district, Alaska.

Element	Geometric Mean (ppm)	Geometric Deviation	Coefficient of Deviation	Coefficient of Variation (%)	Threshold (ppm)	Clarke	Multiple of Clarke
Sb	8.5 (22)	1.41	0.15	1.8	17	0.2	42(110)
As	11 (130)	1.45	0.16	1.5	24	1.8	6(72)
Cu	74	1.55	0.19	0.3	180	55	1.3
Au <sup>(1)</sup>	100	7.50	0.88	0.9	500	2	50
Pb	17	1.71	0.23	1.4	48	12	1.4
Hg	3	1.33	0.12	4.2	6	0.5	6
Ag <sup>(1)</sup>	160	3.63	0.56	0.4	2000	70	2.2
Sn	1.7	1.68	0.23	13.4	4	2	0.8
W	12	2.33	0.37	3.1	27	1.5	8
Zn	40	2.25	0.35	0.9	210	70	0.6

(1) Au and Ag in ppb

### 6.6.2 Data and Data Reduction

The data were grouped by major lithologies by terrane and sample means and standard deviations were calculated for each group. The sample data and statistics are given in Table 6.4.

### 6.7 DISCUSSION

The anomalous stream sediment, pan concentrate, and mineralized rock samples along with the locations of the known lode mineral occurrences are plotted on Ch 4, Plates III through XI. The data indicate two parallel northeast-southwest trending mineralized belts. These belts are parallel to the regional trend of the metamorphic sequences. The more northerly belt is congruous with the Cleary Anticline and the northern outcrop of the Cleary sequence. The southerly belt is congruous with the Tungsten Anticline and the southern outcrop of the Cleary sequence.

The distribution of the arsenic, antimony, lead, and zinc geochemical anomalies corresponds closely to the outcrop pattern of the Cleary sequence and also to the distribution of most of the known lode mineral occurrences in the northeastern portion of the district. In the Ester Dome area which is the southwestern extremity of the district, the above element suite is supplemented by high tungsten concentrations. It is notable that in this area the Cleary sequence is dominated by chlorite and chlorite-calc schist.

Table 6.5 is a comparison of the average trace element content of the mineralized rock samples of the Fairbanks district with average crustal abundances. The table shows that the mineralized rocks in the district average 210, 83, 50, and 14 times the crustal abundances of antimony, arsenic, gold, and tungsten respectively. The anomalous sample locations shown on Ch 4, Plates III through XI indicate that there are at least eighteen areas of potential lode mineralization that have not been previously delineated. Anomalous areas are defined by more than one sample with one or more anomalous elements. The eighteen areas of potential miner-

alization can not be accounted for by the 188 previously noted occurrences in the district. Roman numerals on the plates depict these new areas.

Area I is located in section 23, T1S, R3W, F.M. Anomalous elements include Sb, As, W, and Hg. Rock types include metachert, metamorphosed felsic volcanoclastics, and calcareous actinolitic greenschist.

Area II is located in Sec 34, T1N, R3W, F.M. Anomalous elements include Sb and As. Rock types include metamorphosed felsic volcanoclastics, biotite-muscovite-quartz-schist, and micaceous quartzite.

Area III is located in Sec 4, T1N, R2W, F.M. Anomalous elements include Sb, As, W and Cu. Rock types include calcareous actinolitic greenschist, biotite-muscovite-quartz schist, and micaceous quartzite.

Area IV is located in Sec 24, T2N, R2W, F.M. Anomalous elements include Sb, As, Pb, Zn and Cu. Rock type include metamorphosed felsic volcanoclastics, calcareous actinolitic greenschist, impure marble, micaceous quartzite, and sericitically altered granodiorite with disseminated arsenopyrite. The bedrock geology of Areas I through IV is described by Bundtzen (1982).

Area V is located in Sec 18, T2N, R1E, F.M. Anomalous elements include Sb, As, W, Gh, Pb, Zn, Cu and Au. Rock types include metamorphosed felsic volcanoclastics or metachert, calcareous actinolitic greenschist, impure marble, porphyroblastic felsic schist, muscovite-quartz schist, and micaceous quartzite. The bedrock geology of Area V is described by Metz (1982).

Area VI is located in Sec 17, T1N, R1E, F.M. Anomalous elements include Sb, As, W, Pb, Zn, Cu, Au, and Ag. Rock types include metamorphosed felsic volcanoclastics or metachert, impure marble, muscovite-quartz-schist, and micaceous quartzite.

Area VII is located in Sec. 35, T2N, R1E, F.M. Anomalous elements include Sb, As, W, gh, Pb, Zn, Au and Ag. Rock types include metamorphosed felsic volcanoclastics, hornfels, impure marble, muscovite-quartz schist, quartz monzonite and aplite.

Area VIII is located in Sec 12, T1N, R1E, F.M. Anomalous elements include As, Pb, Zn, Au and Ag. Rock types include biotite muscovite quartz schist and micaceous quartzite.

Area IX is located in Sec 25, T2N, R2E, F.M. Anomalous elements include As, W, Gh, Pb and Zn. Rock types include calcareous schist and biotite-muscovite-quartz schist.

Area X is located in Sec 17, T2N, R2E, F.M. Anomalous elements include Sb, As, Hg, Pb and Ag. Rock types include calcareous schist, actinolitic greenschist, hornfels, muscovite-quartz-schist, micaceous quartzite, and quartz monzonite. The bedrock geology of areas VI through X is described by Robinson (1982).

Area XI is located in Sec 35, T3N, R1E, F.M. Anomalous elements include Sb, As, W, Gh, Pb, Zn, Au and Sn. Rock types include metamorphosed felsic volcanoclastics, calcareous schist, muscovite-quartz schist and micaceous quartzite.

Table 6.5 Comparison of average trace element abundances for the Fairbanks mining district with average crustal abundances for all rock types.

Element	Fairbanks mean	Clarke	Multiple of Clarke
Sb	22	0.2	210
As	150	1.8	83
Cu	75	55	1.4
Au	0.1	0.002	50
Pb	17	12	1.4
Hg	3	0.5	6
Ag	0.2	0.07	2.9
Sn	2	2	1
W	21	1.5	14
Zn	40	70	0.6

Table 6.4 Trace element content of the major rock units of the Fairbanks mining district, Alaska.

Termes/ Sample Number/ Description	Element Units	Au PPB	Sb PPM	As PPM	Ba PPM	Cd PPM	Cr PPM	Co PPM	Hf PPM	Fe PCT	La PPM	Mo PPM	Ni PPM	Na PCT	Ta PPM	Th PPM	W PPM	U PPM	Zn PPM
<b>Charanlita</b>																			
3830 Garnet clinopyroxenite		9	0.9	1	<100	12	390	59	5	7.0	48	<2	270	0.66	3	6.1	<2	1.7	1100
3831 Garnet clinopyroxenite		5	7.2	50	420	<5	55	14	6	2.1	38	<2	<50	0.31	4	13.0	4	3.5	<200
3832 Garnet amphibolite		<5	2.2	55	440	<5	64	<10	11	2.3	38	<2	<50	0.15	5	15.0	4	4.2	<200
3833 Muscovite-hornblende schist		19	45.6	46	3100	<5	190	<10	2	1.4	13	13	66	0.41	<1	5.3	<2	4.6	380
3841 Garnet-calc schist		<5	0.4	2	3200	<5	540	75	6	8.4	65	<2	370	0.92	5	8.9	<2	2.8	<200
3842 Garnet amphibolite		<5	1.6	3	1200	<5	530	67	6	10.0	99	<2	380	1.60	5	12.0	<2	2.6	<200
3843 Muscovite-K-Feldspar-schist		<5	3.8	22	530	<5	75	12	8	3.2	38	<2	<50	0.09	<1	17.0	30	2.8	<200
3846 Garnet amphibolite		8	2.7	4	1500	<5	430	39	5	7.5	55	<2	180	2.40	5	8.4	<2	3.0	<200
21342 Marble		<5	1.6	8	1800	<5	300	25	4	5.6	37	<2	75	1.30	3	4.8	4	2.6	<200
21343 Impure marble		<5	1.2	1	5800	<5	370	29	4	5.7	40	<2	100	1.30	3	5.7	<2	1.8	<200
21344 Graphitic metachert		14	14.0	153	1600	31	420	<10	2	1.1	18	24	130	0.26	<1	3.5	18	13.0	670
	i	8	7.4	32	1790	8	306	32	5	4.9	44	5	156	0.85	3	9.1	7	3.9	341
	r	5	13.3	46	1685	8	182	25	3	3.1	23	7	127	0.73	2	4.5	9	3.2	291
<b>Cleary Sequence</b>																			
<b>Metavolcanics/Metathalites</b>																			
197 Banded-muscovite quartzite		110	24.6	54	<100	<5	240	<10	5	0.9	11	<2	<50	<0.05	<1	3.3	88	1.0	<200
198 Banded-muscovite quartzite		46	39.6	369	1300	<5	53	<10	6	1.3	31	8	<50	0.12	<1	12.0	15	1.6	<200
3818 Banded-muscovite quartzite		1260	71.4	2410	150	<6	85	<10	5	7.9	12	<2	<50	<0.40	<1	6.2	30	1.4	<200
3819 Banded-muscovite quartzite		2300	59.2	8920	<100	<7	<50	<10	3	1.5	13	<2	<50	<0.34	<1	5.5	13	<0.5	<200
3824 Banded-muscovite quartzite		81	232.0	839	1900	<9	70	<10	5	2.3	51	<2	<50	<1.10	2	19.0	<8	1.7	800
3835 Metachertite tuff		54	339.0	5310	270	<14	170	<10	3	2.8	27	<3	<50	<1.60	1	7.1	<13	<0.6	<200
3836 Garnet ortho-amphibolite		52	2.8	81	450	<5	690	56	6	10.0	42	<2	240	0.47	4	4.1	<2	1.0	<200
3837 Garnet ortho-amphibolite		110	3.0	86	460	<5	360	51	7	9.4	49	<2	160	0.45	5	4.3	9	1.1	<200
3839 Metachertite tuff w/ sulfide		230	25.1	1060	620	<5	71	11	7	3.6	39	2	54	0.12	1	16.0	17	3.0	<200
21151 Feldspathic-chlorite schist		12	3.4	20	180	<5	280	37	<2	6.5	5	<3	130	2.00	<1	0.6	<2	<0.5	<200
21152 Chlorite-talc schist		1570	324.0	6630	920	<14	120	15	5	4.8	48	<3	<50	<1.50	2	25.0	<10	5.2	<200
21330 Ortho-amphibolite		460	1.8	17	260	<5	730	55	7	10.0	62	<2	200	1.10	5	8.1	4	2.1	230
21331 Feldspathic-muscovite quartzite		29	17.0	403	310	<5	<50	<10	<2	1.1	16	<2	<50	<0.05	<1	5.1	<2	0.8	<200
21335 Banded muscovite quartzite		11	75.1	234	580	<5	67	<10	9	2.0	29	<2	<50	0.06	<1	13.0	<2	1.3	<200
21337 Graphitic schist		35	2.8	25	870	<5	160	13	5	4.7	64	<2	<50	0.10	1	19.1	64	2.4	<200
21346 Banded muscovite quartzite		33	6.1	17	120	<5	92	25	9	5.4	37	<2	<50	0.23	2	26.0	14	4.7	<200
21347 Muscovite-garnet schist		32	2.0	4	680	<5	99	18	7	5.8	46	2	<50	0.90	2	17.0	48	5.1	<200
82SH02 Feldspathic-muscovite schist		42	20.8	856	990	<7	<50	17	6	4.4	54	<2	<50	0.08	2	18.0	74	4.8	<200
82CH02 Chloritic schist w/ sulfides (1)		>30000	54.8	4970	200	<17	360	<10	<3	0.8	6	<7	<50	<0.06	<1	2.8	6	5.8	<200
82BY01 Chloritic schist w/ sulfides (1)		16400	704.0	>30000	320	<30	180	<10	<3	4.6	20	<8	<50	<3.10	<1	11.0	44	<1.3	<200
	i	341	66.8	1440	650	6	184	20	6	4.5	35	2	78	0.56	2	12.0	22	2.4	235
	r	642	107.3	2593	586	3	205	16	2	3.1	18	1	59	0.61	1	7.7	26	1.8	144

Table 6.4 (Continued)

Terrane/ Sample Number/ Description	Element Units	Au PPB	Sb PPM	As PPM	Ba PPM	Cd PPM	Cr PPM	Co PPM	Hf PPM	Fe PCT	La PPM	Mo PPM	Ni PPM	Na PCT	Ta PPM	Th PPM	W PPM	U PPM	Zn PPM	
<b>Clary Sequence</b>																				
<b>Metasediments</b>																				
185	Biotite-muscovite-garnet schist	<5	0.6	8	900	<5	220	18	7	5.2	60	4	<50	1.20	2	19.0	3	3.1	<200	
192	Biotite-muscovite-garnet schist	6	3.7	72	390	<5	120	<10	7	5.3	54	<2	<50	0.45	1	19.0	13	3.9	<200	
3810	Para-amphibolite	8	0.3	<1	1000	<5	81	16	11	3.8	50	<2	<50	1.20	2	24.0	<2	2.5	<200	
3823	Marble	11	26.6	13	<100	<5	<50	<10	<2	<0.5	<5	<2	<50	<0.05	<1	0.7	<2	1.2	<200	
3825	Para-amphibolite (?)	<5	0.9	10	<100	<5	680	25	8	10.0	100	<2	190	0.69	6	14.0	4	4.4	<200	
3826	Muscovite quartzite	<5	1.0	10	420	<5	<50	<10	5	1.8	17	<2	<50	0.32	<1	11.0	<2	1.8	<200	
3827	Marble	6	0.3	2	120	<5	<50	<10	<2	0.7	11	<2	<50	0.14	<1	2.6	<2	1.0	<200	
3838	Biotite-muscovite-garnet schist	9	2.8	17	280	<5	190	26	5	7.6	20	9	84	0.71	<1	6.4	<2	1.3	<200	
20506	Metaconglomerate	12	4.4	65	850	<5	180	<10	7	2.7	33	<2	<50	0.87	<1	14.0	3	2.0	<200	
20510	K-Feldspar-biotite schist	<5	3.0	62	1200	<5	110	18	6	5.1	61	<2	<50	2.50	2	21.0	<2	3.3	<200	
21142	Quartzite	7	0.8	4	410	<5	<50	18	5	2.9	16	3	<50	0.18	<1	8.2	17	2.7	<200	
21147	Quartzite	9	0.6	4	430	<5	<50	24	6	2.7	17	5	<50	0.25	<1	8.6	<2	2.8	<200	
21154	Muscovite schist	11	0.5	2	890	<5	100	20	6	5.7	55	<2	53	0.68	2	20.0	<2	4.7	<200	
21320	Muscovite quartzite (1)	<14	373.0	26	1100	<12	250	<10	6	2.8	35	<4	<50	1.30	<1	15.0	<3	2.8	<200	
21334	Feldspathic biotite garnet schist	13	4.9	25	780	<5	76	<10	7	4.6	52	<2	<50	0.40	1	20.0	12	2.9	<200	
		i	8	5.4	22	558	5	143	16	6	4.2	39	3	63	0.69	2	13.5	5	2.5	<20
		s	3	7.9	26	362	0	165	6	2	2.6	27	2	38	0.64	1	7.4	5	1.3	0
<b>Fairbanks Schist</b>																				
<b>Metasediments</b>																				
3828	Garnet-chlorite-muscovite schist	5	0.9	47	650	<5	<50	<10	7	3.2	33	<2	<50	0.24	<1	14.0	2	2.6	<200	
20505	Biotite-muscovite-quartz schist	<5	0.8	2	820	<5	200	<10	7	4.0	58	<2	<50	0.76	2	16.0	<2	3.0	<200	
20508	Muscovite-quartz schist	<5	0.6	3	110	<5	110	<10	10	1.7	10	<2	<50	0.78	<1	12.0	<2	2.6	<200	
		i	5	0.8	17	527	5	120	10	8	3.0	34	2	50	0.59	1	14.0	2	2.1	200
<b>Goldstream Sequence</b>																				
3809	Biotite-muscovite schist	26	0.3	10	1000	<5	63	<10	8	2.4	41	<2	<50	1.00	<1	17.0	<2	1.4	<200	
3814	Garnet-chlorite-muscovite schist	<5	3.1	217	<100	<5	<50	12	7	1.6	16	3	<50	0.90	<1	7.8	<2	1.2	<200	
3815	Garnet-biotite-muscovite schist	8	5.8	160	87	<5	110	<10	9	3.4	61	<2	<50	1.30	2	24.0	3	5.3	<200	
3816	Garnet-amphibolite	<5	0.4	2	<100	<5	63	43	5	10.0	18	<2	<50	2.80	1	1.4	<2	0.6	<200	
3817	Calcareous schist	<5	0.2	5	260	<5	<50	<10	3	1.2	16	<2	<50	0.71	<1	6.1	<2	<0.5	<200	
3840	Marble	<5	1.3	1	860	<5	<50	<10	<2	1.1	10	<2	<50	0.20	<1	3.4	<2	0.6	<200	
3844	Para-amphibolite	<5	0.5	3	400	<5	200	17	8	3.6	34	<2	110	1.30	2	11.0	<2	2.3	<200	
21324	Graphitic-quartz schist	21	41.3	80	1200	<5	230	<10	4	3.4	29	<2	57	0.07	<1	7.6	13	2.5	300	
		i	10	6.6	60	500	5	102	15	6	3.3	28	2	58	1.04	1	9.8	4	1.8	212
		s	8	14.2	85	452	0	73	12	3	2.9	17	0	21	0.85	1	7.4	4	1.6	35

Table 6.4 (Continued)

Terrane/ Sample Number/ Description	Element Units	Au PPB	Sb PPM	As PPM	Ba PPM	Cd PPM	Cr PPM	Co PPM	Hf PPM	Pb PCT	La PPM	Mo PPM	Ni PPM	Nb PCT	Ta PPM	Th PPM	W PPM	U PPM	Zn PPM
<b>Birch Hill Sequence</b>																			
3811 Graphitic-quartz schist		<5	0.8	7	<100	<5	<50	<10	5	1.5	<5	<2	<50	<0.05	<1	5.2	<2	0.9	<200
3820 Calcareous schist		<5	0.7	8	1300	<5	52	<10	3	2.5	28	<2	<50	1.00	<1	11.0	<2	0.9	<200
3821 Graphitic phyllite		<5	14.0	38	2000	<5	76	<10	<2	1.1	20	7	<50	<0.05	<1	2.7	<2	4.6	<200
3822 Graphitic quartzite		<5	4.2	9	1200	<5	97	<10	<2	1.0	6	5	<50	<0.05	<1	1.0	<2	1.7	<200
20503 Carbonaceous quartzite		<5	4.3	7	2700	<5	210	<10	3	0.7	18	<2	<50	0.06	<1	6.2	4	2.6	<200
20504 Pyritic-banded quartzite		8	6.5	47	690	5	170	15	3	4.4	22	<2	<50	0.07	<1	8.3	12	1.4	<200
	$\bar{x}$	6	5.1	19	1332	5	101	11	3	1.9	16	3	50	0.21	1	5.7	4	2.0	200
	s	1	4.9	18	924	0	77	2	1	1.4	9	2	0	0.39	0	3.6	4	1.4	0
<b>Aplite Dikes</b>																			
3834 Pyritic Aplite		<5	2.9	17	1200	<5	<50	13	9	5.5	65	<2	<50	2.10	1	19.0	8	5.5	<200
20507 Pyritic Aplite		8	8.9	118	1700	<5	<50	<10	9	4.1	65	<2	<50	1.10	2	20.0	<2	6.6	200
	$\bar{x}$	6	5.9	68	1450	5	50	12	9	4.8	65	2	50	1.60	2	19.5	5	6.1	200
<b>Skarns/Hornfels</b>																			
175 Calc-silicate		250	19.0	13	<100	<7	80	16	<19	8.1	27	32	<50	0.10	1	9.2	2240	4.7	250
186 Hornblende hornfels		7	21.9	62	230	<6	700	44	8	9.2	77	<2	180	0.63	6	9.2	12	2.8	<200
190 Calc-silicate		470	24.2	11	<130	<12	96	13	<64	6.8	14	120	<50	<0.05	<1	2.6	5720	4.5	<200
200 Calc-silicate		37	2.2	47	<100	<6	<50	190	5	15.0	18	4	67	<0.10	<1	5.8	3720	6.1	<200
3812 Calc-silicate		110	1.7	5	390	<5	<50	15	<19	5.2	59	<2	<50	0.72	2	17.0	1600	2.4	<200
3813 Calc-silicate		6	1.1	20	790	<5	<50	<10	4	1.3	21	2	<50	2.20	<1	13.0	2	4.9	<200
3829 Garnet-vesuvianite skarn		220	42.1	11	<100	<5	<50	<10	<53	5.9	30	57	<50	0.07	1	5.9	4590	4.9	<200
3845 Sheared hornfels		20	41.9	162	<100	<5	<50	10	4	4.3	16	2	<50	<0.05	<1	5.5	15	2.6	<200
21149 Calc-silicate		<5	1.3	9	520	<5	73	17	4	4.1	37	3	<50	0.77	<1	12.0	85	3.1	<200
21162 Calc-silicate		100	31.8	54	180	<13	53	59	<21	16.0	42	223	<50	<0.33	3	7.9	19800	4.5	290
21341 Epidote hornfels		10	20.1	78	670	<5	150	13	7	3.1	47	22	<50	0.88	<1	20.0	11	14.0	<200
21349 Altered hornfels		130	65.8	233	520	<20	130	39	<73	13.0	59	100	<50	0.15	1	8.7	8260	3.7	<200
	$\bar{x}$	114	22.8	59	320	8	128	36	23	7.7	37	47	62	0.50	2	9.7	3838	4.8	362
	s	141	20.2	71	250	5	183	51	25	4.8	20	69	37	0.62	2	5.0	5711	3.1	517

1) Note: Not included in mean and standard deviation calculation

Area XII is located in Sec 24, T3N, R1E, F.M. Anomalous elements include As, Zn and Cu. Rock types include calcareous schist, impure marble, muscovite quartz schist, micaceous quartzite and eclogite.

Area XIII is located in Sec 31, T3N, R2E, F.M. Anomalous elements include As, W, Pb, Zn and Ag. Rock types include metamorphosed felsic volcanoclastics, actinolitic greenschist, calcareous schist, muscovite-quartz-schist, and micaceous quartzite.

Area XIV is located in Sec 15, T3N, R2E, F.M. Anomalous elements include As, Pb, Zn and Cu. Rock types include metamorphosed felsic volcanoclastics, actinolitic greenschist, muscovite-quartz schist micaceous quartzite and eclogite.

Area XV is located in Sec 27, T3N, R2E, F.M. Anomalous elements include Sb, As, Pb, Zn, Cu and Ag. Rock types include metamorphosed felsic volcanoclastics, calcareous schist, muscovite-quartz schist and micaceous quartzite.

Area XVI is located in Sec 7, T3N, R3E, F.M. Anomalous elements include As, Pb, Zn and Cu. Rock types include metamorphosed felsic volcanoclastics, calcareous schist, biotite-muscovite-quartz schist, actinolitic greenschist, impure marble, and micaceous quartzite.

Area XVII is located in Sec 10, T3N, R3E, F.M. Anomalous elements include Sb, As, Zn and Cu. Rock types include metamorphosed felsic volcanoclastics, calcareous schist, and micaceous quartzite. The bedrock geology of areas XI through XVII is described by Metz (1982).

Area XVIII is located in Sec 31, T3N, R4E, F.M. Anomalous elements include Sb, As, W, Cu and Ag. Rock types include calcareous schist, impure marble, calcareous metaconglomerate, muscovite-quartz schist, and micaceous quartzite. Bedrock geology of the area is described by Robinson (1982).

The seventy-eight "unmineralized" samples indicate that the mineralized sample data should be interpreted with great caution. The sample means for the individual terranes are considerably different and are very different from the grand mean of all 78 samples.

The eclogitic rocks of the Chatanika terrane and their intercalated metasediments have gold contents of less than 20 ppb. These rocks have low Sb, As, and W contents relative to the Cleary sequence; however the eclogitic rocks contain 3 times the Ba, Cr, and Ni contents of any other sequence.

The metavolcanic and exhalative rocks of the Cleary sequence have gold contents that range from 30 ppb to several thousand ppb. Stratabound sulphide horizons within the sequence contain 3 to 30 ppm gold and up to 600 ppm silver. The average Sb (67 ppm) and As (1440 ppm) contents of the metavolcanic/exhalative rocks are two orders of magnitude greater and the average W (22 ppm) content is an order greater than those of any of the metasedimentary rocks of the district.

The correlation coefficients of Au-As, Au-Sb, and Au-W, are 0.84, 0.31, and -0.12 respectively. These data confirm field observations and ore/silicate rock petrologic examinations that show a strong relationship between gold and

arsenopyrite in all rock units; the presence of major sulfosalt mineralization in the metabasic, metafelsic, and metachert units of the Cleary sequence with or without gold mineralization; and the concentration of W in the metacherts and metabasic rocks; and the relatively low W contents of the gold enriched metafelsic rocks.

The Au contents of the metasediments of the Cleary sequence average 8 ppb while the metasediments of the Fairbanks schist, Goldstream sequence, and Birch Hill sequence average 5 ppb, 10 ppb, and 6 ppb respectively. The average Sb contents of these rock types are 5 ppm, 0.8 ppm, 6.6 ppm, and 5.1 ppm respectively; the arsenic contents are 22 ppm, 17 ppm, 60 ppm, and 19 ppm respectively; and the W contents are 5 ppm, 2 ppm, 4 ppm, and 4 ppm respectively.

Two pyritic aplite dikes were sampled to determine the gold content of these late phases of the intrusive complexes. The average Au, Sb, As, and W contents are 6 ppb, 5.9 ppm, 68 ppm, and 5 ppm respectively. Although these limited data do not confirm that the late phase granitic rocks are not the source of these elements in the mineral deposit types described above, the data does support observed field and petrologic evidence that demonstrates little spatial, mineralogical, or petrological association of the Types I, II, IV, and V (see sec. 4.2) mineralization with the granitic rocks.

The samples of the tungsten skarns of the Type III mineralization have average Au, Sb, As, W contents of 114 ppb, 22.8 ppm, 59 ppm, and 3838 ppm respectively. These relatively small bodies of exoskarn are all within Cleary sequence rocks in contact with or adjacent to the Gilmore Dome porphyritic quartz monzonite.

## 6.8 CONCLUSIONS

Stream sediment, pan concentrate, and rock geochemical sampling in the district indicates eighteen additional areas of potential lode mineralization. The high antimony, arsenic, gold, and tungsten concentrations in the Cleary sequence metavolcanic and metaexhalative rocks provide strong evidence for a stratiform volcanogenic primary lode source. The elemental and petrologic associations are similar to the Archean volcanogenic gold deposits of eastern Canada and southern Africa. These deposits generally have low to moderate grades but large tonnages. Based on analogy with the above types of mineralization, the mineral potential of the district may be very large compared to the potential based on the previously accepted epigenetic quartz-vein model.

---

## CHAPTER 7

### FLUID INCLUSION AND STABLE ISOTOPE GEOCHEMISTRY OF THE FAIRBANKS MINING DISTRICT

#### 7.1 INTRODUCTION

Metz (1984) and Metz and Hamil (1987) discuss the preliminary data on the fluid inclusions in the various types

of mineralization, and in the metamorphic and intrusive rocks of the Fairbanks district. These data, in conjunction with sulphur isotopic and mineral paragenetic data are utilized to estimate temperatures, pressures, compositions, and origin of the fluids that formed the various types of mineralization. This investigation is an expansion of the preliminary data base and also includes quantitative analyses of fluid compositions from the various types of mineralization. These data further constrain the models for the origin of the mineralization and can be used as guides for mineral exploration and evaluation.

## 7.2 SAMPLE COLLECTION

### 7.2.1 Sampling of Metamorphic Rocks

Five samples of metamorphic quartz were collected. Three of these samples were within the Cleary sequence (samples 21152, 21320, and 21346, see Ch. 4, Plate II). One sample was from the Fairbanks schist (Sample 20505, see Ch. 4, Plate II) and one sample was from the Goldstream sequence (sample 3809, see Ch. 4, Plate II).

Samples for whole rock and trace element analysis were taken at these same sample locations. The sample material for the fluid inclusion measurements was quartz boudins. The sample sites were selected to avoid visible stratabound and vein mineralization.

### 7.2.2 Sampling of Plutonic Rocks

Four samples of plutonic rocks were collected. The sample sites were the same as reported by Blum (1983) and the sample numbers reflect those locations. Two of the samples are from the Gilmore Dome intrusive and are porphyritic quartz monzonite (81JB137 and 81JB162, see Ch. 4, Plate II). The other two samples are fine-grained granodiorite and porphyritic granodiorite (81JB211 and 81JB213 respectively, see Ch. 4, Plate II). The samples were selected away from any indication of alteration and quartz veining. Primary quartz grains were taken from each sample for the measurements.

### 7.2.3 Sampling of Mineral Deposit Types

At least one occurrence from each of the five mineral deposit types was sampled. These samples were collected to be representative of the mineral deposit type but are not necessarily uniformly distributed geographically.

Two samples of Type I mineralization were collected. These samples 81MIRL22 and 81MIRL19 were from the Wackwitz and Tolovana occurrences respectively (see locs. 62 and 54, Ch. 4, Plate VIII). Euhedral to subhedral quartz was selected from the massive sulphide lenses at each locality.

A single sample of Type II mineralization was collected from the adit at the Silver Fox Mine (sample 81MIRL17, see loc. 91, Ch. 4, Plate VIII). The material is from the sulphide rich vein and is composed of subhedral quartz spatially associated with major arsenopyrite.

Four Type III occurrences were sampled. These included the Gil prospect (Sample 81MIRL06), the Stepovich (Sample 82STEP SCH), the Yellow Pup (Sample 81MIRL26) and the

Tungsten Hill (Sample 82PM202).

These occurrences are shown as locations 116, 116, 117, and 129 on Ch. 4, Plate X. Sample 81MIRL06 is quartz vein material from near vertical scheelite bearing veinlets. Sample 82STEP SCH is scheelite from a high angle quartz veinlet. Samples 81MIRL26 and 82PM202 are subhedral quartz grains from scheelite bearing retrograde skarns.

A total of eleven Type IV occurrences were sampled. Four occurrences were sampled in the Ester Dome area and seven occurrences were sampled in the Cleary Summit area. Three of the four samples in the Ester Dome area were from past producing properties while all of the occurrences in the Cleary Summit area had some record of past production.

Sample 81MIRL03 is from the Clipper Mine, location 150, Ch. 4, Plate VIII. The sample consists of subhedral quartz with visible gold. Sample 81MIRL07 is from the 200 level of the Grant Mine, location 136, Ch. 4, Plate VIII. The sample consists of subhedral quartz with visible gold. Sample 81MIRL15 is massive milky white quartz from the Ryan Lode (see loc. 141, Ch. 4, Plate VIII). The sample is from the ore zone that is estimated to average 0.25 OPT Au. Sample 81MIRL13 is from the Rogach prospect, location 166, Ch. 4, Plate VIII. The sample consist of euhedral quartz from the one meter (3.25 foot) wide vein that averages 0.51 OPT at the sample site. In addition to visible gold the sample contains abundant galena and traces of sphalerite. This is the only sampled location on Ester Dome that does not have a record of gold production.

Sample 81MIRL08 is from the lower level of the Hi-Yu Mine, location 7, Ch 4, Plate VIII. The material is milky white quartz with major sphalerite and minor boulangerite and gold. Sample 82NA01 is from the Christina vein in the Nordale Adit, location 24, Ch 4, Plate VIII. The material is milky white quartz with major pyrite and jamesonite and minor boulangerite. There is no visible gold in the sample. Sample 82CA03 is from the Christina vein in the Christina Adit, location 24, Ch 4, Plate VIII. The material is milky white quartz and boulangerite with no visible gold. Sample 81MIRL21A is from the Christina vein on the surface above the Christina Adit (sample location 28, Ch 4, Plate VIII). The material is milky white quartz with abundant gold, arsenopyrite, galena, and boulangerite. Sample 81MIRL21B is from the Christina vein approximately 100 meters (325 feet) west of sample 81MIRL21A. The material is milky white highly fractured quartz with major stibnite filling the fractures. The quartz is thus probably associated with Type IV rather than Type V mineralization. Sample 82CH02 is from the Cleary Hill Mine, location 47, Ch 4, Plate VIII. The material is milky white quartz with arsenopyrite and no visible gold. Sample 81MIRL25 is from the Wyoming Mine, location 48, Ch 4, Plate VIII. The material is milky white quartz with visible gold. Sample 82TV05 is from the Tolovana Mine, location 54, Ch 4, Plate VIII. The material is milky white quartz with abundant boulangerite and gold. The 0.6 meter (2 foot) wide quartz vein cuts several 10 cm (4 inch) thick lenses of jamesonite in metafelsite at the sample location. Sample 82NB01 is from the Newsboy Mine, location 60, Ch

4, Plate VIII. The material is milky white quartz with no visible gold. The above Type IV mineralized samples from the Cleary Summit area are all from veins with past gold production although the production from the Wyoming is probably less than a few thousand troy ounces.

Three Type V mineral occurrences were sampled. Only two locations contained quartz that was probably related to the stibnite mineralization. The third occurrence did contain large scheelite grains with abundant fluid inclusions.

Sample 81MIRL05 is from the Farmer prospect, location 170, Ch 4, Plate VIII. The sample material is highly fractured milky white quartz crosscut by massive stibnite. This later stage quartz crosscuts earlier stage iron-stained quartz and fault breccia. The earlier stage quartz is reported to contain visible gold but none is noted in the later stage quartz and stibnite.

Sample 81MIRL16 is from the Scrafford Mine, location 109, Ch 4, Plate VI. The material is milky white quartz in massive fine-grained stibnite. This material is considered the most representative of the Type V mineralization.

Sample 81MIRL09 is from the Johnson prospect, location 53, Ch 4, Plate VI. The material is coarse-grained scheelite and stibnite. The coarse-grained stibnite and scheelite are in a shear that cross-cuts very fine-grained stibnite, fine-grained scheelite, pyrite, and minor galena in white-mica quartzite and chlorite schist. The mineralization in the quartzite and schist is parallel to the compositional layering with individual lenses up to 15 cm (6 inches) thick. There is no quartz obviously associated with the late cross-cutting antimony mineralization.

#### 7.2.4 Sampling within Mineral Deposit Types

The limited exposure of most of the mineral occurrences precluded extensive sampling laterally and vertically within the occurrences. The Christina vein system was the only exception. Sample 82NA01 was taken approximately 60 meters (200 feet) below and 550 meters (1,800 feet) east of sample 82CA03. Sample 81MIRL21A was taken approximately 60 meters (200 feet) above 82CA03 and 81MIRL21B was taken 100 meters (325 feet) west of sample 81MIRL21A. Thus the vein has been sampled over a 120 meter (400 foot) vertical interval and over a strike length of 650 meters (2,100 feet).

#### 7.3 FLUID INCLUSION CLASSIFICATION BY MAJOR COMPONENTS

The classification system of Weisbrod (1981) is used to categorize the fluid inclusions in the various lithologies and mineral occurrences. The four main types are:

1. Type L inclusions contain primarily liquid with no daughter phases. These inclusions homogenize to a liquid phase.
2. Type V inclusions are dominantly vapor without solid phases. These inclusions homogenize to a vapor.

3. Type C inclusions contain one aqueous liquid, one carbonic liquid, and a complex vapor phase. These inclusions homogenize to a liquid.

4. Type S inclusions always contain at least one crystal. The liquid phase usually is dominant over the vapor phase, thus the inclusions homogenize to a liquid.

Transitional types exist between these end member types. For example inclusions intermediate between Type L and Type V are common and some of these may exhibit critical homogenization. Some Type S inclusions may contain significant amounts of carbon dioxide as evidenced by the dark appearance of the vapor phases or by the presence of liquid carbon dioxide.

The type of inclusion can also be distinguished by its morphology. The Type L inclusions are generally very irregularly shaped while the Type C inclusions are usually more equi-dimensional. Negative crystal shapes are not uncommon for the Type C inclusions.

#### 7.4 ESTIMATION OF FLUID INCLUSION ABUNDANCE

A rigorous estimation of fluid inclusion abundance in the various rock types and ores has not been attempted. The abundance of inclusions in the metamorphic and igneous quartz is low compared to the abundance in the vein ores. In a field of view of the microscope at 600X, the metamorphic and igneous samples generally contain one to four inclusions that are in the 10-20 micron range. In contrast, the highly mineralized vein quartz may contain an order of magnitude more inclusions. The mineralized veins also tend to contain inclusions that are in the 20-70 micron range thus the total fluid volume in the vein ores may be 500 times the volume in the other rock types.

#### 7.5 FLUID INCLUSION MICROTHERMOMETRY

Fluid inclusion heating and cooling measurements were made in order to estimate fluid compositions and trapping temperatures. Doubly polished wafers were prepared using a low speed diamond saw and low temperature waxes as adhesives in order to prevent microfracturing and autodecrepitation respectively. Temperature measurements were made on Linkam Th 600 heating and cooling instruments. Calibrations were made at -56.6°C (pure CO<sub>2</sub> inclusion), 0°C (pure water), 100°C (Merck 9700), 200°C (Merck 9800), 398°C (potassium dichromate), and 592°C (nitrobarite).

Twenty-five freezing measurements were made on each sample to confirm the presence or absence of carbon dioxide and to estimate the chloride species in solution. In the absence of CO<sub>2</sub>, the last melting of ice was used to determine salinities. In the presence of CO<sub>2</sub>, the clathrate melting temperatures were used to determine salinities by the method of Collins (1979). Carbon dioxide liquid-vapor homogenization measurements and volume percent estimates were made to allow for the calculation of the mole percentages of CO<sub>2</sub> and H<sub>2</sub>O by the method of Burrus (1981).

At least twenty-five liquid-vapor homogenization measurements were made on each sample. Particular note was made of samples containing liquid rich and vapor rich inclusions that homogenized to liquid and vapor phases at the same temperature thus indicating effervescence of the vapor phase. Decrepitation temperatures were recorded if decrepitation preceded homogenization.

### 7.5.1 Data Summary

#### 7.5.1.1 Fluids in Metamorphic Quartz

The primary fluid inclusions in the metamorphic quartz are relatively small (0.005 to 0.010 mm) negative crystal shaped inclusions. The abundance of the inclusions is low, with one to four inclusions in a field of view of the microscope (0.3 mm in diameter).

These primary inclusions are predominantly low salinity (2-6 weight percent NaCl equiv.). Type C inclusions as evidenced by clathrate melting temperatures of 8.0 to 10.0°C. These inclusions homogenize at 300 to 350°C (see Figures 7.1 thru 7.5). A limited number of Type L inclusions is noted with similar salinities and slightly lower homogenization temperatures (280 to 320°C).

The Type C inclusions are estimated to contain less than 10 mole percent CO<sub>2</sub> with an average of 5 mole percent. These CO<sub>2</sub> contents probably do not reflect the average CO<sub>2</sub> content of the metamorphic rocks in the district due to the limited sampling of the diverse metamorphic lithologies.

#### 7.5.1.2 Fluids in Plutonic Quartz

The primary fluid inclusions in the plutonic quartz are also relatively small (0.1 to 0.2 mm). Negative crystal shapes are predominant and inclusion abundances are low (two to five inclusions in a field of view).

The primary inclusions are usually Type L or Type S but Type C are noted in sample 81JB213. The salinities are moderate, at 20 to 35 weight percent NaCl equivalent. First melting temperatures for the ice indicate that the chloride species include NaCl, and either NaCl-MgCl<sub>2</sub>, or NaCl-CaCl<sub>2</sub>, with the latter the more likely combination.

The primary inclusions homogenize to a liquid at 425 to 550°C with an average of about 475°C (see Figures 7.6 thru 7.9). The Type S and Type C inclusions homogenize at a slightly higher temperature with an average of about 500°C.

The CO<sub>2</sub> contents of the Type C inclusions are estimated at less than 5 mole percent. Since Type C inclusions comprise less than five percent of the primary inclusions measured in the plutonic quartz. These estimates may not be representative of CO<sub>2</sub> content of the porphyritic granodiorite of the Pedro Dome area or of the intrusive rocks of the entire district.

#### 7.5.1.3 Fluids in Type I Mineral Occurrences

The primary fluid inclusions in Type I mineral occurrences (volcanogenic stratabound sulphides) are small (0.010 to 0.025 mm) irregularly shaped inclusions. The abundance of the inclusions is moderately high with five to ten in a field of view (600x magnification).

These primary inclusions are low salinity with clathrate melting temperatures of 9.0 to 10.5°C. The clathrate melting temperature above 10.1 suggests the presence of another gas phase which is probably methane. Carbon dioxide melting temperatures of -58.8 to -59.2°C also indicate the presence of methane. Although the salinities cannot be calculated with certainty due to the presence of methane it is highly unlikely that they exceed 10 weight percent NaCl equivalent. The lowest temperature of the first melting of ice is -22.3°C. This freezing point depression is close to the eutectic temperature of NaCl-KCl (-22.9°C). The host rock is a metafelsic tuff. The rock contains 70 percent quartz and 25 plus percent white-mica thus a high potassium content in the fluid inclusions is expected.

At 40°C, the CO<sub>2</sub> occupies up to 30 volume percent of the inclusions, it homogenizes to vapor at 30°C. From these data, it is estimated that the CO<sub>2</sub> content of the inclusions is 10 mole percent.

The primary inclusions homogenize at 250 to 330°C with a mean value of approximately 300°C (see Figures 7.10 and 7.11). Using the data of Franck (1977), the maximum two phase region at 300°C for a fluid composition 88.6 mole percent H<sub>2</sub>O, 9.7 mole percent CO<sub>2</sub>, and 1.7 mole percent NaCl is at 0.9 kilobars.

#### 7.5.1.4 Fluids in Type II Mineral Occurrences

The primary fluid inclusions in the single sample of Type II mineralization (intrusive hosted gold and silver) are small (0.005 to 0.020 mm) negative crystal shaped inclusions. The inclusion abundance is low with one to five inclusions in the field of view of the microscope at 600x magnification.

These primary inclusions are low to moderate salinity (6 to 15 weight percent NaCl equiv.) Type L inclusions. The inclusions homogenize to a liquid at 300 to 390°C (see Figure 7.12). A few of the inclusions contain relatively dark vapor phases indicating the possible presence of CO<sub>2</sub>. This is not confirmed by freezing measurements since the small size of the inclusions make the observation of such measurements difficult.

#### 7.5.1.5 Fluids in Type III Mineral Occurrences

The primary inclusions in Type III mineral occurrences (tungsten skarn and associated quartz-scheelite veins) are medium sized (0.010 to 0.030 mm) negative crystal shaped inclusions. The abundance is relatively high with ten to twenty inclusions in the field of view of the microscope.

The primary inclusions are probably moderately saline Type C inclusions. Clathrate melting temperatures range from 7.2 to 10.5 indicating the presence of a gas phase other than CO<sub>2</sub>. The CO<sub>2</sub> melting temperatures of -57°C suggest that the other gas phase, probably methane, is not in great abundance. These data preclude a definitive estimation of salinity but it may range from 5 to 15 weight percent NaCl equivalent.

The CO<sub>2</sub> occupies between 10 and 20 volume percent at 40°C and homogenizes to a vapor at 30°C. From these data,

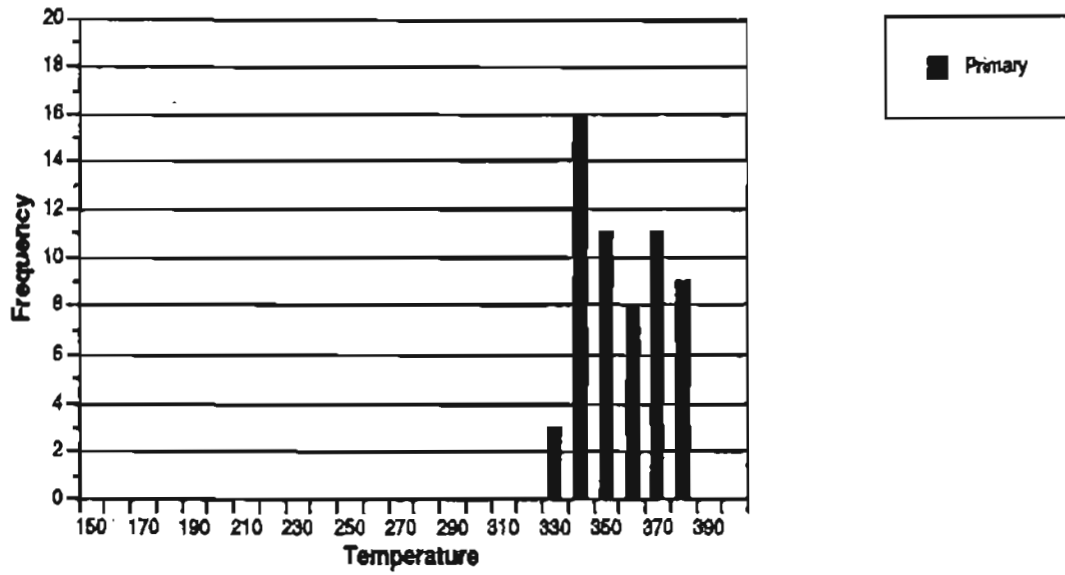


Figure 7.1 Histogram of homogenization temperatures of fluid inclusions in metamorphic quartz, sample 3809.

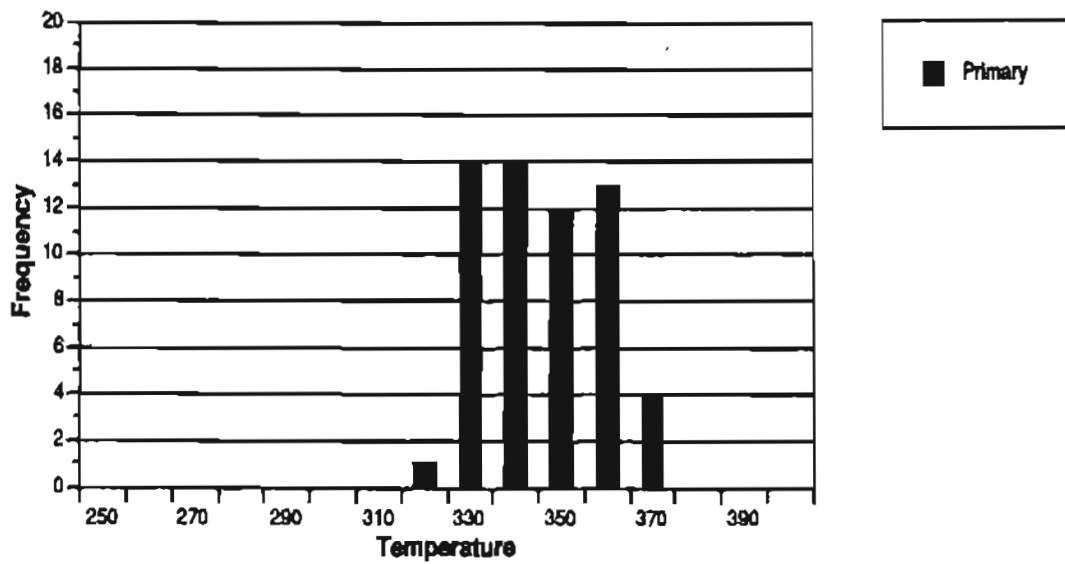


Figure 7.2 Histogram of homogenization temperatures of fluid inclusions in metamorphic quartz, sample 20505.

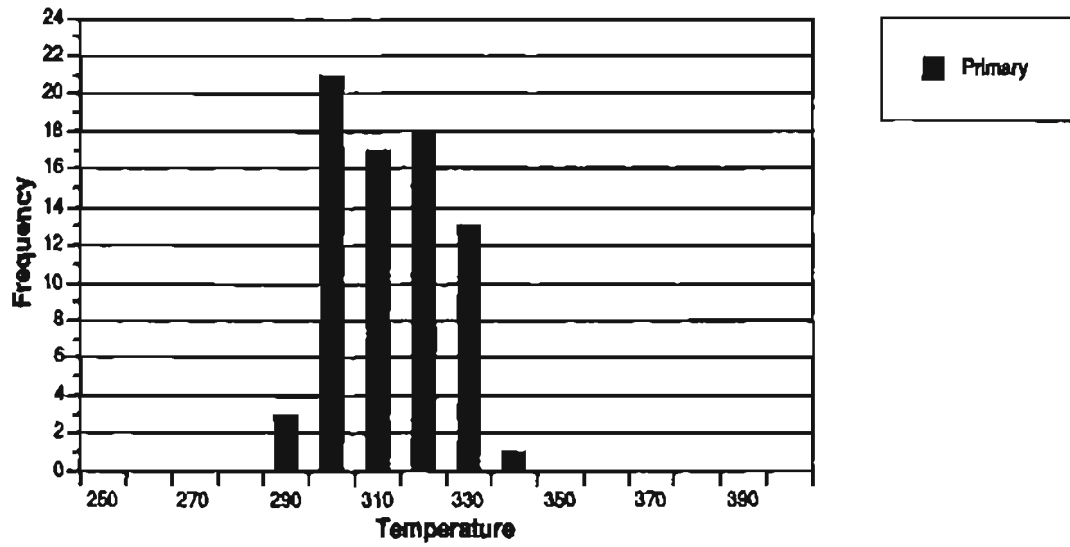


Figure 7.3 Histogram of homogenization temperatures of fluid inclusions in metamorphic quartz, sample 21152.

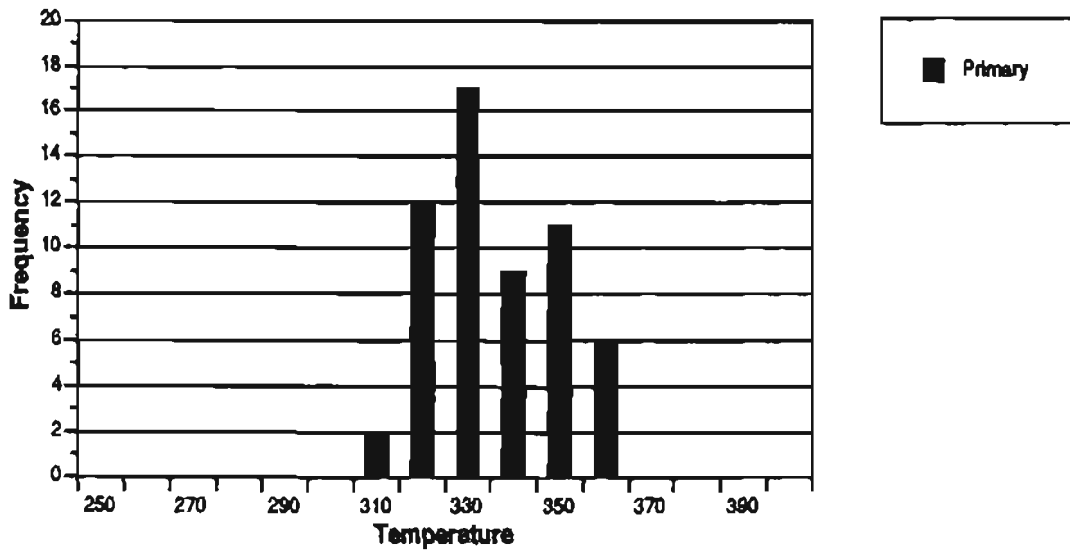


Figure 7.4 Histogram of homogenization temperatures of fluid inclusions in metamorphic quartz, sample 21320.

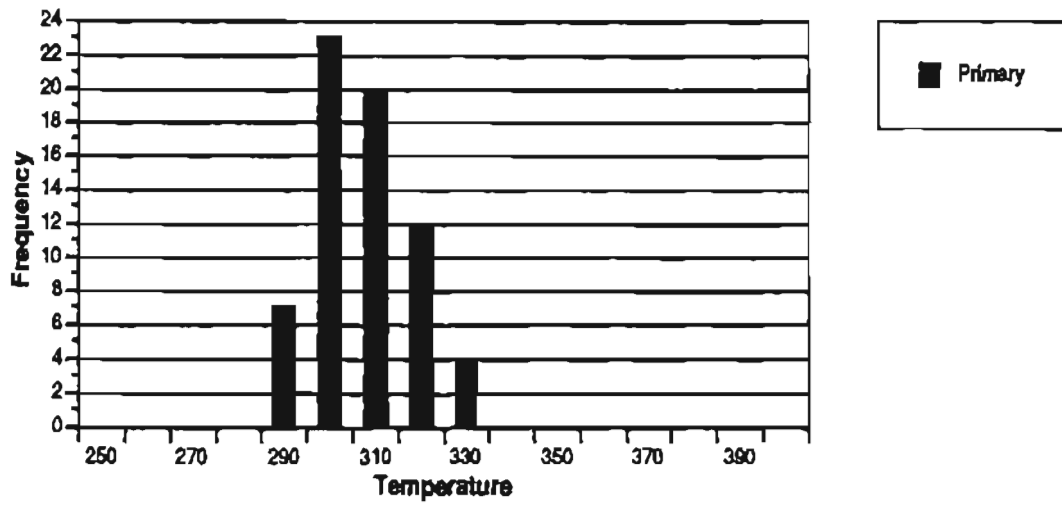


Figure 7.5 Histogram of homogenization temperatures of fluid inclusions in metamorphic quartz, sample 21346.

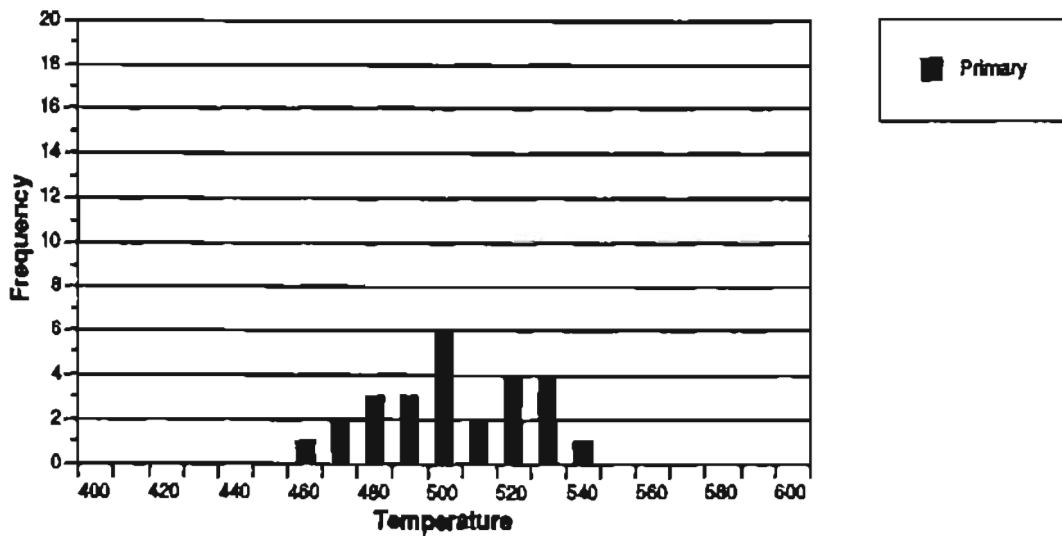


Figure 7.6 Histogram of homogenization temperatures of fluid inclusions in plutonic quartz, sample 81JB137.

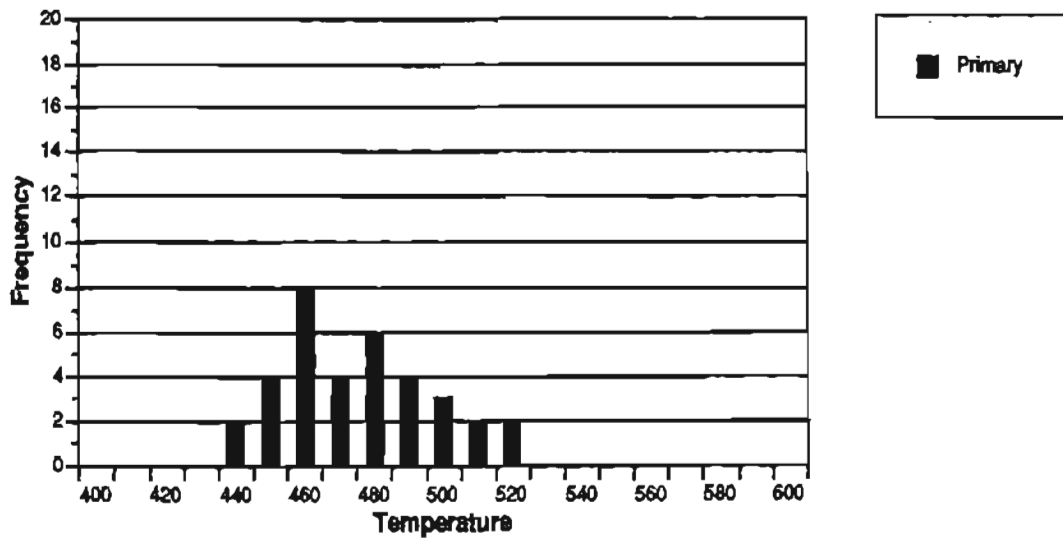


Figure 7.7 Histogram of homogenization temperatures of fluid inclusions in plutonic quartz, sample 81JB162.

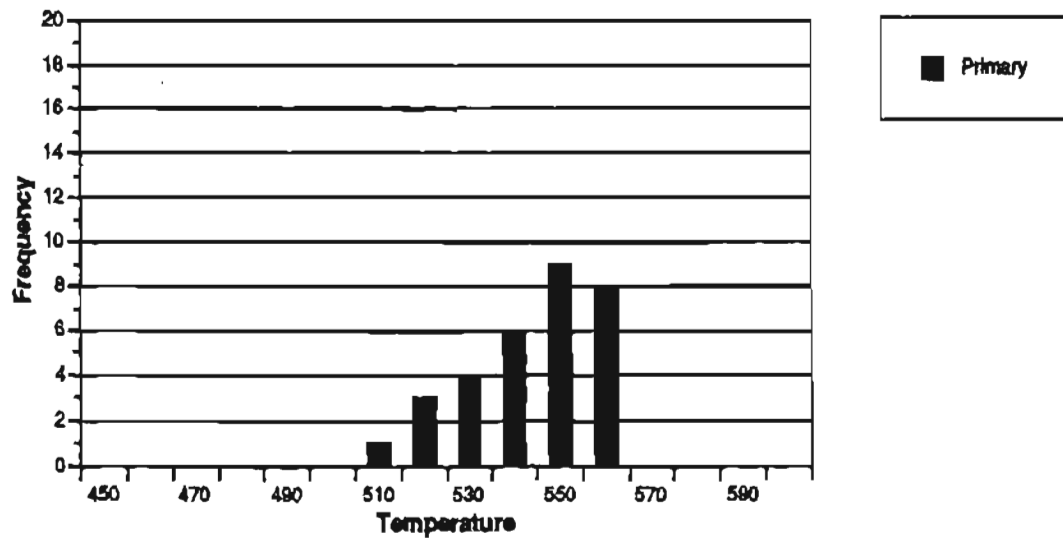


Figure 7.8 Histogram of homogenization temperatures of fluid inclusions in plutonic quartz, sample 81JB221.

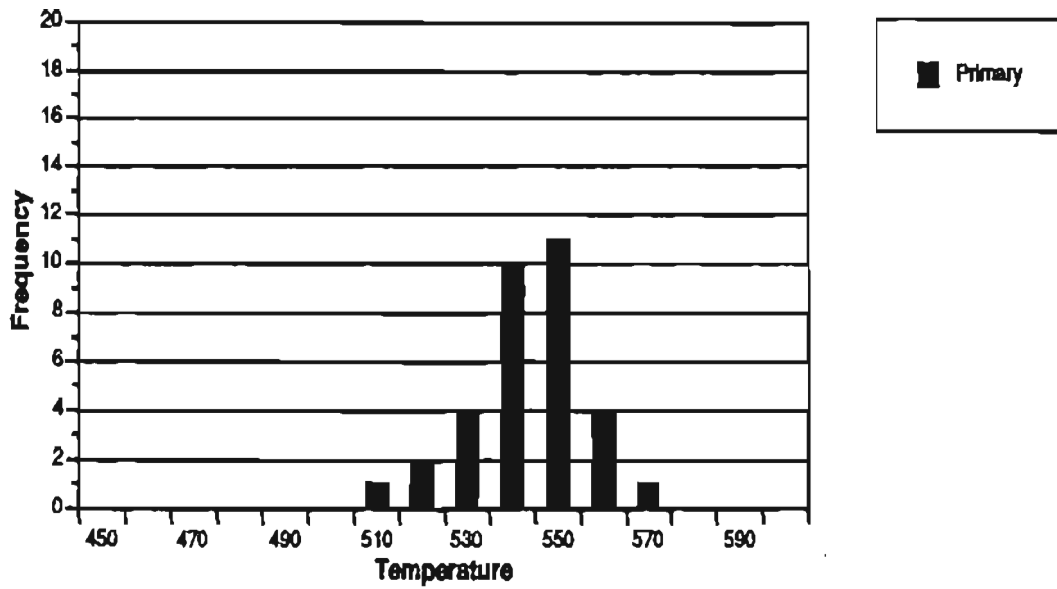


Figure 7.9 Histogram of homogenization temperatures of fluid inclusions in plutonic quartz, sample 81JB213.

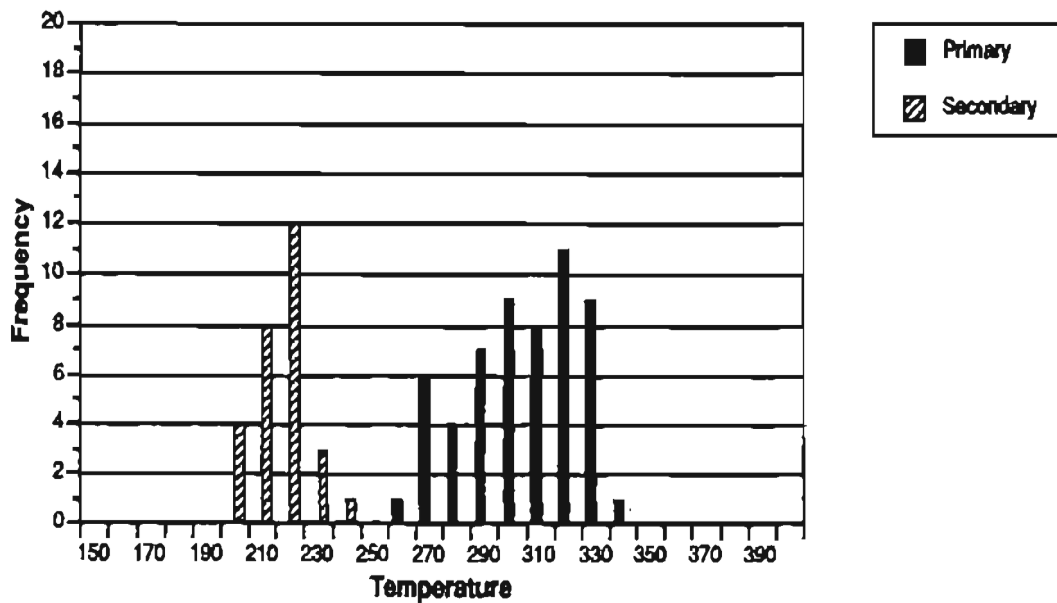


Figure 7.10 Histogram of homogenization temperatures of fluid inclusions in quartz from the Wackwitz prospect, sample 81MIRL22A.

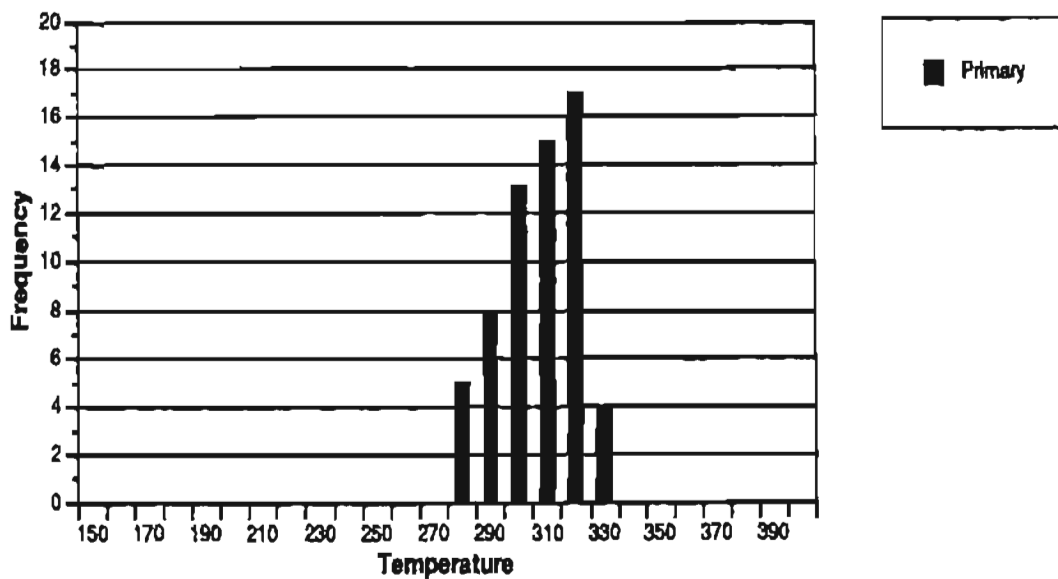


Figure 7.11 Histogram of homogenization temperatures of fluid inclusions in quartz from the Tolovana prospect, sample 81MIRL19A.

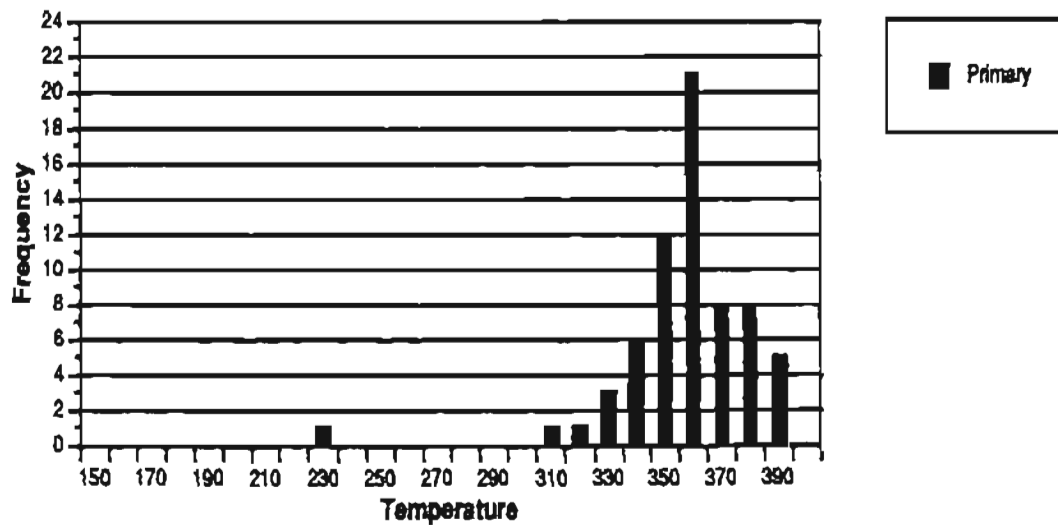


Figure 7.12 Histogram of homogenization temperatures of fluid inclusions in vein quartz from the Silver Fox Mine, sample 81MIRL17A.

it is estimated that the CO<sub>2</sub> content of the inclusions does not exceed 2 mole percent.

The primary inclusions homogenize to a liquid at 300 to 380°C (see Figures 7.13 thru 7.16). These data should be regarded with caution since there are only four samples from the Type III mineralization.

#### 7.5.1.6 Fluids in Type IV Mineral Occurrences

The primary fluid inclusions in Type IV mineral occurrences (metamorphic hosted gold-quartz vein occurrences) are relatively large (0.020 to 0.18 mm) variably shaped inclusions. The larger inclusions are irregularly shaped while the smaller inclusions are generally negative crystal shaped. The abundance of the inclusions varies from less than ten to over fifty in a field of view of the microscope. The areas with high abundances usually contain relatively small inclusions. Individual large inclusions nearly fill the field of view of the microscope.

The primary inclusions are low salinity (2-6 weight percent NaCl equiv.) Type C inclusions. Clathrate melting temperatures are 8.5 to 10.0°C. These Type C inclusions are dominantly liquid rich although vapor rich sub-types are present. These primary inclusions homogenize to liquid and vapor phases respectively at 260 to 340°C (see Figures 7.17 thru 7.29). This suggests that the inclusions were trapped at temperatures and pressures along the upper limit of the two phase boundary for the fluid. The samples that indicate such conditions also contain abundant visible gold.

The CO<sub>2</sub> content of the primary inclusions is highly variable. The sample with the greatest estimated abundance is 81MIRL07. Several inclusions in this sample contain 60 volume percent CO<sub>2</sub> at 40°C. The CO<sub>2</sub> homogenizes to a liquid at 25°C. From these data, it is estimated that the CO<sub>2</sub> content is 22 mole percent. These high CO<sub>2</sub> content inclusions all decrepitate prior to homogenization of the liquid phases.

Secondary inclusions are Type L inclusions and are generally smaller and less abundant than the primary inclusions. The secondaries have slightly lower salinities than the primaries but may have appreciable CO<sub>2</sub> contents. The secondary inclusions homogenize over a wide range from 130 to 250°C.

#### 7.5.1.7 Fluids in Type V Mineral Occurrences

The primary fluid inclusions from the monomineralic stibnite occurrences (Type V) are relatively small (0.010 to 0.025 mm) irregular shaped inclusions. The abundance of the inclusions is low with two to six in the field of view of the microscope.

The primary inclusions are low salinity (2-6 weight percent NaCl equiv.) Type L inclusions. The vapor phase is dark and freezing experiments indicate the presence of CO<sub>2</sub>. Liquid CO<sub>2</sub> is noted in several inclusions. In such inclusions the clathrate melting temperatures range from 9.3 to 10.1°C. The CO<sub>2</sub> melting temperatures are suspect due to the small size of the inclusions but none indicated CO<sub>2</sub> melting point depressions. The inclusions with visible liquid CO<sub>2</sub> ho-

mogenized by critical phenomena at 31°C. The CO<sub>2</sub> vapor phase occupies approximately 20 volume percent at 40°C. From the above data the CO<sub>2</sub> content is estimated at 3 mole percent.

The homogenization temperatures of the primary inclusions in quartz range from 180 to 200°C (see Figures 7.30 thru 7.32). The higher temperature primary inclusions are from the Farmer prospect and the sampled quartz may not be cogenetic with the stibnite. The temperatures of homogenization for the sample from the Scrafford Mine are considered more representative of the probable temperature range of the mineralization.

The primary inclusions in the scheelite from the Johnson prospect have homogenization temperatures that range from 260 to 300°C. The salinity and CO<sub>2</sub> contents are as described above for the other two samples.

These data suggest temperature of formation of these occurrences is considerably less than that of the gold-quartz veins. Considerable uncertainty exists however, due to the small sample size and lack of sample homogeneity.

#### 7.5.1.8 Discussion

The fluid inclusions from Type I mineralization are similar in composition to those from the other metamorphic rocks. The homogenization temperatures are also similar. The latter observation is expected since both were subjected to the same regional metamorphic event. However the homogenization temperatures of the stratabound mineralization could reflect original homogenization temperatures associated with ore formation. Hannington et al. (1986) report gold in polymetallic sulphides forming on the Juan de Fuca Ridge at a depth of 1,500 meters. The hydrothermal fluids from which the metals are precipitation may exceed 300°C in temperature. The inclusions in the Type I mineralization indicate that the fluids were trapped at pressures greater than 0.9 kilobars since there is no indication of phase separation. This pressure would equate to a depth of 10.5 kilometers (34,000 feet) which is highly unlikely. The inclusions in Type I mineralization are thus interpreted as metamorphic fluids trapped during recrystallization of the ores.

The inclusions in Type I mineralization have higher methane contents than any other rock or ore hosted inclusions. The high methane content of the stratabound mineralization suggests a more reducing environment than that of either the intrusive related mineralization or the gold-quartz vein mineralization.

The Type IV mineralization exhibits similar ranges in homogenization temperatures of fluid inclusions as those in the metamorphic host rocks, including the stratabound sulphide occurrences. Inclusions in vein quartz have salinities similar to inclusions in the metamorphic quartz, but the CO<sub>2</sub> content of the vein inclusions is up to an order of magnitude greater.

The inclusions from the Type II and III mineralization are more saline than those from either the metamorphic rocks or from the Type IV mineralization. These salinities are

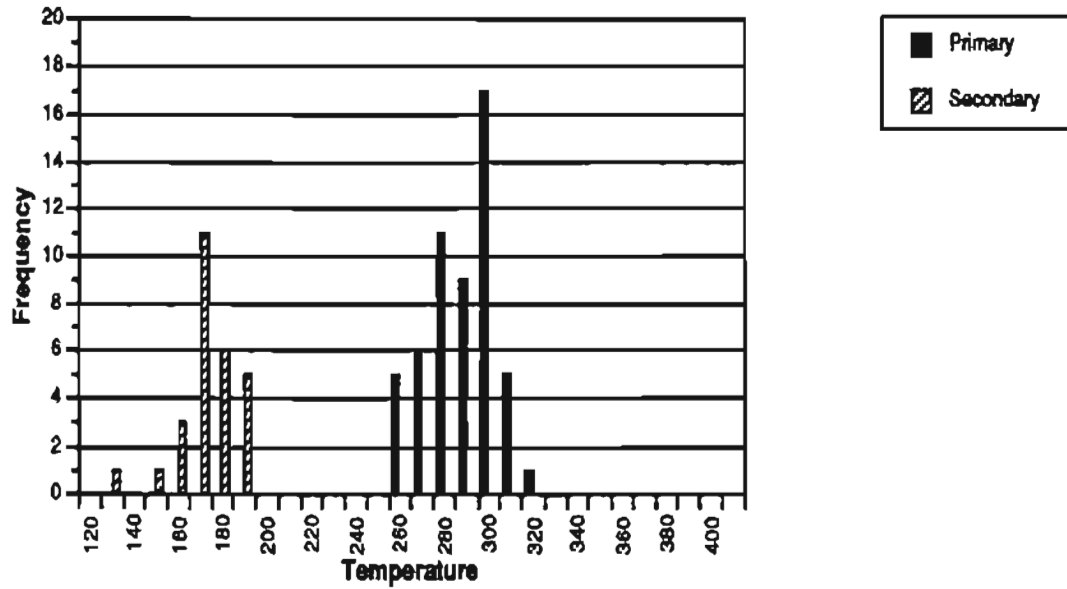


Figure 7.13 Histogram of homogenization temperatures of fluid inclusions in vein quartz from the Gil prospect, sample 81MIRLO6.

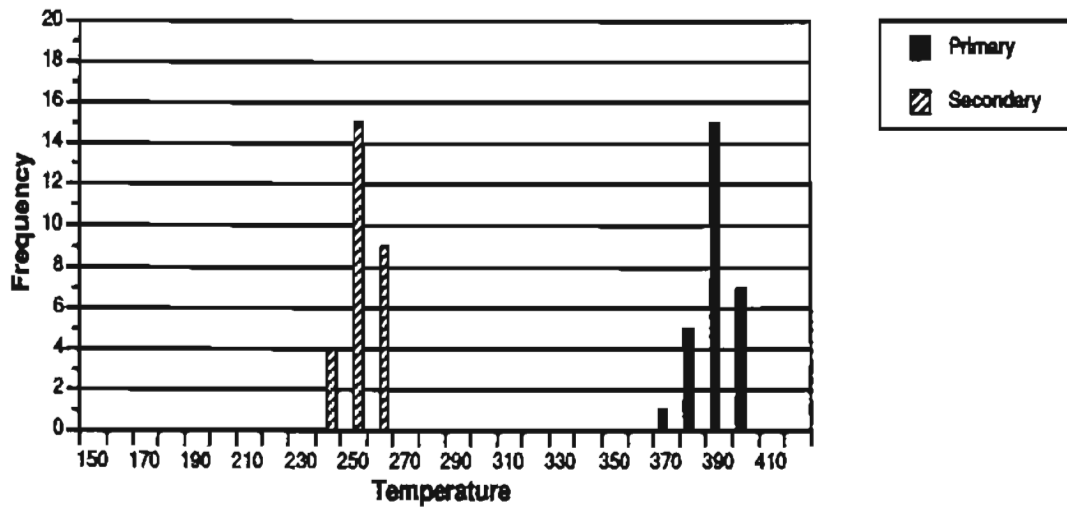


Figure 7.14 Histogram of homogenization temperatures of fluid inclusions in scheelite from the Stepovich prospect, sample 82STEP SCH.

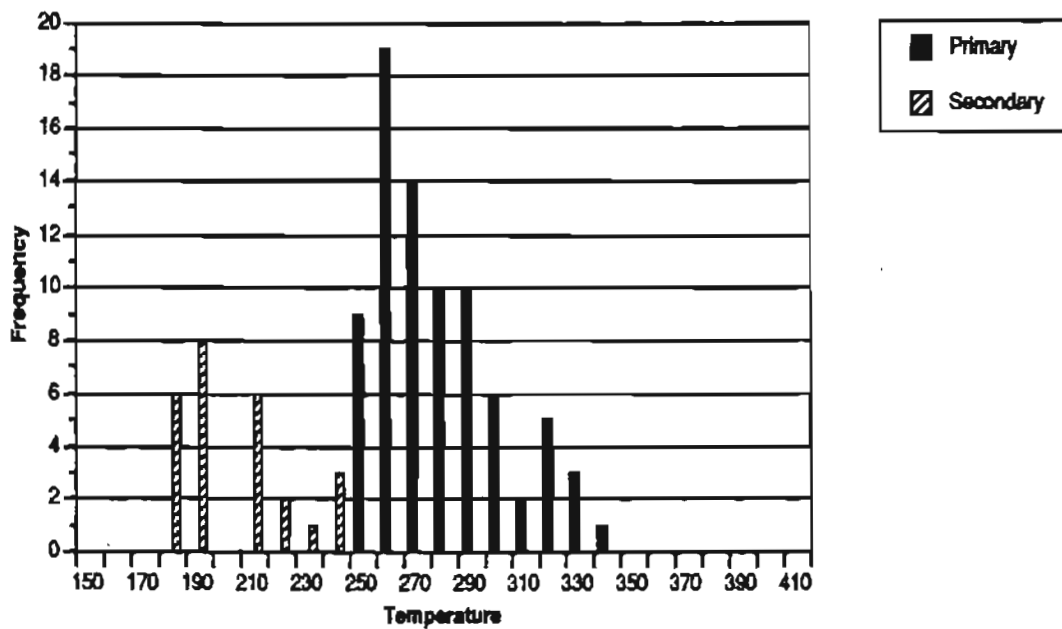


Figure 7.15 Histogram of homogenization temperatures of fluid inclusions in quartz from the skarn mineralization at the Yellow Pup prospect, sample 82YP01.

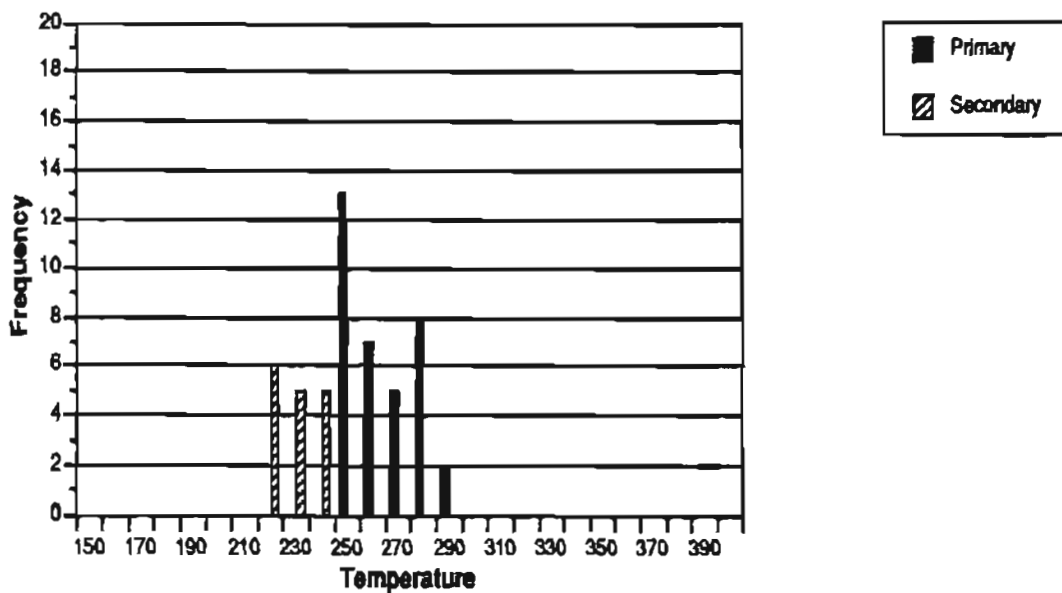


Figure 7.16 Histogram of homogenization temperatures of fluid inclusions in quartz from the skarn mineralization at the Tungsten Hill prospect, sample 81PM202.

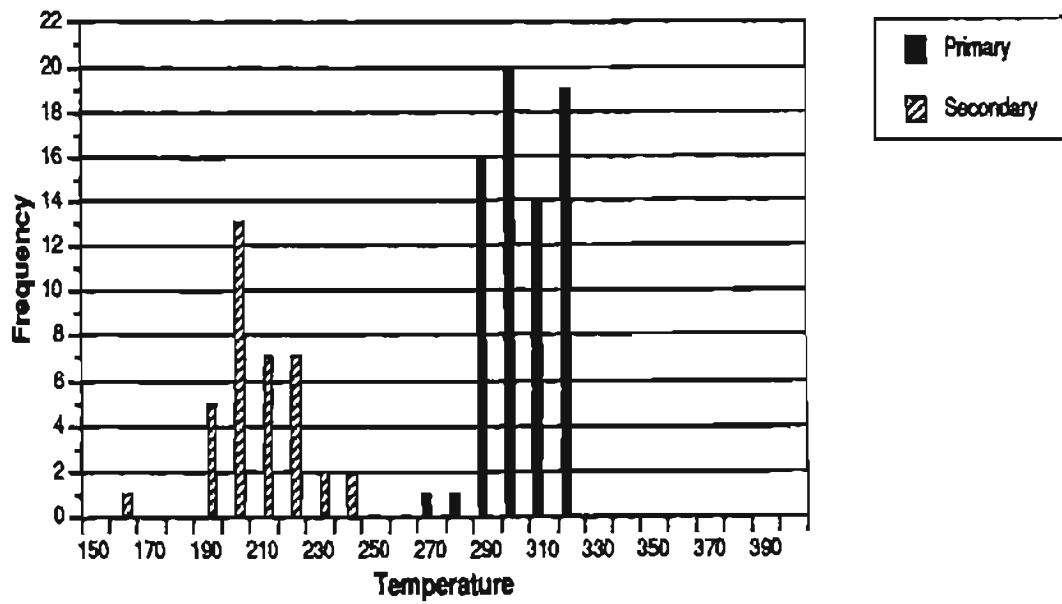


Figure 7.17 Histogram of homogenization temperatures of fluid inclusions in vein quartz from Hi-Yu Mine, sample 81MIRL08.

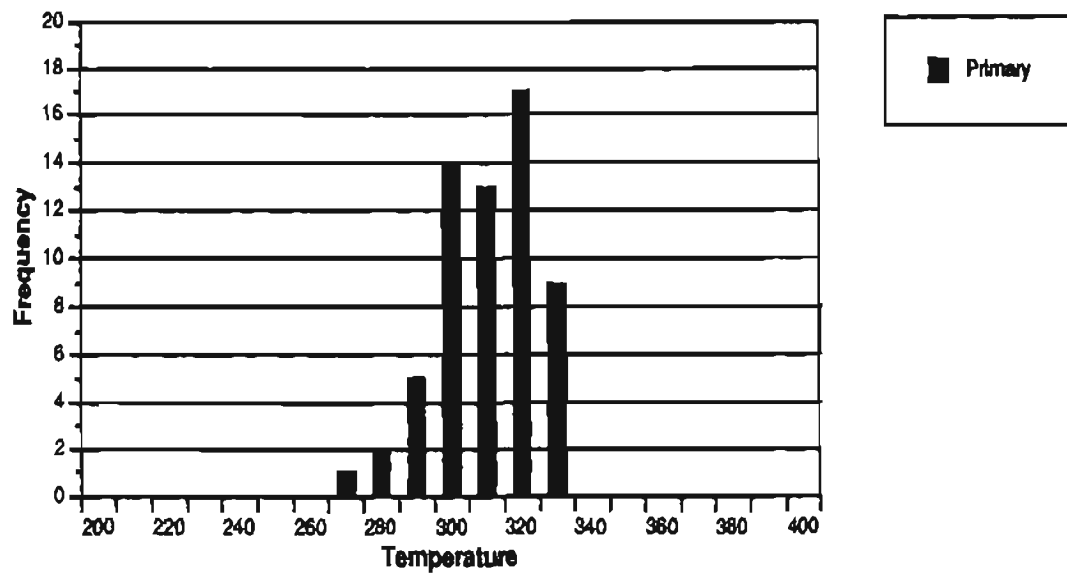


Figure 7.18 Histogram of homogenization temperatures of fluid inclusions in vein quartz from the Christina vein, sample 82NA01.

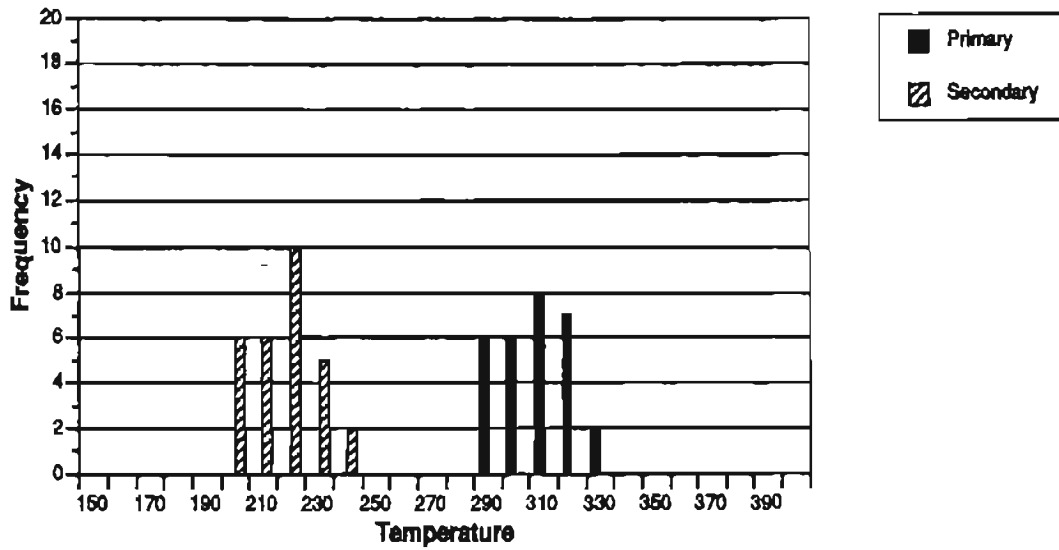


Figure 7.19 Histogram of homogenization temperatures of fluid inclusions in vein quartz from the Christina vein, sample 82CA03.

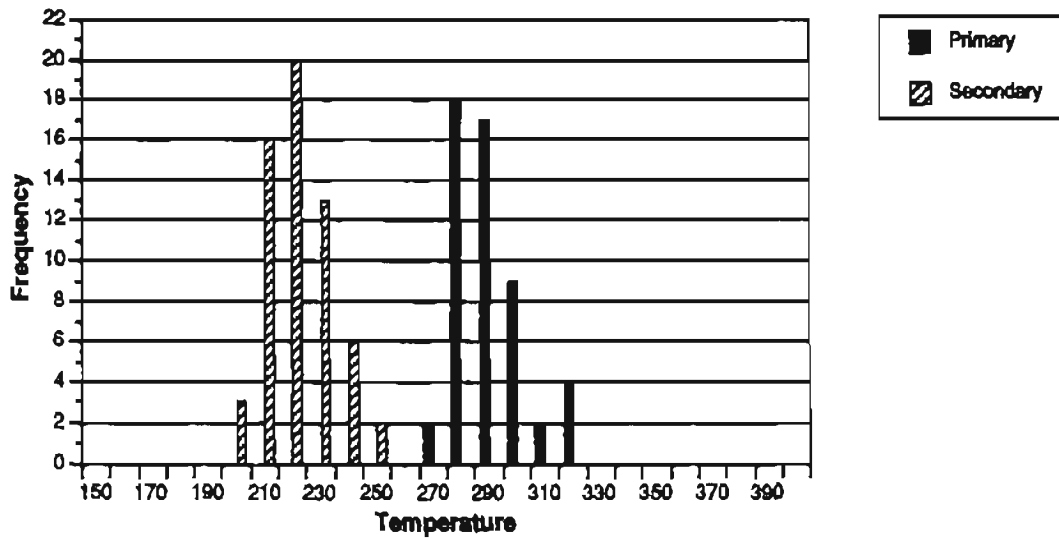


Figure 7.20 Histogram of homogenization temperatures of fluid inclusions in vein quartz from the Christina vein, sample 81MIRL21A.

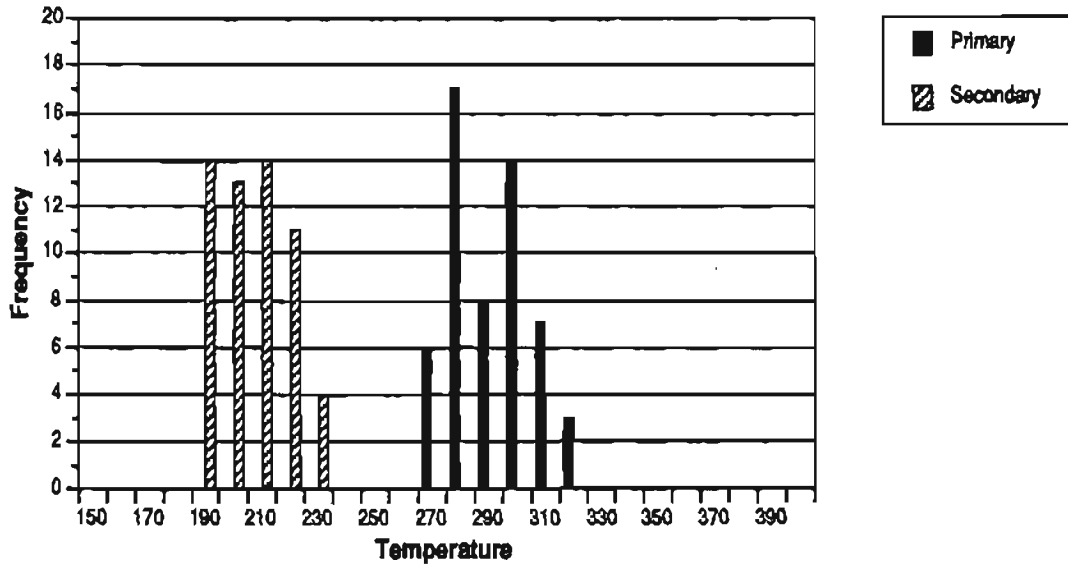


Figure 7.21 Histogram of homogenization temperatures of fluid inclusions in vein quartz from the Christina vein, sample 81MRL21B.

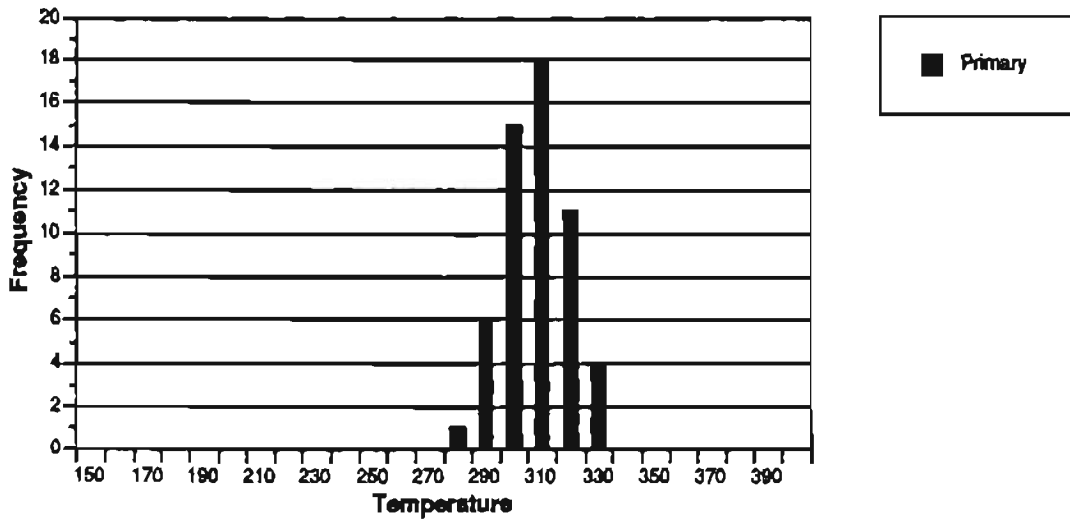


Figure 7.22 Histogram of homogenization temperatures of fluid inclusions in vein quartz from the Cleary Hill Mine, sample 82CH02.

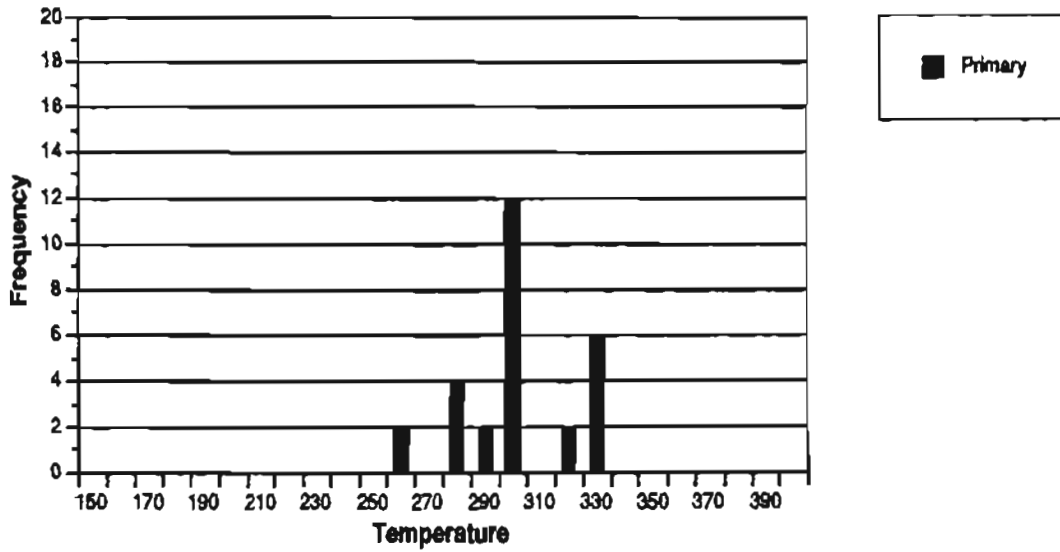


Figure 7.23 Histogram of homogenization temperatures of fluid inclusions in vein quartz from the Wyoming Mine, sample 81MIRL25.

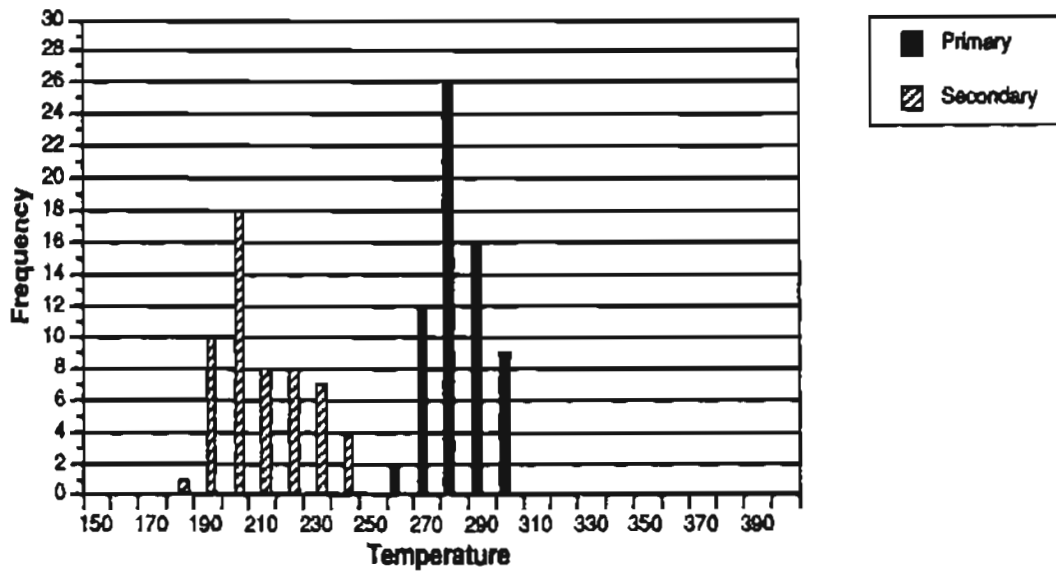


Figure 7.24 Histogram of homogenization temperatures of fluid inclusions in vein quartz from the Tolovana Mine, sample 82TV05.

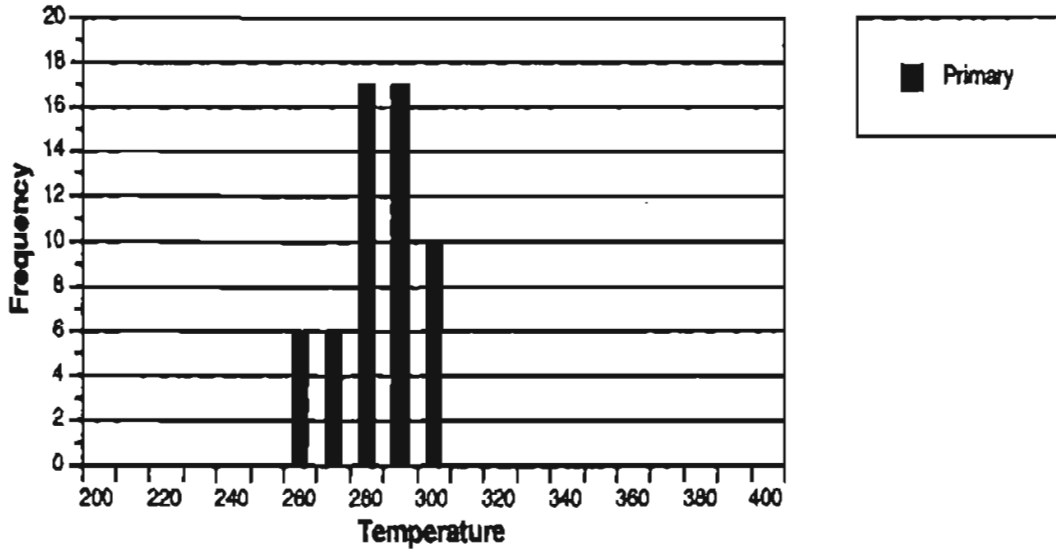


Figure 7.25 Histogram of homogenization temperatures of fluid inclusions in vein quartz from the Newsboy Mine, sample 82NB01.

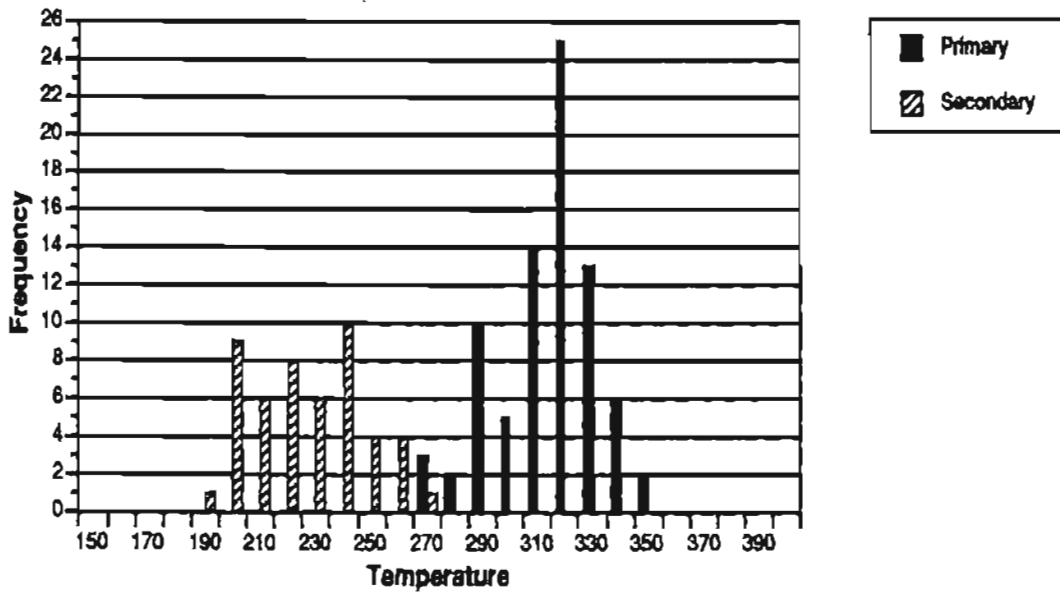


Figure 7.26 Histogram of homogenization temperatures of fluid inclusions in vein quartz from the Clipper Mine, sample 81MIRL03.

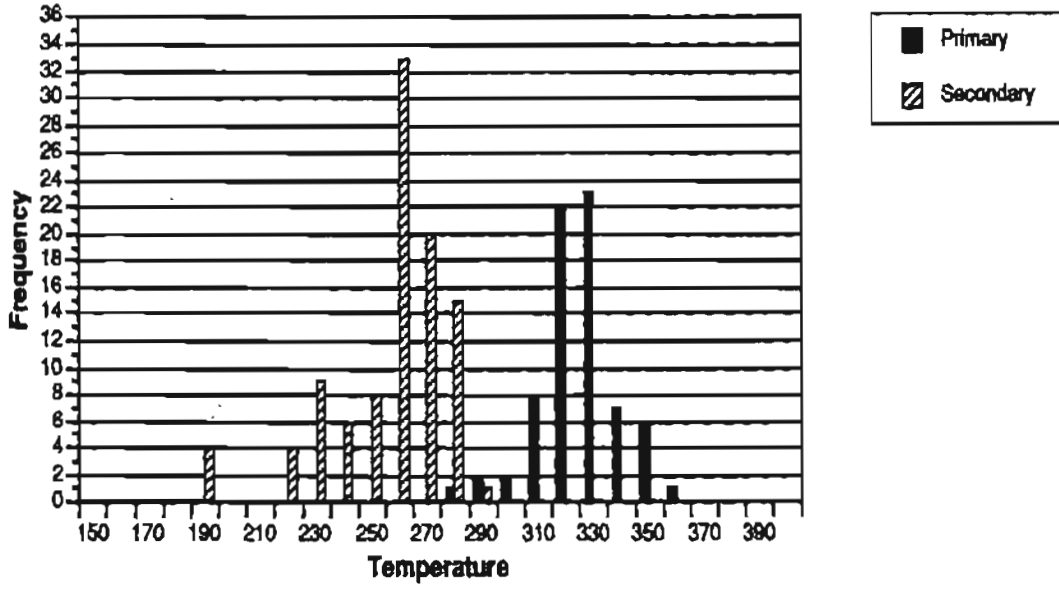


Figure 7.27 Histogram of homogenization temperatures of fluid inclusions in vein quartz from the Grant Mine, sample 81MIRL07.

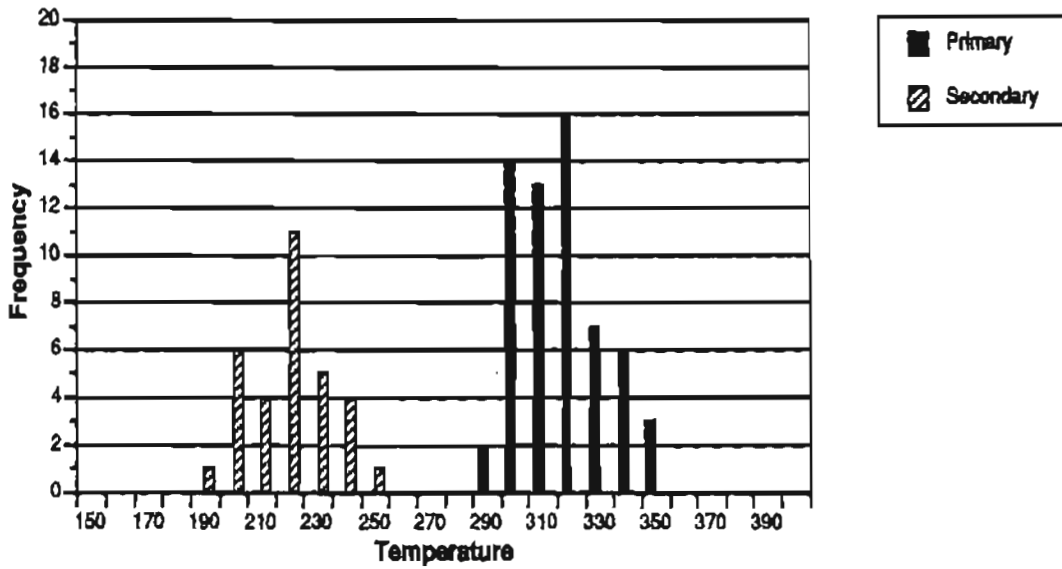


Figure 7.28 Histogram of homogenization temperatures of fluid inclusions in vein quartz from the Ryan Lode, sample 81MIRL15A.

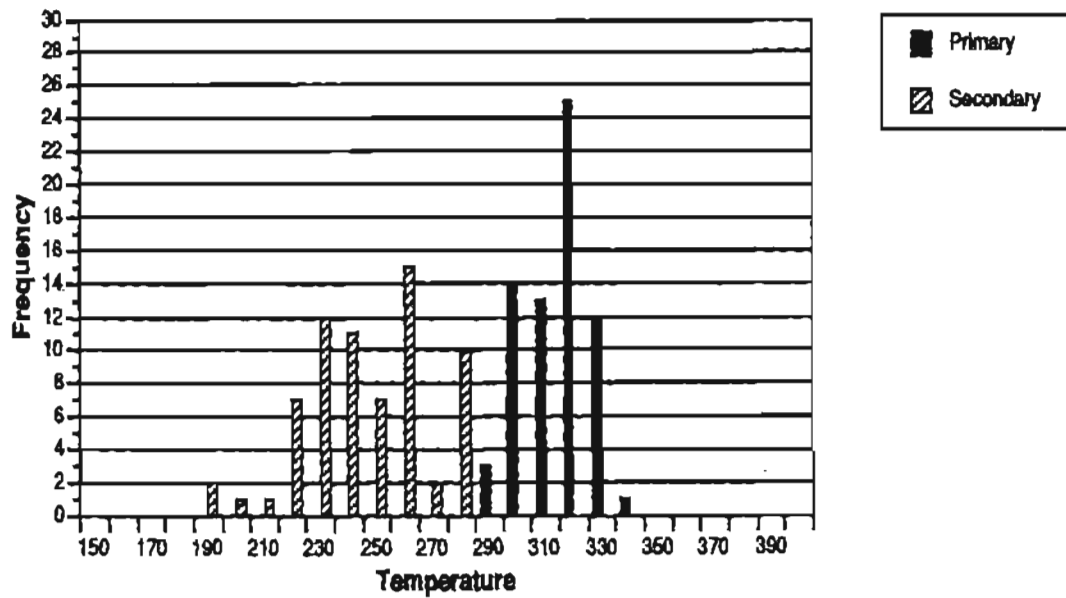


Figure 7.29 Histogram of homogenization temperatures of fluid inclusions in vein quartz from the Rogasch prospect, sample 81MIRL13A.

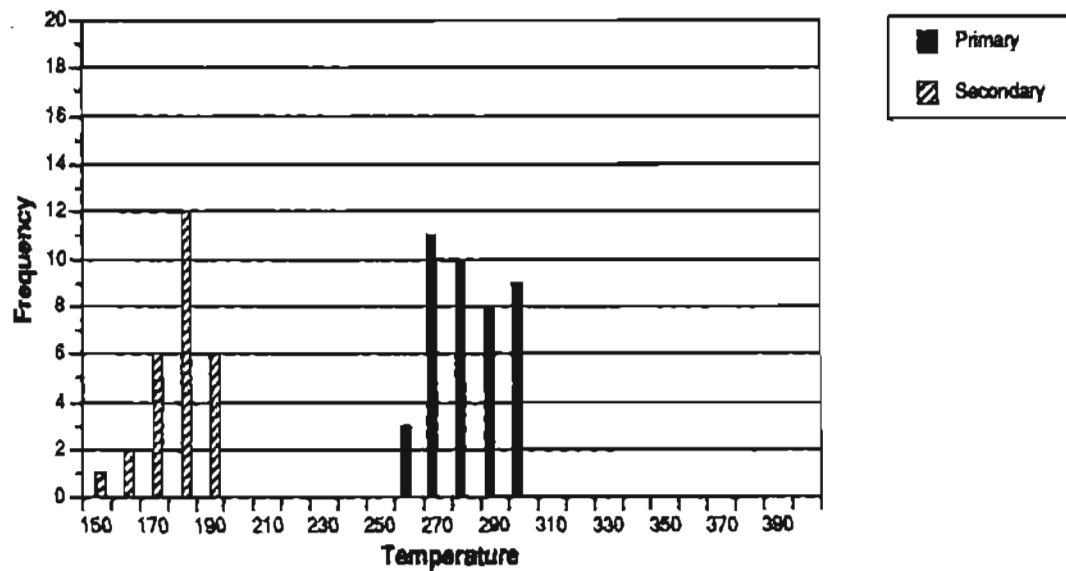


Figure 7.30 Histogram of homogenization temperatures of fluid inclusions in scheelite from the Johnson prospect, sample 81MIRL09.

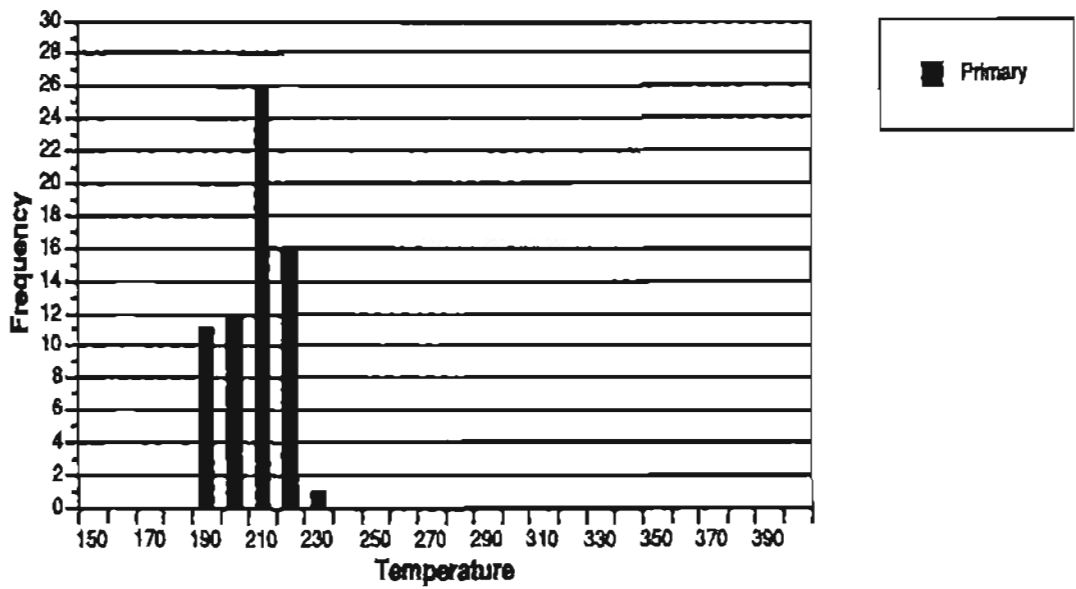


Figure 7.31 Histogram of homogenization temperatures of fluid inclusions in quartz from the Scrafford Mine, sample 81MIRL16.

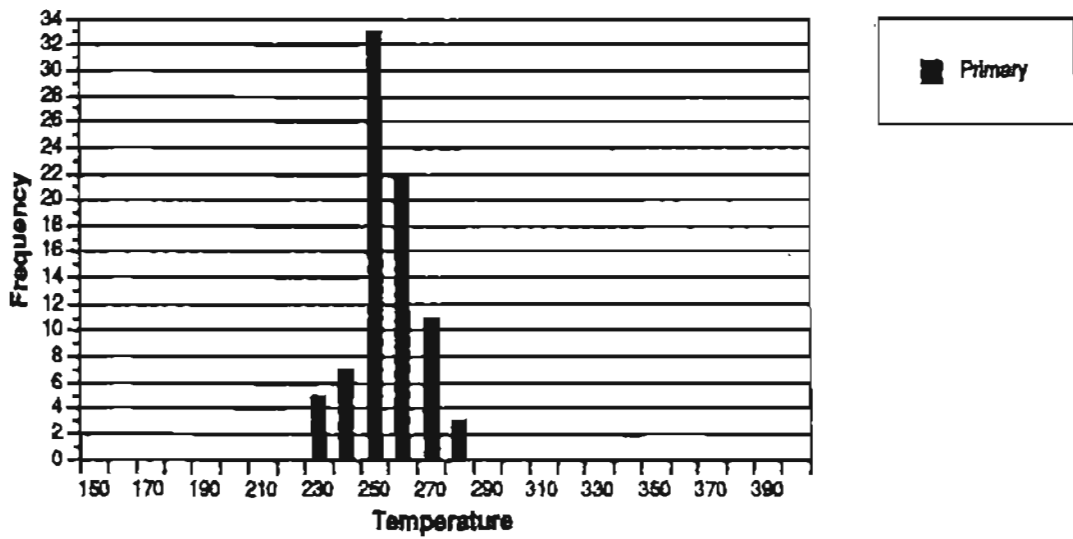


Figure 7.32 Histogram of homogenization temperatures of fluid inclusions in quartz from the Farmer prospect, sample 81MIRL05.

intermediate between the salinities of the inclusions in the plutonic and metamorphic quartz.

The fluid inclusion data are evidence that the ore forming fluid for the Type IV mineralization is primarily metamorphic fluid. Since many of the inclusions indicate that they consist of fluids whose composition lies along the liquid-vapor curve, the homogenization temperatures are also probably the trapping temperatures of the fluid.

Helgeson and Garrels (1968) show that up to 300°C,  $\text{AuCl}_2^-$  is the most important complex in NaCl solutions. At a temperature of 250°C and at neutral pH and at salinities of 2-7 percent, the maximum concentration of the gold chloride complex is 0.01 ppb. Under similar conditions of temperature and salinity, and reduced sulphur concentrations of 0.01 to 0.001 mole, Au solubility as a bisulphide complex is close to 1 ppm (Seward, 1973; Hannington et al., 1986). The massive sulphide mineralization is capable of contributing these reduced sulphur concentrations at greenschist facies metamorphism, thus the metamorphic fluid is estimated to be a very efficacious transporter of gold.

The deposition of gold out of the fluid is probably a function decreasing temperatures, changes in pH thru the loss of  $\text{CO}_2$ , decreases in the bisulphide concentrations thru the volatilization of sulphur species, and finally decreases in the two phase region due to decreases in  $\text{CO}_2$  or NaCl concentrations. The association of high grade gold mineralization (greater than 1.0 OPT) occurring in the veins along with galena, lead sulfosalts, and carbonate is evidence of the role of the volatile phase changes in gold deposition. Drummond (1981) discusses the complexity of the relationships between the deposition of metal and the loss of volatile phases during boiling in the system  $\text{NaCl-CO}_2\text{-H}_2\text{S-H}_2\text{O}$ .

Radical temperature drops to account for the formation of the high grade mineralization is not evidenced in the fluid inclusion data. While ore grades may change over a distance of one meter, temperatures gradients are small over hundreds of meters.

The inclusions in the intrusive related mineralization (Types II and III) are up to an order of magnitude more saline than the inclusions in either the metamorphic rocks or the gold-quartz veins. The fluid inclusion data do not allow the determination of whether there is a metamorphic component to the fluids in the Type II or Type III occurrences. The presence of hypersaline inclusions in some phases of the plutonic rocks indicates that higher salinities existed in the magmatic fluids. The dilution of these fluids to produce inclusion salinities similar to those in Type II and III mineralization could be due to mixing with metamorphic fluids or meteoric fluids. Alternatively the lower salinities of the intrusive related mineralization could be accounted for by simple cooling and phase separation of the more saline magmatic fluids.

## 7.6 FLUID INCLUSION ANALYSES BY MASS SPECTROMETRY

### 7.6.1 Methodology

Samples of quartz (-10 + 14 mesh, 2 grams each) were

selected from eight different Type IV and two Type V mineral occurrences. The quartz grains were hand picked under a binocular microscope to ensure mineral integrity. The samples were washed in concentrated HCl for 30 minutes and rinsed with distilled water.

The samples were then analyzed by the method described by Sheppard and Waters (1984). The analyses were completed at the National Environmental Research Council Stable Isotope Laboratory at the British Geological Survey in London.

### 7.6.2 Results

The results are given in Table 7.1. The two samples from the Type V mineralization in the Fairbanks district have relatively low  $\text{CO}_2$  contents. Also included in the data is an analysis of a sample of Type V mineralization from the Stampede Mine, Kantishna mining district, Alaska (sample 82SM01). This sample is from the ore zone, where the quartz is intergrown with massive fine grained stibnite. The Stampede Mine is the largest historic antimony mine in the United States although it is no longer in production. The  $\text{CO}_2$  content of the Stampede sample is comparable to the contents of the two Type V occurrences in the Fairbanks district. The gold contents reported in the table are average gold contents of the vein and are determined from past production records. The three Type V mineral occurrences contain only traces of gold in the ores and have no record of past gold production.

The remaining eleven analyses are for samples from Type IV mineral occurrences. These show a general trend of increasing gold content with increasing  $\text{CO}_2$  content. The sample from the Ryan Lode contains the lowest  $\text{CO}_2$  content of the Type IV samples. Sample 81MIRL15 is from the uppermost exposure of the vein system; massive stibnite is reported in the ore from this location. The Type IV sample with the highest  $\text{CO}_2$  content is from the Rogasch prospect located on the west side of Ester Dome. A channel sample of the one meter (3.25 foot) wide vein indicates a gold content of 0.51 OPT. Sample 81MIRL13 is a split from the channel sample.

The samples of Type IV mineralization from the Cleary Summit area all have methane contents of less than 0.10 mole percent except the sample from the Newsboy Mine. The samples of Type IV mineralization from the Ester Dome area have methane contents up to 0.94 mole percent or approximately an order of magnitude greater than the samples from the Cleary Summit area.

### 7.6.3 Discussion

Table 7.1 lists the bulk fluid composition of the samples as determined by mass spectrographic analysis. Primary and secondary inclusion contents are measured simultaneously. Since the secondary inclusions tend to be liquid  $\text{H}_2\text{O}$  types and the primaries tend to be  $\text{CO}_2$  rich types, the data cannot be interpreted as representing the  $\text{CO}_2$  content of the primary inclusions. The underestimation of the  $\text{CO}_2$  content is a function of the differences in the volume of fluid in the primary and secondary inclusions.

The difference in the estimation of  $\text{CO}_2$  using

Table 7.1 Mass spectrographic analyses of fluid inclusions from various lode mineral occurrences in the Fairbanks mining district, Alaska

Sample No.	Location Name	Mole % H <sub>2</sub> O	Mole % H <sub>2</sub>	Mole % Ar	Mole % N <sub>2</sub>	Mole % CH <sub>4</sub>	Mole % CO <sub>2</sub>	Total	Gold Content (OPT) (2)	Comments
81MIRL05	Farmer	98.08	0.27	0.00	0.41	0.16	1.08	100.00	None	Mono mineralic stibnite lode
82SM01(1)	Stampede	95.67	0.04	0.00	0.98	0.70	2.61	100.00	None	Mono mineralic stibnite lode
21332	Scrafford	96.11	—	—	—	—	3.41	99.52	Trace	Mono mineralic stibnite lode
81MIRL15	Ryan Lode	95.59	—	—	—	—	4.41	100.00	<0.25	No visible Au in sample
82CH02	Cleary Hill	92.78	0.07	0.00	0.26	0.09	6.79	99.99	>1.00	No visible Au in sample
82CA03	Christina	92.41	0.02	0.00	0.07	0.05	7.44	9.99	>1.00	No visible Au in sample
82NB01	Newsboy	91.82	0.03	0.00	0.20	0.30	7.65	100.00	>1.00	No visible Au in sample
82NAB1	Nordale	91.60	0.02	0.00	0.16	0.07	8.14	9.99	>1.00	No visible Au in sample
81MIRL21A	Vetter	91.12	0.02	0.00	0.12	0.09	8.64	99.99	>1.00	Abundant visible Au
81MIRL21B	Vetter	90.42	0.01	0.00	0.30	0.08	9.19	100.00	>1.00	Abundant visible Au
82TV05	Tolovana	90.20	0.03	0.00	0.19	0.08	9.50	100.00	>1.00	Abundant visible Au
81MIRL03	Clipper	87.41	0.04	0.00	0.13	0.50	11.92	100.00	>1.00	Abundant visible Au
81MIRL07	Grant	86.39	0.03	0.00	0.52	0.49	12.57	100.00	>1.00	Abundant visible Au
81MIRL13	Rogasch	84.69	0.03	0.00	0.58	0.94	13.76	100.00	>1.00	Abundant visible Au

Note: (1) The sample no. 82SM01 is from the Stampede Mine, Kantishna mining district.  
(2) Gold contents are the average gold content of the vein from past production records.

microthermometry and mass spectrographic methods for the Grant Mine sample can give an estimate of the uncertainty in the data. It is estimated that on the average the CO<sub>2</sub> occupies 25 volume percent of the primary inclusions in sample 81MRL07 at 40°C. The CO<sub>2</sub> homogenizes to a liquid at 30°C. Using the method of Burruss (1981), the estimated CO<sub>2</sub> content is 13 mole percent. This estimate is remarkably close to the measured value of 12.57 mole percent for the entire sample fluid. There is at least a one mole percent error in the graphical method of Burruss. The similarity in the results is probably due to the relatively small volume of fluid in the small secondary inclusions. The sample from the Grant Mine has the largest measured primary inclusions at a maximum of 0.18 mm. The results are unlikely to be the same for samples that contain smaller primary inclusions.

The mass spectrometric data suggests a positive correlation between CO<sub>2</sub> content and gold content in the Type IV samples. The high CO<sub>2</sub> content of gold-quartz vein type deposits in metamorphic rocks is noted by Fyfe and Kerrich (1984), Groves et al. (1984), and Nesbitt and Muehlenbachs (1989).

The presence of separate CO<sub>2</sub> liquid rich and CO<sub>2</sub> vapor rich inclusions homogenizing at the same temperature indicates that the temperature of homogenization and the temperature of trapping are the same. This separation of phases is noted in all samples with visible gold and CO<sub>2</sub> contents greater than approximately 8.5 mole percent.

The relatively high methane content of the Type IV samples from the Ester Dome area is indicative of more reducing conditions. Whether this is a function of the source fluid or the buffering effects of the wallrock is not determinable from the data.

## 7.7 SULPHUR ISOTOPE INVESTIGATIONS

In order to further refine the classification of the mineral occurrences of the Fairbanks district, sulphur isotopic analyses were completed on each of the ore types with the exception of the tungsten skarn deposits. Fifty-seven sulphide bearing samples were collected from 27 different occurrences. A total of 88 sulphur isotopic analyses was completed on the sample suite.

### 7.7.1 Methodology

Samples of sulphide bearing material were collected from surface exposures and underground workings where access was available. At the Cleary Hill, Hi-Yu, McCarty, Mohawk, Newsboy, and Woods Mines, access was not possible and samples were collected from the mine tips.

Polished sections of the ore were examined, sulphide mineralogy was determined by optical methods, and sulphide phases were confirmed by microprobe analyses. In all cases, the sulphide phases were very coarse grained and were separated by hand. Sample integrity was checked under a binocular microscope prior to sample weighing and sulphur extraction.

Sulphur isotope ratios were determined in the National Environmental Research Council Stable Isotope Laboratory

at the British Geological Survey in London and at Geochron Laboratories Inc., Cambridge, Massachusetts. The following procedure was adopted at the London laboratory.

Sulphur dioxide from sulphides was extracted for analysis by oxidation with cuprous oxide at 1070°C, using essentially the method described by Robinson and Kusakabe (1975). The isotopic analyses of the purified sulphur dioxide were made on a modified Micromass 602 mass spectrometer with a heated inlet system. The results were corrected for isobaric interference assuming a constant oxygen isotopic content and instrumental crosstalk (Coleman, 1977; 1980) and expressed in conventional  $\delta$  notation with respect to the Canon Diablo meteoritic troilite standard.

Analytical uncertainty, mainly in the oxygen isotope correction, amounts to between 0.05 and 0.1 %.

$$\delta^{34}\text{S}_{\text{ sample}} = \left[ \frac{^{34}\text{S}/^{32}\text{S}_{\text{ sample}}}{^{34}\text{S}/^{32}\text{S}_{\text{ standard}}} - 1 \right] \times 1000\%$$

Fractionation between two phases is expressed as:

$$\Delta_{A-B} = \delta_A - \delta_B$$

### 7.7.2 Results

Sample descriptions and results are given in Table 7.2 and summarized in Figure 7.33. Generally the duplicate samples ran at each laboratory were within 0.5 per mil and in some cases within 0.1 per mil. Stratabound sulphide from the Type I mineralization has a mean of 2.0 per mil. Excluding two samples of sulphides from a single disseminated occurrence in eclogite, sulphides from Type I occurrences have a mean of 8.8 per mil. Sulphides from both Type II mineralization (endoshears) and Type IV mineralization (exoshears) have a mean of 1.4 and 2.2 per mil respectively. Stibnite from late antimony veins (Type V mineralization) have a mean of -4.2 per mil. The mean per mil values for the stratabound and vein mineralization are approximately equivalent to the expected values for volcanic sulphide and modern hydrotherms respectively (Nielsen, 1979). The sample means of Types I, II and IV mineralization are not significantly different, neither are the variances of 1.19, 1.23 and 1.21 per mil respectively, however the small number of samples, particularly from Type II mineralization, preclude rigorous hypothesis testing.

### 7.7.3 Discussion

The presence of disseminated galena and sphalerite in the eclogite rocks was not expected nor can descriptions of analogues of that type of mineralization be found in the literature. Lead isotopic analyses of galena from the disseminated mineralization in the eclogitic rocks of the Chatanika terrane and from stratabound and vein mineral-

Table 7.2 Sulphur isotopic compositions of sulphides from the Fairbanks district, Alaska

Mineral Occurrence/ Sample No.	Description	Ga	Sp	Py	CDT (%) Cp	As	Ia	St	Deposit Type
Chatham Creek Prospect									I
81 MI 01 B1	Banded Sulphides in marble and metachert		+1.7	+3.2					
* 81 MI 01 B1	Banded Sulphides in marble and metachert	+2.6		+3.5					
* 81 MI 01 B1	Banded Sulphides in marble and metachert		+2.0	+2.4					
Cleary Hill Mine									LIV,V
81 MI 02 A	Quartz Sulphide vein			+2.7		+1.6			
* 82 CM 02 A	Qtz Sulphide vein in calc-schist w/ sulphides	-8.4							
82 CM 02 B	Banded Sulphides in calc-schist and metachert	-9.0							
82 CH 01	Stibnite vein w/ trace sphalerite		-0.5					-5.1	
Clipper Mine									IV
81 MI 03	Qtz vein in mica-quartzite			+3.1		+3.2			
* 81 MI 03	Qtz vein in mica-quartzite			+2.6					
Christina Adit									LIV,V
82 CA 01	Massive Stibnite in metafelsite							-3.0	
82 CA 01	Quartz vein in metafelsite		+2.1						
* 82 CA 04	Quartz vein in metafelsite			+2.9					

Table 7.2 (continued)

Mineral Occurrence/ Sample No.	Description	Ga	Sp	Py	CDT (%) Cp	As	Ia	St	Deposit Type
Engineer Creek Prospect 20509	Pyrite in adamellite dyke in shear zone			+0.3					II
Farmer Prospect 81 MI 05	Massive Stibnite vein cutting metafelsite					+3.1			V
Hi-Yu Mine 81 MI 08	Qtz Sulphosalt vein in calc-schist w/ sulphate	+2.7							I,IV
81 MI 08	Qtz Sulphosalt vein in calc-schist w/ sulphate	+3.2					+1.9		
82 HY 01	Qtz Sulphosalt vein in calc-schist w/ sulphate			+3.2		+0.3			
75 PM 03	Qtz Sulphosalt vein in calc-schist w/ sulphate	+2.9							
* 75 PM 03	Qtz Sulphosalt vein in calc-schist w/ sulphate	+2.8							
Johnson Prospect 81 MI 09 A	Massive Stibnite in shear zone							-5.6	V
* 81 MI 09 A	Massive Stibnite in shear zone							-0.3	
McCarty Mine 81 MI 10 A1	Pyrite in metafelsite			+1.1					I,IV,V
81 MI 10 A2	Pyrite in metafelsite			+4.2					
82 MM 01	Massive Stibnite with minor quartz					+1.5		-0.4	
Mohawk Mine 81 MI 11	Quartz veinlets cutting chlorite schist					+8.2			IV
* 82 M 3B	Quartz veinlets cutting chlorite schist					+10.9			

Table 7.2 (continued)

Mineral Occurrence/ Sample No.	Description	Ga	Sp	Py	CDT (%) Cp	As	Ja	St	Deposit Type
Cheechako Prospect									I
81 MI 12 A	Banded Sulphides in marble and metachert	+0.3	+2.5	+2.8					
* 81 MI 12 A1	Banded Sulphides in marble and metachert	+1.7	+2.9						
* 81 MI 12 A2	Banded Sulphides in marble and metachert	+0.5							
* 81 MI 12 A3	Banded Sulphides in marble and metachert	+1.2							
Newsboy Mine 82 NB 01	Quartz Sulphosalt veins in metafelsite					+2.1	+0.5		IV
96 Nordale Adit 82 NA 01	Quartz Sulphosalt veins in calc-schist w/ banded sulphides			+3.0			+0.5		LIV
82 NA 02	Quartz Sulphosalt veins in calc-schist w/ banded sulphides					-0.8			
* 21150	Quartz Sulphosalt veins in calc-schist w/ banded sulphides				+3.0				
Ridge Prospect 81 MI 28	Banded Sulphides in marble and metafelsite	+0.9	+3.1						I
Rogasch Prospect 81 MI 13 A	Quartz vein in mica quartzite	+4.1				+3.7			IV
Rowley Prospect	Shear zone near grano- diorite-schist contact	+0.7							II

Table 7.2 (continued)

Mineral Occurrence/ Sample No.	Description	Ga	Sp	Py	CDT (%) Cp	As	Ja	St	Deposit Type
Ryan Lode Mine * 81 MI 15A	Shear zone in chlorite- calc-schist					+0.5			IV
82 RLO-3A	Shear zone in chlorite					+3.7			
Scrafford Mine * 81 MI 16	Massive Stibnite in metafelsite							+2.6	V
Silver Fox Mine 81 MI 17 A	Shear zone in grano- diorite	+0.5	+2.5	+3.5		+2.4			II
* 81 MI 17 A1	Shear zone in grano- diorite	+0.2	+2.1						
* 81 MI 17 A2	Shear zone in grano- diorite	-0.9	+1.3						
Steese Arsenic Prospect 81 MI 18	Shear zone in mica- quartzite and metafelsite					+7.5			IV
Steese Eclogite Prospect 81 MI 04	Disseminated Sulphide in eclogite	+8.0	+9.3						I
* 81 MI 04 A	Disseminated Sulphide in eclogite	+9.3	+9.7						
* 81 MI 04 B	Disseminated Sulphide in eclogite	+8.1							
Scrafford Mine 81 MI 16	Massive Stibnite in metafelsite							+2.6	V
Tolovana Mine 81 MI 19 A	Massive Sulphide lenses in metafelsite						+4.6		II,IV,V

Table 7.2 (continued)

Mineral Occurrence/ Sample No.	Description	Ga	Sp	Py	CDT (%) Cp	As	Ja	St	Deposit Type
Vetter Prospect 81 MI 21 A	Quartz vein in mica- quartzite and metafelsite	+0.2				+2.2			IV,V
81 MI 21 B	Massive Stibnite in quartzite and metafelsite							-4.4	
Wackwitz Prospect 81 MI 22 B	Massive Sulphide lenses in metafelsite	-0.4	+0.4	+3.0			+1.4		I
* 81 MI 22 B1	Massive Sulphide lenses in metafelsite	+0.9							
* 81 MI 22 B2	Massive Sulphide lenses in metafelsite	-0.5							

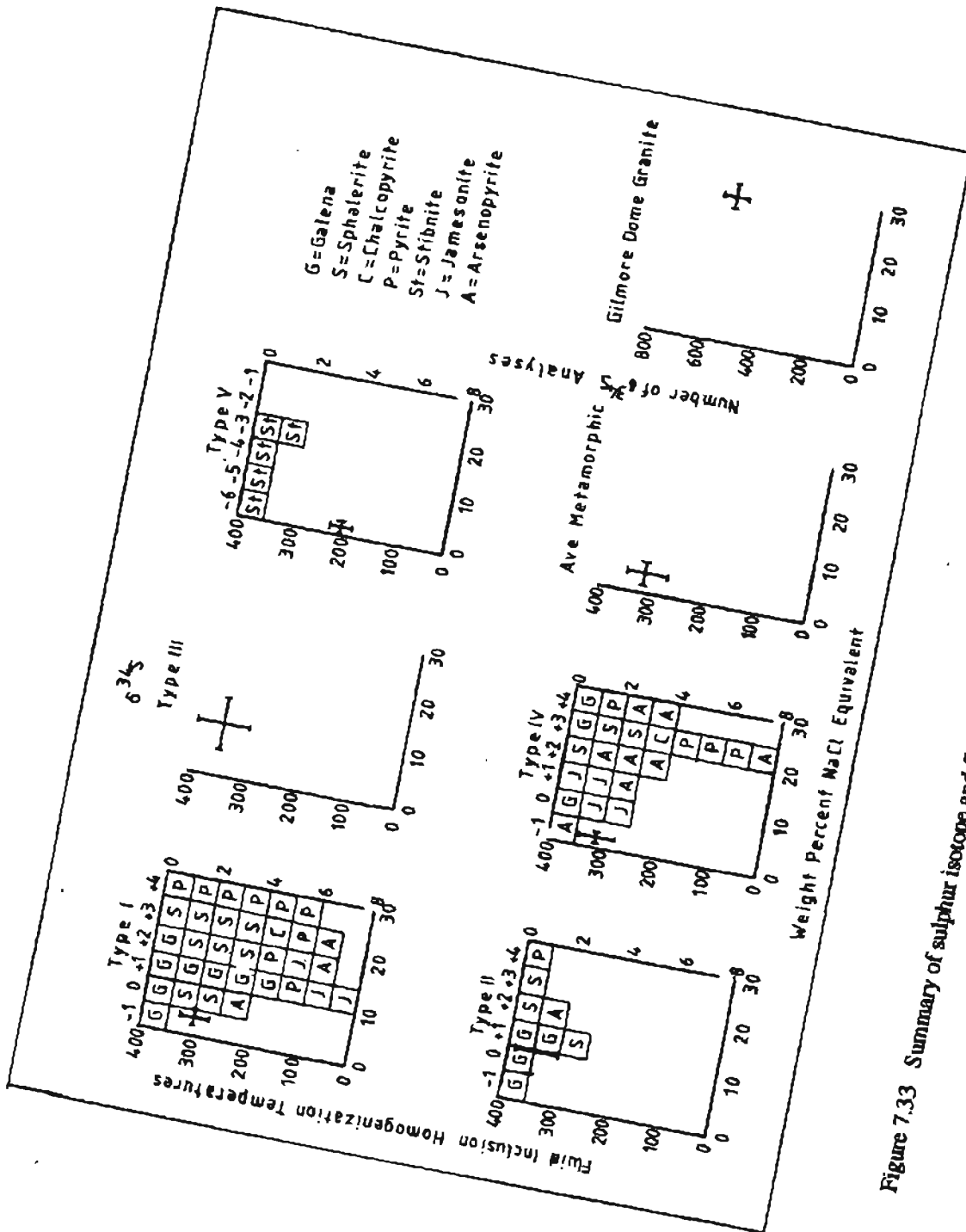


Figure 7.33 Summary of sulphur isotope and fluid inclusion data for Fairbanks mining district, Alaska.

ization in the Cleary sequence indicate two distinctive lead isotope populations for the two tectono-stratigraphic units. Although sulphur isotopic data for the Chatanika terrane are very limited, there is a difference of about 7 per mil in the mean values of the Cleary sequence and Chatanika terrane sulphides. Although these two tectono-stratigraphic units both contain stratabound mineralization, the modes of origin of the mineralization were probably significantly different. In addition, the two rock units and hosted syngenetic mineralization were subsequently subjected to radically different pressure-temperature conditions during one or more regional metamorphic events.

Mineral deposit Types II and IV show the largest difference in sulphur isotope sample means, however the sample means are not significantly different above the 90% confidence interval. Given the order of isotopic exchange rate galena > sphalerite > chalcopyrite > pyrite (Brown et al., 1975) it may be expected that the metamorphosed Type I mineral occurrences would show narrower ranges for galena than pyrite as compared to Types II and IV mineralization. This is not the case as shown in Figure 7.33. Therefore it can be concluded that metamorphism has had limited effect on the sulphur

isotope values and the degree of equilibrium or disequilibrium in the system is a function of the original conditions of ore deposition.

The stibnite from Type V mineralization contains significantly lighter sulphur than the other mineral deposit types. The antimony bearing phase in Type V is always restricted to stibnite. The stibnite contains only trace amounts of arsenic and gold. Conversely in Types I, II and IV mineralization, the antimony bearing phases are complex sulphosalts, and stibnite occurs only in trace amounts in a limited number of occurrences.

Figure 7.33 includes fluid inclusion homogenization and salinity data for Types I (except the eclogite occurrence) through V mineral occurrences, as well as selected metamorphic and intrusive igneous rocks from the district. Table 7.3 is a tabulation of calculated temperatures from sulphide mineral pairs from seven Type I mineral locations (including the eclogite occurrence) and one Type II mineral occurrence. Four of the Type I occurrences have sulphide pairs that indicate temperatures compatible with the ranges of temperatures indicated by the sulphide and metamorphic mineral assemblages and by the fluid inclusion homogenization data.

Table 7.3 Calculated temperatures from sulphur isotopic compositions of sulphide mineral pairs and fluid inclusion homogenization temperature ranges from the Fairbanks mining district, Alaska.

Mineral Occurrence	Sulphide Mineral	Calculated Temp. (°C)	Deposit Type Pair	Range of fluid Inclusion Homogenization Temp (°C)
Chatham Creek Prospect	Py-Ga	700	I	280-360
Christina Adit	Py-Sl	300	I	
Cheechako Prospect	Py-Ga Sl-Ga	700 630	I I	
Ridge Prospect	Sl-Ga	290	I	?
Silver Fox Mine	Py-Ga Sl-Ga	580 600	II II	300-380
Steese Eclogite Prospect	Sl-Ga	330	I	?
Wackwitz Prospect	Py-Ga Py-Sl	400 100	I I Sl-Ga	280-360  100 I
Willow Creek Prospect	Py-Ga Sl-Ga	630 1200	I I	

The remaining three Type I sulphur isotope pairs indicate temperatures incompatible with those obtained from fluid inclusion measurements. The two sulphide mineral pairs from the Silver Fox Mine (Type II occurrence) indicate temperatures 200°C above the fluid inclusion homogenization temperatures. From these data it can be concluded that isotopic equilibrium may have been attained in some of the Type I occurrences but was not approached in the Type II occurrence. No suitable sulphur isotope mineral pairs were available for Types IV and V mineralization, thus no estimate can be made from sulphur species concerning equilibrium conditions in these systems.

Types I and IV mineral occurrences contain quartz with CO<sub>2</sub> rich fluid inclusions. Type IV mineral occurrences often contain variable density CO<sub>2</sub> inclusions that homogenize at the same temperature, thus suggesting effervescence of CO<sub>2</sub> during vein formation. Type V mineralization contains relatively minor CO<sub>2</sub> (3 mole percent maximum) compared to Types I and IV mineralization (22+ mole percent). Type V mineral occurrences do not show any evidence of CO<sub>2</sub> effervescence. The effervescences of CO<sub>2</sub> will result in an increase in pH and an increase in pH should shift the sulphur species to more positive  $\delta^{34}\text{S}$  values. A decrease in temperature or an increase in oxygen partial pressure should cause a shift to lighter  $\delta^{34}\text{S}$  (Ohmoto, 1972). The disequilibrium conditions in some of the Type I mineral occurrences and in the Type II occurrence probably reflects rapid changes in pH, temperature and partial pressure of volatile phases.

The sample means of Types I and V versus IV and V mineralization differs by approximately 6 per mil. Ohmoto and Rye (1979) and Robinson and Farrard (1982) suggest that equilibrium stibnite values are about 4 per mil lower than H<sub>2</sub>S in an ore fluid at the temperature range of 150 to 200°C. Fluid inclusion homogenization temperatures for Type V mineralization indicate ore deposition took place between 180 and 220°C, thus sulphur from either Types I, II, or IV mineralization could account for the  $\delta^{34}\text{S}$  values in Type V mineral deposits. In addition, it is possible that Type I mineralization could have been the source of sulphur for Types II and IV mineral deposits.

## 7.9 SUMMARY AND CONCLUSIONS

The fluid inclusion data indicate that there are significant differences in the temperature and composition of the fluids that formed the various deposit types. The fluids in the Types I and IV mineral occurrences and in the metamorphic rocks have similar salinities and homogenization temperatures. The salinities in the Types II and III mineral occurrences are higher, and intermediate between the metamorphic fluids and the fluids in the plutonic rocks. Thus the high grade gold mineralization and the disseminated mineralization in the host shear zones are probably the result of the focusing of metamorphic fluids in the brittle shear zones. The Type II mineralization may be a consequence of the mixing of magmatic fluids and fluids circulated through the metamorphic host rocks to the plutons.

It is estimated that the Type IV mineralization occurred at a pressure of approximately one kilobar. Assuming an open system and a hydrostatic head, the depth of ore formation is estimated at 10.5 kilometers (34,000 feet). Assuming a closed system and a lithologic pressure, the depth of formation is estimated at 4.0 kilometers (13,000 feet).

---

## CHAPTER 8

### GENERAL GEOLOGY AND TRACE ELEMENT GEOCHEMISTRY OF THE CIRCLE, STEESE, RICHARDSON, TOLOVANA, AND KANTISHNA MINING DISTRICTS

#### 8.1 INTRODUCTION

Along with the Fairbanks mining district, the Circle, Steese, Richardson, Tolovana, and Kantishna mining districts constitute a appreciable part of the land area of the northwestern margin of the Yukon-Tanana Terrane (YTT). From the historic placer gold production, it can be inferred that these districts in the aggregate comprise the highest mineral potential area of east-central Alaska. The following is a review of the general geology, lode and placer mineralization, and trace element geochemistry of these districts. Such a review is essential in determining not only the mineral potential of the region but also the geologic evolution of this portion of the terrane.

#### 8.2 CIRCLE MINING DISTRICT

##### 8.2.1 Location and Previous Investigations

The Circle mining district is located in east-central Alaska approximately 140 kilometers (90 miles) northeast of Fairbanks (see Ch. 2, Plate I). The district is defined by the various tributaries of Birch Creek that have produced significant quantities of placer gold. The western extremity of the district is delineated by the North Fork of Birch Creek and the south boundary is defined by Birch Creek. The northern extent is bounded by Porcupine and Crooked Creeks while the eastern limit is the two Portage Creeks (see Ch. 8, Plates I thru IV). The total area of the district is 1,500 square kilometers (600 square miles).

Previous investigations in the district include Barker (1979), Brooks (1909, 1910), Cady and Barnes (1983), Cady and Weber (1983), Churkin et al. (1982), Cushing (1984), Cushing and Foster (1984), Cushing et al. (1984a, 1984b), Dahlin et al. (1987), Foster et al. (1983), Johnson (1910), Laird and Foster (1986), Laird et al. (1984), Masterman (1990), Menzie et al. (1983), Mertie (1937, 1938), Metz (1984g, 1990); Prindle (1913), Wilkinson (1987), and Wilson et al. (1985).

##### 8.2.2 Bedrock Geology

Figure 8.1, after Foster et al. (1983) and Metz (1990) is a generalized geologic map of the district. The major lithologies include Proterozoic or Lower Paleozoic

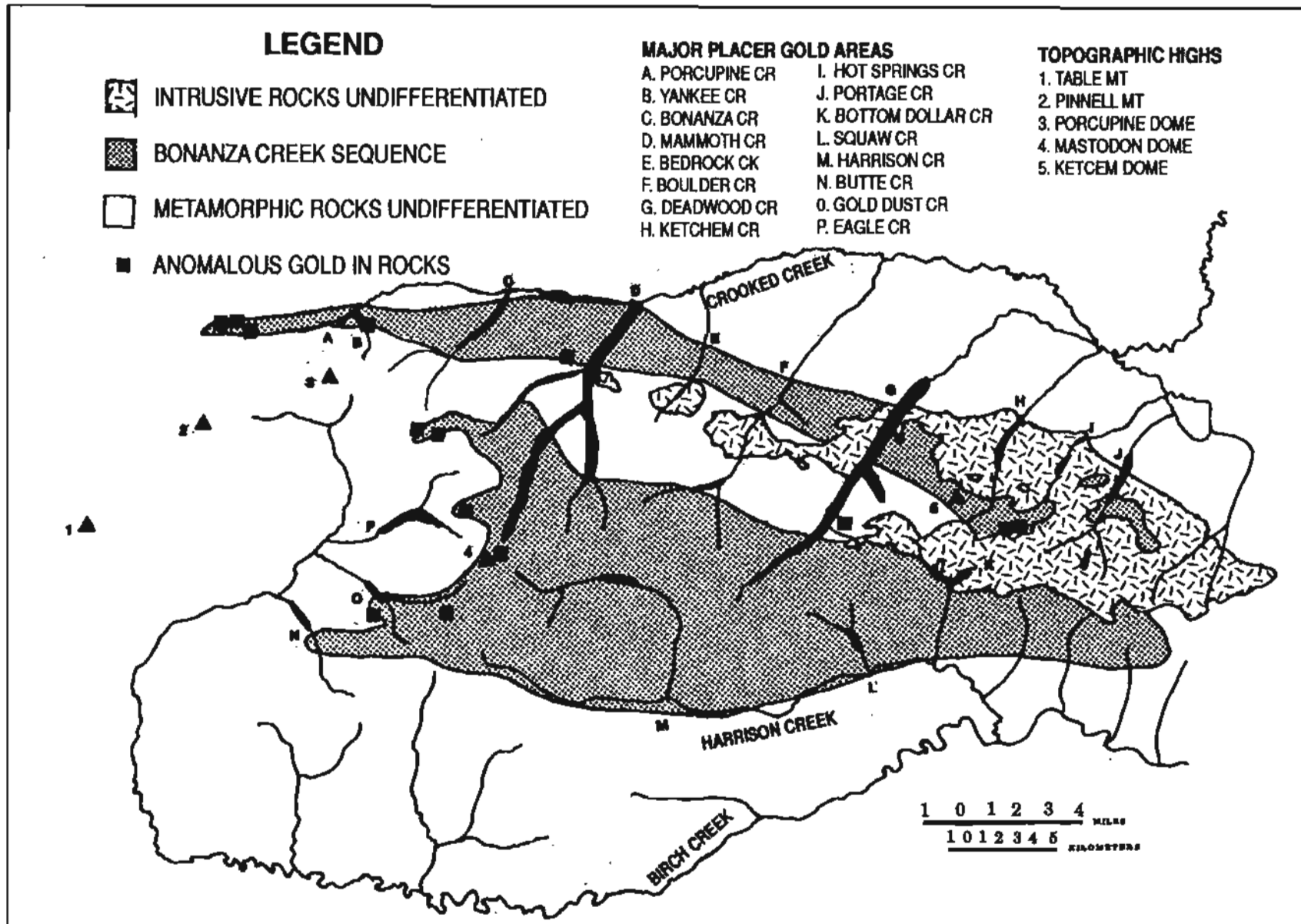


Figure 8.1 Generalized geologic map of the Circle mining district, Alaska.

metasediments and metavolcanics, Late Proterozoic or Early Cambrian "metagrit", and Late Cretaceous and Tertiary age intrusive rocks that range in composition from granite to basalt.

#### 8.2.2.1 Regionally Metamorphosed Rocks

This group of metamorphic rocks can be divided into four main lithologies: pelitic schist and quartzite, mafic schist, Bonanza Creek sequence, and grit and quartzite. These rock units have been defined by 1:24,000 scale geologic mapping (Metz, 1990).

##### 8.2.2.1.1 Quartzite and Pelitic Schist

The unit consists of white mica-quartz schist, massive quartzite, biotite schist, and minor chlorite-garnet-biotite schist. The schists are fine- to medium-grained, thinly-laminated, and medium to dark grey.

Mineral assemblages include quartz, muscovite, chlorite, plagioclase,  $\pm$  garnet and biotite. Tourmaline, zircon, sphene, and epidote occur as accessory minerals. The quartz and feldspar grains range from less than a millimeter to over a centimeter in diameter.

The matrix of the quartzites is a mosaic of highly strained quartz, feldspar, and white-mica. The mylonitization is particularly evident in the northwestern portion of the district at Porcupine Creek.

The massively bedded quartzite is the most abundant and distinctive lithology in the map unit. The resistant rock type forms the ridge tops and crops out on the higher peaks in the western extremity of the district. Locally sedimentary structures including cross and graded bedding are clearly visible. The quartzite may be gradational with the grit and quartzite unit described below.

##### 8.2.2.1.2 Mafic Schist

The mafic schist unit is composed predominantly of chlorite schist, and minor calc-schist and metachert. The chlorite schists are either a massive variant composed of actinolite + chlorite + epidote + plagioclase + quartz + sphene + rutile  $\pm$  biotite, white-mica, carbonate, and garnet. The plagioclase occurs as porphyroblasts up to two centimeters in diameter. The second variant of the chlorite schist is finely laminated and is composed of green chlorite + plagioclase + quartz + carbonate + rutile  $\pm$  white-mica, sphene, and garnet. Both variants contain abundant magnetite giving the unit a very distinctive magnetic signature. Locally the chlorite schist contains narrow lenses and disseminations of pyrite, arsenopyrite, sphalerite, galena, and argentiferous tetrahedrite. Microprobe analyses of the tetrahedrite indicate silver contents of approximately 15 percent. The protoliths of the two variants are probably mafic volcanic flow rocks and volcaniclastics respectively.

Intercalated with the chlorite schists are calc schist and metachert. The calc schist is a light grey to buff colored rock and is composed of carbonate + chlorite + white-mica  $\pm$  garnet. The protolith is assumed to be an impure marble or calcareous mudstone. The metachert is highly variable in

color ranging from light grey to red, green, dark grey, and black. The metachert may be composed of very finely laminated quartz or may contain lithic fragments and feldspars in a fine-grained quartz matrix. Locally the metachert may contain up to 10 percent pyrite and minor arsenopyrite and galena. Individual compositional layers of metachert range from a few centimeters to several tens of meters in thickness.

The unit appears to overlie the quartzite and pelitic schist unit; however the nature of the contact is uncertain. The mafic schist unit is the dominant rock type in a 190 square kilometer (70 square mile) area in the central portion of the district. This area forms the headwaters of the creeks that account for two thirds of the placer gold production from the district.

##### 8.2.2.1.3 Bonanza Creek Sequence

The Bonanza Creek sequence is composed of quartz white-mica schist, graphitic schist, metachert, and marble. The mineral assemblage in the quartz white-mica schist is supplemented by plagioclase. Quartz constitutes up to 75 percent of the rock with the balance comprised of up to 25 percent white-mica and plagioclase. Traces of zoned tourmaline and zircon are ubiquitous.

The graphitic schist is composed of 75 percent quartz and the balance is graphite with or without chlorite. The graphitic schist locally contains abundant pyrite and minor arsenopyrite.

The metacherts in the Bonanza Creek sequence are similar to those in the mafic schist unit. Near the assumed top of the sequence the graphitic schist is overlain by a marble that is at least ten meters (30 feet) thick. The marble weathers to a light grey to buff color and forms a distinctive marker horizon. At several localities on Bonanza Creek, Porcupine Creek, and Yankee Creek, the marble contains layered sulphides including sphalerite, galena, and arsenopyrite.

The Bonanza Creek sequence is spatially associated with the mafic schist sequence and appears to conformably overlie that unit. The Bonanza Creek sequence is in turn overlain by the quartzite and pelitic schist unit. The Bonanza Creek sequence is similar to the Cleary sequence in the Steese and Fairbanks mining districts which is described in subsequent sections. The Cleary sequence is an informal name for a metamorphosed mafic and felsic volcanic sequence initially described in the Fairbanks mining district (Metz, 1982). The inclusion of the mafic schist unit with the Bonanza Creek sequence results in a stratigraphic section similar to that for the Cleary sequence in the Fairbanks district. The total thickness of the mafic schist unit and the Bonanza Creek sequence is estimated in excess of 300 meters (1,000 feet). This is comparable to the thickness of the Cleary sequence in the Fairbanks district.

##### 8.2.2.1.4 Grit and Quartzite

The unit is composed of metamorphosed quartz arenite, quartzwacke, graywacke and quartzite. Megacrysts are monocrystalline or polycrystalline grains of clear, white, grey, blue grey, or black quartz. The matrix is quartz with minor white-mica and feldspar. Locally chlorite and biotite

are present thus indicating lower greenschist facies metamorphism.

The unit overlies the Bonanza Creek sequence and may be gradational with the quartzite and pelitic schist unit. The unit is estimated to be several thousand meters thick, however this thickness may be due in part to structural repeating of the stratigraphy. There are no stratigraphic marker horizons that can be utilized to make a definitive determination of either structure or stratigraphic position.

The unit has been correlated with the Wickersham grit of the Livengood quadrangle. The Wickersham grit in turn has been correlated with the Windemere Supergroup of the Yukon Territory and of northern British Columbia. These correlations are discussed in more detail in the section on the Steese mining district:

#### 8.2.2.2 Tertiary Gravels

The Tertiary gravels as well as the Pleistocene and Recent surficial deposits will be discussed in the section on placer deposits.

#### 8.2.2.3 Intrusive Rocks

Wilkinson (1987) describes the igneous rocks of the Circle mining district. The descriptions are predicated on the classification of Streckeisen (1973) and an analysis of the macrocrystalline textures of the rocks. The criteria used for the textural classification of the rocks are similar to that used by Burns and Newberry (1987) for the description of the igneous rocks of the Steese mining district. Table 8.1 is a summary the textural classification used for both areas.

Wilkinson (1987) subdivided the the Circle Intrusive Complex into two units based on the bulk composition, texture, and radiometric age dates of the rocks. The two units are referred to as the Circle Hot Springs pluton and the Two-Bit pluton.

The Circle Hot Springs (CHS) pluton is the more northerly body and in part is bordered by the Tintina Fault. The CHS pluton is compositionally more complex than the Two-Bit (T-B) pluton. The CHS pluton is composed predominantly of syenogranite, monzogranite, and quartz monzonite. The T-B pluton is composed primarily of monzogranite with minor granodiorite.

#### 8.2.2.3.1 Circle Hot Springs Pluton

The syenogranite phase of the pluton is in the central part of the body. The rock is a medium-grained to mediophyric biotite syenogranite. Accessory minerals include zircon, sphene, apatite, muscovite, and opaques. Locally hornblende and tourmaline are present as well as secondary chlorite and sericite.

The monzogranite phase is the dominant phase on the northern margin of the pluton. The rock unit is a slightly mediophyric to mediophyric biotite monzogranite. Accessory minerals are the same as those present in the syenogranite.

Aplite-pegmatite dikes intrude the CHS pluton, however most of the occurrences are represented by rubblecrop thus the contact relationships are speculative. The aplites are very fine grained; however quartz, white-mica, fluorite, and tourmaline have been identified from a number of float specimens. Masterman (1990) provides a brief description of

Table 8.1 Criteria used for textural classification and grain size of the granitic rocks of the Yukon-Tanana Terrane.

TEXTURES:	DEFINITION:	CRITERIA:
equigranular	one narrow size range	biggest grain 5% smallest
porphyritic	bimodal size distribution	grain size variations 10x; smallest big grains 5x & biggest small grains 20x the fine-grained matrix
seriate	wide & continuous range in grain sizes	grain size variations 10x; % fine-grained matrix
GRAIN SIZES:	AVERAGE GRAIN DIAMETER:	
fine	< 1 mm	
medium	1-5 mm	
coarse	5-30 mm	
very-coarse	> 30 mm	

several pegmatite float specimens. The pegmatites are simple in composition with the mineral assemblage quartz + feldspar + muscovite ± biotite. The feldspars are frequently altered to sericite and the biotite to chlorite.

Mafic dikes intrude the pluton at numerous localities; however most of the localities are represented by rubblecrop. The dike rocks are fine-grained dark grey to dark green. Some specimens contain visible white laths of plagioclase and minor hornblende altered to biotite.

Wilkinson (1987) reports four K-Ar age dates for the Circle Hot Springs pluton that range from  $56.35 \pm 1.69$  to  $57.75 \pm 1.73$  million years. One age date of  $54.17 \pm 1.96$  million years is reported for an aplite dike intruding the pluton.

#### 8.2.2.3.2 Two-Bit Pluton

The Two-Bit pluton is located south of the main body of the Circle Hot Springs pluton and is composed of monzogranite and minor granodiorite. Both phases of the T-B pluton have a medium-grained, subequigranular groundmass with large subhedral to euhedral potassium feldspar phenocrysts. The relatively uniform size of the phenocrysts is a distinctive textural characteristic of the T-B pluton as is the relatively larger grain size of the groundmass. Fine-grained contact zones are less prevalent in the T-B pluton than in the CHS pluton.

The monzogranite phase of the T-B pluton is a megaphyric biotite rich rock that forms the main portion of the intrusive. The potassium feldspars are large sub- to euhedral and white to pale pink. The quartz in the groundmass is milky white to light grey and forms sub- to euhedral crystals. Biotite is green due to chloritization with increases in intensity near contact zones. Trace amounts of hornblende are present and accessory minerals include zircon, apatite, monazite(?), and opaques. Secondary minerals are sericite, epidote(?), chlorite, sphene, tourmaline, and fluorite. Trace amounts of gold occur in silicified shear zones in the eastern portion of the pluton.

The granodiorite phase of the T-B pluton occurs in three different localities. The rock has a fine- to medium-grained subequigranular groundmass, and phenocrysts of sub- to euhedral potassium feldspar and quartz. Locally the rock contains clusters of biotite several centimeters in diameter. Trace mineralogy includes hornblende, apatite, sphene, zircon, monazite(?), allanite(?), and secondary mineralogy includes sericite, chlorite, epidote, and opaques.

Aplite and mafic dikes intrude the T-B pluton and are similar to those that intrude the CHS pluton. Most of the occurrences are rubblecrop; thus the contact relationships are uncertain. Silicified zones also crosscut the T-B pluton. The zones are several tens of meters in width with individual quartz veinlets up to two centimeters wide. At one locality near Bottom Dollar Creek (Joker No. 1 claim) visible gold occurs in the quartz veinlets and on the joint surfaces of the sericitically altered granodiorite.

Wilkinson (1987) reports K-Ar age dates of  $69.71 \pm 2.09$  and  $70.92 \pm 2.13$  million years for the pluton. Thus the more

mafic phase of the Circle Intrusive Complex is approximately 16 million years older than the felsic rich phase.

#### 8.2.2.4 Contact Metamorphic Rocks

Contact metamorphism is present at the margins of the plutons and in the roof pendants in the Ketchem Dome and Portage Creek areas. The evidence for the contact metamorphism is the occurrence of biotite and hornblende-bearing hornfels zones. The hornblende hornfels zones often contain garnet and may be intensely silicified. The lack of exposure of the contact zones prevents a definitive description of the nature of the contacts as well as the contact metamorphic mineral assemblages. The lack of carbonate units in the contact zones precludes the development of calc-silicate assemblages and the various types of economic skarn mineralization.

The quartzites and pelitic schists in the vicinity of Granite Gulch, Boulder Creek, Deadwood Creek, Ketchem Creek, and Bottom Dollar Creek are silicified and contain secondary biotite, hornblende, and garnet. These contact mineral assemblages may extend several hundred meters outward from mapped intrusive contacts.

#### 8.2.2.5 Regional Structure

Davies (1972) relates the micro- and macrostructures of the Circle district to the Tintina Trench. Of particular significance is the description of the Hot Springs Fault as the northern extension of the Tintina Fault, a first order wrench fault, and the description of numerous second and third order structures, as well as major thrust faults in the district.

The Hot Springs Fault strikes N 65°W and is vertical. The second order wrench faults are normal to the first order fault thus strike approximately N 30°E. The third order structures generally parallel the first order structure within a few kilometers of the structure. Both the second and third order structures are near vertical. The first order structure has a right lateral sense of motion while the second order structures are left lateral. Major second order structures are mapped on Ketchum and Boulder and Bedrock Creeks.

The thrust faults trend northeast-southwest and dip to the southeast at 0 to 20 degrees. The thrusts are limited to the southwest side of the Hot Springs Fault and terminate at the fault at right angles. Major thrusts are mapped on both Portage Creeks, Deadwood Creek, and Independence Creek.

The age of the structures is problematic; however the thrusts appear to predate the Circle intrusive complex and in part may control the emplacement of the complex. The thrusts are either associated with wide outcrop patterns of the pluton or in the case of the Independence Creek thrust, mark the extremities of the pluton. The second and third order structures postdate the pluton and even offset Pleistocene sediments north of the Tintina Fault.

Metz and Wolff (1980) describe two orthogonal sets of linear features interpreted from Landsat imagery. One set is sub-parallel to the Tintina Fault and the second is sub-parallel to the second order structures of Davies (1972). The orthogonal

linears are inferred to result from a tensional tectonic event that preceded the strike-slip motion on the Tintina Fault. Thus the fault is an older suture zone that formed as the YTT was separated from the North American continental margin (Metz et al., 1982).

Cushing and Foster (1984) describe four deformational events in the district. The first event (D1) is the development of axial-plane schistosity while (D2) is the first isoclinal folding of the schistosity. The third event (D3) is a second isoclinal event which results in interference forms. The fourth event (D4) is an open folding event with steeply dipping axial planes. Events (D2) and (D3) are interpreted to be indicative of large scale recumbent structures. Cushing and Foster (1984) do not discuss the four events in terms of the structural mapping of Davies (1972). They do indicate that considerable uncertainty exists with respect to events (D2) and (D3). One event is shown to have fold axes that trend N 30° to 50°E and plunge 0° to 5°SW, and the other event has axes that trend N 30° to 60°W with no significant plunge. The relative ages of the folds are unknown.

Simpson (1983) recognizes a Landsat feature along Independence Creek but interprets the structure as a high angle fault rather than a thrust fault. Triebel (1990) also makes note of the structure and also interprets it as a high angle fault. The radical changes in schistosity across the feature, the apparent differences in secondary mineral growth, and the differences in fluid inclusion compositions are interpreted by Triebel (1990) to be due to large scale vertical movements.

Triebel (1990) recognizes two sets of isoclinal fold axes neither of which are congruous with the (D2) or (D3) axes of Cushing and Foster (1984). One set trends N 65°W and plunge 5° to 10°NW. This set is parallel to the Hot Springs Fault. The other set trends S 80°W and plunges 0° to 20°W.

Metz (1990) and Masterman (1990) show a major anticlinorium south of Porcupine Creek that strikes east-west. The antiform extends from Loper Creek to Independence Creek, a distance of 25 kilometers (15.5 miles). East of Independence Creek the trend of the Circle Hot Springs pluton is parallel to the Porcupine Creek antiform. It is uncertain whether the antiform predates or postdates the intrusive event. If in fact the Independence Creek fault terminates the Porcupine Creek antiform and the fault predates the intrusive, then both the antiform and the Independence Creek fault may be controlling the emplacement of the intrusive complex.

From the limited structural and petrologic data, the following tectonic evolution of the district may be inferred:

1. Rifting of the YTT from the North American continental margin in the Proterozoic and the deposition of the thick sequence of clastic sediments and exhalative rocks in graben structures.
2. Burial metamorphism of the sedimentary and volcanic sequences during the Paleozoic (D1 event of Cushing and Foster, 1984).
3. Closing of the narrow suture zone and oblique collision of the YTT with North America com-

mencing in the Jurassic (D2 event with isoclinal fold axes parallel to the Hot Springs Fault and development of the Porcupine Creek anticlinorium),

4. Right lateral strike-slip motion on the Tintina Fault, eventual buttressing of the YTT against the North American continental margin northwest of the Circle district, and the formation of major imbricate thrust faults (D3 event with isoclinal fold axis N 30° to 50°E and refolding of the Porcupine Creek anticlinorium),
5. Emplacement of the Circle Intrusive Complex and continued movement along the Tintina Fault during the Late Cretaceous,
6. Development of tensional zones along the Tintina Fault due to the oblique collision, formation of graben structures during Eocene thru Pliocene time, and the deposition of continental clastics in the grabens,
7. Continued uplift and erosion during the Pleistocene and Holocene.

This probable sequence of events is compatible with the tectonic histories proposed for the other adjacent districts in the YTT as outlined below.

### 8.2.3 Lode Mineral Occurrences

Although the Circle mining district has been a major placer gold producing area, prior to the investigation by Metz (1984) there were only seven reported lode mineral occurrences in the district. Of these seven, only two were described as gold occurrences. During the district wide geologic mapping (Metz, 1984), six additional lode occurrences were discovered and seven geochemically anomalous areas were delineated.

#### 8.2.3.1 Porcupine Dome

Mertie (1938) reports the presence of Au, Ag, and Sn mineralization on a ridge near Porcupine Dome (section 9, T8N, R11E, F.M.). The mineralization is described as a narrow gold quartz vein in mica schist. Abundant quartz vein rubblecrop is noted on the ridge between Yankee and Dome Creeks and grab samples are reported to contain in excess of one troy ounce per ton. However the in situ mineralization is not apparent in outcrop.

#### 8.2.3.2 Miller House

Wedow et al. (1954) report the occurrence of Cu, Pb, and fissionable materials in section 11, T8N, R12E, F.M. The mineralization is in an altered syenogranite which is the western most exposure of the Circle Hot Springs pluton. Ore minerals include hematite, magnetite, malachite, zircon, rutile, galena, ilmenite, and pyrite. Menzie et al. (1983) note anomalous gold concentrations at the same locality. Limited sampling of arsenopyrite-bearing quartz sericite schists near the contact zone of the pluton indicates gold concentrations in the range of 50 to 1000 pph.

#### 8.2.3.3 Bedrock Creek

Nelson et al. (1954) report scheelite and monazite near

the northern contact of the CHS pluton at Bedrock Creek (section 20, T8N, R13E, F.M.). The host rock is altered syenogranite. Two samples from the area are slightly anomalous in tungsten (2-3 ppm), fluorine (2300-2400 ppm), lead (11-25 ppm), and arsenic (12-24 ppm). The mineralization is associated with narrow quartz veinlets in the intrusive.

#### 8.2.3.4 Deadwood Creek

Mertie (1938) notes the occurrence of galena and scheelite in a metachert on Deadwood Creek (section 6, T7N, R14E, F.M.). The mineralization occurs as millimeter thick lenses and disseminations in a light grey to pink metachert. The mineralization is visible in the placer mining excavations in the active stream channel. The exposed mineralization covers an area approximately 300 meters (1,000 feet) by 1,000 meters (3,250 feet). The metacherts are nearly horizontal at the locality, thus the total thickness of the mineralization is unknown.

#### 8.2.3.5 Portage Creek

Nelson et al. (1954) report significant quantities of uranothorianite, wolframite, scheelite, and sphalerite in sluice concentrates from Portage Creek (section 2, T7N, R15E, F.M.). The bedrock at the placer operation is syenogranite of the CHS pluton. Other minerals present are apatite, arsenopyrite, bismuthinite, cassiterite, chalcopyrite, chlorite, diopside, fluorite, garnet, gold, hematite, jamesonite, ilmenite, magnetite, monazite, pyrite, sphene, spinel, topaz, tourmaline, and zircon.

Nelson et al. (1954) do not provide a detailed description of the mineral occurrence. Furthermore, the placer excavation is no longer open, thus it is not possible to determine the form and extent of the occurrence.

#### 8.2.3.6 Ketchem Dome

Eberlein et al. (1977) and Dahlin et al. (1987) briefly describe tin-tungsten mineralization in the contact zone of the CHS pluton on Ketchem Dome (section 1, T7N, R14E, F.M.). The host rocks are syenogranite and quartz-mica schist. The ore minerals include cassiterite, wolframite, and pyrrhotite. Tourmaline is abundant in both hosts.

The mineralization is exposed in trenches and covers an area 100 meters (325 feet) by 30 meters (100 feet). Both tin and tungsten grades are less than 0.2 percent.

#### 8.2.3.7 Switch Creek and Discovery Gulch

Barker (1979) reports anomalous tin and tungsten from syenogranite on Switch Creek (section 4, T7N, R14E, F.M.). Nearby at the confluence of Discovery Gulch and Deadwood Creek, cassiterite and wolframite are present in the placer deposits. Both creeks are within the contact zone of the CHS pluton. The pluton intrudes micaceous quartzites and quartzites. The pluton and the schists are locally silicified. Other minerals present in heavy mineral concentrates are apatite, epidote, garnet, hematite, ilmenite, magnetite, scheelite, spinel, tourmaline, and zircon.

#### 8.2.3.8 Butte Creek

Metz (1984g) describes the occurrence of argentiferous tetrahedrite, arsenopyrite, pyrite, sphalerite in a chlorite schist near the confluence of Butte Creek and Birch Creek (section 24, T7N, R10E, F.M.). The sulphide mineralization is parallel to compositional layering in the isoclinally folded schist. The sulphides constitute between 5 and 10 percent of the rock and occur as 0.2 to 1.0 centimeter wide lenses or as disseminations in the schist. Microprobe analyses of the tetrahedrite indicate silver contents of 12 to 15 percent.

In addition to chlorite, the silicate mineral assemblage includes plagioclase, quartz, white-mica, and garnet. Calcite is present both as 1-5 millimeter size grains and as narrow crosscutting veinlets up to 10 centimeters wide.

The sulphides are only exposed for approximately 300 meters (1,000 feet) in a road cut, thus the width and thickness of the mineralization is unknown. Base metal geochemical anomalies in Bear, Fish, and Butte Creeks suggests that the sulphide mineralization may extend for a considerable distance beyond the road excavation.

#### 8.2.3.9 Gold Dust Creek

Metz (1984g) reports stratabound sulphide and lead and silver vein type mineralization on Gold Dust Creek (section 22, T7N, R11E, F.M.). The stratabound mineralization is similar to that at the Butte occurrence. The vein mineralization is hosted in the sulphide mineralization and in metachert. The vein consists of approximately a half meter (1.7 feet) of massive milky quartz with pods of galena and minor sphalerite. Grab samples of the galena rich vein material assay in excess of 10 OPT Ag.

The vein exposure is in the active channel of the creek and is exposed over a strike length of 30 meters (100 feet). No third dimensional data are available for the occurrence.

The gently dipping stratabound sulphide mineralization extends over an area of at least 300 meters (1,000 feet) by 100 meters (325 feet) that is exposed by placer mining activity. The mineralization appears to continue under the alluvial gravels, and base metal geochemical anomalies are present upstream from the placer excavation.

#### 8.2.3.10 Eagle Summit

Metz (1984g) reports pods of massive stibnite in mica quartzite in section 35, T8N, R11E, F.M. The pods are an echelon and are in near vertical shears that strike northeast and southwest. The individual masses are up to 15 centimeters (6 inches) wide and up to a meter (3.25 feet) in the other two dimensions. The mineralization is exposed for about 20 meters (65 feet) along the Steese Highway. The continuity of the mineralization along strike and down dip is unknown.

#### 8.2.3.11 Porcupine Dome

Metz (1984g) reports stratabound sulphide mineralization in a placer mining excavation on Porcupine Creek above the confluence of Yankee Creek (section 4, T8N, R11E, F.M.). The mineralization includes arsenopyrite, galena,

pyrite, and sphalerite and is hosted primarily in marble. Graphitic and chloritic schists host stratabound pyrite and arsenopyrite.

The sulphides in the marble constitute 10 to 15 percent of the rock and form lenses up to 6 centimeters (2.5 inches) thick. The flat lying carbonate hosted mineralization is exposed only over an area of a few square meters. However the iron and arsenic sulphide mineralization is intermittently visible for a distance of two kilometers (1.2 miles) along the historic placer workings. The width and thickness of the mineralized section are unknown. The sulphides in the schist account for 5 to 10 percent of the rock and occur as 1-5 millimeter size grains. The disseminated grains are elongate parallel to the foliation. Gold occurs as 1-10 micron size inclusions in the arsenopyrite.

#### 8.2.3.12 Bonanza Creek

Metz (1984g) describes stratabound sulphide mineralization in the placer workings on the lower 3.2 kilometers (2 miles) of Bonanza Creek, the reference section for the Bonanza Creek sequence. The mineralization is on strike with similar mineralization on Porcupine Creek which is 9.6 kilometers (6 miles) to the west.

On Bonanza Creek, the mineralized section strikes east-west and dips to the north at 15 to 45 degrees. The base of the sequence is at the upstream limit of the exposure. The basal lithology is chlorite schist intercalated with graphitic schist. Disseminated pyrite and arsenopyrite comprise 5-10 percent of the rock. Channel samples taken at right angles to the compositional layering indicate gold grades of 0.12 OPT over 1.5 meter (5 feet) widths.

The stratabound mineralization is cut by narrow vertical quartz veinlets that range from less than a centimeter (1/2 inch) to 15 centimeters (6 inches) wide. The veinlets strike east-west.

The veinlets contain pyrite, arsenopyrite, and gold. Gold wires up to 5 millimeters long and gold crystals up to 2 millimeters in diameter occur within vuggy quartz. Gold also occurs as inclusions in the arsenopyrite and along the sulphide grain boundaries.

Two larger quartz base metal sulphide veins are noted at the same locality. These structures strike N 45 W and are vertical. They range in thickness from 60 centimeters (2 feet) to 1.0 meters (3.25 feet). The veins are exposed in the placer cut for approximately 30 meters (100 feet).

The sulphide mineralogy is galena, sphalerite, traces of jamesonite, and tetrahedrite. Channel samples across the veins indicate gold values ranging from 1 to over 2 OPT.

#### 8.2.3.13 Independence Creek

Metz (1984g) reports the occurrence of stibnite in mica quartzite and chlorite schist in section 12, T7N, R12E, F.M. The mineralization is in a vertical shear zone that strikes east-west. The stibnite forms lenticular masses 15 centimeters (6 inches) wide and 1.0 meters (3.25 feet) in diameter.

The shear zone is filled with quartz, blue-grey clay, stibnite and traces of pyrite. The zone contains only traces of

gold where it crops out in the road cut. The vertical and lateral extent of the mineralization is unknown.

#### 8.2.4 Placer Deposits

After the Klondike and the Fairbanks district, the Circle mining district is the next largest placer gold producing area of the Yukon-Tanana Uplands. The Circle district continues to be a centre of placer mining activity. The average scale operation in the district in recent years is about 1,500 cubic meters (2,000 cubic yards) per day and there have been on an average 20 operations per year in the district for the past decade. In 1983 there were over 50 discrete operations. This rate of mining however, is declining.

The relatively high relief, limited overburden, and thin gravel sections have enhanced the economics of placer mining in the Circle district over other districts in the YTT. These same factors, as well as the large number of mining exposures have facilitated the investigation of the placer deposits of the district.

Surficial deposits account for all of the gold production of the district. These deposits include colluvium, fan deposits, Tertiary(?) gravel, and Recent alluvial gravels (Yeend, 1989a, 1989b).

Colluvium includes unsorted to poorly sorted gravel, sand, silt, and clay. The colluvium deposits are found along the margins of valleys with steep bedrock walls. Mass wasting processes responsible for these deposits are enhanced in the sub-arctic environment and are most prevalent on north facing slopes. These processes may be responsible for valley asymmetry and this asymmetry may be a guide in placer exploration. Colluvium is common in Portage, Miller, Mastodon, Mammoth, and Independence Creeks which are also asymmetrical drainages.

Fan deposits are also found as fill in the Tintina Fault trench. They are poorly sorted sediments of late Pleistocene and Holocene age.

The Tertiary gravels are orange to dark brown and are highly weathered. The clasts include quartzite, mica schist, and granite. The matrix has a high clay content and thus the gravels are poorly sorted. The gravels are generally low grade (0.0025 OPT) however locally mineable grades are present on Crooked Creek. The Tertiary gravels are also present north of the Circle Hot Springs fault on Portage and Deadwood Creeks.

Late Pleistocene and Holocene gravels are found along the reaches of all the creeks in the district. The gravels occur both as floodplain and as older terrace deposits. The gravels are grey to light brown and are composed of clasts of unweathered quartzite, mica schist, mafic schist, and granite. Radiocarbon dates indicate ages ranging from less than 40,000 B.P. to 10,000 B.P. (Yeend, 1989b). The total thickness of the gravels range from 2 to 6 meters (6 to 20 feet). Gold grades range up to 0.04 OPT.

Descriptions of the placer deposits of the Circle district are summarized by creek in Appendix D2. There are two significant factors with respect to the placer gold deposition that are apparent from the tabulation and from unpublished

U.S. Bureau of Mines placer production data. First, ninety-five percent of the placer production comes from areas underlain by either Bonanza Creek sequence, mafic schist, or granitic rocks. Yeend (1989b) indicate that the mafic schist unit is the sole lode source for the placer gold. Second, the placer gold fineness values reflect the different bedrock types.

The Bonanza Creek sequence and mafic schist are the bedrock types for over ninety percent of the placer gold production while the intrusive rocks account for only five percent. Each of these lithologies contain more than trace amounts of gold and are potential source rocks for the placer deposits although neither lithology is known to contain economic lode deposits.

The fineness values for gold from the Bonanza Creek sequence and the mafic schist bedrock range from 810 to 915, with a mean value of 852 and a standard deviation of 26. The fineness values for the placers related to intrusive bedrock range from 714 to 806 with a mean value of 757 and a standard deviation of 39. Thus, there is a significant difference in the sample means for the two populations.

By contrast, fineness values for the Fairbanks district range from 824 to 961 with a grand mean of 894. Limited fineness data for intrusive bedrock related placers indicate values in excess of 900 fine. Thus the potential intrusive-related lode sources for the Fairbanks district have very high fineness values relative to the intrusive lode sources in the Circle district. The placer deposits in the Fairbanks district with probable stratabound sulphide and metamorphic hosted vein lode sources have fineness values that are in the same range as comparable deposits in the Circle district.

Boyle (1979) has extensively reviewed the literature on the fineness of gold from various types of deposits. In the review the relative gold and silver content are expressed as a ratio rather than as fineness. A summary of the review is as follows:

1. "Only three types of hypogene deposits have Au/Ag ratios consistently greater than 1.0. These are the auriferous quartz pebble conglomerate deposits, certain skarn deposits and most, but not all, gold-quartz veins in Precambrian, Paleozoic, and Mesozoic rocks. Tertiary deposits in certain belts also have ratios greater than 1.0, but they are relatively uncommon. All gold placers always have ratios greater than 1.0.
2. The Au/Ag ratios in disseminated deposits in shales and sandstones (Kupferschiefer and red bed types) are generally low, indicating a relatively high degree of mobility and concentration of silver during formation of these particular deposits.
3. In the auriferous quartz-pebble conglomerate deposits, the range of Au/Ag ratios is generally narrow, but there are some significant differences in some deposits such as the Wirwatersrand, ... (Range 5.8 to 15.6).
4. There are few data on gold content of Mississippi Valley type lead-zinc deposits, and hence a precise

knowledge of the Au/Ag ratios is not obtainable.

5. The Au/Ag ratios in skarn deposits are exceedingly variable and related to the mineralogy and hence the chemistry of these deposits.
6. Massive nickel-copper sulphides of the Sudbury type are generally associated with basic igneous rocks, seem to have a narrow range of Au/Ag ratios from about 0.03 to 0.07.
7. The porphyry copper deposits tend to have a relatively low Au/Ag ratio judging from the few good data available.
8. The massive polymetallic sulphide deposits (Flin Flon or Noranda-Bathurst type) nearly all have relatively low Au/Ag ratios which average about 0.025.
9. The polymetallic veins and the native silver-cobalt-nickel arsenide veins have the lowest ratios of all the various types of auriferous hypogene deposits, indicating an extreme mobility of silver and practically no mobility for gold during formation.
10. Gold-quartz veins in Precambrian, Paleozoic, and Mesozoic rocks generally have Au/Ag ratios greater than 2.0, and these average about 4.2 (range 1.37 to 12.5).
11. Gold-quartz veins, lodes, and stockworks in Tertiary andesite, dacite, rhyolite, and other associated volcanic rocks generally have ratios less than 1.0.
12. Siliceous sinters precipitated from present-day hot springs generally have Au/Ag ratios less than 1.0.
13. Gold placers always have Au/Ag ratios greater than 1.0 regardless of the age of the source deposits.
14. Deposits in older geological formations are frequently richer in gold than those in younger formations.
15. The evidence that the Au/Ag ratios is an index of temperature is conflicting. On a statistical basis however there is some evidence to support the contention that deep-seated (high temperature) deposits have a higher Au/Ag ratio than those formed at intermediate depths or near the surface, presumably under conditions of lower temperature.
16. There is considerable evidence to show that the Au/Ag ratio increases in primary halos with proximity to ore shoots in most types of epigenetic gold deposits.
17. The observation of Scherbina (1956) that gold is predominant in telluride ores whereas silver is dominant in selenide ores appears to be true.
18. Gold and silica show a marked association whereas silver tends to be concentrated in an environment where carbonates are abundant.
19. Evidence from many auriferous belts throughout the world indicates that there is a wall rocks effect on the Au/Ag ratio, the ratio being higher where the wall rocks are basic than where acidic rocks are the hosts.

20. The Au/Ag ratio in deposits seems to depend on regional metallogenic peculiarities in a crude way, if only certain types of deposits are considered."

From this summary several conclusions can be drawn from the gold fineness data for the district.

The fineness values of the placers associated with stratabound sulphide and metamorphic hosted vein deposits in the Fairbanks and Circle districts are in the range of values for other comparable deposits worldwide. In contrast, intrusive related and hot springs mineralization generally have Au/Ag ratios less than one (fineness values less than 500). There are no fineness data for intrusive related mineralization in the Circle district. However the placers associated with intrusive related mineralization in the district have fineness values higher than 700. These higher values may be attributable to the mechanism of preferential silver depletion in the placer environment as noted in the Fairbanks district. The extremely high fineness values of both the intrusive related mineralization and associated placers in the Fairbanks district (over 900) are in contrast to the deposits in the Circle district.

#### 8.2.5 Trace Element Geochemistry

Metz (1984g) reported trace elemental analyses for 1118 stream sediment samples collected in the Circle B-2, B-3, B-4, C-2, C-3, C-4 quadrangles. Values for arsenic, copper, lead, zinc, and silver were determined by atomic absorption spectrophotometry on aqua-regia digests at the Bondar-Clegg Inc. laboratory, Vancouver British Columbia, Canada.

Detection limits are 10 ppm for arsenic, 1 ppm for the base metals, and 0.1 ppm for silver. Data reduction includes histograms and log concentration-probability plots for each element (see Appendix C1). Anomalous sample concentrations are determined by the method of Lepeltier (1969) and are defined as concentrations above the 97.5 probability level. Table 8.2 lists the threshold values for each element.

Ch. 8, Plates I thru VI indicate the sample locations for stream sediment, pan concentrate, and sluice concentrate samples from the district. Due to budget constraints only the stream sediment samples are reported in this investigation. Ch. 8, Plates VII thru XII display the anomalous stream

sediment samples for the district. Anomalous samples are defined as those with one or more elements above the threshold value.

#### 8.2.6 Discussion

The anomalous localities shown on Ch. 8, Plates VII thru XII suggest that there are at least seven areas of potential lode mineralization in the district that have not been previously described. Anomalous areas are defined as those having more than one sample with one or more anomalous element. Samples with multiple anomalous elements are generally considered more significant than those with a single anomalous elemental concentration. The Roman numerals on the plates depict these anomalous areas.

Area I is located in T8N, R10E, F.M. The major elemental associations are As-Pb-Zn-Ag. Bedrock in the area is Bonanza Creek sequence with the predominant lithologies being metachert, graphitic schist, and marble. The Zn anomalies are associated with the marble while the As-Pb-Ag anomalies are either associated with sulphide bearing metachert and graphitic schist or with stratabound quartz veinlets in the metamorphic rocks. Quartz veinlets in the schist occur as rubble crop on the ridge between Dome Creek and Yankee Creek and in the placer tailings on Porcupine Creek.

Area II is located in T8N, R11E, F.M. The elemental associations are the same as those in Area I as are the bedrock lithologies. The metamorphic rocks strike east-west in the area and the trend of the geochemical anomalies is also east-west. Stratabound sulphide and gold quartz vein mineralization occur on in the lower 3.2 kilometers (2 miles) of Bonanza Creek. This same section of the creek has been a major source of placer gold. The tributaries of Bonanza Creek in this area all contain stream sediments anomalous in base metals and gold.

Area III is located in T8N, R12E, F.M. The elemental associations are the same as those in Areas I and II. The bedrock lithologies are also the same except in the eastern extreme of the area. In the Granite Gulch area the bedrock is porphyritic monzogranite of the Circle Hot Springs pluton. This is the westernmost exposure of the pluton.

Table 8.2 Statistical parameters for stream sediment samples from the Circle mining district, Alaska.

Element	Geometric Mean (ppm)	Geometric Deviation	Coefficient of Deviation	Coefficient of Variation (%)	Threshold (ppm)
As	6.0	8.00	0.90	15.0	132
Cu	22.5	2.18	0.34	1.5	70
Pb	12.8	1.52	0.18	1.4	30
Ag <sup>(1)</sup>	440	3.41	0.53	1.2	540
Zn	68	1.38	0.14	0.2	130

(1) Ag in ppb.

The three anomalous areas extend over a trend length of 20 kilometers (12 miles). With the exception of the monzogranite at Granite Gulch, the bedrock is entirely Bonanza Creek sequence. There is no indication of intrusive rocks either as rubble crop or as placer tailings over the entire trend length. The creeks that crosscut the Bonanza Creek sequence in these three areas are important sources of placer gold. It is highly probable that the source of the placer gold and of the geochemical anomalies is the Bonanza Creek sequence.

Area IV is located in T7N, R12E, F.M. The elemental associations are As-Pb-Ag. The bedrock in the area is quartzite and pelitic schist and minor metachert of the Bonanza Creek sequence. Triebel (1990) provides some evidence that a buried intrusive may occur to the south of the area.

Area V is located in T6N, R12E, F.M. The elemental associations are Pb-Ag. This is the only area without anomalous arsenic concentrations. The bedrock is calc schist and minor graphitic schist. The elemental concentrations are relatively low and there is no significant placer accumulation in the creeks.

Area VI is located in T7N, R14E, F.M. The elemental associations are As-Pb-Ag. The bedrock is quartzite and pelitic schist. Granodiorite of the Two-Bit pluton crops out 1.6 kilometers (one mile) south of the area. The area includes the headwaters of Switch Creek, Ketchum Creek, and Bottom Dollar Creek. The Two-Bit pluton to the east of the area contains narrow gold quartzite veinlets in a silicified and sericitically altered zone.

Area VII is located in T7N, R15E, F.M. The elemental associations are As-Pb-Zn-Ag. The bedrock is quartzite and pelitic schist and porphyritic monzogranite of the Two-Bit pluton. This is the headwater area of Portage Creek, the most easterly gold placer occurrence in the district.

Anomalous Areas I thru IV are exploration targets for stratiform and stratabound mineralization in the Bonanza Creek sequence. This mineralization is similar to that in analogous rocks in the Fairbanks district. Area V is enigmatic in that it contains little arsenic and no placer gold concentrations. The potential of this area is considered small. Areas VI and VII have good potential for intrusive related gold mineralization.

## 8.3 STEESE MINING DISTRICT

### 8.3.1 Location and Previous Investigations

The Steese mining district is located in east-central Alaska approximately 95 kilometers (60 miles) northeast of Fairbanks (see Ch. 2, Plate I). This is a historic gold placer district, that includes the drainages of Faith, Hope, and Charity Creeks. However the headwaters of these creeks and adjacent areas have been the centre of recent lode mineral exploration. In addition to the source of the alluvial gold, the targets of the current exploration activities are tin and tungsten bearing granites, carbonate hosted lead-zinc and intrusive related gold, uranium, and rare earth mineralization.

Previous investigations of the area include Barker and Clautice (1977), Burack et al. (1984), Burand (1965, 1968),

Burton (1981, 1984), Burton et al. (1985), Cady and Barnes (1983), Cady and Weber (1983), Church and Dufree (1961), Cushing and Foster (1984), Foster et al. (1973, 1983, 1984), Holm (1973), Laird et al. (1984), Laird and Foster (1986), Le Compte (1981), Light et al. (1987), Menzie et al. (1983, 1986a, 1986b, 1987), Mertie (1937), O'Leary et al. (1986), Prindle (1906, 1913), Saunders (1967), Simpson (1983), Smith et al. (1987), Tripp et al. (1983), Tripp and Crim (1983), Tripp and Houston (1983), Staff, USGS (1974), Warner et al. (1986), Wedow et al. (1954a, 1954b), Wilson and Shew (1981) and Yeend (1987). The investigation by Smith et al. (1987) includes a synopsis of the previous investigations and the results of a recent geological and geochemical study of the area. The above investigation includes portions of the Circle B-4, B-5, B-6, C-4, C-5, and C-6 fifteen minute quadrangles. Hereinafter the study area of Smith et al. (1987) will be referred to as the Steese mining district. The following description of the general geology is summarized from Smith et al. (1987).

### 8.3.2 Bedrock Geology

Figure 8.2, after Pessel et al. (1987), is a generalized geologic map of the district. The major lithologies include Proterozoic or Lower Paleozoic metasediments and metavolcanics, Late Proterozoic or Early Cambrian "metagrit", Middle to Late Ordovician volcanics and intercalated sediments, and Cretaceous and Tertiary age intrusive rocks that range in composition from granite to lamprophyre.

#### 8.3.2.1 Regionally Metamorphosed Rocks

The aforementioned metamorphic rocks can be divided into seven main lithologies: lower Fairbanks schist, Cleary sequence, upper Fairbanks schist, lower grit, marble/chlorite schist, upper grit, and maroon and green grit (Pessel et al., 1987).

##### 8.3.2.1.1 Lower Fairbanks Schist

The Fairbanks schist is an informal name for a pelitic schist sequence mapped in the Fairbanks mining district (Metz, 1982; Robinson, 1982; and Bundtzen, 1982). The lower Fairbanks schist is the lowermost stratigraphic unit in the Steese district. The lower contact of the unit is not exposed in the district, thus the exposed thickness of 2,500 meters (8,000 feet) is a minimum. The unit is composed of white-mica-quartz schist, massive quartzite, biotite schist, and garnet-chlorite-biotite schist. The schists are fine- to medium-grained, thinly-laminated, and medium to dark grey.

In the southern part of the district the mineral assemblages include quartz, muscovite, chlorite, plagioclase,  $\pm$  garnet, and biotite. Trace amounts of tourmaline, zircon, sphene, and epidote are common. Kyanite is found in the southernmost extremity of the area.

Narrow compositional layers of chlorite schist occur in the lower Fairbanks schist. These lensoid layers are light green muscovite-chlorite-quartz schist. The muscovite may be the chromium variety fuchsita. The chlorite schist layers are not mappable units at the 1:63,360 scale.



The chlorite schists are fine- to coarse-grained and well foliated. The mineral assemblages include up to 50 percent quartz and feldspar, 40 percent muscovite, and 30 percent chlorite. Tourmaline and porphyroblastic plagioclase are common locally.

#### 8.3.2.1.2 Cleary Sequence

The Cleary sequence is an informal name for a sequence of meta-volcanic, meta-volcaniclastic, and meta-exhalative rocks mapped in the Cleary Summit area of the Fairbanks mining district (Metz, 1982). In the Steese district, the unit is composed primarily of graphitic schist, with minor felsic schist, and laminated quartzite or meta-chert. The aggregate thickness of the unit is less than 500 meters (1,600 feet).

The graphitic schist is a dark grey to black fissile rock and is interlayered with the felsic schist. The graphitic schist is composed of graphite-chlorite-white-mica schist, feldspathic quartz-white-mica schist, white or laminated quartzite, black quartzite, and felsic meta-grit. Sulphides are locally abundant in the graphite-chlorite-white-mica schist and in the black quartzite. The sulphides include pyrite, arsenopyrite, sphalerite, galena, chalcopyrite, pyrrhotite, and argentiferous tetrahedrite. The graphitic schist unit locally has abundant quartz-sulphide veinlets that also contain the above mentioned sulphides plus stibnite.

The felsic schist is composed of white-mica-plagioclase-quartz schist and laminated micaceous quartzite. The unit contains up to 75 percent quartz, 15 percent plagioclase, and 10 percent white-mica with minor chlorite and accessory tourmaline and zircon. Arsenopyrite, pyrite, and chalcopyrite are locally abundant in the unit.

R.J. Newberry (unpublished data, 1987) notes from microprobe analyses that the highly zoned tourmalines are very low in calcium and contain subequal amounts of iron and magnesium. Using the criteria of Taylor and Slack (1984), the Ca-Mg-Fe content of the tourmalines and the high degree of zonation suggest a volcanogenic origin for the host rock.

The Cleary sequence in the district has a more restricted lithologic composition than in the Fairbanks district. In the Steese district the unit is also host to stratabound and probably stratiform sulphide mineralization. The intercalation of the Cleary sequence with the Fairbanks schist which in turn underlies the lower Paleozoic rocks is the basis for assigning the unit to the Late Precambrian.

#### 8.3.2.1.3 Upper Fairbanks Schist

The upper Fairbanks schist is composed of white-mica-quartz schist, brown massive quartzite, and white-mica-biotite-quartz schist. The unit generally contains minor biotite, chlorite, garnet, and poikiloblastic plagioclase. The total thickness of the upper unit is approximately the same as the thickness of the lower unit.

Near the lower contact of the upper unit with the Cleary sequence there are layers of marble, schistose marble, calc schist and meta-chert. The carbonate bearing rocks contain up to 30 percent quartz, 20 percent white-mica, and 10 percent plagioclase.

The pelitic schists of the upper unit are generally fine-grained and are brown to greenish grey. The mineral assemblages are similar to those in the lower unit, however the upper unit grades into a fine- to medium-grained meta-grit near the upper contact. The "quartz eyes" near the upper contact are up to 1.5 millimeters in diameter.

There are no radiometric age data or fossil evidence for the age of the upper unit. The unit is overlain by the meta-grit unit that has been assigned an Early Cambrian age based on the presence of *Oldhamia*. The fossil localities in the meta-grit unit are approximately 6,000 meters (19,500 feet) stratigraphically above the Fairbanks schist thus the unit has been assigned a Late Precambrian age.

#### 8.3.2.1.4 Meta-grit Sequence

The meta-grit sequence is an informal name used by Pessel et al. (1987) for metamorphosed clastic rocks that form the majority of the exposed bedrock in the district. The rocks occur in a northeast-southwest trending belt approximately 25 kilometers (15 miles) wide. The rocks have been correlated with the Wickersham Grit of Weber et al. (1985) and thus may extend for several hundred kilometers along strike. The unit is estimated to be at least 7,000 meters (22,000 feet) thick. The meta-grit sequence is divided into the following three sub-units: lower grit, marble/chlorite marker, and upper grit.

The meta-grit unit ranges in metamorphic grade from lower greenschist facies in the northwestern part of the district to upper greenschist facies in the southeast. The lower and upper units had similar protoliths which probably included shale and siltstone with minor conglomerate and quartz arenite. The protoliths of the marble-chlorite marker were both pelitic sediments and carbonate beds.

The lower grit unit is composed of white-mica schist, brown massive quartzite, mica quartzite, and white-mica-biotite-quartz schist. Thus the unit has a bulk composition similar to the Fairbanks schist. The lower grit however only exhibits lower greenschist mineral assemblages while the upper Fairbanks schist attained upper greenschist isograds. The total thickness of the lower unit is less than 2,000 meters (6,500 feet).

The marble-chlorite marker unit is composed of marble, dolomitic marble, calcareous schist, and minor white-mica-chlorite-quartz schist. The carbonates are very fine grained to cryptocrystalline. Locally the marbles grade into calcareous schist. The unit has similar metamorphic mineral assemblages to the lower grit unit; however the finer grain size distribution gives the appearance of a slightly lower metamorphic grade for the marble-chlorite marker unit. The total thickness of the unit is less than 2,000 meters (6,500 feet).

The upper grit unit is composed primarily of slate and phyllite and thus appears to be of slightly lower metamorphic grade than the other two sub-units of the meta-grit sequence. The sedimentary parentage of the meta-grit sequence is readily apparent in the minor lithologies of the upper unit that include: quartz arenite, quartzite, calcareous sandstone,

quartzwacke, and graywacke. The rocks have all been metamorphosed to lower greenschist facies as evidenced by anthigenic chlorite, white-mica, and quartz forming in the matrix of the clastic sediments.

The age of the meta-grit has been estimated by the occurrence of the trace fossil *Oldhamia* in the overlying maroon and green grit. The fossil has been noted at two localities in the Circle quadrangle and one in the Livengood quadrangle (Mertie, 1937; Churkin and Brabb, 1965; Foster et al., 1983). The presence of the trace fossil in the overlying unit places an upper age limit of Early Cambrian on the meta-grit unit.

The meta-grit unit and the maroon and green grit have been correlated with the Wickersham grit, an informal unit in the Livengood quadrangle (Weber et al., 1985). The Wickersham grit includes a sequence of meta-conglomerate, quartzite, phyllite, maroon and green slate, and marble. Regionally these units probably correlate with a grit sequence in the Gull Lake area of the Yukon Territory, Canada which is 900 kilometers (540 miles) southeast of the Steese district. These grit units may also be correlative with the Twitya Formation of the Windermere Supergroup in the MacKenzie Mountains of northwest Yukon Territory. The Twitya Formation has been correlated with the Middle to Late Proterozoic grit of the Selwyn Basin (Eisbacher, 1981).

#### 8.3.2.1.5 Maroon and Green Grit

The unit is the youngest of the meta-clastic sequences in the district and is composed of slate and phyllite with subordinate gritty sandstone and siltstone. The unit crops out to the northwest of Lime Peak and strikes northeast-southwest. The unit has been mapped for a strike length of about 20 kilometers (12 miles) in the district. The belt of rocks is about 6 kilometers (3.6 miles) wide.

The lower contact of the unit has been mapped as a thrust fault west of the Lime Peak pluton. Lithologically the unit is similar to the underlying upper grit unit. The maroon and green grit exhibits a characteristic upward fining sequence west of the district and the reversal of this sequence in the district is partial evidence for an overturned structure in the area. The lower thrust contact thus may be the result of major axial plane shearing in a folded sequence that is otherwise conformable. Such an assumption has been made in assigning upper age limits on the underlying grit units.

The upper contact of the maroon and green grit with the Fossil Creek Volcanics is probably a faulted unconformity. The estimated thickness of the grit is 1,700 meters (5,500 feet) with individual beds up to 15 meters (50 feet) thick. Minor limestone, marble, and calc-arenite beds are found up to 3 meters (10 feet) thick and near the southern and northern extremities of the unit, mafic schistose rocks occur in horizons up to 70 meters (225 feet) thick.

The mafic schist is a fine- to medium-grained rock with relict lapilli texture. The rock is composed of calcite, quartz, chlorite, calcic pyroxene, plagioclase, muscovite, epidote, opaques, and volcanic rock fragments. The mafic schists and associated carbonate layers form two mirror image belts that

suggest they represent limbs of a major overturned syncline.

As noted above, the presence of the trace fossil *Oldhamia* in the northern part of the district is evidence of an Early Cambrian age for the unit. The maroon and green grit correlates with the middle unit of the Wickersham grit of the Livengood quadrangle (Weber et al., 1985). The Wickersham grit in turn has been correlated with the Windermere Supergroup of the Yukon Territory and British Columbia, Canada. The Windermere Supergroup is Late Proterozoic (Hadrynian) thus grit sequences of the district may be Hadrynian or older and as young as Early Cambrian.

#### 8.3.2.1.6 Fossil Creek Volcanics

The Fossil Creek Volcanics are defined by Mertie (1937). The type locality is to the west of the district in the Livengood quadrangle. In the district, the unit is composed of dark-grey to dark-brown shale, cherty shale, shaly siltstone, calcareous shale, limestone, dolomite, and black banded chert. The sediments are intruded by dikes and sills of mafic and ultramafic composition. Thus the rocks correlate with the lower part of the Fossil Creek Volcanics, but the volcanic members of the formation are absent from the district. The total exposed thickness of the unit is 1,300 meters (4,200 feet).

The clastic sediments of the unit are dominantly composed of quartz (up to 95 percent) with minor lithic fragments (3 to 5 percent) and traces of plagioclase, muscovite, biotite, tourmaline, and opaques. The cements include carbonate, silica, and hematite.

The carbonate rocks are very fine-grained dark- to light-grey limestone and dolomite. The limestone contains up to 10 percent detrital quartz and is interbedded with black shale and thin-bedded white chert.

The chert is dark-grey to black and is the predominant rock type in the lower part of the unit. The chert contains angular grains of quartz, feldspar, tourmaline, and lithic fragments and is interbedded with dark-grey to black argillite. The chert contains up to 20 percent hematite in the matrix and up to 10 percent hematite or carbonate cement.

The chert is interbedded with tuffaceous sandstone, and lithic tuff near the lower contact with the maroon and green grit. The volcanoclastic rocks contain clinopyroxene, hornblende, and plagioclase.

The Fossil Creek Volcanics in the district correlate with the lower sedimentary unit of the formation that is defined in the Livengood quadrangle by Chapman et al. (1971). In the Livengood quadrangle the lower unit is thinly interbedded calcareous dark-grey slate, black tuffaceous shale, dark-grey to black banded chert with minor mafic volcanics (Wheeler et al., 1987). The outcrop area in the Livengood quadrangle is contiguous with that in the Steese district.

The Fossil Creek Volcanics are Middle to Late Ordovician based on fossils collected in the Livengood quadrangle (Chapman et al., 1971; Blodgett et al., 1987). The formation may be correlative with an Ordovician to Cambrian section of mafic tuffs, basalts, shale, and limestone in the Selwyn Basin, Yukon Territory.

### 8.3.2.2 Intrusive Rocks

Burns and Newberry (1987) define the following six types of intrusive rocks in the Steese district: 1) the three granitic plutons of the Hope granite suite, 2) sills and dikes of gabbroic and ultramafic composition in the northwest portion of the district, 3) irregular stocks of hornblende granite, lamprophyric and alkalia syenitic dikes, and felsite dikes, 4) the Pinnel Mountain monzogranite, 5) rhyolitic and trachytic dikes, and 6) gabbroic dikes intruding the Hope granite suite. The Hope granite suite includes the Lime Peak, Quartz Creek, and Mt. Prindle composite plutons. These three plutons account for over 95 percent of the exposed intrusive rocks in the district.

The Hope granite suite contains a variety of mineral occurrences including lode tin mineralization (Burton et al., 1984; Holm, 1973; Menzie et al., 1986a; Warner et al., 1986), fluorite veins (Mertie, 1937), vein uranium (Barker and Clautice, 1977; Burton, 1981), rare-earth bearing dikes (Burton, 1981; Armbrustmacher, 1984), and placer tin mineralization (Joesting, 1942, 1943; Wedow et al., 1954).

The three plutons of the Hope granite suite are part of a belt of Late Cretaceous to Early Tertiary age intrusives that extends from northern British Columbia through the Yukon Territory and into east central Alaska (see Ch. 2). Some of the intrusive rocks of the belt are spatially related to lode and placer tin and gold occurrences; porphyry type copper and copper-molybdenum occurrences; and tungsten skarn occurrences.

The plutons of the Hope granite suite generally indicate passive emplacement and elongation parallel to the regional structural trend of the host rocks. The regional trend of the host rocks is northeast-southwest; however the trend is deflected locally by north to north-northeast trending high angle faults. The plutons crosscut the major thrust faults in the district as well as in the region; thus the intrusives post date the thrust faults.

Using the terminology of Streckeisen (1976), the plutons of the Hope granite suite are classified as composite intrusives that consist of syenogranite and monzogranite. Individual plutons may have up to three distinct main phases that in turn may be intruded by mafic dikes. The contact of the intrusives with the country rocks are sharp and fine-grained margins are rare. Granitic dike rocks, quartz veins and quartz-tourmaline veins may occur in the country rock near the contact zone of the main intrusive body. The contacts between the individual phases of the plutons are much less distinctive.

#### 8.3.2.2.1 Lime Peak Pluton

The Lime Peak Pluton is 18 kilometers (11 miles) long and 6 kilometers (3.6 miles) wide with a total outcrop area of approximately 108 square kilometers (40 square miles) or about 7 percent of the area of the Steese district. The intrusive is composed of three main phases. From oldest to youngest these are: (L1) a coarse-grained seriate unit; (L2) a fine-grained porphyritic- to medium-grained equigranular unit; and (L3) a fine- to medium-grained equigranular unit.

The main phases are intruded by dikes that range in

composition from rhyolite porphyry to diabase. Phases (L1) and (L2) are locally fractured and the fractures are filled with iron- and manganese-oxides. Greisen veins preferentially intruded phases (L2) and (L3) and consist primarily of chlorite and sericite.

#### 8.3.2.2.2 Quartz Creek Pluton

The Quartz Creek pluton is 17 kilometers (10 miles) long and 4 kilometers (2.4 miles) wide with a total outcrop area of approximately 68 square kilometers (24.5 square miles) or about 4 percent of the mining district. The pluton consists of two main phases. The earlier phase (Q1) is a coarse-grained seriate unit similar to (L1) but with a greater abundance of potassium feldspar megacrysts. The later phase (Q2) is a fine-grained porphyritic and a fine- to medium-grained equigranular unit equivalent to (L2). The Quartz Creek pluton is distinguished from the Lime Peak pluton by a greater abundance of potassium feldspar, a paucity of rhyolite dikes, finer grained biotite, schlieren with up to 50 percent biotite, and an absence of greisen veins.

#### 8.3.2.2.3 Mt. Prindle Pluton

The Mt. Prindle pluton is more equi-dimensional than the other two plutons and has an outcrop area of approximately 40 square kilometers (15 square miles) or about 2.6 percent of the total area of the district. The pluton is composed primarily of one phase (P1) which is compositionally equivalent to (L2) and (Q2). However phase (P1) has greater textural variability ranging from seriate to porphyritic to equigranular. A minor phase (P2) is similar to (L3) and consists of a fine- to medium-grained equigranular unit. Although there are bulk mineralogical similarities in the three intrusives, the Mt. Prindle pluton has significant differences in the trace mineral content. First, it contains more topaz and tourmaline than the Lime Peak or Quartz Creek units. Second, it contains less fluorite than the Lime Peak units but not less than the Quartz Creek units.

Phase (P1) of the pluton is dominantly a monzogranite that includes four mappable textural varieties. The contacts between these textural units are gradational. Phase (P2) is also a monzogranite but does not exhibit the same textural diversity of (P1). Conversely units (L1) and (Q1) are syenogranite intruded by monzogranites (L2) and (Q2) respectively.

Burns and Newberry (1987) have summarized the petrographic characteristics of the main phases of the three plutons as well as the mineral grain size distributions for each unit. Although the plutons have considerable textural variability and the noted trace mineral differences, they all exhibit a similar alteration suite of sericite-chlorite-minor opaque-ilmenorutile  $\pm$  muscovite.

Rhyolite porphyry dikes of the Hope granite suite crosscut all the main granite phases and are thus the youngest rocks in the suite. The dikes are light green- to grey-, white-, orange-, and pink-weathering and occur both within the main plutons and adjacent to them. The dikes are composed of phenocrysts of quartz (5 to 20 percent), potassium feldspar (2 to 10

percent), plagioclase (up to 7 percent), and biotite (up to 3 percent). The phenocrysts range in size from 0.5 to 5 mm in the largest dimension. The groundmass is green to grey, and aphanitic.

#### 8.3.2.2.4 Minor Intrusive Rocks

Gabbroic and ultramafic rocks occur in the northwestern portion of the district. The gabbros are dark green- to grey-weathering sills and dikes. The majority of the rocks are holocrystalline, fine- to medium-grained, and equigranular however, locally they may be basaltic and porphyritic. The gabbroic rocks are composed of 40 to 60 percent clinopyroxene, 40 to 60 percent plagioclase, up to 5 percent olivine, and up to 5 percent opaque minerals. The pyroxene may be zoned with rims of brown hornblende.

The ultramafic rocks include lherzolite and clinopyroxenite. The lherzolites consist of clinopyroxene, olivine, and less than 10 percent calcic plagioclase.

The mafic and ultramafic rocks intrude both the Fossil Creek Volcanics and the maroon and green grit, thus the intrusives must be Middle Ordovician or younger. Locally the intrusives are altered to chlorite, serpentine, and carbonate rich rocks. The age of alteration is unknown.

The Pinnell Mountain monzogranite is a small pluton in the eastern extremity of the district. The total outcrop area is less than a square kilometer (0.4 square miles). The unit is a porphyritic, medium- to coarse-grained rock. The megacrysts are potassium feldspar and the matrix is composed of medium-grained quartz, zoned plagioclase, and biotite. Minor amounts of hornblende, sphene, magnetite, and tourmaline are present.

The Pinnell Mountain unit is distinguished from the Hope granite suite by: (a) a lower differentiation index, (b) smaller europium anomalies, (c) more calcic plagioclase, (d) co-presence of sphene, magnetite, and hornblende, and (e) indications from bulk chemistry of a higher crystallization pressure (Burns and Newberry, 1987). These differences indicate a higher economic potential for the Pinnell Mountain unit, which will be reviewed in a subsequent section.

The following three types of alkalia rocks occur in the district: (a) hornblende quartz monzonite, (b) lamprophyre and syenite and (c) felsite. The hornblende quartz monzonite unit occurs as dikes and small irregular shaped bodies, and is spatially associated with the lamprophyric dikes discussed below. The unit is white to brown-weathering and is phaneritic and porphyritic. The megacrysts are potassium feldspar, and the matrix is composed of equigranular quartz and plagioclase with minor hornblende, clinopyroxene, biotite, sphene, and traces of magnetite, apatite, and pyrite.

The lamprophyres are reddish-brown weathering dike rocks. The unit is composed of 5 to 20 percent biotite in a fine-grained groundmass of clinopyroxene, biotite, and potassium feldspar, with minor leucite and garnet. Generally the lamprophyres intrude the hornblende quartz monzonite.

The felsite dikes occur in the Homestake Creek and Table Mountain area in the extreme east of the district. The felsites are spatially associated with the alkalia suite, however

the intensity of alteration precludes precise petrologic classification.

The dikes are generally microcrystalline but may have phenocrysts of quartz, alkali feldspar, and biotite with traces of hornblende, magnetite, sphene, zircon, and apatite. The alteration minerals include chlorite, ankerite, sericite, magnetite, and pyrite.

Mafic dikes intrude the units of the Hope granite suite. The dikes are gabbroic in composition, with 70 to 85 percent plagioclase, and the balance clinopyroxene. The dikes are not altered.

#### 8.3.2.3 Contact Metamorphic Rocks

Contact metamorphism is present at the margins of the plutons of the Hope granite suite and to a lesser extent at the margins of the smaller intrusives. The evidence for contact metamorphism is the occurrence of biotite or hornblende-bearing hornfels zones. The hornblende-bearing hornfels may contain garnet.

The hornfels zones generally extend for not more than 500 meters (1,500 feet) outward from the steeply dipping contacts, however, at a few localities the zones are over a kilometer (3,000 feet) wide thus suggesting low angle contacts.

The diversity in the composition of the country rocks results in significant differences in the contact metamorphic mineral assemblages. In the sandstones and grit unit, the response to the thermal effects is represented by secondary silicification, white-mica, and biotite. The pelitic rocks produce white-mica, biotite, quartz, feldspar, with or without chlorite, andalusite, tourmaline, cordierite, and garnet.

In the calcareous rocks, the mineral assemblages include quartz, plagioclase, phlogopite, calcite, tremolite, and garnet. The carbonate units contain tremolite ± calcite, chlorite, quartz, idocrase, garnet, and diopside. Skarn mineralization includes garnet, idocrase, actinolite, chlorite, hornblende, fluorite, clinopyroxene, calcite, and rare sulphides, scheelite, and hulsite-pageite.

The mineral assemblages in the hornfels zones include upper albite-epidote hornfels facies to lower hornblende hornfels facies. The alteration of garnet to chlorite and hornblende to biotite is evidence for retrograde metamorphism. The absence of garnet-bearing hornfels in the pelitic host rocks suggests that the granitic magmas were relatively cool at the time of emplacement (Pessell et al., 1987).

#### 8.3.2.4 Regional Structure

Swainbank (1987) summarizes the structural geology of the district; the following is primarily from that summary. In the above review the structural elements are identified using standard stereonet projection and include: foliation, minor fold axes, lineations, cleavage, bedding, joints, veins, and faults. The outcrop data are supplemented by airphoto interpretation of major folds, faults, and lineations. Swainbank (1987) concludes that there are five structural domains in the district. The overall northeast-southwest trend of bedding

and foliation is reflected in the same orientation of the structural domains. These domains are shown on Figure 8.2.

Domain (A) is located in the northwest portion of the district. In this domain, bedding and foliation have a mean strike of  $N75^{\circ}E$  and generally dip  $30^{\circ}$  to  $40^{\circ}SE$ . Although the stereonet projections of poles to bedding and foliation suggest only monoclinial folds in the domain, large overturned north-vergent folds (F1 event) are observed in the field. The folds are asymmetric, isoclinal, and overturned, with axial planes dipping to the south. Open cylindrical folds (F2 event) are superimposed on the isoclinal folds. The axes of the open folds strike northwest-southeast. Lineations in domain (A) trend  $N40^{\circ}E$  and  $N65^{\circ}W$ . These major trends are approximately parallel to the isoclinal and open fold axes respectively.

Domain (B) is located southeast of domain (A). In domain (B), foliation strikes  $N45^{\circ}E$  and dips to the north at  $30^{\circ}$ . Thus domain (B) appears to encompass the south limb of a major synclinorium with an axis parallel to the axes of the smaller scale isoclinal folds. As in domain (A), the isoclinal fold axes and the axis of the synclinorium have been refolded by open folds with northwest trending fold axes. The lineations in domain (B) are similar in orientation to those in domain (A).

Domain (C) is located southwest of domain (B). Due to poor bedrock exposure there are much less structural data than for domains (A) and (B). In the southwest extremity of the domain, isoclinal overturned folds have axes that trend northwest-southeast and dip to the northeast at 30 degrees. These isoclinal folds are vergent to the southwest. In the central and eastern portion of the domain the isoclinal folds trend east-west or northeast-southwest and are south or southeast vergent. Lineations generally trend parallel to the isoclinal fold axes.

Domain (D) is located southeast of domain (B) and northeast of domain (C). In domain (D) isoclinal fold axes trend northwest-southeast, the axial planes dip to the northeast at  $20^{\circ}$  to  $40^{\circ}$ , and the folds are southwest vergent. The isoclinal fold axes are refolded by open folds with axes trending  $N45^{\circ}E$ . Lineations are either parallel or at right angles to the isoclinal fold axes.

Domain (E) is southeast of domain (D). Poles to foliation in the domain are bimodally distributed. The isoclinal fold axes trend northeast-southwest, the axial planes dip to the north on the north limb of a northeast-southwest trending anticlinorium and dip to the south on the southerly limb. The isoclinal fold axes and the axis of the anticlinorium are refolded by open folds with northwest-southeast trending axes. The anticlinorium is generally parallel to the synclinorium of domains (A) and (B). Lineations are both parallel and at right angles to the isoclinal fold axes.

Swainbank (1987) does not segregate the joint, fault, or vein data by structural domain but the joint data are reduced according to major lithologies. The joints in the metasedimentary units have the following three major trends: north-south, east-west, and  $N45^{\circ}W$ . In all three directions, the joints are nearly vertical. In the intrusive rocks, the joints

strike predominantly north-south and  $N45^{\circ}E$ . As in the metasedimentary units, low angle joints are absent. In the hornfels zones there are four joint sets all of which are near vertical. The major trends are north-south, east-west,  $N45^{\circ}E$ , and  $N45^{\circ}W$ . The absence of low angle joints in all lithologies may be due to lack of attention to those structures during the field mapping.

The major mapped faults are high angle structures with both strike-slip and dip-slip components. These structures make up the boundaries between domains (B) and (C), between domains (C) and (D), and between domains (C) and (E). The high angle faults trend north-south to  $N60^{\circ}E$ .

Limited thrust faulting occurs in domain (A) both west and northwest of the Lime Peak pluton. The thrusts are northerly directed and thus indicate the same sense of motion as the north vergent isoclinal folds.

Aerial photographs indicate linear features which are in part expressions of contact zones and in part inferred fault zones. Due to poor outcrop distribution, most of the lineaments reported by Swainbank (1987) cannot be confirmed as faults.

The veins reported in Swainbank (1987), are primarily greisen veins in the plutons. The trend approximately  $N45^{\circ}W$  and dip between  $70^{\circ}$  and  $80^{\circ}$  to the south. Detailed investigations at the Bedrock Creek, Cliff, and Tin Ridge prospects indicate a major east-west trend to the greisen veins but not to the joints in the intrusives. The veins at these prospects appear to be controlled by the contacts between various phases of the plutons (Swainbank, 1987).

### 8.3.3 Lode Mineral Occurrences

Prior to the work by Smith et al. (1987) there were only five known lode mineral prospects in or adjacent to the district. These are the Dempsey Pup antimony occurrence in section 14, T6N, R6E, F.M. (Joesting, 1943), the Hope Creek antimony-copper-lead-molybdenum-tungsten occurrence in section 26, T7N, R6E, FM (Joesting, 1943), the Mt. Prindle uranium and rare earth occurrence in section 2, T7N, R6E, F.M. (Burton, 1981), the Table Mountain gold occurrence in section 9, T7N, R9E, F.M. (Burack, 1983), and the Lime Peak tin-silver occurrence in section 19, T9N, R5E, F.M. (Burton et al., 1984). Newberry et al. (1987) state that there are "several hundred mineral occurrences" located or relocated as a result of their investigation, however they do not define what constitutes a mineral occurrence. Newberry et al. (1987) continued with descriptions of fifteen areas of multiple anomalous stream sediment, pan concentrate, or rock geochemical samples.

The presence of such multiple anomalous samples is the basis for the definition of a mineral occurrence in this report.

The fifteen anomalous areas or "prospects" and the elemental associations discussed by Newberry et al. (1987) are as follows:

1. Faith-Charity Creeks (stratiform Au)
2. Bachelor Creek (stratiform Au)
3. Pinnell Trail (Sb Anomaly)

4. Table Mountain (Au veins; Au-W skarn)
5. Lower Hope Creek (hydrothermal Au)
6. Bedrock Creek (Sn-Ag)
7. Cliff (Sn-Ag)
8. Tin Ridge (Sn-Ag)
9. North Fork Prospect (Sn-Ag)
10. Mascot Creek (Sn-Ag)
11. South Lime Peak (Sn-Ag)
12. Upper Preacher Creek (Sn-Ag)
13. Mt. Prindle (Sn-Ag; U-REE)
14. Hope Creek (Sn-Ag)
15. Fluorite Creek (Sn-Ag)

The Dempsey Pup antimony, the Hope Creek antimony-copper-lead-molybdenum-tungsten, and the Mt. Prindle U-REE occurrences are outside the area included in the investigation of Smith et al. (1987). The first two occurrences are probably associated with Cleary sequence rocks and may have similarities to the stratiform gold occurrences on Faith-Charity Creeks and Bachelor Creek. The following brief descriptions refer to the fifteen mineral occurrences listed above.

#### 8.3.3.1 Faith-Charity Creeks Stratiform Au

Smith et al. (1987) describe a section of Cleary sequence in sections 22, 23, 26, and 27 T7N, R7E, F.M. The sequence includes grey graphitic chlorite-muscovite schist, black to dark grey graphitic schist, grey laminated quartzite, and feldspathic quartz-muscovite schist. The feldspathic units are generally limonitic and contain stratiform sulphides. The graphitic schists may contain up to 10 percent disseminated pyrite.

A measured section of 52 meters (170 feet) on Charity Creek is reported to contain slightly anomalous gold (14 ppb), lead (720 ppm), arsenic (140 ppm) and silver (500 ppb). The section is primarily composed of grey laminated quartzite and graphitic schist.

On Faith Creek, quartz veins containing pyrite, sphalerite, arsenopyrite, chalcopyrite, and stibnite crosscut the schist sequence. The veins occur in red weathering horizons of graphitic schist. Select samples of the vein material contain up to 4.8 ppm Au, 67 ppm Ag, 8.4 percent Pb, 11 percent Sb, 7.3 percent Zn, 1.1 percent As, and 0.17 percent Cu (Smith et al., 1987).

#### 8.3.3.2 Bachelor Creek Stratiform Au

Smith et al. (1987) report on a measured section on Bachelor Creek, section 23, T7N, R8E, F.M. Twenty-three rock geochemical analyses from the section indicate gold contents of less than 6 ppb as well as very low abundances for Ag, Pb, Sb, Zn, As, and Cu. The 48 meter (155 ft.) thick section is composed of graphitic schist, feldspathic schist, micaceous schist, quartzite, and felsic grit.

The sulphide-bearing lithologies of the Cleary sequence on Bachelor Creek strike toward Table Mountain. The lithologies are associated with stream sediment and pan concentrate geochemical anomalies discussed in section 8.3.5. There is no indication of intrusive rocks in the Bachelor Creek

drainage thus these anomalies are attributed to the Cleary sequence. In the Table Mountain area discussed below, the Cleary sequence is intruded by felsic dikes and the origin of the mineralization in that area cannot be attributed to only the Cleary sequence.

The measured sections in the Bachelor Creek drainage have very low metal contents, however mineralized samples of Cleary sequence rocks in the area have significant amounts of metal. The felsic schists and laminated quartzites contain up to 240 ppb Au, 4,300 ppm Cu, 2,100 ppm As, 4,000 ppb Ag, 4.5 ppm Sb, 130 ppm Zn, 14 ppm Pb, 90 ppm Sn, and 3,100 ppm W. The graphitic schists contain lower amounts of all the above metals (Smith et al., 1987).

#### 8.3.3.3 Pinnell Trail Sb Anomaly

The tributaries of the North Fork of Birch Creek and Bear Creek (T8N, R10E, F.M.) are reported to contain anomalous concentrations of antimony in the stream sediments (Wiltse and Reifensuhl, 1987). The drainage area is underlain by micaceous quartzite and chlorite-quartz-muscovite schist. The chloritic schist contains 45 percent plagioclase, 25 percent chlorite, 15 percent quartz, 5 percent muscovite and minor pink garnet, sphene, calcite, and zoisite. The unit is mineralogically similar to the mafic unit of the Cleary sequence in the Fairbanks district.

Trace elemental analyses of the two units indicate low level anomalous concentrations of antimony and arsenic in both units with the chloritic schist containing significantly higher concentrations at the 90 percent confidence level (Wiltse and Reifensuhl, 1987).

#### 8.3.3.4 Table Mountain Au Occurrences

Black biotite schist in section 9, T7N, R9E, F.M. is reported to contain anomalous gold concentrations (Burack, 1983; Menzie et al., 1987; Smith et al., 1987). The schist contains arsenopyrite and tourmaline and up to 140 ppm gold. Menzie et al. (1987) do not describe the mineralogy or petrology of the schist, but attribute the high gold concentrations to nearby quartz sulphide veins and felsic dike rocks. The felsic dikes are composed of phenocrysts of quartz, potassium feldspar, and sericitized plagioclase in a fine-grained groundmass of sericite. Locally the dikes are intruded by veinlets of quartz and fluorite.

The schists are also intruded by two separate phases of granitic rocks. One phase is a coarse-grained equigranular biotite granite and the other is a porphyritic biotite granite. The coarse-grained granite is composed of 23 percent plagioclase, 29 percent quartz, 41 percent potassium feldspar, and 7 percent biotite (Menzie et al., 1987). The plagioclase is altered to white-mica and the biotite to chlorite. The granites are also intruded by the felsic dikes and at several localities these dikes have low level gold anomalies (250 ppb). Near the anomalous dike rocks, the granitic rocks contain up to 10 ppm Sn but no detectable Au or Ag.

Menzie et al. (1987) note that fluid inclusions from the mineralized quartz veins and dike rocks are of two types. Type I are low salinity, low CO<sub>2</sub> bearing, liquid-rich and

homogenize in the range of 250° to 275°C. Type II inclusions have similar salinities and CO<sub>2</sub> contents as those of Type I, however Type II inclusions are vapor-rich and homogenize in the range of 320° to 380°C. They also note that there is no morphological evidence to suggest that the Type I inclusions are secondary inclusions. Although the two types do not homogenize at near the same temperatures, Menzie et al. (1987) believe that the two types are cogenetic and thus indicate boiling conditions. They then estimate a depth of emplacement of the veins between 1.4 and 2.4 kilometers (4,600 to 7,800 feet).

The depth of emplacement of the granites is estimated (from the contact effects) at 6 kilometers (19,000 feet). The difference between the depth of mineralization and the depth of the crystallization of the granitic rocks is between 3.6 and 4.6 kilometer (14,400 and 11,200 feet). The range in ages of other granites in this area is between 66 and 57 m.y. Thus assuming the mineralization is associated with the latest intrusive event, the uplift rate ranges from 3.6 to 4.6 kilometer per 10 million years (Menzie et al., 1987).

The exact origin of the high grade gold mineralization on Table Mountain is still problematical. Both southwest and northeast of the occurrence, placer gold production comes from drainages that contain no evidence of intrusive rocks. The high gold values at Table Mountain occur in the black biotite schist rather than in late stage felsic dike rocks or quartz veins. The presence of tourmaline in the contact zone of the intrusives is suggested as evidence for an intrusive related origin of the gold as well as the tourmaline in the schist (Menzie et al., 1987). As noted previously, there is strong evidence for syngenetic tourmaline in the metavolcanic rocks of the Cleary sequence. Recent work by Solie et al. (1990) and Newberry et al. (1990) suggests that there is generally a higher probability of intrusive related gold mineralization associated with the earlier more mafic phases of plutonic complexes rather than with the later more felsic phases as is suggested by Menzie et al. (1987) for the Table Mountain occurrence.

#### 8.3.3.5 Lower Hope Creek Au Anomaly

Swainbank and Burton (1987) report anomalous gold in stream sediment and pan concentrate samples from Zephyr Creek (sections 28, T7N, R7E, F.M.) a tributary of Hope Creek. Small bodies of hornblende quartz monzonite and the contact zones of the intrusives also contain anomalous gold concentrations. Quartz veinlets in the micaceous quartzites which are hosts to the intrusives, also contain minor gold mineralization. These are all possible sources for the placer gold deposits that occur in Hope Creek below Zephyr Creek.

Bedrock exposure in the area is limited and the resistant micaceous quartzite that is observed only in rubble, may not be representative of all the metamorphic lithologies present. The unit is composed of massive grey quartz rich rocks with minor white-mica. The non-resistant chloritic and graphitic rocks of the Cleary sequence are not apparent in the area.

The hornblende quartz monzonite may be altered to a chlorite-ankerite-sericite rich rock that may contain pyrite,

fluorite, and garnet. The contact zones of the intrusive are anomalous in As, Sb, and Au. Minor quartz vein material occurs in the rubble of the contact zones and in the intrusive rubble.

#### 8.3.3.6 Bedrock Creek Sn-Ag Occurrence

Burton et al. (1985) report tin mineralization in the Bedrock Creek area (sections 4 and 9, T9N, R5E, F.M.) of the Lime Peak pluton. The mineralization is hosted in units (L1) and (L2). Newberry et al. (1987) describe the mineralization as consisting of subparallel zones of chlorite greisens up to 1 kilometer (4,000 feet) long and 60 meters (200 feet) wide. The zones strike N30W, N60W, and N70W and are near vertical. The individual greisen veins are up to 0.6 meters (2 foot) wide and may be as closely spaced as 5 veins per 3 meters (10 feet). Biotite, tourmaline, and zinnwaldite are associated with the highest cassiterite concentrations. The greisen veins may also contain chalcopyrite, molybdenite, sphalerite, and arsenopyrite. The veins may crosscut biotite-tourmaline-beryl-topaz pegmatites and aplite dikes in the granites. The chlorite greisens may in turn be cut by narrow shear zones.

The highest grades reported by Newberry et al. (1987) are 0.7 percent Sn although grades of 0.3 percent are common. Silver, grading up to 1 OPT is correlated with Sn bearing rather than with the high sulphide bearing greisens. Metal zonation is best exemplified by zinc halos around the high tin bearing greisens.

#### 8.3.3.7 Cliff Sn-Ag Occurrence

The Cliff occurrence is located in section 21, T9N, R4E, F.M. It consists of tin greisen veins in the seriate granite of the Lime Peak pluton (L1). Unit (L1) is intruded by narrow dikes of porphyritic granite and rhyolite porphyry. The strike of the dikes ranges from N40W to N80W and the structures are nearly vertical.

The mineralization is associated with the contact zones of the dikes and the seriate granite. Alteration minerals include chlorite, iron oxides, and fluorite. The alteration is zoned vertically with fluorite relatively more abundant at higher elevations and chlorite more prevalent at lower elevations. The greisen veins are only a few centimeters wide at the top of the cliff but up to 0.8 meters (2.5 ft.) wide at the bottom of the cliff. The mineralized zone is approximately 300 meters (1,000 feet) long by 250 meters (900 feet) wide. Channel samples across the mineralized zone indicate grades up to 0.1 percent Sn over 0.6 meter (2 foot) widths. Anomalous Ag (3 ppm), As (200 ppm), Au (60 ppb), Mo (39 ppm), and Zn (.25 percent) are reported (Newberry et al., 1987).

#### 8.3.3.8 Tin Ridge Sn-Ag Occurrence

The Tin Ridge occurrence is located in section 26, T9N, R4E, F.M. which is the southwest extremity of the Lime Peak pluton. The primary host rock is an equigranular granite (L3) which intrudes seriate granite (L1), porphyritic granite (L2), and metapelitic rocks. The alteration and associated mineralization is in the contact zones of the equigranular granite.

The mineralized zone strikes N45W and extends for 1,000 meters (3,250 feet) along strike and 300 meters (1,000 feet) across the trend.

The alteration of the (L3) granite is primarily chloritic, however higher grade Sn values are associated with zinnwaldite and tourmaline. Individual chlorite greisen veins strike east-west to northeast-southwest and are nearly vertical. The vein widths range from a few centimeters to a meter (1 inch to 3.25 feet). Zinnwaldite-chlorite greisen veins occur as either vertical structures in the granite or as flat-lying structures in the hornfels zones. The vertical structures have orientations, and dimensions similar to the chlorite greisen veins. The flat-lying veins are narrower than the vertical veins and range from a few centimeters to 30 centimeters (1 inch to 1 foot) in thickness.

#### 8.3.3.9 North Fork Sn-Ag Prospect

The North Fork prospect is located in section 24, T10N, R5E, F.M. and is in the eastern extremity of the Lime Peak pluton. The bedrock in the prospect area includes units (L1) and (L2) and rhyolite porphyry dikes; however the contact relationships are uncertain due to the limited amount of outcrop. The mineralization in the area consists of veins of chlorite-quartz-sericite greisen ± fluorite. The trend of the mineralization is northwest-southeast, however Swainbank et al. (1987) do not indicate trends for the individual veins.

The mineralization and alteration occurs intermittently over a distance of 1.6 kilometer (1 mile). The individual veins are generally less than 12 centimeters (5 inches) wide and 30 m (100 feet) long. Rock samples from the greisen indicate anomalous Sn (up to 500 ppm), Ag (up to 29 ppm), Cu (up to 350 ppm), and Zn (up to 1 percent).

#### 8.3.3.10 Mascot Creek Sn-Ag Occurrence

The Mascot Creek anomaly is located in section 14, T9N, R4E, F.M. The occurrence is located in the northwestern portion of the Lime Peak pluton. Bedrock in the area consists of units (L1) and (L2) and rhyolite porphyry dikes.

Chlorite greisen rubble occurs on the ridge south of the creek as well as in the upper portions of the drainage. Disseminated sulphides are present in unit (L2) near the contact with (L2). The greisen rubble covers an area approximately 600 m (2000 ft.) in diameter. Swainbank and Burton (1987) report that selected samples of the greisen float contain anomalous Sn (up to 620 ppm), As (up to 0.1 percent), Pb (up to 700 ppm), and Zn (up to 2.5 percent).

#### 8.3.3.11 South Lime Peak Sn-Ag

The South Lime Peak anomalous area is centred in section 19, T9N, R5E, F.M. but extends into section 17. The occurrence is in the southern contact zone of the Lime Peak pluton. Bedrock in the area is (L1) and (L2) units as well as hornfelsed metasediments. The granites are altered and the alteration assemblages include biotite, chlorite, and clay minerals.

No chlorite greisen veins are visible, however metamorphic quartz veining is apparent in outcrop and in rubble.

Three separate anomalies occur over a strike length of 3.2 kilometers (2 miles). Wiltse and Reifensuhl (1987) report that composite rock chip samples contain anomalous amounts of the following elements, with concentrations up to: Ag (17 ppm), As (1,000 ppm), Cu (490 ppm), Mo (20 ppm), Pb (180 ppm), Sn (210 ppm), W (17 ppm), and Zn (590 ppm).

#### 8.3.3.12 Upper Preacher Creek Occurrence

The Upper Preacher Creek anomalous area is centred near the common corners of T8N, R6E; T8N, R7E; T9N, R6E; and T9N, R7E, F.M. The area includes approximately 15 square kilometers (six square miles) on the northeast contact zone of the Quartz Creek pluton. Bedrock in the area consist of units (Q1) and (Q2), and hornfelsed metasediments.

The rocks are altered and the mineral assemblages include pyrite, arsenopyrite, limonite, tourmaline, and secondary quartz. Quartz-tourmaline veins occur in the hornfelsed zone as well as in the granite. Smith (1987) reports that the veins in the hornfels are slightly enriched in the following elements: As (up to 73 ppm), W (up to 87 ppm), and Ag (up to 1.5 ppm). In the granites, the concentrations are higher with the following upper limits: As (1,200 ppm), W (26 ppm), Ag (2.5 ppm), Pb (800 ppm), and Au (36 ppb).

Two samples of almadine + spessartine + hedenbergite bearing skarn occur within 3 kilometers (2 miles) of the tourmaline quartz veins. The skarn mineralization contains elemental concentrations intermediate between the hornfels hosted and intrusive hosted quartz-tourmaline veins. Upper limits in the skarn are Au (13 ppb), Sn (1,800 ppm), Zn (340 ppm), and W (18 ppm).

Smith (1987) contrasts the Upper Preacher Creek occurrence with the Table Mountain occurrence. He notes that the former has much lower potential than the latter, based on the rock geochemistry although the stream sediment samples indicate that the Preacher Creek occurrence has a much broader area of mineralization than the Table Mountain occurrence. The discrepancy between the rock and stream geochemistry may be due to differences in dispersion at the two locations or the presence of additional lode mineralization in the upper Preacher Creek area.

#### 8.3.3.13 Mt. Prindle Sn-Ag and U-REE Occurrences

Holm (1973) reports the presence of anomalous tin on upper American Creek which drains the Mt. Prindle pluton. Uranium mineralization has been reported in the area since the 1950's. However it was not until later that Barker and Clautice (1977) and Burton (1981) defined the areal extent of the uranium mineralization and the associated rare earth element mineralization.

The Sn-Ag mineralization is associated with greisen veins and aplite-pegmatite dikes in the porphyritic granite phase of the pluton. Samples from the greisen veins indicate the following metal concentrations: Sn (up to 0.2 percent), Ag (up to 1.5 ppm), and Zn (up to 550 ppm).

The major uranium and rare earth element discoveries of the 1950's and 1970's are outside the bounds of the Steese district. The intrusive rocks and the associated veins and

contact metamorphic rocks of the district are not known to contain even near economic grade uranium mineralization. The greisen veins generally contain less than 25 ppm uranium, while quartz-fluorite veins range up to 35 ppm. Gossan and breccia zones in the intrusives may contain up to 200 ppm uranium.

The only rocks that show enrichment in the rare earth elements in the district are the chlorite greisen, zinnwaldite greisen, and quartz fluorite veins. The chlorite greisens contain up to 280 ppm Ce and 0.06 percent total light rare earth elements. The zinnwaldite greisens and quartz-fluorite veins generally contain less than 100 ppm and 35 ppm Ce respectively, with correspondingly lower concentrations of light rare earth elements.

#### 8.3.3.14 Hope Creek Sn-Ag Occurrence

The Hope Creek occurrence is located in sections 23 and 26, T7N, R6E, F.M. The occurrence is hosted in the Hope Creek pluton and in wollastinite hornfels and pyroxene bearing skarns. The higher grade mineralization is in the skarns which are pyroxene-amphibole-garnet-chlorite rocks. The skarns are within 30 meters (100 feet) of the contact of the pluton and range from 4.5 to 15 meters (15 to 50 feet) wide. Grab samples from the skarns indicate grades up to 1.8 percent Sn, 20 ppm Ag, 0.13 percent W, 0.15 percent Zn, 0.1 percent Pb, and 13 ppb Au (Smith, 1987).

#### 8.3.3.15 Fluorite Creek Sn-Ag Occurrence

The Fluorite Creek occurrence is located in section 7, T7N, R7E, F.M. Holm (1973) informally named Fluorite Creek because of the abundant fluorite rubble in the lower reaches of the drainage. The fluorite occurs in the matrix of a quartz and chalcedony fault breccia in the coarse-grained granite of the Mt. Prindle pluton. The granite is only slightly altered near the fault, with feldspars being converted to clay minerals. Limited sampling of the breccia indicates Sn concentrations up to 350 ppm (Swainbank, 1987).

#### 8.3.4 Placer Deposits

The surficial geology of the district is reviewed by Rawlinson (1987) and the placer deposits of the district are discussed by Fechner and Balen (1988). A list of the placer occurrences is included in Appendix D3 along with a brief discussion of the placer geology and gold fineness data.

Rawlinson (1987) divides the surficial deposits of the area into seven colluvial units, four alluvial units, and four glacial units. The colluvial units are not known to contain placer gold, have little potential for future placer gold discoveries, and will not be discussed herein.

The alluvial deposits are sub-divided into stream alluvium, terrace alluvium, colluvium covered terrace alluvium, and fan alluvium. These deposits are host to the known placer deposits and have the greatest potential for the discovery of additional placer reserves.

The stream alluvium consists primarily of sand and silt with minor gravel. The channel deposits are subangular to

subrounded and contain clasts up to boulder size. The composition of the clasts are representative of the composition of the bedrock of the drainages except where the streams rework local glacial deposits.

The alluvial terrace deposits are similar to the stream deposits but occur along the valley margins and up to several tens of meters above the stream deposits. The terrace alluvium generally has thicker overbank deposits and is better vegetated than the stream deposits.

The alluvial fan deposits have a higher percentage of gravel than either the stream or terrace deposits. The fan deposits occur at the convergence of streams or below moraine deposits.

Glacial-stream outwash, terrace outwash, and fan outwash are similar to the alluvial counterparts except that the glacial deposits tend to have a greater silt content. Glacial deposits are preserved near Mt. Prindle, Lime Peak, and Table Mountain. Weber and Hamilton (1984) provide evidence of four Pleistocene glacial episodes. From oldest to youngest these are the Prindle, Little Champion, American Creek, and Convert. The glacial till and outwash are not known to contain placer deposits and have limited potential for the discover of additional placer reserves in the area.

The fluvial deposits are the main source of past placer production and current placer reserves. The stream deposits are up to 200 meters (650 feet) wide and 4.5 meters (15 feet) thick. Terrace deposits are up to 400 meters (1,300 feet) wide and are of comparable thickness to the stream deposits.

Heavy minerals in the gravels include gold, cassiterite, scheelite, monazite, zircon, xenotime, topaz, tourmaline, pyrite, rutile, chalcopyrite, galena, and cinnabar. The heavy minerals occur in the lower 60 centimeters (2 feet) of the alluvial gravels and in crevices in the weathered bedrock.

Fechner and Balen (1988) report 48 gold fineness values for the district. The fineness ranges from 779 to 958. This range is wider than the ranges in gold fineness values for either the Circle or Tolovana districts. Plots of the limited data for the Steese district do not indicate any definitive spatial relationships either to the bedrock or to the stream drainage patterns.

#### 8.3.5 Trace Element Geochemistry

Wiltse (1987) reported trace elemental analyses for 1,472 stream sediment and 440 pan concentrate samples from the district. Sample analyses were conducted by Nuclear Activation Services, Ltd., Hamilton, Ontario, Canada.

The stream sediment samples were analyzed by two methods. One sample aliquot was prepared and digested in hot LeFort aqua-regia prior to analysis by atomic absorption spectroscopy for Cu, Pb, Zn, and Ag. A second aliquot was prepared, irradiated and analyzed by Instrumental Neutron Activation Analysis (INAA) for As, Au, Ba, Ca, Co, Cr, Cs, Fe, Hf, Mo, Na, Ni, Rb, Sb, Sc, Se, Ta, Th, U, W, La, Ce, Sm, Eu, Yb, and Lu.

The pan concentrate samples were also analyzed by INAA for Ag, As, Au, Ba, Co, Cr, Fe, Mo, Sb, Sc, Sn, Ta, Th,

U, W, and La. Larger samples with detectable Sn were fused into a lithium tetraborate glass disk and analyzed by x-ray fluorescence spectroscopy.

The summary statistics for the stream sediment and pan concentrate samples from Wiltse (1987) are shown in Tables 8.3 and 8.4 respectively. Threshold values are defined as the upper 2 percent of the sample values. The values above the threshold are considered anomalous. Multiple anomalous samples define the anomalous areas described previously.

The stream sediment data are comparable to the data reported for the other districts. The pan concentrate data have some discrepancies. In particular the As and Ba values are not comparable to either the stream sediment data or to pan concentrate data from the other districts. The threshold values for these elements also appear to be incorrect based on the reported means and standard deviations. The discrepancies in the As and Ba data may be a function of how the samples were collected and prepared. The threshold calculation appear to be in error, however, the means and standard deviations of the other elements are probably correct.

### 8.3.6 Discussion

The stream sediment data indicate that there are significant geochemical differences between the four major lithologies. The Fossil Creek Section and the Maroon/Green Grit units have high barium and high copper-lead-zinc contents relative to the Quartz-rich metaclastics. This may be indicative of sediment hosted lead-zinc-barite mineralization.

The Quartz-rich metaclastics are enriched in gold, tungsten, and arsenic relative to the other three lithologic types. Stream sediment samples from both the quartz-rich metaclastics and the igneous lithologies indicate relatively high uranium contents in the source areas.

## 8.4 RICHARDSON MINING DISTRICT

### 8.4.1 Location and Previous Investigations

The Richardson mining district is located in east-central Alaska approximately 80 kilometer (50 miles) southeast of Fairbanks (see Ch. 2, Plate I). The district is bounded on the north by the Salcha River and by McCoy Creek; on the east by Keystone Creek; and on the south and west by the Tanana River.

Previous investigations of the district include Saunders (1965), Bundtzen and Reger (1977), Weber et al. (1978), Foster, et al. (1979), Dusel-Bacon and Foster (1983), Metz et al. (1984e) and Swainbank et al. (1984). The first generalized geologic map of the district is from Saunders (1965) which includes limited stream sediment sample data. Saunders noted several areas of potential mineralization in addition to the known placer gold occurrences on Banner and Tenderfoot Creeks.

Bundtzen and Reger (1977) map lineaments extending from Tenderfoot Creek northwest to Shamrock Creek. These lineaments apparently control the spatial distribution of a porphyro-aphanitic quartz-orthoclase porphyry which in turn is associated with the past placer gold production from the

area. The single lode prospect in the district is in the porphyry. Bundtzen and Reger (1977) also report an  $86.9 \pm 2.6$  m.y. age date for the porphyry by K/Ar methods. The porphyry locally is sericitically altered, and contains disseminated arsenopyrite and pyrite, and is host to gold bearing quartz veinlets.

North of the porphyry, epidote-actinolite hornfels is found proximal to a coarse-grained K-feldspar-quartz-muscovite metagranite. The relationships of the hornfels and the metagranite to the porphyry and its associated mineralization are not reported by Bundtzen and Reger (1977).

Geologic mapping on a regional scale is provided by Weber et al. (1978) and discussed by Foster et al. (1979). The mapping is done at 1:250,000 scale and includes the entire Big Delta quadrangle.

Dusel-Bacon and Foster (1983) examine a gneissic dome located approximately 38 kilometers (24 miles) northeast of the district. Due to limited outcrop areas the field relationship of these gneisses and those of the district are not well understood.

Metz et al. (1984) report data on 378 stream sediments and 111 pan concentrate samples from the district. The preliminary reduction of those data defined six new areas of potential mineralization in the district.

Swainbank et al. (1984) provide a 1:40,000 scale geologic map of the district and a description of the bedrock geology (see Figure 8.3). The following is a synopsis of that discussion, supplemented by unpublished industry data.

### 8.4.2 Bedrock Geology

The Richardson mining district is located near the southern margin of the YTT. The Paleozoic or older quartzites and pelitic and calcareous schists, amphibole schists, and K-feldspar schists are of upper greenschist and lower amphibolite facies and are locally upgraded to upper amphibolite and granulite facies.

The metamorphic rocks have been intruded by a complex Cretaceous age pluton that ranges in composition from quartz diorite to a true granite.

Due to the low outcrop area (less than 1 percent), the nature of contacts and the other structural features of the metamorphic and intrusive rocks are not well defined. Within the metamorphic units, contacts are gradational and terms such as gneissic schist, schistose gneiss and granofels are used to indicate progressive changes from a dominance of a planar rock fabric to granular rock textures in which indications of regional thermal or dynamic metamorphism are minimal.

The third major group of rocks in the district is composed of contact metamorphic rocks. These indicate only local thermal effects and are usually of the epidote amphibolite facies.

#### 8.4.2.1 Regionally Metamorphosed Rocks

The group of metamorphic rocks can be subdivided into three main lithologies: schist, gneiss, and granofels.

Table 8.3 Statistical parameters for stream sediment samples from the Steese mining district, Alaska (after Wiltse, 1987).

Element (1)	Fossil Creek Section			Maroon/Green Grit			Quartz-Rich Metaclastics			Igneous Rocks		
	Mean	Std.	Threshold	Mean	Std.	Threshold	Mean	Std.	Threshold	Mean	Std.	Threshold
Au	0.010	0.008	0.020	0.010	0.009	0.020	0.019	0.090	0.058	0.013	0.009	0.015
Ag	—	—	1.0	—	—	1.0	—	—	1.5	—	—	1.5
As	11	3	62	10	3	16	19	23	78	12	18	62
Sb	2	1	3.5	1	1	4.5	2	2	7.2	1	1	3.4
Cu	45	18	63	25	7	41	20	11	51	15	10	40
Pb	20	12	30	43	40	129	20	30	34	55	60	196
Zn	140	96	173	160	110	290	90	90	339	190	170	509
W	15	12	8.4	5	3	8.4	15	20	69	12	8	31
Ba	1200	250	1780	1000	400	1739	600	150	965	650	200	1049
U	6	3	6.5	8	9	19.8	9	20	70.4	50	55	175

Note: (1) All data in ppm, means and standard deviations from bar graphs, thus values are approximations.

Table 8.4 Statistical parameters for pan concentrate samples from the Steese mining district, Alaska (after Wiltse, 1987).

Element (1)	Fossil Creek Section			Maroon/Green Grit			Quartz-Rich Metaclastics			Igneous Rocks		
	Mean	Std.	Threshold	Mean	Std.	Threshold	Mean	Std.	Threshold	Mean	Std.	Threshold
Au	—	—	0.014	—	—	0.014	0.032	0.125	0.014	—	—	0.014
Ag	—	—	0.030	—	—	0.030	—	—	0.030	—	—	0.050
As	0.5	0.3	1.10	0.4	0.5	1.10	1.6	2.7	5.85	1.3	3.5	2.0
Sb	0.1	0.1	0.23	0.1	0.2	0.23	0.4	0.7	3.17	0.2	0.5	0.10
Ta	0.3	0.4	0.22	0.4	0.7	0.22	0.7	1.3	2.05	1.3	1.9	4.10
Sn	18	70	3.4	20	70	3.4	50	150	48	120	160	24
W	2	—	22	2	—	22	9	20	100	12	20	37
Ba	280	4000	349	1000	4000	349	—	—	32	—	—	73
U	1.0	1.8	0.77	1.0	2.2	0.77	0.5	1.0	2.45	2.4	2.4	5.70

Note: (1) All data in ppm, means and standard deviations are from bar graphs thus values are approximations.

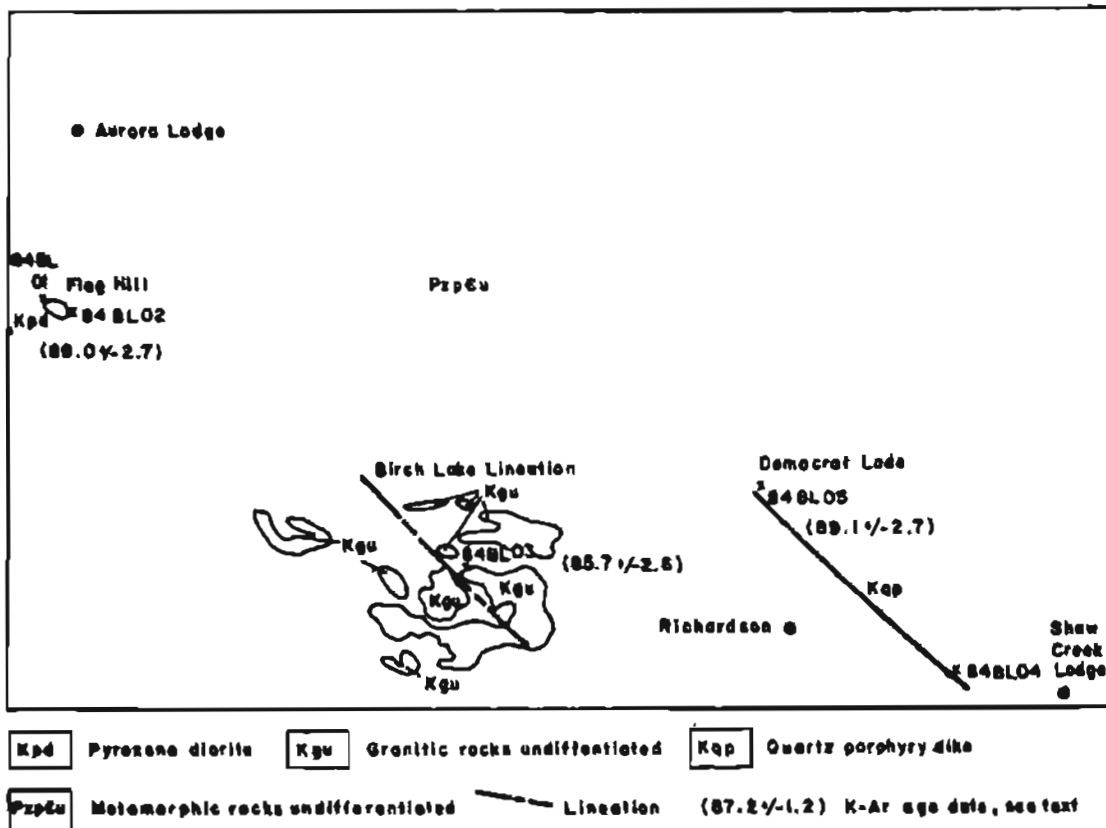


Figure 8.3 Generalized geological map of the Richardson mining district, Alaska.

#### 8.4.2.1.1 Schistose Rocks

The schistose rocks exhibit an early cataclastic texture which is overprinted by a planar synkinematic fabric. The rocks are predominantly either quartzo-feldspathic or biotite-epidote assemblages.

The quartzo-feldspathic schists have wide ranges in the proportions of quartz, twinned K-feldspar and plagioclase. Plagioclase compositions range from albite to andesine with those of the albite-oligoclase boundary most prevalent. The whole rock mineralogic compositions result in rocks that vary from quartzite to micaceous quartzite, quartz mica schist, feldspathic quartzite, and feldspathic mica schist. Compositional variants occur over narrow intervals up to a meter (3.25 feet) thus the schists have been mapped as a single rock unit.

The synkinematic fabric is marked by parallel alignment of the long axis of quartz grains and the micas including both biotite and muscovite. The large sub- to euhedral poikiloblastic plagioclase and orthoclase porphyroblasts are similarly aligned when present. Post synkinematic deformation is evidenced by intrafolial folds and bending of twin planes of the poikiloblastic plagioclase.

Minor lithologies grouped with the schists include marble, amphibole schist, and amphibolites. The marble unit is composed predominantly of calcite (80 percent plus) and minor quartz, plagioclase (albite-oligoclase), chlorite, sphene, and clinozoisite. The amphibole schist is composed of

actinolitic-hornblende, plagioclase (andesine-labradorite), quartz, clinozoisite, and minor sphene. The amphibolites have little or no quartz and a relatively larger amount of hornblende.

#### 8.4.2.1.2 Gneissic Rocks

The gneissic rocks include calcareous gneiss, amphibole gneiss and quartzo-feldspathic gneiss. The calcareous gneiss is composed of calcite, labradorite, and diopsidic pyroxene. The amphibole gneiss contains major hornblende, in part retrograded to chlorite, and lesser amounts of plagioclase (oligoclase-andesine), epidote, and sphene. The quartzo-feldspathic gneissic rocks are generally composed of quartz, plagioclase (albite-oligoclase), orthoclase or microcline, sillimanite, garnet, and minor biotite, muscovite, sphene, and zircon.

All compositional varieties display an early cataclastic texture and evidence of a later synkinematic event. The textures of the gneissic rocks have been discussed by Swainbank et al. 1984 as follows:

"Petrographic study of the texture of the gneissic rocks indicates an early phase of dynamic metamorphism with development of a granular cataclastic or mortar texture, often preserved only in the 'strain shadow' areas of rounded porphyroclasts or early porphyroblasts of potash feldspar and plagioclase. The feldspar is generally

intensely altered and the potash feldspar is sometimes twinned. Bent and strained twin lamellae are common.

The long axes of the rounded porphyroclasts make an acute angle with coarser more typical dynamothermal layering in most examples studied. Mafic and quartzofeldspathic components are more or less segregated, and oriented biotite and muscovite are aligned parallel to patches of annealed granular quartz with poorly-developed preferred lattice orientation, and to untwinned orthoclase and small twinned albite-oligoclase. Sillimanite is commonly associated with the mica, particularly the muscovite, as oriented aggregates of minute acicular crystals, and rarely as larger euhedral laths. Garnet, if present, appears to be generated from biotite in this synkinematic fabric.

Evidence of later, thermal overprinting is developed to a variable extent in the gneissic rocks, ultimately resulting in a granoblastic mosaic with only rare, obscure remnants of oriented fabric elements. Large subhedral to euhedral plates of biotite with random orientation of the c-axes disrupt biotite and muscovite rich bands, and clots of subhedral to anhedral muscovite are scattered throughout the rock in some places. Thin veinlets of felty quartz feldspar cut across earlier layering in several localities. Large subhedral or anhedral patches of poikiloblastic potash feldspar include rounded remnants of earlier quartz feldspar fabric, and cross hatch twinning is developed in many examples. Lobate or rounded patches of graphic or granophyric texture are present to some extent at quartz-orthoclase (or microcline) grain boundaries, and occasional examples of myrmekitic textures were observed. Large patches of quartz develop preferred lattice orientation, and a mottled or undulose extinction is all that indicates the origin from annealing of granular material."

#### 8.4.2.1.3 Granofels

Granofels is defined as a rock without obvious planar structure such as layering or foliation, but which has no clearly igneous origin as observed in hand specimen and in outcrop. The textures are hypidiomorphic-granular or granoblastic and the subhedral crystals are either medium or coarse grained.

Compositionally the rocks range from quartz monzonite to quartz diorite. The quartz monzonite varieties contain quartz, plagioclase (oligoclase-andesine), potassium feldspar, sillimanite, biotite possibly altered to chlorite, muscovite, and opaques. The quartz diorite assemblages contain quartz, plagioclase (andesine-labradorite), potassium feldspar, hornblende locally altered to chlorite, sphene, and opaques.

Due to the low outcrop area, the spatial relationship of the granofelsic and gneissic rocks can only be inferred. The contact between the units generally appears to be transitional and the granofelsic rocks usually occupy lower elevations. In some cases, mafic granofels are enveloped by felsic varieties

on the scale of one to ten meters (3 to 30 feet). At several localities the lower elevations contain rubble crops of granofelsic rocks that are intruded by thin felsic dikes. At higher elevations gneissic rubble crop also exhibit the presence of narrow felsic intrusives. In the north central part of the district, grano-felsic and overlying gneissic rocks are intruded by narrow arsenopyrite bearing quartz-feldspar-sericite veins.

#### 8.4.2.2 Igneous Rocks

Plutonic and hypabyssal igneous rocks outcrop in the Richardson district and some rubble crops may contain remnants of extrusive igneous rocks.

##### 8.4.2.2.1 Plutonic Rocks

The largest plutonic complex in the Richardson district is the Birch Lake Pluton. The pluton is generally coarse-grained equigranular to porphyritic and ranges in composition from quartz diorite to quartz monzonite and granite. The pluton contains abundant xenoliths and is not foliated. The contacts of the pluton have been defined primarily by rubble crop however at a few localities sharp angle contacts with distinctive hornfels or skarn zones have been mapped.

The early more mafic phase of the pluton occurs in the Flag Hill area of the northwestern portion of the district. The quartz diorite is composed primarily of quartz, plagioclase (labradorite) and diopsidic pyroxene which may be altered to tremolite or chlorite. The main accessory mineral is sphene.

The pluton becomes progressively more felsic in a southeasterly direction. In the Birch Lake area, the pluton is predominantly a coarse-grained porphyro-phaneritic monzogranite to fine-grained quartz monzonite.

The granitic rock is composed of grey quartz (20-30 percent), twinned orthoclase feldspar (30-40 percent), oligoclase (30-40 percent), and biotite (0-5 percent). Trace amounts of hornblende, muscovite, tourmaline, rutile, sphene, apatite, and magnetite are locally present. The quartz monzonitic rocks have similar compositions albeit lower quartz contents.

The porphyro-phaneritic rocks contain large orthoclase phenocrysts in the 2-5 cm range and quartz phenocrysts in the 5-10 cm range within a matrix of plagioclase feldspar in the 1-5 mm range. The porphyro-aphanitic rocks contain quartz and orthoclase phenocrysts in the 5-10 mm range in a fine-grained groundmass.

These rocks are all located at elevations below 400 meters (1,400 feet) above sea level. Intrusive contacts are sharp and at high angles where visible, however as noted above outcrops are limited and outcrops of contact zones are rare.

In the Tenderfoot Creek and Democrat Creek areas which form the southeastern portion of the district, a late phase of the intrusive occurs as a northwest-southeast trending dike. The intrusive is primarily a porphyro-aphanitic quartz-orthoclase rock. The quartz and orthoclase phenocrysts range in size from 5-10 mm. The quartz is euhedral while the feldspar is subhedral. The orthoclase is in part altered to

sericite or kaolinite. Euhedral arsenopyrite and pyrite are locally present and are in part oxidized to hematite and various hydrous iron oxides. The sulphides occur as disseminated grains in the porphyry and also in narrow quartz veinlets (1-2 cm in width) that form stockworks in the altered porphyry.

The porphyry dike is from 20-400 meters (65-1,300 feet) wide and has sharp high angle contacts with the adjacent marbles and schists. Skarn and hornfels zones are well developed northeast of the dike that outcrops intermittently for 16 kilometers (10 miles).

All of the placer gold production in the district is spatially associated with the dike. Locally there is visible gold in the altered porphyry, within the disseminated arsenopyrite, and within the quartz veinlets. There are insufficient surface and subsurface data to estimate the tonnage and grade of the gold mineralization.

#### 8.4.3 Lode Mineral Occurrence

The single known lode mineral occurrence in the district is the Democrat Mine located in T7S, R7E F.M. (see Plate XIV). The property is mentioned by Brooks (1923) but no geologic description or production data are given.

Saunders (1965) and Bundtzen and Reger (1977) give a brief description of the rhyolite porphyry dike that is host to the gold mineralization at the property. Gold occurs in fracture fillings in the dike rock with or without quartz and arsenopyrite. The fractures in the rhyolite dike crosscut the intrusive at 30 to 90 degrees. The shears are near vertical and are characterized by early sericitic and late clay alteration. The late stage kaolinite ranges from trace amounts to a complete replacement of the feldspars.

Coarse grained gold (greater than 5 mm), euhedral quartz and euhedral to massive arsenopyrite fill the 2 cm wide fractures. Coarse grained gold may occur along joint surfaces in sericitically altered rock. Sulphides, including pyrite and arsenopyrite, may be present in the joints or may occur disseminated throughout the intrusive.

The lode mineralization in the dike probably extends outside the immediate vicinity of the mine. Residual placers have been mined at several localities along the 13 kilometer (8 mile) outcrop of the dike but there is no description of the bedrock at any of these localities.

The extent and grade of the mineralization are not known. Surface sampling indicates grades up to 0.176 OPT over 14 meters (46 feet), however the mineralization is rather discontinuous along the strike of the dike (Tri-Valley Corp., unpublished data). Eight rotary drill holes in the Democrat Mine area do not intercept similar grades as have been determined from surface sampling.

Solie et al. (1990) indicate that the more mafic phases of the Birch Lake intrusive complex are highly favorable for intrusive related gold mineralization. Posterior probability estimates range from 100 to 28.4 percent. The sampling and probability estimates do not include the rhyolite porphyry dike which is the only visibly mineralized phase of the complex.

#### 8.4.4 Placer Deposits

There are only six creeks in the Richardson district that are cited in the literature as having produced placer gold. These are tabulated in Appendix D4. Early drift mine workings and extensive surface trenching is evidenced by highly vegetated tailing piles along Junction, Redman, Shamrock, Gold Run, and Canyon Creeks. The majority of the production from the district is from Tenderfoot Creek and most of the balance is from Democrat Creek.

The bedrock on Tenderfoot Creek is primarily micaceous quartzite and minor rhyolite porphyry. The alluvial placer deposits are hosted in both buried stream deposits and in older elevated bench deposits. Residual placers are hosted in the highly weathered rhyolite dike.

The alluvial gravels contain cobble to boulder size clasts in a matrix of sand, silt, and clay, thus the deposits are poorly sorted. Clasts are dominantly quartz and schist with minor amounts of intrusive rock types. The buried alluvial channel deposits are dominantly sand size material a few meters to 16 meters (9 to 50 feet) thick with the thickest sections at the confluence of Tenderfoot Creek and the Tanana River. The gravels account only for the lower few meters of the section. There is an inverse correlation between gravel thickness and grade.

The alluvial deposits are overlain by one to 25 meters (3.25 to 80 feet) of wind blown silt and its reworked products. The silt size material contains abundant organic material and is ice rich. Pleistocene mammal fossils occur in these sections of "muck" as they do throughout the uplands.

Residual placers occur on the divide between Tenderfoot Creek and Banner Creek. At this locality the white-mica schist or rhyolite porphyry is subject to intense argillic alteration. Crystalline gold and gold "wires" are attached to euhedral to subhedral quartz. There is no evidence of transport of either the gold or the quartz. The placer was mined in 1982 and 1983 and as much as 10,000 troy ounces may have been produced from an area less than 300 meters (1,000 feet) by 100 meters (325 feet).

Tenderfoot Creek flows to the southeast in an direction opposite to the Tanana River and is an example of a structurally controlled barbed drainage. The divide area between Banner and Tenderfoot Creek is not only an area of intense argillic alteration but shows evidence of oxidation and deep weathering. For instance, the disseminated pyrite and arsenopyrite in the intrusive and schist rocks are completely replaced by limonite and scorodite. To the northwest of the divide, Banner Creek flows to the southwest into the Tanana River. This same drainage pattern is indicated by the tributaries of Tenderfoot Creek. This evidence suggests that Tenderfoot Creek is a captured stream drainage.

Tilting of the surface with uplift to the northeast in a seismic area between the Richardson district and Fairbanks caused differential headward migration of proto-Tenderfoot Creek, beheading of its tributaries, and the development of a poorly drained area between Tenderfoot Creek and Banner Creek. The stream capture resulted in resorting of gold in the tributaries of Tenderfoot Creek and the formation of the

paystreaks in the drainage. The poorly drained area of the Tenderfoot-Banner divide contributed to formation of the residual placer and resulted in the preservation of the deposit.

The gold fineness for the district ranges from 693 on Buckeye Creek, to 928 on Democrat Creek. Tenderfoot Creek has an average fineness of 901. These large differences in fineness values over short distances of less than a few kilometers suggest either very different lode sources for the placer gold or a complex mechanism of weathering and transport. The latter is considered the more likely.

#### 8.4.5 Trace Element Geochemistry

A total of 378 stream sediment and 111 pan concentrate samples was collected (see Ch. 8, Plates XIV and XV). The stream sediment samples were sieved and the minus 80 mesh fractions were analyzed by inductively coupled plasma emission spectroscopy for Cu, Pb, Zn, Ni, Fe, Mn, and Cr. Analyses were completed by the Alaska Division of Geological and Geophysical Surveys (ADGGS). Pan concentrate samples were concentrated by elutriation, and the minus 100 mesh fractions were analyzed for Ag, W, As, Hg, Au, Sn, and Sb at the Bondar-Clegg Laboratory, Vancouver, British Columbia,

Canada. Silver, mercury, and gold were determined by atomic absorption methods; tungsten and arsenic determinations were completed by colourimetric techniques; and tin and antimony concentrations were measured by X-ray fluorescence.

Histograms and concentrate-log-probability plots (see Appendix C3) were completed for each element, and anomalous samples were estimated by the technique described by Lepeltier (1969). Anomalous concentrations are defined as those above the 97.5 probability level. The statistical parameters for the stream sediment and pan concentrate sample analyses are listed in Tables 8.5 and 8.6 respectively. Locations of samples with one or more elements above the estimated threshold are located on Ch. 8, Plates XVI and XVII. Ch. 8, Plates XVI and XVII also show the locations of the major intrusive rocks in the Richardson district as well as aeromagnetic contours (ADGGS, 1973).

#### 8.4.6 Discussion

The anomalous sample localities shown on Ch. 8, Plates XVI and XVII suggest that there are at least six additional areas of lode mineralization in the district. Anomalous areas

Table 8.5 Statistical parameters for stream sediment samples from the Richardson mining district, Alaska.

Element	Geometric Mean (ppm)	Geometric Deviation	Coefficient of Deviation	Coefficient of Variation (%)	Threshold (ppm)
As	18	1.28	0.11	0.6	36
Pb	8.8	1.36	0.13	1.5	18
Zn	43	1.27	0.11	0.2	70
Ni	24	1.29	0.11	0.5	40
Fe	2700	1.22	0.09	-	4000
Mn	300	1.67	0.22	0.1	1100
Cr	28	1.50	0.18	0.6	45

Table 8.6 Statistical parameters for stream and pan concentrate samples from the Richardson mining district, Alaska.

Element	Geometric Mean (ppm)	Geometric Deviation	Coefficient of Deviation	Coefficient of Variation (%)	Threshold (ppm)
Sb	15	1.67	0.22	1.5	42
As	14	1.43	0.15	1.1	30
Au <sup>(1)</sup>	110	2.09	0.32	0.3	450
Ag <sup>(1)</sup>	450	1.28	0.11	-	700
Sn	7.8	1.67	0.22	2.8	22
W	18	1.17	0.07	0.4	27
Hg <sup>(1)</sup>	40	1.75	0.24	0.6	120

(1) Au, Ag, and Hg in ppb.

are defined by more than one sample with one or more anomalous elements. Roman numerals on Ch. 8, Plates XVI and XVII depict these anomalous areas.

Area I is located in Sec. 20, T6S, R7E, F.M. (Ch. 8, Plate XVII). The major elemental associations include Hg-W±Au-Ag and Cu-Ni-Zn-Fe±Au-Ag. Bedrock in the area consist of felsic and mafic gneiss, felsic granofels, schistose gneiss, marble, and a small quartz monzonite pluton.

Area II is located in Sec. 31, T6S, R8E, F.M. (Ch. 8, Plate XVI). The elemental associations and bedrock are the same as in Area I.

Area III is located in Sec. 21, T6S, R5E, F.M. (Ch. 8, Plate XVII). The major elemental associations are Hg-Sb and Fe-Mn. Bedrock exposure is poor, however rubble crops indicate the predominance of mafic gneiss with minor schistose gneiss, quartzite, rhyolite porphyry and andesite porphyry.

Area IV is located in Sec. II, T6S, R5E, F.M. (Ch. 8, Plate XVII). The major elemental associations are Hg-Sb-W-As, and Fe-Mn±Cr. Bedrock exposure is poor, however rubble crops indicate the predominance of mafic gneiss, schistose gneiss, quartz-mica-feldspar schist and quartzite.

Area V is located in Sec. 27, T6S, R6E, F.M. (Ch. 8, Plate XVII). The major elemental association is Cr and the predominant bedrock type is amphibole gneiss.

Area VI is located in Sec. 22, T7S, R6E, F.M. (Ch. 8, Plate XVII). The major elemental associations are Sn-W-As±Sb-Au-Ag and Cu-Ni-Zn±Fe-Mn-Cr. Bedrock in the area is quartz-mica-feldspar schist, marble, hornfels, skarn, and granite of the Birch Lake pluton.

Stream sediment and pan concentrate sampling in the Richardson mining district indicates six additional areas of potential lode mineralization. Although bedrock exposures are poor to non-existent, inferences can be made to possible genetic types of lode mineralization based on the elemental associations and limited petrologic data.

The mercury-antimony-tungsten±gold and silver elemental associations are similar to the metamorphosed syngenetic mineralization in the Fairbanks district (Metz, 1977, 1982 and 1984; Metz and Robinson, 1979 and 1980). Strong silicate and ore petrologic similarities exist between the Fairbanks syngenetic mineralization and the stratabound tungsten model of Maucher (1976).

The copper-nickel-zinc±gold-silver elemental associations in areas of mafic gneiss indicate possible metamorphosed syngenetic basemetal sulphide mineralization. Saunders (1965) suggested that the low fineness values of the placer gold from the district (Smith, 1941) is a function of a basemetal sulphide source. The low fineness values for Banner and Buckeye Creeks (Metz and Hawkins, 1981) and the stream sediment base metal anomalies in this area are further supporting evidence for that hypothesis.

The tin-tungsten-arsenic±gold-silver elemental associations in the contact areas of the Birch Lake pluton are suggestive of the Cornubian tin-granite association. The sericitized, greisenized, and kaolinized quartz porphyry dikes, slightly younger than the granitic intrusives are very similar to the elvan dike systems of Cornwall, England. The pres-

ence of cassiterite, scheelite, and tourmaline in the placer deposits below the quartz porphyry dike (Wedow et al., 1954; Saunders, 1965) in T7S, R7E, F.M. (Ch. 8, Plate XVI) further supports this genetic model.

The chromium anomalies in Area V are associated with amphibolite gneiss. The association suggests a mafic volcanic or ultramafic origin of the gneiss. The economic potential of any chromite mineralization is low, however if the original bedrock source is an ultramafic rock there may be some potential for platinum group metal mineralization.

## 8.5 TOLOVANA MINING DISTRICT

### 8.5.1 Location and Previous Investigations

The Tolovana mining district is located at the common corner of the Livengood B-3, B-4, C-3 and C-4 quadrangles in east central Alaska. The district is in the northwestern portion of the YTT (see Ch. 2, Plate I). The Livengood B-3, B-4, C-3 and C-4 quadrangles have been geologically mapped (Bundtzen, 1983; Albanese, 1983a; Smith, 1983; and Robinson, 1983) and geochemical samples were collected from the mapped areas (Albanese, 1983b).

### 8.5.2 Bedrock Geology

The bedrock geology of the Tolovana district has been mapped by Chapman et al. (1971), Albanese (1983), Bundtzen (1983), Robinson (1983) and Smith (1983). Smith (1983) and Bundtzen (1983) define eight tectono-stratigraphic sequences separated by major thrust faults (see Figure 8.4). From north to south these sequences include:

1. Rampart Group (Permian or Triassic),
2. Paleozoic Clastics and Chert Unit (Silurian or Devonian),
3. Grit Unit (Late Proterozoic or Cambrian),
4. Chert Terrane (Middle Ordovician to Silurian),
5. Devonian Clastics and Mafic Couples (Middle Devonian),
6. Mesozoic Flysch (Jurassic or Cretaceous),
7. Paleozoic sedimentary, igneous and low grade metamorphic rocks (Cambrian or Ordovician),
8. Tolovana Limestone (Silurian and Devonian).

#### 8.5.2.1 Grit Unit

The Grit Unit includes conglomerate coarse-grained arenaceous sandstone, quartzite, siltstone, maroon and greenish slate, phyllite, and coarse crystalline limestone or dolomitic limestone. Chapman et al. (1971) refer to this sequence of rocks as the 'Grit Unit' of the YTT and have made a tentative correlation with the late Precambrian to Cambrian quartz rich shelf deposits of the Windemere Group of southern Canada and the northwestern United States. The rocks are regionally metamorphosed to lower greenschist facies with progressive increase in metamorphic grade from the northwest to southeast.

#### 8.5.2.2 Paleozoic Sedimentary, Igneous, and Low Grade Metamorphic Rocks

The Paleozoic sedimentary, igneous and low-grade

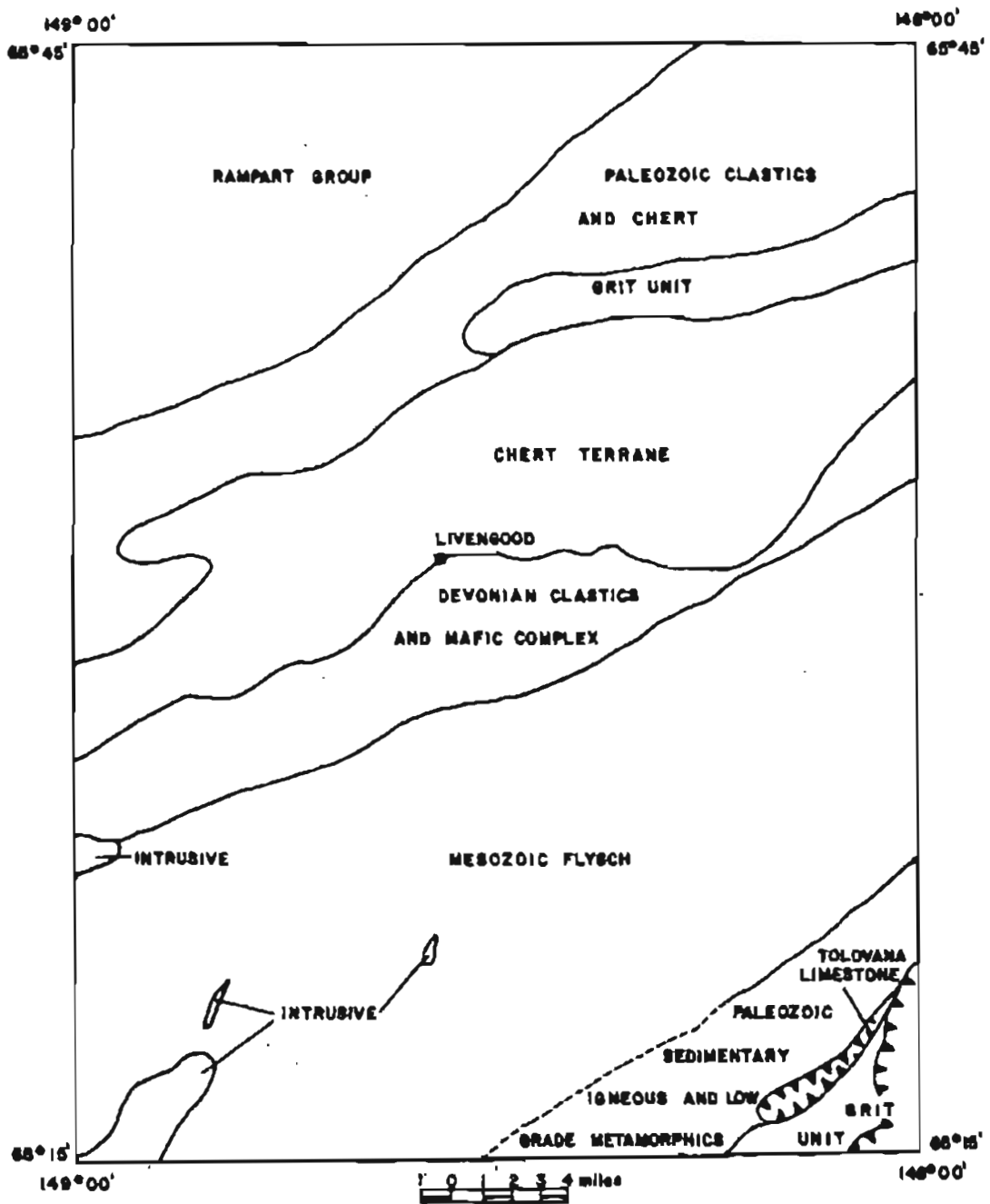


Figure 8.4 Generalized geologic map of the Tolovana mining district, Alaska.

metamorphic map unit includes fine to medium grained quartzite, dark grey to black phyllite, grey slate, grey to green banded chert, light grey coarse crystalline limestone and amygdaloidal greenstone, gabbro, and diorite. The amygdaloidal greenstone is aphanitic to coarse-grained with vesicle fillings of calcite and prehnite. The gabbros and diorites are medium to coarse-grained rocks composed of diopside, orthopyroxene, hornblende, biotite and plagioclase feldspar (An 40-60).

The Paleozoic sedimentary rocks are correlated with the *Oldhamia*-bearing grits of Noodor Dome by Chapman et al. (1971). The igneous rocks within the map unit are similar to the Fossil Creek volcanics of Church and Durfee (1961) which occur on strike to the northeast. The Fossil Creek Volcanics are of Middle Ordovician age and thus the Paleozoic sedimentary, igneous and low grade metamorphic may be of Cambrian or Ordovician age. The above map unit is regionally metamorphosed and the metamorphic grade progressively increases from the northwest to southeast.

#### 8.5.2.3 Chert Terrane

The Chert Terrane defined by Robinson (1983) includes the Livengood Dome chert of Chapman et al. (1979). The lower portion of the map unit is composed of light grey to tan fine-grained and thinly layered chert; variegated black, red, green, blue, and white massive bedded radiolarian chert; chert conglomerate; and greyish black siliceous shale and siltstone. The lower portion of the map unit contains dark grey to green massive and highly altered mafic volcanic rock and fine-grained recrystallized dolomitic limestone. Fauna evidence suggests a range in age from Middle Ordovician to Silurian (Robinson, 1983).

#### 8.5.2.4 Paleozoic Clastics and Chert Unit

Paleozoic Clastics and Chert Terrane defined by Robinson (1983) is composed of chert and shale pebble conglomerate; grey to brown, fine to medium grained lithic sandstones; maroon and green siliceous shale; and medium grey to buff recrystallized dolomitic limestone. The unit appears to overlie rocks of the Chert Terrane. With the exception of the absence of mafic volcanics, the map unit is similar to the Paleozoic sedimentary, igneous and low grade metamorphic rocks to the southeast described by Bundtzen (1983). Robinson (1983) does not indicate how the age of the Paleozoic Clastic and Chert Terrane was determined.

#### 8.5.2.5 Tolovana Limestone

The Tolovana Limestone as defined by Mertie (1937) includes a belt of carbonate rocks that extends from Willow Creek, north of Cache Mountain to Globe Creek. In the Globe Creek area Bundtzen (1983) divided the formation into three members. The Limestone Breccia member is a medium grey recrystallized limestone breccia with angular fragments up to 25 cm in diameter. The angular clasts contain *Amphipora* and coral fragments. The Laminated Limestone member is a medium grey, thinly layered silty limestone that is locally brecciated. The Massive Limestone member is medium to

dark-blue-grey massive oolitic and dolomitized micritic limestone. Faunal assemblages include *Amphipora* and *Dendrostromella* sp; *D. Rhenana* of Middle Devonian age.

#### 8.5.2.6 Devonian Clastics and Mafic Complex

The Devonian Clastics and Mafic Complex contains conglomerate, sandstone, shale, chert, and black dolomitic marble; andesitic flows and agglomerate; mafic aphanitic to coarse grained igneous rocks; and serpentinite. The sandstones and conglomerates are grey to brown thin bedded to massive sublithic rocks. The coarse clastics are interbedded with grey to olive shale that locally grades to siltstone. The andesitic to dacitic flow rocks are interlayered with grey banded chert, black dolomitic marble, and clastic rocks. The flow rocks contain phenocrysts of plagioclase, hornblende and quartz and have vesicle fillings of calcite and epidote. The mafic igneous rocks include fine to coarse-grained olive to tan weathering hypersthene gabbro, hornblende gabbro, augite bearing diorite, and massive greenstone. The serpentinite is a green to black altered peridotite occurring in and adjacent to the mafic igneous rocks (Bundtzen, 1983).

#### 8.5.2.7 Rampart Group

The Rampart Group in the Livengood C-3 and C-4 quadrangles is composed of mafic to intermediate intrusive and volcanic rocks intercalated with clastic sediments including sandstone, siltstone, shale, and chert. The intrusive rocks range in composition from gabbro to diorite and occur as irregular stocks and sills. The extrusive rocks range in composition from altered basalt to rhyodacite with the more mafic rocks predominating (Robinson, 1983; Smith, 1983).

Brosge et al. (1969) provide faunal evidence for a Permian age of the Rampart Group rocks while potassium-argon determinations on hornblende from an intrusive gabbro indicate a Triassic radiometric age.

#### 8.5.2.8 Mesozoic Flysch

The Mesozoic Flysch has been divided into two sub-units that contain varying proportions of conglomerate and finer clastics. The conglomerate, minor sandstone and siltstone unit is composed of medium to dark-olive-grey polymictic conglomerate with cobbles of greenstone, diorite, serpentinite, quartzite, siltstone, slate, phyllite, limestone and chert. The siltstone, sandstone and minor conglomerate unit is composed of medium-grey to greenish-grey siltstone, shale, and fine to medium-grained sandstone. The rocks exhibit graded bedding as well as flute casts, ripple marks, flame structures, cut and fill structures and channelling. The rocks are very immature and contain clasts and lithic fragments similar to those in the conglomerate unit. These lithic fragments are of probable local origin.

Invertebrate fauna includes *Inoceramus* and *Buchia* thus indicating a Late Jurassic or Early Cretaceous age of the sediments.

The composition and sedimentary structures of the Mesozoic sediments indicate a proximal turbidite fan environment of deposition. Similar rocks occur in a northeast-

southwest belt over 150 kilometers (90 miles) long and over 60 kilometers (36 miles) wide. The original size of the Mesozoic basin is indeterminant since the sediments have been structurally thickened.

#### 8.5.2.9 Granitic Rocks

These sequences have been intruded by Cretaceous and Tertiary age granitic rocks that range in composition from quartz monzonite to quartz syenite and rhyolite quartz porphyry. The felsic intrusives of the Livengood quadrangle yield potassium-argon ages ranging from 58.0 to 88.8 m.y. (Turner et al., 1975).

#### 8.5.2.10 Regional Structure

The above described tectono-stratigraphic sequences are deformed into isoclinal overturned and recumbent north vergent folds with axes generally striking northeast-southwest. The major terranes and rock units within the terranes are separated by thrust faults of probable Mesozoic age. The thrust faults are cut by high angle northerly trending normal faults. The high angle structures may be controls for the localization of the Cretaceous and Tertiary felsic intrusives in the Livengood quadrangle. A major normal fault (Barnes, 1961) forms the eastern boundary of Minto Flats and can be traced in a north-south direction for 100 kilometers (60 miles) as a linear feature on Landsat imagery and aerial photography. The Tolovana Hot Springs Dome Pluton as well as other unnamed felsic intrusives are located along the fault in the Eagle and Wilbur Creek area and in the Shorty and Steel Creek area. The linear feature terminates near Livengood at Money Knob and several quartz monzonite stocks also crop out in this area.

#### 8.5.3 Lode Mineral Occurrences

Prior to this investigation there were: six known lode gold prospects; a lode antimony prospect; a lode chrome-nickel prospect; and a copper-molybdenum porphyry prospect in the area. Previous descriptions of the economic geology of the Tolovana mining district include: Mertie (1918b); Overbeck (1920); Joesting (1942, 1943); Foster and Chapman (1967); Foster (1968a, 1968b); Robinson and Metz (1979); and Metz and Robinson (1980).

Foster (1968b) describes the six known lode gold deposits as follows:

1. Gertrude Creek Prospect (Location 2, Ch. 8, Plate XVIII) - "Massive, ironstained silica-carbonate rock which is green on fresh surfaces, contains minor amounts of gold".
2. Ruth Creek Prospect (Location 3, Ch. 8, Plate XVIII) - "Pyritized, brecciated, iron-stained igneous rock shows replacement by silica and carbonate and contains traces of gold".
3. Lillian Creek Prospect (Location 3, Ch. 8, Plate XVIII) - "Narrow auriferous arsenopyrite-quartz-scorodite veins occur in and near a limonite-stained dike in altered and contorted graywacke-argillite country rock. Samples from the prospect contain

from 0.5 to 48 ppm gold."

4. Griffin Prospect (Location 4, Ch. 8, Plate XVIII) - "Massive sulphide-bearing, green-stained silica-carbonate-talc rocks veined by quartz, contains as much as 3.9 ppm gold."
5. Old Smoky Prospect (Location 4, Ch. 8, Plate XVIII) - "Narrow, northwestward-trending auriferous arsenopyrite-quartz veins occur in a ferruginous quartzite footwall near the intersection of an altered porphyritic biotite monzonite dikes and a potassium feldspar-rich porphyritic dike. Samples from the prospect contain from 3 to 13 ppm gold."
6. Sunshine No. 2 Prospect (Location 4, Ch. 8, Plate XVIII) - "A northwestward-trending, crumbly, auriferous dike with internal limonite veinlets is in contact with altered argillite."

Foster (1968b) concluded that the known lode gold vein type deposits of the Livengood area are either below economic grade or have low potential for large tonnage mineralization, however, the known occurrences may be an indication of concealed deposits at depth. The host rock lithologies, trace elemental associations, and structural features of the area are similar to those common to the Carlin-type deposits of north-central Nevada, which are relatively low grade but large tonnage deposits. Future exploration in the district should encompass the Carlin-type genetic model as well as the gold quartz vein hydrothermal model.

Overbeck (1920) and Joesting (1942) report the occurrence of stibnite in bedrock at an alluvial bench placer deposit on the north side of Livengood Creek near the mouth of Amy Creek (Location 1, Ch. 8, Plate XVIII). Prior to the current investigation this was the only evidence of a potential lode mineral source north of Livengood Creek.

Foster and Chapman (1967) report chromite, magnetite, and iron-nickel alloys in a serpentinite located on the southeast side of Amy Dome (Location 5, Ch. 8, Plate XVIII). Although there is considerable strike length to the serpentinite bearing sequence only one lode sample contained anomalous elemental concentrations and Foster (1968b) found only minor chrome and nickel concentrations in stream sediment samples collected below the serpentinite outcrops.

Robinson and Metz (1979) briefly describe an occurrence of disseminated copper mineralization in a quartz feldspar porphyry near the head of Shorty Creek (Location 6, Ch. 8, Plate XVIII). The host rock is a light grey to green quartz feldspar porphyry with relict potassium feldspar altered to sericite, and plagioclase feldspar altered to albite-quartz-calcite. The quartz and feldspar phenocrysts are up to a centimeter in diameter. The groundmass is light grey to green and weathers to light tan. The rock contains disseminated pyrite, chalcopyrite, arsenopyrite, and rutile.

The Shorty Creek porphyry is located along the previously described major north-south linear feature that is probably an extension of the Minto Flats Fault. The porphyry is hosted in the siltstone, sandstone and minor conglomerate unit of the Mesozoic Flysch Terrane. The mineral occurrence was originally located for antimony and 80 state mining

claims were located in 1972 by Earth Resources Company. The property was subsequently drilled by BP Minerals, however the drill data are not currently available.

#### 8.5.4 Placer Deposits

Placer gold was discovered in the district in 1914 and the first definitive descriptions of the placer deposits was by Mertie (1918). He notes that the major placer deposits occur on Livengood Creek both as major paystreaks on bedrock or other impermeable layers, and as fine-grained disseminations throughout the gravels. He also provides considerable physiographic evidence for stream capture and the resulting changes in the flow direction of Livengood Creek. Metz (1984) has shown that stream capture, and the resulting change in flow direction and stream gradient, is an important process in the formation of alluvial placer paystreaks. Fine-grained disseminated placer deposits generally occur in distal areas such as beach deposits or as residual or eluvial deposits. The later process is probably responsible for the fine-grained disseminated deposits stratigraphically above the bedrock paystreaks of Livengood Creek.

Mertie (1918) suggests that the lode sources of the gold placers of Livengood Creek and its tributaries were quartz feldspar porphyry dikes and stocks and associated quartz veins. The intrusives and quartz veins are located on or near Money Knob and Amy Dome. Foster (1968b) provides additional geochemical evidence to support that hypothesis but also suggests a potential for Carlin-type and massive sulphide related mineralization in the area. The high gold fineness values of 907 to 934 (Metz and Hawkins, 1980) for Amy, Gertrude, Lillian, Livengood, Lucky Myrtle, and Olive Creeks would be compatible with the Carlin-type ore deposit model. The moderately low value of 866 for Ruth Creek would support a massive sulphide source as proposed by Foster (1968b). The occurrence of placer gold on Wilbur Creek (818 fine) indicates an additional source area southeast of Amy Dome. The low fineness value could be attributed to either a massive sulphide or a subvolcanic porphyry source.

From 1914 to date the Tolovana mining district has produced approximately 375,000 troy ounces of placer gold (Robinson and Bundzen, 1979) most of which has come from Livengood Creek. Hargraves (1975) and Albanese (1981) have discussed the history, mining methods, and estimated placer gold reserves of Livengood Creek. The deposit is estimated to contain 600,000 troy ounces of proven, probable, and possible reserves. The placer mines and prospects of the district are summarized in Appendix D5.

#### 8.5.5 Trace Element Geochemistry

Albanese (1983) reported analyses for 1,597 stream sediment, 197 pan concentrate and 305 rock samples from the Livengood B-3, B-4, C-3 and C-4 quadrangles. Antimony, arsenic, gold, lead, molybdenum, and silver contents were determined at the ADGGS laboratory by atomic absorption spectrophotometry on aqua regia digests. Cadmium, chromium, cobalt, copper, iron, manganese, nickel and zinc were analyzed at the ADGGS laboratory by inductively coupled

plasma emission spectrophotometry on aqua regia digests. Detection limits were 1 ppm for antimony, cadmium, copper, lead, molybdenum and zinc; 10 ppm for arsenic, chromium, cobalt, iron, manganese and nickel; and 0.1 ppm for gold and silver. Tin, tungsten and mercury were analyzed by Bondar-Clegg and Company Ltd., Vancouver, B.C., Canada. Tungsten was analyzed by colourimetric techniques with a lower limit of detection of 2 ppm. Mercury was analyzed by cold-vapor atomic-absorption spectrophotometry with a lower detection limit of 5 ppb. Tin content was determined by x-ray fluorescence with a lower detection limit of 5 ppm (Albanese, 1983).

Since not all the samples were analyzed for all the elements, data reduction could not be completed for all elements for all three groups of geochemical samples. Data reduction, including histograms and log-concentration-probability plots, (see Appendix C4) were completed for the following elements:

- A. Stream sediment samples - As, Cu, Pb, Ag, Zn.
- B. Pan concentrate samples - Cu, Au, Hg, Sn, W, Zn.
- C. Rock samples - Cu, Au, Pb, Mo, Ag, W, Zn.

Anomalous sample concentrations are estimated by the technique described by Lepeltier (1969) and are defined as concentrations above the 97.5 probability level. Tables 8.7, 8.8, and 8.9 list the statistical parameters for the stream sediment, pan concentrate, and rock geochemical samples respectively.

Plate XVI indicates sample locations of all geochemical samples from the Tolovana mining district, while Ch. 8, Plate XIX displays the anomalous sample locations for the region. Anomalous samples are defined as those with one or more elements above the threshold value.

#### 8.5.6 Discussion

The anomalous localities shown on Ch. 8, Plate XIX suggest that there are at least eight areas of potential lode mineralization in the district in addition to those previously defined by Foster (1968b) and Robinson and Metz (1979). Anomalous areas are defined as those having more than one sample with one or more anomalous elements. Samples with a single anomalous element are less significant than those samples with multiple anomalous elemental concentrations. Roman numerals on Ch. 8, Plate XIX depict these anomalous areas.

Area I is located in T10N, R6W, F.M. The major elemental associations include As-Cu-Pb-W-Zn. Bedrock in the area consist of Rampart Group rocks including greenstone, grey chert and variegated chert (Robinson, 1983). Arsenic concentrations are restricted to areas with chert exposure. High zinc concentrations in stream sediment and pan concentrate samples can be attributed in part to the relatively high zinc content of the Rampart Group greenstones with a mean of approximately 70 ppm.

Area II is located in T9N, R4W, F.M. The major elemental associations include As-Cu-Au-Pb. Bedrock in the area is Chert Terrane including grey and tan chert and chert conglomerate (Robinson, 1983; Smith, 1983).

Table 8.7 Statistical parameters for stream sediment samples from the Tolovana mining district, Alaska.

Element	Geometric Mean (ppm)	Geometric Deviation	Coefficient of Deviation	Coefficient of Variation (%)	Threshold (ppm)
As	14	1.21	0.08	0.6	25 (65)
Cu	26	1.35	0.13	1.5	48
Pb	12	1.33	0.12	1.0	22
Ag <sup>(1)</sup>	150	1.67	0.2	0.1	400
Zn	80	1.13	0.1	0.1	116

(1) Note: Ag in ppb.

Table 8.8 Statistical parameters for pan concentrate samples from the Tolovana mining district, Alaska.

Element	Geometric Mean (ppm)	Geometric Deviation	Coefficient of Deviation	Coefficient of Variation (%)	Threshold (ppm)
Cu	37	1.35	0.13	0.4	68
Au <sup>(1)</sup>	130	1.23	0.09	0.1	200
Hg <sup>(1)</sup>	95	1.26	0.10	0.1	160
Sn	7	1.21	0.08	1.2	10
W	5	1.54	0.19	3.7	12
Zn	125	1.44	0.16	0.1	170

(1) Note: Au and Hg in ppb.

Table 8.9 Statistical parameters for rock samples from the Tolovana mining district, Alaska.

Element	Geometric Mean (ppm)	Geometric Deviation	Coefficient of Deviation	Coefficient of Variation (%)	Threshold (ppm)
Cu	27	2.52	0.40	1.5	160
Au <sup>(1)</sup>	78	1.67	0.22	0.3	200
Pb	10	4.00	0.60	6.0	40
Mo	4	1.62	0.21	5.3	20
Ag <sup>(1)</sup>	200	3.50	0.54	0.3	700
W	3.5	2.00	0.30	8.6	20
Zn	50	2.80	0.45	0.9	60

(1) Note: Au and Ag in ppb.

Area III is located in T9N, R3W, F.M. The major elemental associations are As-Cu-Pb-Hg-Ag-Zn. Bedrock is Chert Terrane including grey and tan chert, chert conglomerate and chert breccia (Smith, 1983).

Area IV is located in T8N, R6W, F.M. The major elemental associations are As-Cu-Au-Pb-Hg-Mo-Ag-Zn. Bedrock is Chert Terrane including grey and tan chert, chert conglomerate and chert breccia (Robinson, 1983).

Area V is located in T7N, R5W, F.M. The major elemental associations are As-Cu-Pb-Hg-Mo-Ag-Zn. Bedrock is Mesozoic Flysch including shale, siltstone, and sandstone. In the north and south extremities of the area the sedimentary rocks are intruded by quartz porphyry (Albanese, 1983). The quartz porphyry dikes and plutons may be structurally controlled since they occur along a major north-south linear feature.

Area VI is located in T7N, R4W, F.M. The major elemental associations include As-Cu-Pb-Mo-Ag-Zn. Bedrock in the area is Mesozoic Flysch including conglomerate, minor sandstone and siltstone. The sedimentary rocks are intruded by quartz porphyry dikes and plutons. The plutonic rocks are sericitically and propylitically altered and sulphides are reported in the plutons and in a shear zone in the western extreme of the Livengood B-3 quadrangle (Bundtzen, 1983).

Area VII is located in T6N, R3W, F.M. The major elemental associations are Pb-Hg-Ag-Zn. Bedrock in the area is gabbro and diorite of the Paleozoic Sedimentary, Igneous, and Low Grade Metamorphic Terrane (Bundtzen, 1983).

Area VIII is located in T5N, R6W, F.M. The major elemental associations are As-Cu-Pb-Ag ± Sn-W. Bedrock is the quartz monzonite of the Tolovana Hot Springs Dome and the shale and siltstone unit of the Mesozoic Flysch Terrane (Albanese, 1983). Chapman et al. (1971) report a biotite  $K^{40}/Ar^{40}$  age date of  $63.3 \pm 2.5$  m.y. for the pluton. The intrusive contains up to 8 percent biotite, 7 percent blue-green hornblende and traces of tourmaline and pyrite.

Epithermal gold-quartz veins associated with quartz monzonite stocks and quartz feldspar porphyries have generally been accepted as the lode source of the major gold placer deposits of the Tolovana mining district. The veins and intrusive rocks are centred around the Money Knob/Amy Dome area and are hosted in the Devonian Clastics and Mafic Complex.

As note above, Foster (1968b) suggested that the Devonian carbonaceous siltstones, argillites, cherts, and marbles exhibit petrologic, structural and trace elemental associations similar to the Carlin-type gold deposits. From a review of recent geological mapping and a statistical analysis of concurrent geochemical sampling of the district the following generalizations can be made:

1. Precious metal mineralization occurs in the Chert Terrane, in the Mesozoic Flysch Terrane in association with porphyritic intrusives; and in the Paleozoic Sedimentary, Igneous, and Low grade Metamorphic Terrane, as well as in the Devonian Clastics and Mafic Complex.

2. In addition to the epithermal vein and Carlin-type genetic ore deposit models, a Precambrian greenstone/exhalite type gold model should be considered to account for the mineralization in the Chert Terrane.
3. The copper-molybdenum porphyry at Shorty Creek and the anomalous areas V and VI should be examined to determine if these systems are of the gold porphyry type of Harris (1979, 1980) and Sillitoe (1979).
4. A precious metal enriched massive sulphide model should be considered in the evaluation of both the Ruth Creek area and anomalous area VII since both areas contain mafic volcanic sequences.

The above ore models are summarized in Chapter 11 along with tonnage and grade ranges for each type.

Stream sediment, pan concentrate, and rock geochemical sampling in the Tolovana mining district indicate eight additional areas of potential lode mineralization. These areas of mineralization are in tectono-stratigraphic terranes not previously considered as lode gold source areas. The elemental associations in the anomalous areas of the Chert Terrane and host rock lithology suggest a Precambrian greenstone/exhalite type ore deposit mode of origin. The arsenic, antimony, copper, molybdenum ± gold and silver anomalies associated with quartz feldspar porphyries in the Mesozoic Flysch Terrane are suggestive of gold porphyry type mineralization. The base and precious metal anomalies associated with mafic volcanic rocks in both the Devonian Clastic and Mafic Complex and the Paleozoic Sedimentary, Igneous, and Low Grade Metamorphic Terrane may be indicative of precious metal enriched massive sulphide type mineralization. The base and precious metal anomalies associated with mafic volcanic rocks in both the Devonian Clastic and Mafic Complex and the Paleozoic Sedimentary, Igneous, and Low Grade Metamorphic Terrane may be indicative of precious metal enriched massive sulphide type mineralization. These genetic ore deposit models as well as the Carlin-type model proposed for the Money Knob/Amy Dome area by Foster (1968b) are large tonnage low grade models relative to the epithermal gold-quartz vein model of Murtie (1918). Based on analogy with major precious metal producing districts worldwide, the possibility of exhalite, porphyry, massive sulphide, and Carlin-type precious metal mineralization in the Tolovana district indicates a greater potential for the area than could be predicted from the previous gold quartz vein epigenetic model.

## 8.6 KANTISHNA MINING DISTRICT

### 8.6.1 Location and Previous Investigations

The Kantishna Mining District is located in west-central Alaska approximately 150 kilometers (90 miles) southwest of Fairbanks (see Ch. 2, Plate I). The district encompasses the Kantishna Hills physiographic sub-province. Previous investigations of the district include Prindle (1907), Brooks (1911a, 1911b, 1911c, 1916a, 1916b), Capps (1918, 1933, 1940), Davis (1922a), Wimmeler (1927), Pilgrim (1929),

Moffit (1933), Wells (1933), Smith (1941a, 1941b), White (1942), Glover (1948), Reed (1961), Seraphim (1961, 1962), Barker (1963), Morrison (1964), Saunders (1964), Bundtzen et al. (1976), Chadwick (1976), Hawley (1978), Bundtzen and Turner (1979), Bundtzen (1981), Metz and Hawkins (1981), Bressler (1984), Hinderman (1984), and Thornsberry et al. (1984).

The general geology and mineral occurrence descriptions that follow are primarily from Bundtzen (1981). The geochemical data are from Bressler (1984).

### 8.6.2 Bedrock Geology

The Kantishna Mining District is located near the western extreme of the YTT. The oldest rocks in the area are crystalline metamorphics that include schists and gneisses of Paleozoic or Precambrian age. Intercalated with the metamorphics are thrust sheets of Paleozoic sedimentary and volcanic rocks. The metamorphic, sedimentary, and volcanic rocks are intruded by Tertiary dikes and stocks that range in composition from felsites to basalts and ultramafics (see Figure 8.5).

The bedrock geology of the district can be divided into five major groups. From oldest to youngest these are:

1. Birch Creek Schist, predominantly a metamorphosed continental shelf sequence of Precambrian and/or early Paleozoic age;
2. Spruce Creek Sequence, metamorphosed sediments and felsic volcanics of Precambrian or early Paleozoic age;
3. Keevy Peak Formation, metamorphosed deep water marine deposits of Middle- to Late-Devonian age;
4. Tertiary continental sedimentary rocks with coal beds locally;
5. Tertiary intrusive rocks ranging in composition from felsites to ultramafics.

#### 8.6.2.1 Birch Creek Schist

Prindle (1907) included all the metamorphosed rocks of the district into the "Birch Creek Series" of Spurr (1898). The name was later changed by Mertie (1937) to Birch Creek Schist and this terminology was used by Bundtzen (1981). However he restricted the use to the older metamorphosed pelitic sediments and volcanic rocks. These metamorphic rocks have undergone at least two episodes of regional metamorphism. The earlier event developed amphibolite facies mineral assemblages while the retrograde event attained greenschist facies assemblages.

Bundtzen (1981) divides the Birch Creek Schist into seven mappable units which are summarized by Hinderman (1984) and described as follows:

**Greenstone and Greenschist** - Rocks consists of medium- to dark-green, garnetiferous greenstone, well-foliated amphibolite, and chlorite-rich amphibolitic greenschist. This unit is usually conformable with foliation and compositional changes within the formation. The rocks appear to have been derived from metamorphism of either mafic sills or volcanic

flows. Garnet-bearing amphibolite schist was collected north of the study area. This contains free gold in heavy mineral separations made for for petrographic testing (Bundtzen, 1981).

**Quartzite** - Quartzites in this unit are commonly interbedded with pelitic schists. Rocks are fine- to medium-grained, micaceous, light- to medium-grey in color and contain 70 to 90% quartz. The quartzites are locally feldspar-rich and are gradational with quartz-feldspar schist and gneiss. The quartzite beds form resistant ridges, and the resultant rubble-crop and colluvium tend to mask less resistant material present in the section. Quartzite is mapped as a separate unit in the Stampede Mine area where it has undergone brittle deformation creating open fractures that preferentially host deposits of antimony.

**Graphitic Schist** - Rocks of this unit consist of quartz, chlorite, muscovite, biotite, feldspar, and graphite. Beds of graphitic schist form useful marker horizons. These are generally less than 100 meters (300 ft) in thickness except where repeated by faulting or folding, as at the Red Dirt occurrence (see Ch. 8, Plate XX). The graphitic schist commonly contains disseminated pyrite, and most outcrops are limonite stained. This unit is a potential host environment for massive sulphide occurrences.

**Calcareous Schist** - This unit includes light greenish-grey, calcareous, mica schist, impure marble, and micaceous quartzite. These rocks are apparently derived from siliceous or silty limestone protoliths.

**Quartz-Feldspar Schist and Gneiss** - These rocks consist of light-tan, medium-grained schist and gneiss. Feldspar content ranges from about 10% in quartzitic rocks to 50% in the more feldspathic units. This unit is believed to have originated as felsic igneous intrusive and extrusive rocks predating the initial prograde metamorphism (Bundtzen, 1981).

**Marble** - Light-grey, bleached, coarse-grained marble occurs as discontinuous beds and lenses up to 50 meters (150 ft) in thickness. This unit commonly grades into the calcareous schist unit.

**Undifferentiated Schist, Quartzite, and Gneiss** - This unit includes undifferentiated schist, quartzite, and gneiss. The predominant rock type is grey to light-green, garnetiferous, quartz-chlorite to quartz-muscovite schist.

#### 8.6.2.2 Spruce Creek Sequence

Bundtzen (1981) defines the Spruce Creek Sequence as a unit consisting of sedimentary and volcanic rocks that have been regionally metamorphosed to greenschist facies. These greenschist facies mineral assemblages are in equilibrium thus depicting a less complex metamorphic history than the Birch Creek Schist.

The sequence is mapped along the crest of the Kantishna Hills from Eldorado Creek to Canyon Creek, a distance of approximately 30 kilometers (20 miles) in a northeast-southwest direction. The sequence is in apparent thrust contact with the Birch Creek Schist. The sequence has an

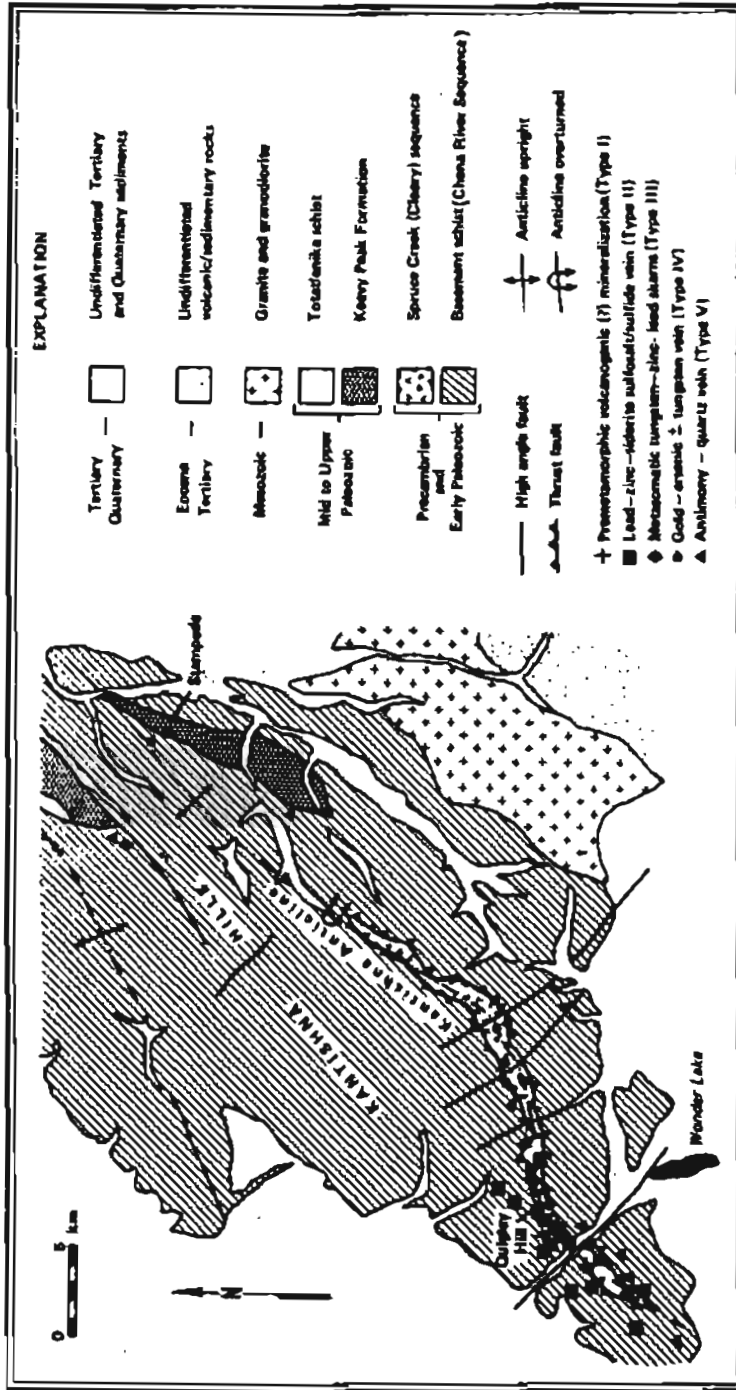


Figure 8.5 Generalized geologic map of the Kantishna mining district, Alaska (after Bundtzen et al., 1984)

outcrop width of about 2.4 kilometers (1.5 miles) and is spatially related to all the precious metal vein occurrences and to most of the alluvial placer gold deposits in the district.

The Spruce Creek Sequence is divided into seven units by Bundtzen (1981) and these are summarized by Hinderman (1984) as follows:

**Chlorite Phyllite** - This unit is the most common in the Spruce Creek Sequence. It consists of light-green to grey, locally feldspathic, quartz-chlorite phyllite and semischist. Rocks of this unit are distinguished from Birch Creek Schist by the general absence of garnet, and by micas which are commonly smaller in grain size. This unit frequently grades into a calcareous chlorite phyllite.

**Marble** - Rocks consist of grey-blue to black, phyllitic, graphitic, medium- to coarse-grained marble. The mineralogy of the marble ranges from essentially pure calcite to approximately 85% calcite, with minor amounts of quartz, muscovite, feldspar, chlorite, and graphite (Bundtzen, 1981).

**Quartzite** - This unit is characterized by medium-grey to black, thin-bedded, fine- to medium-grained, phyllitic quartzite. The rock consists primarily of quartz with minor amounts of chlorite, graphite, and feldspar. Drill cores from the Quigley Ridge area show this unit to be gradational to metafelsite.

**Interbedded Marble and Quartzite** - Fine-grained vitreous quartzite and grey-blue marble occur in alternating beds in the headwaters of Rainy Creek. Thickness of the individual beds average about 3 meters (10 feet).

**Graphitic Phyllite** - The rocks of this unit are composed of graphite with lesser amounts of chlorite, muscovite, biotite, and feldspar. They commonly contain about 45% quartz. Individual beds range from a few centimeters to several meters in thickness, and are scattered throughout the Spruce Creek Sequence. The unit is not resistant to weathering. Drill core intercepts considerably exceeded thicknesses inferred from surface exposures. Graphitic phyllite is commonly interbedded in the metafelsite and marble units and is often spatially associated with precious metal-enriched vein deposits.

**Metafelsite** - The metafelsite consists of tan-weathering, light- to dark-grey gneiss and semischist. Quartz and plagioclase phenocrysts comprise 15 to 30% of the rock. Groundmass consists of fine-grained quartz, feldspar, sericite, zoisite-clinozoisite, and opaques. Rocks locally contain up to 0.5% pyrite as disseminations and veinlets. On the basis of mineralogy, thin section analyses, and whole-rock analyses, the unit appears to be of igneous derivation (Bundtzen, 1981). Individual beds and lenses commonly parallel adjacent sedimentary units suggesting that the rocks originated as rhyolitic flows and tuffs. Both the metafelsite and quartzite units preferentially host vein-type mineralization in the Spruce Creek Sequence. Rocks of these units undergo brittle deformation, and appear to be better conduits for ore-bearing fluids than the phyllitic rocks. Surficial evidence indicates that the metafelsite contains anomalous amounts of base and precious metals.

**Meta-Andesite and Diorite Semischist** - These rocks of

intermediate to mafic composition occur as small bodies, both conformable and cross-cutting volcanic and sedimentary units. They are interpreted to be dikes and sills emplaced in the Spruce Creek Sequence prior to regional metamorphism.

#### 8.6.2.3 Keevy Peak Formation

Bundtzen (1981) correlates the rocks between Moonlight Creek and the Stampede Mine with the type section of the Keevy Peak Formation defined by Wahrhaftig (1968) at Keevy Peak northeast of the district. The Formation is of Middle- to Late-Devonian age based on fossil evidence outside the district.

The Formation is in thrust contact with the underlying Birch Creek Schist and is divided into four units by Bundtzen (1981) and these are summarized by Hinderman (1984) as follows:

**Calcareous Schist** - Tan-weathering, light-grey, calcareous schist is the basal unit of the Keevy Peak Formation. The upper portion is graphitic and gradational with the overlying unit.

**Interbedded Black Quartzite, Slate, Phyllite, and Marble** - A 275 kilometer (900 foot) thick section of interbedded black quartzite, slate, and marble overlies the calcareous schist unit. The quartzites are dark-grey, thinly laminated to massive, and locally contain up to 50% graphite (Bundtzen, 1981). The quartzite beds are gradational with dark-grey, limonite-stained, carbonaceous slate and phyllite.

**Marble** - The slate and phyllite contain interbeds of light-grey to dark blue-grey, schistose marble. These marble beds are included with the rest of the unit, except where they are large enough to map separately.

**Conglomerate and Quartzite** - The conglomerate and quartzite unit is the most distinctive in the Keevy Peak Formation. A light-tan to medium-grey, stretched-pebble conglomerate occurs at the top of the formation. Clasts in the conglomerate consist of chert, sandstone, and slate. Deformation of the pebbles parallel to the foliation exhibits a 4:1 length/width ratio. The conglomerate contains thin interbeds of quartz-rich phyllite.

#### 8.6.2.4 Tertiary Intrusive Rocks

Dikes and small stocks intrude all of the metamorphic groups. The intrusives range in composition from rhyolite porphyry to serpentinized ultramafic rocks. The Tertiary intrusives are not foliated and lack any other indication of metamorphism other than serpentinization.

Bundtzen and Turner (1979) provide potassium-argon age dates for several dike rocks in the district. Two gabbroic dikes and one quartz-orthoclase dike average 49.8 m.y. while a dacite dike yields an age of 81.3 m.y. The two plutonic episodes are similar to the two igneous events in the Fairbanks and Circle Mining Districts.

Bundtzen (1981) divided the Tertiary intrusive rocks in the district into seven groups while Hinderman (1984) grouped them into the following four categories:

**Undifferentiated Mafic and Ultramafic Intrusives** - These rocks exhibit a wide range of compositions and textures and

include serpentized ultramafics, lamprophyres, gabbros, and andesitic dikes and plugs.

**Basalt** - The basaltic rocks usually occurs as greenish-brown weathering, dark-grey, fine-grained, equigranular dikes.

**Felsic Intrusives** - The felsic intrusive rocks vary in texture from equigranular to porphyritic. Unweathered, they are usually light-grey to light-green, and weather to a tan to light reddish-brown color caused by oxidation of accessory sulphides. The majority of the felsic intrusives occur as small dikes. The stock at the Bunnell Prospect, however, is exposed over an area 1 kilometer (4,000 ft) long by 300 meters (1,000 ft) wide. The upper portion of the Bunnell stock is an equigranular granite or quartz monzonite which has undergone argillic alteration. The lower part of the stock, located near the prospect workings, is a rhyolite porphyry with moderate chloritic or propylitic alteration.

**Hornfels and Skarn** - Hornfels and skarns consisting of recrystallized, calc-silicate minerals occur chiefly in calcareous schist and marble horizons. The most prominent is the Iron Dome skarn north of Eldorado Creek. It is composed primarily of clinozoisite, microcline, idocrase, and garnet, with small isolated pods of pyrite and other sulphide minerals (Bundtzen, 1981).

#### 8.6.2.5 Tertiary Sedimentary Rocks

Continental clastic rocks occur at several localities in the district and consist primarily of sandstone, siltstone, and conglomerate. Sub-bituminous coal crops out just east of the district and rubble in several stream drainages suggests that there are undiscovered occurrences within the district. The rocks are correlated with the unit of the Nenana Coal Field to the east (Moffit, 1933; Bundtzen, 1981).

#### 8.6.2.6 Regional Structure

Bundtzen (1981) provides evidence from primary and secondary fold structures, foliation, rock cleavage, and low angle faults that the district has undergone at least two regional penetrative deformational events in pre-Cenozoic time. In Cenozoic time tensional tectonics predominated as evidenced by high angle block faulting and graben formation. The deformational events are summarized as follows:

1. "Multiple penetrative deformation resulted in the formation of open to upright, northwest trending (F1) isoclinal folds and development of foliation (S1) usually parallel to original sedimentary and igneous layering. Evidence for this deformation is preserved in the Birch Creek Schist and Spruce Creek Sequence but is absent in the Totatlanika Schist and Keevy Peak Formation. This event probably correlates with pre-Jurassic, perhaps pre-Devonian regional metamorphism which in the Birch Creek Schist, reached amphibolite metamorphic facies.
2. Compressional deformation resulted in the formation of upright, northeast trending isoclinal folds (F2) and synkinematic thrust faulting; (S2) cleavage

developed during this time. This deformation may correlate with the mid-Cretaceous metamorphic event that produced greenschist facies mineral assemblages present in the Birch Creek Schist, Spruce Creek Sequence, and Totatlanika Schist. Compressional stress from this deformation is probably responsible for rotated microtextures observed in polymetamorphic rocks. Structurally, higher portions of the metamorphic section (Totatlanika Schist) experienced milder deformation and accompanying slightly lower grade regional metamorphism. Thrust faults juxtapose the older Birch Creek Schist over the younger(?) Spruce Creek Sequence.

3. A last phase of folding (F3) warped the structural grain into broad, open synclines and anticlines during late Cretaceous or early Tertiary time. High angle joints and fractures are infilled by quartz during dewatering phases of Cretaceous regional metamorphism. True structural domes such as Busia Mtn., Wickersham Dome, formed when these warps intersected previous (F1) and (F2) fold axes. The (F3) warping locally folded thrust faults associated with the (F2) compression.
4. The initiation of high angle block faulting and high angle fracturing along northeast trending faults parallel to regional structural grain took place in Cenozoic time. This fracturing event was responsible for intrusion of dikes in the south-central Kantishna Hills. The block faulting also produced structural lows that later contributed to the development of the Crooked Creek erosion surface and sites of Tertiary sedimentary rock deposition. The block faulting episode probably continued through late Tertiary time.
5. Northwest trending faulting took place in the Late Tertiary to Recent time. A few northwest trending faults are older features associated with last stages of regional penetrative deformation, but most are fairly recent features offsetting the northeasterly structural grain. They are believed to reflect the Late Tertiary and Quaternary uplift of the Kantishna uplands, still active today."

Similar structural events are noted in the Wyoming Hills to the east (Gilbert and Redman, 1977) and in the Fairbanks district to the north (Hall, 1984) of the Kantishna Hills.

#### 8.6.3 Lode Mineral Occurrences

Bundtzen (1981) briefly describes 98 mineral occurrences in the Kantishna district. Ch. 8, Plate XX shows the location of these occurrences, and descriptions are given in Appendix D6.

Thornberry et al. (1984) classified the lode occurrences into precious metal vein types, antimony lode types and stratabound massive sulphide types. The three types of mineralization are reviewed by McKee (1984), Kurtak (1984), and Bressler (1984) respectively.

#### 8.6.3.1 Precious Metal Vein Mineralization

The precious metal vein mineralization can be subdivided into (1) silver-predominant lodes composed of galena-sphalerite-tetrahedrite-pyrite-chalcopyrite-silver in a carbonate gangue, and (2) gold-predominant lodes composed of arsenopyrite-pyrite-scheelite-gold in a quartz gangue. Although there are numerous examples of each vein type the majority of the occurrences in the district exhibit some characteristics of both types thus there is a general continuum between the two types.

Hypogene vein ore mineralogy includes: arsenopyrite, boulangerite, bourmonite, cassiterite, chalcopyrite, covellite, friebertite, galena, gold, jamesonite, marcasite, polybasite, pyragyrite, pyrite, pyrrhotite, scheelite, stephanite, stibnite, and tetrahedrite. Supergene oxidation products include: azurite, cerussite, kermesite, malachite, melanterite, scorodite, and stibiconite. Gangue mineralogy is primarily quartz, calcite, siderite, and ankerite, with minor tourmaline and barite.

Bundtzen (1981) provides a paragenetic sequence for the veins which includes: early arsenopyrite and pyrite; late boulangerite, jamesonite, and stibnite; and mid to late stage base metal sulphides and tetrahedrite. Gangue paragenesis includes early quartz followed by carbonates, barite and tourmaline.

McKee (1984) notes that high silver contents correlate with high copper rather than with high lead concentrations. Bonanza silver lodes generally also have high gold contents, however gold correlates to a higher degree with arsenic than with silver.

The vein occurrences in the district are fault controlled. The mineralized faults trend N30°E to N70°E and are subparallel to the Kantishna Anticline. In outcrop, most of the veins dip steeply to the southeast, however limited subsurface data indicate vertical to northwest dipping structures at depth.

The best developed veins occur in the metafelsite and quartzite units of the Spruce Creek Sequence. The stratabound nature of the mineralization may be due to both elemental availability and the brittle nature of the hosts.

At several localities, the veins are spatially associated with small dikes of felsic to mafic composition. There is no definitive evidence that these dikes contributed any of the metals or volatile phases to the vein occurrences.

#### 8.6.3.2 Antimony Lodes

Antimony lodes are found primarily in shear zones in the Birch Creek Schist. The mineralogy is simple, and consists of stibnite with minor arsenopyrite, pyrite, and quartz. The shear zones are parallel to the anticlinal axes of the major folds. The secondary minerals are kermesite, stibiconite, and cervantite. Trace amounts of gold may be present.

The veins are usually in the Birch Creek Schist near the contact with the Spruce Creek Sequence. Based on mineral paragenesis, the veins are probably of low temperature origin although no fluid inclusion data are available to confirm this

estimate. The stibnite lodes in the Spruce Creek Sequence crosscut the silver and gold veins.

#### 8.6.3.3 Stratabound Massive Sulphide Mineralization

There is no known economic massive sulphide mineral occurrence in the district, however there are three potential host environments: (1) quartzite units in the Birch Creek Schist, (2) black slate/schist units in the Birch Creek Schist and Keevy Peak Formation, and (3) volcanogenic rocks in the Spruce Creek Sequence. Examples of each of these environments will be discussed.

##### 8.6.3.3.1 Lloyd Prospect

The Lloyd prospect is located near the confluence of the East and West Forks of Glen Creek in section 6, T16S, R16W, F.M. It consists of a stratiform zone of sphalerite and chalcopyrite in laminated quartzite of the Birch Creek Schist. The quartzite is intercalated with garnet white-mica schist and actinolite schist.

The mineralization is in a concordant zone 0.3 to 1.5 meters (1 to 5 feet) thick which contains disseminated to massive sulphides. The sulphides are medium grained. The mineralized horizon is exposed in outcrop for 40 meters (125 feet). Grab samples contain 2.16 percent Cu, 0.09 percent Pb, 3.98 percent Zn, 0.97 OPT Ag, and traces of Au (Bundtzen, 1981).

##### 8.6.3.3.2 Red Dirt Occurrence

The mineralization is located in section 5, T11S, R17W, F.M. The host rock for the mineralization includes calcareous schist, quartz-muscovite chlorite schist, graphitic quartzite, and graphitic schist of the Birch Creek Schist. The graphitic horizons are estimated to have an aggregate thickness of 460 meters (1,500 feet).

The prospect area is marked by several gossan zones that extend for 1,200 meters (4,000 feet) along the regional strike of the schist units. The only visible sulphide is pyrite which locally constitutes over 3 percent of the host rocks. Soil samples over the gossan (Bressler, 1984) indicate up to 125 ppm Cu, 105 ppm Pb, 155 ppm Zn, 2.5 ppm Ag, 0.44 ppm Au, and 255 ppm As. Rock samples from the graphitic schist unit are highly oxidized, however they indicate the same level of anomalies as the soil samples.

##### 8.6.3.3.3 Moonlight Creek Occurrence

Bundtzen (1981) reports disseminated and massive pyrite in section 11, T15S, R16W, F.M. The mineralization is hosted in a graphitic slate unit of the Keevy Peak Formation. The pyrite is fine-grained and forms laminations up to a centimeter thick. Traces of galena are locally present and stream sediment samples from creeks draining the unit have lead and zinc concentrations in excess of 1,000 ppm. Twenty-two soil samples across the Keevy Peak Formation show the following low level anomalies: 50 ppm Pb, 110 ppm Cu, and 2.2 ppm Ag (Bressler, 1984). These trace element data suggest that the unit has moderate potential for sedimentary exhalative type mineralization.

#### 8.6.3.3.4 Spruce Creek Occurrences

The Spruce Creek occurrences are located in section 29 and 30, T15S, R16W, F.M. The mineralization consists of arsenopyrite, pyrite, and sphalerite in the metafelsite and in the actinolitic greenschist units of the Spruce Creek sequence. The metafelsite is blastoporphyratic and contains discontinuous pods of massive sulphide up to thirty centimeters (one foot) thick. The greenschist unit is composed of actinolite, chlorite, and epidote with multiple lenses of pyrite, chalcopyrite, and sphalerite up to 0.5 meters (1.6 feet) thick.

The units and enclosed mineralization strike northeast-southwest and dip to the northwest at 20 to 40 degrees. The mineralized zones can be traced for over 1.6 kilometers (one mile) along strike. The extension of the mineralization down dip is unknown. Limited sampling from these occurrences indicates the rocks contain significant precious metal values with up to 8.2 ppm Au, 12 ppm Ag, 1,850 ppm Pb, 1,500 ppm Zn, and 2,600 ppm As (Bundtzen, 1981).

#### 8.6.4 Placer Deposits

Descriptions of the placer deposits of the district are provided by Brooks (1911a), Capps (1918), Davis (1922), Bundtzen (1981), and Levell (1984). The placer gold fineness is reviewed by Metz and Hawkins (1981).

Examination of the geologic mapping of Bundtzen (1981) and Thomsberry et al. (1984) and the placer production records of the U.S. Bureau of Mines for the district, indicates that over 90 percent of the placer gold production has come from creeks draining the Spruce Creek Sequence. The major producing creeks are listed in Appendix D7 along with a brief description of the placer geology and fineness data.

Although there has been no exhaustive study of the surficial deposits of the district, Levell (1984) divides the auriferous gravels into three main categories: tributary gravels, lowland alluvial gravels, and Quaternary gravels. No gold production has been reported from the Tertiary gravels.

Tributary gravels are poorly sorted material with angular to subangular clasts. These gravels form irregular beds and lenses in the narrow V-shaped stream drainages. Tributary gravels are usually less than 3 meters (10 feet) thick and 45 meters (150 feet) wide. Gold is concentrated in the lower 60 centimeters (2 feet) of the gravel or within the fractured bedrock. Gold grades are erratic and gold grain size is highly variable.

Lowland alluvial deposits accumulate in the broader valleys such as Moose, Glacier, and Caribou Creeks. The gravels are similar to the tributary gravels, however the boulder size fraction is smaller and the degree of rounding is greater. On Glacier Creek, the Recent alluvial deposits are underlain by Tertiary gravels. The lowland alluvial gravels contain fine-grained gold, but the average tenor of the deposits is not significantly less than that of the tributary gravels.

Quaternary gravels are found in terraces along the broader stream valleys. The clasts in the terrace deposits are more well rounded than those in the tributary gravels, and the sediments show better sorting. The Quaternary gravels

contain more sand and silt size clasts than the tributary gravels, and are ice rich.

As noted above, the tributary gravels contain coarse gold. The nuggets may be attached to quartz, and the gold may exhibit crystalline textures. Heavy mineral concentrates include large grains of very friable sulphides such as galena and stibnite. These phases, as well as scheelite do not travel great distances in the alluvial environment without significant size reduction, thus the tributary placers are probably proximal deposits.

The majority of the placer gold recovered from the Kantishna district is fine-grained (less than 16 mesh) and ranges from flattened to angular particles. Thirty percent of the gold is coarse (larger than 16 mesh). Nuggets weighing one troy ounce are not uncommon; the largest particle recovered from the district to date is 32 troy ounces.

Metz and Hawkins (1981) report gold fineness values for 11 creeks in the district. The lowest value of 567 is from Stampede Creek and the highest value of 906 is from Eureka Creek. The district has the lowest mean value (789) of all the placer producing areas of Alaska, the largest standard deviation from the mean (126), and the largest coefficient of variation (15.97). These data probably reflect the multiple lode sources for the placers. The extremely low fineness values appear to be associated with the stratiform sulphide lodes, the moderate fineness values are associated with the silver-dominant veins, and the high fineness values are spatially associated with the gold dominant veins.

Levell (1984) reports 44 gold fineness values for the district. The number of samples is larger than those reported by Metz and Hawkins (1981) but the individual samples are much smaller (one gram versus at least 3,400 grams for the earlier investigation). The mean for the 44 samples is 750, and the range is from 532 to 952. The Levell (1984) investigation notes the increases in gold fineness values downstream from lode sources. These data are comparable to the findings reported in this investigation for the Fairbanks district.

Levell (1984) reports on the grades of placer gold production for 1983. Production grades range from 0.006 to 0.078 troy ounces per cubic meter (0.005 to 0.063 troy ounces per cubic yard). Although these data probably do not reflect historic placer mining grades, the data is the only grade data available for the district.

#### 8.6.5 Trace Element Geochemistry

Bressler (1984) provides data on 217 stream sediment and 55 pan concentrate samples taken from the district. Salisbury (1984) discusses the analysis and data reduction for these samples. All sample analyses were conducted by Skyline Laboratories in Wheat Ridge, Colorado. Stream sediment samples were analyzed by atomic absorption spectrophotometry for Au, Ag, As, Cu, Pb, Sb, W, and Zn. Pan concentrate samples were analyzed by atomic absorption spectrophotometry for Au, Ag, As, Sb, Cu, Pb, and Zn; and by colourimetric techniques for W.

Frequency distributions and correlation matrices are prepared for the sample data. Summary statistics are provided for the stream sediment and pan concentrate data and are listed in Tables 8.10 and 8.11 respectively. Anomalous concentrations are defined as those above the upper 25th percentile. Strongly anomalous samples are defined as those above the 94th percentile. Thus, the lower values of the "1st order range" are approximately equal to defining the anomalous samples as those above two standard deviations from the mean (Salisbury, 1984).

### 8.6.6 Discussion

The Ag, Cu, Pd, Sb, and Zn threshold values of 256, 91, 176, 91, and 336 ppm are the highest values for the six mining districts. Thus, the stream sediment data reflect the high silver and base metal content of the vein mineralization.

A threshold value of 248 ppm for tungsten is approximately an order of magnitude larger than that for any other district. These high tungsten values appear to be associated with the Spruce Creek Sequence rocks.

Numerous arsenic, antimony, tungsten, gold, silver, copper, lead, and zinc anomalies are associated with the quartzite, graphitic schist, and black slate units of the Birch Creek Schist; the Spruce Creek Sequence, and the Keevy Peak Formation. Bressler (1984) summarizes the anomalous areas as follows: "More than 400 stream sediment and panned concentrate samples were collected within the Kantishna Hills study area..."

The Eldorado Creek drainage contains numerous first- and second-order gold, silver, copper, lead, zinc, antimony, tungsten, and arsenic anomalies. Values range up to 8.6 ppm silver, 0.45 ppm gold, 5,650 ppm copper, 500 ppm lead, 1,250 ppm zinc, 15,000 ppm antimony, 3,100 ppm tungsten,

Table 8.10 Statistical parameters for stream sediment samples from the Kantishna mining district, Alaska (after Salisbury, 1984).

Element	Mean (ppm)	Standard Deviation (ppm)	Upper 25 Percentile Range (ppm)	Rank (ppm)	1st Order Range	Rank
Au	0.05	0.03	0.02-0.42	All detectable values considered anomalous		
Ag	0.58	0.44	0.7-2.0	+77%	1.5-2.0	+94%
As	71	101	100-550	+77%	256-550	+95%
Cu	42	20	55-185	+85%	91-185	+98%
Pb	40	63	40-530	+75%	176-530	+98%
Sb	21	34	16-205	+75%	91-205	+95%
W	5	2	6-19	+80%	10-19	+99%
Zn	155	91	165-550	+75%	336-550	+95%

Table 8.11 Statistical parameters for pan concentrate samples from the Kantishna mining district, Alaska (after Salisbury, 1984).

Element	Mean (ppm)	Standard Deviation (ppm)	Upper 25 Percentile Range (ppm)	1st Order Range (ppm)
Au(1)	0.025	0.060	All samples above 0.01 considered anomalous	
Ag	6	12	5-70	31-70
As	151	199	130-870	550-749
Cu	34	37	40-380	109-380
Pb	67	101	50-530	270-530
Sb	82	155	32-730	393-730
W	72	87	60-420	248-430
Zn	141	87	200-500	317-500

Note: (1) troy ounces per cubic yard

and 2,300 ppm arsenic. The drainage is underlain by the Spruce Creek Sequence exposed through a structural window. Numerous prospects, including the Slate Creek, Bunnell, Alpha, and Eagles Den, are located in this drainage basin.

A cluster of gold, silver, copper, lead, zinc, tungsten, and arsenic anomalies occurs in the upper Caribou Creek drainage. Most of the anomalous streams drain the Spruce-Kankone Trend described earlier.

First-order anomalies (to 1,350 ppm) are characteristic of streams draining the Keevy Peak Formation and black graphitic schist and slate units of the Birch Creek Schist. The previously described Canyon Creek and Red Dirt occurrences show background zinc values in stream silt; downstream values increase to 425 to 540 ppm. As described earlier, coincident, first order lead and zinc stream silt anomalies occur near the Canyon Creek occurrence and in the Keevy Peak Formation. In black shale terrane, zinc greater than 500 ppm and lead greater than 50 ppm are considered anomalous.

A tributary to Bearpaw River found to be anomalous in lead (1,090 ppm; Bundtzen et al., 1976) and zinc (4,750 ppm; Hawley, 1978) was resampled during this study. Results verify the magnitude of Hawley's zinc anomaly but not the extremely high lead value reported by Bundtzen. The drainage is underlain by undifferentiated schist and quartzite of the Birch Creek Schist and a small pod of the graphitic schist. A sample from an iron oxide-stained seep contained 5,900 ppm zinc with negligible amounts of lead and copper. The adjacent drainage to the west also drains a portion of the pCgs unit and yielded samples containing up to 550 ppm zinc. A single sample in the upper Rock Creek drainage contains 1,350 ppm zinc with no associated lead content. Upper Rock Creek was determined by Bundtzen (1981) to be underlain by a large section of the graphitic schist unit of the Birch Creek Schist. Other scattered lower order zinc anomalies occur in the Rock Creek, Little Moose Creek, and Bearpaw River drainages. The bedrock source is not known.

Anomalously high lead and zinc values were detected in several streams draining the Spruce Creek Sequence. Samples with anomalous lead values were also obtained from Rock and Little Moose Creeks.

Anomalously high copper was detected in samples in the Canyon Creek basin, which drains the Red Dirt and Canyon Creek occurrences. Several streams draining the Spruce Creek Sequence also contained high copper values. Other copper anomalies were detected in samples from Little Moose Creek and two eastern tributaries to Rock Creek.

Possibly significant tungsten anomalies were detected in the Canyon Creek drainage by regional placer and panned concentrate sampling. Placer samples from the (Middle Fork) of Canyon Creek outline a 6.4 kilometer (4 mile) long dispersion train with values from 200 to 17,850 ppm tungsten. Panned concentrate samples from the area contain up to 46 ppm tungsten. Coarse grained scheelite was detected in the samples. The farthest upstream anomaly, with a value of 1,000 ppm, is located in a stream drainage about 4.8 kilometers (3 miles) long. The basin is underlain by schist, quartzite, and graphitic schist of the Birch Creek Schist. No intrusive rocks

or calcareous rocks indicative of skarns are currently known to occur in the basin.

Tungsten anomalies are present in many of the streams draining the Spruce Creek Sequence. Minor streams draining the ridge separating Caribou and Rock Creeks, and an unnamed tributary to the upper Bearpaw River contain anomalously high tungsten values. The latter anomalies are in close proximity to major north-trending faults within the Birch Creek Schist.

Tungsten anomalies were also delineated in the main channel of the North Fork of Canyon Creek (375 ppm), in a small south-flowing tributary draining calcareous schist (265 ppm), and in the Stampede area (up to 2,000 ppm). These anomalies may be related to the projected trend of the Spruce Creek Sequence.

Gold and silver anomalies are present in most of the streams draining known gold and silver lode deposits contained in the Spruce Creek Sequence. Anomalous gold was also detected in samples from Canyon, Stampede, and Little Moose Creeks and in tributaries to upper Bearpaw River. High silver values are present in Canyon, Moose, and Rock Creeks.

Numerous arsenic anomalies were detected in stream silt samples in the Eldorado Creek drainage and in streams draining the Spruce-Kankone Trend. Isolated arsenic anomalies were also detected in the North Fork of Canyon Creek and in an unnamed tributary to Rock Creek.

## 8.7 SUMMARY AND CONCLUSIONS

Although the Kantishna, Fairbanks, and Circle mining districts extend for over 350 kilometers (210 miles) long the regional strike of the Yukon-Tanana Terrane, the districts contain remarkably similar geology, geochemistry, and mineral occurrences. Figure 8.6 includes composite stratigraphic sections for the Spruce Creek sequence (Kantishna district), the Cleary sequence (Fairbanks district) and the Bonanza Creek sequence and the mafic schist unit (Circle District).

Each of the composite sections shows a lower mafic schist unit. The mafic rocks are intercalated with metacherts. Together these rocks are interpreted as a marine mafic volcanic and exhalative sequence. In the middle portions of the sections the lithologies are a mix of pelitic schist and metavolcaniclastic rocks. The upper portions of the sections are felsic schist intercalated with pelitic sediments, graphitic schist, and marbles. These rocks are interpreted as a felsic volcanic and exhalative sequence.

In the Fairbanks and Kantishna districts these volcanic and exhalative rocks contain stratiform massive sulphide mineralization that is precious metal enriched. The rocks are also host to major precious metal vein type mineralization. In the Steese and Circle districts the volcanic and exhalative rocks contain disseminated sulphides, and are host to narrow gold-quartz-sulphide veins. In all four districts the volcanic and exhalative rocks are spatially associated with the placer gold deposits.

Rock, stream sediment, and pan concentrate geochemi-

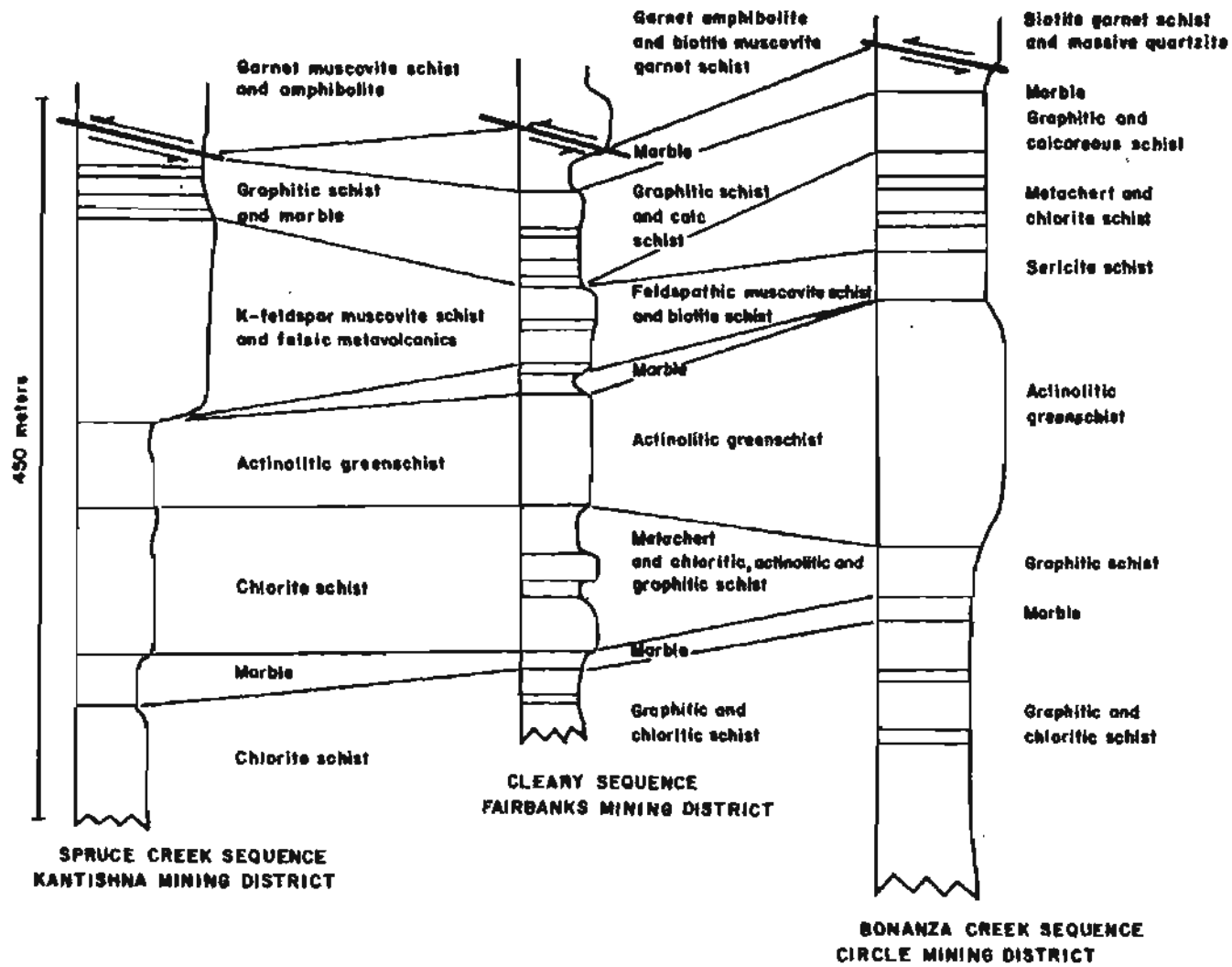


Figure 8.6 Composite stratigraphic section of the Kantishna-Fairbanks-Circle metallogenic province.

Table 8.12 Number of mineral occurrences by probable deposit type in the Fairbanks, Circle, Steese, Richardson, Tovelana, and Kantishna mining districts, Alaska.

		Fairbanks		Circle		Steese		Richardson		Tolovana		Kantishna	
		Known(1)	Disc(2)	Known	Disc	Known	Disc	Known	Disc	Known	Disc	Known	Disc
1.	Metamorphosed volcanic/exhalative and associated veins	159	17	2	10	--	3	--	1(?)	1(?)	--	64	28
2.	Copper-molybdenum gold porphyry	--	--	--	--	--	--	1	1(?)	1	3	--	--
3.	Precious metal massive sulfide	3(?)	--	--	--	--	--	--	2	1	1	--	6
4.	Epithermal veins	13	1	1	4	1	2	1	--	6(?)	1	--	--
5.	Skarns	13	--	2(?)	--	--	--	--	2(?)	--	--	--	--
6.	Tin-greisens	--	--	1	--	1	9	--	3	--	--	--	--
7.	Carlin type gold	--	--	--	--	--	--	--	--	--	3	--	--
8.	Paleoplacer	--	2(?)	1	--	--	--	--	--	--	1(?)	--	2(?)

Notes:

1) Prior to 1980

2) Discovered since various interior mining project studies

data indicates that the three stratigraphic sequences (Cleary, Spruce Creek, Bonanza Creek) are enriched in varying degrees in As, Sb, W, Pb, Zn, Au, and Ag. Furthermore stream sediment and pan concentrate data are efficacious in delineating areas of potential but undiscovered mineralization.

The Kantishna, Fairbanks, Steese, and Circle districts also contain monomineralic antimony occurrences. This low temperature vein mineralization is not necessarily associated with the volcanic/exhalative sequences.

The only known lode mineralization in the Richardson district is intrusive related gold associated with the various phases of the Birch Lake pluton. The gold mineralization is accompanied by anomalous concentrations of arsenic and traces of base metals, tungsten, and tin. Similar intrusive related mineralization occurs in the Fairbanks, Steese, and Circle districts. The intrusive rocks of the Circle and Steese district have higher tin content than the intrusives in the Richardson and Fairbanks districts. The former two districts have moderate potential for lode tin mineralization.

The North American continental margin rocks of the Tolovana district are host to different types of mineralization than the rocks of the other five districts. In particular copper-gold porphyry and sediment hosted gold deposit types are likely to occur only in the Tolovana district.

Table 8.12 lists the probable mineral deposit types for each district as well as the number of known occurrences and the number of new areas of potential mineralization. There exists considerable uncertainty in the assignment of the mineral deposit types, however such assignments are necessary to estimate the mineral potential of the districts. Even in highly developed districts there are moderate levels of uncertainty associated with mineral deposit classification. The total number of known mineral occurrences and the number of new areas of expected mineralization listed in Table 8.12 do not reflect the mineral endowment of each of the districts. The total metal availability of each district is a function of the number of mineral discoveries multiplied by the metal content of each discovery. Each mineral deposit type has a unique tonnage-grade curve, thus each deposit type will have a unique metal availability. This subject will be addressed in subsequent chapters.

---

---

## CHAPTER 9

### MAJOR OXIDE AND RARE EARTH ELEMENT GEOCHEMISTRY OF THE FAIRBANKS MINING DISTRICT AND ADJACENT AREAS

#### 9.1 INTRODUCTION

Major oxide and rare earth element analyses are conducted on the metamorphic rocks primarily to provide a basis for lithologic classification and to determine if there are lithogeochemical controls of the various types of lode mineralization. These data are supplemented by limited published data for the intrusive rocks of the Fairbanks, Circle, Steese, and Richardson districts.

Geological mapping and petrographic examination of thin sections from each mappable rock unit have resulted in the inference of a protolith for each rock type. A mafic volcanic protolith has been inferred for most of the amphibolites in the Chatanika terrane and in the Cleary sequence. Similarly the muscovite schists of the Cleary sequence with or without K-feldspar have been designated as metafelsites. Finely laminated quartzite and muscovite quartzite that are spatially associated with the above lithologies have been assumed to have a sedimentary exhalative protolith.

The metavolcanics and metaexhalites contain lenses and disseminations of base metal sulphides with or without sulphosalts and precious metals. The sulphides exhibit textures common to volcanogenic massive sulphide and sedimentary exhalative type deposits.

Laird et al. (1984) describe amphibole-bearing eclogites in the Circle A-6 quadrangle. The location is a few kilometers east of the Fairbanks district. The mineralogic and whole-rock data for the eclogites of the Circle quadrangle suggests a mafic igneous protolith for the rocks. Dusel-Bacon (1984) provides major oxide, rare earth element (REE), and trace element data to demonstrate a mafic igneous origin for amphibolites in the Big Delta quadrangle (adjacent to the north boundary of the Richardson district and southeast of the Fairbanks district).

Amphibolites occur throughout the Yukon-Tanana Terrane (YTT). However in the Big Delta quadrangle and in the Fairbanks district they are spatially associated with metafelsites. The demonstration of a concurrent igneous origin for these rocks places significant constraints on the tectonics and metallogeny of this portion of the YTT.

Solie et al. (1990) attempt to discriminate between gold and non-gold bearing intrusive rocks in a portion of the YTT in the Big Delta quadrangle. The discriminant analysis is based on the whole-rock geochemistry of the unmetamorphosed Cretaceous and Tertiary granitic plutons. At the Fort Knox property, the major known intrusive hosted gold occurrence in the Fairbanks district, the gold mineralization is in quartz veinlets in a shear zone that clearly post dates the emplacement of the intrusive. At the Silver Fox mine (Fairbanks district), at the Democrat mine (Richardson district) and at the Joker prospect (Circle district) the intrusive hosted mineralization also occurs in quartz veinlets in major shear zones. Geologic mapping and petrographic analysis of the intrusive rocks at the above localities suggest that the gold mineralization is not hosted by a single compositional variant in the composite plutons at each locality. Major oxide analyses are conducted on the various phases of the granitic plutons in the interior mining districts to determine if there is a preferred compositional host to the various types of intrusive related mineralization.

#### 9.2 SAMPLING

The same samples that were collected for the trace element analyses that were reported in Chapter 6 were split and used for major oxide and rare earth element determinations. Sample locations are given on Ch.3, Plate I. The

samples were prepared and analyzed by Bondar-Clegg Ltd., Vancouver, British Columbia, Canada.

The analyses for alumina, calcium, ferric iron, potassium, magnesium, manganese, sodium, phosphorous, silica, and titanium were completed by multi-acid total digestions and D.C. plasma emission spectroscopy. Ferrous iron was determined by titrametric methods while water and loss on ignition were determined by gravimetric methods. Carbon dioxide and sulphur were determined on carbon and sulphur analysis instruments (Leco). Tin, barium, rubidium, and strontium were determined by x-ray fluorescence. Rare earth elemental analyses were determined by the instrumental neutron activation method.

### 9.3 GEOCHEMISTRY OF THE ROCK TYPES

Major oxide analyses for the metamorphic and igneous rocks of the Fairbanks district are reported in Table 9.1a. Whole-rock analyses of selected intrusive igneous rocks from the Circle and Richardson districts are included in Tables 9.2a and 9.3a respectively. Tables 9.1b, 9.2b and 9.3b list the normative mineralogies for the respective major oxide analyses. Whole-rock analyses for the Steese district are included in Smith et al. (1987).

The normative mineralogies that are listed in the above tables are calculated by PETCAL version 83.01.02 (Hutchison, 1983). Lithologic classifications are based primarily on various indices calculated by the program and by plots of the data on AFM diagrams.

#### 9.3.1 Fairbanks District Metamorphic Terranes/Sequences

##### 9.3.1.1 Chatanika Terrane

The garnet pyroxenites and garnet amphibolites of the Chatanika terrane have bulk chemical compositions that suggest both sedimentary and tholeiitic basaltic protoliths. The rocks generally plot near the centre of the AFM diagram (see Figure 9.1), however a few samples show alkali enrichment and may be classified as alkali basalts. The rocks are subaluminous and contain normative nepheline with one exception. Only sample 3832 contains normative quartz and this sample is probably a para-amphibolite.

The Ca-Na-K plot (see Figure 9.2) indicates the low sodium and potassium content of the eclogitic rocks. The intercalated muscovite schists are relatively enriched in potassium.

The Al-Si-Fe diagram (see Figure 9.3) shows the high iron content of the eclogitic rocks relative to silica and alumina. The intercalated muscovite schists contain little iron or alumina relative to silica.

Laird et al. (1981) describe similar rocks in the Circle quadrangle approximately 40 kilometers (24 miles) to the east of the Fairbanks district localities. The omphacite content of the Circle eclogites which ranges from  $jd_{45} wo_{26} en_{22} fs_6 cats_1$  to  $jd_{40} ac_7 wo_{25} en_{23} fs_2 cats_3$  is significantly greater than that for the eclogites of the Fairbanks district. Similarly the Circle quadrangle rocks have a higher pyrope ( $Fe_{1.54}^{2+} Mg_{0.75} Ca_{0.03} Al_{1.98} Fe_{0.06}^{3+} Si_{2.95} Al_{0.05} O_{12}$ )

content than the eclogitic rocks of the Fairbanks district. On the basis of the compositional data, Laird et al. (1981) place the eclogites of the Circle quadrangle at the Type B/Type C boundary of Coleman et al. (1965). This is a significant modification of the classification provided by Swainbank and Forbes (1975).

At both localities the eclogites are intercalated with muscovite-K-feldspar schist. This assemblage places an upward limit of 600°C for the temperature of formation of the eclogites. Laird et al. (1981) use the muscovite-paragonite solvus of Eugster et al. (1972) to estimate a lower temperature limit of 530°C for the eclogites of the Circle quadrangle. Using the P,T stability field for the reaction of albite = jadeite + quartz (Holland, 1979; 1980) and the partition of  $Fe^{2+}/Mg$  in garnet and pyroxene, Laird et al. (1981) estimate a temperature of 600°C ± 50°C and a pressure of 13.5 ± 1.5 Kbars for the formation of the eclogites of the Circle quadrangle. These are slightly higher conditions than those estimated by Swainbank and Forbes (1975) of 540 to 590°C and 5.5 to 7.5 Kbars for the eclogites of the Fairbanks district.

The eclogites of the Fairbanks district and Circle quadrangle are compositionally similar to the eclogites of the Yukon Territory reported by Erdmer and Helmstaedt (1983). The occurrences in the Yukon Territory are northeast of the Tintina Fault in the vicinity of Faro. Projecting the regional strike of the eclogites of the Fairbanks and Circle areas to the Tintina Fault and correlating these rocks with the eclogites of the Yukon Territory indicates an offset along the fault of 350 kilometers (220 miles). This estimate of the offset is similar to that made by Tempelman-Kluit (1979) based on the separation of other major rock sequences. The juxtaposition of the eclogitic rocks in both areas with middle to upper greenschist facies metamorphic rocks suggests that there was a major plate boundary in Alaska and the Yukon Territory that pre-dated the strike-slip motion on the Tintina Fault.

##### 9.3.1.2 Cleary Sequence

Samples from the Cleary sequence are divided into two groups based on mineralogy and petrology. The first group includes metavolcanic and metaexhalative rocks while the second is composed of metasedimentary lithologies.

On the AFM diagram (see Figure 9.4) the metavolcanic and metaexhalative rocks plot in several fields that include tholeiitic basalts and fractionated granitic rocks. The Ca-Na-K diagram (see Figure 9.5) indicates that the alkali enrichment in some of the felsic metavolcanic and metaexhalative rocks is due primarily to a high potassium content.

The tholeiitic rocks in contrast are low in potassium as are the tholeiites in the Chatanika terrane. In fact, the mafic rocks from both sequences have very similar bulk chemical compositions. The limited number of samples from each lithologic group from each terrane precludes a more rigorous analysis of the data.

The large silica content of the Cleary sequence metavolcanics and metaexhalites relative to alumina and iron is displayed on Figure 9.6. This suggests that there is little terrestrial contribution to the metaexhalites.

Table 9.1a Major oxide analysis of the major rock units of the Fairbanks mining district (sample analyses 81JB 106 thru 81JB 218 after Blum, 1983)

Terrane/ Sample Number/ Description	SiO <sub>2</sub>	Al <sub>2</sub> O <sub>3</sub>	Fe <sub>2</sub> O <sub>3</sub>	FeO	MgO	CaO	Na <sub>2</sub> O	K <sub>2</sub> O	TiO <sub>2</sub>	P <sub>2</sub> O <sub>5</sub>	MnO	LOI	H <sub>2</sub> O	Total
<b>Chatanika</b>														
3830 Garnet clinopyroxenite	34.03	7.16	1.83	5.91	6.19	28.33	0.83	0.07	1.58	0.55	0.40	10.22	0.39	97.49
3831 Garnet clinopyroxenite	35.39	7.73	1.44	1.11	1.26	28.08	0.54	1.83	0.65	0.07	0.06	19.73	0.48	98.37
3832 Garnet amphibolite	56.11	9.87	1.83	1.13	1.22	13.99	0.37	2.70	1.04	0.11	0.06	9.38	0.45	98.26
3833 Muscovite-hornblende schist	72.60	5.00	0.23	1.08	6.30	3.59	0.66	1.96	0.26	0.26	0.09	6.68	0.42	99.13
3841 Garnet-calc schist	34.11	10.53	0.19	9.00	7.08	21.10	0.95	1.15	2.42	0.78	0.18	9.92	0.36	97.77
3842 Garnet amphibolite	37.61	10.59	1.97	9.05	8.86	18.47	1.78	0.32	2.20	0.84	0.17	6.51	0.37	98.74
3843 Muscovite-K-Feldspar-schist	71.70	13.37	4.57	0.77	0.48	0.44	0.21	2.15	0.74	0.17	0.16	3.29	0.61	98.66
3846 Garnet amphibolite	43.37	10.18	2.39	7.22	8.39	14.88	3.09	0.25	1.69	0.62	0.34	3.75	0.42	96.59
21342 Marble	34.96	9.16	2.33	5.29	5.06	26.87	2.02	0.12	1.56	0.33	0.17	12.04	0.36	99.91
21343 Impure marble	31.98	8.80	2.19	5.00	4.56	26.60	1.64	1.28	1.26	0.40	0.17	16.82	0.38	100.70
21344 Graphitic metachert	84.20	2.77	0.40	1.39	1.19	3.79	0.48	0.53	0.19	1.46	0.01	4.06	0.20	100.47
<b>Cleary Sequence Metavolcanics/Metaexhalites</b>														
197 Banded-muscovite quartzite	98.96	0.98	0.68	0.53	0.19	0.24	0.17	0.34	0.15	0.06	0.02	0.51	0.17	103.00
198 Banded-muscovite quartzite	80.96	10.49	1.71	0.45	0.50	0.30	0.41	3.15	0.53	0.03	0.05	1.89	0.18	100.65
3818 Banded-muscovite quartzite	77.07	7.45	11.12	0.59	0.25	0.32	0.16	1.29	0.80	0.17	0.08	1.85	0.64	101.79
3819 Banded-muscovite quartzite	89.91	3.57	1.17	0.99	0.00	0.47	0.19	0.53	0.15	0.09	0.13	0.95	0.53	98.68
3824 Metarhyolitic tuff	66.76	16.94	2.09	1.58	1.12	0.29	0.38	5.38	0.83	0.12	0.18	2.48	0.45	98.60
3835 Metarhyolitic tuff	70.07	12.51	2.63	1.23	1.52	0.25	0.34	3.57	1.21	0.10	0.09	3.16	0.44	97.12
3836 Garnet ortho-amphibolite	43.04	11.04	0.59	10.44	11.05	11.80	0.46	1.60	2.69	0.57	0.22	3.55	0.45	97.50
3837 Garnet ortho-amphibolite	42.25	12.52	1.03	10.26	9.65	11.87	0.45	1.78	3.52	0.76	0.22	3.68	0.44	98.43
3839 Metarhyolitic tuff w/ sulfide	71.36	12.66	2.47	2.61	0.97	1.13	0.31	3.00	0.70	0.12	0.23	3.11	0.41	99.08
21151 Feldspathic-chlorite schist	47.96	15.32	1.55	7.98	6.74	11.12	3.15	0.41	1.15	0.18	0.18	3.69	0.07	99.50
21152 Chlorite-talc schist	56.59	20.80	2.71	4.54	2.10	0.79	0.47	5.36	1.06	0.14	0.16	4.62	0.10	99.40
21155 Ortho-amphibolite	42.14	13.63	1.88	10.42	8.99	14.52	1.49	0.70	2.45	0.45	0.38	0.48	0.18	97.53

Table 9.1a (Continued)

Terrane/ Sample Number/ Description	SiO <sub>2</sub>	Al <sub>2</sub> O <sub>3</sub>	Fe <sub>2</sub> O <sub>3</sub>	FeO	MgO	CaO	Na <sub>2</sub> O	K <sub>2</sub> O	TiO <sub>2</sub>	P <sub>2</sub> O <sub>5</sub>	MnO	LOI	H <sub>2</sub> O	Total
21330 Calc-chlorite schist	25.45	4.52	1.23	1.38	0.81	37.73	0.16	0.96	0.15	0.14	0.06	30.77	0.31	103.36
21331 Feldspathic-muscovite quartzite	88.24	6.20	0.58	2.05	0.28	0.08	0.25	1.46	0.30	0.03	0.18	1.10	0.24	100.75
21335 Banded muscovite quartzite	77.65	14.00	0.67	0.50	0.39	0.20	0.29	2.30	0.58	0.03	0.05	3.49	0.32	100.15
21337 Graphitic schist	51.54	25.31	0.83	4.56	1.58	0.32	0.68	7.08	0.95	0.13	0.06	6.12	0.94	100.10
21346 Banded muscovite quartzite	72.37	13.46	7.28	0.27	0.28	0.28	0.15	0.97	0.89	0.09	0.12	5.04	0.47	101.20
21347 Muscovite-garnet schist	59.34	16.18	3.67	4.28	2.90	3.50	1.25	3.81	1.04	0.08	0.19	3.33	0.56	99.57
82SH02 Feldspathic-muscovite schist	67.14	16.25	5.73	0.69	0.84	0.40	0.46	3.80	0.75	0.17	0.16	3.90	1.11	100.29
82CH02 Chloritic quartzite w/ sulfides	96.78	1.27	0.41	0.85	0.06	0.10	0.23	0.43	0.10	0.02	0.01	0.64	0.27	100.90
82HY01 Chloritic quartzite w/ sulfides	76.13	6.53	4.97	0.89	1.25	1.53	0.64	1.58	0.29	0.14	0.10	4.10	0.23	98.15
<b>Clary Sequence Metasediments</b>														
185 Biotite-muscovite-garnet schist	63.11	16.64	1.60	5.39	2.23	1.12	1.47	3.99	1.09	0.16	0.12	1.74	0.21	98.87
192 Biotite-muscovite-garnet schist	52.94	19.36	2.23	4.77	2.23	13.30	0.61	1.61	0.82	0.10	0.33	0.90	0.30	99.50
3810 Para-amphibolite	66.46	15.86	2.60	2.46	2.12	1.30	1.69	3.75	0.65	0.18	0.09	3.10	0.21	100.47
3823 Marble	6.01	0.00	0.02	0.18	0.26	52.75	0.08	0.19	0.04	0.14	0.08	42.37	0.21	101.33
3825 Para-amphibolite (?)	29.98	14.08	1.91	11.75	6.82	17.40	0.86	0.29	2.55	0.93	1.22	10.24	0.29	98.32
3826 Muscovite quartzite	86.13	6.18	1.09	1.76	0.56	0.42	0.63	1.67	0.27	0.07	0.13	0.61	0.35	99.87
3827 Marble	11.49	0.12	0.13	0.54	0.21	48.34	0.33	0.59	0.09	0.10	0.04	38.50	0.32	100.80
3838 Biotite-muscovite-garnet schist	66.84	11.44	1.26	8.91	3.53	3.22	0.99	1.37	1.07	0.14	0.55	0.00	0.58	100.00
20506 Metaconglomerate	77.15	11.10	1.93	2.19	1.35	0.44	1.19	2.35	0.54	0.08	0.04	1.94	0.24	100.54
20510 K-Feldspar-biotite schist	56.45	19.98	1.05	5.53	2.82	0.66	3.14	7.43	0.92	0.23	0.13	1.14	0.14	99.62
21142 Quartzite	85.38	5.64	1.60	2.37	0.67	2.87	0.37	0.43	0.26	0.02	0.17	1.12	0.03	100.93
21147 Quartzite	85.95	6.26	1.51	2.24	0.80	2.27	0.40	0.55	0.32	0.04	0.13	1.33	0.31	101.80
21154 Muscovite schist	58.75	19.55	0.96	7.28	2.51	0.73	1.02	4.40	0.93	0.12	0.14	2.12	0.38	98.51
21320 Muscovite quartzite	76.91	11.03	1.49	2.25	1.26	0.95	1.70	2.44	0.50	0.07	0.06	1.32	0.28	99.98
21334 Feldspathic biotite garnet schist	66.90	16.62	5.35	1.36	1.33	0.28	0.84	3.83	0.91	0.12	0.11	2.86	0.48	100.51

Table 9.1a (Continued)

Terrane/ Sample Number/ Description	SiO <sub>2</sub>	Al <sub>2</sub> O <sub>3</sub>	Fe <sub>2</sub> O <sub>3</sub>	FeO	MgO	CaO	Na <sub>2</sub> O	K <sub>2</sub> O	TiO <sub>2</sub>	P <sub>2</sub> O <sub>5</sub>	MnO	LOI	H <sub>2</sub> O	Total
<b>Fairbanks Schist Metasediments</b>														
3828 Garnet-chlorite-muscovite schist	72.30	11.50	1.22	3.56	1.59	2.75	0.39	2.38	0.52	0.19	0.11	3.08	0.32	99.91
20505 Biotite-muscovite-quartz schist	61.64	20.57	2.34	2.90	1.70	0.33	1.12	4.83	0.89	0.08	0.05	3.63	0.32	100.40
20508 Muscovite-quartz schist	87.44	6.16	0.97	1.57	0.68	0.61	1.16	0.76	0.32	0.02	0.06	1.03	0.11	100.89
<b>Goldstream Sequence</b>														
3809 Biotite-muscovite schist	72.69	12.70	2.01	1.82	1.62	0.49	1.50	3.45	0.50	0.11	0.07	2.07	0.20	99.23
3814 Garnet-chlorite-muscovite quartzite	90.00	4.57	0.99	1.28	0.13	0.46	1.35	0.43	0.20	0.06	0.16	0.32	0.37	100.32
3815 Garnet-biotite-muscovite schist	61.12	19.84	2.02	3.08	1.99	0.41	1.78	4.07	0.87	0.10	0.08	3.22	0.53	99.11
3816 Garnet-amphibolite	47.06	13.32	1.55	9.88	5.73	10.01	3.33	0.25	2.61	0.32	0.24	5.85	0.39	100.54
3817 Calcareous schist	34.59	4.09	0.33	1.04	2.19	30.90	1.02	0.84	0.18	0.17	0.05	25.56	0.42	101.38
3840 Marble	18.46	2.73	0.35	0.92	2.48	40.55	0.39	0.90	0.16	0.10	0.03	33.16	0.56	100.79
3844 Para-amphibolite	74.07	10.34	0.70	4.14	2.55	2.23	2.01	1.35	1.04	0.22	0.14	0.78	0.40	99.97
21324 Graphitic-quartz schist	69.84	9.20	0.29	3.94	0.95	4.51	0.26	2.28	0.64	2.94	0.03	4.64	1.02	100.54
<b>Birch Hill Sequence</b>														
3811 Graphitic-quartz schist	93.37	2.88	1.53	0.63	0.22	0.35	0.15	0.35	0.14	0.06	0.05	1.00	0.13	100.86
3820 Calcareous schist	44.26	9.08	1.24	1.85	1.97	19.72	1.29	2.26	0.35	0.18	0.12	17.03	0.46	99.81
3821 Graphitic phyllite	93.29	2.15	0.67	1.04	0.07	0.35	0.21	0.52	0.09	0.10	0.11	0.10	0.52	99.22
3822 Graphitic quartzite	96.03	1.79	0.40	1.22	0.04	0.50	0.22	0.38	0.06	0.07	0.20	0.00	0.47	101.38
20503 Carbonaceous quartzite	89.47	5.30	0.41	0.19	0.56	1.08	0.18	1.61	0.34	0.63	0.01	1.59	0.11	101.48
20504 Pyritic-banded quartzite	84.23	5.93	4.44	0.75	0.80	1.64	0.15	0.27	0.25	0.04	0.15	2.51	0.47	101.63

Table 9.1a (Continued)

Terrane/ Sample Number/ Description		SiO <sub>2</sub>	Al <sub>2</sub> O <sub>3</sub>	Fe <sub>2</sub> O <sub>3</sub>	FeO	MgO	CaO	Na <sub>2</sub> O	K <sub>2</sub> O	TiO <sub>2</sub>	P <sub>2</sub> O <sub>5</sub>	MnO	LOI	H <sub>2</sub> O	Total
<b>Igneous Intrusives</b>															
81JB201	Fine-grained granodiorite	59.36	16.52	1.09	5.67	3.81	6.62	2.50	2.52	0.92	0.22	0.12	-	-	98.99
81JB203	Fine-grained granodiorite	59.65	16.05	1.00	6.03	3.72	6.20	2.56	2.43	0.95	0.23	0.14	-	-	98.96
81JB205	Fine-grained granodiorite	61.95	16.34	1.08	5.07	2.56	5.43	2.45	2.75	0.86	0.19	0.12	-	-	98.80
81JB207	Fine-grained granodiorite	62.47	15.78	1.11	5.36	2.94	5.61	2.14	2.69	0.98	0.18	0.12	-	-	99.29
81JB211	Fine-grained granodiorite	65.36	15.99	1.29	3.96	1.19	3.50	2.36	3.50	0.67	0.21	0.08	-	-	98.91
81JB216	Fine-grained granodiorite	65.34	14.95	0.83	4.41	1.52	4.55	2.64	3.19	0.78	0.22	0.09	-	-	98.52
81JB218	Fine-grained granodiorite	63.49	15.78	0.59	4.37	2.42	4.55	3.55	2.24	0.71	0.20	0.11	-	-	98.01
81JB106	Porphyritic granodiorite	68.67	14.75	0.80	2.68	0.88	2.25	3.59	3.41	0.40	0.14	0.07	-	-	97.64
81JB108	Porphyritic granodiorite	70.16	14.77	0.29	1.31	0.50	2.16	3.93	4.15	0.33	0.11	0.05	-	-	97.76
81JB116a	Porphyritic granodiorite	72.52	13.98	0.47	1.49	0.52	2.34	3.24	4.05	0.29	0.08	0.04	-	-	99.02
81JB127	Porphyritic granodiorite	69.76	14.80	0.58	2.61	0.96	2.85	3.17	3.13	0.49	0.12	0.06	-	-	98.53
81JB128	Porphyritic granodiorite	70.30	14.83	0.68	2.12	0.80	2.72	3.04	3.66	0.47	0.15	0.05	-	-	98.82
81JB132	Porphyritic granodiorite	71.61	14.76	0.40	1.94	0.67	2.37	3.39	3.71	0.37	0.13	0.04	-	-	99.39
81JB134	Porphyritic granodiorite	74.08	13.02	0.57	2.52	0.45	2.06	2.87	3.37	0.26	0.10	0.09	-	-	99.39
81JB213	Porphyritic granodiorite	70.61	14.80	0.65	2.16	0.66	2.97	3.53	3.09	0.40	0.15	0.05	-	-	99.07
81JB215	Porphyritic granodiorite	67.03	15.05	0.95	3.15	1.07	3.53	3.54	3.00	0.57	0.19	0.09	-	-	98.17
81JB135	Porphyritic quartz monzonite	74.95	11.85	0.47	2.84	0.47	1.98	2.76	3.40	0.28	0.10	0.10	-	-	99.20
81JB137	Porphyritic quartz monzonite	77.67	12.13	0.20	1.13	-	1.37	3.37	3.68	0.07	0.04	0.04	-	-	99.70
81JB142	Porphyritic quartz monzonite	71.15	14.50	0.45	2.93	0.54	2.36	3.28	3.66	0.28	0.08	0.08	-	-	99.31
81JB143	Porphyritic quartz monzonite	70.00	14.23	0.27	2.57	0.51	2.33	3.24	3.59	0.29	0.09	0.08	-	-	97.20
81JB144	Porphyritic quartz monzonite	69.65	13.58	0.46	3.33	0.95	2.22	2.79	4.01	0.41	0.14	0.10	-	-	97.64
81JB145	Porphyritic quartz monzonite	74.72	14.38	0.29	1.53	0.24	1.66	3.14	4.46	0.14	0.09	0.06	-	-	100.71
81JB146	Porphyritic quartz monzonite	71.76	12.75	0.41	2.79	0.56	2.13	2.90	3.47	0.32	0.09	0.10	-	-	97.28
81JB148	Porphyritic quartz monzonite	71.43	13.90	0.42	2.61	0.42	2.21	3.21	3.41	0.25	0.07	0.17	-	-	98.10
81JB149	Porphyritic quartz monzonite	74.85	13.05	0.11	1.32	-	1.48	3.39	3.90	0.07	0.07	0.04	-	-	98.28
81JB152	Porphyritic quartz monzonite	74.30	12.52	0.18	1.55	0.03	1.58	3.25	3.95	0.12	0.06	0.06	-	-	97.60
81JB161	Porphyritic quartz monzonite	72.95	14.40	0.64	1.49	0.38	1.91	3.03	4.46	0.20	0.07	0.07	-	-	99.60

Table 9.1a (Continued)

Terrane/ Sample Number/ Description	SiO <sub>2</sub>	Al <sub>2</sub> O <sub>3</sub>	Fe <sub>2</sub> O <sub>3</sub>	FeO	MgO	CaO	Na <sub>2</sub> O	K <sub>2</sub> O	TiO <sub>2</sub>	P <sub>2</sub> O <sub>5</sub>	MnO	LOI	H <sub>2</sub> O	Total
81JB162 Porphyritic quartz monzonite	76.68	12.89	0.35	0.54	0.11	0.96	3.69	4.56	0.05	0.12	0.10	-	-	100.05
81JB165 Porphyritic quartz monzonite	72.88	13.79	0.41	0.19	0.30	1.95	3.28	4.13	0.19	0.08	0.07	-	-	97.27
81JB166b Porphyritic quartz monzonite	74.69	13.14	0.15	0.63	-	1.21	3.71	4.65	0.04	0.04	0.03	-	-	98.29
81JB167 Porphyritic quartz monzonite	72.57	14.23	0.53	1.85	0.57	1.99	2.99	4.15	0.24	0.09	0.08	-	-	99.29
81JB173 Porphyritic quartz monzonite	74.85	13.93	0.43	1.31	0.31	2.38	3.13	3.55	0.16	0.11	0.06	-	-	100.22
81JB175 Porphyritic quartz monzonite	72.53	13.88	0.57	1.98	0.53	2.26	2.93	4.31	0.26	0.10	0.08	-	-	99.43
81JB179 Porphyritic quartz monzonite	74.00	13.75	0.29	1.31	0.23	1.50	3.20	5.05	0.13	0.05	0.05	-	-	99.56
81JB186 Porphyritic quartz monzonite	74.46	13.43	0.47	1.53	0.36	1.73	3.03	3.89	0.20	0.08	0.05	-	-	99.23
81JB189 Porphyritic quartz monzonite	73.58	14.11	0.38	1.53	0.35	1.70	2.82	4.69	0.18	0.06	0.05	-	-	99.45
81JB192 Porphyritic quartz monzonite	73.57	13.73	0.47	1.44	0.33	1.70	3.15	4.48	0.16	0.06	0.05	-	-	99.14
81JB194 Porphyritic quartz monzonite	76.13	12.77	0.24	0.68	0.09	1.58	3.20	4.45	0.08	0.05	0.03	-	-	99.30
81JB195 Porphyritic quartz monzonite	70.90	14.50	0.49	2.21	0.65	2.52	3.11	4.19	0.32	0.14	0.08	-	-	99.11
81JB214 Porphyritic quartz monzonite	72.76	13.80	0.40	1.22	0.50	1.75	3.44	3.93	0.19	0.08	0.04	-	-	98.11
<b>Aplite Dikes</b>														
81JB133 Aplite dikes	75.06	13.83	0.76	1.22	-	0.20	3.94	4.61	0.02	0.05	0.03	-	-	99.72
81JB139 Aplite dikes	76.27	12.59	0.10	1.04	-	0.97	3.70	4.27	0.04	0.06	0.10	-	-	99.14
81JB141 Aplite dikes	75.26	12.94	0.18	0.95	0.02	1.01	3.51	4.48	0.06	0.04	0.04	-	-	98.49
81JB150 Aplite dikes	73.15	13.68	1.13	1.45	-	0.29	3.89	4.60	0.02	0.05	0.01	-	-	98.27
81JB191 Aplite dikes	74.42	13.59	0.96	0.59	-	0.28	3.80	4.53	0.02	0.09	0.02	-	-	98.30
3834 Pyritic Aplite	61.28	15.99	2.57	5.25	0.70	0.91	2.71	3.81	0.77	0.34	0.33	4.43	0.53	99.62
20507 Pyritic Aplite	64.95	16.26	5.96	0.27	0.74	0.92	1.41	3.81	0.79	0.29	0.03	3.49	1.62	100.04
<b>Skarns/Hornfels</b>														
175 Calc-silicate	42.84	11.18	1.81	8.66	1.57	26.90	0.20	0.08	0.39	0.12	0.62	3.17	0.34	97.54
186 Hornblende hornfels	45.97	11.00	2.19	8.67	10.87	14.79	0.65	1.11	2.12	0.80	0.20	1.11	0.31	99.48
190 Calc-silicate	33.37	8.08	1.31	7.19	0.92	36.60	0.15	0.00	0.19	0.14	0.56	4.17	0.23	92.68
200 Calc-silicate	25.26	7.69	9.78	7.13	0.87	22.71	0.35	0.12	0.26	0.14	0.23	9.52	1.72	84.06

Table 9.1a (Continued)

Terrane/ Sample Number/ Description	SiO <sub>2</sub>	Al <sub>2</sub> O <sub>3</sub>	Fe <sub>2</sub> O <sub>3</sub>	FeO	MgO	CaO	Na <sub>2</sub> O	K <sub>2</sub> O	TiO <sub>2</sub>	P <sub>2</sub> O <sub>5</sub>	MnO	LOI	H <sub>2</sub> O	Total
3812 Calc-silicate	60.93	15.14	4.30	2.52	1.65	8.62	1.04	1.63	0.79	0.13	0.38	2.67	0.13	99.91
3813 Calc-silicate	74.47	13.53	1.57	0.61	0.37	0.36	3.04	4.06	0.23	0.10	0.03	1.74	0.07	100.18
3829 Garnet-vesuvianite skarn	44.27	13.44	1.77	5.18	1.29	27.77	0.15	0.09	0.38	0.15	0.55	0.91	0.36	96.31
3845 Sheared hornfels	81.23	7.36	8.05	0.64	0.07	0.32	0.16	0.42	0.28	0.11	0.13	2.62	0.47	101.86
21149 Calc-silicate	65.12	11.81	1.67	3.84	1.24	5.00	1.17	1.77	0.45	0.06	0.23	1.40	0.18	99.88
21162 Calc-silicate	43.92	10.76	16.74	3.87	1.24	11.29	0.54	0.20	0.36	0.19	1.14	4.62	2.14	94.87
21341 Epidote hornfels	72.54	14.42	4.09	0.43	0.70	0.26	1.34	3.55	0.62	0.08	0.05	2.88	0.38	100.96
21349 Altered hornfels	54.79	11.69	18.42	0.34	2.34	3.53	0.41	0.54	0.47	0.14	0.75	6.92	4.15	100.34

Table 9.1b Normative mineralogies of the major rock units of the Fairbanks mining district.

Terrace/ Sample Number/ Description	Qt	Car	Qtz	Al	An	Ln	Nb	Kp	As	Nb	Ks	Wo	Dt	Ht	Cr	Ms	Hb	Tl	Ru	Ap
<b>Charnokite</b>																				
3830 Garnet orthopyroxene	-	-	-	-	17.960	0.373	4.379	-	-	-	-	-	26.235	-	9.887	33.197	3.054	-	-	3.454
3831 Garnet orthopyroxene	-	-	-	-	16.969	10.849	3.167	-	-	-	-	-	37.446	-	18.530	2.417	0.175	-	-	1.579
3832 Garnet amphibole	26.280	-	18.042	3.540	19.539	-	-	-	-	-	-	20.288	7.411	-	-	0.931	1.427	-	-	2.234
3833 Muscovite-biotite schist	50.677	-	12.585	6.068	5.315	-	-	-	-	-	-	-	9.586	14.217	-	0.362	-	-	-	0.654
3841 Garnet-calc schist	-	-	-	-	24.084	6.091	4.977	-	-	-	-	-	15.537	-	19.779	21.903	0.315	-	-	5.253
3842 Garnet amphibole	-	-	-	-	21.729	1.614	8.882	-	-	-	-	-	33.987	-	14.685	9.329	3.109	-	-	2.117
3843 Muscovite-K-Feldspar-schist	63.410	10.901	13.440	1.880	1.135	-	-	-	-	-	-	-	49.404	-	6.250	3.436	-	-	-	0.416
3846 Garnet amphibole	-	-	1.598	9.609	14.248	10.120	-	-	-	-	-	27.647	-	-	5.271	3.750	-	-	-	3.473
21342 Marble	-	-	-	-	17.722	0.633	10.537	-	-	-	-	-	12.172	-	10.382	38.330	3.845	-	-	3.372
21343 Impure marble	-	-	-	-	15.343	7.071	8.962	-	-	-	-	-	4.599	-	10.382	38.330	3.786	-	-	2.853
21344 Crinoidal muscovite	76.649	-	3.248	4.213	3.981	-	-	-	-	-	-	-	-	-	-	0.602	-	-	-	3.507
<b>Chemyl Sequence Metavolcanic/Metasediments</b>																				
197 Banded-muscovite quartzite	93.775	0.039	1.964	1.406	0.781	-	-	-	-	-	-	-	-	0.659	-	0.964	-	-	-	0.136
198 Banded-muscovite quartzite	66.157	6.018	18.882	3.519	1.311	-	-	-	-	-	-	-	1.263	-	-	0.079	1.680	-	-	1.021
3818 Banded-muscovite quartzite	65.938	5.706	7.745	3.316	0.486	-	-	-	-	-	-	-	13.419	-	-	3.389	-	-	-	1.544
3819 Banded-muscovite quartzite	88.105	2.103	3.222	1.634	1.794	-	-	-	-	-	-	-	0.870	-	-	1.745	-	-	-	0.293
3824 Muscovite-tuff	43.845	10.715	33.290	3.361	0.685	-	-	-	-	-	-	-	3.061	-	-	3.168	-	-	-	1.648
3835 Muscovite-tuff	55.509	8.417	22.357	3.076	0.628	-	-	-	-	-	-	-	4.048	-	-	0.803	2.258	-	-	2.457
3836 Garnet ortho-amphibole	-	-	10.112	4.163	24.955	-	-	-	-	-	-	27.311	9.394	16.338	-	0.915	-	-	-	1.412
3837 Garnet ortho-amphibole	-	-	11.153	4.037	28.506	-	-	-	-	-	-	23.244	9.239	13.286	-	1.584	-	-	-	1.866
3839 Metachert	56.118	7.467	18.351	2.745	5.047	-	-	-	-	-	-	23.526	4.646	-	-	3.748	-	-	-	1.391
21151 Feldspathic-chlorite schist	-	-	2.531	27.898	27.628	-	-	-	-	-	-	23.526	0.053	13.363	-	3.919	-	-	-	2.281
21152 Chlorite-talc schist	28.122	13.858	33.444	4.199	3.173	-	-	-	-	-	-	10.819	-	-	-	3.919	-	-	-	2.126
21155 Ortho-amphibole	-	-	4.262	2.649	29.299	-	5.602	-	-	-	-	34.160	-	-	-	2.809	-	-	-	0.942
21330 Calc-chlorite schist	-	-	-	-	12.095	0.205	-	-	-	-	-	-	-	-	15.356	2.809	-	-	-	1.074
21331 Feldspathic-muscovite quartzite	79.550	4.149	8.658	2.123	0.202	-	-	4.292	-	-	-	-	-	-	3.417	75.685	-	-	-	0.467
21335 Banded muscovite quartzite	68.525	11.213	14.061	2.539	0.824	-	-	-	-	-	-	-	-	1.005	-	0.097	0.626	-	-	0.072
21337 Crinoidal schist	20.328	18.548	47.731	6.564	0.843	-	-	-	-	-	-	-	-	4.489	-	-	-	1.007	-	0.343
21346 Banded muscovite quartzite	67.507	12.407	5.991	1.327	0.838	-	-	-	-	-	-	-	-	6.325	-	3.622	-	-	-	0.218
21347 Muscovite-garnet schist	23.970	3.982	23.421	11.003	17.519	-	-	-	-	-	-	-	-	14.029	-	3.831	-	-	-	2.055
82SH02 Feldspathic-muscovite schist	48.284	11.516	23.380	4.053	0.911	-	-	-	-	-	-	-	-	6.569	-	3.397	-	-	-	0.410
82CH02 Chlorite quartzite w/ sulfides	92.818	0.291	2.534	1.941	0.365	-	-	-	-	-	-	-	-	1.222	-	0.593	-	-	-	0.046
82HY01 Chlorite quartzite w/ sulfides	63.250	1.408	9.961	5.777	7.123	-	-	-	-	-	-	-	-	8.780	-	2.769	-	-	-	0.346
<b>Chemyl Sequence Metasediments</b>																				
185 Biotite-muscovite-garnet schist	31.812	8.512	24.327	12.833	4.655	-	-	-	-	-	-	-	-	12.951	-	2.394	-	-	-	0.382
192 Biotite-muscovite-garnet schist	13.426	-	9.678	5.251	46.115	-	-	-	-	-	-	-	16.890	3.536	-	3.289	-	-	-	1.584
3810 Para-amphibole	36.728	7.299	22.818	14.724	5.431	-	-	-	-	-	-	-	-	8.092	-	3.210	-	-	-	1.271
3823 Marble	-	-	-	-	38.388	7	4.490	99.822	0.097	0.238	0.521	-	-	-	1.294	7	-	-	-	0.127
3825 Para-amphibole(?)	-	-	-	-	38.388	7	4.490	3.607	-	-	-	-	-	-	29.442	16.413	-	-	-	5.517
3826 Muscovite quartzite	74.380	2.770	9.977	5.389	1.645	-	-	-	-	-	-	-	-	3.561	-	1.598	-	-	-	0.518

Table 9.1b (Continued)

Terrane/ Sample Number/ Description	Qt	Cor	Qtz	Al	An	Lo	Nb	Kp	As	Nr	Ks	Wo	Di	Hy	Qt	Os	Mu	Hb	Il	Ru	Ap	
3827 Marble	37.692	2.828	8.151	8.434	15.163	?	-	66.912	0.607	0.888	1.266	-	-	23.527	1.734	?	1.839	-	0.276	-	0.374	
3838 Biotite-muscovite- garnet schist	-	-	-	-	-	-	-	-	-	-	-	-	-	-	-	-	1.839	-	2.046	-	0.326	
20506 Metaconglomerate	58.737	6.090	14.118	10.237	1.688	-	-	-	-	-	-	-	-	5.055	-	-	2.845	-	1.043	-	0.188	
20510 R-Feldspar-biotite schist	1.158	6.226	44.646	27.016	1.803	-	-	-	-	-	-	-	-	15.286	-	-	1.548	-	1.777	-	0.542	
21142 Quartzite	73.681	-	2.547	3.138	12.486	-	-	-	-	-	-	-	1.993	3.892	-	-	2.325	-	0.495	-	0.046	
21147 Quartzite	74.053	0.971	3.235	3.369	10.948	-	-	-	-	-	-	-	-	4.550	-	-	2.179	-	0.605	-	0.092	
21154 Muscovite schist	26.836	12.521	26.974	8.954	2.944	-	-	-	-	-	-	-	-	18.207	-	-	1.444	-	1.832	-	0.288	
21320 Muscovite quartzite	53.693	4.087	14.614	14.579	4.314	-	-	-	-	-	-	-	-	5.397	-	-	2.190	-	0.963	-	0.164	
21334 Feldspathic biotite garnet schist	44.438	11.166	23.247	7.300	0.622	-	-	-	-	-	-	-	-	7.578	-	-	3.589	-	1.775	-	0.285	
Pairwaik Schist Metasediments																						
3828 Garnet-ebolite- muscovite schist	52.884	3.873	14.577	9.420	12.855	-	-	-	-	-	-	-	-	9.080	-	-	1.833	-	1.024	-	0.456	
20505 Biotite-muscovite- quartz schist	33.914	13.573	29.592	9.825	1.156	-	-	-	-	-	-	-	-	6.479	-	-	3.518	-	1.753	-	0.192	
20508 Muscovite-quartz schist	74.950	2.374	4.502	9.839	2.903	-	-	-	-	-	-	-	-	3.367	-	-	1.410	-	0.609	-	0.046	
Goldstream Sequence																						
3809 Biotite-muscovite schist	48.628	6.055	21.026	13.090	1.767	-	-	-	-	-	-	-	-	5.203	-	-	2.991	-	0.979	-	0.263	
3814 Garnet-ebolite- muscovite quartzite	79.102	1.195	2.550	11.465	1.897	-	-	-	-	-	-	-	-	1.830	-	-	1.441	-	0.381	-	0.139	
3815 Garnet-biotite- muscovite schist	31.880	12.584	25.220	15.794	1.448	-	-	-	-	-	-	-	-	8.027	-	-	3.071	-	1.733	-	0.243	
3816 Garnet-ampibolite	-	-	1.567	29.879	21.907	-	-	-	-	-	-	-	23.537	7.463	7.224	-	2.383	-	5.257	-	0.786	
3817 Calcic muscovite schist	-	-	-	-	5.438	5.162	6.201	-	-	-	-	35.049	19.177	-	-	27.964	-	0.635	-	0.453	-	0.522
3840 Marble	-	-	-	-	-	-	-	-	-	-	-	-	-	-	7.825	91.140	0.757	-	0.345	-	0.345	
3844 Para-ampibolite	47.292	2.069	8.075	17.215	9.745	-	-	-	-	-	-	-	-	12.063	-	-	1.027	-	1.999	-	0.516	
21324 Amphibole-quartz schist	62.671	5.667	14.862	2.427	3.513	-	-	-	-	-	-	-	-	2.610	-	-	-	-	0.071	0.669	7.510	
Birch Hill Sequence																						
811201 Amphibole-quartz schist	90.494	1.766	2.074	1.273	1.348	-	-	-	-	-	-	-	-	0.549	-	-	1.793	0.298	0.267	-	0.139	
3820 Calcic muscovite schist	0.878	-	16.223	13.259	14.954	-	-	-	-	-	-	-	-	-	-	-	2.184	-	0.808	-	0.506	
3821 Amphibole phyllite	90.125	0.857	3.116	1.802	1.099	-	-	-	-	-	-	-	-	1.609	-	-	0.983	-	0.173	-	0.235	
3822 Amphibole quartzite	90.545	0.273	2.225	1.845	2.005	-	-	-	-	-	-	-	-	2.262	-	-	0.575	-	0.113	-	0.161	
20503 Carbonaceous quartzite	81.068	2.811	9.535	1.526	1.249	-	-	-	-	-	-	-	-	1.398	-	-	-	0.411	0.424	0.118	1.462	
20504 Pyrite-banded quartzite	78.795	2.539	3.617	1.287	7.982	-	-	-	-	-	-	-	-	2.020	-	-	2.212	2.975	0.481	-	0.094	
Igneous Intrusives																						
811201 Fine-grained granodiorite	13.65	-	14.89	21.15	26.41	-	-	-	-	-	-	-	2.64	16.40	-	-	1.58	-	1.75	-	0.51	
811203 Fine-grained granodiorite	14.10	-	14.36	21.66	25.13	-	-	-	-	-	-	-	3.41	16.51	-	-	1.45	-	1.80	-	0.53	
811205 Fine-grained granodiorite	19.02	-	16.25	20.73	25.47	-	-	-	-	-	-	-	0.19	15.50	-	-	1.57	-	1.63	-	0.44	
811207 Fine-grained granodiorite	20.58	-	15.90	18.11	25.51	-	-	-	-	-	-	-	0.95	14.53	-	-	1.61	-	1.69	-	0.42	

Table 9.1b (Continued)

Terrane/ Sample Number/ Description	Qt	Cor	Or	Al	An	Ln	Ne	Kp	Ac	Nr	Kr	Wo	Di	Hy	Ol	Ca	Mn	He	Il	Ru	Ap
81JB211	Fine-grained granodiorite	25.97	--	20.68	19.97	15.99	--	--	--	--	--	--	--	10.20	--	--	1.87	--	1.27	--	0.49
81JB216	Fine-grained granodiorite	23.86	--	18.85	22.34	19.52	--	--	--	--	--	--	1.36	9.39	--	--	1.20	--	1.48	--	0.51
81JB218	Fine-grained granodiorite	18.65	--	13.24	30.04	20.51	--	--	--	--	--	--	0.63	12.28	--	--	0.86	--	1.35	--	0.46
81JB106	Porphyritic granodiorite	27.30	1.40	24.52	30.38	10.23	--	--	--	--	--	--	--	5.92	--	--	1.16	--	0.76	--	0.32
81JB108	Porphyritic granodiorite	25.57	0.15	24.52	33.25	1--	--	--	--	--	--	--	--	2.96	--	--	0.42	--	0.63	--	0.25
81JB116a	Porphyritic granodiorite	31.73	0.20	23.93	27.42	11.09	--	--	--	--	--	--	--	3.24	--	--	0.68	--	0.55	--	0.19
81JB127	Porphyritic granodiorite	30.50	1.30	18.50	26.82	13.35	--	--	--	--	--	--	--	6.01	--	--	0.84	--	0.93	--	0.28
81JB128	Porphyritic granodiorite	30.81	1.28	21.63	25.72	12.51	--	--	--	--	--	--	--	4.64	--	--	0.99	--	0.89	--	0.35
81JB132	Porphyritic granodiorite	30.76	1.17	21.92	28.69	10.91	--	--	--	--	--	--	--	4.36	--	--	0.58	--	0.70	--	0.30
81JB134	Porphyritic granodiorite	37.91	1.15	19.91	24.29	9.57	--	--	--	--	--	--	--	5.02	--	--	0.83	--	0.49	--	0.23
81JB213	Porphyritic granodiorite	30.02	0.61	18.26	29.87	13.75	--	--	--	--	--	--	--	4.51	--	--	0.94	--	0.76	--	0.35
81JB215	Porphyritic granodiorite	24.41	0.02	17.73	29.95	16.27	--	--	--	--	--	--	--	6.89	--	--	1.38	--	1.08	--	0.44
81JB135	Porphyritic quartz monzonite	39.15	0.27	20.09	23.35	9.17	--	--	--	--	--	--	--	5.72	--	--	0.68	--	0.53	--	0.23
81JB137	Porphyritic quartz monzonite	40.13	0.21	21.75	28.52	6.54	--	--	--	--	--	--	--	1.87	--	--	0.29	--	0.13	--	0.09
81JB142	Porphyritic quartz monzonite	30.29	1.04	21.63	27.75	11.19	--	--	--	--	--	--	--	6.04	--	--	0.65	--	0.53	--	0.19
81JB143	Porphyritic quartz monzonite	30.02	0.99	21.21	27.42	10.97	--	--	--	--	--	--	--	5.44	--	--	0.39	--	0.55	--	0.21
81JB144	Porphyritic quartz monzonite	29.91	0.95	23.70	23.61	10.10	--	--	--	--	--	--	--	7.61	--	--	0.67	--	0.78	--	0.32
81JB145	Porphyritic quartz monzonite	34.61	1.58	26.36	26.37	7.65	--	--	--	--	--	--	--	3.05	--	--	0.42	--	0.27	--	0.21
81JB146	Porphyritic quartz monzonite	34.44	0.57	20.51	24.54	9.98	--	--	--	--	--	--	--	5.84	--	--	0.59	--	0.61	--	0.21
81JB148	Porphyritic quartz monzonite	32.56	1.08	20.15	27.16	10.51	--	--	--	--	--	--	--	5.40	--	--	0.61	--	0.47	--	0.16
81JB149	Porphyritic quartz monzonite	36.19	0.73	23.05	28.69	6.89	--	--	--	--	--	--	--	2.29	--	--	0.16	--	0.13	--	0.16
81JB152	Porphyritic quartz monzonite	35.83	0.17	23.34	27.50	7.45	--	--	--	--	--	--	--	2.69	--	--	0.26	--	0.23	--	0.14
81JB161	Porphyritic quartz monzonite	32.88	1.28	26.36	26.64	9.02	--	--	--	--	--	--	--	2.95	--	--	0.93	--	0.38	--	0.16
81JB162	Porphyritic quartz monzonite	35.52	0.43	26.95	31.22	3.98	--	--	--	--	--	--	--	1.08	--	--	0.51	--	0.09	--	0.28
81JB165	Porphyritic quartz monzonite	33.60	0.57	24.41	27.75	9.13	--	--	--	--	--	--	--	0.57	--	--	0.29	--	0.36	--	0.19
81JB166b	Porphyritic quartz monzonite	32.43	--	27.48	31.39	5.47	--	--	--	--	--	--	0.24	0.89	--	--	0.22	--	0.08	--	0.09
81JB167	Porphyritic quartz monzonite	33.20	1.42	24.52	25.30	9.28	--	--	--	--	--	--	--	4.13	--	--	0.77	--	0.46	--	0.21
81JB173	Porphyritic quartz monzonite	36.94	0.87	20.98	26.49	11.09	--	--	--	--	--	--	--	2.67	--	--	0.62	--	0.30	--	0.25
81JB175	Porphyritic quartz monzonite	32.33	0.53	25.47	24.79	10.56	--	--	--	--	--	--	--	4.20	--	--	0.83	--	0.49	--	0.23
81JB179	Porphyritic quartz monzonite	31.71	0.41	29.84	27.08	7.11	--	--	--	--	--	--	--	2.62	--	--	0.42	--	0.25	--	0.12
81JB186	Porphyritic quartz monzonite	36.94	1.28	22.99	25.64	8.06	--	--	--	--	--	--	--	3.08	--	--	0.68	--	0.38	--	0.14
81JB189	Porphyritic quartz monzonite	34.19	1.45	27.71	23.86	8.04	--	--	--	--	--	--	--	3.16	--	--	0.55	--	0.34	--	0.14
81JB192	Porphyritic quartz monzonite	33.19	0.75	26.47	26.65	8.04	--	--	--	--	--	--	--	2.91	--	--	0.68	--	0.30	--	0.14
81JB194	Porphyritic quartz monzonite	36.70	--	26.30	27.08	7.34	--	--	--	--	--	--	0.15	1.12	--	--	0.35	--	0.15	--	0.12
81JB195	Porphyritic quartz monzonite	29.31	0.60	24.76	26.32	11.59	--	--	--	--	--	--	--	4.89	--	--	0.71	--	0.61	--	0.32
81JB214	Porphyritic quartz monzonite	32.68	0.90	23.22	29.11	8.16	--	--	--	--	--	--	--	2.92	--	--	0.58	--	0.36	--	0.19
Aplite Dikes																					
81JB133	Aplite dikes	33.47	2.11	27.24	33.34	0.67	--	--	--	--	--	--	--	1.64	--	--	1.10	--	0.04	--	0.12
81JB139	Aplite dikes	35.61	0.26	25.23	31.31	4.42	--	--	--	--	--	--	--	1.95	--	--	0.14	--	0.08	--	0.14
81JB141	Aplite dikes	34.90	0.58	26.47	29.70	4.75	--	--	--	--	--	--	--	1.62	--	--	0.26	--	0.11	--	0.09
81JB150	Aplite dikes	31.66	1.89	27.18	32.92	1.11	--	--	--	--	--	--	--	1.71	--	--	1.64	--	0.04	--	0.12
81JB191	Aplite dikes	34.50	2.14	26.77	32.15	0.80	--	--	--	--	--	--	--	0.29	--	--	1.39	--	0.04	--	0.21
3834	Pyritic Aplite	26.885	6.940	23.791	24.231	2.425	--	--	--	--	--	--	--	9.876	--	--	3.478	--	1.545	--	0.832
20507	Pyritic Aplite	40.348	9.297	23.683	12.550	2.810	--	--	--	--	--	--	--	5.535	--	--	3.493	--	1.578	--	0.706
Skarn/Hornfels																					
175	Calc-silicates	--	--	--	--	31.123	0.393	0.971	--	--	--	19.302	38.658	--	--	5.701	2.781	--	0.785	--	0.294
186	Hornblende hornfels	--	--	6.668	5.591	24.213	--	--	--	--	--	--	36.283	9.826	8.217	--	3.228	--	4.093	--	1.883

Table 9.1b (Continued)

Terrane/ Sample Number/ Description	Qt	Cor	Or	Al	An	La	Ne	Kp	Ac	Ns	Ka	Wo	Di	Hy	Ol	Cr	Ma	Ho	Il	Rn	Ap
190 Calc-silicate	-	-	-	-	24.148	-	0.777	-	-	-	-	-	13.831	-	7.546	50.787	2.146	-	0.408	-	0.366
200 Calc-silicate	-	-	-	-	25.845	?	2.176	0.997	-	-	-	-	-	-	28.125	38.913	3.461	-	0.670	-	0.440
3812 Calc-silicate	28.654	-	9.937	9.078	32.836	-	-	-	-	-	-	-	8.692	5.523	-	-	3.426	-	1.548	-	0.311
3813 Calc-silicate	40.878	3.781	24.389	26.148	1.152	-	-	-	-	-	-	-	-	0.937	-	-	1.420	0.616	0.444	-	0.235
3829 Garnet-vesuvianite skarn	0.030	-	0.560	1.335	37.597	-	-	-	-	-	-	32.660	24.000	-	-	-	2.700	-	0.759	-	0.365
3845 Sheared hornfels	79.186	6.402	2.513	1.371	0.890	-	-	-	-	-	-	-	-	0.177	-	-	1.696	6.980	0.538	-	0.258
21149 Calc-silicate	40.371	-	11.324	10.718	23.544	-	-	-	-	-	-	-	2.434	7.914	-	-	2.622	-	0.925	-	0.150
21162 Calc-silicate	7.010	-	1.331	5.148	29.681	-	-	-	-	-	-	-	28.144	24.398	-	-	3.038	-	0.770	-	0.496
21341 Epidote hornfels	50.230	8.267	21.431	11.583	0.784	-	-	-	-	-	-	-	-	3.173	-	-	3.140	-	1.203	-	0.189
21349 Altered hornfels	29.944	4.738	3.477	3.780	18.086	-	-	-	-	-	-	-	-	35.547	-	-	3.112	-	0.973	-	0.353

Table 9.2a Major oxide analyses of granitic rocks from the Circle mining district, Alaska

Sample Number	Description/ (Pluton)	SiO <sub>2</sub>	Al <sub>2</sub> O <sub>3</sub>	Fe <sub>2</sub> O <sub>3</sub>	FeO	MgO	CaO	Na <sub>2</sub> O	K <sub>2</sub> O	TiO <sub>2</sub>	P <sub>2</sub> O <sub>5</sub>	MnO
KM147	Syenogranite (CHS)	74.700	12.610	0.600	1.400	0.150	0.520	3.560	5.250	0.160	0.040	0.030
CH61	Syenogranite (CHS)	76.620	12.630	0.240	1.810	0.110	0.740	2.660	5.640	0.190	0.040	0.050
PM281	Syenogranite (CHS)	73.970	13.220	0.600	0.900	0.160	0.420	3.650	4.850	0.110	0.110	0.050
PM280	Monzogranite (2-Bit)	71.050	13.090	1.100	2.510	0.420	1.450	3.530	4.840	0.500	0.150	0.060
CH60	Syenogranite (CHS)	77.330	12.340	0.040	1.680	0.060	0.510	2.530	5.720	0.170	0.040	0.060
CH59	Monzogranite (2-Bit)	71.910	13.690	0.210	2.960	0.340	1.450	2.790	5.960	0.470	0.020	0.070
KM142	Syenogranite (CHS)	76.340	13.590	0.240	1.080	0.090	0.480	2.630	6.090	0.100	0.080	0.030
CH57	Monzogranite (2-Bit)	76.000	12.990	0.410	1.800	0.040	0.760	3.110	5.200	0.140	0.040	0.070
1933	Granodiorite (CHS)	71.620	14.600	0.520	2.690	0.810	3.440	2.690	2.620	0.350	0.100	0.090
PM278	Monzogranite (2-Bit)	69.830	15.190	0.900	2.000	0.800	2.320	4.370	3.430	0.290	0.110	0.070
KM114	Granodiorite (CHS)	64.780	17.140	1.710	3.310	1.000	4.050	3.240	4.140	0.730	0.220	0.090
CH56A	Granodiorite (CHS)	71.130	15.510	0.100	1.950	0.650	2.500	3.190	4.650	0.270	0.100	0.070
CH33	Monzogranite (2-Bit)	68.300	15.530	0.100	2.250	0.780	2.490	3.350	4.460	0.310	0.110	0.080
CH54	Monzogranite (2-Bit)	72.710	14.750	0.340	1.860	0.520	2.140	2.890	4.950	0.220	0.060	0.070

Table 9.2b CIPW normative analyses of granitic rocks from the Circle mining district, Alaska

Sample Number	Description/ (Pluton)	Qt	Cor	Or	Al	An	La	Ne	Kp	Ac	Ns	Ka	Wo	Di	Hy	Ol	Cs	Ma	Ho	Il	Ru	Ap
KM147	Syenogranite (CHS)	32.144	0.224	31.330	30.420	2.341	--	--	--	--	--	--	--	--	2.262	--	--	0.879	--	0.307	--	0.094
CH61	Syenogranite (CHS)	36.342	0.893	33.086	22.343	3.385	--	--	--	--	--	--	--	--	3.155	--	--	0.345	--	0.358	--	0.092
PM281	Syenogranite (CHS)	33.524	1.495	29.232	31.500	1.393	--	--	--	--	--	--	--	--	1.496	--	--	0.887	--	0.213	--	0.260
PM280	Monzogranite (2-Bit)	27.827	--	28.977	30.261	5.651	--	--	--	--	--	--	--	0.552	3.802	--	--	1.616	--	0.962	--	0.352
CH60	Syenogranite (CHS)	38.161	1.150	33.639	21.304	2.258	--	--	--	--	--	--	--	--	3.018	--	--	0.058	--	0.321	--	0.092
CH59	Monzogranite (2-Bit)	27.252	0.061	35.264	23.637	7.072	--	--	--	--	--	--	--	--	5.470	--	--	0.305	--	0.894	--	0.046
KM142	Syenogranite (CHS)	35.770	1.976	35.719	22.087	1.845	--	--	--	--	--	--	--	--	1.885	--	--	0.345	--	0.189	--	0.184
CH57	Monzogranite (2-Bit)	34.937	0.954	30.556	26.168	3.490	--	--	--	--	--	--	--	--	2.949	--	--	0.591	--	0.264	--	0.092
1933	Granodiorite (CHS)	35.955	1.330	15.555	22.868	16.490	--	--	--	--	--	--	--	--	6.145	--	--	0.758	--	0.668	--	0.233
PM278	Monzogranite (2-Bit)	24.428	0.336	20.409	37.232	10.866	--	--	--	--	--	--	--	--	4.604	--	--	1.314	--	0.555	--	0.256
KM114	Granodiorite (CHS)	18.816	0.490	24.364	27.302	18.579	--	--	--	--	--	--	--	--	6.093	--	--	2.469	--	1.381	--	0.507
CH56A	Granodiorite (CHS)	27.257	0.922	27.445	26.959	11.735	--	--	--	--	--	--	--	--	4.795	--	--	0.145	--	0.512	--	0.231
CH33	Monzogranite (2-Bit)	24.430	0.949	26.959	28.994	11.901	--	--	--	--	--	--	--	--	5.757	--	--	0.146	--	0.602	--	0.261
CH54	Monzogranite (2-Bit)	30.292	0.886	29.102	24.329	10.173	--	--	--	--	--	--	--	--	4.175	--	--	0.490	--	0.416	--	0.138

Table 9.3a Major oxide analyses of granitic rocks from the Richardson mining district, Alaska

Sample Number	Description	SiO <sub>2</sub>	Al <sub>2</sub> O <sub>3</sub>	Fe <sub>2</sub> O <sub>3</sub>	FeO	MgO	CaO	Na <sub>2</sub> O	K <sub>2</sub> O	TiO <sub>2</sub>	P <sub>2</sub> O <sub>5</sub>	MnO
84BL01	Pyroxene diorite	56.030	15.000	5.200	3.470	3.450	2.190	2.250	3.300	1.070	0.320	0.150
84BL02	Granodiorite	63.220	15.530	0.333	6.400	2.230	3.480	3.880	3.750	0.650	0.220	0.120
84BL03	Quartz monzonite	69.770	14.850	1.200	1.800	0.810	2.000	3.690	4.500	0.310	0.140	0.040
84BL04	Granite	73.390	15.060	0.800	0.260	0.210	0.270	2.280	7.660	0.100	0.110	0.030
84BL05	Granite	77.810	13.280	0.250	0.260	0.070	0.070	2.870	5.010	0.070	0.030	0.020

Table 9.3b CIPW normative analyzes of granitic rocks from the Richardson mining district, Alaska

Sample Number	Description	Qt	Cor	Or	Al	An	Lo	Ne	Kp	Ac	Ns	Kr	Wo	Di	Hty	Ot	Ca	Ma	Ho	Il	Ru	Ap
84BL01	Pyroxene diorite	19.690	4.894	21.158	20.656	9.521	--	--	--	--	--	--	--	--	17.032	--	--	4.043	--	2.205	--	0.804
84BL02	Granodiorite	11.737	--	22.208	32.902	13.914	--	--	--	--	--	--	--	1.648	15.409	--	--	0.436	--	1.237	--	0.511
84BL03	Quartz monzonite	25.328	0.613	26.822	31.492	9.086	--	--	--	--	--	--	--	--	3.984	--	--	1.755	--	0.594	--	0.327
84BL04	Granite	30.184	2.786	45.187	19.259	0.620	--	--	--	--	--	--	--	--	0.522	--	--	0.645	0.354	0.190	--	0.254
84BL05	Granite	41.672	3.055	29.676	24.511	0.132	--	--	--	--	--	--	--	--	0.368	--	--	0.363	--	0.133	--	0.070

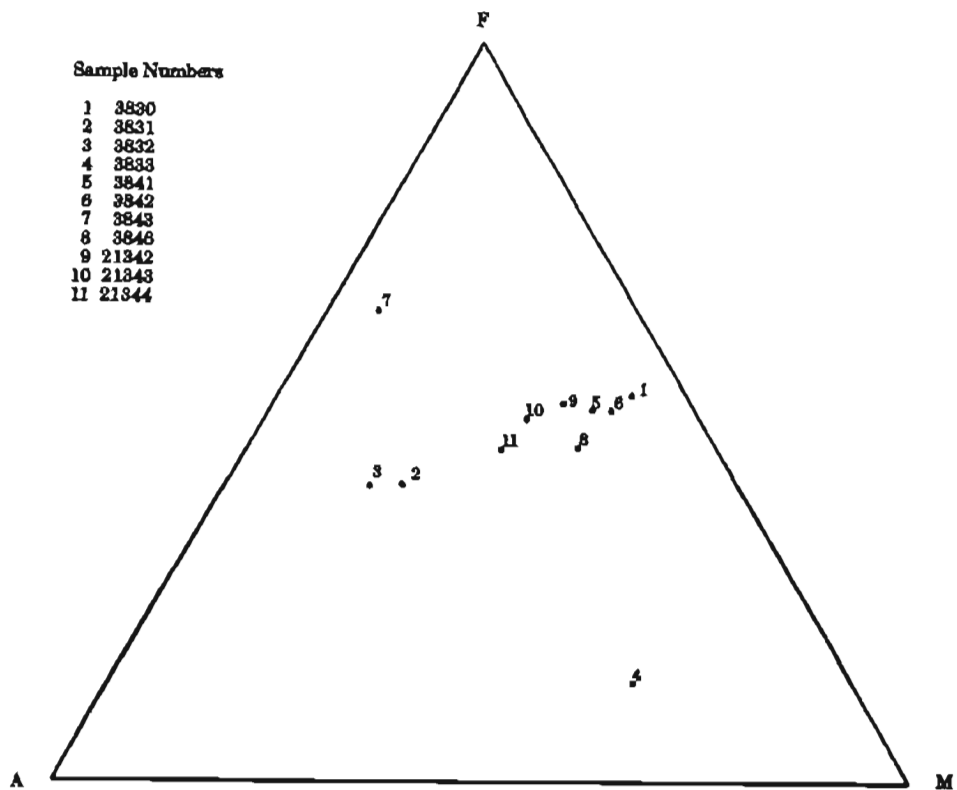


Figure 9.1 Plot of Chatanika Terrane samples on an AFM diagram (sample descriptions in Table 9.1a).

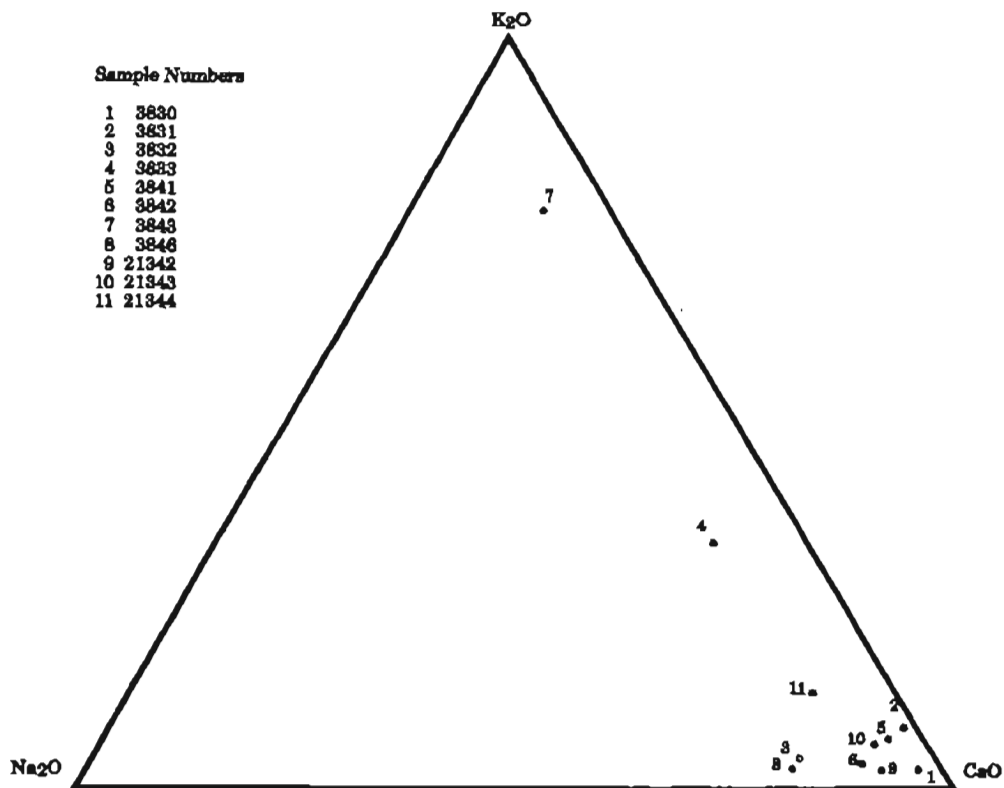


Figure 9.2 Plot of Chatanika terrane samples on an Na-Ca-K diagram (sample descriptions in Table 9.1a).

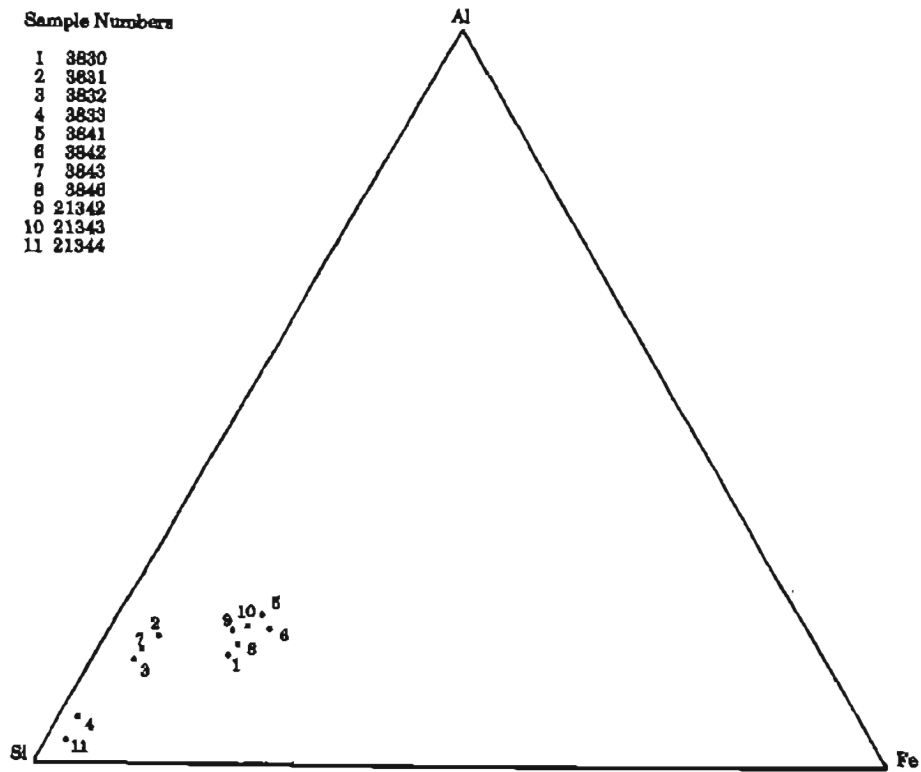


Figure 9.3 Plot of samples from the Chatanika terrane on a Al-Si-Fe diagram.

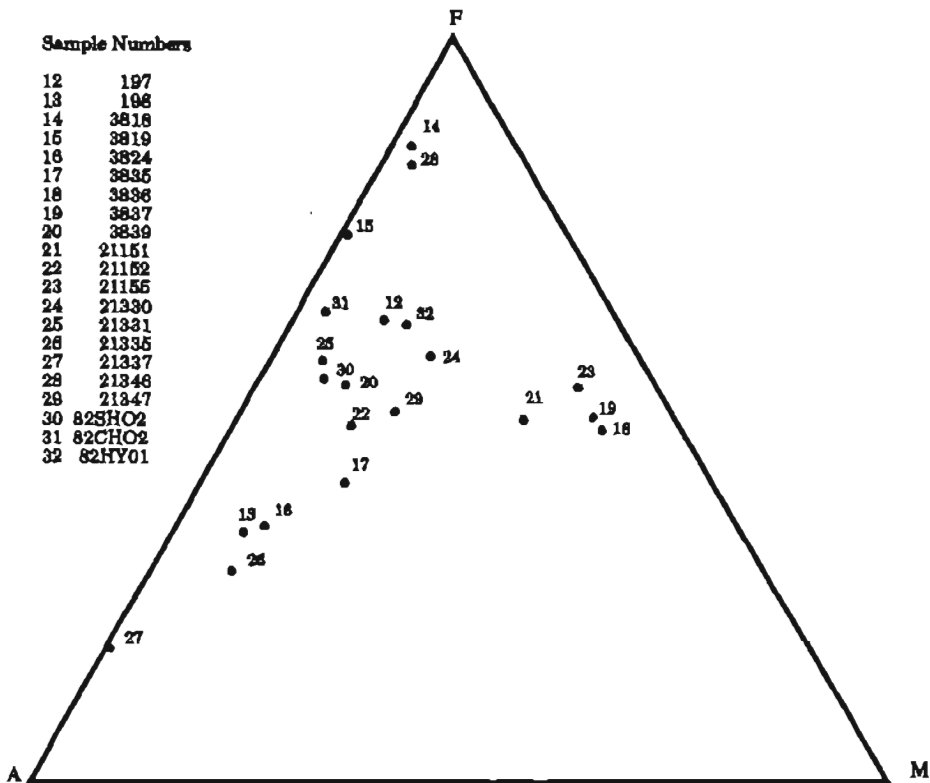


Figure 9.4 Plot of metavolcanic samples from the Cleary sequence on an AFM diagram (sample descriptions in Table 9.1a).

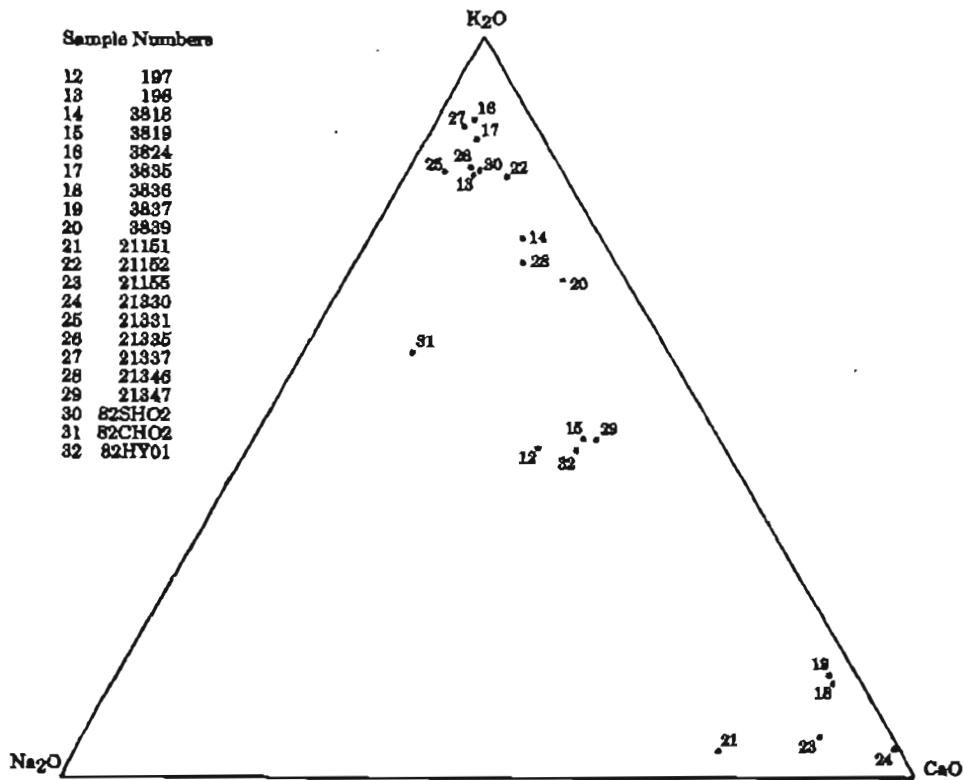


Figure 9.5 Plot of metavolcanic samples from the Cleary sequence on a Na-Ca-K diagram (sample descriptions in Table 9.1a).

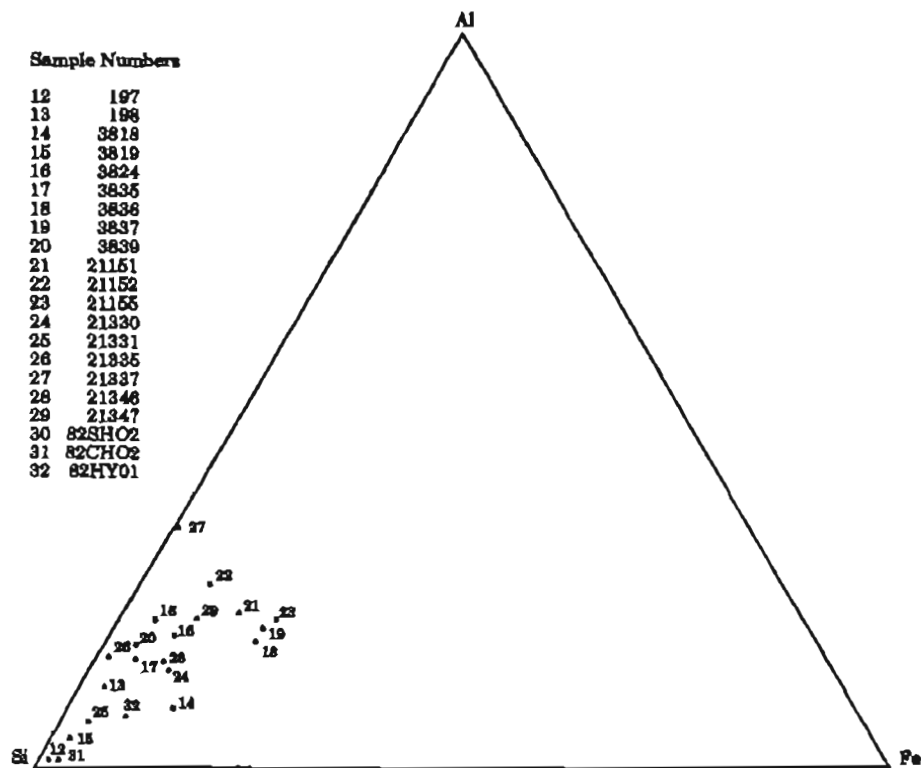


Figure 9.6 Plot of metavolcanic samples from the Cleary sequence on Al-Si-Fe diagram.

The metasedimentary rocks of the Cleary sequence contain a much smaller mafic component than the basic metavolcanic rocks (see Figure 9.7). The metasediments also have a smaller potassium content than the metavolcanics (see Figure 9.8). The Ca-Na-K diagram indicates a continuum of calcium and potassium content for the metasediments but discrete compositions for the metavolcanics.

Figure 9.9a shows the large silica content of the Cleary sequence metasediments relative to alumina and iron. On the same diagram are plots for the metavolcanic and metasediments of the gold-bearing Chopawamsic Formation (Pavliades, 1982) and the rocks at the London-Virginia mine (Mangan et al., 1984). There are strong similarities in the mineralogy, petrology and whole-rock geochemistry of the Cleary sequence and the Chopawamsic Formation, which is host to the volcanic-exhalative gold mineralization at the London-Virginia mine.

#### 9.3.1.3 Goldstream Sequence

The Goldstream sequence metasediments are generally slightly enriched in iron and magnesium relative to the Cleary sequence metasediments (see Figures 9.7, 9.8, and 9.9b). The mafic component in the Goldstream sequence is generally less than the mafic component in either the mafic metavolcanics of the Cleary sequence or in the Chatanika terrane.

The Goldstream metasediments have a larger total alkali content than the metasediments of the Cleary sequence. This is due to the greater  $\text{Na}_2\text{O}$  and  $\text{CaO}$  content of the Goldstream rocks. The  $\text{Na}_2\text{O}$  content of samples from the Goldstream sequence lies within a very narrow range, however this may be a function of the small number of samples.

#### 9.3.1.4 Birch Hill Sequence

The metasediments of the Birch Hill sequence have a smaller mafic component than the Goldstream sequence metasediments. The Birch Hill rocks contain more silica and potassium on the average than the Goldstream metasediments. The Birch Hill sequence also has a narrower range in  $\text{Na}_2\text{O}$  relative to  $\text{CaO}$  and  $\text{K}_2\text{O}$  (see Figure 9.8). The Birch Hill metasediments generally plot on the AFM diagram (see Figure 9.7) within the range of the Cleary sequence metasediments.

#### 9.3.1.5 Major Oxide and Rare Earth Element Variation

Chondrite normalized REE data are plotted on Figures 9.10a through 9.10c. Chondrite normalizing values are from Haskin et al. (1968) and Evensen et al. (1978). Figure 9.10a includes chondrite normalized REE patterns for a composite of North American Shale (NAS) (Haskin et al., 1966) and for continental tholeiitic basalt (CTB) (Gottfried et al., 1977).

Chondrite normalized REE patterns for basaltic rocks generally show a depletion in LREE relative to the NAS. Continental tholeiites, on the average, are depleted in LREE by a factor of two relative to NAS, and are the least depleted of the mafic volcanics. The amphibolites of probable igneous origin from the Chatanika terrane and the Cleary sequence

are not depleted in light rare earth elements (LREE) relative to the (NAS). Similarly, the ortho-amphibolites are not enriched in the heavy rare earth elements (HREE) relative to NAS. The lack of LREE depletion is not a sufficient condition to reclassify all the amphibolites in the Chatanika terrane and Cleary sequence as para-amphibolites.

Some of the metafelsites and exhalites have negative europium anomalies but most exhibit either no anomaly or a slightly positive value relative to NAS. Skarns with large tungsten contents have positive europium anomalies. The metasediments of the Cleary, Goldstream, and Birch Hill sequences have REE trends nearly parallel with the NAS. Other than the above mentioned trends, the REE data for the metaigneous and metasedimentary rocks show little variance with NAS.

Figure 9.11a is a Harker variation diagram for the metaigneous rocks from the Chatanika terrane and Cleary sequence with a high mafic component, while Figure 9.11b is a similar diagram for the metaigneous rocks of intermediate to felsic composition. The diagrams indicate a general decrease in alumina, iron, calcium, and magnesium with increased silica content. Sodium is low even in the more felsic rocks with an average of approximately one percent. Potassium contents increase from less than one percent in the mafic rocks to more than four percent in the felsic varieties. Although the curves are not smooth, the results suggest a differentiated igneous suite. Some of the irregularity in the curves is probably due to the sedimentary component in the volcaniclastic rocks.

#### 9.3.1.6 Discussion

Whole-rock geochemical analyses are not sufficient to allow the discrimination between ortho- and para-amphibolites. Dusei-Bacon (1984) utilized REE patterns to estimate the protoliths of amphibolites in the Big Delta quadrangle, Alaska. These data were supplemented by other trace element data and the criterion established by Leake (1964) and by Shaw and Kudo (1965) to further constrain the estimates.

Leake (1964) states that large Cr contents (above 250 ppm) are uncommon for pelite-dolomite mixtures but are within the expected value for ortho-amphibolite. Similarly  $\text{TiO}_2$  for pelite-dolomite mixtures are expected to be less than 0.82 weight percent.

Shaw and Kudo (1965) determine that Sc and Co are the best trace elements to utilize in the discrimination between ortho- and para-amphibolites. Average Sc contents for ortho- and para-amphibolites are 30 and 5 ppm respectively. Average Co contents for ortho- and para-amphibolites are 37 and 14 ppm respectively. Chromium and cobalt analyses are reported in Table 6.4 and  $\text{TiO}_2$  is listed in Table 9.1. Using the above criteria, samples 3830, 3836, 3837, 3841, 3842, 3846, and 21155 are all classified as ortho-amphibolites. This classification is the same as that made on the basis of petrologic and field evidence.

Whole-rock and trace element geochemistry supports the hypothesis that bimodal volcanic and sedimentary exhalative rocks are the protoliths for various mappable rock

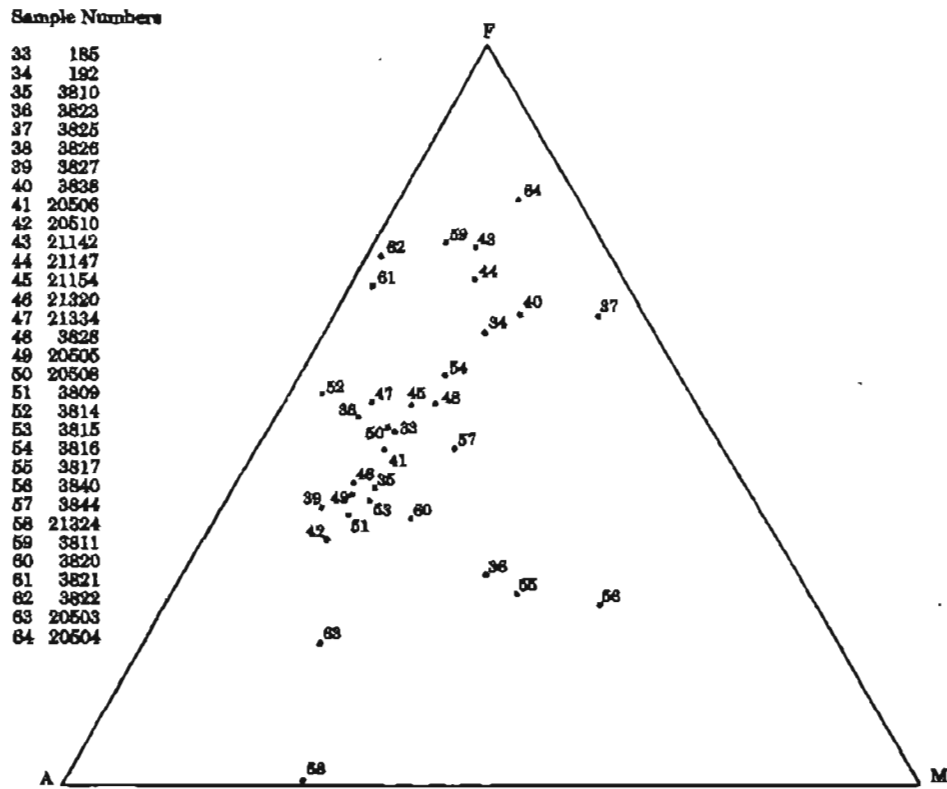


Figure 9.7 Plot of metasedimentary samples from the Fairbanks Schist and Cleary, Goldstream, and Birch Hill sequences on an AFM diagram (sample descriptions in Table 9.1a).

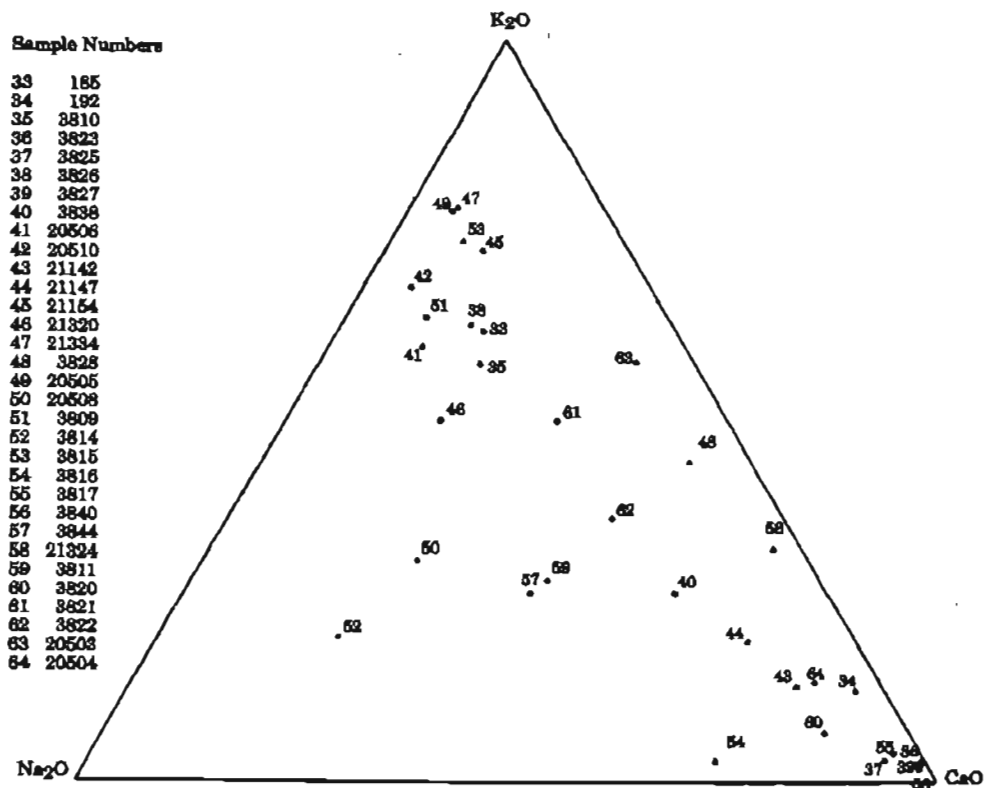


Figure 9.8 Plot of metasedimentary samples from the Fairbanks Schist and Cleary, Goldstream, and Birch Hill sequences on a Na-Ca-K diagram (sample descriptions in Table 9.1).

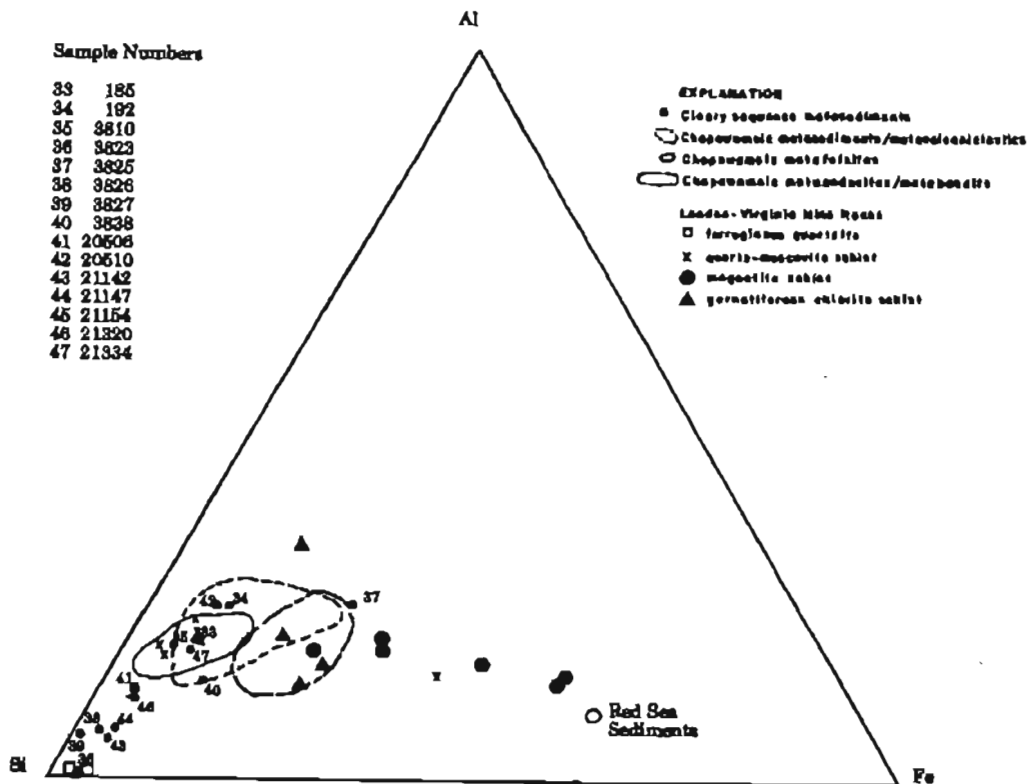


Figure 9.9a Plot of metasedimentary samples from the Cleary sequence, Chopawamsic rocks (Pavides, 1982) and London-Virginia Mine rocks (Mangan et al., 1984) on a Al-Si-Fe diagram.

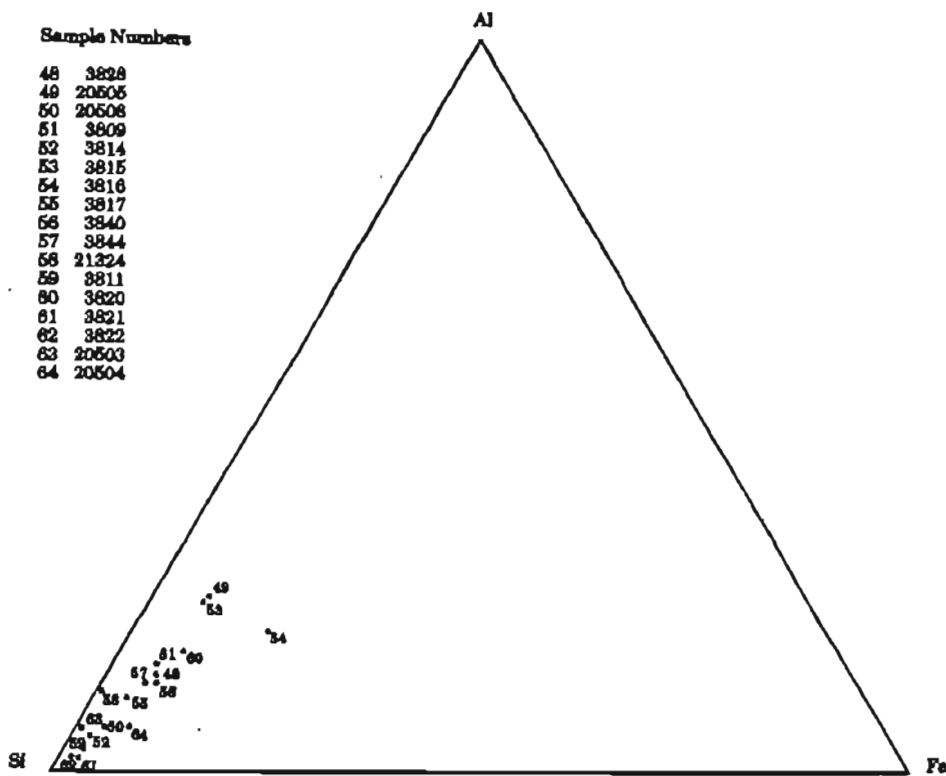


Figure 9.9b Plot of metasedimentary samples from the Fairbanks Schist and Goldstream and Birch Hill Sequence on a Al-Si-Fe diagram.

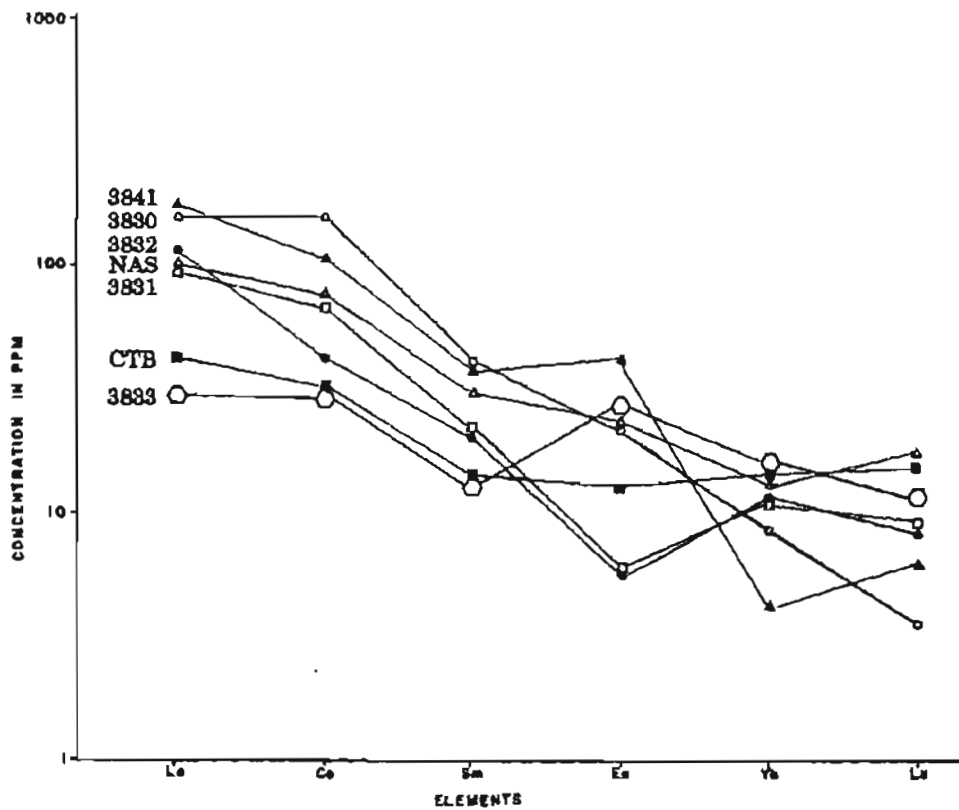


Figure 9.10a Chondrite-normalized rare earth element patterns for samples of metamorphic rocks from the Chatanika Terrane and for an average of North American shales (NAS) and for an average of continental tholeiitic basalts (CTB).

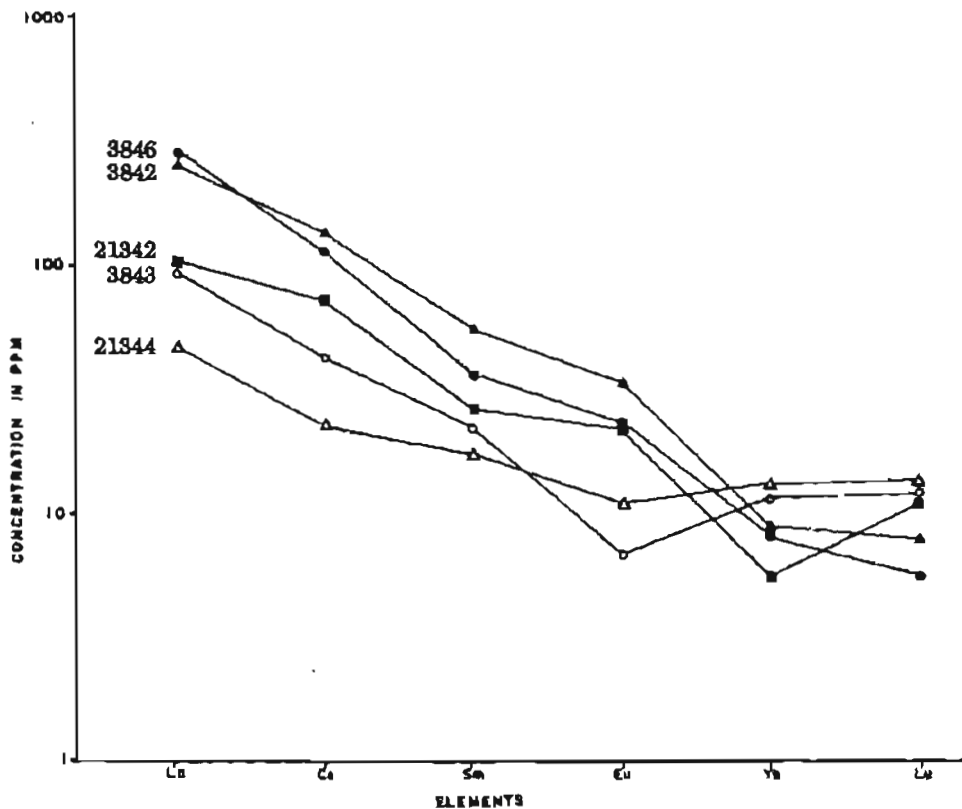


Figure 9.10b Chondrite-normalized rare earth element patterns for samples of metamorphic rocks from the Chatanika Terrane.

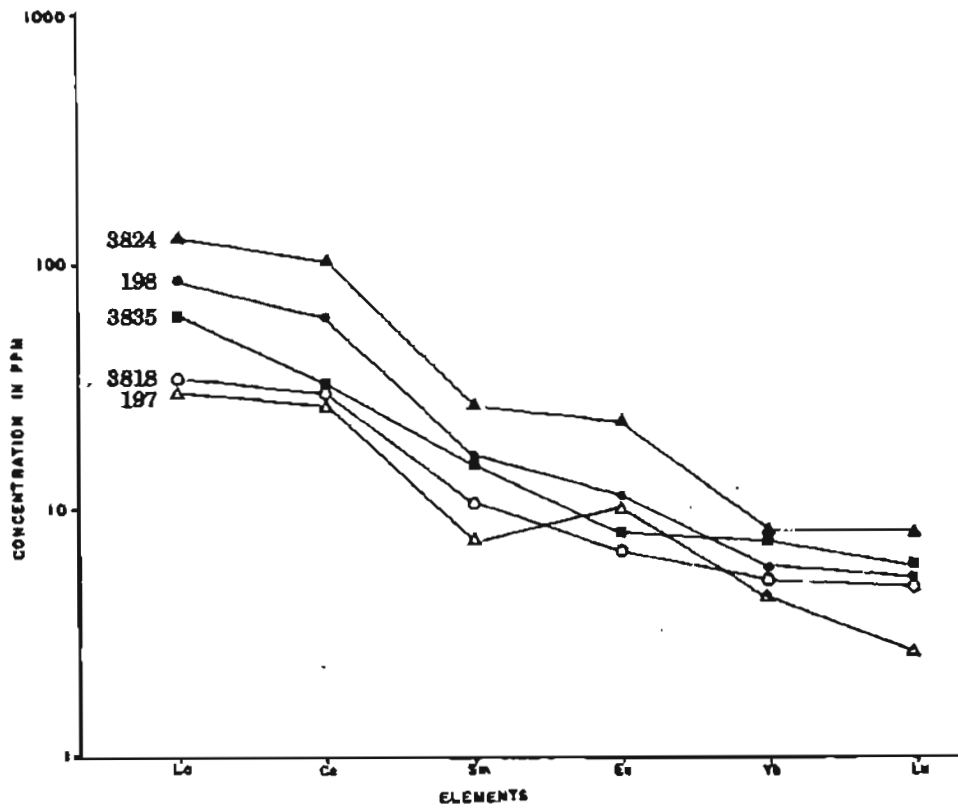


Figure 9.10c Chondrite-normalized rare earth element patterns for samples of metavolcanic rocks from the Cleary sequence.

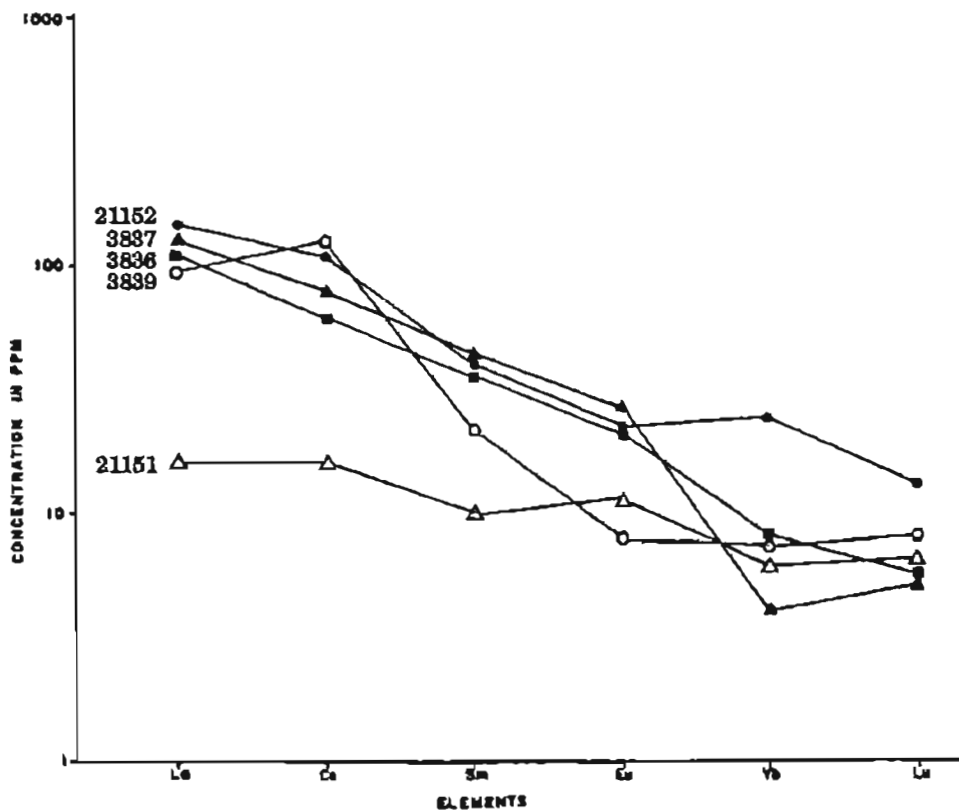


Figure 9.10d Chondrite-normalized rare earth element patterns for samples of metavolcanic rocks from the Cleary sequence.

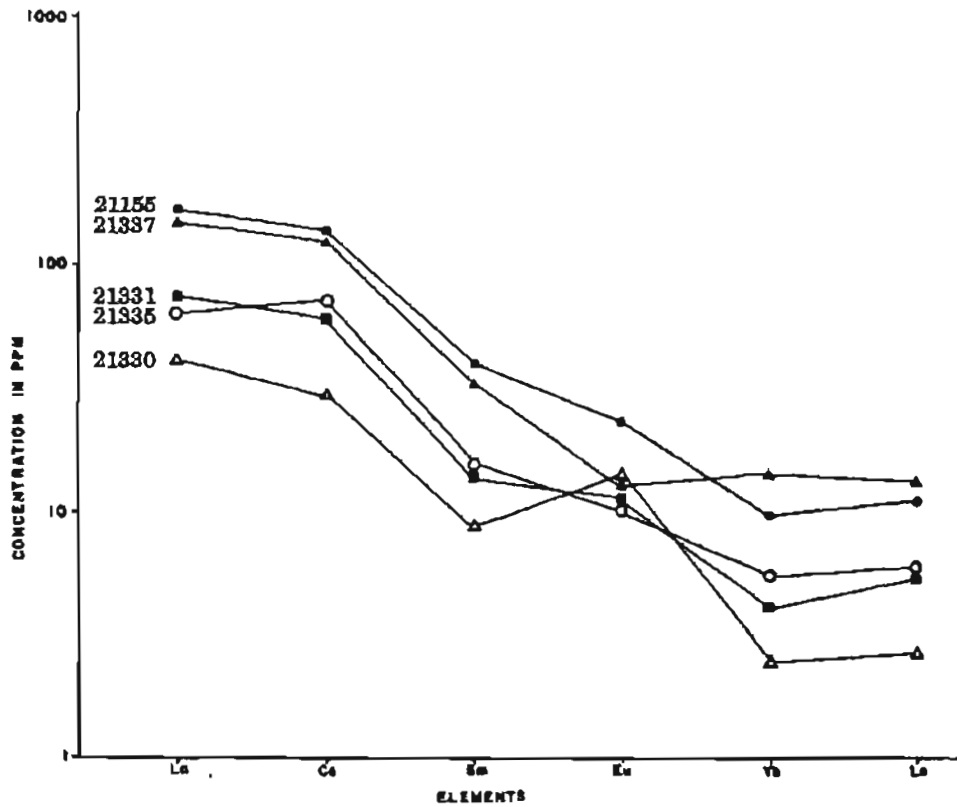


Figure 9.10e Chondrite-normalized rare earth element patterns for samples of metavolcanic rocks from the Cleary sequence.

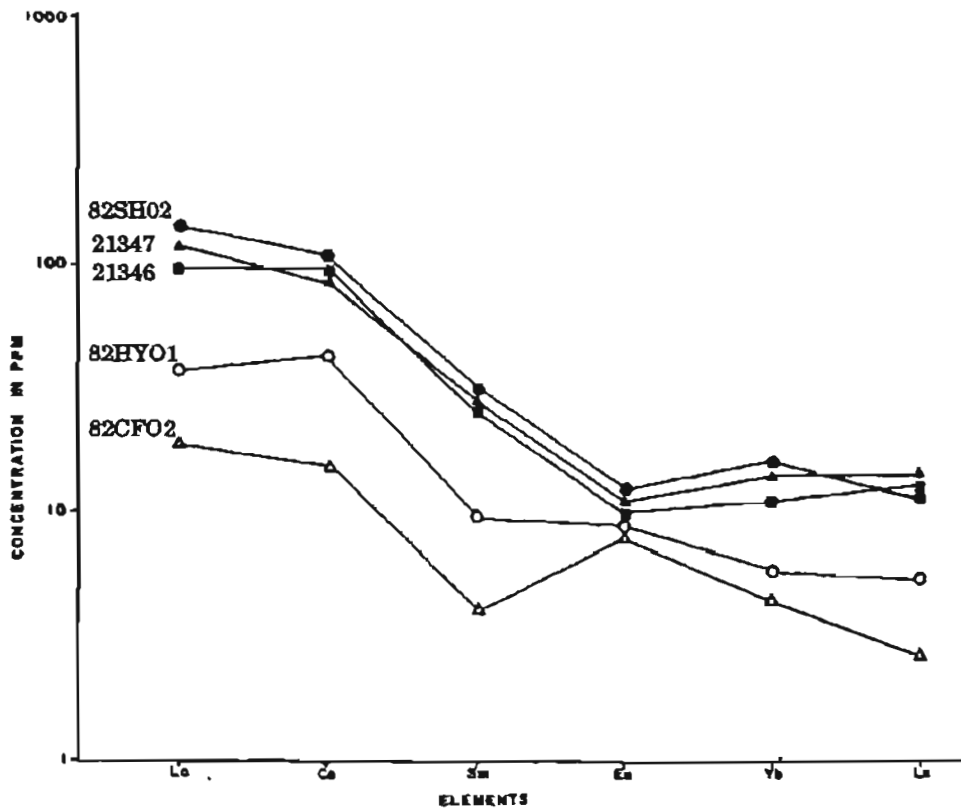


Figure 9.10f Chondrite-normalized rare earth element patterns for samples of metavolcanic rocks from the Cleary sequence.

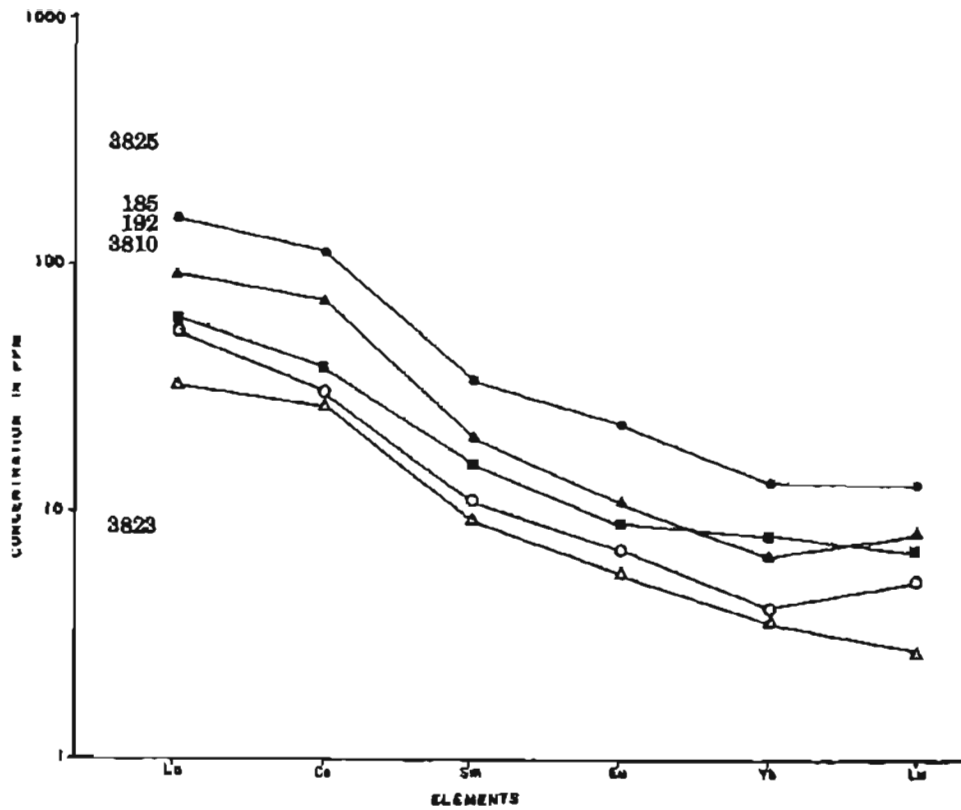


Figure 9.10g Chondrite-normalized rare earth element patterns for samples of metasedimentary rocks from the Cleary sequence.

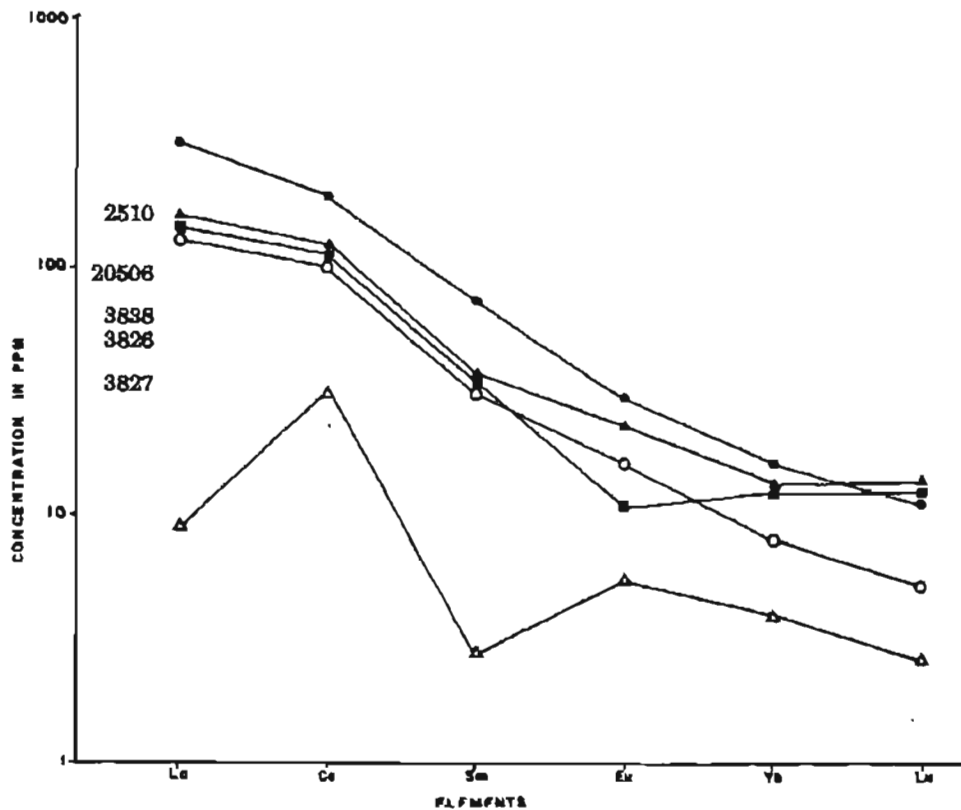


Figure 9.10h Chondrite-normalized rare earth element patterns for samples of metasedimentary rocks from the Cleary sequence.

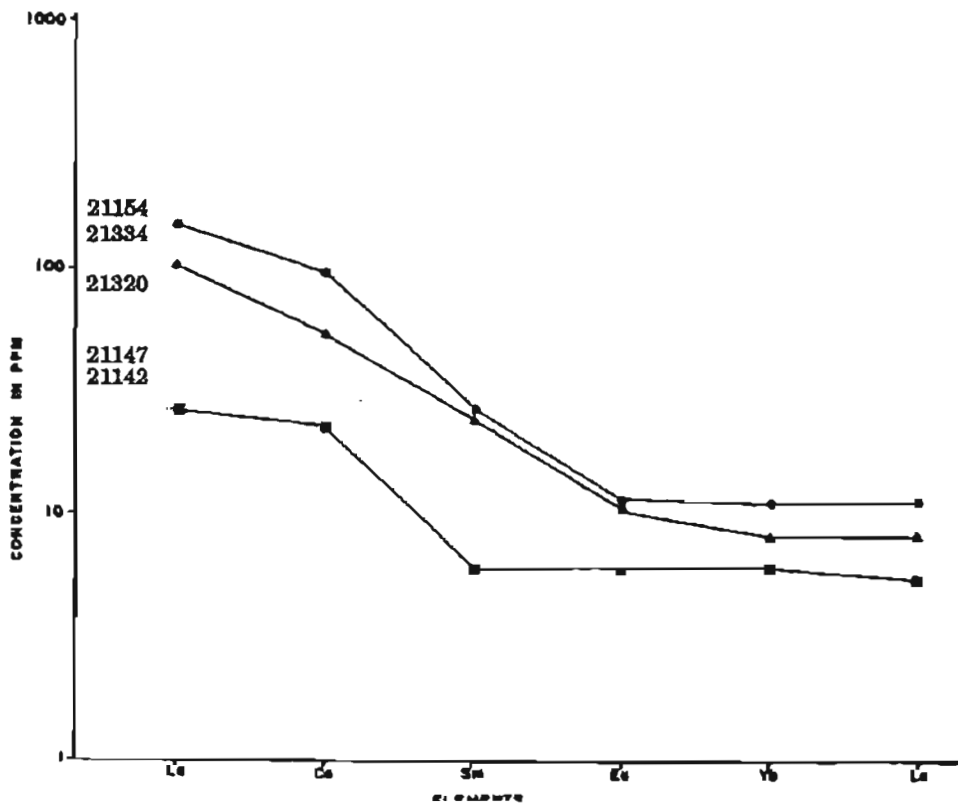


Figure 9.10i Chondrite-normalized rare earth element patterns for samples of metasedimentary rocks from the Cleary sequence.

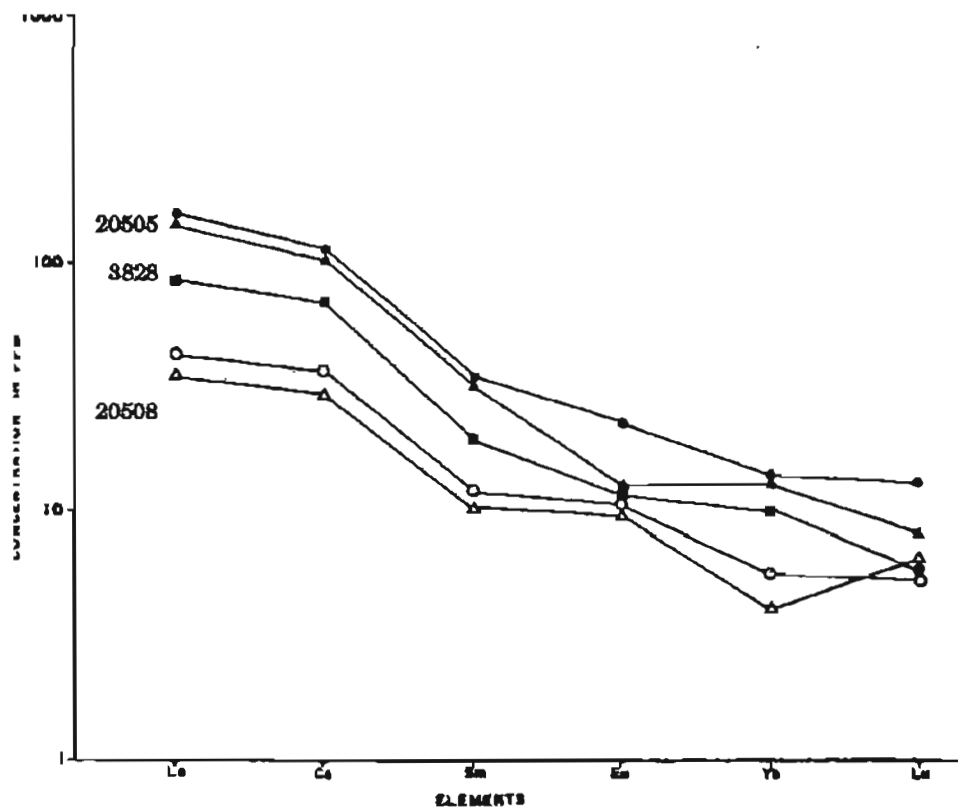


Figure 9.10j Chondrite-normalized rare earth element patterns for samples of metamorphic rocks from the Fairbanks Schist.

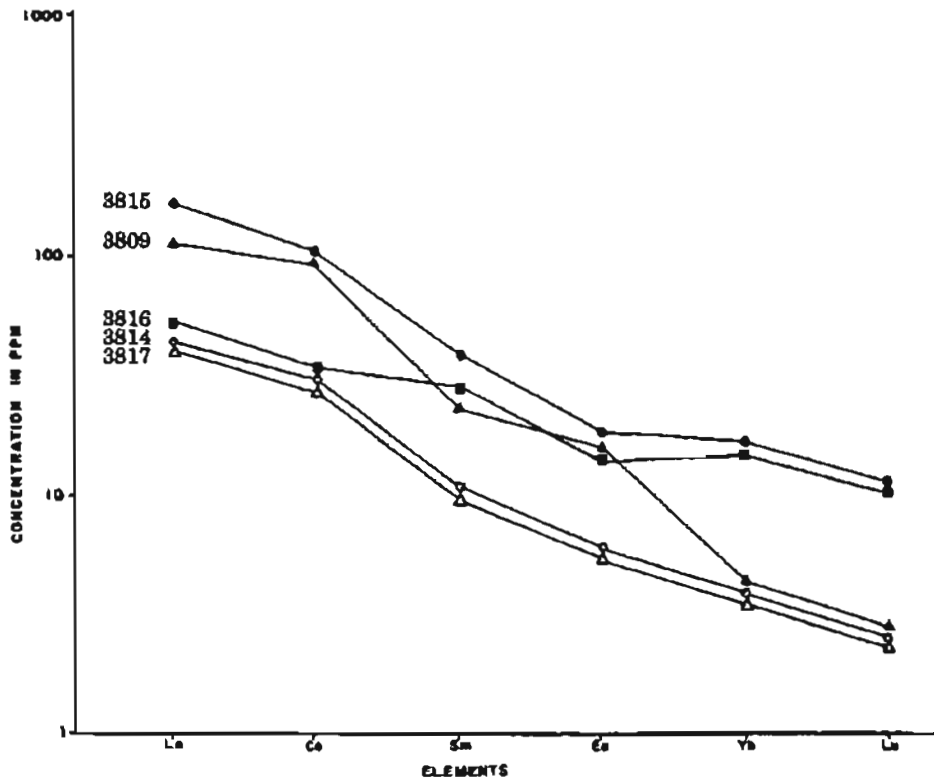


Figure 9.10k Chondrite-normalized rare earth element patterns for samples of metamorphic rocks from the Goldstream sequence.

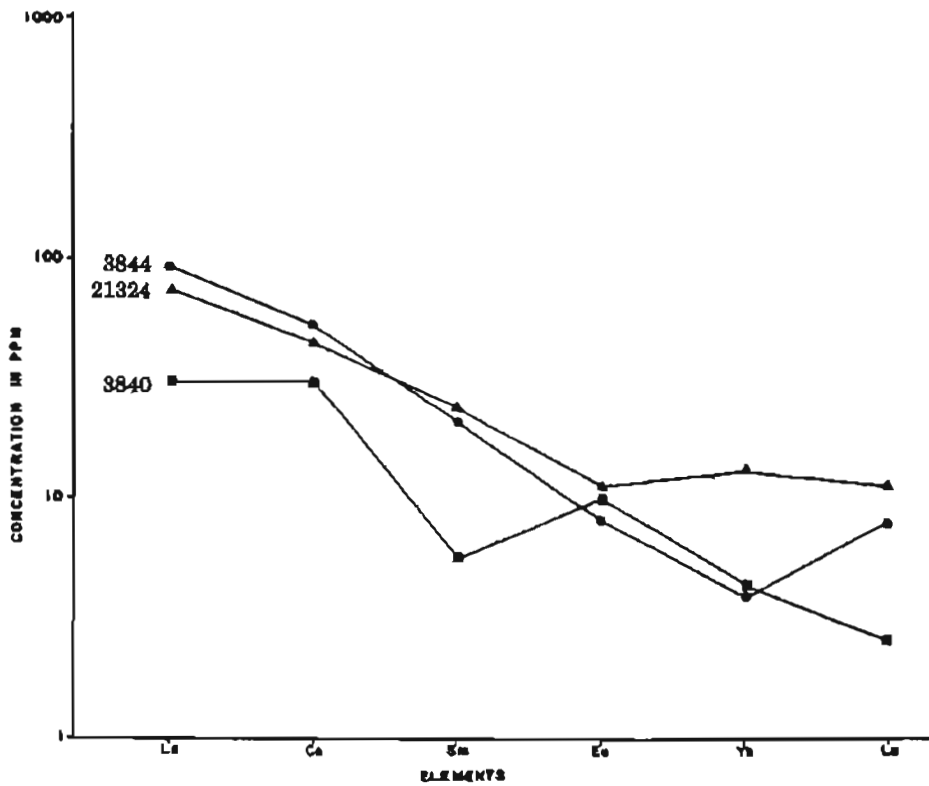


Figure 9.10l Chondrite-normalized rare earth element patterns for samples of metamorphic rocks from the Goldstream sequence.

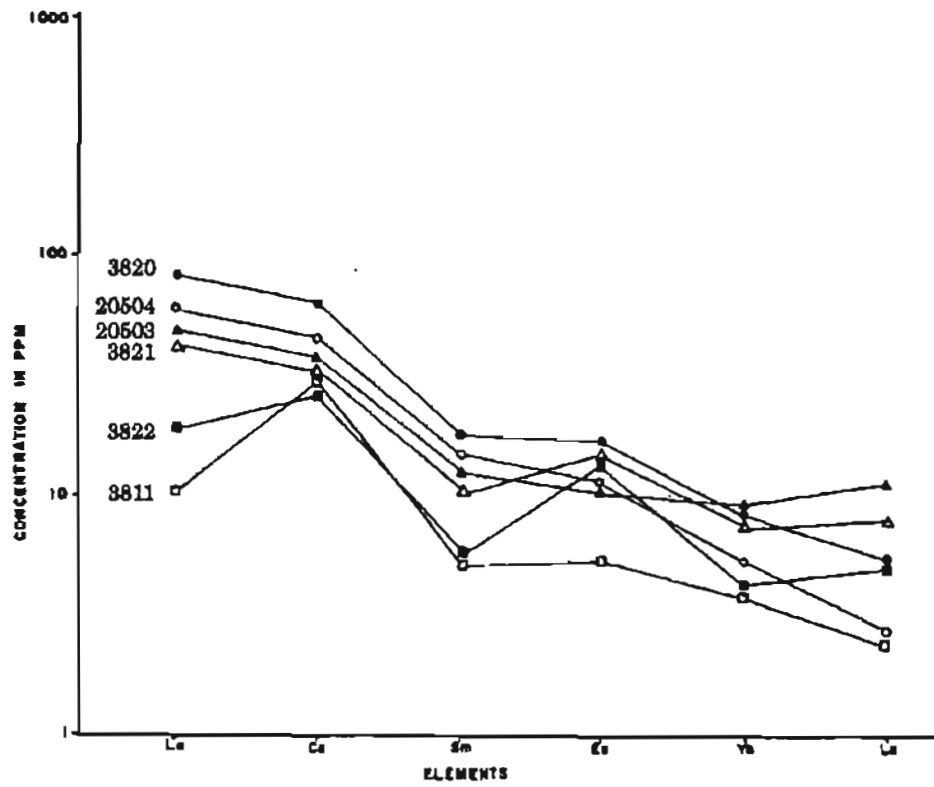


Figure 9.10m Chondrite-normalized rare earth element patterns for samples of metamorphic rocks from the Birch Hill sequence.

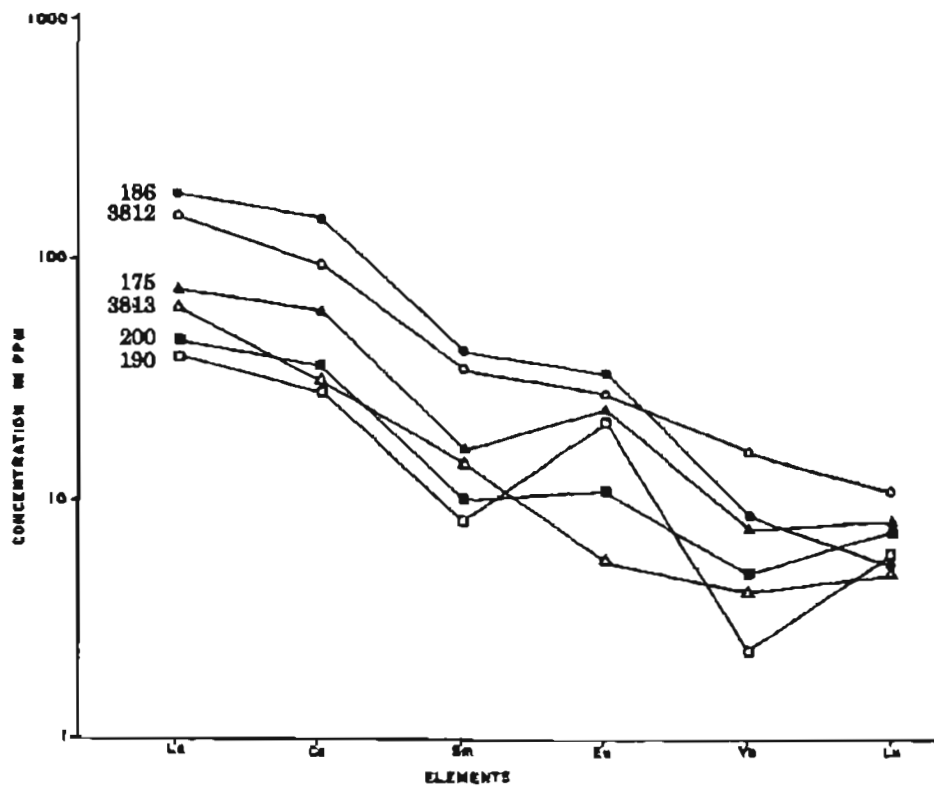


Figure 9.10n Chondrite-normalized rare earth element patterns for samples of metasomatic skarns.

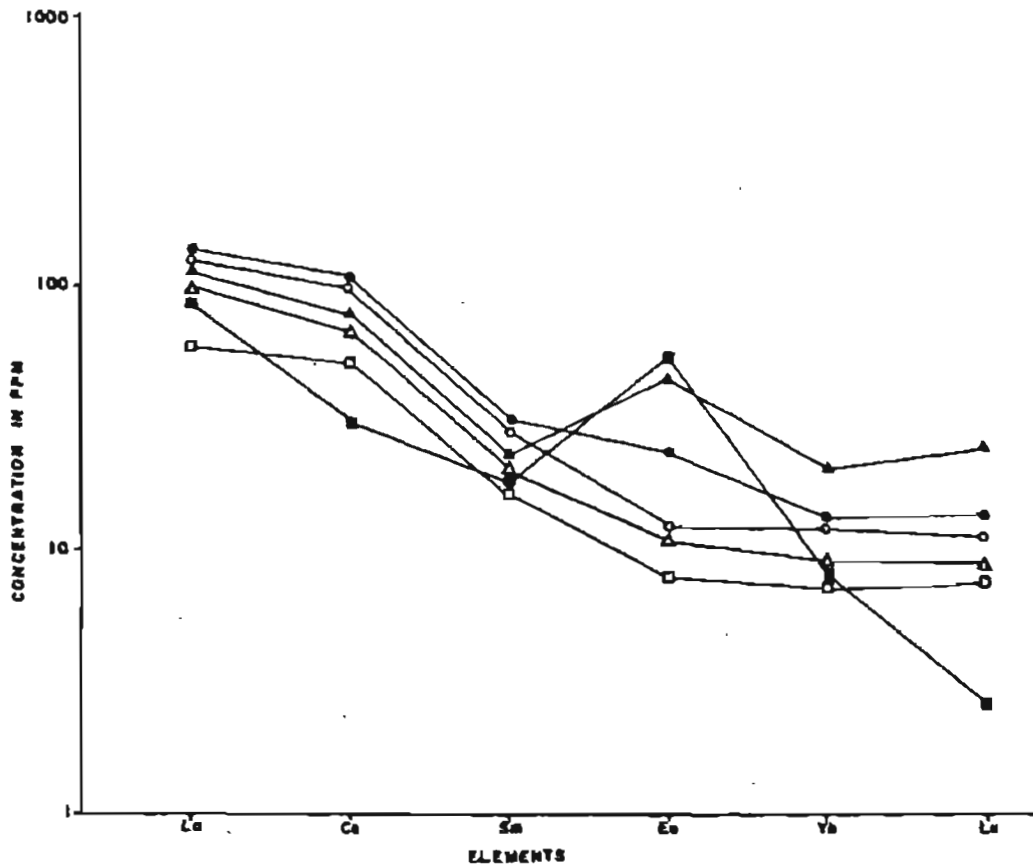


Figure 9.100 Chondrite-normalized rare earth element patterns for samples of metasomatic skarns.

units in the Chatanika terrane and Cleary sequence. The associated precious metal and base metal sulphide mineralization is considered to be the product of the same volcanic/exhalative processes.

Archaean, Proterozoic, and Phanerozoic stratabound gold mineralization associated with bimodal volcanics and exhalites are well documented in the literature. Selected references include: Abrams and McConnell (1984), Bell (1982), Bernasconi (1985), Bernier (1987), Boyle (1979), Fehlberg and Giles (1982), Feiss (1982), Foster (1982), Foster et al. (1986), Fripp (1976), Gallagher et al. (1981), Ghisler et al. (1980), Ghosh et al. (1970), Godwin (1973, 1977, 1982), Hannington et al. (1986), Kerrich (1980), Kerrich et al. (1979, 1981), Pavlides et al. (1982), Potgieter and DeVilliers (1986), Rye and Rye (1974), Saager et al. (1987), Spence and de Rosen-Spence (1975), and Spence et al. (1978).

Mangan et al. (1984) describe a bimodal volcanic suite associated with the submarine exhalative gold mineralization at the London-Virginia Mine, Buckingham County, Virginia. The deposit is hosted in the Cambrian Chopawamsic Formation that crops out over a strike length of 175 kilometers (105 miles). The formation has an estimated thickness of 1,800 to 3,000 meters (5,850 to 9,750 feet), however, at the mine site only 140 meters (450 feet) of section is described.

From the oldest to the youngest, the major rock units are: (1) graniferous chlorite schist, (2) magnetite schist, (3) quartz-muscovite schist, (4) ferruginous quartzite, and (5) chlorite biotite schist. The rocks show evidence of polydeformation and contain upper greenschist to lower amphibolite facies mineral assemblages. The gold mineralization is associated with lenses and disseminations of pyrite, sphalerite, argenteriferous tetrahedrite-tennantite, galena, and chalcopyrite.

Mangan et al. (1984) proposed a rift-generated sedimentary basin model for the origin of the precious metal enriched sulphide deposits of the Central Virginia Volcanic-Plutonic Belt. The Red Sea basin and its contained mineralization is a modern day analogue. The belt is part of the Southern Appalachian Metallogenic Province that has produced at least 2.5 million ounces of gold. The host lithologies and mineralization are similar to the precious metal enriched sulphide mineralization of the Fairbanks district and adjacent areas.

### 9.3.2 Granitic Rock Types

Blum (1983) provides major oxide analyses for the granitic rocks of the Fairbanks mining district as well as modal and normative mineralogies. Burns and Newberry (1987) discuss the whole-rock, REE, and trace element chemistry of the granitic rocks of the Steese mining district

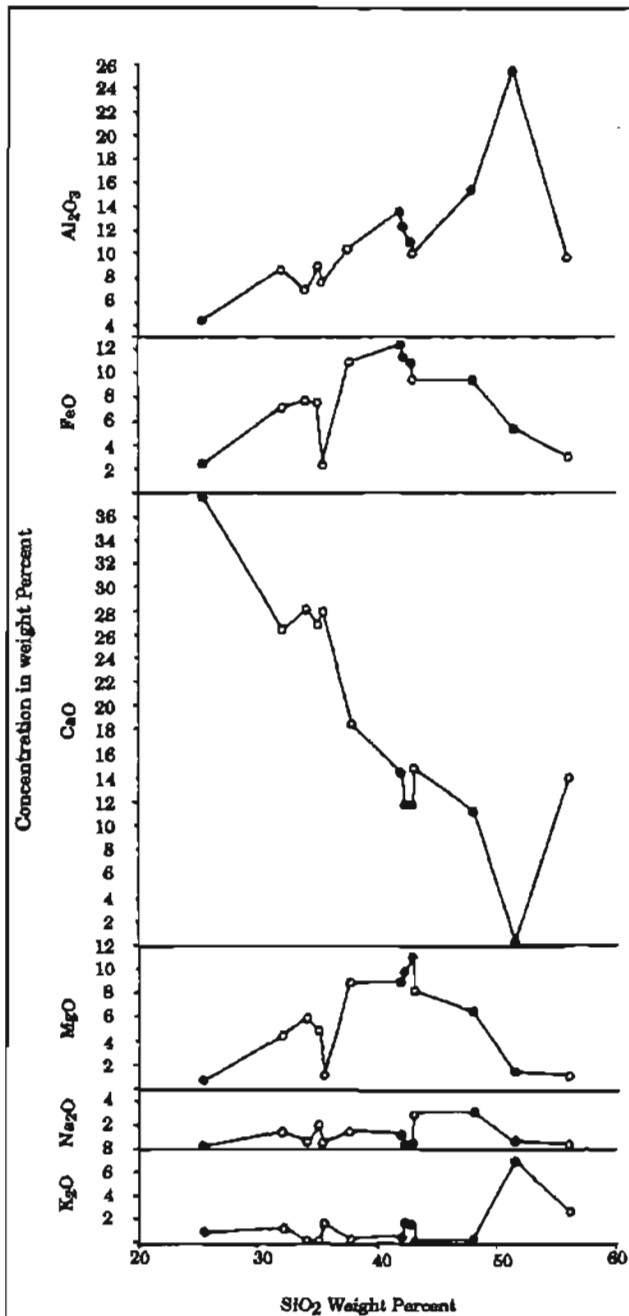


Figure 9.11a Samples of mafic metaigneous rocks from the Chatanika terrane (closed circles) and Cleary sequence (open circles) on a Harker variation diagram.

and relate the intrusive hosted mineralization to particular phases of the plutons. Wilkinson (1987) reports whole-rock and limited trace element geochemical data for the Circle Intrusive Complex. The data from Blum (1983) are included in Tables 9.1a and 9.1b. The data from Wilkinson (1987) are included in Tables 9.2a and 9.2b. Whole-rock analyses for samples from the Richardson mining district are listed in Table 9.3a, and normative mineralogies are reported in Table 9.3b.

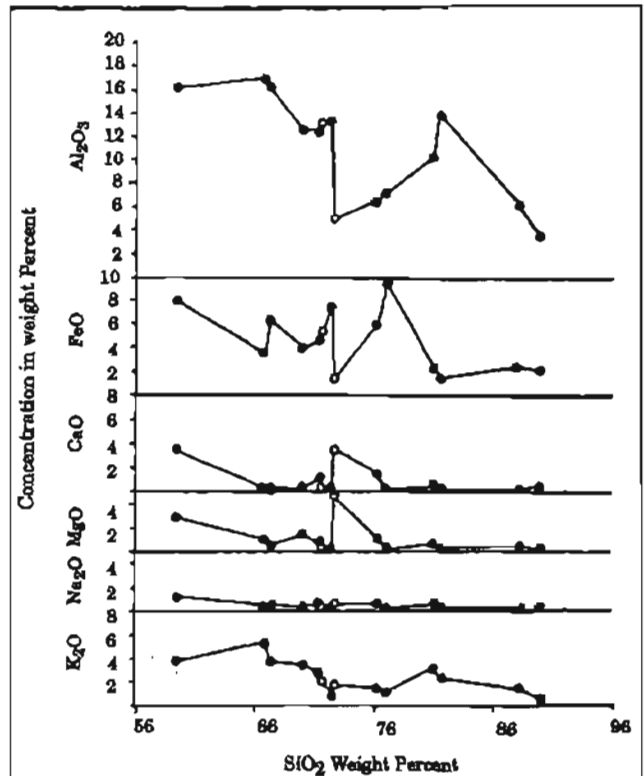


Figure 9.11b Samples of felsic metaigneous rocks from the Chatanika terrane (closed circles) and Cleary sequence (open circles) on a Harker variation diagram.

### 9.3.2.1 Fairbanks Mining District

A plot of the whole-rock analyses of the intrusive rocks of Gilmore Dome and Pedro Dome on an AFM diagram indicates a unimodal suite (see Figure 9.12). The suite is derived from a moderately fractionated magma. Using the criterion of Petro et al. (1979), the AFM diagram is partial evidence that the calc-alkaline suite was generated at a compressional plate boundary.

A plot of the whole-rock analyses on a Ca-Na-K diagram also depicts the fractionation trend of the suite (see Figure 9.13). The least fractionated rocks are the fine-grained granodiorites, while the most fractionated are the aplite dikes.

Figure 9.14 is a Harker variation diagram for the intrusive suite. The diagram displays the wide range in silica content of the suite (59 to 78 weight percent). The large silica content relative to CaO of three of the aplite dikes results in the dikes falling below the linear trend of the diagram. These highly fractionated rocks also show indications of at least two types of hydrothermal alteration. Silicification is manifested by secondary quartz in microfractures. Potassic alteration is evidenced by secondary biotite and white-mica. Chloritization may be present.

The intrusive suite is additionally characterized by normative plagioclase, generally normative corundum, and calc/alkaline indices in the range of 60-64. These data further

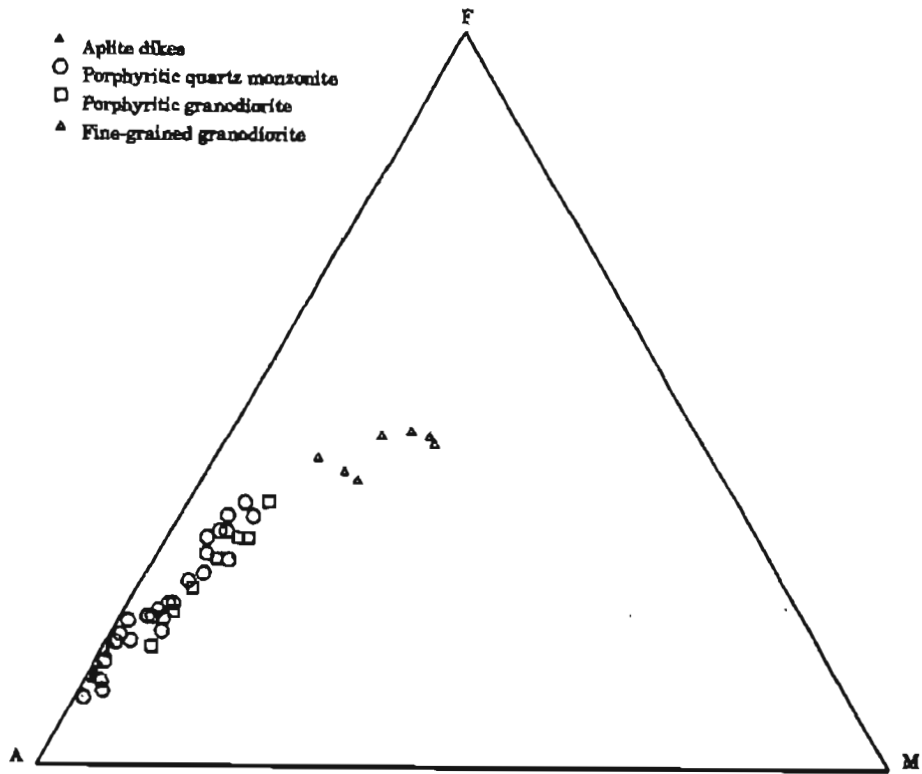


Figure 9.12 Plot of samples of igneous rocks from the Fairbanks mining district on a AFM diagram (after Blum, 1983).

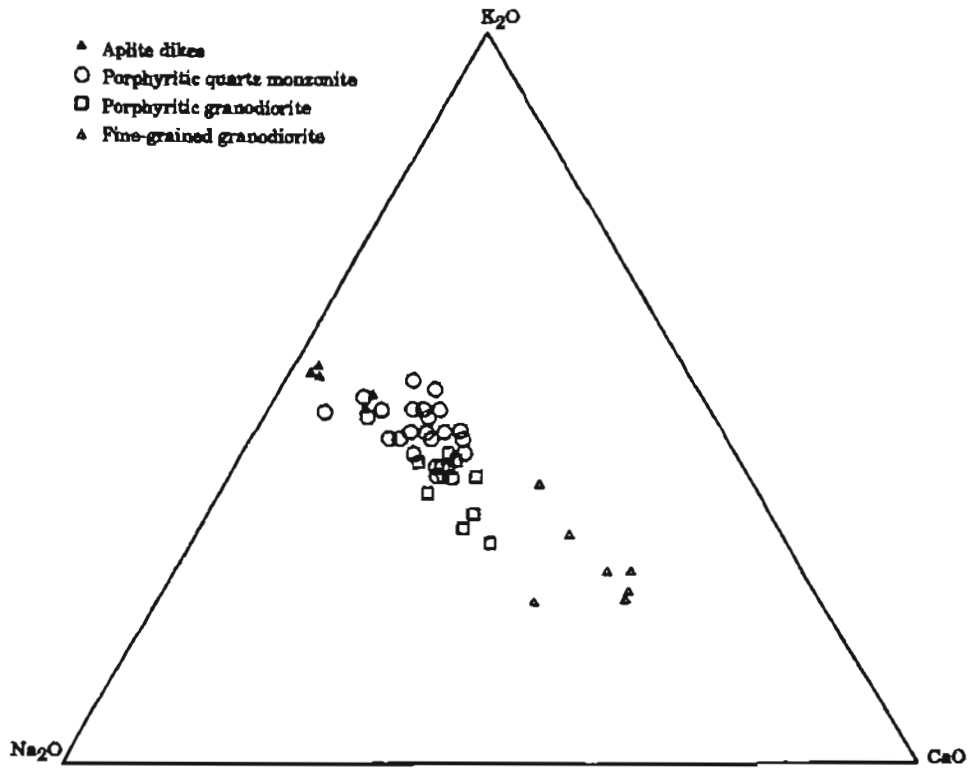


Figure 9.13 Plot of samples of igneous rocks from the Fairbanks mining district on a Na-Ca-K diagram (after Blum, 1983).

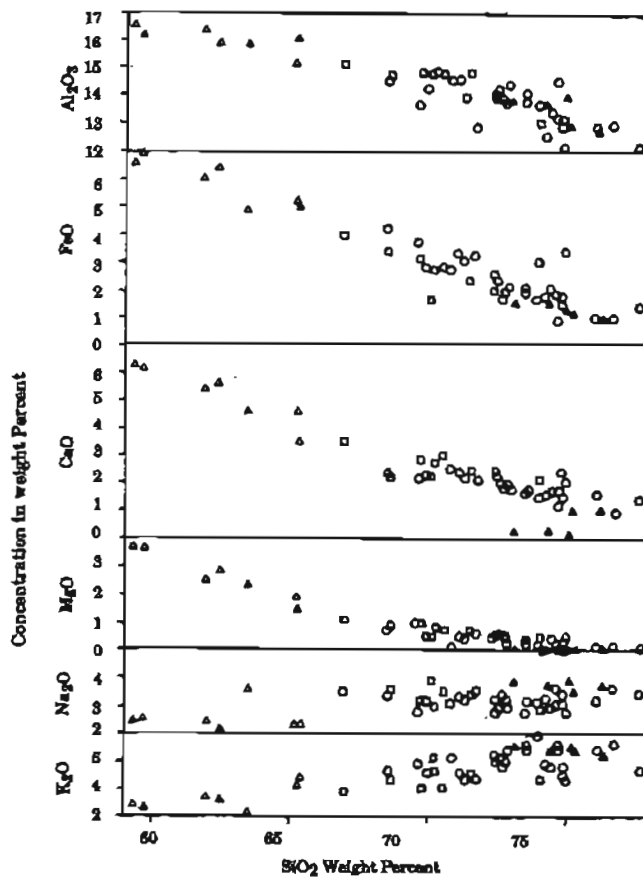


Figure 9.14 Major oxide data for samples of igneous rocks from the Fairbanks mining district plotted on a Harker variation diagram (after Blum, 1983).

support a compressional plate boundary origin for the intrusives.

The gold mineralization at the Fort Knox property is hosted in altered porphyritic granodiorite. The host to the mineralization is not the least fractionated rock type of the suite. This is contrary to what is predicted by the discriminant analysis model of Solie et al. (1990).

### 9.3.2.2 Circle Mining District

A plot of the whole-rock analyses of the Circle Intrusive Complex on an AFM diagram indicates a unimodal suite (see Figure 9.15) that is slightly less fractionated than the suite of igneous rocks of the Fairbanks district. The Circle Intrusive Complex ranges in composition from granodiorite to syenogranite. Wilkinson (1987) subdivided the complex into two plutonic suites, the Two-Bit pluton and the Circle Hot Springs pluton. This subdivision is based on field mapping, textural classification, and K-Ar age dating. Major oxide geochemistry alone cannot be used as the basis for such a subdivision.

The Ca-Na-K diagram (see Figure 9.16) and the Harker variation diagram (see Figure 9.17a) also depict the fractionation trend of the suite. The range in silica content of the suite

(64 to 76 weight percent) is considerably smaller than that for the igneous rocks of the Fairbanks district. The trends on the Harker variation diagram are rather linear and there does not appear to be a significant increase in the sodium or potassium content of the more silica rich rocks. By the criteria of Petro et al. (1979), the intrusive complex is inferred to have been generated at a compressive plate boundary.

Visible gold occurs in silicified and sericitically altered granodiorite of the Two-Bit pluton. The host to the mineralization is the least fractionated phase of the Circle Intrusive Complex. This is in conformance with what is predicted by the application of the discriminant analysis of Solie et al. (1990).

### 9.3.2.3 Richardson Mining District

A plot of the whole-rock analyses of the Birch Lake pluton on an AFM diagram indicates a unimodal suite. The suite is the most fractionated of the three igneous suites under consideration. The Birch Lake pluton ranges in composition from a pyroxene diorite to a quartz-orthoclase porphyry.

The Ca-Na-K diagram (see Figure 9.16) and the Harker variation diagram (see Figure 9.17b) also depict a parent magma that is greatly fractionated. The range in silica content from 58 to 78 weight percent is the largest of the three plutonic suites. The trends on the Harker diagram are linear, however the data base is small. As in the cases of the igneous rocks of the Fairbanks and Circle districts, the Birch Lake pluton manifests the criteria of Petro et al. (1990) for magma generation at a compressional boundary.

Visible gold mineralization at the Democrat Lode (sample location 84 BL 04) is associated with a 50 percent increase in the potassium content and a similar decrease in the sodium content of the quartz-orthoclase porphyry. The mineralization is associated with silicification and sericitization of the intrusive. The mineralization is hosted the most fractionated phase of the plutonic suite.

### 9.3.2.4 Major Oxide and Trace Element Variation

The bulk chemical composition of the granitic rocks of the three mining districts varies from the centre to the margin of the YTT. In the Richardson district, which is most distant from the margin of the terrane, the plutonic suite has the largest range in bulk composition (pyroxene diorite to granite). These end member rocks account for a significant volume of the Birch Lake pluton. Eighty kilometers (fifty miles) to the northwest of the Richardson district, the granitic rocks of the Fairbanks district exhibit a narrower range in bulk composition (granodiorite to granite). Volumetrically, granodiorite and quartz monzonite are the most significant variants in the Pedro Dome and Gilmore Dome plutons respectively. At the northwest margin of the YTT, the Circle Intrusive Complex displays the narrowest range in bulk composition (granodiorite to syenogranite). Syenogranite and monzogranite account for 90 percent of the exposed complex.

There has been no systematic sampling of the granitic rocks of the three districts for trace element geochemistry. Differences in the trace element content of the three plutonic

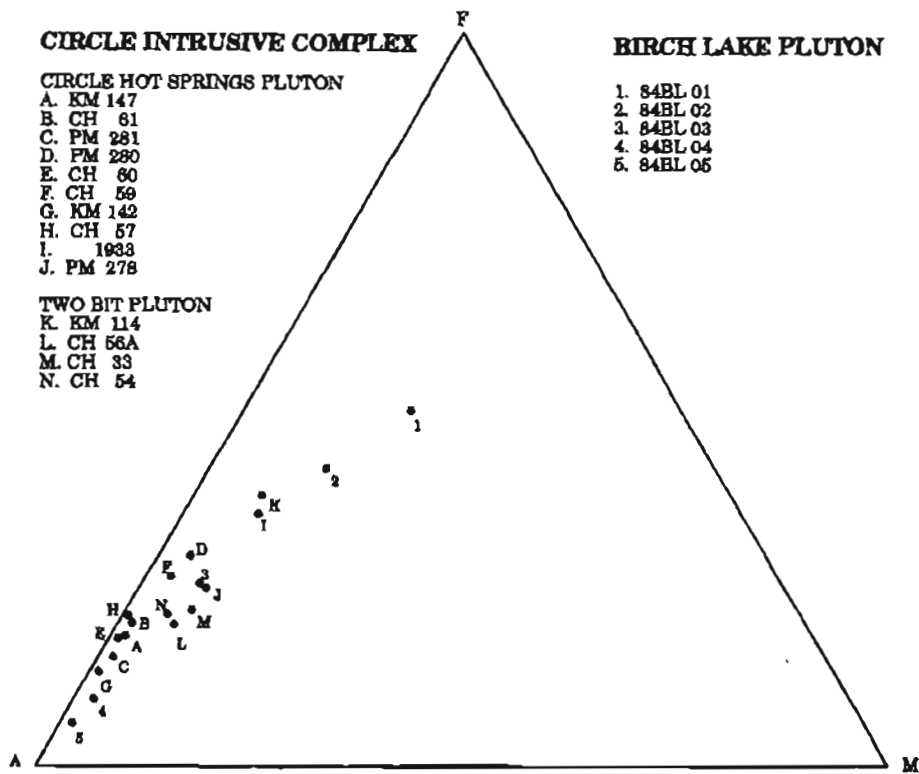


Figure 9.15 Plot of samples from the Circle Intrusive Complex and Birch Lake Pluton on an AFM diagram.

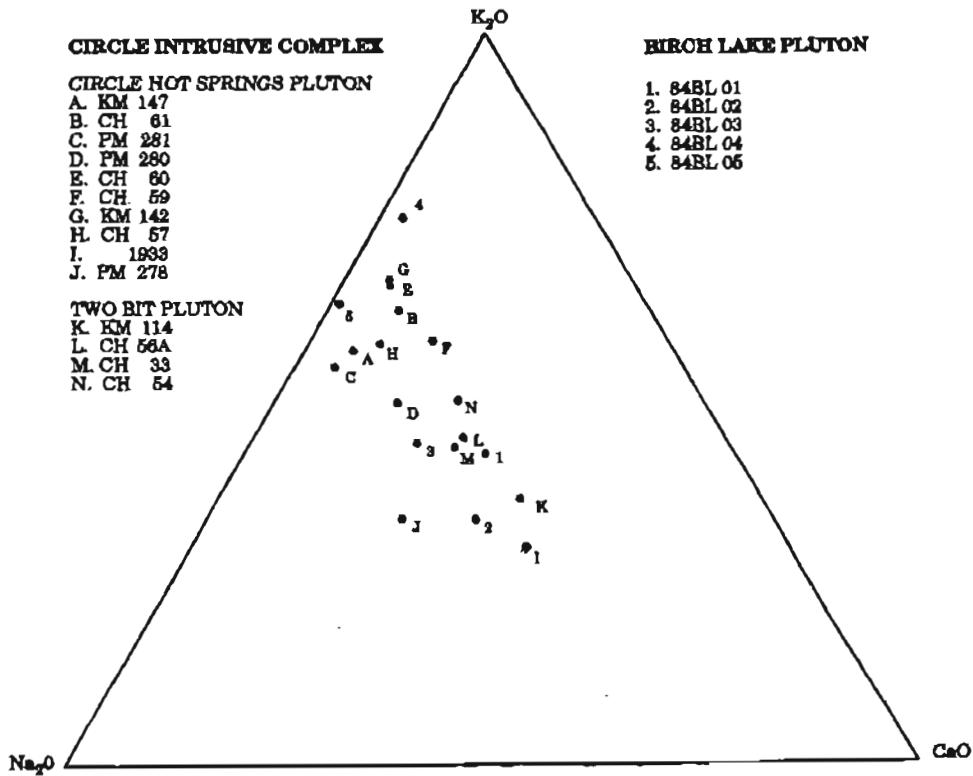


Figure 9.16 Plot of samples from the Circle Intrusive Complex and Birch Lake Pluton on a Na-Ca-K diagram.

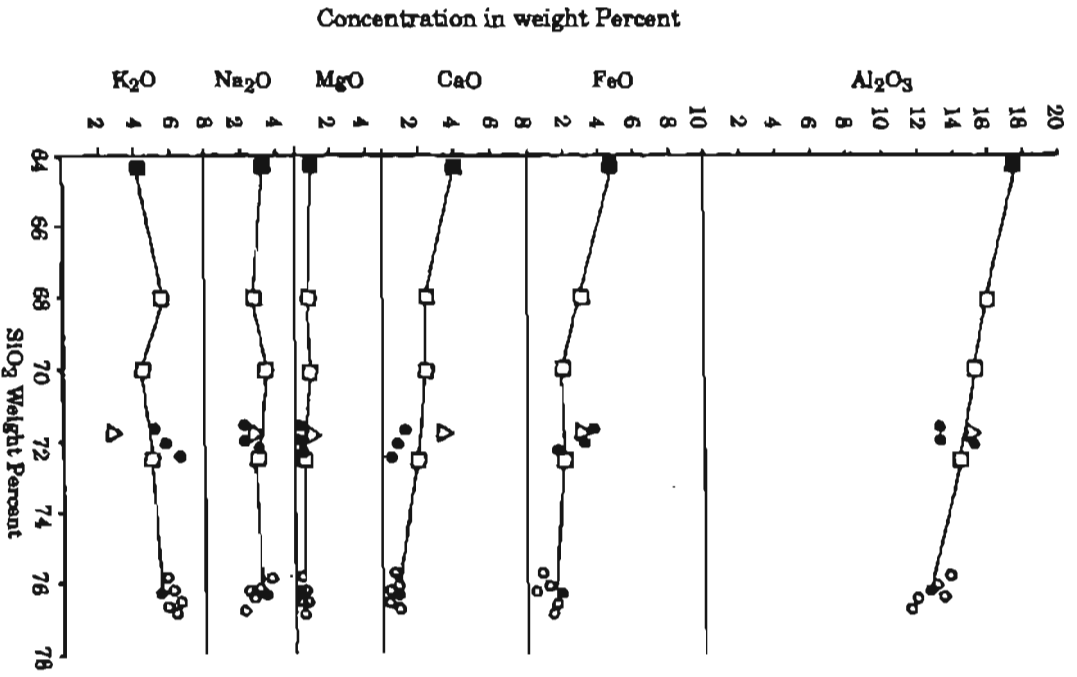


Figure 9.17a. Major oxide data for samples of igneous rocks from the Circle mining district plotted on a Harker variation diagram (open squares, Two-bit granodiorite; shaded squares, Two-bit monzogranite; open circles, CHS syenogranite; closed circles, CHS monzogranite; triangles CHS granodiorite).

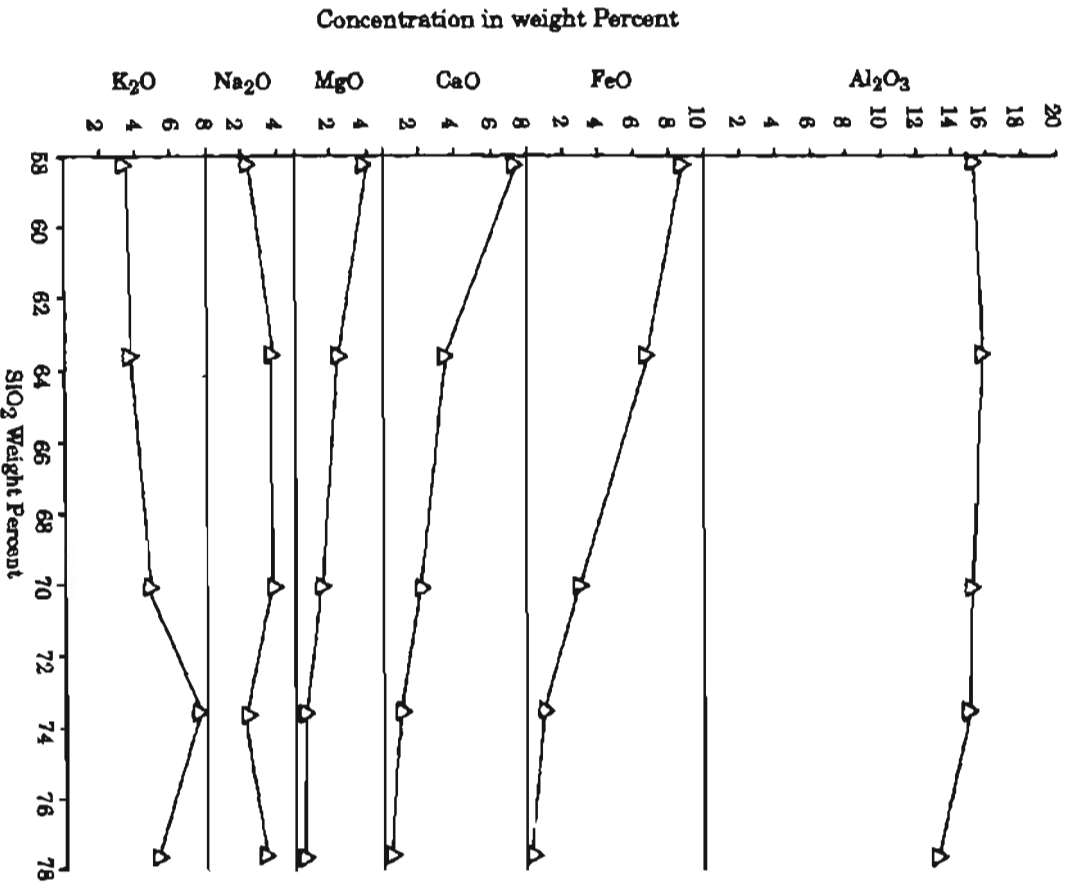


Figure 9.17b. Major oxide data for samples of igneous rocks from the Richardson mining district plotted on a Harker variation diagram (1=84BL01 ccl.)

suites have been noted in a qualitative way from the relative abundances of heavy minerals in the alluvial deposits adjacent to the plutons and in the lode deposits in the intrusives.

#### 9.3.2.5 Discussion

Gold, tin, and tungsten have been the most noted heavy metals in the three mining districts. Estimates have been made of the mineral potential of the granitic suites based on the adjacent lode and placer deposits. Such estimates have been subject to critical review since the inference has been made, based on limited data, that the plutons were the source of the heavy metals.

Of the three heavy metals, tin appears to occur uniquely in the granitic rocks. The tin-greisens are noted in the Circle Intrusive Complex, and numerous locations are described in the Hope granitic suite of the adjacent Steese mining district. Tin-greisens are not well documented in either the Fairbanks or Richardson districts although cassiterite is noted in minor amounts in the alluvial gold deposits in these districts. In contrast, commercial quantities of alluvial tin are noted in the production records from the Circle district.

Tungsten is present as scheelite in skarn occurrences adjacent to the Gilmore Dome pluton but scheelite is also ubiquitous in the alluvial gold deposits of the Fairbanks district. Many of these deposits are in streams that do not drain areas of intrusive rocks. Scheelite and wolframite are present in the alluvial gold deposits of the Circle and Richardson districts and, as in the Fairbanks district, a large number of the alluvial deposits are not in drainages that contain outcrops of intrusive rocks.

As noted previously, gold mineralization occurs in all three plutonic suites. Within the three districts, the intrusive related gold occurrence with largest reserves reported to date is Fort Knox in the Fairbanks district. The contribution of intrusive related lode mineralization to the placer deposits of the district is probably limited. This estimate is based on the limited number of placer-bearing streams that drain areas of intrusive rocks and from the limited quantity of granitic material in the alluvial deposits in streams that do drain granitic outcrop areas. Although intrusive related gold occurrences do not account for any of the past lode gold production in the Fairbanks district, the Fort Knox property contains significant quantities of gold. Whether the Gilmore Dome pluton is the source of the gold at the Fort Knox property, or whether the pluton simply acts as a thermal centre to remobilize gold from the Cleary sequence remains problematical without more detailed trace element and isotopic investigations. It must be noted that the only intrusive related gold occurrence in that area of the district is in a small

satellite stock of the Gilmore Dome pluton. This stock intrudes the Cleary sequence, while the main body of the pluton intrudes the Fairbanks schist which is relatively deficient in gold.

Barium, rubidium, and strontium analyses are conducted in conjunction with the major oxide analyses. The data are summarized in Figure 9.18. The figure includes ratios of whole-rock Ba/Rb, K/Rb, and Rb/Sr for average granites, tin-bearing granites and barren granites (after Govet, 1983) as well as similar data for the Hope granite suite of the Steese mining district (after Burns and Newberry, 1987). These data indicate that the Hope granitic suite has strong affinities to tin-bearing granites while the Circle Intrusive Complex has moderate affinities, and the granitic rocks of the Fairbanks and Richardson districts have weak affinities. Inferences concerning other elements cannot be made from the data.

#### 9.4 CONCLUSIONS

The discrimination between ortho and para-amphibolites in the various metamorphic sequences is made on the basis of whole-rock and trace element geochemistry. Whole-rock geochemistry also provides strong evidence for a felsic volcanic origin for the K-feldspar and muscovite schists that are intercalated with the ortho-amphibolites. Finely laminated rocks composed of silica and minor amounts of alumina and potassium are inferred to have an exhalative origin. This bimodal volcanic suite is enriched in As, Sb, Au, Ag, and W relative to the metasedimentary rocks. The metavolcanic host rocks and the gold mineralization are analogous with volcanic-exhalative gold mineralization that occurs in Archean, Proterozoic, and Phanerozoic metamorphic belts. The bimodal volcanic rocks and contained gold deposits of lower Paleozoic age of the Georgia-Carolina-Virginia metallogenic province of southeastern USA are good Phanerozoic analogues to the gold deposits of the Kantishna-Fairbanks-Circle belt. The host rocks and contained mineralization in both metallogenic provinces are inferred to have developed in a tensional tectonic environment such as the Red Sea graben.

The whole-rock geochemistry of the intrusive rocks of the Fairbanks district and adjacent areas indicates that the granitic rocks are derived from moderately to highly fractionated magmas. The data provide strong evidence that magma generation occurred along a compressive plate boundary. The range in the bulk chemical compositions of the granitic suites decreases from the interior to the margin of the YTT. With the existing data, only tin mineralization can be related to the whole-rock geochemistry of the granitic rocks.

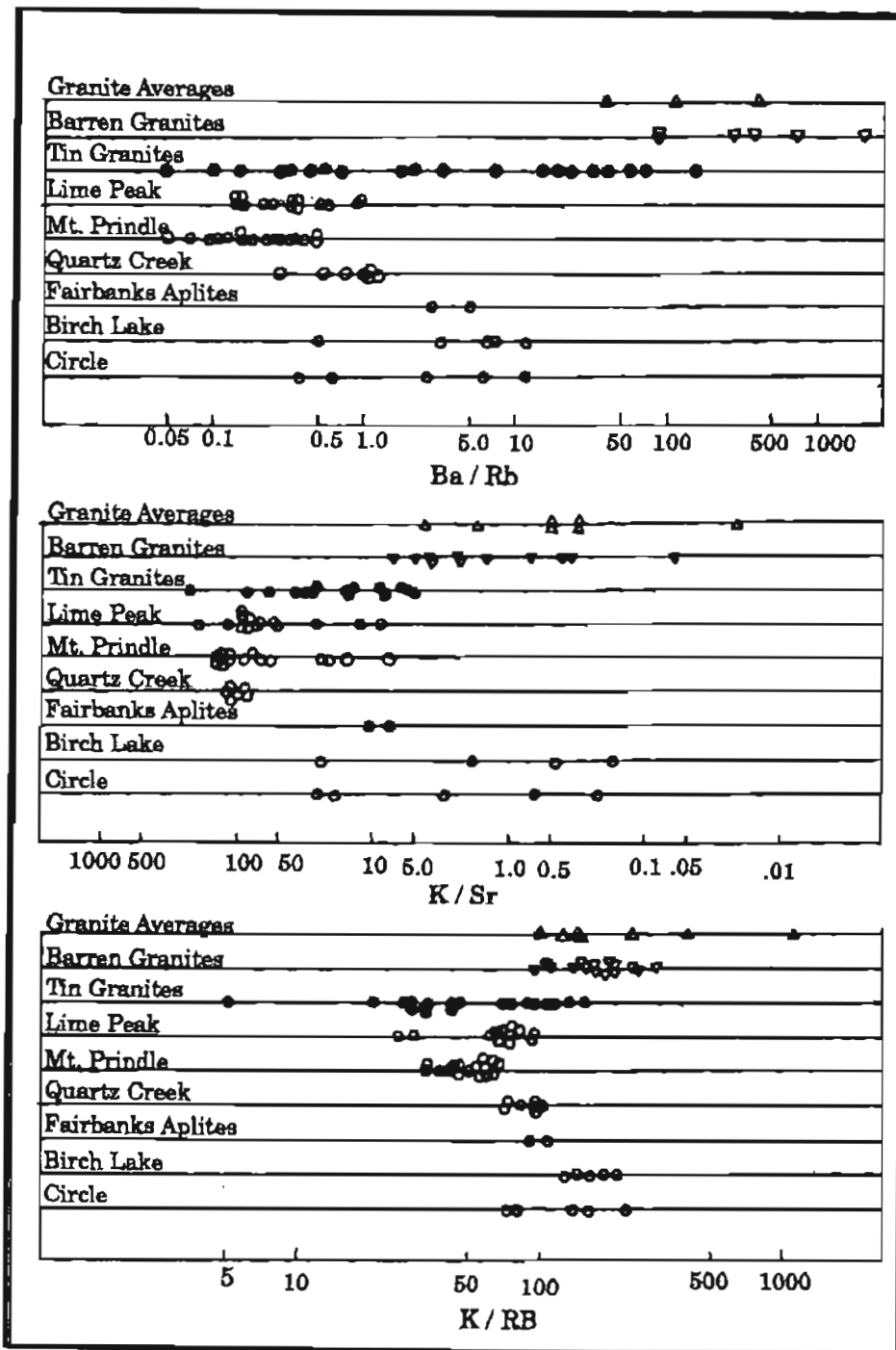


Figure 9.18 Line plots showing ratios of whole rock a) Ba/Rb, b) K/Rb, and c) Rb/Sr for tin granites, barren granites, average granites, of Govet (1983) and the granites in the Fairbanks, Circle, Steese (Newberry and Burns, 1987) and Richardson mining districts.



**METALLOGENY OF THE FAIRBANKS  
MINING DISTRICT, ALASKA AND  
ADJACENT AREAS**

**PAUL ANTHONY METZ**

**A thesis in two volumes submitted for the degree of Doctor of Philosophy of the  
University of London**

**VOLUME II  
TEXT (Chapters 10-13),  
APPENDICES, AND PLATES**

**Department of Geology  
Royal School of Mines  
Imperial College of Science, Technology and Medicine  
London**

**May 1991**



---

---

## CHAPTER 10

### RADIOGENIC ISOTOPIC GEOCHEMISTRY OF THE FAIRBANKS MINING DISTRICT AND ADJACENT AREAS

#### 10.1 INTRODUCTION

The determination of the relative geochronology of the metasedimentary and metavolcanic rocks of the Fairbanks district in particular, and the Yukon Tanana Terrane (YTT) in general, is made difficult by the lack of fossils, limited outcroppings, and a complex history of thermal and dynamic metamorphism and deformation. Radiogenic isotopic data is essential in determining definitive ages of the rocks and the time(s) of metamorphism, intrusion, and deformation. Radiogenic isotopes are also utilized in the determination of the provenance of the magmatic rocks and mineralizing fluids. Thus, these data place important constraints on the modeling of petrologic systems and mineral deposits.

The first isotopic data for rock samples in the YTT was the Pb-alpha investigations of Matzko et al. (1958). Wasserburg et al. (1963) applied K-Ar and Rb-Sr methods to the first investigation of the thermal history of the YTT. This work was followed by numerous K-Ar investigations of the intrusive rocks of the terrane but few investigations utilizing the Rb-Sr method have been completed to date. McCulloch and Wasserburg (1978) applied the Nb-Sm method to metamorphic rocks from the central Alaska Range in order to determine their thermal history. Aleinikoff et al. (1981a) utilized zircons in the application of the U-Pb method to date and model the origin of high grade metamorphic rocks in the terrane to the east of the Fairbanks district. R.B. Forbes collected three galena samples from the Fairbanks district in 1969 for Pb-Pb analysis and these were later reported by Doe and Zartman (1979). Rubidium-strontium, potassium-argon, uranium-lead, and lead-lead investigations have all been applied to the dating and modeling of the origin of the rocks of the Fairbanks district and adjacent areas of the YTT.

#### 10.2 RUBIDIUM-STRONTIUM AGE DETERMINATIONS

##### 10.2.1 Metamorphic Rock Sequences

Although the Rb-Sr method was one of the first isotopic methods to be applied in the YTT, there has been no systematic application of the method to determine the thermal history of the metamorphic rocks of the Fairbanks district. The wide range in metamorphic grade and the complex deformational history of the various sequences has provided an opportunity for application of the technique.

##### 10.2.2 Intrusive Rocks

The Rb-Sr method is applied to the dating and modeling of the granitic rocks of the Fairbanks, Circle, and Richardson mining districts. The determination of a mantle, or lower crustal origin of the intrusive rocks is particularly important in addressing the mineral deposit potential of the plutons.

The data for the Fairbanks district are from Blum (1983).

Whole-rock samples from the Circle and Richardson districts that were collected for geochemical analysis and were reported in Chapter 9 were also utilized for the Rb-Sr investigation. The Geochron Laboratories Division of Krueger Enterprises, Inc. of Cambridge, Massachusetts provided the analyses under a research grant from Krueger Enterprises. For the calculation of the age dates, a half life of  $48.8 \times 10^6$  years and a corresponding decay constant of  $1.42 \times 10^{-11}$ /year were used (after Steiger and Jager, 1977).

Discrepancies between the age determinations by the Rb-Sr method and the K-Ar method are discussed in section 10.3.2.4. There are little additional Rb-Sr data from other granitic rocks of the terrane for comparison with the Rb-Sr data from the three mining districts.

##### 10.2.2.1 Gilmore and Pedro Dome Plutons

Blum (1983) reports a  $91.0 \pm 0.7$  m.y. date for the Gilmore Dome and Pedro Dome plutonic suite. A  $^{87}\text{Sr}/^{86}\text{Sr}$  initial ratio of  $0.7128 \pm 0.00010$  is determined. This initial ratio is larger than that at the upper limit of the range of ratios for other Phanerozoic batholiths of the North American Cordillera which range from 0.7030 to 0.7090 (after Fairbairn et al., 1964; Kistler and Peterman, 1973). The ratio is much larger than the ratio at the upper limit of the range of initial ratios for plutonic rocks of the YTT in the Yukon Territory (0.7050 to 0.7070) as determined by LeCouteur and Tempelman-Kluit (1976). The initial ratio is well within the range of ratios of Precambrian crustal rocks, which extend from 0.7090 to 0.7210 (Hedge, 1966). From these data, Blum (1983) infers that the Gilmore Dome and Pedro Dome plutonic suite is derived from the partial melting of Precambrian crustal rocks.

##### 10.2.2.2 Circle Intrusive Complex

Table 10.1 lists the whole-rock Rb-Sr analyses for the Circle Intrusive Complex. Rubidium to strontium ratios range from 0.19 to 12.50. Figure 10.1a is a rubidium-strontium variation diagram for the data from the Fairbanks, Circle, and Richardson districts. The ranges in the data indicate that the elemental content of the rocks are adequate for the Rb-Sr dating method. The best fit of the isotopic ratios on Figure 10.1b indicates an age of  $98.0 \pm 13$  m.y. The large error of the estimate is due to sample 83 KM 147 which plots considerably below the line.

Dasch (1969) and Bottino and Fullagar (1968) discuss the effects of chemical weathering and alteration of granitic rocks on the rubidium-strontium method. These effects can increase rubidium to strontium ratios by up to 70 percent while the  $^{87}\text{Sr}/^{86}\text{Sr}$  ratio only increases slightly. The location of sample 83 KM 147 to the right of the isochron may be explained by slight hydrothermal alteration. Trace amounts of tourmaline and arsenopyrite are noted in outcrops adjacent to the sample locality.

The initial  $^{87}\text{Sr}/^{86}\text{Sr}$  ratio is 0.7100. This ratio is smaller than that for the Fairbanks granitic suite and is near the upper limit of the initial ratio of the British Columbia batholith

(0.7090) reported by Fairbairn et al. (1964) but considerably greater than that of the upper limit of the Sierra Nevada batholith (0.7080) reported by Kistler and Peterman (1973). It is possible that the source magma for the Circle Intrusive Complex was generated by the partial melting of a combination of Precambrian crustal rocks and primary mantle or lower crustal material.

#### 10.2.2.3 Birch Lake Pluton

Table 10.1 also lists the elemental and isotopic data for whole-rock analyses of the Birch Lake pluton. Rubidium to strontium ratios range from 0.29 to 12.45. These data are also plotted on Figure 10.1a. The ranges in the data indicate that the elemental contents of the rocks are sufficient for the Rb-Sr dating method. The best fit of the isotopic ratios on Figure 10.1b indicates an age of  $79.0 \pm 1$  m.y. The calculated age does not include sample 84 BL 05. This sample plots considerably above the isochron.

Al-Rawi and Carmichael (1967), Pankhurst (1969) and Faure and Powell (1972) all discuss the mechanisms of wall rock contamination by foreign strontium resulting in anomalously high  $^{87}\text{Sr}/^{86}\text{Sr}$  ratios. Since sample 84 BL 05 is from the contact zone of the rhyolite porphyry dike and since the dike is less than 30 meters (100 feet) wide, the effects of wall rock contamination may explain the anomalous isotopic ratio.

The initial  $^{87}\text{Sr}/^{86}\text{Sr}$  ratio is 0.7129. This is greater than that for the Gilmore Dome and Pedro Dome plutonic suite.

#### 10.2.2.4 Summary of Initial Ratios and Crystallization Histories

The Birch Lake plutonic suite has the largest initial  $^{87}\text{Sr}/^{86}\text{Sr}$  ratio of the three igneous suites. It is the most distant from the margin of the YTT and has the largest range in bulk chemical composition. The suite yields the least Rb-Sr age date. The plutonic rocks of the Fairbanks district have an initial ratio intermediate between that of the Birch Lake pluton and the Circle Intrusive Complex. The Gilmore Dome and Pedro Dome plutons are nearly equi-distant from the Birch Lake pluton and the Circle Intrusive Complex, which is at the margin of the YTT. The Rb-Sr age date for the granitic rocks of the Fairbanks district is intermediate between the age dates for the other two districts. The bulk chemical composition of the Fairbanks intrusive rocks is also intermediate between the compositions of the other two plutonic suites.

The Rb-Sr data suggest that the plutonic suites were generated, at least in part, by anatexis of Precambrian crustal material. The earliest magma generation occurred near the margin of the YTT. Magma generation migrated with time to the interior portions of the terrane. The collision of the YTT with the North American Continental Margin (NACM),

Table 10.1  $^{87}\text{Sr}/^{86}\text{Sr}$  and  $^{87}\text{Rb}/^{86}\text{Sr}$  ratios for the intrusive rocks of the Fairbanks, Circle, and Richardson mining districts.

Sample Number	ppm Rb	ppm Sr	$^{87}\text{Rb}/^{86}\text{Sr}$ (atomic)	$^{87}\text{Sr}/^{86}\text{Sr}$ ( $\pm 2$ S.D.)
83 Ch 33	121.2	644	.5434	.71072 (18)
83 KM 147	178.0	103.1	4.985	.71221 (28)
83 PM 279	206	378	1.574	.71373 (07)
83 PM 280	276	158.7	5.024	.71998 (06)
83 PM 281	275	22.1	35.95	.76068 (30)
84 BL 01	187.6	508	1.066	.71419 (06)
84 BL 02	483	42.7	32.64	.74962 (31)
84 BL 03	133.2	464	.8291	.71386 (25)
84 BL 04	334	136.3	7.079	.72064 (11)
84 BL 05	523	42.4	35.60	.76580 (25)

Errors on  $^{87}\text{Rb}/^{86}\text{Sr}$  are approximately  $\pm 1\%$ . Errors on  $^{87}\text{Sr}/^{86}\text{Sr}$  are given as 2 sigma in the last digits.

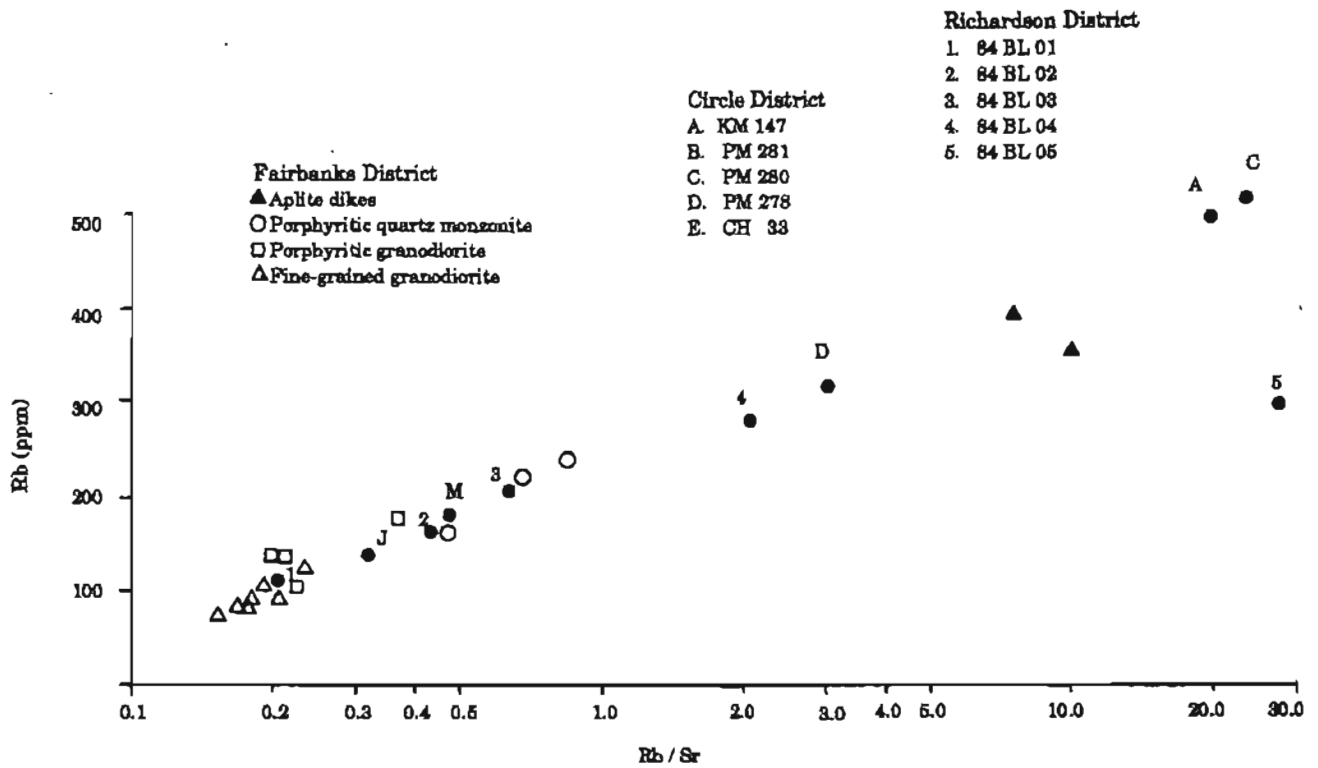


Figure 10.1a Rubidium - strontium variation diagram for igneous rocks from the Fairbanks district (after Blum, 1983), the Circle district, and the Richardson district.

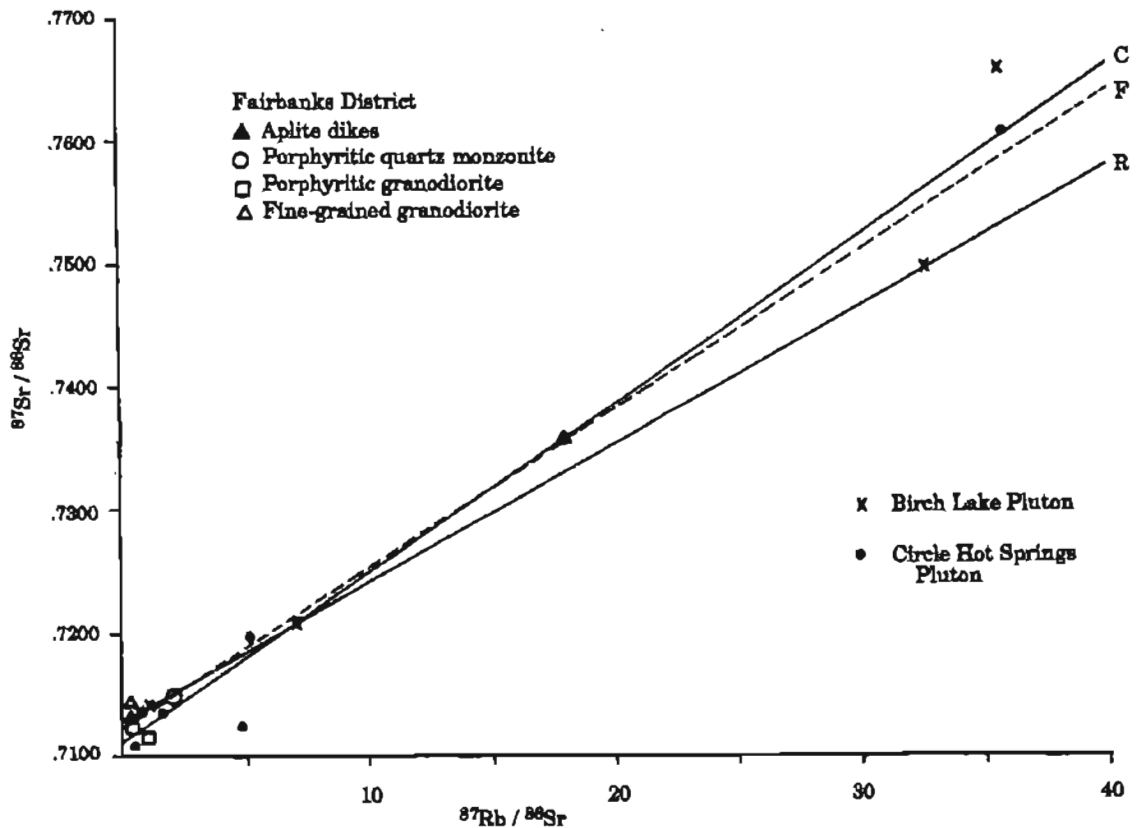


Figure 10.1b Whole Rock  $^{87}\text{Rb}/^{86}\text{Sr}$  versus  $^{87}\text{Sr}/^{86}\text{Sr}$  for the plutonic rocks from the Fairbanks (F), Circle (C), and Richardson (R) mining districts.

accompanied by thrust faulting and crustal thickening in the Circle area during the Cretaceous, could account for the magma generation.

### 10.3 POTASSIUM-ARGON AGE DETERMINATIONS

#### 10.3.1 Metamorphic Rock Sequences

Forbes (1982) summarizes the K-Ar data for the Fairbanks district. Four dates are listed for the eclogitic rocks of the Chatanika terrane. The ages range from  $470 \pm 35$  to  $115 \pm 2.6$  m.y. The oldest date is from an analysis of hornblende from an eclogitic rock from the Chatanika terrane. Three dates are listed for the Cleary sequence and they range from  $138.1 \pm 2.0$  to  $100 \pm 3$  m.y. The oldest date is from an analysis of muscovite. Three dates are given for the Goldstream sequence and these range from  $240 \pm 18$  to  $123.6 \pm 3.7$  m.y. The oldest date is from an analysis of hornblende. A single analysis is reported from the Birch Hill sequence. The muscovite date is  $113.6 \pm 3.4$  m.y.

Bundtzen and Turner (1979) report ages for the Birch Creek Schist in the Kantishna district. Four hornblende separates from a garnet amphibolite yield ages ranging from 195.4 to 104.0 m.y. Two muscovite separates from a garnet-mica schist yield an average age of 100.0 m.y. while two biotite separates from the same rock yield an average age of 98.7 m.y.

Bundtzen and Turner (1979) obtain a  $108.0 \pm 3.2$  m.y. age from a whole-rock analysis of the Totatlanika Schist in the Kantishna district. Sherwood and Craddock (1979) report  $309.0 \pm 2.5$  m.y. age from actinolite from a metabasite unit of the Totatlanika Schist in the Healy D-2 quadrangle which is east of the Kantishna district and south of the Fairbanks district. Wahrhaftig (1968) assigned a Mississippian(?) age to the Totatlanika Schist on the basis of a *Syringopora* bearing fossil locality in the Healy D-2 quadrangle.

#### 10.3.2 Intrusive Rocks

##### 10.3.2.1 Gilmore Dome and Pedro Dome Plutons

Forbes and Swainbank (1975) report a K-Ar age of  $90.7 \pm 5.1$  m.y. from an analysis of hornblende from the Pedro Dome pluton. Forbes (1982) reports a K-Ar age of  $93.2 \pm 2.2$  m.y. from an analysis of biotite from the quartz monzonite phase of the same pluton. These dates are comparable with the Rb-Sr dates of Blum (1983).

##### 10.3.2.2 Circle Intrusive Complex

Wilson and Shew (1981) report a single K-Ar date of  $60.5 \pm 1.8$  m.y. based on an analysis of biotite from a granitic phase of the Circle Hot Springs pluton. Wilkinson (1987) reports seven K-Ar age dates for the Circle Intrusive Complex. A single analysis of biotite from the granodiorite phase of the Two-Bit pluton yields a date of  $69.7 \pm 2.1$  m.y. White-mica from a pegmatite dike in the pluton yields an age of  $70.9 \pm 2.1$  m.y. Five analyses of biotite from various lithologies in the Circle Hot Springs pluton yield ages that range from  $57.8 \pm 1.7$  to  $54.2 \pm 1.6$  m.y.

Wilson and Shew (1981) report three K-Ar age dates for

the Hope granitic suite in the Steese district. Muscovite from a pegmatite dike in the Mt. Prindle pluton yields a date of  $58.1 \pm 1.8$  m.y. Biotite from a granite in the Quartz Creek pluton yields a date of  $65.9 \pm 1.38$  m.y. Biotite from a granite in the Lime Peak pluton yields a date of  $56.7 \pm 0.95$  m.y.

The K-Ar age dates for the Circle Intrusive Complex and the Hope granitic suite have a considerable range (70.9 to 54.2 m.y.). These dates are significantly younger than those derived from the Rb-Sr method.

##### 10.3.2.3 Birch Lake Pluton

Bundtzen and Reger (1977) report a K-Ar age date of  $89.1 \pm 2.7$  m.y. from an analysis of K-feldspar from the quartz-orthoclase porphyry dike of the Birch Lake pluton. The sample location is the Democrat Lode prospect and is the same as the location for 84 BL 04. Hornblende from gneiss adjacent to the dike yields age dates of  $115.8 \pm 3.5$  m.y. and  $105.5 \pm 3.2$  m.y.

Wilson et al. (1985) report a biotite age of  $91.2 \pm 2.7$  m.y. from the pyroxene diorite at Flag Hill on the northwestern margin of the Birch Lake pluton. They also report a biotite age ( $89.3 \pm 2.7$  m.y.) and a hornblende age ( $87.3 \pm 2.7$  m.y.) from granodiorite which outcrops on Canyon Creek near Birch Lake on the eastern margin of the pluton. These dates have a relatively narrow range but are significantly older than the Rb-Sr dates reported above.

##### 10.3.2.4 Summary of K-Ar Evidence for Thermal Events in the Yukon-Tanana Terrane

Wilson et al. (1985) note at least six igneous and thermal metamorphic(?) events in the YTT based on the K-Ar method. Plutonism occurred during Mississippian, Early Jurassic, mid-Cretaceous, Late Cretaceous, and early Tertiary times. These events are all documented in the area of the five mining districts. However, caution should be used in the evaluation of the K-Ar data for the terrane.

K-Ar data for the biotite and hornblende pairs in the metamorphic rocks often show strong discordance. This could be a function of differences in blocking temperatures or differences in argon retention during subsequent thermal events.

K-Ar data for the Circle Intrusive Complex indicate Late Cretaceous and early Tertiary events, however the Rb-Sr data indicate a mid-Cretaceous age for the initial crystallization. The K-Ar data are probably recording two stages of alteration of the complex. Early greisenization appears to be overprinted by weak sericitic and argillic alteration.

K-Ar and Rb-Sr data for the intrusive rocks of the Fairbanks district yield comparable ages. It is noteworthy that the intrusive rocks of the district do not exhibit greisenization and show the effects of weak sericitic alteration only adjacent to major shear zones.

Forbes (1982) reports a whole-rock K-Ar age of  $80.2 \pm 3.6$  m.y. for the olivine basalts of the Birch Hill area of the Fairbanks district. The pillow basalts are inter-layered with clastic sediments that contain lower Tertiary flora including *Metasequoia*. The flora is correlated with the Eocene thru

Miocene flora of the Nenana Coal Field to the south of the district.

The anomalously old K-Ar age for the Tertiary basalts of the Fairbanks district is probably a function of excess argon. Excess argon in basalts is documented by Damon et al. (1967), and Dalrymple (1969). The schists adjacent to the basalts of the Fairbanks district are possible sources of excess argon.

K-Ar and Rb-Sr data for the Fairbanks district indicate that prior to 240 m.y. ago, metamorphic temperatures of the various schist sequences peaked. At approximately 240 m.y. ago the metamorphic rocks cooled below 475°C, the blocking temperature of amphibole (Damon, 1968), for the final time. Between 131 and 100 m.y. ago, metamorphic temperatures fell below 230°C, the blocking temperature of mica (Damon, 1968), for the last time. At about 91 m.y. ago the metamorphic sequences were intruded by the plutonic rocks. Finally, during the early Tertiary, the schist sequences were intruded by the olivine basalts.

The K-Ar data for the Birch Lake pluton indicates an age of approximately 89 m.y. while the Rb-Sr data yields an age of 79 m.y. Pearson et al. (1966) note 60 percent excess argon in hornblende from a hornblendite that intrudes Precambrian gneiss. The gneiss in contact with the Birch Lake pluton, as noted above, has an early Cretaceous K-Ar age but correlative rocks to the north yield detrital zircons with Proterozoic U-Pb ages (Aleinikoff et al., 1984). The anomalously old K-Ar age for the Birch Lake pluton is probably due to inherited argon from the gneissic rocks.

## 10.4 URANIUM LEAD (U-Pb) DETERMINATIONS

### 10.4.1 Data from Southeastern Yukon-Tanana Terrane

As noted in Chapter 2, Mortensen (1983) and Mortensen and Jilson (1985) provide U-Pb and Rb-Sr data for a mid-Paleozoic felsic volcanic-plutonic suite in the southeastern portion of the YTT. Associated with the felsic rocks are mafic and ultramafic rocks that have late Devonian U-Pb ages. The metamorphosed felsic volcanic-plutonic suite extends from the Watson Lake area, through central Yukon Territory into east-central Alaska (see orthogneissic dome complexes, Ch. 2, Plate I).

### 10.4.2 Data from Northwestern Yukon-Tanana Terrane

Aleinikoff et al. (1981b) report an early Proterozoic U-Pb age for multigrain fractions of zircons from an ortho-augen gneiss in the YTT in east-central Alaska. A concordia plot of the data defines a cord that intercepts concordia at  $344 \pm 3$  and  $2,283 \pm 33$  m.y. The interpretation preferred by the authors is that the protolith of the augen gneiss was intruded in the mid-Paleozoic and incorporated material of Proterozoic age.

Aleinikoff et al. (1984a) provide U-Pb evidence for an Early Proterozoic age for detrital zircons from east-central Alaska. The multigrain fractions of zircons from four distinct quartzite units give intercepts of  $346 \pm 38$  and  $2,232 \pm 34$  m.y. on a concordia plot. The authors interpret the data as follows:

“Detritus from Early Proterozoic crustal rocks about 2,250 m.y. old was deposited probably during the latest Proterozoic and (or) earliest Paleozoic. Part of this package of sedimentary rocks was either partially melted or incorporated into a magma that formed the plutonic protolith of the augen gneiss about 350 m.y. B.P. Old detrital zircons were incorporated as cores around which younger magmatic rims of zircon grew. Metamorphism of the gneiss and at least the nearby quartzite protoliths may have been contemporaneous with emplacement of the magma, as suggested by coplanar foliation and the lower intercept, or after it cooled. The linear array of the uranium-poor detrital zircons, from widespread areas of the Yukon-Tanana Upland, suggests that this 350-m.y.-B.P. event was a large-scale, regional occurrence with major significance to the geology of the region. This conclusion is substantiated by many other ages of approximately 350 m.y. (J.N. Aleinikoff, unpub. data, 1981) on metaplutonic and metavolcanic rocks in the upland.”

Aleinikoff et al. (1984b) report U-Pb ages of zircons from sillimanite gneiss from the Big Delta quadrangle, east-central Alaska. Five samples form a cord that intercepts concordia at  $302 \pm 156$  and  $2,383 \pm 298$  m.y. The earlier age is interpreted as the provenance age of the sedimentary protolith of the sillimanite gneiss. The lower-intercept age is considered the age of development of the metamorphic zircons.

Aleinikoff and Nokleberg (1984) report an Early Proterozoic U-Pb age for zircons from a metarhyodacite from the Mount Hayes C-6 quadrangle. The authors assign the metavolcanic rocks to the Jarvis Creek Glacier tectonostratigraphic terrane rather than to the YTT. The calculated age of the metarhyodacite is about 2,000 m.y. Episodic lead loss is inferred at 350 m.y. From the lithologic associations the authors interpret the data as evidence for an Andean-type volcanic arc during the Early Proterozoic.

### 10.4.3. Zircons from the Fairbanks Mining District

Aleinikoff and Nokleberg (1989) report a U-Pb age date for zircon from a sample of metasilstone and a sample of “metarhyolite” from the Cleary sequence. These sample data are combined with sample data from Aleinikoff et al. (1984a, 1984b, 1986). The later data base is for zircons from gneissic domes and metasediments of east-central Alaska. The combined data forms a cord that intercepts concordia at about 2,250 and 370 m.y. The authors interpret the data as evidence for a Late Devonian age for the volcanism in the Fairbanks district and an Early Proterozoic age (2,300 to 2,100 m.y.) for the provenance of the metasediments.

Mortensen (1990) reports U-Pb ages for single grains of detrital zircons from two units in the YTT. All previous investigations which indicate provenance ages of 2,300 to 2,100 m.y. are based on multigrain analyses. Eighteen analyses of single zircon grains from a laminated quartzite unit of the Cleary sequence yield U-Pb age groups at 3,400,

2,500, 1,900-1,800, 1,400-1,300, and 1,200 m.y. Similarly, eight analyses are given for single zircon grains from the Nizina Quartzite collected from an area to the west of Dawson, Yukon Territory. The analyses show age groups at 2,800-2,600 and 2,100-1,800 m.y. The 2,300-2,100 m.y. group is noticeably not present. The previously determined 2,300-2,100 m.y. upper intercept U-Pb ages are therefore probably average ages for inherited and detrital zircons and zircons of this age group probably do not exist in the YTT.

#### 10.4.4 U-Pb Evidence for Evolution of the Yukon-Tanana Terrane

The data from Mortensen (1990) places considerable doubt on the previously reported U-Pb ages for detrital zircons from the YTT. There is strong evidence that provenance material for the metasediments and metaexhalites may be as old as Archean (3,400 m.y. age group) and may include most of the Proterozoic (2,500, 1,900-1,800, 1,400-1,300, and 1,200 m.y. age groups).

U-Pb data indicate Late Devonian to mid-Mississippian (370 to 340 m.y.) bimodal volcanism and regional metamorphism in the terrane. This is evidence for a mid-Paleozoic extensional plate boundary. Metz et al. (1982) propose that the Tintina Fault was the loci of one arm of mid-Paleozoic triple junction centred in northeastern Alaska and northwestern Yukon Territory. One aborted arm of the rift system is responsible for the minor bimodal volcanism and major Ba-Pa-Zn metallogeny of northern Alaska. The arm sub-parallel to the Tintina Fault probably formed an ocean basin the size of the Red Sea and is responsible for the complex mid-Paleozoic metallogeny of the YTT. Closure of the basin in the Mesozoic is indicated by renewed plutonism and regional metamorphism. Evidence for the timing of these events is recorded in the previously discussed Rb-Sr and K-Ar data.

## 10.5 LEAD-LEAD ISOTOPIC DETERMINATIONS

### 10.5.1 Determinations from Southeastern Yukon-Tanana Terrane

Godwin and Sinclair (1982) and Godwin et al. (1982) report lead isotopic data for the central Yukon Territory and demonstrate the regional zoning of the data relative to the major mineral deposit types. Church et al. (1987) list a compilation of Pb isotope data for Alaska, however, the data for the YTT in Alaska is limited.

### 10.5.2 Determinations from the Fairbanks Mining District

#### 10.5.2.1 Sample Collection

Five samples of Type I, two of Type II, and three of Type IV mineralization were collected. Polished blocks of the samples were examined and galena or lead sulphosalts were extracted from the polished blocks.

#### 10.5.2.2 Sample Preparation, Analysis, and Data Reduction

The analytical facilities of the National Environmental Research Council (NERC) Isotope Laboratory at the British Geological Survey in London were utilized. Lead isotope analyses were conducted on a Thomas-Houston THN 206 solid source mass spectrometer by the method of Cameron et al. (1969). Approximately 5 µg of sample in the form of lead nitrate was mounted onto a rhenium filament along with a drop of suspension of silica gel in phosphoric acid. A beam current of  $2 \times 10^{-11}$  A was generated for a few hours to allow 50 or 60 measurements to be made on each sample. The NBS 981 Common Lead Standard was analyzed at regular intervals and corrections were applied for the variation in the measured value from the accepted absolute value. The sample analyses are presented in Table 10.2.

Table 10.2 Lead-lead isotopic data for the Fairbanks district and adjacent areas of the Yukon-Tanana Terrane.

Sample No/ Location	Deposit Type	206/204	207/204	208/204
81 MURL 04 Steese Eclogite	I	18.7382	15.6359	38.5412
81 MURL 12 Cheechako	I	19.1125	15.6577	39.0921
TS-1 Cheechako (3)	IV	19.046	15.619	38.961
81 MURL 13 Rogasch	IV	19.0877	15.6471	38.9976
84 ASCF 08 Rogasch (3)	IV	19.102	15.638	39.105

Table 10-2 (Continued)

Sample No/ Location	Deposit Type	206/204	207/204	208/204
81 MURL 14 Rowley	II	19.1106	15.6600	39.0658
FC-1 Flume Creek (3)	II	19.168	15.669	39.058
81 MURL 17 Silver Fox	II	19.1351	15.6757	39.1059
ECP-21-67 (1) Silver Fox	II	19.120	15.686	39.153
ECP-1-67 (1) Steamboat	?	19.126	15.678	39.136
No Number (1) Pedro Dome	?	19.112	15.681	39.122
81 MURL 21 Christina	I	19.1506	15.6912	39.1508
84 ASCF 04A Nordell Mine (3)	I	19.139	15.694	39.214
84 ASCF 06 Christina (3)	IV	19.139	15.696	39.226
81 MURL 22 Wackwitz	I	19.1298	15.6549	39.0586
TS-3 Wackwitz (3)	I	19.027	15.612	38.932
TS-2 Cleary Road (3)	I	19.087	15.663	39.044
81 MURL 28 Ridge Prospect	I	19.1357	15.6710	39.1114
82 CM 02 Cleary Hill	IV	19.0103	15.5869	38.5868
G3134 Cleary Hill (3)	IV	19.127	15.680	39.176
82 PM 03 Hi-Yu	IV	19.0889	15.6303	38.9789
G3132 Hi-Yu	IV	19.161	15.693	39.224
83 GD 01 Gold Dust (2)	IV	18.9932	15.6272	38.8239
83 PM 291 Deadwood (2)	I	19.4435	15.6809	39.4311

Note: (1) R.B. Forbes unpub. data  
(2) Circle mining district  
(3) Church et al., 1987

### 10.5.3 Discussion

Table 10.2 also includes data from Church et al. (1987) and unpublished data from R.B. Forbes. Multiple samples from some locations are included in the three data sets. The data are comparable from the three separate laboratories.

The Pb isotope analyses all indicate future ages and thus the leads are very anomalous lead regardless of deposit type. The range of the data, with the exception of the single sample from the Chatanika terrane, are very narrow. The stratabound and vein type mineralization have nearly identical Pb isotopic compositions.

Figure 10.2 is a plot of Fairbanks district data and two Pb-Pb analyses from the Kantishna district (after Bundtzen, 1981). The data all plot within the field of Red Sea sediments of Doe and Zartman (1979). These data support the Red Sea graben model presented in Chapter 9 for the stratabound mineralization.

Figure 10.3 is a detailed plot the analyses present in the investigation. The extreme narrow range of the Fairbanks data, excluding the eclogite occurrence, is shown graphically. Gulson (1986) notes that there is a positive correlation between increasing lead isotopic homogeneity and increasing deposit size. The similarity of lead isotopic ratios over the

48 kilometer (30 mile) strike length of the sampled mineralization of the district is an indication of the large size of the hydrothermal system that produced the stratabound mineralization.

The Pb isotopic data for the Fairbanks district (excluding the Chatanika terrane) are more radiogenic than those of the Greens Creek massive sulphide of Alexander terrane (LeHuray et al., 1985a) and the massive sulphide deposits of the Jarvis Creek terrane (LeHuray et al., 1985b). The Pb isotopes for the Chatanika terrane plot very near the single data point for the Greens Creek deposit. Using the models of Doe and Zartman (1979) it is inferred that the evolution of the Pb isotopes of the Fairbanks district involved complex multistage processes with a major contribution of material from Precambrian crustal rocks.

### 10.5.4 Summary of Pb-Pb Isotopic Evidence for the Evolution of the Rock Sequences and Mineral Occurrences

Lead isotopic data supports Precambrian crustal sources for the lead and probably the other elements that formed the stratabound mineralization in the Cleary sequence. The less radiogenic lead from the Chatanika terrane is isotopically similar to that from the Greens Creek deposit in southeastern

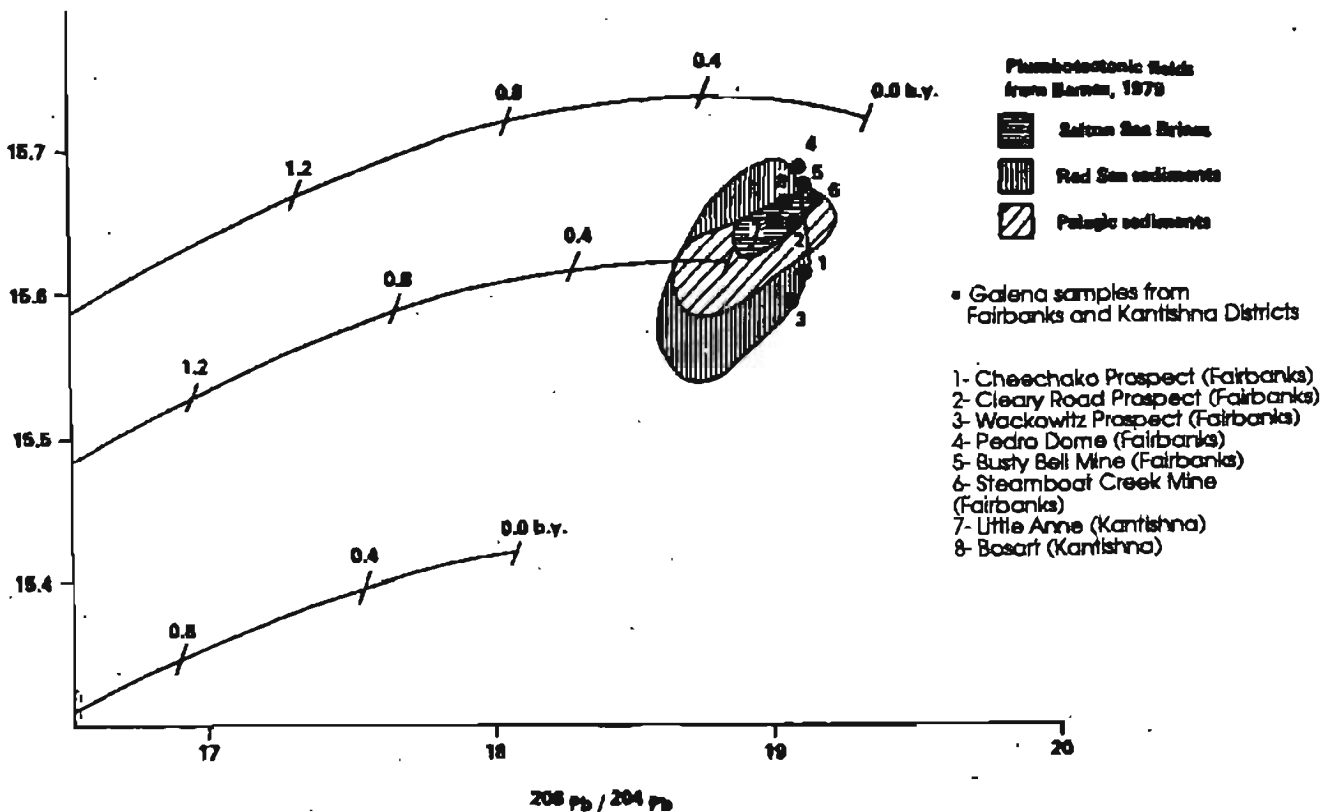


Figure 10.2 Plot of lead-lead isotopic data for the Fairbanks district and adjacent areas versus various mineral deposit models (after Bundtzen et al., 1984).

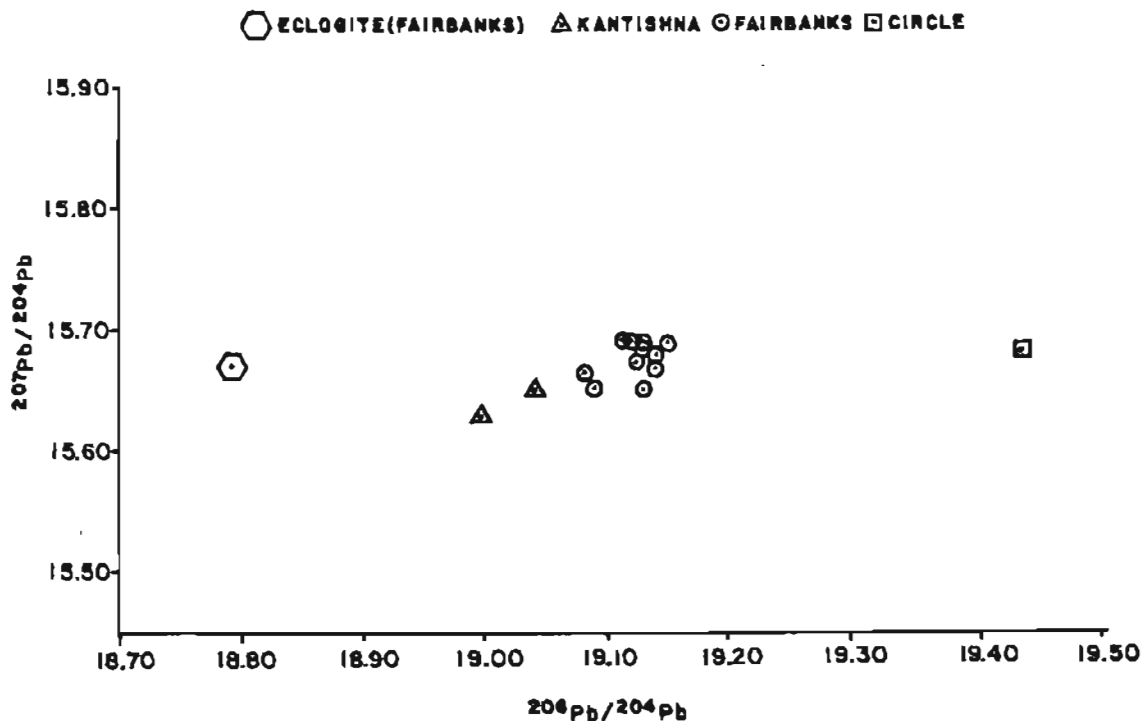


Figure 10.3 Detailed plot of lead-lead isotopic data for the Fairbanks district and adjacent areas of the Yukon-Tanana Terrane.

Alaska. The lead isotopic data support a rift system model for the generation of the stratabound mineralization in the district. The subsequent gold quartz vein mineralization inherited the isotopic compositions of the stratabound mineralization.

## 10.6 SUMMARY AND CONCLUSIONS

Mineral deposit models for the Fairbanks district and adjacent areas have been created on the basis of regional geologic mapping, mineralogy, petrology, major oxide geochemistry, trace element geochemistry, and fluid inclusion analysis. Radiogenic isotopic geochemistry does not contradict any of the proposed mineral deposit models, however, it further constrains the models for the Fairbanks district and adjacent areas. The narrow range of the Pb isotopic data for the Fairbanks district indicates that the hydrothermal systems for the various types of mineralization were very large. Isotopic data substantiates that multiple stage processes are responsible for the varied mineral deposit types, however, the timing of the events prior to the mid-Paleozoic remain unknown.

From the limited data, it can be concluded that a definitive determination of the timing of each of the mineralizing events in the district and adjacent areas will require a substantial research commitment. No single isotopic method can be expected to resolve all the unanswered questions. In addition, critical review of the existing isotopic data base and, in particular, the U-Pb data base is essential before the data are quoted.

---



---

## CHAPTER 11

### MINERAL DEPOSIT MODELS FOR THE FAIRBANKS MINING DISTRICT AND ADJACENT AREAS

#### 11.1 INTRODUCTION

There are diverse types of mineralization described for the Fairbanks district and the adjacent areas of east-central Alaska. There is limited geologic information available for most of the mineral occurrences in this region and none of the mineral occurrences is currently in production. In order to estimate the economic significance of the mineralization, analogies are made with similar types of mineralization that are currently under production in other parts of the world. In order to establish analogies, the mineralization in this region is classified into eight major types. Due to economic constraints, emphasis is placed on the gold content of the various deposit types.

#### 11.2 PARAMETERS INCLUDED IN THE MINERAL DEPOSIT MODELS

The mineral deposit models are descriptive and include the following thirteen parameters: 1) elemental associations, 2) host rock associations, 3) ore mineralogy, 4) gangue mineralogy, 5) age of host, 6) age of mineralization, 7) sulphur isotopic ratios, 8) hydrogen and oxygen isotopic

ratios, 9) lead/lead isotopic ratios, 10) fluid inclusion data, 11) regional structural setting, 12) local structural controls, and 13) tonnage and grade. Although this is a descriptive classification system, the terminology for some of these parameters imparts a genetic connotation to the system.

The eight major lode types of gold bearing deposits found in east-central Alaska are as follows:

1. Metamorphosed volcanic-exhalative and associated low sulphide gold-quartz veins,
2. Copper-molybdenum-gold porphyry,
3. Precious metal enriched massive sulphides,
4. Epithermal veins in volcanics and plutonic rocks,
5. Gold bearing skarns,
6. Tin greisen-gold-quartz veins,
7. Carlin-type sediment-hosted gold,
8. Paleoplacers.

A summary of the thirteen parameters for each of these deposit types is given in Table 11.1. All thirteen parameters are not available for all the deposit types, however this does not seriously constrain the classification of any deposit type.

### 11.3 EXAMPLES OF THE MINERAL DEPOSIT TYPES

#### 11.3.1 Metamorphosed Volcanic-Exhalative Gold and Associated Low Sulphide Gold-Quartz Veins

The Type ID mineralization at the Tolovana prospect, Fairbanks district, is a prime example of metamorphosed volcanic-exhalative gold mineralization. The Cleary sequence (Fairbanks district), the Spruce Creek sequence (Kantishna district), and the Bonanza Creek sequence (Circle district) are all host to this type of mineralization. The stratabound As-W mineralization in the lower Cleary sequence is similar to the stratabound Hg-Sb-W mineralization in Austria (Maucher, 1976), South Africa (Muff, 1978), and Spain (Arribas, 1984). The stratabound Au-As-Sb mineralization of the lower and upper Cleary sequence has strong mineralogic and petrologic similarities to the Archean stratabound gold mineralization in southern Africa (Anhaeusser, 1976), western Australia (Fehlberg and Giles, 1982), eastern Canada (Godwin, 1982), and Zimbabwe (Foster and Wilson, 1982). Phanerozoic examples of volcanic exhalative gold mineralization include several deposits in lower Paleozoic rocks in southeastern USA (Mangan et al., 1984). This deposit type is transitional with the precious metal enriched massive sulphides. In the Kantishna district the stratabound mineralization is all classified as massive sulphide type.

The Type IV mineralization of the Christina vein system in the Fairbanks district is the best example of the low sulphide vein mineralization. An analogue for this type of mineralization is the Homestake Mine at Lead, South Dakota. The veins hosted in the Bonanza Creek sequence are also relatively low sulphide types, however the veins in the Spruce Creek sequence are generally higher in total sulphide content.

The analogue stratabound gold occurrences are relatively small deposits, however the associated vein deposits are very large. For instance the Homestake deposit is estimated to have an ultimate production in excess of 1,000 tonnes (1,100 tons) of gold.

#### 11.3.2 Copper-Molybdenum-Gold Porphyry

The single example of this type mineralization is the Shorty Creek prospect in the Tolovana mining district. The analogues for this mineralization are the gold-rich porphyry deposits of the southwest Pacific including the Lahir Island discovery. Other intrusive related gold occurrences in the region, including the Fort Knox prospect (Fairbanks district) and the Joker prospect (Circle district) are often referred to as porphyry type gold occurrences. These occurrences do not exhibit the same elemental associations or alteration assemblages as porphyry copper or porphyry molybdenum deposits. They possess more of the characteristics of intrusive related epithermal veins and are classified as such in a subsequent section.

Gold enriched porphyry deposits are large sources of gold. Individual deposits may contain 1,000 tonnes (1,100 tons) of metal, thus a single deposit may contain the equivalent of the total production of Alaska to date.

#### 11.3.3 Precious Metal Enriched Massive Sulphides

The Type IC and IE mineralization (see Sections 4.3.3 and 4.3.5, Chapter 4) of the Nordale adit and Cheechako prospect, Fairbanks district are examples of precious metal enriched massive sulphides. The massive sulphides in the Spruce Creek sequence are similar to the massive sulphides in the volcanoclastic and exhalative units of the Cleary sequence. The Greens Creek deposit in southeastern Alaska is probably the best analogue for the precious metal enriched massive sulphides in the Fairbanks and Kantishna districts.

The tonnage and grade of massive sulphides are highly variable. The tonnages range from 3 to 110 million tonnes (3.3 to 120 million tons) of ore with precious metal contents of 3 to 200 tonnes (3.3 to 220 tons) of Au and 500 to 15,000 tonnes (550 to 16,500 tons) of Ag.

#### 11.3.4 Epithermal Veins in Volcanic and Plutonic Rocks

The Fort Knox and Silver Fox occurrences in the Fairbanks district are examples of intrusive related mineralization. The Joker occurrence in the Circle district and the Democrat Mine in the Richardson district are also intrusive related; however these occurrences are less well documented.

This model includes a variety of sub-types that are represented by gold dominant and silver dominant end members. Contained metal contents range from 4 to 300 tonnes (4.4 to 330 tons) of Au and 11,000 to 50,000 tonnes (12,100 to 55,000 tons) of Ag. This type of deposit is thus a significant source of gold and a major source of silver. The mineralization in the Fairbanks district and adjacent areas is the gold dominant sub-type.

#### 11.3.5 Precious Metal Skarns

Three types of gold bearing skarns are recognized. These include gold skarns, copper-gold skarns, and tungsten-gold skarns. The later type includes tungsten-gold stockwork veins within or adjacent to granitic plutons. The Tungsten Hill prospect in the Fairbanks district is an example of this type of mineralization. Neither gold, or copper-gold skarns

Table 11.1. Major gold deposit types with analogues in east-central Alaska

Gold Deposit Type	Examples	Elemental Associations	Host Rock Associations	Ore Mineralogy	Gangue Mineralogy	Age of Host
1. Metamorphosed Volcanic-Exhalative and Associated Low Sulfide Gold-Quartz Veins	Homestake Mine, Lead South Dakota; Fairbanks Dist, AK, Juneau Gold Belt, AK, Chichagoff Mine, AK; Zimbabwe	Au,Ag,As	Metamorphosed, basalt, andesite, felsic volcanics & pyroclastic rocks, silicic carbonate, exhalite chert; talc/fuchsite schist; black schist; cummingtonite schist; cherty iron formation phyllite.	Arsenopyrite, bismuth (tr), boulangerite, chalcocite (tr), chalcocopyrite (tr), covellite (tr), galena, gold, jamesonite, loellingite, magnetite, pyrite, rutile, scheelite, sphalerite, stibnite, tetrahedrite, zircon	Ankerite, biotite, calcite, chlorite, cummingtonite, garnet, graphite, mariposite, quartz, staurolite, scorodite, tourmaline	Archean or Proterozoic major; Paleozoic minor
2. Copper-Molybdenum-Gold Porphyry	Bougainville and OK, Tedi Papua New Guinea; Golden Zone, AK; Shorty Cr., Tolovana District, AK; Lahar Is, Papua, New Guinea	Cu,Mo,Au, Ag	Associated with either high-K shonkinitic rocks ranging from diorite to syenite or with low-K calc-alkaline quartz diorite to granodiorite. Host rocks for the intrusives may be of any age or composition.	Arsenopyrite, bornite, chalcocopyrite, gold, magnetite, molybdenite, pyrite, sphalerite, stibnite	Actinolite, albite, alkali-feldspar, biotite, carbonate, garnet tremolite, sericite	Hercynian to Cenozoic
3. Precious Metal Enriched Massive Sulfide	Kidd Creek, Ontario; Flin Flon, Manitoba; Cyprus, Noranda, Quebec; Rio Tinto, Spain; Delta, AK; Greens Creek, AK; Fairbanks District, AK	Zn,Cu,Pb, Au,Ag	m-basalt, m-andesite, m-hyaloclastites, m-rhyolite, tuff, m-keratophere, muscovite quartz schist, m-chert, talc-actinolite schist, m-breccia, black schist, slate, fuchsite schist, and jaspilite.	Barite, bornite, chalcocopyrite, galena, gold, magnetite, molybdenite, pyrite, pyrrhotite, scheelite (tr), sphalerite, tetrahedrite	Actinolite, biotite, carbonate, garnet, graphite, mariposite, olivine, plagioclase, feldspar, pyroxene, quartz, sericite, tourmaline	Archean to Miocene
4. Epithermal Veins	Iditarod-Irnoko, AK; Oatman, AZ; Bodie, CA; Creede, CO; Delamar, ID; Pachuca, Mexico; Comstock NV; Colqui, Peru; Keno Hill, Yukon Terr.; Fairbanks, Dist., AK	Au,Ag,Pb, Zn,Cu,Sb, As	Andesitic to rhyolitic volcanics and hypabyssal plutons.	Altaite, argentite, arsenopyrite, bornite, chalcocite, chalcocopyrite, covellite, cerargyrite, electrum, enargite, galena, gold, heazite, jamesonite, marcasite, mlargyrite, molybdenite, pyrrargyrite, polybasite, proustite, pyrite, realgar, stephanite, sphalerite, stromeyerite, stibnite, tetrahedrite, tetramnite-	Actinolite, biotite, carbonate, garnet, graphite, mariposite, olivine, plagioclase, feldspar, pyroxene, quartz, sericite, tourmaline	Cretaceous to Tertiary

Table 11.1 (Continued)

Age of Mineralization	Sulfur Isotope Ratios	Hydrogen/Oxygen Isotope Ratios	Lead/Lead Isotope Ratios	Type	Salinity	Fluid Inclusions Temp. Hom.	Temp. Trap.	Regional Structural Setting
Archean or Proterozoic remobilized from host.	$\delta^{34}\text{S}+3$ to +10 per mil	$\delta^{18}\text{O}$ 8-11 per mil.	206/204, 19.00 to 19.15; 207/204, 15.60 to 15.70; 206/204, 38.80 to 39.20.	$\text{H}_2\text{O}+$ $\text{CO}_2+$ NaCl	1-10 wt% NaCl Equiv.	300-360°C	400-500°C	Mobile belts adjacent to stable cratons. Early tensional and subsequent compressional tectonics accompanied by regional greenschist facies metamorphism.
Slightly younger than host intrusive.	$\delta^{34}\text{S}-5$ to +5 per mil.	$\delta\text{D}$ , -40 to -80 per mil $\delta^{18}\text{O}$ , +5 per	206/204, 16.20 to 18.80; 207/204, 208/204, 35.50 to 39.90	$\text{H}_2\text{O}-$ $\text{CO}_2-$ NaCl (liq-equiv. vapor)	5-15 wt% NaCl	250-350°C	300-400°C	Intrusive hosts often near major thrust and high angle faults
Archean to Miocene	$\delta^{34}\text{S}-5$ to +10 per mil	$\delta\text{D}$ , 0 to 100 per mil; $\delta^{18}\text{O}$ , +5, per mil.	206/204, 13.2-15.7; 207/204, 14.4-15.5; 208/204, 33.1-35.3.	$\text{H}_2\text{O} +$ NaCl (liq. vapor)	1.0-5.0 wt% NaCl equiv.	200-350°C	300-500°C	Back arc, inter-arc, and intracratonic basins formed in tensional tectonic environment. Formed by submarine volcanic and exhalative activity.
Usually 2-3 million years younger than host	$\delta^{34}\text{S}-5$ to +10 per mil.	$\delta\text{D}$ , -50 to -120 per mil; $\delta^{18}\text{O}$ 0 to -16	206Pb/204Pb, 18.75 to 19.50; 207Pb/204Pb, 15.55 to 15.65; 208Pb/204Pb, 38.20 to 39.10.	$\text{H}_2\text{O}-$ $\text{CO}_2-$ NaCl (liq-vapor)	1 to 10 wt% NaCl (usually 1 to 3 wt%)	200-320°C	220-350°C	Volcanic sequences formed above subduction zone. Regional structures often related to radial and concentric fracture zone of caldera and resurgent caldera complexes.

Table 11.1 (Continued)

Local Structural Control	Tonnage/Grade or Contained Metal	Comments	References
Remobilized mineralization in stratabound quartz carbonate veins and in major shear zones with both normal and strike slip components. Remobilized mineralization also localized as fold hinges.	9-20 grams/tonne Au 1000 tons, Au	Ore bodies include sulfide/gold disseminations and lenses in metavolcaniclastic exhalites, and iron formations; major shear zone related mineralization exhibiting both open space filling and replacement structures and textures.	Brown et al., 1959; Riley, 1972; Horwood and Pye, 1955; Bragg, 1967; Riddle, 1970; Rye and Rye, 1974; Bayley, 1972; Cair, 1962; Tolbert, 1964; Fleischer and Routhier, 1973; Puizer, 1976; Ghosh et al., 1970; Krishnaswamy, 1972; Woodall, 1975; Woodall, 1962a, 1962b; Grinblitz, 1964; Viljoen et al., 1969, 1970, 1978; Pye and Roberts, 1981; Anhaeusser, 1976a, 1976b; Anhaeusser et al., 1975; Patterson, 1984.
Gold occurs in stock-work vein-lets associated with chalcopyrite, bornite, or arsenopyrite or as inclusions in disseminations of the above minerals, or propylitic alteration.	50-1000x10 <sup>6</sup> tonnes ore; 0.5-3 ppm Au; 0.4-1.0% Cu; 0.02-0.2% Mo	Gold mineralization is centrally located in cores of potassium silicate alteration. The gold mineralization may in turn be surrounded by a molybdenum rich zone and or a zone of sericitic	Harris, 1979; Sillitoe, 1979; 1980; 1982; Nash, 1976.
Mineralization occurring generally in volcanoclastic sequence in transition zone from mafic to felsic volcanism and in sediments occurring in local structural depressions in the volcanic pile.	3-11x10 <sup>6</sup> tonnes, Zn; 0.5-2x10 <sup>6</sup> tonnes, Cu; 25-480x10 <sup>3</sup> tonnes, Pb; 3-200 tonnes, Au; 0.5-15x10 <sup>3</sup> tonnes, Ag; 0.14-3.7 gm/tonne, Au; 7-70 gm/tonne Ag	Ore bodies include sulfide and gold disseminations in volcanoclastic rocks and sediments. Massive sulfide lenses may be up to tens of meters in thickness and continuous for several thousand meters on strike.	Koo and Mossman, 1975; Suffel et al., 1971; Marulick et al., 1974; Spence & de Kozenspence, 1975; Roberts, 1975; Martin, 1957; Staff, Engineering Mining Jour., 1977; Thuzlow, 1975; Thompson & Panteleyev, 1976; Albers, 1966, Staff, Engineering Mining Jour., 1977; Skillinga, 1976; Magnuson, 1970; Peltola, 1978; Strauss et al., 1977; Schmalz, 1972; Cissarz, 1957; Ima, 1978; Reid, 1975.
High angle complex fault systems provide conduits for fluid. Ore shoots are usually much smaller than the vein structure and include dilational zones in bends in the fault zones in vein inter-sections, and in area of dip decrease.	4-300 tonnes Au; 11-50x10 <sup>3</sup> tonnes Ag; 2-34 gm/tonne Au; 6-1000 gm/tonne Ag.	Ore bodies include fracture fillings and replacement in either volcanic flow rocks or a hypabyssal intrusive. Alteration mines include propylitic, potassic, argillic, phyllic, alunitic, and silicic with ore shoots generally associated with silicic and alunitic alteration. Ore shoots associated with boiling or effervescent CO <sub>2</sub> fluids; limited to a 200 meter vertical interval with horizontal vertical ratios of 16:1 to 1:1. Vein width average less than 10 meters.	Armbrustmacker and Wruicke, 1979; Ashley, 1974, 1975, 1979; Ashley and Keith, 1978; Ashley & Silberman, 1976; Bethke & Rye, 1979; Buchanan, 1981; Casadevall, and Okamoto, 1977; Foley et al., 1982; Hayba, 1983. Heald-Welaufer et al., 1983; Kamilli and Okamoto, 1977; Keeler, 1978; Lipman et al., 1976; Lipman and Steven, 1976; McKee, 1979; O'Neil et al., 1973; Rye et al., 1970; Rynba, 1981; Silberman, 1982; Silberman and Chesterman, 1972; Silberman and McKee, 1974; Sillitoe, 1977; Slack, 1980; Steven and Eaton, 1975; Taylor, 1973.

Table 11.1 (Continued)

Gold Deposit Type	Examples	Elemental Associations	Host Rock Associations	Ore Mineralogy	Gangue Mineralogy	Age of Host
5a. Gold Skarns	Nabesna Mine, Alaska	Au, As	Limestone, dolomite intruded by dioritic to quartz monzonitic I-type, stocks and batholiths	Arsenopyrite (tr), chalcopyrite (tr), galena, gold, hematite, magnetite, marcasite, pyrite, pyrrhotite, sphalerite, stibnite (tr)	Andradite-hessonite, actinolite, angelite, apatite, calcite, cerussite, diopside-hedenbergite, epidote, gypsum, limonite, perennite, quartz, rutile, serpentinite, sphene, spinel, thuringite, vesuvianite, wollastonite	Lower Paleozoic to Triassic
5b. Copper-gold Skarns	Whitehorse Copper Mine, Yukon Terr.	Cu, Au	Limestone, dolomite, included by dioritic to quartz monzonitic I-type, stocks and batholiths	Bornite, chalcocite, chalcopyrite, gold, hematite, magnetite, pyrite	Actinolite, andraditic garnet, chlorite, diopside pyroxene, epidote, forsteritic olivine, serpentine, tremolite, wollastonite	Lower Paleozoic to Triassic
5c. Tungsten-gold skarns and tungsten-gold stockwork veins with or without granitic stocks	Muruntan, Uzbek, SSR; Zarmitan, Uzbekistan, SSR; Moose River, Nova Scotia	W, Au, F, Bi, Mo	Limestone, dolomite, S-Type and/or ilmenite type granite	Arsenopyrite, bismuthinite, gold, magnetite, molybdenite, pyrrhotite, pyrite, scheelite, wolframite	Actinolite, albite, biotite, chlorite, diopside-hedenbergite, fluorite, grossular-andradite, graphite, microcline, quartz, sericite, tourmaline	Lower Paleozoic to Triassic
6. Tin Greisen-Gold Quartz Veins	Richardson Dist., AK; Yana-Kolyma Belt, Siberia; Circle Dist., AK; Tofty Dist., AK; Steese Dist., AK	Su, Be, Li, F, Rb, Mo, Au	Clastic and carbonate rocks	Arsenopyrite, cassiterite, fluorite, galena, gold, magnetite, pyrite, pyrrhotite, scheelite, sphalerite	Chlorite, quartz, tourmaline	Lower Paleozoic to Triassic
7. Carlin type, sediment-hosted gold	Carlin, Cortez, Gold Acres, Getchell, Pinson-Preble, Northumberland, Manhattan, Mariboro Canyon, and Windfall, NV; Mercur, Utah; Livengood, Tolovana Dist, AK	Au-Ag-As-Sb-Hg-W-Tl	Dolomite, siltstone, silty limestone.	Gold, pyrite, arsenopyrite, orpiment, realgar, stibnite, cinnabar, barite, sphalerite (tr), galena (tr).	Quartz, sericite, kaolin, carbonate, illite, montmorillonite, & organic carbon.	Cambrian to Devonian
8. Paleoplacer	Witwatersrand, S. Africa; Sierra Nevada, CA; Lao Medulas, Spain; Tertiary Basins, AK including Crooked Creek, Circle Mining District	Au	Continental clastics including conglomerate and sandstone	Ore minerals arsenopyrite, cassiterite (tr), gold, magnetite, pyrite, scheelite (tr), rutile, wolframite (tr)	Gangue minerals, garnet, sphene, tourmaline, zircon	Proterozoic to Tertiary

Table 11.1 (Continued)

Age of Mineralization	Sulfur Isotope Ratios	Hydrogen/Oxygen Isotope Ratios	Lead/Lead Isotope Ratios	Type	Salinity	Fluid Inclusions Temp. Hom. Temp. Trap.		Regional Structural Setting
Jurassic to Cretaceous								Continental margin associated with late to post orogenic magmatism
Jurassic to Cretaceous				H <sub>2</sub> O+ NaCl (liq-vapor)	20-45 wt% NaCl equiv.	160-500°C	200-550°C	Continental margin associated with late to post orogenic magmatism
Jurassic to Cretaceous				H <sub>2</sub> O+ CO <sub>2</sub> + NaCl	5-15 wt% NaCl Equiv.	350-400°C	450-500°C	Syn to late orogenic magmatism at compressive plate margins
Jurassic to Cretaceous				H <sub>2</sub> O- NaCl (liq-vapor) boiling	5-40 wt% NaCl Equiv.	170-530°C	~200-600°C	Accreted/continental-continental collision belts associated with anatectic S-type granitoids
Younger than host.		δD, -150 per mil. δ <sup>18</sup> O, 3 to 6 per mil.		H <sub>2</sub> O- CO <sub>2</sub> - NaCl (liq-vapor)	5-15 wt% NaCl equiv.	250-350°C	300-400°C	Intrusive hosts often near major thrust and high angle faults
Proterozoic to Tertiary								Graben generated sedimentary basins

Table 11.1 (Continued)

Local Structural Control	Tonnage/Grade or Contained Metal	Comments	References
Irregular ore bodies of Fe-sulfides or veins in carbonate or calcareous sediments	0.01 to 50 x 10 <sup>6</sup> tonnes ore at 3 to 40 gm/tonne Au	Three types of ore bodies: (1) magnetite + pyrite + calcite + gold (2) "veins" of pyrrhotite + pyrite + gold (3) "veins" of auriferous pyrite + calcite	Mairant, 1988; Einaudi et al., 1981.
Irregular ore bodies in carbonate or calcareous sediments	0.25 to 25x10 <sup>6</sup> tonnes ore at 0.7 to 4.0% Cu, 0.4 to 2.8 gm/tonne Au, 2.5 to 100 gm/tonne Au	Gold associated with chalcopyrite, vallerite and in retrograde skarn assemblage	Einaudi et al., 1981.
Contact zones in carbonate rocks	0.1 to 25x10 <sup>6</sup> tonnes ore at 0.3 to 1.8% WO <sub>3</sub> H-1000 tonnes Au (Mauritanian)	Most tungsten skarns devoid of gold. Tungsten-gold stockworks highly variable gold content	Rakhmatullayev and Sher, 1969.
Veins in splices of granitic cusps, lithologic contacts, vein intersections, cross faults	0.25 to 10x10 <sup>6</sup> tonnes ore at 0.7 to 2.3% Sn	Cassiterite and gold-quartz veinlets, stockworks and breccia pipes in quartzized intrusive and in contact zone	
High angle faults generally provided conduits for the low to moderate temperature ore forming fluids and most ore replacements are associated with the hanging walls of these structures.	10-160 tonnes Au, 3-7 grams/tonne.	Ore bodies include tabular or irregular replacement with attitudes similar to the host rocks or as pipe-like and vein type ore bodies spatially related to high angle faults. Alteration envelope include illitization, sericitization, kaolinitization and carbonation.	Dickson et al., 1975a, 1975b, 1979; Harris and Radtke, 1976; Hayba, 1983; Nash, 1972; Noble and Radtke, 1978; Radtke, 1976a, 1976b; Radtke et al., 1972a, 1972b, 1980; Roberts et al., 1971; Roedder, 1984; Wango, 1979.
Heavy mineral concentrates near basal contact	1-100x10 <sup>6</sup> tonnes of ore at 1-10 gm/tonne Au	Tabular and elongate bodies in sedimentary structures indicating changes in hydraulic gradients	

are recognized in the Fairbanks district or adjacent areas.

Skarn deposits are not major sources of gold in North America; however the large gold deposit at Muruntau, Uzbekistan, USSR is a skarn (Rakhmanullaev and Sher, 1969). This deposit may contain as much as a 1,000 tonnes (1,100 tons) of Au. However the tungsten-gold skarns in east-central Alaska appear to be small.

### 11.3.6 Tin Greisen-Gold-Veins

The Birch Lake pluton occurrence in the Richardson district is an example of this type of (tin greisen-gold-vein) mineralization. This type is a source of gold production in the eastern extremes of the Soviet Union. It is not a source of gold production in North America and neither this example nor the numerous tin greisens in the Steese district are known to contain near economic gold grades.

### 11.3.7 Carlin-Type Sediment-Hosted Gold

The mineral occurrences in the Gertrude Creek and Ruth Creek areas of the Tolovana district may be sediment-hosted gold deposits. The host rocks to gold anomalies are Devonian carbonaceous siltstones and are thus similar in age and composition to the sediment hosted gold deposits of Nevada. Unfortunately these occurrences are poorly described, thus the existence of this mineral deposit type in the Tolovana district is open to question and unproven.

The area is a major source of placer gold but lode sources are not well documented. If sediment-hosted gold mineralization could be demonstrated, it may account for the estimated 400,000 troy ounces of production and the estimated 600,000 troy ounces of indicated reserves in the placer deposits. Carlin-type deposits elsewhere contain between 300,000 and 5,000,000 troy ounces of gold.

### 11.3.8 Paleoplacers

The Tertiary section on Crooked Creek in the Circle district is an example of a paleoplacer occurrence that is a current source of gold production. Tertiary terrestrial clastic sediments are documented in each of the districts considered herein except the Steese and the Richardson. Tertiary terrestrial sediments are potential hosts to a Las Medulas (Spain) size paleoplacer deposit. It is estimated that the Las Medulas deposit produced at least 1,000 tonnes (1,100 tons) of Au. Other analogues of this type of mineralization include the Grass Valley region of California and the Tertiary basins of northern Columbia. Total production from each of these areas is estimated in excess of 1,000 tonnes (1,100 tons).

## 11.4 SUMMARY BY MINING DISTRICT

### 11.4.1 Circle Mining District

The Circle district contains 13 mineral occurrences. These include metamorphosed volcanic-exhalative, epithermal vein, tin greisen-gold-quartz vein, and paleoplacer

type mineralization. The intrusive related epithermal vein model is the most probable deposit type to result in large scale gold production.

### 11.4.2 Steese Mining District

The Steese district contains 15 mineral occurrences. These include metamorphosed volcanic-exhalative, epithermal vein, and tin greisen-gold-quartz vein type mineralization. The intrusive related epithermal vein model is the most probable deposit type to result in large scale gold production.

### 11.4.3 Richardson Mining District

The Richardson district contains 7 mineral occurrences. These include epithermal vein, tungsten-gold skarn, and tin greisen-gold-quartz vein type mineralization. The intrusive related epithermal vein model is the most probable deposit type to result in large scale gold production.

### 11.4.4 Tolovana Mining District

The Tolovana district contains 17 mineral occurrences. These include metamorphosed volcanic-exhalative, copper-molybdenum-gold porphyry, precious metal enriched massive sulphides, epithermal vein, Carlin-type sediment-hosted gold, and paleoplacer type mineralization. Any of these deposit types could result in large scale gold production.

### 11.4.5 Kantishna Mining District

The Kantishna district contains 98 mineral occurrences. These include metamorphosed volcanic-exhalative, precious metal enriched massive sulphides and paleoplacer type mineralization. Any of these three deposit types could result in large scale gold production.

### 11.4.6 Fairbanks Mining District

The Fairbanks district contains 202 mineral occurrences. These include metamorphosed volcanic-exhalative, precious metal enriched massive sulphides, epithermal vein, tungsten-gold skarn, and paleoplacer type mineralization. With the exception of the tungsten-gold skarn, all the deposit types could result in large scale gold production.

## 11.5 SUMMARY AND CONCLUSIONS

Placer gold deposits account for the majority of metallic mineral production in the Fairbanks district and adjacent areas of east-central Alaska. There is evidence that there may be at least eight different types of lode source deposits for the placer mineralization. These eight distinct types include all six of the deposit types that account for the vast majority of the worldwide gold production. The Fairbanks district and the Tolovana district each with five of the eight deposit types, and thus have the greatest potential for large tonnage gold production.

---

---

## CHAPTER 12

### ECONOMIC ANALYSIS OF MAJOR MINERAL DEPOSIT TYPES IN THE FAIRBANKS MINING DISTRICT

#### 12.1 INTRODUCTION

Mineral exploration and regional resource evaluation based solely on generalized genetic ore deposit and tonnage/grade models is subject to several serious constraints. The most severe is the uncertainty that the expected tonnage and grade will warrant development under the prevailing economic conditions. Reducing this uncertainty in the early stages of exploration and evaluation decreases project risk and thus increases the return on exploration investment.

The following are two pre-feasibility studies for the Fairbanks mining district. The investigations provide order of magnitude estimates of the economic viability of two types of mineralization under varying conditions of tonnage and grade. Since mine feasibility is generally most sensitive to these two parameters and metal price (Calvin, 1985), these will be the only variables adjusted in this investigation.

Mining activity and mineral exploration in the district have been focused primarily on gold occurrences. Most of the past production has come from placer deposits, and considerable potential exists for the exploitation of deep placers and possibly bench placers. However the greatest economic potential exists for the development of lode deposits. Past lode production has come from narrow quartz vein deposits, and the extent of this type of mineralization is potentially large. Disseminated gold mineralization occurs in three distinctive types of occurrences; these too are potential sources of large quantities of metal.

The following includes pre-feasibility studies for a gold-quartz vein deposit developed by underground mining methods, and a disseminated gold deposit exploited by open pit methods. The normal procedure for an order-of-magnitude pre-feasibility study is to assume a target tonnage and grade, use a rule of thumb estimate for mine life, estimate capital and operating costs, and calculate a rate of return on investment at various metal prices. The rates of return are then plotted against metal prices.

This procedure assumes that the deposit under exploration and evaluation will fit the pre-feasibility tonnage and grade model. This is seldom the case in the early stages of evaluation. What is more useful to the project decision makers at this stage is the estimation of the economic tonnage and grade of the deposit type under evaluation at the specific site. If this tonnage and grade curve is significantly different from the average for the deposit type or is significantly different from the curve developed for the deposit, then decision makers can determine the appropriate course of action.

The following pre-feasibility studies develop tonnage and grade curves for the two deposit types based on cost

estimates appropriate for the Fairbanks area and a 20 percent required rate of return on investment. Minimum mine lives of 20 years are assumed for both deposit types. Acquisition costs are to be paid as a 4 percent net smelter return (NSR) royalty over the life of the mine.

#### 12.2 DISSEMINATED GOLD DEPOSITS

Types IC, ID, IE, IIA, and IV mineralization can be described as disseminated mineralization. Economic deposits of disseminated gold mineralization are generally developed by open pit mining methods. The above deposit types in the Fairbanks district can be expected to be developed by such methods.

Type I occurrences in the Cleary Summit area can be expected to have stripping ratios between 1:1 and 4:1 although some, such as the Tolovana occurrence, are well exposed at the surface. Type II and IV occurrences can be expected to have stripping ratios greater than 4:1.

The mine feasibility of a disseminated deposit is investigated at mining rates of 1,000, 2,000, 4,000, 8,000, and 12,000 tonnes per day (1,100, 2,200, 4,400, 8,800, and 13,200 tons per day). Mining is by conventional drilling and blasting, with pit walls developed at a 45 degree slope and a stripping ratio of 1:1. For the smaller operations, (less than 2,000 metric tonnes per day (mtpd)) blast hole drilling is completed by percussion-type drills, while in the larger scale operations, blast hole drilling is accomplished with rotary electric drills. Loading is done with front-end loaders in the smaller operations and is undertaken in the larger operations with electric shovels. Haulage is with 50-tonne rock trucks for the smaller operations. Truck size increases to a maximum of 150-tonne for the largest scale operation. A mining recovery rate of 95 percent is assumed.

Ore mineralogic and petrologic examinations of the various types of ores indicate significant compositional and textural differences that affect mineral recovery. The design of a mineral beneficiation flowsheet for these ores must take into account:

1. A gold grain size, ranging from one micron to several millimeters,
2. Gold occurring as free-milling grains and as inclusions in arsenopyrite,
3. Sulphide contents are up to 50 percent in the Type I ores but less than 1 percent in Type II and IV ores,
4. Complex mineralogy of the sulphides in Type I ores.

A flowsheet for the processing of the sulphide ores is much more complex than one for the processing of Type II and IV ores. The one for sulphide ores is for a beneficiation facility that has both high capital and operating costs. Utilizing such a flowsheet for plant design will ensure maximum flexibility in ore processing and a relatively conservative cost estimate if the final feasibility indicates such a plant is not required.

A generalized mill flowsheet includes crushing, grinding, gravity concentration, conditioning, thickening, flotation (to give a bulk sulphide concentrate), filtration, carbon-in-pulp (CIP) leaching of flotation tailings, precipitation, and

refining. The flowsheet is developed through limited bench scale tests, bulk sampling, and custom milling in a CIP circuit. This flowsheet applies to disseminated and high grade gold-quartz ores. A mineral beneficiation recovery rate of 90 percent is assumed.

### 12.2.1 Mining and Milling Cost Analysis

Sources of mining cost data include local union published wage rates, local equipment supplier cost quotations, and various published cost estimating guides such as Schumacher (1990), Mular (1982), and Clement et al (1978). The data are adjusted for the Fairbanks area by a geographic factor. The capital and operating costs for the surface mining and milling are summarized in Table 12.1.

### 12.2.2 Cash Flow Analysis

A price of gold of \$350 per troy ounce is assumed for the life of the operation. Costs are estimated to remain constant over the mine life. Thus there is no expected differential inflation over the project period. This assumption is justified by the fact that over the past fifty years the composite metal price and the wholesale price indices in the United States have increase at the same rate.

For each daily mining rate an average grade is estimated that will produce sufficient cash flow to result in a 20 percent return on invested capital. A tax rate of 42 percent (34 percent federal and 8 percent state) is assumed. Straight line depreciation is used with a seven year life for the mining equipment. The total mining capital investment is repeated in years 7 and 14 with no salvage value at the end of the project. Other deductions from revenue, in addition to operating expenses, include a 4 percent NSR royalty (property acquisition cost),

a one percent refining expense, and a depletion allowance of 15 percent. An example for the cash flow calculations is given in Table 12.2.

Table 12.2 Calculation of annual positive cash flow for open pit gold mining operation in the Fairbanks district, Alaska.

Assumptions: average grade 0.22 OPT; price of gold \$350 per troy ounce; straight line depreciation; 15 percent depletion allowance, effective tax rate of 42 percent.

Gross Revenue	\$ 23,042,250
Operating Cost	9,677,500
Net Revenue	13,364,750
Royalty	921,690
Smelting and Refining	230,423
Depletion	3,456,338
Depreciation	3,639,571
Taxable Income	5,116,728
After Tax Net Income	2,967,702
After Tax Cash Flow	\$ 10,063,611

### 12.2.3 Discussion

The calculated grades for each mine capacity are plotted on Figure 12.1. The tonnage and grade curve indicates that economic grades range from 0.22 OPT at 1,000 tonnes (1,100 tons) per day to 0.09 OPT at 12,000 tonnes per day. These daily mine capacities require reserves of 9,000,000 tonnes

Table 12.1 Surface mining and mineral beneficiation capital and operating costs for disseminated gold mineralization in the Fairbanks mining districts, Alaska

	Mine Capacity (metric tonnes per day)				
	1,000	2,000	4,000	8,000	12,000
<b>Underground Mining</b>					
Capital costs (\$)	5,779,000	7,682,000	11,787,000	17,616,000	23,726,000
Operating costs (\$)	3,102,000	4,725,000	5,369,000	9,084,000	12,929,000
Cost per tonne (\$)	8.86	6.75	3.84	3.24	3.08
<b>Milling</b>					
Capital costs (\$)	19,698,000	29,505,000	45,470,000	70,307,000	91,796,000
Operating costs	6,577,000	10,558,000	16,896,000	28,862,000	38,664,000
Cost per tonne (\$)	18.79	15.08	12.07	10.31	9.21
<b>Total cost per tonne (\$)</b>	<b>27.65</b>	<b>21.83</b>	<b>15.91</b>	<b>13.55</b>	<b>12.29</b>

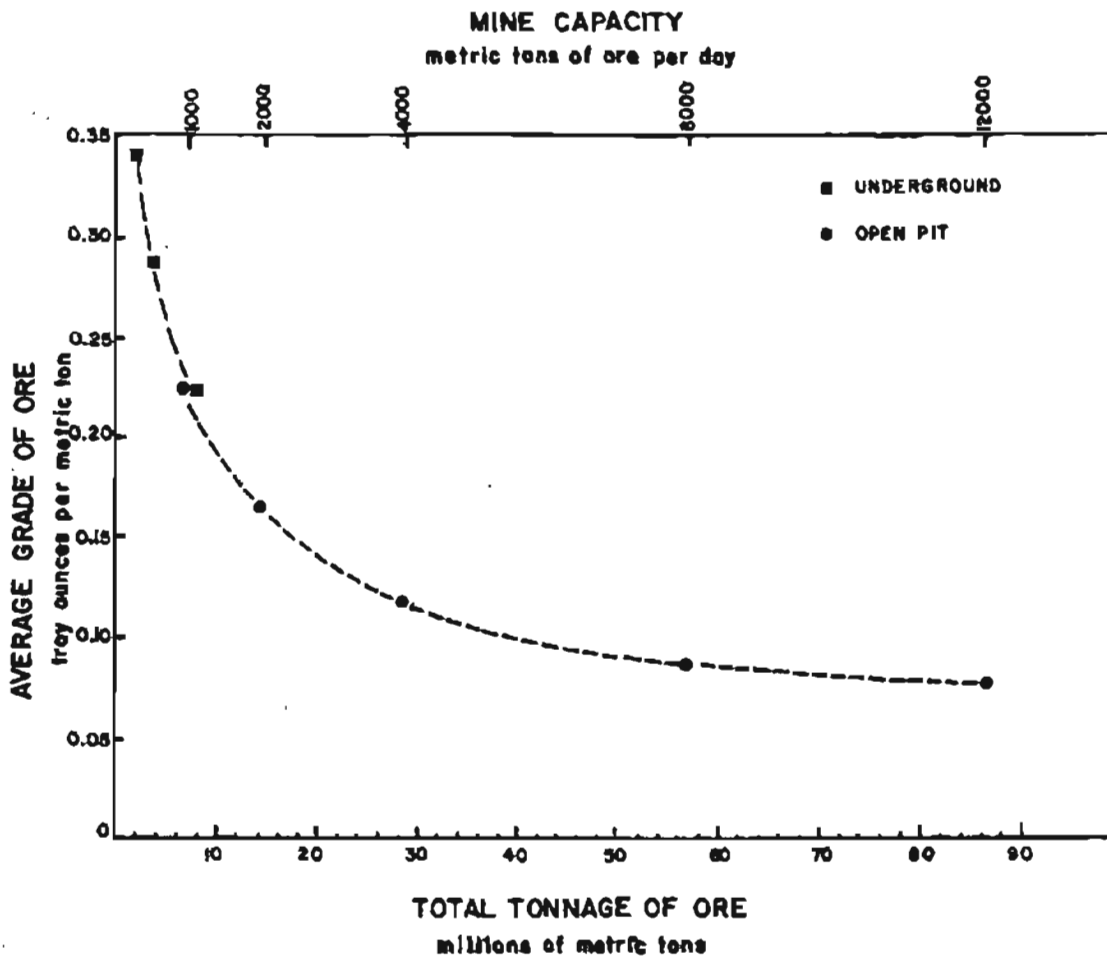


Figure 12.1 Tonnage - grade curve for underground and open pit mine models with a 20 percent internal rate of return on investment.

(9,900,000 tons) and 88,000,000 tonnes (96,800,000 tons) respectively.

Cox and Singer (1986) provide cumulative frequency curves for tonnages and for grades of numerous mineral deposit types. There are two serious problems associated with the use of these data for resource evaluation. First, the cumulative frequency curves are not tonnage and grade curves, and grades that correspond to a particular tonnage cannot be determined from the data. Furthermore the assumption cannot be made that grade and tonnage are inversely related. Thus the lowest grade on the cumulative frequency curve does not correspond to the largest tonnage on the cumulative frequency curve.

Second, the data base in Cox and Singer (1986) does not include an analogue of Type I or Type IV disseminated mineralization. Type II mineralization may correspond to their Hot Springs Au-Ag model, however the data base does not include tonnage and grade data for this mineral deposit model.

The genetic ore deposit models in Chapter 11 include two deposit types that have tonnages and grades comparable

with those calculated for the disseminated gold mineralization of the Fairbanks district. The Carlin-type gold and the epithermal vein model both have tonnages and grades that correspond to the calculated tonnages and grades. Thus in terms of tonnage and grade these are permissible models that can be guides in exploration and evaluation.

The calculated tonnage and grade curve indicates tonnages and corresponding grades greater than any measured reserves in the district. Maximum grade in the disseminated mineralization is 0.25 OPT and the average is much less than 0.22 OPT. From the surface to 15 meters (50 feet), the footwall zones of the major vein systems may average 0.075 OPT over considerable strike lengths. Combining the disseminated footwall zones with the high grade gold-quartz veins greatly increases the average grades. For instance, adding the high grade zone to the footwall zone of the Christina vein gives a grade of 0.13 OPT over a 15 meter (50 foot) width. In the Cleary Summit area the vein systems, such as the Christina vein, have an aggregate strike length of over 22,000 meters (72,000 feet). Assuming a 15 meter (50 foot) average width, these vein system may contain an aggregate of

15,000,000 tonnes (16,500,000 tons) to a depth of 15 meters (50 feet). These grades and contained gold are comparable to the grades and tonnages of Carlin-type and epithermal vein deposits.

As an alternative, a combination of conventional milling of the smaller tonnages of high grade gold-quartz vein ores and heap leaching of the near surface oxidized disseminated footwall mineralization may produce a higher rate of return on investment than conventional milling of both ore types. This alternative should be investigated.

It is important to note the sensitivity of the rates of return on investment and thus the required ore grades and tonnages to the price of gold. At \$400 per troy ounce, the required grade decreases to 0.06 OPT at 88,000,000 tonnes. At \$450 per troy ounce, the required grade decreases to approximately 0.05 OPT at the same tonnage.

It is also important to note that this sensitivity decreases as the grade approaches the lower limit that is as the curve in Figure 12.1 begins to approach a horizontal asymptote. Thus as tonnages approach 15 to 20 million tonnes the project feasibility becomes much less sensitive to total tonnage.

### 12.3 VEIN TYPE GOLD DEPOSITS

Type IV mineralization includes narrow and relatively steeply dipping vein structures that extend from the surface to at least 300 meters (1,000 feet). Vein widths range from 15 cm to 4.6 meters (6 inches to 15 feet). The narrow veins are in wider shear zones that may pose some ground stability problems. These deposits are amenable to either square set timber or cut-and-fill mining methods. The latter, being more cost effective, is the method to be employed in this investigation.

Mining rates of 250, 500, and 1,000 tonnes per day (275, 550, and 1,100 tons per day) are assumed. The deposits are accessed by adits. Mining equipment includes jackleg drills and stopers for production development and small jumbo drills for drift development. Slushers move ore from the stopers to ore chutes, and load-haul-dumps move ore from the chutes to ore storage.

Mineral beneficiation includes crushing, grinding, gravity concentration, and CIP leaching. This flowsheet is identical to the Grant mill circuit which was used for the bulk testing of Christina ore. Mineral beneficiation recovery is estimated at 95 percent.

#### 12.3.1 Mining and Milling Cost Analysis

For the analysis of mining and milling costs, the sources of the cost data are the same as those used for the open pit operation. The cost data are summarized in Table 12.3.

#### 12.3.2 Cash Flow Analysis

The cash flow analysis is conducted with the same assumptions and in the same manner as that for the open pit operation. An example of the cash flow calculations is given in Table 12.4.

Table 12.3 Underground mining and mineral beneficiation capital and operating costs for gold-quartz vein mineralization in the Fairbanks mining district, Alaska.

	Mine Capacity (metric tonnes per day)		
	250	500	1,000
Underground Mining			
Capital costs (\$)	4,917,000	7,157,000	10,108,000
Operating costs (\$)	5,853,000	10,435,000	14,216,000
Cost per tonne (\$)	65.03	57.97	39.49
Milling			
Capital costs (\$)	6,338,000	11,037,000	19,698,000
Operating costs	2,475,000	3,825,000	6,577,000
Cost per tonne (\$)	27.50	21.25	18.79
Total cost per tonne (\$)	92.53	79.22	63.17

Table 12.4 Calculation of annual positive cash flow for underground gold mining operation in the Fairbanks district, Alaska.

Assumptions: average grade 0.45 OPT; price of gold \$350 per troy ounce; straight line depreciation; 15 percent depletion allowance, effective tax rate of 42 percent.

Gross Revenue	\$ 11,782,969
Operating Cost	8,328,000
Net Revenue	3,454,969
Royalty	471,319
Smelting and Refining	117,830
Depletion (1)	1,432,910
Depreciation	1,607,857
Taxable Income	
After Tax Net Income	2,865,547
After Tax Cash Flow	\$ 2,865,547

Note: (1) Fifty percent rule in effect

#### 12.3.3 Discussion

The calculated grades required for each mine capacity are also plotted on Figure 12.1. The tonnage and grade curve indicates that economic grades range from 0.45 at 250 tonnes per day (275 tons per day) to 0.22 at 1,000 tonnes per day (1,100 tons per day). These daily mine capacities require reserves of 1,000,000 tonnes (1,100,000 tons) and 9,000,000 tonnes (9,900,000) respectively.

These tonnages are comparable to the upper ten percentile of the tonnages of the low sulphide gold-quartz vein model in Cox and Singer (1986). The grades are in the lower fifty percentile of the model, thus there is a moderate probability of the economic deposits in the district attaining the model tonnage and a very high probability of the deposits attaining

the model grades. This model is the same as the metamorphic vein model discussed in Chapter 11.

The calculated tonnage and grade curve indicates tonnages greater than that for any measured reserves in the district but calculated grades are one half to one third drill indicated grades. The drill indicated and inferred grade in the Christina system is 0.6 OPT while the corresponding tonnage is 360,000 tonnes (400,000 tons). This tonnage is based on near surface drilling and it is reasonable to expect additional reserves are available for discovery in the Christina system as well as in the other veins.

## 12.4 CONCLUSIONS

The two pre-feasibility analyses provide exploration and evaluation target tonnage and grade models. These models indicate that there is a reasonable expectation of the discovery of economic disseminated gold mineralization and a high probability of the discovery of economic gold-quartz vein mineralization in the Fairbanks district. The economic viability of the disseminated mineralization may be enhanced by selective mining and a combination of conventional mineral beneficiation and heap leaching.

---

# CHAPTER 13

## SUMMARY, CONCLUSIONS, AND RECOMMENDATIONS

### 13.1 SUMMARY

Prior to this investigation there were 188 known lode mineral occurrences in the Fairbanks mining district. These occurrences were considered to be either narrow discontinuous vein type deposits or tungsten skarn mineralization. The origin of both deposit types was thought to be the Cretaceous age granitic rocks that intrude the metamorphic rocks of the Yukon-Tanana Terrane. The economic potential of these veins and skarns was considered small.

This investigation has demonstrated that there are at least five types of gold mineralization in the Fairbanks district and an additional three other types of gold bearing deposits in the nearby mining districts. In the Fairbanks district these deposit types include metamorphosed volcanic-exhalative mineralization and associated shear zone hosted gold-quartz vein deposits; precious metal enriched volcanogenic massive sulphide occurrences; gold-quartz vein stockworks in intrusive rocks; tungsten skarns with minor gold-quartz veins; and paleoplacer mineralization.

The metamorphic and intrusive rocks of the Circle mining district contain similar types of mineralization to the Fairbanks district, with two exceptions. First, tungsten skarn mineralization is not recognized in the Circle district. Tungsten bearing minerals are present in the alluvial deposits, however, in most cases the alluvial material only contains metamorphic rock fragments and no indications of either skarn mineral assemblages or intrusive rock types. Second, tin greisen

mineralization is present in the Circle district but not in the Fairbanks district. The tin greisens in the Circle district contain visible and thus anomalous gold concentrations. The Circle district has only 13 known mineral occurrences but it is the second largest placer producing area after the Fairbanks district.

The Steese district contains metamorphosed volcanic-exhalative mineralization, intrusive related epithermal vein mineralization, and tin greisen-gold-quartz vein occurrences. The volcanic-exhalative mineralization in the Steese district is minor compared to that in either the Fairbanks or Circle districts. There is more tin mineralization in the Steese district than in any of the other five districts.

The Richardson district is characterized by only intrusive related mineralization. Epithermal veins in the quartz porphyry phase of the Birch Lake pluton are the most probable target for a large scale deposit. Tin greisen veins with visible gold are present at one locality and inferred at another, based on pan concentrate geochemistry. Skarn mineral assemblages are present at several localities and may be more widespread than is apparent in outcrop.

The lower Paleozoic sedimentary rocks of the Tolovana district contain numerous gold anomalies. There is no well defined vein or intrusive sources for the mineralization, and thus it is inferred that the mineralization may be of the Carlin type. Other types of mineralization in the district include metamorphosed volcanic-exhalative, precious metal enriched massive sulphide, epithermal vein, copper-molybdenum-gold porphyry and paleoplacer deposits. The sediment hosted gold and porphyry deposit types are not found in the other five districts.

The Kantishna district contains metamorphosed volcanic-exhalative and associated vein mineralization, precious metal enriched massive sulphide, and paleoplacer deposits. The vein mineralization has a higher silver and base metal content than the vein mineralization of the Fairbanks district. The veins are structurally controlled and rather continuous along strike. After the Fairbanks district, the Kantishna district has the largest number of lode mineral occurrences. Although there is a large number of potential vein sources of the placer gold, the district is a relatively minor placer gold producing area. This is in marked contrast to the Circle district that has a small number of lode mineral occurrences but the largest placer gold production after the Fairbanks district.

The major alluvial placer deposits of the six districts generally occur in streams that show the effects of uplift, tilting of the drainage basin, and alteration of stream drainage patterns by stream capture. Economic paleoplacer accumulations of Tertiary age occur in the Circle district and are probable sources of some of the recent alluvial placers in that district as well as in the Fairbanks, Tolovana, and Kantishna districts.

The host rocks for the stratabound mineralization in the Kantishna-Fairbanks-Circle mineral belt are a bimodal volcanic and exhalative sequence that extends for at least 350 kilometers (210 miles) in a northeast-southwest direction.

The sequence is anomalous in arsenic, antimony, tungsten, gold, and silver. At several localities in the Fairbanks district the sequence contains ore grade gold mineralization (0.04 to 0.15 OPT) over 10 meter (32 foot) intervals. The sequence is host to major shear zone and included gold-quartz vein mineralization in the Fairbanks and Kantishna districts and minor gold-quartz vein mineralization in the Circle district.

The intrusive related gold mineralization in the Fairbanks, Circle, and Richardson districts is in shear zones that crosscut the intrusives and the surrounding metamorphic sequences. Preliminary evidence suggests that the fluids associated with the intrusive related gold mineralization are a mixture of magmatic and either metamorphic or meteoric fluids. There is no evidence that any of the phases of the intrusive complexes are enriched in gold.

In the Fairbanks district, the gold-quartz veins in the metamorphic rocks are relatively high grade (0.25 to 3.0 OPT Au) over 1.5 meter (5 foot) mining widths. The disseminated mineralization in the metamorphic hosted shear zones ranges up to 0.15 OPT Au over 15 meter (50 foot) widths and 0.10 OPT Au over 70 meter (225 foot) widths. The mineralization in the metamorphic hosts is laterally continuous for strike lengths in excess of 1,800 meters (6,000 feet). In the Cleary Summit area, the metamorphic hosted shears have an aggregate strike length of at least 22,000 meters (72,000 feet). Mineralization in the shear zones and included quartz veins is known to extend to a depth of at least 300 meters (1,000 feet) which is the maximum depth of drilling in the area. Shear zones in the intrusive rocks in the same area extend over a strike length of approximately 1,500 meters (5,000 feet).

## 13.2 CONCLUSIONS

The mineral potential of the Fairbanks district in particular and the other five districts in the northwestern portion of the Yukon-Tanana Terrane in general is considered large. There are over 350 known mineral occurrences in these districts outlined in Chapter 11. Each of these occurrences can be analogued with one of eight mineral deposit types. Each of these deposit types is capable of yielding between 300 and 1,000 tonnes (330 to 1,100 tons) of gold. The delineation in the area of a single large scale deposit of any one of these types could result in a gold reserve equivalent to the entire historic production of Alaska.

The probability of a mineral occurrence in a known mining district becoming an economic discovery is estimated at between 0.01 to 0.10 (Koulomzine and Dagenais, 1959; Bailey, 1964; Peters, 1978). Thus it is estimated that there are between 3.5 and 35 economic mineral occurrences in these six districts based on known mineral occurrences.

The total placer gold production of the Fairbanks district can be accounted for by the weathering and erosion of 100 meters (325 feet) of the known vein mineralization in the district assuming that the average grade of the eroded veins was the same as that of the existing remaining veins. The relatively coarse-grained gold in the quartz veins has a size distribution similar to the size of gold in the coarser headward parts of the placers, while the gold eroded from the dis-

seminated portions of the shear zones and in the stratabound mineralization probably resides in lower energy environments downstream from the historic placer workings. The potential for deeply buried fine-grained placer deposits is estimated to be large based on the high gold content of the metamorphic rocks and the shear zones. The discovery of a single Las Medulas size (greater than 1,000 tonnes of Au) placer or paleoplacer deposit can produce a gold reserve equivalent to the combined alluvial gold production of Alaska and the Yukon Territory. The potential is high for one or more such discoveries in one or more of the six districts.

Stream sediment and pan concentrate geochemistry is effective in the delineation of buried mineralization even in areas of extensive loess deposits. These geochemical techniques can also be used to assist in the definition of mappable lithologies in areas of limited outcrop.

Lithogeochemistry is important in the definition of potential host rocks for most types of mineralization. Shear zone mineralization is in part influenced by the bulk chemistry of the rocks to the extent that chemistry is related to the shear and compressive strength of the rocks. Trace element chemistry of the shear zone host rocks may influence the grade of the shear zone mineralization.

There appears to be a zonation of mineralization within the mining districts, between the districts, and on the regional scale of the Yukon-Tanana Terrane. In the Fairbanks, Circle, Richardson, and Kantishna districts where metamorphic lithologies predominate, the metal and mineral zonation appears to be related to lithologies rather than depths or temperature gradients.

The Spruce Creek, Cleary Creek, and Bonanza Creek sequences, although all host stratabound and stratiform mineralization, contain differing quantities of metal. The Spruce Creek sequence and the associated veins contain relatively high amounts of silver as evidenced by the wide variety of silver minerals and the high grade of the lode mineralization. The high silver content of the lodes is accompanied by high lead and moderately high zinc values.

The stratabound and stratiform mineralization of the Fairbanks district contains economic ore grades which are not known in the Kantishna district. The associated vein mineralization is relatively silver poor. The only silver bearing mineral phase in the Fairbanks district that is moderately abundant is argentiferous tetrahedrite.

In the Circle district, the stratabound mineralization has a relatively low sulphide mineral content. Gold is dominant over silver, and base metal sulphides are scarce. The only silver bearing phase is argentiferous tetrahedrite but it is not abundant in either the stratiform mineralization or in the veins.

The differences in metal content of the three districts may be in part related to differences in lithology. The Spruce Creek sequence includes a large section of rhyolitic flow rocks with lesser quantities of exhalative rocks than occur in the Cleary sequence of the Fairbanks district. Rhyolitic flow rocks are scarce in the Fairbanks district but volcanoclastic rocks and exhalites are common in the Cleary sequence.

Graphitic rocks occur in the Spruce Creek and Cleary sequences but are much thicker and more widely distributed in the Bonanza Creek sequence. The Bonanza Creek is dominated by exhalites and graphitic schists and only locally contains volcanoclastics. The mafic schist underlying the Bonanza Creek sequence is much thicker than the mafic schists in either the Fairbanks or Kantishna districts. Thus it is concluded that the metal zonation between the three districts is a function of differences in the volcanic and sedimentary environments during the syngenetic mineralizing event.

The regional metal zonation in the Yukon-Tanana Terrane is reflected in the paucity of gold mineralization in the terrane east of the Klondike district and the ubiquitous nature of gold mineralization to the west. The gold mineralization is associated with abundant arsenic and antimony bearing minerals. The major base metal mineralization in the terrane is east of the Klondike district. The base metal deposits are characterized by relatively low arsenic and antimony contents. Tin mineralization is limited to the northwestern extremity of the terrane and does not occur in abundance to the east of the Circle mining district. Copper mineral occurrences are noticeably absent in the northwestern margin of the terrane, but occur in the North American continental margin rocks of the Tolovana district.

The stratabound As-Sb-W-Au-Ag mineralization associated with both metamorphosed felsic and mafic volcanics is in a thick pelitic sedimentary sequence. This is suggestive of an early continental rifting and metallogenic event that was followed by the deposition of continentally derived clastic sediment. The prevalence of tin granites associated with the continental crustal rocks in a major thrust belt along the northwestern boundary of the terrane is indicative of a

subsequent continental-continental collisional event. The presence of porphyry type copper mineralization north of the thrust belt and in the southern portion of the terrane suggests that an earlier stage of oceanic subduction occurred prior to the continental collisional event. These are highly speculative conclusions concerning the regional metallogeny that need to be tested by additional research.

### 13.3 RECOMMENDATIONS FOR FUTURE INVESTIGATIONS

Additional detailed mineral deposit investigations need to be completed in the Fairbanks district as well as in the other five districts. Economic models should be developed for each mineral deposit type. Particular emphasis must be placed on incorporating tonnage and grade data in order to determine the economic viability of the deposit models.

The sensitivity of the economic models should be tested with respect to changes in metal price, mining and mineral preparation methods, secondary metal recovery, and geographic cost differentials in the region.

More definitive estimates of the probability of a discovery for the various deposit types within the districts and within the terrane would be beneficial for both the private sector mineral explorationists and the public sector land managers and resource policy decision makers. Probability estimates will be difficult to develop due to the difficulty in finding analogue areas with similar complex and superimposed mineralization.

Finally, the exploration and evaluation of these districts will be enhanced by the availability of regional geophysical data. Such data will both further contribute to the construction of ore deposit models and indicate potential target areas.

## REFERENCES CITED

- Abrams, C.E. and McConnell, K.I., 1984, Geologic setting of volcanogenic base and precious metal deposits of the West Georgia Piedmont: A multiply deformed metavolcanic terrain: *Econ. Geol.*, v. 79, p. 1521-1539.
- Adams, John, Zimpfer, G.L. and McLane, C.F., 1978, Basin dynamics, channel processes and placer formation: *Econ. Geol.*, v. 73, p. 416-426.
- Albanese, M.D., 1982a, Geochemical reconnaissance of the northern Fairbanks D-1 and southern Livengood A-1 Quadrangles, Alaska - summary of data on pan-concentrate, stream-sediment, and rock samples: Alaska Division of Geological and Geophysical Surveys Open-file Report 164, 26 p., 3 plates.
- Albanese, M.D., 1982b, Geochemical reconnaissance of the Fairbanks D-3 Quadrangle, Alaska - summary of data on stream-sediment, pan-concentrate and rock samples, Alaska: Alaska Division of Geological and Geophysical Surveys Open-file Report 166, 15 p., 3 plates, scale 1:63,360.
- Albanese, M.D., 1982c, Geochemical reconnaissance of the northern Fairbanks D-2 and southern Livengood A-2 Quadrangles, Alaska - summary of data on stream-sediment, pan-concentrate, and rock samples: Alaska Division of Geological and Geophysical Surveys Open-file Report 165, 23 p., 3 plates.
- Albanese, M.D., 1983a, Bedrock geologic map of the Livengood B-4 Quadrangle, Alaska: Alaska Division of Geological and Geophysical Surveys Report of Investigations 83-3, 1 pl., scale 1:40,000.
- Albanese, M.D., 1983b, Geochemical reconnaissance of the Livengood B-3, B-4, C-3, and C-4 Quadrangles, Alaska: Summary of data on stream-sediment, pan-concentrate, and rock samples: Alaska Division of Geological and Geophysical Surveys Report of Investigations 83-1, 55 p., 4 pl., scale 1:63,360.
- Albanese, Thomas, 1981, The valuation of mining feasibility of a deep gold placer near Livengood, Alaska: University of Alaska unpub. M.S. Thesis, 211 p.
- Aleinikoff, J.N., Dusel-Bacon, Cynthia, and Foster, H.L., 1981a, Geochronologic studies in the Yukon-Tanana upland, east-central Alaska, in Albert, N.R.D. and Hudson, Travis, eds., *The United States Geological Survey in Alaska: Accomplishments during 1979: U.S. Geol. Survey Circular 823-B*, p. B34-B37.
- Aleinikoff, J.N., Dusel-Bacon, Cynthia, Foster, H.L. and Futa, Kiyoto, 1981b, Proterozoic zircon from augen gneiss, Yukon-Tanana Upland, east-central Alaska: *Geology*, v. 9, no. 10, p. 469-473.
- Aleinikoff, J.N., Foster, H.L., Nokleberg, W.J. and Dusel-Bacon, Cynthia, 1984a, Isotopic evidence from detrital zircons for Early Proterozoic crustal material, east-central Alaska, in Coonrad, W.L. and Elliott, R.L., eds., *The United States Geological Survey in Alaska: Accomplishments during 1981: U.S. Geol. Survey Circular 868*.
- Aleinikoff, J.N., Dusel-Bacon, Cynthia and Foster, H.L., 1984b, Uranium-lead isotopic ages of zircon from sillimanite gneiss and implications for Paleozoic metamorphism, Big Delta quadrangle, east-central Alaska, in Coonrad, W.L. and Elliott, R.L., eds., *The United States Geological Survey in Alaska: Accomplishments during 1981: U.S. Geol. Survey Circular 868*, p. 45-48.
- Aleinikoff, J.N., Dusel-Bacon, Cynthia and Foster, H.L., 1986, Geochronology of augen gneiss and related rocks, Yukon-Tanana Terrane, east-central Alaska: *Geological Society of America Bulletin*, v. 97, p. 626-637.
- Aleinikoff, J.N. and Nokleberg, W.J., 1984, Early Proterozoic metavolcanic rocks in the Jarvis Creek Glacier tectonostratigraphic terrane, Mount Hayes C-6 quadrangle, Alaska, in Reed, K.M. and Bartsch-Winkler, Susan, eds., *The U.S. Geological Survey in Alaska, accomplishments during 1982: U.S. Geol. Survey Circular 939*, p. 40-44.
- Aleinikoff, J.N. and Nolkeberg, W.J., 1989, Age of deposition and provenance of the Cleary sequence of the Fairbanks schist unit, Yukon-Tanana Terrane, east-central Alaska: *U.S. Geol. Survey Bull.* 1903, p. 75-83.
- Allegro, G.L., 1987, The Gilmore Dome tungsten mineralization, Fairbanks mining district, Alaska: University of Alaska unpub. M.S. thesis, 114 p.
- Al-Rawi, Y., and Carmichael, I.S.E., 1967, Natural fusion of granites: *Amer. Miner.*, v. 52, p. 1806-1814.
- Anhaeusser, C.R., 1976a, Archaean metallogeny in southern Africa: *Econ. Geol.*, v. 71, p. 61-43.
- Anhaeusser, C.R., 1976b, The nature and distribution of Archean gold mineralization of South Africa: *Minerals Sci. Eng.*, v. 8, no. 1, p. 46-84.
- Anhaeusser, C.R., Fitze, K., Fyfe, W.S., and Gill, R.C.O., 1975, Gold in "primitive" Archaean volcanics: *Chem. Geol.*, 16, p. 129-135.
- Armbrustmacher, T.J. and Wrucke, C.T., 1979, The disseminated gold deposit at Gold Acres, Lander County,

- Nevada: in Lovering, T.G., and McCarthy, J.H., Jr. (eds.), *Conceptual models in exploration geochemistry: Jour. Geochem. Explor.*, v. 9, no. 2/3, p. 195-203.
- Armbrustmacher, Theodore, 1984, Rare-earth/thorium deposits associated with a complex of syenite rocks near Mt. Prindle, east-central Alaska: *Geological Society of America, Abstracts with programs*, v. 16, no. 5, p. 266-267.
- Arribas, A., 1984, Los Yacimientos de tungsteno de La Zona de Morille: *Separata de Boletín Geológico y Minero, Madrid*, 20 p.
- Ashley, R.P., 1974, Goldfield mining district, in *Guidebook to the geology of four Tertiary volcanic centers in central Nevada: Nevada Bureau of Mines and Geology Report 19*, p. 49-66.
- Ashley, R.P., 1975, Preliminary geologic map of the Goldfield mining district, Nevada: U.S. Geol. Survey Miscellaneous Studies Map MF-681.
- Ashley, R.P., 1979, Relation between volcanism and ore deposition at Goldfield, Nevada, in *International Association for the Genesis of Ore Deposits (IAGOD), 5th Quadrennial Symposium proceedings, Vol. II: Nevada Bureau of Mines and Geology Report 33*, p. 77-86.
- Ashley, R.P. and Keith, W.J., 1978, Goldfield mining district, Esmeralda County, Nevada, in Lovering, T.G., and McCarthy, J.H., Jr., eds., *Conceptual models in exploration geochemistry — The Basin and range province of the western United States and northern Mexico: Journal of Geochemical Exploration*, v. 9, p. 204-208.
- Ashley, R.P. and Silberman, M.L., 1976, Direct dating of mineralization at Goldfield, Nevada, by potassium-argon and fission-track methods: *Econ. Geol.*, v. 71, p. 904-924.
- Bailey, P., 1964, Methods, costs, land requirements, and organization in regional exploration for base metals: pre-print, American Institute of Mining Engineers, New York, 31 p.
- Barker, F., 1963, Exploration for antimony deposits at the Stampede Mine, Kantishna district: in *Contributions to the economic geology of Alaska: U.S. Geol. Survey Bull. 1155*, p. 10-17.
- Barker, J.C., 1979, A trace element study of the Circle Mining district, Alaska: U.S. Bureau of Mines, Open-file report no. 57-79, 57 p.
- Barker, J.C., and Clantice, K.H., 1977, Anomalous uranium concentrations in artesian springs and stream sediments in the Mount Prindle area, Alaska: U.S. Bureau of Mines Open-file Report 130-77, 19 p.
- Barnes, D.F., 1961, Gravity low at Minto Flats, Alaska, in *Short papers in the geologic and hydrologic sciences: U.S. Geol. Survey Prof. Paper 424-D*, p. D254-D258.
- Barton, P.B., 1969, Thermochemical study of the system Fe-As-S: *Geochim Cosmochim Acta*, v. 33, p. 841-857.
- Bates, R.G., and Wedow, Helmut, Jr., 1953, Preliminary summary review of thorium-bearing mineral occurrences in Alaska: *U.S. Geol. Survey Circ. 202*, 13 p.
- Bayley, R.W., 1972, A preliminary report on the geology and gold deposits of the Rochford district, Black Hills, South Dakota: *U.S. Geol. Surv. Bull. 1332-A*.
- Beistline, E.H., 1939, An examination and valuation of the Harry W. Woods gold mine, located on Twin Creek in the Fairbanks district, Alaska: University of Alaska unpub. B.S. thesis, 38 p.
- Bell, E.K., 1974, Origin of the auriferous clays in the Fairbanks area, Alaska: *Ariz. State Univ.*, unpub. M.S. thesis, 63 p.
- Bell, Henry, 1982, Strata-bound sulfide deposits, wall rock alteration, and associated tin-bearing minerals in the Carolina Slate Belt: *Econ. Geol.* v. 77, p. 294-311.
- Berg, H.C., and Cobb, E.H., 1967, Metalliferous lode deposits of Alaska: *U.S. Geol. Survey Bull. 1246*, 254 p.
- Berglund, S. and Ekström, T.K., 1980, Arsenopyrite and sphalerite as T-P indicators in sulfide ores from northern Sweden: *Mineralium Deposita*, v. 15, no. 2, p. 175-187.
- Bernasconi, A., 1985, Archaean gold mineralization in central eastern Brazil, a review: *Mineral. Depos.*, v. 20, p. 277-283.
- Bernier, Louis, et al., 1987, Geology and metamorphism of the Montauban North Gold Zone: A metamorphosed polymetallic exhalative deposit, Granville Province, Quebec: *Econ. Geol.* v. 82, p. 2076-2090.
- Bethke, P.M. and Rye, R.O., 1979, Environment of ore deposition in the Creede mining district, San Juan Mountains, Colorado: Part IV. Source of fluids from oxygen, hydrogen, and carbon isotope studies: *Econ. Geol.*, v. 74, p. 1832-1851.
- Blodgett, R.B., et al., 1987, A Late Ordovician age reappraisal for the Upper Fossil Creek Volcanics and possible significance for glacio-eustasy: in Hamilton, T.D., and Galloway, J.P., eds., *Geologic Studies in Alaska by the*

- U.S. Geological Survey during 1986: U.S. Geol. Survey Circular 998, p. 54-58.
- Blum, J.D., 1983, Petrology, geochemistry, and isotope geochronology of the Gilmore Dome and Pedro Dome plutons, Fairbanks mining district, Alaska: University of Alaska unpub. M.S. thesis, 107 p.
- Blum, J.D., 1985, A petrologic and Rb-Sr isotopic study of intrusive rocks near Fairbanks, Alaska: *Can. J. Earth Sci.*, v. 22, p. 1314-1321.
- Bottino, M.L. and Fullagar, P.D., 1968, The effects of weathering on whole-rock Rb-Sr ages in granitic rocks: *American Journal of Science*, v. 266, p. 661-670.
- Boyle, R.W., 1954, A decrepitation study of quartz from the Campbell and Negus-Rycon shear zone systems, Yellowknife, Northwest Territories, *Geol. Surv. Can. Bull.*, v. 30, 20 p.
- Bragg, J.G., 1967, Upper Canada Mine: in *Guidebook to C.I.M. Centen. Field Excursion, N.W. Quebec - N. Ontario*, p. 89-92.
- Bressler, J.B., 1984, Geochemical anomalies: in Thornsberry et al., eds., *Mineral resource studies in the Kantishna Hills and Dunkle Mine areas, Denali National Park and Preserve*: Salisbury and Dietz, Inc., 234 p.
- Britton, J.M., 1970, Petrology and petrography of the Pedro Dome plutons, Fairbanks, Alaska: University of Alaska unpub. M.S. thesis, 52 p.
- Brooks, A.H., 1905, Placer mining in Alaska in 1904: *U.S. Geol. Survey Bull.* 259, p. 18-31.
- Brooks, A.H., 1907, The mining industry in 1906: *U.S. Geol. Survey Bulletin* 314, p. 19-39.
- Brooks, A.H., 1907, The Circle precinct, Alaska: *U.S. Geol. Survey Bull.* 314, p. 187-204.
- Brooks, A.H., 1908, The mining industry in 1907: *U.S. Geol. Survey Bull.* 345, p. 30-53.
- Brooks, A.H., 1909, The Alaska mining industry in 1908: *U.S. Geol. Survey Bull.* 379, p. 5-20.
- Brooks, A.H., 1910, The mining industry in Alaska in 1909: *U.S. Geol. Survey Bull.* 442, p. 20-46.
- Brooks, A.H., 1911a, The mining industry in 1910: *U.S. Geol. Survey Bull.* 480-B, p. 21-42.
- Brooks, A.H., 1911b, The Mount McKinley region, Alaska, with descriptions of the igneous rocks and of the Bonnifield and Kantishna districts, by L.M. Prindle: *U.S. Geol. Survey Professional Paper* 70, 234 p.
- Brooks, A.H., 1911c, Geological features of Alaskan metalliferous lodes: *U.S. Geol. Survey Bull.* 480, p. 43-93.
- Brooks, A.H., 1912, The mining industry in 1911: *U.S. Geol. Survey Bull.* 520, p. 17-44.
- Brooks, A.H., 1914, The Alaskan mining industry in 1913: *U.S. Geol. Survey Bull.* 592, p. 45-74.
- Brooks, A.H., 1915, The Alaskan mining industry in 1914: *U.S. Geol. Survey Bull.* 622, p. 15-68.
- Brooks, A.H., 1916a, The Alaskan mining industry in 1915: *U.S. Geol. Survey Bull.* 642, p. 16-71.
- Brooks, A.H., 1916b, Antimony deposits of Alaska: *U.S. Geol. Survey Bull.* 649, p. 5-41.
- Brooks, A.H., 1918, The Alaskan mining industry in 1916: *U.S. Geol. Survey Bull.* 662, p. 11-62.
- Brooks, A.H., 1922, The Alaskan mining industry in 1920: *U.S. Geol. Survey Bull.* 722, p. 7-67.
- Brooks, A.H., 1923, Alaska mining industry - 1921: *U.S. Geol. Survey Bull.* 739, p. 33.
- Brooks, A.H., 1925, Alaska's mineral resources and production, 1923: *U.S. Geol. Survey Bull.* 773, p. 3-52.
- Brooks, A.H., and Capps, S.R., 1924, The Alaskan mining industry in 1922: *U.S. Geol. Survey Bull.* 755, p. 3-49.
- Brooks, A.H., and Martin, G.C., 1921, The Alaskan mining industry in 1919: *U.S. Geol. Survey Bull.* 714, p. 59-95.
- Brosge, W.P., Lanphere, M.A., Reiser, H.N. and Chapman, R.M., 1969, Probable Permian age of the Rampart Group, central Alaska: *U.S. Geol. Survey Bull.* 1294-B, p. B1-B18.
- Brown, C.E.G., Dadson, A.S. and Wrigglesworth, L.A., 1959, On the ore-bearing structures of the Giant Yellowknife Gold Mine: *Trans. Can. Inst. Min. Metall.*, 62: 107-116.
- Brown, J.M., 1962, Bedrock geology and ore deposits of the Pedro Dome area, Fairbanks mining district, Alaska: University of Alaska unpub. M.S. thesis, 137 p.
- Brown, P.R.L., Rafter, T.A., Robinson, B.W., 1975, Sulphur isotopic variations in nature, Part II: Sulphur isotope ratios in sulphides from Broadlands geothermal field, new Zealand, *N.Z. Journ. Sci.*, v. 18, p. 35-40.

- Buchanan, L.J., 1981, Precious metal deposits associated with volcanic environments in the southwest, in Dickinson, W.R., and Payne, W.D., eds., *Relations of Tectonics to Ore Deposits in the Southern Cordillera*: Ariz. Geol. Soc. Digest, v. XIV, p. 237-262.
- Bundtzen, T.K., 1981, Geology and mineral deposits of the Kantishna Hills, Mt. McKinley quadrangle, Alaska: University of Alaska unpub. M.S. thesis, 238 p.
- Bundtzen, T.K., 1982, Bedrock geology of the Fairbanks mining district, western sector, Alaska: Alaska Division of Geological and Geophysical Surveys Open-file Report 155, 2 plates, scale 1:24,000.
- Bundtzen, T.K., 1983, Bedrock geologic outcrop map of the Livengood B-3 quadrangle, Alaska: Alaska Division of Geological and Geophysical Surveys Report of Investigations 83-6, map, 1 sheet, scale 1:40,000.
- Bundtzen, T.K. and Kline, J.T., 1981, Geologic mine map, Grant Gold Mine, Fairbanks mining district, Alaska: Alaska Division of Geological and Geophysical Surveys Open-file Report 141, 2p.
- Bundtzen, T.K. and Reger, R.D., 1977, The Richardson lineament - a structural control for gold deposits in the Richardson mining district, Alaska, in *Short notes on Alaskan geology - 1977*: Alaska Division of Geological and Geophysical Surveys Geologic Report 55, p. 29-34.
- Bundtzen, T.K. and Smith, T.E., 1976, Progress report: Geology and mineral deposits of the Kantishna Hills, Alaska: Alaska Division of Geological and Geophysical Surveys Open-file Report 98, 80 p., 2 sheets, scale 1:63,360.
- Bundtzen, T.K., and Turner, D.L., 1979, Geochronology of metamorphic and igneous rocks in the Kantishna Hills, Mt. McKinley quadrangle, in *Short Notes on Alaskan Geology, 1978*: Alaska Division of Geological and Geophysical Surveys Geol. Rept. 61, p. 25-30.
- Bundtzen, T.K. et al, 1982, Geology of the Clipper Gold Mine, Fairbanks mining district, Alaska: Alaska Division of Geological and Geophysical Surveys Open-file Report 157, 10 p., 1 plate.
- Burack, A.C., Laird, Jo, Foster, H.L., and Cushing, G.W., 1984, Metamorphic petrology of the Table Mountain area, Circle quadrangle, Alaska, [in] Coonrad, W.L., ed., *The United States Geological Survey in Alaska: Accomplishments during 1981*: U.S. Geol. Survey Circular 868, p. 54-57.
- Burand, W.M., 1965, A geochemical investigation between Chatanika and Circle Hot Springs, Alaska: Alaska Division Mines and Minerals Geochem. Rept. 5, 11 p.
- Burand, W.M., 1966a, A geochemical investigation of the Nenana Highway area, central Alaska: Alaska Division of Mines and Minerals Geochem. Rept. 10, 13 p.
- Burand, W.M., 1966b, A geochemical investigation of stream sediments in the Elliott Highway area, Alaska: Alaska Division of Mines and Minerals Geochem. Rept. 11, 30 p.
- Burand, W.M., 1968, Geochemical investigations of selected areas in the Yukon-Tanana region of Alaska, 1965 and 1966: Alaska Division of Mines and Minerals Geochem. Rept. 13, 51 p. including 13 p. of maps, scale 1:63,360.
- Burns, L.E., and Newberry, R.J., 1987, Intrusive rocks of the Lime Peak-Mt. Prindle area: in Smith et al.; eds, *Mineral assessment of the Lime Peak-Mt. Prindle area, Alaska*: Alaska Division of Geological and Geophysical Surveys Contract Report, 276 p, maps 13 sheets.
- Burruss, R.C., 1981, Analysis of phase equilibrium in C-O-H-S fluid inclusions: Chap. 3 in *Handbook to Mineralogical Association of Canada Short Course in Fluid Inclusions*, p.
- Burton, P.J., 1981, Radioactive mineral occurrences, Mt. Prindle area, Yukon-Tanana uplands, Alaska: University of Alaska, unpub. M.S. thesis, 72 p.
- Burton, P.J., 1984, Compilation of some mineral occurrences in the White Mountains, N.R.A.: Alaska Division of Mining Report, unpub. report, 15 p.
- Burton, P.J., Warner, J.D., and Barker, J.C., 1985, Reconnaissance investigation of tin occurrences at Rocky Mountain [Lime Peak], east-central Alaska: U.S. Bureau of Mines Open-file Report 31-85, 44 p.
- Byers, F.M., 1957, Tungsten deposits in the Fairbanks district, Alaska: U.S. Geol. Survey Bull. 1024-I, p. 179-216.
- Cady, J.W., and Barnes, D.F., 1983, Complete Bouguer gravity anomaly map of the Circle quadrangle, Alaska: U.S. Geol. Survey Open-file Report 83-170-D.
- Cady, J.W., and Weber, F.R., 1983, Aeromagnetic interpretation map of the Circle quadrangle, Alaska: U.S. Geol. Survey Open-file Report 83-170-C.
- Calvin, J.S., 1985, Preliminary mine feasibility study of disseminated gold deposits located in the Fairbanks mining district, Alaska: University of Alaska unpub. M.S. thesis, 99 p.

- Capps, S.R., 1918, Mineral resources of the Kantishna region: in Brooks and others, Mineral resources of Alaska, 1916; U.S. Geol. Survey Bull. 662, p. 279-333.
- Capps, S.R., 1919, The Kantishna region, Alaska: U.S. Geol. Survey Bull. 687, 116 p.
- Capps, S.R., 1924, Geology and mineral resources of the region traversed by the Alaska Railroad: U.S. Geol. Survey Bull. 755, p. 73-150.
- Capps, S.R., 1933, Mineral investigations in the Alaska Railroad belt, 1931: U.S. Geol. Survey 844-B, p. 32.
- Capps, S.R., 1940, Geology of the Alaska railroad region: U.S. Geol. Survey Bull. 907, 201 p.
- Casedevall, T. and Ohmoto, 1977, Sunnyside mine, Eureka mining district, San Juan County: Geochemistry of gold and base-metal ore deposition in a volcanic environment: *Econ. Geol.*, v. 72, p. 1285-1320.
- Cathelineau, Michael, et al., 1989, Gold in arsenopyrite: Crustal chemistry, location and state, physical and chemical conditions of deposition: in Keays, R.R. et al., eds., *The Geology of gold deposits: The perspective in 1988*: *Econ. Geol. Monograph* 6, p. 328-341.
- Chadwick, R., 1976, Mineral appraisal of properties in proposed Mt. McKinley additions: National Park Service, unpub. report, 300 p.
- Chapin, Theodore, 1914, Lode mining near Fairbanks: U.S. Geol. Survey Bull. 592-J, p. 321-355.
- Chapin, T. and Harrington, G.L., 1919, Mining in Fairbanks, Ruby, Hot Springs, and Tolstoi districts: U.S. Geol. Survey Bull. 692, p. 321-353.
- Chapman, R.M. and Foster, R.L., 1969, Lode mining and prospects in the Fairbanks district, Alaska: U.S. Geol. Survey Prof. Paper 625-D., p. D1-D25.
- Chapman, R.M., Weber, F.R., Churkin, Michael Jr. and Carter, Claire, 1979, The Livengood Dome Chert, a new Ordovician formation in central Alaska, and its relevance to displacement on the Tintina fault in Shorter contributions to stratigraphy and structural geology, 1979: U.S. Geol. Survey Professional Paper 1126, p. F1-F13.
- Chapman, R.M., Weber, F.R., and Taber, Bond, 1971, Preliminary geologic map of the Livengood Quadrangle, Alaska: U.S. Geol. Survey Open-file Report 71-66 (483), 2 sheets, scale 1:250,000.
- Chappel, B.W. and White, A.J.R., 1974, Two contrasting granite types: *Pacific Geology*, v. 8, p. 173-174.
- Cheney, E.S. and Patton, T.S., 1967, Origin of the bedrock values of placer deposits, *Econ. Geol.*, v. 62, p. 852-853.
- Church, R.E. and Durfee, M.C., 1961, Geology of the Fossil Creek area, White Mountains Alaska: University of Alaska, unpub. M.S. thesis, 96 p.
- Church, S.E., Delevaux, M.H., and Gray, J.E., 1987, Physotope data base for sulfides from Alaska, March 1987: U.S. Geol. Survey Open File Report 87-259, 44 p.
- Churkin, Michael, Jr., and Brabb, E.E., 1965, Occurrence and stratigraphic significance of *Qldhamia* a Cambrian trace fossil, in east-central Alaska, in *Geological Survey Research 1965*: U.S. Geol. Survey Prof. Paper 525-D, p. D120-124.
- Churkin, M., Jr., Foster, H.L., Chapman, R.M. and Weber, F.R., 1982, Terranes and suture zones in east-central Alaska: *Journal of Geophysical Research*, v. 87, no. B5, p. 3718-3730.
- Cissarz, A., 1957, Lagerstätten des Geosynkinalvulkanismus in den Dinariden und ihre Bedeutung für die Geosynklinale Lagerstättenbildung: *Neue Jahrb. Mineral. Abh.*, 91, p. 485-540.
- Clement, G.K., et al., 1978, Capital and operating cost estimating handbook: Straam Engineers, Inc., Arcadia, Ga., 374 p.
- Cobb, E.H., 1973, Placer deposits of Alaska U.S. Geol. Survey Bull. 1374, 213 p.
- Cobb, E.H., 1976a, Summary of references to mineral occurrences in the Circle quadrangle, Alaska: U.S. Geol. Survey Open-file Report 76-633, 66 p.
- Cobb, E.H., 1976b, Summary of references to mineral occurrences in the Fairbanks quadrangle, Alaska: U.S. Geol. Survey Open-file Report 76-662, 174 p.
- Cobb, E.H., 1976c, Summary of references to mineral occurrences in the Livengood quadrangle, Alaska: U.S. Geol. Survey Open-file Report 76-819, 241 p.
- Cobb, E.H., 1980a, Summary of references to mineral occurrences in the Mount McKinley quadrangle, Alaska: U.S. Geol. Survey Open-file Report 80-363, 150 p.
- Cobb, E.H., 1980b, Summaries of data on and lists of references to metallic and selected nonmetallic mineral deposits in the Big Delta and Tanacross quadrangles, Alaska: U.S. Geol. Survey Open-file Report 80-1086, 76 p.

- Coleman, M.L., 1977, Sulphur isotopes in petrology: *Jour. Geol. Soc. Lond.*, v. 133, p. 593-608.
- Coleman, M.L., 1980, Corrections for mass spectrometer analysis of SO<sub>2</sub>: *Institute of Geological Sciences Stable Isotope Report No. 45*, 5 p.
- Coleman, R.G., Lee, D.E., Beatty, L.B. and Brannock, W.W., 1965, Eclogites and eclogites: their differences and similarities: *Geol. Soc. of America Bull.*, 76, p. 483-508.
- Collins, P.L.F., 1979, Gas hydrates in CO<sub>2</sub> bearing fluid inclusions and the use of freezing data for estimation of salinity: *Econ. Geol.*, v. 75, p. 1435-1444.
- Cook, D.J., and Rao, P.D., 1973, Distribution analysis, and recovery of fine gold from alluvial deposits: *University of Alaska, Mineral Industry Research Laboratory, MIRL Report No. 32*, 102 p.
- Cotton, C., 1942, *Geomorphology: Whitcombe and Tombo Ltd., Christchurch, New Zealand*, 354 p.
- Cox, D.P. and Singer, D.A., 1986, *Mineral deposit models: U.S. Geol. Survey Bull. 1693*, 379 p.
- Cox, S.H., 1879, Auriferous reef on Rimutaka Ranges: *Rep. Geol. Expl.*, no. 13, p. 11-12.
- Currey, P.R., 1964, A preliminary study of valley asymmetry in the Ogoturuk Creek area, northwestern Alaska: *Arctic*, v. 17, p. 84-89.
- Cushing, G.W., 1984, Early Mesozoic history of the eastern Yukon-Tanana Upland: Albany, State University of New York, unpub. M.S. thesis.
- Cushing, G.W., and Foster, H.L., 1984, Structural observations in the Circle quadrangle, Yukon-Tanana upland, Alaska, [in] Coonrad, W.L., and Elliott, R.L., eds., *The United States Geological Survey in Alaska: Accomplishments during 1981: U.S. Geol. Survey Circular 868*, p. 64-65.
- Cushing, G.W., Foster, H.L. and Harrison, T.M., 1984a, Mesozoic age of metamorphism and thrusting in the eastern part of east-central Alaska: *EOS (American Geophysical Union Transactions)*, v. 65, p. 290-291.
- Dahlin, D.C., Brown, L.L., and Warner, J.D., 1987, Characterization of Ketchum Dome tin prospect, east-central, Alaska: *U.S. Bureau of Mines R.I. 9145*, 11 p.
- Dalrymple, G.B., 1969, <sup>40</sup>Ar/<sup>36</sup>Ar analyses of historic lava flows: *Earth Planet. Sci. Letters*, v. 6, 47-55.
- Damon, P.E., 1968, Potassium-argon dating of igneous and metamorphic rocks with application to the basin ranges of Arizona and Sonora: in Hamilton, E.I., and Farquhar, R.M., eds., *Radiometric dating for geologists: London, Interscience Publishers*, p. 1-72.
- Damon, P.E., Laughlin, A.W., and Percious, J.K., 1967, Problem of excess argon-40 in volcanic rocks: p. 463-481 in *Radioactive Dating and Methods of Low-level Counting*, Vienna, Internat. Atomic Energy Agency, 744 p.
- Dasch, E.J., 1969, Strontium isotopes in weathering profiles, deep-sea sediments, and sedimentary rocks: *Geochimica et Cosmochimica Acta*, v. 33, p. 1521-1552.
- Davies, W.E., 1972, The Tintina Trench and its reflection in the structure of the Circle Area, Yukon-Tanana Upland, Alaska: *Proceedings, 24th International Geological Congress, Montreal, Canada, section 3*, p. 211-216.
- Davis, J.A., 1922a, The Kantishna district: in Stewart, B.D., *Annual Report of the Territorial Mine inspector of Alaska*, p. 12-14.
- Davis, J.A., 1922b, Lode mining in the Fairbanks district, Alaska: in Stewart, B.D., *Annual report of the mine inspector of Alaska*, p. 88-133.
- Davis, J.A., 1923, The Kantishna region, Alaska, in Stewart, B.D., *Annual report of the Mine Inspector of Alaska, 1922: Juneau, Alaska*, p. 113-138.
- Desborough, G.A., 1970, Silver depletion by microanalysis of gold from placer occurrences, Western United States: *Econ. Geol.* v. 65, p. 304-311.
- Dickson, F.W., et al., 1975, Solid solutions of antimony, arsenic, and gold in stibnite, orpiment, and realgar: *Econ. Geol.* v. 70, p. 591-594.
- Dickson, F.W., Radtke, A.S. and Rye, R.O., 1975b, Implications of the occurrence of barium minerals and sulfur isotopic compositions of barite on late stage processes in Carlin-type gold deposits (abs.): *Geol. Soc. America Abs. with Programs*, v. 7, no. 5, p. 604-605.
- Dickson, F.W., Rye, R.O. and Radtke, A.S., 1979, The Carlin gold deposit as a product of rock-water interactions: Nevada Bureau of Mines and Geology Rept. 33: *Proceedings, Fifth Quadrennial Symposium. The International Symposium on the Genesis of Ore Deposits, Volume 11*.
- Doe, B.R. and Zartman, R.E., 1979, Plumbotectonics, the Phanerozoic, in Barnes, H.L., ed., *Geochemistry of*

- hydrothermal ore deposits, 2nd ed., Wiley, New York, 798 p.
- Drury, G.H., 1965, Theoretical implications of underfit streams: U.S. Geol. Survey Prof. Paper 452C, p. C1-C43.
- Dusel-Bacon, Cynthia, 1984, Trace element evidence for the tectonic affinities of some amphibolites from the Yukon-Tanana Upland, east-central Alaska, in Coonrad, W.L. and Elliott, R.L., eds., *The U.S. Geological Survey in Alaska, accomplishments during 1981*: U.S. Geol. Survey Circular 868, p. 50-54.
- Dusel-Bacon, C. and Foster, H.L., 1983, A sillimanite gneiss dome in the Yukon crystalline terrane, east-central Alaska: petrography and garnet-biotite geothermometry: U.S. Geol. Survey Professional Paper 1170-E, 25 p.
- Eakin, H.M., 1915a, Tin mining in Alaska: U.S. Geol. Survey Bull. 622, p. 81-94.
- Eakin, H.M., 1915b, Mining in the Fairbanks district: U.S. Geol. Surv. Bull. 622, p. 229-238.
- Eakins, G.R., and Daniels, C.L., 1980, Survey of mineral activity in Alaska - 1977: Alaska Division of Geological and Geophysical Surveys Open-File Report 122, 32 p.
- Ebbley, Norman, Jr. and Wright, W.S., 1948, Antimony deposits in Alaska: U.S. Bur. Mines Rept. Inv. 4173, 41 p.
- Einaudi, M.T., Meinert, L.D. and Newberry, R.J., 1981, Skarn deposits: *Econ. Geol.*, 75th Anniversary volume, p. 317-391.
- Einaudi, M.T. and Burt, D.M., 1982, Introduction-terminology, classification, and composition of skarn deposits: *Econ. Geol.*, v. 77, p. 745-754.
- Eisbacher, G.H., 1981, Sedimentary tectonics and glacial record in Windemere Supergroup, Mackenzie Mountains, northwestern Canada: *Geol. Survey of Canada, Paper 80-27*, 40 p.
- Ellsworth, C.E., 1910, Placer mining in the Yukon-Tanana region: U.S. Geol. Survey Bull. 422, p. 230-245.
- Ellsworth, C.E., 1912, Placer mining in the Fairbanks and Circle districts: U.S. Geol. Survey Bull. 520, p. 240-245.
- Ellsworth, C.E. and Davenport, R.W., 1913 Placer mining in the Yukon-Tanana region: U.S. Geol. Survey Bull. 542, p. 203-222.
- Ellsworth, C.E., and Parker, G.L., 1911, Placer mining in the Yukon-Tanana region: U.S. Geol. Survey Bull. 480, p. 153-172.
- Erdmer, P. and Helmstaedt, H., 1983, Eclogite from central Yukon: a record of subduction at the western margin of ancient North America: *Canadian Journal of Earth Sciences*, v. 20, p. 1389-1408.
- Eugster, H.P., Albee, A.L., Bence, A.E., Thompson, J.B., Jr., and Waldbaum, D.R., 1972, The two-phase region and excess mixing properties of paragonite-muscovite crystalline solutions: *Journal of Petrology*, v. 13, no. 1, p. 147-179.
- Evensen, N.M., Hamilton, P.J., and O'Nions, R.K., 1978, Rare-earth abundances in chondritic meteorites: *Geochim. Cosmochim. Acta*, v. 42, p. 1199-1212.
- Fairbairn, H.W., Hurley, P.M. and Pinson, W.H., 1964, Initial Sr87/Sr86 and possible sources of granitic rocks in southern British Columbia: *J. Geophys. Res.*, v. 69, p. 4889-4893.
- Faure, G. and Powell, J.L., 1972, *Strontium Isotope Geology*: Springer-Verlag, Berlin, 188 p.
- Fechner, S.A. and Balen, M.D., 1988, Results of 1987 Bureau of Mines placer investigations of the White Mountains study area, Alaska: U.S. Bureau of Mines Open-file Report OFR 5-88, 158 p.
- Fehlberg, B. and Giles, C.W., 1982, Archaean volcanic exhalative gold mineralization at Spargoville western Australia: in *Gold '82 Geology, Geochemistry and Genesis of Gold Deposits*: R.P. Foster (editor), A.A. Balkema Rotterdam, p. 285-304.
- Feiss, P.G., 1982, Geochemistry and tectonic setting of volcanics of the Carolina Slate Belt: *Econ. Geol.*, v. 77, p. 273-293.
- Fleischer, R. and Routhier, P., 1973, The "consanguinous" origin of a tourmaline-bearing gold deposit: Passagem de Mariana (Brazil). *Econ. Geol.*, 68:11-22.
- Foley, N.K., Bethke, P.M. and Rye, R.O., 1982, A reinterpretation of  $dD_{H_2O}$  values of inclusion fluids in quartz from shallow ore bodies (abs.): *Geol. Soc. America, Abstracts with Programs*, v. 14, no. 7, p. 489.
- Forbes, R.B., 1980, Chemical zonation in gold nuggets, Second Annual Conference on Alaskan Placer Mining - Focus on Gold: University of Alaska, MIRL Report No. 46, p. 72-77.
- Forbes, R.B., 1982, Bedrock geology and petrology of the Fairbanks mining district, Alaska: Alaska Division of

- Geological and Geophysical Surveys Open-file Report 169, 68 p.
- Forbes, R.B. and Weber, F.R., 1982, Bedrock geology of the Fairbanks mining district: Alaska Division of Geological and Geophysical Surveys Open-file Report 170, 2 sheets, scale 1:63,360.
- Forbes, R.B., Pilkington, H.D. and Hawkins, D.B., 1968, Gold gradients and anomalies in the Pedro Dome - Cleary Summit Area, Fairbanks district, Alaska: U.S. Geol. Survey Open-file Rept. 68-101, 43 p.
- Foster, H.L., Albert, N.R.D., Griscom, Andrew, Hessin, T.D., Menzie, W.D., Turner, D.L. and Wilson, F.H., 1979, The Alaskan Mineral Resource Assessment Program: Background information to accompany folio of geologic and mineral resource maps of the Big Delta quadrangle, Alaska: U.S. Geol. Survey Circular 783, 19 p.
- Foster, H.L., Laird, J. and Cushing, G.W., 1984, Thrust faulting in the Eagle A-1 quadrangle, Alaska, and its implications for the tectonic history of the Yukon-Tanana Upland: EOS (American Geophysical Union Transactions), v. 65, p. 291.
- Foster, H.L., Laird, J., Keith, T.E.C., Cushing, G.W. and Menzie, W.D., 1983, Preliminary geologic map of the Circle quadrangle, Alaska: to accompany U.S. Geol. Survey Open-file Report 83-170-A, 30 p., 2 plates, 1 map, scale 1:250,000.
- Foster, H.L., O'Leary, R.M., McDougal, C.M., and Menzie, W.D., 1984, Analysis of rock samples from the Circle quadrangle, Alaska: U.S. Geol. Survey Open-file 84-479, 121 p., 1 sheet, scale 1:250,000.
- Foster, H.L., Weber, F.R., Forbes, R.B., and Brabb, E.E., 1973, Regional geology of Yukon-Tanana Upland, Alaska: American Assoc. of Petroleum Geologists Memoir No. 19, Arctic Geology, p. 388-395.
- Foster, R.L., 1968a, Potential for lode deposits in the Livengood gold placer district, east-central Alaska: U.S. Geol. Survey Circular 590, 18 p.
- Foster, R.L., 1968b, Descriptions of the Ruth Creek, Lillian Creek, Griffin, Old Smoky, Sunshine No. 2, and Olive Creek lode prospects, Livengood district, Alaska: U.S. Geol. Survey Open-file Report 322, 21 p.
- Foster, R.L., and Chapman, R.M., 1967, Locations and descriptions of lode prospects in the Livengood area, east-central Alaska: U.S. Geol. Survey Open-file Report 275, unpagged.
- Foster, R.P. and Wilson, J.F., 1982, Geologic setting of Archaean gold deposits in Zimbabwe: in Foster, R.P., ed., Gold '82: Geology geochemistry and genesis of gold deposits: A.A. Balkema, Rotterdam, p. 521-552.
- Foster, R.P., et al., 1986, Archaean gold mineralization in Zimbabwe: in Anhaeusser, C.R., and Maske, S., eds., Mineral deposits of southern Africa: Geological Society of South Africa, p. 43-112.
- Fripp, R.E.P., 1976, Strata-bound gold deposits in Archean banded iron formation, Rhodesia: Econ. Geol., 71: 58-75.
- Furst, G.A., 1968, Geology and petrology of the Fairbanks basalts, Fairbanks, Alaska: University of Alaska unpub. M.S. thesis, 53 p.
- Fyfe, W.S., and Kerrich, R., 1984, Gold: natural concentration processes; in Foster, R.P., ed., Gold '82, The geology, geochemistry, and genesis of gold deposits: Geological Society of Zimbabwe Special Publication No. 1, p. 99-128.
- Gair, J.E., 1962, Geology and ore deposits of the Nova Lima and Rio Acimo Quadrangles, Minas Gerais, Brazil: U.S. Geol. Survey Professional Paper, 341-A, 67 p.
- Gallagher, M.J., et al., 1981, Stratabound arsenic and vein antimony mineralization in Silurian greywacke at Glendinning, South Scotland: Trans. Inst. Min. Metall. Sect. B Appl. Earth Sci., v. 90, no. 2.
- Garkovets, V.G., et al., 1979, Osnovnye cherty metallogenii Uzbekistania, A.N. Uzbek, S.S.R., Tashkent, 272 p.
- Gedney, Larry and Berg, Edward, 1969, The Fairbanks earthquakes of June 21, 1967; aftershock distribution, focal mechanisms, and crustal parameters: Bull. Seism. Soc. Am., v. 59, p. 73-100.
- Ghisler, M., et al., 1980, Stratabound scheelite, arsenopyrite, and copper sulphide mineralization in the late Precambrian sedimentary succession of the east Greenland Caledonides: Spec. Paper Geol. Survey of Ireland, v. 5, p. 19-24.
- Ghosh, D.B., et al., 1970, Ore environment and ore genesis in Ramagiri Gold Field, Andhra Pradesh, India: Econ. Geol., v. 65, p. 801-814.
- Gilbert, W.G. and Redman, E.R., 1977, Metamorphic rocks of the Toklat-Teklanika area, Mt. McKinley quadrangle; Alaska Division of Geological and Geophysical Surveys Geol. Rept. 49, 20 pp.

- Glover, A., 1948, Gold and silver fineness values from Alaskan placer districts: Territory of Alaska Dept. Mines unpub. report, 16 p.
- Godwin, C.I., et al., 1982, Lead isotope models for the genesis of carbonate-hosted Zn-Pb, shale hosted Ba-Zn-Pb, and silver rich deposits in the Northern Canadian Cordillera: *Econ. Geol.*, v. 77, p. 82-94.
- Godwin, C.I. and Sinclair, A.J., Average lead isotope growth curves for shale-hosted zinc-lead deposits, Canadian Cordillera: *Econ. Geol.*, v. 77, p. 675-690.
- Goodwin, A.M., 1973, Archaean iron-formations and tectonic basins of Canada: *Econ. Geol.*, v. 68, p. 915-933.
- Goodwin, A.M., 1977, Archaean volcanic studies in the Superior Province, Canadian Shield, in W.R.A. Paragar, L.C. Coleman and J.M. Hall (editors), *Volcanic Regimes Symposium: Geol. Assoc. Can. Spec. Pap.* 16, p. 205-241.
- Goodwin, A.M., 1982 Archaean greenstone belts and mineralization, Superior Province, Canada: in *Gold '82: The Geology Geochemistry and Genesis of Gold Deposits*, R.P. Foster ed., A.A. Balkema, Rotterdam, p. 521-551.
- Gottfried, David, Annell, C.S., and Schwarz, L.J., 1977, Geochemistry of subsurface basalt from the deep corehole (Clubhouse Crossroads core-hole 1) near Charleston, South Carolina-magma type and tectonic implications: *U.S. Geol. Survey Prof. Paper* 10028-G, p. 91-113.
- Gottfried, D., Jaffe, H.W., and Senftle, F.E., 1959. Evaluation of the lead-alpha (Larsen) method for determining ages of igneous rocks: *U.S. Geol. Survey, Bull.* 1097-A, pp. 1-63.
- Govet, G.J.S., 1983, Rock geochemistry in mineral exploration, Vol. 3: Elsevier, New York, 461 p.
- Gribnitz, K.H., 1964, Notes on the Barberton Goldfield: in S.H. Haughton, ed., *The Geology of Some Ore Deposits in Southern Africa*, 2. Johannesburg, p. 77-90.
- Groves, D.I., et al., 1984, Controls on distribution of Archaean hydrothermal gold deposits in Western Australia; in Foster, R.P., ed., *Gold '82, The geology, geochemistry, and genesis of gold deposits: Geological Society of Zimbabwe Special Publication No. 1*, p. 689-712.
- Gulson, B.L., 1986, Lead isotopes in mineral exploration: Elsevier, New York, 245 p.
- Hall, M.H., 1985, The structural geology of the Fairbanks mining district, central Alaska: University of Alaska unpub. M.S. thesis, 63 p.
- Hallbauer, D.K. and Utter, T., 1977, Geochemical and morphological characteristics of gold particles from recent river deposits and the fossil placers of the Witwatersrand: *Mineral. Deposita*, v. 12, p. 293-306.
- Hannington, M.D., et al., 1986, Gold in sea-floor polymetallic sulfide deposits: *Econ. Geol.*, v. 81, p. 1867-1883.
- Hargraves, David, 1975, The Livengood placer deposit - a developing Alaskan gold mine: *Mining Mag.*, p. 363-368.
- Harris, Michael, 1979, Alteration and mineralization at the Salave gold prospect, N.W. Spain: Imperial College of Science and Technology, unpub. Ph.D. thesis, 328 p.
- Harris, M., 1980, Gold mineralization at the Salave gold prospect northwest Spain: *Inst. Min. Met. Trans.*, v. 89, p. 1-4.
- Harris, Michael and A.S. Radtke, 1976, Statistical study of selected trace elements with reference to geology and genesis of the Carlin gold deposit, Nevada: *U.S. Geol. Survey Professional Paper* 960. 21 p.
- Haskin, L.A., Frey, F.A., Schmitt, R.A., and Smith, R.H., 1966, Meteoric, solar, and terrestrial rare earth distributions: *Phys. Chem. Earth*, v. 7, p. 167-321.
- Haskin, L.A., Haskin, M.A., and Frey, F.A., 1968, Relative and absolute terrestrial abundances of the rare earths, in Ahrens, L.A., ed., *Origin and distribution of the elements*, Oxford/Pergamon Press, p. 889-912.
- Hasler, J.W., Miller, M.H., and Chapman, R.M., 1973, Bismuth, in Brobst, D.A., and Pratt, W.P., eds., *United States mineral resources: U.S. Geol. Survey Professional Paper* 820, p. 95-98.
- Hawley, C.C., and Associates, Inc., 1978, Mineral appraisal of lands adjacent to Mt. McKinley National Park, Alaska: *U.S. Bureau of Mines Report* 24-78, 275 p. (paged by section) + 7 pl.
- Hayba, D.O., 1983, A compilation of fluid inclusion and stable isotope data on selected precious and base metal epithermal deposits: *U.S. Geol. Survey Open-file Report* 83-450, 24 p.
- Heald-Wetlaufer, P., Hayba, D.O., Foley, N.K. and Goss, J.A., 1983, Comparative anatomy of epithermal precious and base metal districts hosted by volcanic rocks: *U.S. Geol. Survey Open-file Report* 83-710, 8 p.
- Hedge, C.E., 1966, Variations in radiogenic strontium found in volcanic rocks: *J. Geophys. Res.*, v. 71, p. 6119-6126.

- Helgeson, H.G. and Garrels, R.M., 1968, Hydrothermal transport and deposition of gold: *Econ. Geol.*, vol. 63, p. 622-635.
- Hess, F.L., 1912, Tin resources of Alaska: *U.S. Geol. Survey Bull.* 520, p. 89-92.
- Hess, F.L. and Graton, L.C., 1905, The occurrence and distribution of tin: *U.S. Geol. Survey Bull.* 260, p. 161-187.
- Hill, J.M., 1933, Lode deposits of the Fairbanks district, Alaska, *U.S. Geol. Survey Bull.* 849-B, p. 29-163.
- Hinderman, T.K., 1984, Geology: in Thornsberry et al., eds., Mineral resource studies in the Kantishna Hills and Dunkle Mine areas, Denali National Park and Preserve: Salisbury and Dietz, Inc., 234 p.
- Holland, T.J.B., 1979, Reversed hydrothermal determinations of jadeite-diopside activities, *abstr.:EOS (American Geophysical Union Transactions)*, v. 60, no. 18, p. 405.
- Holland, T.J.B., 1980, The reaction albite = jadeite + quartz determined experimentally in the range 600-1200°C: *American Mineralogist*, v. 65, no. 1-2, p. 129-134.
- Holm, Bjarne, 1973, Bedrock geology and mineralization of the Mount Prindle area, Yukon-Tanana Upland, Alaska: University of Alaska, Fairbanks, unpublished M.S. thesis, 55 p., 1 sheet, scale 1:24,000.
- Hopkins, D.M., 1967, The Bering land bridge, Stanford, Stanford Univ. Press, 495 p.
- Hopkins, D.M. and Taber, B., 1962, Asymmetrical valleys in central Alaska, *Geol. Soc. America Spec. Paper* 68.
- Horwood, H.C. and Pye, E.G., 1955, Geology of Ashmore Township: *Ont. Dept. Min.*, 60 (part 5): p. 1-105.
- Imai, H., 1978, Geological studies of the mineral deposits in Japan and East Asia: University of Tokyo Press, Tokyo, p. 261-264.
- Jaffe, H.W., Gottfried, D., Waring, C.L., and Worthing, H.W., 1959, Lead-alpha age determinations of accessory minerals of igneous rocks (1953-1957). *U.S. Geological Survey, Bull.* 1097-B, pp. 65-148.
- Joesting, H.R., 1942, Strategic mineral occurrences in interior Alaska: Territory of Alaska Dept. Mines Pamph. 1, 46 p.
- Joesting, H.R., 1943, Supplement to Pamphlet No. 1 - Strategic mineral occurrences in interior Alaska: Territory of Alaska Dept. Mines Pamph. 2, 28 p.
- Johnson, B.L., 1910, Occurrence of wolframite and cassiterite in the gold placers of Deadwood Creek, Birch Creek district: *U.S. Geol. Survey Bull.* 442, p. 246-250.
- Kamilli, R.J. and Ohmoto, H., 1977, Paragenesis, zoning, fluid inclusion and isotopic study of the Finlandia vein, Colqui district, Central Peru: *Econ. Geol.*, v. 72, p. 950-982.
- Kennedy, B.A., 1976, Valley-side slopes and climate: in Derbyshire, E., ed., *Geomorphology and Climate*, John Wiley and Sons, New York, p. 171-201.
- Kennedy, B.A. and Melton, 1971, Valley asymmetry and slope forms of a permafrost area in the Northwest Territories, Canada, *Spec. Pub. Inst. Brit. Geog.*, v. 4, p. 107-121.
- Kerrich, R., 1980, Archaean gold-bearing chemical sedimentary rocks and veins: a synthesis of stable isotope and geochemical relations: in *Genesis of Archaean, Volcanic-Hosted Gold Deposits*, Pye, E.G., Roberts, R.G., (eds.) Ontario, Geol. Surv. Misc. Paper 97, p. 1-15 (1981).
- Kerrich, R. and Fryer, B.J., 1979, Archaean precious-metal hydrothermal systems, Dome Mine Abitibi Greenstone Belt II, REE and oxygen isotope relations: *Can. J. Earth Sci.*, v. 16, p. 440-458.
- Kerrich, R., Fryer, B.J., Milner, K.J. and Pierce, M.G., 1981, The geochemistry of gold bearing chemical sediments, Dickenson Mine, Red Lake, Ontario: a reconnaissance study: *Can. J. Earth Sci.*, v. 18, p. 624-637.
- Kesler, S.E., 1978, Metallogenesis of the Caribbean region: *J. Geol. Soc. London*, v. 135, p. 429-441.
- Killeen, P.L. and Mertie, J.B., 1951, Antimony ore in the Fairbanks district, Alaska: *U.S. Geol. Survey Open-file report*, 43 p.
- Kistler, R.W., 1974, Phanerozoic Batholiths in Western North America: *Ann. Rev. Ear. Plan. Sci.*, v. 2, p. 403-418.
- Kistler, R.W. and Peterman, Z.E., 1973, Variations in Sr, Rb, K, Na, and Initial  $87\text{Sr}/86\text{Sr}$  in Mesozoic granitic rocks and intruded wall rocks in central California: *Geol. Soc. Amer. Bull.*, v. 84, p. 3489-3512.
- Koo, J. and Mossman, D.J., 1975, Origin and metamorphism of the Flin Flon stratabound Cu-Zn sulfide deposit, Saskatchewan and Manitoba: *Econ. Geol.*, 70, p. 48-62.
- Koschman, A.H. and Bergendahl, M.H., 1968, Principal

- gold-producing districts of the United States: U.S. Geol. Survey Prof. Paper 610, 283 p.
- Koulomzine, T. and Dagenais, R.W., 1959, Statistical determination of chances of success in mineral exploration in Canada: *Can. Min. J.*, v. 74, no. 4, p. 107-110.
- Kretschmar, U. and Scott, S.D., 1976, Phase relations involving arsenopyrite in the system Fe-As-S and their applications: *Can. Mineral.*, v. 14, p. 364-386.
- Krishnaswamy, S., 1972, *India's Mineral Resources*, Oxford Press, Delhi, 503 p.
- Kurtak, J.M., 1984, Antimony lode deposits: in Thornsberry et al., eds., *Mineral resource studies in the Kantishna Hills and Dunkle Mine areas, Denali National Park and Preserve*: Salisbury and Dietz, Inc., 234 p.
- Laird, Jo and Albee, A.L., 1981, Pressure, temperature, and time indicators in mafic schist: their application to reconstructing the polymetamorphic history of Vermont: *Amer. Jour. Sci.*, v. 281, p. 127-175.
- Laird, Jo, Biggs, D.L. and Foster, H.L., 1984, A terrane boundary of the southeastern Circle quadrangle, Alaska. Evidence from petrologic data: *EOS*, v. 65, p. 291.
- Laird, Jo and Foster, H.L., 1986, Petrologic evidence for a terrane boundary in south-central Circle Quadrangle, Alaska: *Geophysical Research Letters*, v. 13, no. 10, p. 1035-1038.
- Laird, Jo, Foster H.L., and Weber, F.R., 1984, Amphibole eclogite in the Circle quadrangle, Yukon-Tanana Upland, Alaska: in Coonrad, W.L., and Elliott, R.L., eds., *The United States Geological Survey in Alaska: Accomplishments during 1981*: U.S. Geological Survey Circular 868, p. 57-60.
- Lauder, W.R., 1962, The Kaiwharawhara capture: *N.Z.J. Geol. Geophys.*, v. 5, p. 141-142.
- Leake, B.E., 1964, The chemical distinction between ortho- and para-amphibolites: *Journal of Petrology*, v. 5, no. 2, p. 238-254.
- Le Compte, J.R., 1981, Landsat features maps of the Circle Quadrangle, Alaska: U.S. Geological Survey Open-file Report 81-782, scale 1:250,000, 2 sheets.
- Le Couteur, P.C. and Tempelman-Kluit, D.J., 1976, Rb/Sr ages and profile of initial  $^{87}\text{Sr}/^{86}\text{Sr}$  ratios for plutonic rocks across the Yukon Crystalline Terrane: *Canadian Journal of Earth Sciences*, v. 13, p. 319-330.
- Le Huray, A.P., Stowell, H.S., and Church, S.E., 1985a, Lead isotopes from volcanogenic massive sulfide deposits in the Alexander Terrane, in Bartsch-Winkler and Reed, K.M., eds., *The U.S. Geological Survey in Alaska, accomplishments during 1983*: U.S. Geol. Survey Circular 945, p. 95-96.
- Le Huray, A.P., Church, S.E. and Nolkeberg, W.J., 1985b, Lead isotopes in sulfide deposits from the Jarvis Creek Glacier and Wrangellia terranes, Mount Hays quadrangle, eastern Alaska Range, in Bartsch-Winkler and Reed, K.M., eds., *The U.S. Geological Survey in Alaska, accomplishments during 1983*: U.S. Geol. Survey Circular 945, p. 72-73.
- Leopold, L.B. and Maddock, T. Jr., 1952, The hydraulic geometry of stream channels and some physiographic implications: U.S. Geol. Survey Prof. Paper 252, 57 p.
- Lepeltier, Claude, 1969, A simplified statistical treatment of geochemical data by graphical representation: *Econ. Geol.*, v. 64, p. 538-550.
- Levell, J.H., 1984, Placer deposits: in Thornsberry et al., eds., *Mineral resource studies in the Kantishna Hills and Dunkle Mine areas, Denali National Park and Preserve*: Salisbury and Dietz, Inc., 234 p.
- Light, T.D., Cady, J.W., Weber, F.R., McCammon, R.B., and Rinehart, C.D., 1987, Sources of placer gold in the southern part of the White Mountains Recreation Area, east-central Alaska: in Hamilton, T.D., and Galloway, J.P., eds., *Geologic studies in Alaska by the U.S. Geological Survey during 1986*: U.S. Geological Survey Circular 998, p. 67-69.
- Lipman, P.W., Fisher, F.S., Mehnert, H.H., Naeser, C.W., Luedke, R.G. and Steven, T.A., 1976, Multiple ages of mid-Tertiary mineralization and alteration in the western San Juan Mountains, Colorado: *Econ. Geol.*, v. 71, no. 3, p. 571-588.
- Lipman, T.A. and Steven, P.W., 1976, Calderas of the San Juan volcanic field, southwestern Colorado: U.S. Geol. Survey Professional Paper 958, 35 p.
- MacKevett, E.M., Jr., and Holloway, C.D., 1977, Map showing metalliferous and selected nonmetalliferous mineral deposits in the eastern part of southern Alaska: U.S. Geol. Survey Open-file Report 77-169A, 1 sheet + 99 p. tabular material, scale 1:1,000,000.
- Magnusson, N.H., 1970, The origin of the iron ores in central Sweden and the history of their alterations: *Sver. Geol. Unders. Ser. C*, 643, 364 p.
- Malone, Kevin, 1962, Mercury occurrences in Alaska: U.S. Bureau Mines I.C. 8131, 57 p.

- Malone, Kevin, 1965, Mercury in Alaska, in U.S. Bureau of Mines, Mercury potential of the United States: U.S. Bureau Mines Inf. Circ. 8252, p. 31-59.
- Maloney, William, 1916, Report of the Territorial mine inspector of Alaska for the year 1915, p. 14-15.
- Mangan, M., Craig, J.R., and Rimstidt, 1984, Submarine exhalative gold mineralization at the London-Virginia Mine, Buckingham County, Virginia: *Mineralium Deposita*, v. 19, no. 3, p. 227-236.
- Martin, G.C., 1919, The Alaskan mining industry in 1917: U.S. Geol. Survey Bull. 692, p. 11-42.
- Martin, G.C., 1920, The Alaskan mining industry in 1918: U.S. Geol. Survey Bull. 712-A, p. 1-52.
- Martin, W.C., 1957, Errington and Vermillion Lake Mines: in *Structural Geology of Canadian Ore Deposits*, 2, Montreal, p. 363-376.
- Masterman, J.S., 1990, A fluid inclusion study of an interior Alaskan gold mining district and its implications on the origin of the mineralization: University of Alaska, unpub., M.S. Project Report, 80 p.
- Materikov, M.P., 1974, Deposits of tin, in Smirnov, V.I., ed., *Ore Deposits of the U.S.S.R.*, v. 3, London, p. 229-294.
- Mamlich, A., Amos, A.C., Walker, R.R. and Watkins, J.J., 1974, The geology department: *Can. Min. Metall. Bull.*, 67, p. 56-63.
- Matzko, J.J., Jaffe, H.W., and Waring, C.L., 1958, Lead-alpha age determinations of granitic rocks from Alaska: *Am. J. Sci.*, v. 256(8), pp. 529-539.
- Maucher, A., 1976, the stratabound cinnabar-stibnite-scheelite deposits: in Wolff, K.G., ed., *Handbook of stratabound and stratiform ore deposits*, Elsevier Scientific Publishing Company, Amsterdam, p. 477-503.
- McCombe, R.J. and Augustine, Grant, Jr., 1931, An investigation of the gold-bearing quartz veins of Ester Dome: University of Alaska unpub. B.S. thesis, 49 p.
- McCulloch, M.T. and Wasserburg, G.J., 1978, Sn-Nd and Rb-Sr chronology of continental crust formation: *Science*, v. 200, p. 1003-1011.
- McKee, C.J., 1984, Precious-metal vein deposits: in Thornsberry et al., eds., *Mineral resource studies in the Kantishna Hills and Dunkle Mine areas, Denali National Park and Preserve*: Salisbury and Dietz, Inc., 234 p.
- McKee, E.H., 1979, Ash-flow sheets and calderas: their genetic relationship to ore deposits in Nevada: *Geol. Soc. of America Special paper* 180, p. 205-211.
- Meinert, L.D., 1982, Skarn, manto, and breccia pipe formation in sedimentary rocks of the Cananea Mining District, Sonora, Mexico: *Econ. Geol.*, v. 77, p. 919-949.
- Meinert, L.D., 1988, Gold and silver in skarn deposits in Bicentennial gold 88, Abstracts, Geological Society of Australia, v. 23, p. 614-616.
- Menzie, W.D., Foster, H.L., Tripp, R.B., and Yeend, W.E., 1983, Mineral resource assessment of the Circle Quadrangle, Alaska: U.S. Geol. Survey Open-file Report 83-170B, 55 p.
- Menzie, W.D., Hua, Renmin, and Foster, H.L., 1987, Newly located occurrences of lode gold near Table Mountain, Circle Quadrangle, Alaska: U.S. Geol. Survey Bulletin 1682, 13 p.
- Menzie, W.D., Reed, B.L., Foster, H.L., Sutley, S.J., Cushing, G.W., and Jones, G.M., 1986b, Analyses of selected rock samples from the Lime Peak area, Circle C-6 Quadrangle, Alaska: U.S. Geol. Survey Open-file Report 86-358.
- Menzie, W.D., Reed, B.L., and Keith, T.E.C., 1986a, Lime Peak—An evolved granite with tin-enriched alteration: in Barch-Winkler, Susan, and Reed, K.M., eds., *Geologic Studies in Alaska by the U.S. Geological Survey During 1985*: U.S. Geol. Survey Circular 978, p. 25-27.
- Mertie, J.B., Jr., 1918a, Lode mining in the Fairbanks district, U.S. Geol. Survey Bull. 662, p. 403-424.
- Mertie, J.B., Jr., 1918b, The gold placers of the Tolovana district, U.S. Geol. Survey Bull. 662, p. 221-277.
- Mertie, J.B., Jr., 1937, The Yukon-Tanana Region, Alaska: U.S. Geol. Survey Bull. 872, 276 p.
- Mertie, J.B., Jr., 1938, Gold placers of the Fortymile, Eagle, and Circle districts, Alaska: U.S. Geol. Survey Bull. 897-C, p. 133-261.
- Mertie, J.B., Jr., 1940, Platinum deposits of the Goodnews Bay district, Alaska, 1939: U.S. Geol. Survey Bull. 910-B, p. 115-145.
- Mertie, J.B., Jr., 1940b, Placer gold in Alaska: *Washington Academy of Science Journal*, no. 3, p. 93-124.
- Metz, P.A., 1977, Comparison of mercury-antimony-tungsten mineralization of Alaska with strata-bound cinnabar-stibnite-scheelite deposits of the Circum-Pacific and Mediterranean regions, in *Short Notes on Alaskan Ge-*

- ology - 1977, Alaska Division of Geological and Geophysical Surveys, Geol. Rept. 35, p. 39-41.
- Metz, P.A., 1982, Bedrock geology of the Fairbanks mining district, northeast sector, Alaska: Alaska Division of Geological and Geophysical Surveys Open-file Report 154, 1 sheet, scale 1:24,000.
- Metz, P.A., 1983, Bedrock stratigraphic, structural and surficial depositional controls of the gold placer deposits of the Fairbanks mining district, Alaska: Abstr. in Proc. 34th Alaska Science Conference, Whitehorse, Yukon Terr., 28 Sept. - 1 Oct. 1983, p. 93.
- Metz, P.A., 1984a, Sulphur isotopic evidence for the genesis of the Au-Ag-Sb-W mineralization of the Fairbanks mining district, Alaska: British Geological Surveys, Isotope Geology Laboratory Open-file Report, 20 p.
- Metz, P.A., 1984b, Fluid inclusion and stable isotopic evidence for the origin of the Au-Ag-Sb-W mineralization of the Fairbanks mining district, Alaska: Geol. Soc. America, Abstracts with Programs, v. 16, no. 6, p. 594-596.
- Metz, P.A., 1984c, Geological factors governing the formation of the gold placer deposits of the Fairbanks mining district, Alaska: Abstr. in University of Alaska, MIREL Report No. 69.
- Metz, P.A., 1984d, Statistical analysis of the stream sediment, pan concentrate and rock geochemical data of the Fairbanks mining district, Alaska: University of Alaska, MIREL Open-file Report 84-1, 40 p., maps, 9 sheets, scale 1:63,360.
- Metz, P.A., 1984e, Statistical analysis of the stream sediment and pan concentrate geochemical data of the Richardson mining district, Alaska: University of Alaska, MIREL Open-file Report 84-2, 48 p., maps, 4 sheets, scale 1:40,000.
- Metz, P.A., 1984f, Statistical analysis of the stream sediment, pan concentrate and rock geochemical samples from the Tolovana mining district, Alaska: University of Alaska, MIREL Open-file Report 84-8, 44 p., maps, 2 sheets, scale 1:63,360.
- Metz, P.A., 1984g, Statistical analysis of stream sediment samples from the Circle mining district, Alaska: University of Alaska, MIREL Open-file Report 84-9, 60 p., maps, 5 sheets, scale 1:40,000.
- Metz, P.A., 1985, The Roman gold mines of the Iberian Peninsula and analogue deposits in Alaska: in Proc. of Seventh Annual Conf. on Alaskan Placer Mining: Alaskan Prospectors Publishing, Fairbanks, Alaska, p. 48-52.
- Metz, P.A., 1987, Ore mineralogy and gold grain size distribution in the gold-silver-arsenic-antimony-tungsten mineralization of the Fairbanks mining district, Alaska: Process Mineralogy VII, The Metallurgical Society, Warrendale, Pennsylvania, p. 247-264.
- Metz, P.A., 1990, Preliminary geologic map of the Circle mining district: University of Alaska, MIREL Open-File Report, maps, 6 sheets, scale 1:40,000.
- Metz, P.A., et al., 1979, Compilation of the data on the land withdrawals in Alaska: University of Alaska, MIREL Report No. 40, 44 p., maps, 6 sheets, scale 1:1,000,000.
- Metz, P.A. and Campbell, Bruce, 1982, Cost of exploration for metallic minerals in Alaska - 1982: University of Alaska, MIREL Report No. 56, 83 p.
- Metz, P.A., Egan, Alyce, and Johansen, Otto, 1982, Landsat linear features and incipient rift system model for the origin of base metal and petroleum resources of northern Alaska: Can. Soc. Petroleum Geologists, Memoir 8, p. 101-112.
- Metz, P.A. and Halls, Christopher, 1981, Ore petrology of the Au-Ag-Sb-W-Hg mineralization of the Fairbanks mining district, Alaska: Abstr. in Proc. Mineralization of the precious metals, uranium and rare earths, University College, Cardiff, Wales, 15-18 Dec. 1981.
- Metz, P.A. and Hamil, B.M., 1986, Origin and extent of the gold, silver, antimony, and tungsten mineralization in the Fairbanks mining district, Alaska, in Hagni, R.D., ed., Process Mineralogy VI, The Metallurgical Society, Warrendale, Pennsylvania, p. 215-238.
- Metz, P.A. and Hawkins, D.B., 1981, A summary of gold fineness values from Alaska placer deposits: University of Alaska, MIREL Report no. 45, 63 p.
- Metz, P.A. and Robinson, M.S., 1979, Tungsten in Alaska: Alaska Division of Geological and Geophysical Surveys, Mines and Geology Bulletin, v. 28, no. 1, p. 1-3.
- Metz, P.A. and Robinson, M.S., 1980, Investigation of mercury-antimony-tungsten metal provinces of Alaska: University of Alaska, MIREL, Open-file Report 80-8, p. 153-190.
- Metz, P.A., Swainbank, R.C. and Burton, P.J., 1984, Statistical analysis of stream sediment and pan concentrate geochemical samples from the Richardson mining district, Alaska: University of Alaska, MIREL Open-file Report 84-3, 54 p., maps, 4 sheets, scale 1:40,000.
- Metz, P.A. and Wolff, E.N., 1980, Interpretation of large geologic features and trends associated with Alaskan

- mineral occurrences by means of enhanced satellite imagery: University of Alaska, MIREL, unpub. contract rept., 74 p.
- Moffit, F.H., 1927, Mineral resources of Alaska, report on progress of investigations in 1925: U.S. Geol. Survey Bull. 792-A, p. 1-39.
- Moffit, F.H., 1933, The Kantishna District, in *Mineral Resources of Alaska, 1930*: U.S. Geol. Survey Bull. 836, p. 301-339.
- Morrison, D.H., 1964, Geology and ore deposits of Kantishna and vicinity, Kantishna district, Alaska: University of Alaska unpub. M.A. thesis, 108 p.
- Mortensen, J.K., 1983a, Age and evolution of the Yukon-Tanana Terrane in southeastern Yukon Territory: University of California (Santa Barbara), unpublished Ph.D. dissertation, 155 p.
- Mortensen, J.K., 1983b, U-Pb and Rb-Sr evidence for the age and timing of tectonism of the Yukon-Tanana Terrane in southeastern Yukon Territory: Geological Association of Canada Program with Abstracts, v. 8, p. A49.
- Mortensen, J.K., 1986, U-Pb ages of granitic orthogneiss in the Yukon-Tanana terrane in west-central Yukon: Selwyn Gneiss and Fiftymile Batholith revisited; in *Current Research, Part B*, Geological Survey of Canada, Paper 86-1A, p. 141-146.
- Mortensen, J.K., 1990, Significance of U-Pb ages for inherited and detrital zircons from Yukon-Tanana Terrane, Yukon and Alaska: abstr., Geol. Assoc. Canada Annual Meeting, Vancouver, B.C., May 16-18, 1990.
- Mortensen, J.K. and Jilson, G.A., 1983, Age and evolution of the Yukon-Tanana Terrane in SE Yukon Territory: Geological Society of America Abstracts with Program, v. 15, p. 274.
- Mortensen, J.K. and Jilson, G.A., 1985, Evolution of the Yukon-Tanana terrane: evidence from southeastern Yukon Territory: *Geology*, v. 13, p. 806-810.
- Mosley, M.P. and Schumm, S.A., 1977, Stream junctions - a probable location for bedrock placers: *Econ. Geol.*, v. 72, p. 691-697.
- Muff, R., 1978, The antimony deposits of the Murchison range of the northeastern Transvaal, Republic of South Africa: *Mon. Ser. Miner. Deposits*, No. 16, 90 p.
- Mullar, A.L., 1982, Mining and mineral processing equipment costs and preliminary capital cost estimations: *Can. Instit. of Min. and Metal.*, CIM Special Vol. 25, 265 p.
- Muller, J.E., 1967, Kluane Lake map area, Yukon Territory: *Geol. Survey of Canada, Memoir 326*, 96 p.
- Mulligan, J.J., 1974, Mineral resources of the trans-Alaska pipeline corridor: U.S. Bureau of Mines, IC 8626, 24 p.
- Nash, J.T., 1972, Fluid inclusion studies of some gold deposits in Nevada: U.S. Geol. Survey Professional Paper 800-C, p. C15-C19.
- Nash, J.T., 1976, Fluid inclusion petrology-Data from porphyry copper deposits and application to exploration. U.S. Geol. Survey Professional Paper, 907-D, 16 p.
- Nelson, A.E., West, W.S., and Matzko, J.J., 1954, Reconnaissance for radioactive deposits in eastern Alaska, 1952: U.S. Geol. Survey Circular 348, 21 p.
- Nesbitt, B.E., Muehlenbachs, Karhs, and Murowchick, J.B., 1989, Genetic implications of stable isotope characteristics of meso-thermal Au deposits and related Sb and Hg deposits in the Canadian Cordillera: *Econ. Geol.* v. 84, p. 1489-1506.
- Newberry, R.J., 1987, Lode mineralization in the Lime Peak-Mt. Prindle area: in Smith et al., eds, *Mineral assessment of the Lime Peak-Mt. Prindle area, Alaska*: Alaska Division of Geological and Geophysical Surveys Contract Report, 276 p, maps 13 sheets.
- Nielson, H., 1979, Sulfur isotopes in Jages, E. and Hunziker, J.C., eds., *Lectures in isotope geology*: Springer-Verlag, New York, N.Y., p. 283-312.
- Noble, L.L. and Radtke, A.S., 1978, Geology of the Carlin disseminated replacement gold deposit, Nevada. Nevada Bureau of Mines and Geol. Rept. 32. Guidebook to mineral deposits of the central great basin, prepared for I.A.G.O.D. Symposium, Mackay Schools of Mines, Reno, Nevada, 1978.
- O'Leary, R.M., Hoffman, J.D., Risoli, D.A., and Tripp, R.B., 1986, Analytical results and sample locality map of stream-sediment and heavy mineral concentrate samples from the Circle Quadrangle, Alaska: U.S. Geol. Survey Open-file Report 86-204, 129 p., 1 sheet, scale 1:250,000.
- Ohmoto, H., 1972, Systematics of sulfur and carbon isotopes and ore genesis: A review: *Econ. Geol.*, v. 69, p. 826-842.
- Ohmoto, H. and Rye, R.O., 1979, Isotopes of sulphur and carbon: In: Barnes, H.L. ed., *Geochemistry of hydrothermal ore deposits*, Wiley Interscience, New York, p. 509-567.
- O'Neil, J.R., Silberman, M.L., Fabbi, B.P. and Chesterman,

- C.W., 1973, Stable isotope and chemical relations during mineralization in the Bodie mining district, Mono County, California: *Econ. Geol.*, v. 68, p. 765-784.
- Overbeck, R.M., 1920, Placer mining in the Tolovana district: *U.S. Geol. Survey Bull.* 712, p. 177-184.
- Pankhurst, R.J., 1969, Strontium Isotopic Studies Related to petrogenesis in the Caledonian Basic Igneous Province of Northeast Scotland: *J. Petrol.*, v. 10, p. 115-143.
- Patterson, G.C., 1984, Field trip guidebook to the Hemlo area: *Ontario Geol. Surv., Misc. Paper no. 118*, 33 p.
- Pavlidis, Louis, et al., 1982, Central Virginia volcanic-plutonic belt as host for massive sulfide deposits: *Econ. Geol.*, v. 77, p. 233-272.
- Pearson, R.C., Hedge, C.E., Thomas, H.H. and Stern, T.W., 1966, Geochronology of the St. Kevin Granite and neighboring Precambrian rocks, northern Sawatch Range, Colorado: *Geol. Soc. America Bull.*, v. 77, p. 1109-1120.
- Peltola, E., 1978, Origin of Precambrian copper sulfides of the Outokumpu district, Finland: *Econ. Geol.*, v. 73, p. 461-477.
- Pessel, G.H., Reifensstuhl, R.R., and Albanese, 1987, Regional geology in Smith et al., eds, *Mineral Assessment of the Lime Peak-Mt. Prindle area, Alaska*: Alaska Division of Geological and Geophysical Surveys Contract Report, 276 p, maps 13 sheets.
- Peters, C.W., 1978, *Exploration and mining geology*: John Wiley & Sons, New York, 696 p.
- Petro, W.L., Vogel, T.A., and Wilband, J.T., 1979, Major-element chemistry of plutonic rock suites from compressional and extensional plate boundaries: *Chemical Geology*, v. 26, p. 217-235.
- Péwé, T.L., 1952, *Geomorphology of the Fairbanks area*: Stanford University unpub. Ph.D. thesis, 220 p.
- Péwé, T.L., 1958, Geologic map of the Fairbanks (D-2) quadrangle, Alaska: *U.S. Geol. Survey Geol. Quad. Map GQ-110*.
- Péwé, T.L., 1975, Quaternary stratigraphic nomenclature in unglaciated central Alaska: *U.S. Geol. Survey Professional Paper 862*, 32 p.
- Péwé, T.L., 1976a, Geologic map of the Fairbanks (D-2 SW) quadrangle, Alaska: *U.S. Geol. Survey Misc. Invest. Map I-829A*.
- Péwé, T.L., 1976b, Geologic map of the Fairbanks (D-2 SE) quadrangle, Alaska: *U.S. Geol. Survey Misc. Invest. Map I-942*.
- Péwé, T.L., 1976c, Geologic map of the Fairbanks (D-2 NE) quadrangle, Alaska: *U.S. Geol. Survey Misc. Invest. Map I-950*.
- Péwé, T.L., Bell, J.W., Forbes, R.B. and Weber, F.R., 1975, Geologic map of the Fairbanks (D-2 NW) quadrangle, Alaska: *U.S. Geol. Survey Misc. Invest. Map I-907*.
- Péwé, T.L. and Revard, N.R., 1961, Geologic map of the Fairbanks (D-3) quadrangle, Alaska: *U.S. Geol. Survey Misc. Invest. Map I-34D*.
- Péwé, T.L., Wahrhaftig, C. and Weber, F.R., 1966, Geologic map of the Fairbanks quadrangle, Alaska: *U.S. Geol. Survey Misc. Invest. Map I-455*.
- Pilgrim, E.R., 1929, Report on Shannon lode properties, Kantishna district: Alaska Division of Geological and Geophysical Surveys, unpub. rept., 10 p.
- Potgieter, G.A. and De Villiers, J.P.R., 1986, Controls of mineralization at the Fumani gold deposit, Sutherland Greenstone Belt in Anhaeusser, C.R., and Maske, S., eds., *Mineral deposits of southern Africa*: Geological Society of South Africa, p. 197-204.
- Prindle, L.M., 1904, Gold placers of the Fairbanks district, Alaska: *U.S. Geol. Survey Bull.* 225, p. 64-73.
- Prindle, L.M., 1905, The gold placers of the Fortymile, Birch Creek and Fairbanks regions, Alaska: *U.S. Geol. Survey Bull.* 251, 89 p.
- Prindle, L.M., 1906a, The Yukon-Tanana region, Alaska: Description of Circle Quadrangle: *U.S. Geol. Survey Bulletin* 295, 27 p.
- Prindle, L.M., 1906b, Yukon placer fields: *U.S. Geol. Survey Bull.* 284, p. 109-127.
- Prindle, L.M., 1907, The Bonifield and Kantishna Regions, Alaska: *U.S. Geol. Survey Bull.* 314-L, p. 205-226.
- Prindle, L.M., 1908, The Fairbanks and Rampart quadrangles, Yukon-Tanana region, Alaska, with a section on the Rampart placers, by F.L. Hess, and a paper on the water supply of the Fairbanks region, by C.C. Covert: *U.S. Geol. Survey Bull.* 337, 102 p.
- Prindle, L.M., 1910, Auriferous quartz veins in the Fairbanks district: *U.S. Geol. Survey Bull.* 442-F, p. 210-229.

- Prindle, L.M., 1913, A geologic reconnaissance of the Circle quadrangle, Alaska: U.S. Geol. Survey Bull. 538, 82 p.
- Prindle, L.M. and Katz, F.J., 1909, The Fairbanks gold-placer region: U.S. Geol. Survey Bull. 379, p. 181-200.
- Prindle, L.M. and Katz, F.J., 1913, Geology of the Fairbanks district: U.S. Geol. Survey Bull. 525, p. 59-131.
- Purinton, C.W., 1905, Methods and costs of gravel and placer mining in Alaska: U.S. Geol. Survey Bull. 263, 273 p.
- Putzer, H., 1976, Metallogenetische Provinzen in Sudamerika, Schweizerbart, Stuttgart, 299 p.
- Pye, E.G. and Roberts, R.G., 1981, Genesis of Archaean volcanic hosted gold deposits: Ontario Geol. Survey Misc. Paper 97, 175 p.
- Radtke, A.S., 1976a, Features of Carlin-type gold deposits: U.S. Geol. Survey Professional Paper 976, p. 4-5.
- Radtke, A.S., 1976b, Genesis of Carlin-type gold deposits in the framework of tectonic evolution of the Basin and Range province (abst.): Econ. Geol., v. 71, no. 3, p. 702.
- Radtke, A.S., Heropoulos, C., Fabbi, B.P., Scheiner, B.J. and Essington, M., 1972, Data on major and minor elements in host rocks and ores, Carlin Gold Deposit, Nevada: Econ. Geol., v. 67, no. 7, p. 975-978.
- Radtke, A.S., Rye, R.O. and Dickson, F.W., 1980, Geology and stable isotope studies of the Carlin gold deposit: Econ. Geology, v. 75, p. 641-672.
- Radtke, A.S., Taylor, C.M. and Christ, C.L., 1972, Chemical distribution of gold and mercury at the Carlin deposit, Nevada (abst.): Econ. Geology, v. 67, p. 1009.
- Rakhmanillaev, Kh.R. and Sher, S.D., 1969, The metasomatic wall rock alteration in the Muruntau ore deposits; in The gold deposits and principle features of the metallogeny of gold in Uzbekistan, I. Kh. Khamrabaev, ed.; "Fan" Publ. Off., Uzbek S.S.R., Tashkent, p. 173-176.
- Rawlinson, S.E., 1987, Surficial geology, lineaments, and placer resources in the Lime Peak-Mt. Prindle and Pinnel Trail areas, east-central Alaska: in Smith et al., eds, Mineral assessment of the Lime Peak-Mt. Prindle area, Alaska: Alaska Division of Geological and Geophysical Surveys Contract Report, 276 p, maps 13 sheets.
- Reed, Irving, 1938, Report on lode mining and development in the year 1938 in the Fairbanks district, Alaska: Alaska Territorial Dept. of Mines Rept., 26 p.
- Reed, J.C., 1961, Geology of the Mount McKinley quadrangle, Alaska: U.S. Geol. Survey Bull. 1108-A, 36 p.
- Reid, K.O., 1975, Mount Lyell copper deposits, In: C.L. Knight (editor), Economic Geology of Australia and Papua New Guinea, Aust. Inst. Min. Metall. Monogr., 5, p. 604-618.
- Richardson, J.M.B., et al., 1982, The East Kemptonville tin deposit, Nova Scotia, An example of a large tonnage, low grade greisen-hosted deposit in the endocontact zone of a granite batholith: Geol. Survey of Canada Paper 82-1B, p. 27-32.
- Ridler, R.H., 1970, Relationship of mineralization to volcanic stratigraphy in the Kirkland-Larder Lakes area, Ontario: Geol. Assoc. Can., 21, p. 33-42.
- Riley, R., 1972, Campbell Red Lake Mines Ltd. gold mine, Red Lake Area, Ontario: 24th Int. Geol. Congr. Montreal, Guidebook, Excursion A33-C33, p. 53-56.
- Roberts, R.G., 1975, The geological setting of the Mattagami Lake Mine, Quebec, A volcanogenic massive sulfide deposit: Econ. Geol., v. 70, p. 115-129.
- Roberts, R.J., Radtke, A.S. and Coats, R.R., 1971, Gold bearing deposits in north-central Nevada and south-western Idaho: Econ. Geol., v. 66, p. 14-33.
- Robinson, B.W. and Farrand, M.G., 1982, Sulphur isotopes and the origin of stibnite mineralization in New England, Australia: Mineral. Deposita, v. 17, p. 161-174.
- Robinson, B.W. and Kusakabe, M., 1975, Quantitative preparation of sulfur dioxide, for 34S/32S analyses from sulfides by combustion with cuprous oxide: Analytical Chemistry, v. 47, no. 7, p. 1179-1181.
- Robinson, M.S., 1982, Bedrock geology of the Fairbanks mining district, southeast sector: Alaska Division of Geological and Geophysical Surveys, Open-file Report 146, 1 sheet, scale 1:24,000.
- Robinson, M.S., 1983, Bedrock geology map of the Livengood C-4 Quadrangle, Alaska: Alaska Division of Geological and Geophysical Surveys Report of Investigations 83-4, 1 pl., scale 1:40,000.
- Robinson, M.S., 1984, Metallurgy of the Tolvana Mining District, east-central Alaska: Alaska Division of Geological and Geophysical Surveys Public Data File 84-48, 7 p.
- Robinson, M.S. and Bundtzen, T.K., 1979, Historic gold production in Alaska: Alaska Division of Geological

- and Geophysical Surveys Mines and Geology Bull., v. 28, no. 3, p. 1-4.
- Robinson, M.S. and Bundtzen, T.K., 1982, Geology of the Scrafford antimony-gold lode deposit, Fairbanks mining district, Alaska: Alaska Division of Geological and Geophysical Surveys Open-file Report 173, 7 p., 1 sheet.
- Robinson, M.S. and Metz, P.S., 1979, Evaluation of the mineral resources of the pipeline corridor, Phases I and II: University of Alaska, Mineral Industry Research Laboratory Open-file Report 79-2, 264 p., maps, 84 sheets, scale 1:63,360.
- Robinson, M.S., Smith, T.E., Forbes, R.B., Metz, P.A., and Reger, R.D., 1989, Geology of the Fairbanks mining district: in Schmidt, R.A.M., Nokleberg, W.J., and Page, R.A., eds., Alaskan Geological and Geophysical Transect: 28th International Geological Congress, Washington D.C., June 24-July 5, 1989, p. 63-69.
- Robinson, M.S., Smith, T.E., and Metz, P.A., 1990, Bedrock geology of the Fairbanks mining district: Alaska Division of Geological and Geophysical Surveys Professional Report 106, map, 2 sheets, scale 1:63,360.
- Roedder, E., 1984a, Fluid inclusion evidence bearing on the environment of gold deposition: in Foster, R.P., ed., Gold '82: Geol. Survey of Zimbabwe Spec. Pub. no. 1, A.A. Balkema, Rotterdam, p. 129-163.
- Roedder, E., 1984b, Fluid inclusions: Reviews in Mineralogy, v. 12, Mineralogical Society of America, 644 p.
- Rye, R.O., Doe, B.R. and Wells, J.D., 1970, Stable isotope study of the Cortez, Nevada, gold deposit and surrounding area: U.S. Geol. Survey Jour. Research, v. 2, no. 1, p. 13-23.
- Rye, D.M. and Rye, R.O., 1974, Homestake gold mine, South Dakota: I. Stable Isotope studies: Econ. Geol., v. 69, p. 293-317.
- Rytuba, J.J., 1981, Relation of calderas to ore deposits in the western United States: in Dickinson, W.R. and Payne, W.D., eds., Relations of tectonics to ore deposits in the southern Cordillera: Ariz. Geol. Soc. Digest, v. XIV, p. 227-236.
- Saager, Rudolf, et al., 1987, Geochemistry and mineralogy of Banded Iron-Formation-Host gold mineralization in the Gwanda Greenstone Belt, Zimbabwe: Econ. Geol., v. 82, p. 2017-2032.
- Salisbury, W.G., 1984, Sample analysis and interpretation: in Thornsberry et al., eds., Mineral resource studies in the Kantishna Hills and Dunkle Mine areas, Denali National Park and Preserve: Salisbury and Dietz, Inc., 234 p.
- Sandvik, P.O., 1964, Metal distribution in ore deposits of central Alaska: Stanford University, unpub. Ph.D. thesis, 144 p.
- Sandvik, P.O. and Hersey, A.J., 1951, Relations of structure to mineral deposition at the Grant mine, Ester Dome, Alaska: University of Alaska, unpubl. B.S. thesis, 28 p.
- Saunders, R.H., 1964, Report on the Bonnell silver-lead prospect, Mt. McKinley quadrangle, Alaska: Alaska Division of Geological and Geophysical Surveys, unpubl. rept., 12 p.
- Saunders, R.H., 1965, Geochemical investigation in the Richardson area, Big Delta quadrangle, Alaska: Alaska Division of Geological and Geophysical Surveys, Geochemical Report No. 3, 12 p.
- Saunders, R.H., 1967, Mineral occurrences in the Yukon-Tanana region, Alaska: State of Alaska, Department of Natural Resources, Division of Mines and Minerals, Spec. Rept. No. 2, 59 p.
- Schulz, O., 1972, Horizontgebundene altpalaeozoische Kupferkiesvererzung in der Nordtiroler Grauwackenzone, Osterreich: Tschermarks Mineral. Petrogr. Mitt., 17: 1-18.
- Schumacher, O.L., 1990, Mining cost service: Western Mining Engineering, Spokane, Washington, 325 p.
- Seraphim, R.H., 1961, Kantishna district: Alaska Division of Geological and Geophysical Surveys, unpubl. rept., MK-193-2, 25 p.
- Seraphim, R.H., 1962, Report on exploration on Quigley Ridge, Kantishna District: Alaska Division of Geological and Geophysical Surveys Report, PE-66-2, 2 p.
- Seward, T.M., 1973, Thiocomplexes of gold and the transport of gold in hydrothermal ore solutions: Geochim et Cosmochim. Acta., v. 37, p. 379-399.
- Seward, T.M., 1979, Hydrothermal transport and deposition of gold, in J.E. Glover and D.I. Groves (eds.), Gold Mineralization Publ. Geol. Dept. and Extension Service, Univ. of Western Australia, 3: 45-55.
- Seward, T.M., 1982, Transport and deposition of gold in hydrothermal systems: in Foster, R.P., ed., Gold '82: Geology, geochemistry and genesis of gold deposits: A.A. Balkema, Rotterdam, p. 165-181.

- Shanks, W.C., et al., 1987, Sulfur and lead isotope studies of stratiform Zn-Pb-Ag deposits, Anvil Range, Yukon: *Econ. Geol.*, v. 82, p. 600-634.
- Shaw, D.M. and Kudoo, A.M., 1965, A test of the discriminant function in the amphibolite problem: *Mineralogical Magazine*, v. 34, no. 268, p. 423-435.
- Sheppard, T.J. and Waters, P., 1984, Fluid inclusion gas studies, Carrock Fell tungsten deposit, England; implications for regional exploration: *Mineralium. Deposita*, vol. 19, p. 304-314.
- Sherman, G.E., 1983, Geology and mineralization of the Silver Fox Mine, Fairbanks District, Alaska: University of Alaska unpub. M.S. thesis, 84 p., 3 sheets, scale 1:4,800.
- Sherwood, K.W. and Craddock, C., 1979, General geology of the central Alaska Range between the Nenana River and Mount Deborah, Alaska Division of Geological and Geophysical Surveys, Alaska Open-file Report AOF-116, 22 p.
- Shulits, S., 1941, Rational equation of riverbed profile: *Transactions of the American Geophysical Union*, v. 22, p. 622-630.
- Silberman, M.L., 1982, Hot-spring type, large tonnage, low-grade gold deposits: in Erickson, R.L., ed., *Characteristics of Mineral Deposit Occurrences*: U.S. Geol. Survey Open-file Report 82-795, p. 131-143.
- Silberman, M.L., Berger, B.R. and Koski, R.A., 1974, K-Ar Age relations of granodiorite emplacement and tungsten and gold mineralization near the Getchell Mine, Humboldt County, Nevada: *Econ. Geol.*, v. 69, p. 646-656.
- Silberman, M.L. and Chesterman, C.W., 1972, K-Ar age of volcanism and mineralization, Bodie mining district and Bodie Hills volcanic field, Mono County, California: *Isochron/West*, no. 3, p. 13-22.
- Silberman, M.L. and McKee, E.H., 1974, Ages of Tertiary volcanic rocks and hydrothermal precious-metal deposits in central and western Nevada: Nevada Bur. Mines Geol. Report No. 19, p. 67-72.
- Sillitoe, R.H., 1977, Metal mineralization affiliated to sub-aerial volcanism - a review: *Volcanic Processes in Ore Genesis*, Geol. Soc. London Spec. Pub. 7, p. 99-116.
- Sillitoe, R.H., 1979, Some thoughts on gold-rich porphyry copper deposits: *Mineral. Deposita*, v. 17, p. 161-174.
- Sillitoe, R.H., 1980, Types of porphyry molybdenum deposits: *Mining Magazine*, v. 142, p. 550-553.
- Sillitoe, R.H., 1982, Unconventional metals in porphyry deposits: *Soc. of Mining Engineers pre-print 82-63*, 13 p.
- Simpson, S., 1983, Geomorphic domains and linear features on Landsat images, Circle Quadrangle, Alaska; U.S. Geol. Survey Open-file Report 83-170-E.
- Skillings, D.N., 1976, Rosario Dominicana S.A. Pueblo Viejo operations: *Skillings Mining Review*, v. 65, no. 12, p. 10-15.
- Slack, J.F., 1980, Multistage vein ores of the Lake City district, western San Juan Mountains, Colorado: *Econ. Geol.*, v. 75, p. 963-991.
- Smirnov, V.I., 1976, *Geology of mineral deposits*: MIR Publishers, Moscow, 520 p.
- Smith, P.S., 1913a, Lode mining near Fairbanks, U.S. Geol. Survey Bull., 542-F, p. 137-202.
- Smith, P.S., 1913b, The fineness of gold in the Fairbanks district, Alaska: *Econ. Geol.*, v. 8, p. 448-454.
- Smith, P.S., 1926, Mineral industry of Alaska in 1924: U.S. Geol. Survey Bull. 783-A, p. 1-30.
- Smith, P.S., 1929, Mineral industry of Alaska in 1926: U.S. Geol. Survey Bull. 797, p. 1-50.
- Smith, P.S., 1930, Alaska mining industry - 1927: U.S. Geol. Survey Bull. 810, p. 26.
- Smith, P.S., 1930, Mineral industry of Alaska in 1928: U.S. Geol. Survey Bull. 813, p. 1-72.
- Smith, P.S., 1932, Mineral industry of Alaska in 1929: U.S. Geol. Survey Bull. 824, p. 1-81.
- Smith, P.S., 1933, Mineral industry of Alaska in 1930: U.S. Geol. Survey Bull. 836-A, p. 1-83.
- Smith, P.S., 1933, Mineral industry of Alaska in 1931: U.S. Geol. Survey Bull. 844-A, p. 1-82.
- Smith, P.S., 1934, Mineral industry of Alaska in 1932: U.S. Geol. Survey Bull. 857-A, p. 1-91.
- Smith, P.S., 1934, Mineral industry of Alaska in 1933: U.S. Geol. Survey Bull. 864-A, p. 1-94.
- Smith, P.S., 1936, Mineral industry of Alaska in 1934: U.S. Geol. Survey Bull. 868-A, p. 1-91.
- Smith, P.S., 1937, Mineral industry of Alaska in 1935: U.S. Geol. Survey Bull. 880-A, p. 1-95.

- Smith, P.S., 1938, Mineral industry of Alaska in 1936: U.S. Geol. Survey Bull. 897-A, p. 1-107.
- Smith, P.S., 1939a, Mineral industry of Alaska in 1937: U.S. Geol. Survey Bull. 910-A, p. 1-113.
- Smith, P.S., 1939b, Mineral industry of Alaska in 1938: U.S. Geol. Survey Bull. 917-A, p. 1-113.
- Smith, P.S., 1941, Mineral industry of Alaska in 1939: U.S. Geol. Survey Bull. 926-A, p. 1-106.
- Smith, P.S., 1941, Fineness of gold from Alaskan placers: U.S. Geol. Survey Bull. 910-C, p. 147-272.
- Smith, P.S., 1942a, Mineral industry of Alaska in 1940: U.S. Geol. Survey Bull. 933-A, p. 1-102.
- Smith, P.S., 1942b, Occurrences of molybdenum minerals in Alaska: U.S. Geol. Survey Bull. 926-C, p. 161-210.
- Smith, S.S., 1917, The mining industry in the Territory of Alaska during the calendar year 1915: U.S. Bur. Mines Bull. 142, 66 p.
- Smith, S.S., 1917, The mining industry in the Territory of Alaska during the calendar year 1916: U.S. Bur. Mines Bull. 153, 89 p.
- Smith, T.E., 1983, Bedrock geologic map of the Livengood C-3 Quadrangle, Alaska: Alaska Division of Geological and Geophysical Surveys Report of Investigations 83-5, 1 pl., scale 1:40,000.
- Smith, T.E., Pessel, G.H., and Wiltse, M.A., 1987, Mineral assessment of the Lime Peak-Mt. Prindle area, Alaska: Alaska Division of Geological and Geophysical Surveys Contract Report, 276 p, maps 13 sheets.
- Solie, D.N., Burns, L.E., and Newberry, R.J., 1990, Gold favorability in the Big Delta quadrangle, Alaska as predicted by discriminant analysis for non-porphry granitic rock: Alaska Division of Geological and Geophysical Surveys Public Data File 90-13, maps, 2 sheets, scale 1:250,000.
- Spence, C.D. and de Rosen-Spence, A.F., 1975, The place of sulfide mineralization in the volcanic sequence at Noranda, Quebec: *Econ. Geol.*, 70, p. 90-101.
- Spence, W.H., et al., 1978 Origin of the gold mineralization at the Haile Mine, Lancaster County, South Carolina: Soc. Min. Engineers of AIME, preprint 78-I-339, 6 p.
- Spencer, W.W. and O'Neill, W.A., 1934, A survey of the gold quartz veins on the north flank of Pedro Dome: University of Alaska unpub. B.S. thesis, 52 p.
- Spurr, J.E., 1898, Geology of the Yukon gold district: U.S. Geol. Surv. 18th Ann. Rept., pt. 3, p. 103-392.
- Staff, Engineering Mining Journal, 1977a, Development of Wisconsin's mineral potential is stymied by the state: *Eng. Mining Jour.*, v. 178, no. 2, p. 23-27.
- Staff, Engineering Mining Journal, 1977b, Rosario Dominicana operates largest open-pit gold mine: *Eng. Mining Jour.*, v. 178, no. 11, p. 145-149.
- Steiger, R.H. and Jäger, E., 1977, Subcommittee on Geochronology, Convention on the use of decay constants in geo- and cosmochronology: *Earth and Planetary Science Letters*, v. 36, p. 359-362.
- Sternberg, H., 1875, Untersuchungen über Langen und Querprofil Geschie beführende Flüsse: *Zeitschrift für Bauwesen*, 25, p. 483-506.
- Steven, T.A. and Eaton, G.P., 1975, Environment of ore deposition in the Creede mining district, San Juan Mountains, Colorado: Part I. Geologic, hydrologic and geophysical setting: *Econ. Geol.*, v. 70, p. 1023-1037.
- Stewart, B.D., 1933, Mining investigations and mine inspection in Alaska, biennium ending March 31, 1933: Territorial Department of Mines Report, 192 p.
- Strauss, G.K., Madel, J. and Alonso, F.F., 1977, Sulphide deposits in the Spanish-Portuguese pyrite belt: geology, geophysics and geochemistry, in: D.D. Klemm and H.J. Schneider (editors), *Time and Strata-Bound ore Deposits*, Springer, New York, N.Y., p. 55-93.
- Straam Engineers, 1978, Capital and operating cost estimating system for mining and beneficiation of metallic and nonmetallic minerals: U.S. Bureau of Mines Contract No. JO255026, 374 p.
- Streckeisen, A., 1973, Classification and nomenclature recommended by the International Union of Geological Sciences Subcommittee on the Systematics of Igneous Rocks: *Geotimes*, v. \_\_, no. 10, p. 26-30.
- Suffel, G.G., Hutchinson, R.W. and Ridler, R.H., 1971, Metamorphism of massive sulphides at Manitouwadge, Ontario, Canada: *Soc. Min. Geol. Jpn. Spec. Issue*, 3, p. 235-240.
- Swainbank, R.C., 1971, Geochemistry and petrology of eclogitic rocks in the Fairbanks area, Alaska: University of Alaska, unpub. Ph.D. thesis, 130 p.
- Swainbank, R.C., 1987, Regional structure: in Smith et al., eds, Mineral assessment of the Lime Peak-Mt. Prindle

- area, Alaska: Alaska Division of Geological and Geophysical Surveys Contract Report, 276 p, maps 13 sheets.
- Swainbank, R.C. and Burton, P.J., 1987, Igneous-hydrothermal related prospects: in Smith et al., eds., Mineral assessment of the Lime Peak-Mt. Prindle area, Alaska: Alaska Division of Geological and Geophysical Surveys Contract Report, 276 p., maps, 13 sheets.
- Swainbank, R.C., Burton, P.J. and Metz, P.A., 1984, Bedrock geology of the Richardson mining district, Alaska: University of Alaska, MURL, Open-file Report 84-2, 60 p., maps, 4 sheets, scale 1:40,000.
- Swainbank, R.C. and Forbes, R.B., 1975, Petrology of eclogitic rocks from the Fairbanks district, Alaska: Geol. Soc. America Special Paper 151, p. 77-213.
- Taylor, B.E. and Slack, J.F., 1984, Tourmaline from Appalachian-Caledonian massive sulfide deposits: textural, chemical, and isotopic relationships: *Econ. Geol.*, v. 79, p. 1703-1726.
- Taylor, H.P., 1973,  $^{18}O/^{16}O$  evidence for meteoric-hydrothermal alteration and ore deposition in the Tonopah, Comstock Lode, and Goldfield mining districts, Nevada: *Econ. Geol.*, v. 68, p. 747-764.
- Tempelman-Kluit, D.J., 1976, The Yukon Crystalline Terrane - Enigma in the Canadian Cordillera: *Geological Society of America Bulletin*, v. 87, p. 1343-1357.
- Tempelman-Kluit, D.J., 1979a, Transported cataclasite, ophiolite, and grandiorite in Yukon: evidence of arc-continent collision: *Geological Survey of Canada Paper* 79-14, 27 p.
- Tempelman-Kluit, D.J., 1979b, Five occurrences of transported synorogenic clastic rocks in Yukon Territory: *Geological Survey of Canada Paper* 79-1A, p. 1-12.
- Tempelman-Kluit, D.J. and Wanless, R.K., 1980, Zircon ages for the Pelly Gneiss and Klotassin granodiorite in western Yukon: *Canadian Journal of Earth Sciences*, v. 17, p. 297-306.
- Tenney, D., 1981, The Whitehorse Copper Belt: Department of Indian and Northern Affairs, Canada, Bull. No. 1, 29 p.
- Thompson, R.L. and Panteleyev, A., 1976, Stratabound mineral deposits of the Canadian Cordillera: in Wolf, K.H. (editor), *Handbook of Stratabound and Stratiform Ore Deposits*, v. 5, Regional Studies and Specific Deposits, Elsevier Scientific Publishing Company, N.Y., p. 37-108.
- Thorne, R.L., Muir, N.M., Erickson, A.W., Thomas, B.L., Heide, H.E. and Wright, W.S., 1948, Tungsten deposits in Alaska: U.S. Bur. Mines R.I. 4174, 51 p.
- Thornsberry, V.V., McKee, C.J., and Salisbury, W.G., 1984, Mineral resource studies in the Kantishna Hills and Dunkle Mine areas, Denali National Park and Preserve: Salisbury and Dietz, Inc., 234 p.
- Thurlow, J.G., Swanson, E.A. and Strong, D.F., 1975, Geology and lithogeochemistry of the Buchans polymetallic sulfide deposit, Newfoundland: *Econ. Geol.*, v. 70, p. 130-144.
- Tolbert, G.E., 1964, Geology of the Raposos gold mine, Minas Gerais, Brazil: *Econ. Geol.*, v. 59, p. 775-798.
- Tourtlot, H.A., 1968, Hydraulic equivalence of grains of quartz and heavier minerals and implications for the study of placers: U.S. Geol. Survey Prof. Paper 594F.
- Triebel, Klaus, 1990, Faulting and extended igneous activity in the Circle mining district, Alaska: University of Alaska, unpub., M.S. Project Report, 29 p.
- Tripp, R.B. and Crim, W.D., 1983, Maps showing geochemistry of minus 80 mesh stream sediment samples, Circle Quadrangle: U.S. Geol. Survey Open-file Report 83-170-H.
- Tripp, R.B. and Houston, D.L., 1983, Mineralogical maps showing selected minerals in the non-magnetic fractions of mineral concentrates of stream sediments, Circle Quadrangle: U.S. Geol. Survey Open-file Report 83-170-F.
- Tripp, R.B., O'Leary, R.M., and Risoli, D.A., 1983, Geochemistry of concentrates of stream sediments, Circle Quadrangle: U.S. Geol. Survey Open-file Report 83-170-G.
- Tuck, R., 1968, Origin of the bedrock values of placer deposits: *Econ. Geol.*, v. 63, p. 191-193.
- Turner, D.L., Grybeck, D. and Wilson, F.H., 1975, Radiometric dates from Alaska - a 1975 compilation: Alaska Division of Geological and Geophysical Surveys Special Report 10, 64 p.
- Vance, R.K. and Condie, K.C., 1987, Geochemistry of footwall alteration associated with early Proterozoic United Verde massive sulfide deposit, Jerome, Arizona: *Econ. Geol.*, v. 82, p. 571-586.
- Vikre, P.G., 1980, Fluid inclusions in silver-antimony-arsenic minerals from precious metal vein deposits: *Econ. Geol.*, v. 75, no. 2, p. 338-339.

- Viljoen, M.J., von Vuuren, C., Pearton, T.N., Minnitt, R., Muff, R., and Cilliers, P., 1978, The regional setting of mineralization in the Murcheson Range with particular reference to antimony: in Verwoerd, W.J., ed., Mineralization in metamorphic terranes, J.L. van Schaik, Limited, Pretoria, p. 55-76.
- Viljoen, R.P., Saager, R. and Viljoen, M.J., 1969, Metallogenesis and ore control in the Steynsdorp Goldfield, Barberton Mountain Land, South Africa: *Econ. Geol.*, 64, p. 778-797.
- Wahrhaftig, Clyde, 1968, Schist of the central Alaska Range: *U.S. Geol. Survey Bull.* 1254-E, p. E1-E22.
- Wargo, Joseph G., 1979, The next exploration stage for Carlin-type gold deposits: *Mining Engineering*, v. 31, no. 9, p. 1321-1323.
- Warner, J.D., Dahlin, D.C., and Brown, L.L., 1986, Greisen and tin occurrences near Rocky Mountain (Lime Peak), east-central Alaska: U.S. Bureau of Mines, Draft report, April 8, 1986, 40 p.
- Wasserburg, G.J., Eberlein, G.D. and Lanphere, M.A., 1963, Age of Birch Creek Schist and some batholithic intrusions in Alaska: *Geol. Soc. Amer. Spec. Paper* 73, p. 258-259.
- Wayland, R.G., 1943, Gold deposit near Nabesna, in Moffit, F.H., ed., *Geology of the Nutzotin Mountains, Alaska*: *U.S. Geol. Survey Bull.* 933-B, p. 103-199.
- Wayland, R.G., 1961, Tofty tin belt, Manley Hot Springs district, Alaska: *U.S. Geol. Survey Bull.* 1058-L, p. 363-414.
- Weber, F.R., Foster, H.L., Keither, T.C. and Dusel-Bacon, Cynthia, 1978, Preliminary geologic map of the Big Delta quadrangle, Alaska: *U.S. Geol. Survey Open-file Report* 78-529A, map, 1 sheet, scale 1:250,000.
- Weber, F.R. and Hamilton, T.D., 1984, Glacial geology of Mount Prindle area, Yukon-Tanana Upland, Alaska: in *Short notes on Alaskan geology 1982-1983*: Alaska Division of Geological and Geophysical Surveys, Professional Report No. 86, p. 42-48.
- Weber, F.R., et al., 1985, Geologic guide to the Fairbanks-Livengood area, east-central Alaska: Alaska Geological Society, Anchorage, Alaska, 44 p.
- Wedow, H., Killeen, P.L. et al., 1954a, Reconnaissance for radioactive deposits in eastern interior Alaska, 1946: *U.S. Geol. Survey Circular* 331, 36 p.
- Wedow, Helmuth, Jr., White, M.G., et al., 1954b, Reconnaissance for radioactive deposits in east-central Alaska, 1949: *U.S. Geol. Survey Circular* 335, 22 p.
- Weisbrod, A., 1981, Fluid inclusions in shallow intrusives, in Hollister, L.S. and Crawford, M.L., eds., *Short Course in Fluid Inclusion*: Mineralogical Association of Canada, Short Course Handbook, v. 6, p. 241-271.
- Wells, F.G., 1933, Lode deposits of Eureka and vicinity, Kantishna district, Alaska: *U.S. Geol. Survey Bull.* 849F, p. 335-379.
- Wheeler, J.O., 1961, Whitehorse map area, Yukon Territory: *Geol. Survey of Canada, Memoir* 312, 156 p.
- Wheeler, J.O., 1987, Tectonic assemblage map of the Canadian Cordillera and adjacent parts of the United States of America: *Geol. Survey of Canada, Open File* 1565, scale 1:5,000,000.
- White, D.H., 1942, Antimony deposits of the Stampede Creek area, Kantishna District, Alaska: *U.S. Geol. Survey Bull.* 936N, p. 331-348.
- Wilkinson, K., 1987, Geology of a subarctic tin-bearing batholith Circle Hot Springs, Alaska: University of Alaska, MIREL Report No. 74, 70 p.
- Williams, J.R., Péwé, T.L., and Paige, R.A., 1959, Geology of the Fairbanks (D-1) quadrangle, Alaska: *U.S. Geol. Survey GQ-124*, map, 1 sheet, scale 1: 63,360.
- Wilson, F.H. and Shew, N., 1981, Map and tables showing preliminary results of potassium-argon age studies in the Circle quadrangle, Alaska, with a compilation of previous dating work: *U.S. Geol. Survey, Open-file Report* 81-889, Scale 1:250,000.
- Wilson, F.H., Smith J.G. and Shew, N., 1985, Reviews of radiometric data from the Yukon Crystalline Terrane, Alaska and Yukon Territory: *Can. Jour. Earth Sci.*, v. 22, p. 525-537.
- Wiltse, M.A., 1987, Geochemistry of the Lime Peak-Mt. Prindle area, west-central Circle quadrangle, Alaska: in Smith et al., eds, *Mineral assessment of the Lime Peak-Mt. Prindle area, Alaska*: Alaska Division of Geological and Geophysical Surveys Contract Report, 276 p, maps 13 sheets.
- Wimmler, N.L., 1927, Placer mining methods and costs in Alaska: *U.S. Bur. Mines Bull.* 259, p. 219.
- Woodall, R., 1975, Gold in Precambrian shield of Western Australia: in C.L. Knight (ed.), *Economic geology of Australia and Papua New Guinea, metals*: Australian Inst. of Mine. Metal., Melbourne, p. 175-185.

- Woodford, A.O., 1951, Stream gradients and Monterey sea valley: Geological Society of America Bull., v. 62, p. 699-852.
- Woodtli, R., 1962a, Gold impregnation deposits in the Moto area (Central Africa): Econ. Geol., v. 56, p. 603-607.
- Woodtli, R., 1962b, Relationships of general structure to gold mineralization in the Kilo area (Central Africa): Econ. Geol., 56, p. 584-591.
- Yeend, W.E., 1987, Placer gold related to mafic schist(?) in the Circle District, Alaska, [in]: Hamilton, T.D., and Galloway, J.P. eds., Geologic studies in Alaska by the U.S. Geological Survey during 1986: U.S. Geol. Survey Circular 998, p. 74-76.
- Yeend, W.E., 1989, Late Cenozoic sedimentary history along major fault zones, Alaska: in Carter, L.D., Hamilton, T.D., and Galloway, J.P., eds., Late Cenozoic interior basins of Alaska and the Yukon: U.S. Geol. Survey Circular 1026.
- Yeend, W.E., Ager, T.A., and Kline, J.T., 1989, Stratigraphy and palynology of an Upper Tertiary terrane deposit of the ancestral Yukon River near Circle, Alaska: in Dover, J.H. and Galloway, J.P., eds., Geologic studies in Alaska by the U.S. Geological Survey, 1988: U.S. Geol. Survey Bull. 1903, p. 62-67.

**APPENDIX A**  
**Classification and Structural Data for Lode Mines and**  
**Prospects in the Fairbanks Mining District**

Table A1  
 Classification of and structural data for lode mines and prospects in the Fairbanks mining district, Alaska  
 (Note: keyed to prospects described by Chapman and Foster, 1969)

Map No.	Mine or Prospect	Mineral Deposit Type	Metals	Attitudes		Dimensions (Avg)			Au Grade	Surface Elev.	References
				Faults or Crushed Zones	Country Rock	Width	Length	Depth (dip)			
1.	Egan and Egan	IV	Au	N40W, 45-60S	N55E, 20N	8 ft.	-	-	-	1500	Hill, 1933, p. 155.
2.	Coffs Dome	I	Au, Pb, Ag	-	N70E, 20N	-	-	-	-	2250	-
3.	Charles Claim	IV	Au	-	N85E, 26N	-	-	-	-	1950	Brooks, 1912, p. 31; Smith, 1913b, p. 156.
4.	Eureka Claim	IV	Au	-	N70W, 11N	-	-	-	-	1950	Brooks, 1912, p. 31; Smith, 1913b, p. 156; Chapin, 1914, p. 326.
5.	McCurry Claim (Alder Creek)	?	-	N40°E vt.	N60E, 20N	13 in.-13 ft.	-	-	-	1850	Prindle, 1910, p. 227; Smith, 1913b, p. 156; Chapin, 1914, p. 326.
6.	Queen Claim	?	-	N70W 33°N	N60E 19N	-	-	-	-	1975	Chapin, 1914, p. 326.
7.	Hi-Yu Mine Critics & Feldman	I & IV	Sb, Au, Ag, Pb, Zn	N60-70W, 80-85S, N75W, 80-85S, N80W, N	N20E, 15N	1-3 ft.	5000 ft.	450 ft.	1.5 OPT	1550 1550 2100	Smith, 1913b, p. 156-159; Hill, 1933, p. 63, 70, 108-113; Killen & Merrie, 1954, p. 14
8a.	Bob and Roy Claim	IV	Au, Sb	-	N60W	30 ft.	-	-	-	1975	Brooks, 1916a, p. 37-38; Martin, 1920, p. 39.
b.	Wolff Claim	?	-	-	E-W, 10N	-	-	-	-	Do	Brooks, 1916a, p. 37-38; Martin, 1920, p. 39.
c.	Savoy Claim	?	-	-	E-W, 10N	-	-	-	-	Do	Brooks, 1916a, p. 37-38; Martin, 1920, p. 39.
9.	Governor Claim	IV	Au	-	N80W, vt.	1 ft.	1500 ft.	70 ft.	0.5 OPT	1825	Smith, 1913b, p. 160.
10.	Whitehorse Mine	I	Au, Sb, Pb	-	N70W	2 ft.	1000 ft.	-	-	1450	Smith, 1913b, p. 157; Hill, 1933, p. 104; Killen & Merrie, 1951, p. 36-37.
11.	Plumbum	?	-	N70W, 45S 45S, E-W 85S	N75E, 13S	3"-24"	-	-	-	1450	Smith, 1913b, p. 157; Hill, 1933, p. 104.
12a.	Fairbanks Cr. Prospect	IV	Au, Ag	-	E-W	-	-	-	-	1475	Smith, 1913b, p. 163.
b.	Schaefer Prospect	?	-	-	E-W	-	-	-	-	1475	Smith, 1913b, p. 163.
13.	Gilmore Mill	?	-	-	E-W, 10-16N	-	-	-	-	1650	Hill, 1933, p. 107-108.

Table A1 (Continued)

Map No	Mine or Prospect	Mineral Deposit Type	Metals	Attitudes			Dimensions (Ave)			Au Grade	Surface Elev.	References
				Veins	Faults or Crushed Zones	Foliation of Country Rock	Width	Length	Depth (dip)			
14.	Ohio Mine	I & IV	Au, Sb, Pb, Ag	N70W, 45S E-W, 45N	-	N75E, 13S	24"-30"	3500 ft.	200 ft.	2.0 OPT	1575	Smith, 1913b, p. 162-163; Mertie, 1918, p. 408-409; Hill, 1933, p. 107-108.
15.	Mizpah	I & IV	Au, Sb, Pb, Ag, Mn, W	N65W, 70S; E-W 75S, N65W, 70S, N80W, 80S	-	N20W, 18S	20"-24"	3000 ft.	120 ft.	1.7 OPT	1750	Smith, 1913b, p. 162; Mertie, 1918, p. 405, 406; 409, 421; Hill, 1933, p. 107; Chapin, 1914, p. 329; Byers, 1957, p. 208; Killeen & Mertie, 1951, p. 14.
16.	Excelsior Prospect	I	Sb, Pb, Ag	N30E, S	-	-	-	-	-	-	1750	Smith, 1913b, p. 161; Killeen & Mertie, 1951, p. 37.
17.	McNeil Shaft (see Hi-Yw)	IV	Sb, Pb	N60W, 70S	-	N45E, 22N	12"	2000 ft.	100 ft.	2.90 OPT	2075	Brooks, 1916b, p. 37; Mertie, 1918a, p. 415; Hill, 1933, p. 104; Killeen & Mertie, 1951, p. 37.
18.	"Cross Vein"	IV	Sb, Pb, Ag	N30°E S	-	N45E, 22N	-	-	-	-	1925	Smith, 1913b, p. 161-162.
19.	Perrank	IV	Au, Sb, Ag	N80W, 60S	-	-	-	-	-	-	1980	Chapin, 1914, p. 329; Killeen & Mertie, 1951, p. 36.
20.	Kellen	IV	Au, Sb	-	-	E-W, 60°S	-	-	-	-	1625	Smith, 1913b, p. 163-164.
21a.	McCarty Mine	IV	Au, Sb, Pb, Zn	N78°W, 51-75S, N40°E, S	-	N60E, 9S	30-35"	2500 ft.	250 ft.	1.0 OPT	2100	Maloney, 1916, p. 14-15; Hill, 1933, p. 104-105; Joesting, 1942, p. 10; Killeen & Mertie, 1951, p. 35.
21b.	Dorothy	?	-	-	-	N60E, 9S	-	-	-	-	2150	Smith, 1913b, p. 167.
c.	Prospect adit (?)	?	-	-	-	N60E, 9S	-	-	-	-	2100	Smith, 1913b, p. 167.
22.	American Eagle Tunnel (see Vetter)	IV	Au, Sb	N70W, 72°S N30°E 75N	-	E-W, 20N	18-24"	3000 ft.	400 ft.	1.0 OPT	1975	Smith, 1913b, p. 164; Hill, 1933, p. 105-106.
23a.	Pioneer Vein (see McCarty)	IV	Au	N65W, 60 S	-	N30E 19N	6-12"	5500 ft.	110 ft.	-	2200	Smith, 1913b, p. 165; Hill, 1933, p. 102.
23b.	Permsylvania Vein (see McCarty)	IV	Au	N80E, 60-70S N76W, 56S	-	N30E, 19N	6-14"	6500 ft.	92 ft.	2.0 OPT	2300	Hill, 1933, p. 102; Smith, 1913b, p. 166-167.
c.	Antimony	V	Sb, Au	N85E, 80N	-	N30E, 19N	18"	2000 ft.	-	-	2150	Hill, 1933, p. 102; Davis, 1922, p. 95.

Table A1 (Continued)

Map No	Mine or Prospect	Mineral Deposit Type	Metals	Attitudes		Orientation of Country Rock	Dimensions (Ave)			Au Grade	Surface Elev.	References
				Veins	Faults or Crushed Zones		Width	Length	Depth (dip)			
d	Willie	IV	Au	N50E 80S	-	N30E, 19N	4-5"	1000 ft.	95 ft.	-	2200	Smith, 1913b, p. 167; Prindle, 1910, p. 227.
24.	Keystone	I & IV	Au, Sb, Pb, Ag	NW	-	N70E, 21N	-	-	-	-	-	Chapman & Foster, 1969, p. D8.
25.	Homestake (see Vetter, American Eagle Keystone)	I & IV	Au, Sb, Ag, Cu	EW, 45S, N60W, 45N, N70E, 40S	-	Horizontal	3-5'	650 ft.	400 ft.	1.0 OPT	1500	Smith, 1913b, p. 168; Chapin, 1914, p. 331-334; Hill, 1933, p. 101-102; Killeen & Mertie, 1951, p. 14; Sandvik, 1964, p. 119-120.
26a.	Barnes	IV	Au	-	-	N40E, 12N	-	-	-	-	1450	Smith, 1913b, p. 171.
b.	Rexall	IV	Au	N25°E, 25N, EW, 60N	-	N40E, 12N	3-5' 1-18"	150 ft. 340 ft.	140 ft. 140 ft.	0.3 OPT 1.5 OPT	1500	Smith, 1913b, p. 168-171; Chapin, 1914, p. 334-335.
27.	Soloman	V	Sb	NE	-	N50E, 12N	3-4"	-	-	-	1375	Smith, 1913b, p. 171; Chapin, 1914, p. 332; Killeen & Mertie, 1951, p. 33.
28.	Vetter Christina (extension of American Eagle Vein)	I & IV	Au, Sb, Cu, Zn, Ag, Pb	N80W 45S, N75W 60S, EW5 N40E 75S	-	N70E, 20N	4-5'	6000 ft.	1000 ft.	0.6 OPT	1950	Sandvik, 1964, p. 113-114; 125-126; Brown, 1962, p. 117-121.
29.	Keystone (extension of Vetter)	I & IV	Au, Sb, Pb, Cu, Zn	N70W, 30-60S, N80W 45S	-	N65E, 12N	-	-	-	-	1950	Chapman & Foster, 1969, p. D9.
30.	Chatham & Burns	I & IV	Au, Sb, Ag, Cu, Zn, Zw	N60W, 65-80S, N70W, N70E, vt E-W.	-	N40E, 8S	6-18"	1250 ft.	180 ft.	1.0-1.9 OPT	1830	Smith, 1913b, p. 172-173; Chapin, 1914, p. 335-336; Brooks, 1916a, p. 35-36; Mertie, 1918, p. 415; Hill, 1933, p. 100-101; Joesting, 1943, p. 8-9; Sandvik, 1964, p. 109-110; Stewart, 1933, p. 129.
31.	Harris & Brown	IV	Sb, Pb	N70E vt	-	N55E, 21N	-	-	-	-	2050	Smith, 1913b, p. 175-176; Chapin, 1914, p. 332; Sandvik, 1964, p. 105-106, 115-118; 123-124.
32.	Quemboe Bros. #1	IV	Au, Sb	N70W, S	-	N50E, 23N	-	1750 ft.	60 ft.	1.0 OPT	2100	Smith, 1913b, p. 171-172; Chapin, 1914, p. 332.
33.	Furstencau	?	-	-	-	N50E 23N	-	-	-	-	1825	Chapin, 1914, p. 332.
34a.	Quemboe Bros. #2	?	-	-	-	N50E, 21N	-	-	-	-	1750	-

Table A1 (Continued)

Map No	Mine or Prospect	Mineral Deposit Type	Metals	Altitudes		Dimensions (Ave)			Au Grade	Surface Elev.	References
				Faults or Crashed Zones	Country Rock	Yalms	Width	Length			
b.	Sky High	I	Au	-	N50E, 21N	Horizontal	3-6"	5 ft.	-	1875	Smith, 1913b, p. 175.
35a.	Alaska	IV	Au	-	N50E, 21N	-	3-5"	110 ft.	-	1700	Smith, 1913b, p. 175; Hill, 1933, p. 99-100; Chapin, 1914, p. 337.
b.	Poster-Hungerford	IV	Au	-	N45E, 50S	-	18"	5 ft.	0.5 OPT	1700	Hill, 1933, p. 99-100.
c.	Nils Genki	IV	Au	-	N60E	-	-	-	-	1700	Hill, 1933, p. 99-100.
d.	Alaska Group	IV	Au	-	N50-60E, E-W, 30N	-	-	-	0.3 OPT	1700	Smith, 1913b, p. 175; Hill, 1933, p. 99-100; 32-337.
36.	Empire Claim Group Mine	IV	Au	-	N50E, 21N	-	-	-	-	1650	Chapin, 1914, p. 3; Hill, 1933, p. 75
37.	Roughneck	?	-	-	N80E, 2N	-	-	-	-	1550	Chapin, 1914, p. 332.
38.	Colbert & Warmbold	IV	Au	-	N50W, 28S	-	-	-	-	1325	Stewart, 1933, p. 130.
39.	Anna-Mary	I & IV	Pb, Ag, Sb, Au	-	N75W, 80S	N70W, 70S	4-8"	7000 ft.	<0.1 OPT	1375	Hill, 1933, p. 100; Stewart, 1933, p. 136.
40.	Pioneers	IV	Au, Sb, Zn	-	N55E, 20N	-	3' Large 4-25" Small vein	200 ft.	1.0-3.0 OPT	1325	Prindle, 1910, p. 226; Smith, 1913b, p. 173-174; Chapin, 1914, p. 336; Hill, 1933, p. 99; Stewart, 1933, p. 131.
41.	Union or DXL	IV	Au	-	N60W, 26N	-	-	-	-	1125	Hill, 1933, p. 75; Reed, 1939, p. 19.
42.	Scott Reese	IV	Au	-	N75E, 25S E-W, 45S	N60E, 80S	4" Fault zone 3" vein	300 ft.	1.5 OPT	1350	Hill, 1933, p. 98-99; Stewart, 1933, p. 137.
43a.	Butler & Petree	I & IV	Au, Sb, Pb, Zn	-	N85E, 45S	NW 45-70, S	6' Fault zone	750 ft.	-	1375	Prindle, 1910, p. 226-227; Smith, 1913b, p. 176-177; Hill, 1933, p. 98; Sandvill, 1964, p. 105-108.
b.	Rea	IV	-	-	N60W, 26N	-	-	500 ft.	-	1375	Brooks, 1912, p. 31; Smith, 1913b, p. 177; Hill, 1933, p. 14.
44.	Cunningham	IV	Au, Sb	-	E-W, 24N	-	-	-	-	1250	Chapin, 1914, p. 332.
45.	Sunrise Claim	V	Sb	-	N40W, 32W	-	12"	-	-	1000	Chapin, 1914, p. 337; Killen & Martle, 1951, p. 31.

Table A1 (Continued)

Map No.	Mine or Prospect	Mineral Deposit Type	Metals	Attitudes			Dimensions (Ave)			Au Grade	Surface Elev.	References
				Veins	Faults or Crushed Zones	Foliation of Country Rock	Width	Length	Depth (dip)			
46a.	Lyons	?	-	-	-	-	-	-	-	1200	Chapin, 1914, p. 332.	
b.	California	?	-	-	-	-	-	-	-	Do	-	
47.	Cleary Hill (Rhoads Hill)	I & IV	Au, Sb, Cu, Pb, Zn, Sn, W, Ag	N75W-85°E 60S, N75W, 55-63S, N75W, 55S N70-80W, 43-60S, N75W low	N75E, 45-60N N70E, 80N N70W, 45S, N70W-70E, 5-15 N & S, N20E-20W, at N & S	N70E, 20N	20"-36"	2500 ft.	300 ft.	2.0 OPT	1350	Prindle, 1910, p. 225; Brooks, 1911, p. 33; Smith, 1913b, p. 177-180; Brooks, 1916a, p. 34-35; Moffit, 1927, p. 12; Hill, 1933, p. 39-36; Byers, 1957, p. 208-209; Sandvik, 1964, p. 109-110, 113-114.
48.	Wyoming or Wackwitz	I & IV	Au, Sb, Ag, Pb, Mn, Mo, Be, W	N80E, 50S N80W, 35S	NNW, 45W	N85W, 27N	12" 2-4"	2500 ft.	250 ft.	0.3 OPT	1425'	Smith, 1913b, p. 180-182; Mertie, 1918, p. 411; Moffit, 1927, p. 12; Hill, 1933, p. 96-98; Byers, 1957, p. 206-208.
49.	Bobbie	IV	Sb, Pb, Ag	-	N-S, W	-	-	-	-	-	1650	Smith, 1913b, p. 177; Chapin, 1914, p. 332; Brooks, 1916a, p. 35.
50.	Hess & Burnett #1	I	Sb	-	-	Horizontal	-	-	-	-	1625	Chapin, 1914, p. 332-339.
51.	Stepovich #1	?	-	-	-	-	-	-	-	-	1150	Chapin, 1914, p. 332.
52.	Crosscut	?	-	-	-	-	-	-	-	-	1200	Do
53a.	Stibnite	I & IV	Au, Pb, Ag, Sb	N45E vt (7)	-	E-W, 20N	-	-	-	-	1325	Chapin, 1914, p. 332; Mertie, 1918, p. 416; Chapman & Foster, 1969, p. D11.
b.	Johnson & Mertie	I & IV	Sb, W	E-W, 20N	-	E-W, 20N	-	-	-	-	1325	Joesting, 1943, p. 7; Byers, 1957, p. 210.
54a.	Tolovana	I, IV & V	Au, Sb, Ag, W	N75E, EW, 60S, EW 50S, N80E 70S	-	EW, 15N	1-3" 18"-36"	350 ft.	100 ft.	-	1300	Prindle, 1910, p. 227; Smith, 1913b, p. 183-185; Chapin, 1914, p. 339-340; Hill, 1933, p. 68, 91-92; Byers, 1957, p. 210.
b.	Hershberger, Beall & Phipps	?	-	-	-	EW, 15N	-	-	-	-	-	Brooks, 1911, p. 34
54c.	Tolovana Vein	V	Sb	-	-	EW, 15N	-	-	-	-	1300	Smith, 1913b, p. 184-185; Hill, 1933, p. 92.

Table A1 (Continued)

Map No.	Mine or Prospect	Mineral Deposit Type	Metals	Altitudes		Veins	Faults or Crushed Zones	Location of Country Rock	Dimensions (Ave)			Surface Elev.	References
				Feet	Meters				Width	Length	Depth (dip)		
55.	Schweynare	7	-	-	-	-	-	N40E, 32N	-	-	-	1300	Smith, 1913b, p. 186; Chapin, 1914, p. 332.
56.	Westonvitch, chechako #1 Eldorado	I & IV	Au, Sb, Pb, Ag, Zn, Cu	N35E, 85N	-	-	-	N60E, 30N	-	-	-	1375	Smith, 1913b, p. 186-187; Hill, 1933, p. 89-90; Davis, 1922, p. 101-102; Chapman & Foster, 1969, p. D-11.
57.	Moore-Shelden	V	Sb	-	N55E, v1	-	-	N60E, 30N	-	-	-	1475	
58.	Stieil	V	Sb	-	-	-	-	N50E, 11N	-	-	-	1425	Smith, 1913b, p. 187; Chapin, 1914, p. 332.
59.	Newboy Extension	IV	Au	N15E, 77W	-	-	-	N50E, 11N	-	115 ft.	0.8 OPT	1750	Smith, 1913b, p. 189-190; Hill, 1933, p. 89.
60.	Newboy	I & IV	Au, Sb, Cu, Zn	N45-48E, 65-80N, 1N N79E, 60S N40E, 73N	EW-N76W, 57-78N, N60W, 80N EW, 32S	-	-	N40E, 31S	4-14'	450 ft.	2.8 OPT	1800	Smith, 1913b, p. 187-189; Hill, 1933, p. 83, 85-89.
61.	Hidden Treasure & New Deal	IV	Au	-	EW-v1	-	-	N60E, 40N	-	-	-	1350	Chapin, 1914, p. 342-343.
62.	Dome View, Rock Run, Wachtwitz Bros & Last Chance	IV	Au	N40E, 70N	-	-	-	N60E, 15-20S	12-40"	145 ft.	0.1 OPT	2000	Hill, 1933, p. 83-84.
63.	Mowhawk, Robinson, Frumlin, Creighton Greenback, Rose	I & IV	Au, Sb	N10E, W N70W, N20E, 60W N80W, 35S N30E, 65N	-	-	-	N20E, 35S	4-8'	680 ft.	1.0 OPT	2150	Smith, 1913b, p. 190; Chapin, 1914, p. 342; Merle, 1918, p. 407; Martin, 1920, p. 40; Hill, 1933, p. 82; Killeen & Merle, 1952, p. 42.
64.	Sunrise #2	7	-	-	-	-	-	N50E, 41N	-	-	-	1900	Chapin, 1914, p. 342.
65.	Robinson Vein	IV	Au	N79E, 60S	-	-	-	N75E, 19N	10"	2500 ft.	-	1850	Hill, 1933, p. 88-89.
66.	Mother Lode Hill (Cleary Summit)	IV	Au, Sb	-	-	-	-	N75E, 19N	-	-	-	1700	Prindle, 1910, p. 221; Brooks, 1916a, p. 32-33.
67.	Cornell	7	-	-	-	-	-	N25E, 19E	-	-	-	2125	Smith, 1913b, p. 186; Hill, 1933, p. 91.
68.	Emma	IV	Au	EW, 45-60S	-	-	-	N80E, 16S	4-12"	100 ft.	1.5 opt/ton	2100	Hill, 1933, p. 90-91.

Table A1 (Continued)

Map No	Mine or Prospect	Mineral Deposit Type	Metals	Altitudes			Dimensions (Ave)			Au Grade	Surface Elev.	References
				Veins	Faults or Crushed Zones	Foliation of Country Rock	Width	Length	Depth (dip)			
69.	Jackson	-	Au, Sb, Pb, Ag	EW, S EW, 25S N45E low S, N45E 45S, N55E 15S, N70E vt-N	N75W vt N45E, 65N N75W, 75S N75W, 65S N75W, S vt N40W, 45N N80W, 70S	N70E, 16S	2-4"	100 ft.	50 ft.	-	2300	Chapin, 1914, p. 338-339; Mertie, 1918, p. 416-417; Hill, 1933, p. 92-93.
70.	Wackwitz (Cleary Summit)	I	Au, Sb, Pb, Ag, Zn	E-W, 6S	-	E-W, 6S	-	-	-	-	2250	Chapman & Foster, 1969, p. D12.
71.	Pinnacle-Cheyenne Cheyenne	I	Au, Sb, Pb	-	-	N50E, 12S	-	-	-	-	2100	Smith, 1913b, p. 182-183.
72.	White Elephant	I	Pb, Ag	-	-	N55E, 40S	-	-	-	-	1925	Chapin, 1914, p. 348; Hill, 1933, p. 114.
73a.	Moonlight	IV	As	-	N75E, 75N	N45E, 30S	4-12"	100 ft.	50 ft.	0.1 oz/ton	1900	Smith, 1913b, p. 201; Hill, 1933, p. 114.
b.	Sunlight	?	-	-	-	N45E, 30S	-	-	-	-	-	Smith, 1913b, p. 201.
c.	Zimmerman	?	Au, Ag	-	-	N45E, 30S	-	-	-	0.1 oz/ton	1700	Do
74.	Independence, Harris, Harry Woods & Twin Lode	II	Au, Pb	N70E vt N82W vt	N75W, 30S E-W, vt N40W, 65W	N670E, 40S	8-10"	50 ft.	75 ft.	0.2 oz/ton	1500	Brooks, 1916b, p. 60-61; Hill, 1933, p. 114-115; Belstline, 1939.
75a.	Goepfert	II	Au	-	-	N60E, 40S	-	-	-	-	1475	Smith, 1913b, p. 201-202.
b.	Whitman & Murray	II	Au	-	-	N60E, 40S	-	-	-	-	1475	Brooks, 1911, p. 35.
76a.	Rainbow	II	Au, Pb, Zn, W	EW-vt EW, 85S N45E	N40E dike	N35E, 60E	18"	195	100	1.0 oz/ton	1700	Smith, 1918b, p. 198-200; Chapin, 1914, p. 348; Hill, 1933, p. 74, 115; Byers, 1957, p. 210.
b.	Hirschberger & Zimmerman	II	Au	-	-	N35E, 60E	-	-	-	-	1700	Brooks, 1912, p. 32.
77a.	Skoogy Creek	IV	Au, Sb	-	EW	N65E, 50S	50-75'	-	-	0.1 oz/ton	1700	Hill, 1933, p. 117.
b.	North Star & Big Lead	IV	Au, Sb	-	N87W, 83S N55E, 43S	N65E, 50S	4-36"	200 ft.	65 ft.	0.1 oz/ton	1550	Prindle, 1910, p. 223-224; Smith, 1913b, p. 202-203; Hill, 1933, p. 116-117; Stewart, 1933, p. 135-186.
78a.	Goepfert Galena	?	Pb	-	-	N65E, 50S	-	-	-	-	1650	Smith, 1913b, p. 202.
b.	Galena	?	Pb	-	-	N65E, 50S	-	-	-	-	Do	Do

Table A1 (Continued)

Map No.	Mine or Prospect	Mineral Deposit Type	Metals	Attitudes			Dimensions (Ave)			Au Grade	Surface Elev.	References
				Veins	Faults or Crushed Zones	Position of Country Rock	Width	Length	Depth (dip)			
79a.	Central Star	IV	Au	-	-	-	-	-	-	-	2100	Hill, 1933, p. 118.
b.	Thompson & Burns	IV	Au	-	N70W, 80S	-	-	-	-	-	2100	Do
80a.	North Star Extension	IV	Au	N84W, 85S	N30W, 45S Dike, NS, 15E Dike	N65E, 50S	1-4"	140 ft.	675 ft.	1.0 oz/ton	1780	Smith, 1913b, p. 202-203; Hill, 1933, p. 116-117.
b.	S.S.	?	Au	-	-	N65E, 50S	-	-	-	-	-	Smith, 1913b, p. 202-203.
81.	Davis & Apex	IV	Au	N70E, 35S E-W	-	N65E, 50S	22"	40 ft.	25 ft.	0.1 oz/ton	1725	Smith, 1913b, p. 201; Hill, 1933, p. 119-120.
82.	Burnet Galena	II	Sb, Pb, Ag	-	-	N65E, 50S	-	-	-	-	1650	Chapin, 1914, p. 349-350; Hill, 1933, p. 118.
83.	Egan	III	W	-	E-W dike	-	-	-	-	-	1575	Byers, 1957, p. 210; Brown, 1962, p. 122-123.
84.	Burnet	II	Au	-	-	-	-	-	-	-	1475	Chapin, 1914, p. 349.
85.	Zimmerman #2	II	Au	N60-90W	EW, 85N N60-90W, N70-90W	-	7-11'	300 ft.	-	0.1 oz/ton	1275	Hill, 1933, p. 118-119.
86.	Birch & Anderson; Hoover	IV	Au, Sb	-	E-W	N65E, 30S	-	-	-	-	1475	Smith, 1913b, p. 198; Hill, 1933, p. 119-120
87.	Robinson	II	-	-	N55E	-	300'	1000 ft.	-	-	2050	Hill, 1933, p. 81-82.
88.	May Florence	?	-	-	-	N65E, 40S	-	-	-	-	1550	Chapin, 1914, p. 346.
89.	Silver Dollar	?	-	-	-	N65E, 40S	-	-	-	-	1500	Do
90.	Rowley-Shurneff & Nightingale	II	Sb, Pb, Ag	-	N80W, 70N	-	-	-	-	-	1350	Smith, 1913b, p. 198; Chapman & Foster, 1969, p. D-13.
91a.	Silverton & Anderson- Wackwitz	II	Au, Sb, Pb, Ag	-	-	-	-	-	-	-	1750	Brown, 1962, p. 121-122; Ak. Div. of Mines & Metals, 1962, p. 8.
b.	Busy Belle	II	Au, Pb, Ag, W, Mo (?)	N68W 70S	-	-	-	-	-	-	1750	Chapman & Foster, 1969, p. D-13.
92.	Verdin	III	W (?) Mo (?)	-	-	N80E, 18S	-	-	-	-	1250	Joesting, 1943, p. 24.
93.	Freeman & Sharf	II	Au, Ag, Pb	-	-	-	-	-	-	-	1625	Smith, 1913b, p. 198.

Table A1 (Continued)

Map No	Mine or Prospect	Mineral Deposit Type	Metals	Attitudes			Dimensions (Ave)			Au Grade	Surface Elev.	References
				Veins	Faults or Crushed Zones	Position of Country Rock	Width	Length	Depth (dip)			
94.	Leslie & Old Glory	III	Sb, W, Mo, Mn	-	-	N10E, 25E	-	-	-	-	1700	Joesting, 1943, p. 23; Thorne & others, 1948, p. 26-27; Byers, 1957, p. 206, 209-210.
95.	Alaska Flyer	?	Au	-	-	-	-	-	-	-	1075	Smith, 1913b, p. 194.
96.	Soo & Spaulding	IV & V	Sb, Au, Ag, Pb	EW, N; EW, 68 N N76W 80N EW, 60N N50E50N N45E 40S	EW, 60N N76N, 80N N70W 53N	EW, N low	36"	1200 ft.	136 ft.	1.5 oz/ton	1750	Smith, 1913b, p. 190-194;  Hill, 1933, p. 77-80; Spencer & O'Neill, 1934; Stewart, 1930, p. 133-134.
97.	Markevitch, Hindenburg & Ohio	IV	Au, Sb, Zn, Cu Ag	NE (?) 60S E-W, S	-	N45E, 55N	-	-	-	0.1 oz/ton	1425	Mertie, 1918, p. 415; Joesting, 1943, p. 9; Hill, 1933, p. 83; Killen & Mertie, 1951, p. 25; Ebbley & Wright, 1948, p. 38; Sandvik, 1964, p. 111-112.
98.	Spruce Creek	?	Au	-	-	-	-	-	-	-	1250	Smith, 1913b, p. 190.
99.	Mother Lode #1	?	Cu	-	-	-	-	-	-	-	1000	Smith, 1913b, p. 194.
100.	Woods Adit & Franklin	IV	Au, Sb, Pb, Mn	N60-80W, 75N N65E, 52N N77E, 56N N45-76E	-	N75E, 8N	-	-	-	-	1025	Spencer & O'Neill, 1934.
101.	Thrift	IV	Au	-	-	N30E, 15N	-	-	-	-	-	Smith, 1913b, p. 196.
102.	Fredricka	IV	Au, Sb	N70W, 45-70N	-  N70W, 80N	N50E, 65N	1"-42"	120 ft.	300 ft.	-	1225	Smith, 1913b, p. 194-196; Brooks, 1916a, p. 30-31; Hill, 1933, p. 80-81; Killen & Mertie, 1951, p. 14; Sandvik, 1964, p. 123-124.
103.	Hoel Bros; Johnson & Witmen	IV	Au	-	-	-	-	-	-	-	1025	Brooks, 1912, p. 32; Smith, 1913b, p. 196.
104.	Gilmer; Muchano & Helen W.	IV	Au, Sb, Ag	N70E 60-70N	N70E, 60-70N	N80E, 80S	-	-	-	-	1200	Brooks, 1916a, p. 29-30; Joesting, 1942, p. 8-10; Sandvik, 1964, p. 121-122.
105.	Independence Creek	?	-	-	-	N85E, 25N	-	-	-	-	1225	Hill, 1933, p. 157.
106.	Goodwin Prospect	V	Sb	-	-	N65E, 23N	-	-	-	-	1400	Killen & Mertie, 1951, p. 23.

Table A1 (Continued)

Map No.	Mine or Prospect	Mineral Deposit Type	Metals	Attitudes			Dimensions (Ave)			Au Grade	Surface Elev.	References
				Veins	Faults or Crushed Zones	Position of Country Rock	Width	Length	Depth (dip)			
107.	Goodwin Mine	V	Sb	-	-	N75E, 29N	-	-	-	-	1325	Hill, 1933, p. 157; Kilkean & Mertie, 1951, p. 22-23.
108.	Treasure Creek	IV	Au	-	-	N65E, 25S	-	-	-	-	950	Smith, 1913b, p. 196.
109a.	Scraftford & Black Eagle	V	Au, Sb, Pb, Ag	-	EW, 50-70S N80E 50-70S	N80E, 30S	3-4'	70 ft.	<0.1 oz/ton	1000	Brooks, 1916a, p. 28-29; Mertie, 1918, p. 415; Hill, 1933, p. 156-157; Kilkean & Mertie, 1951, p. 12, 21-22; Sandvik, 1964, p. 121-122, 127-128; Robinson and Bundzen, 1982.	
b.	Eagle	V	Sb	-	-	N80E, 30S	-	-	-	-	-	Smith, 1913b, p. 196; Hill, 1933, p. 156-157.
110.	Anatomy Ridge	V	Sb	-	N15E	N70W, 75S	-	-	-	-	-	Chapman & Foster, 1969, p. D-14.
111.	Bunker Hill Mine	IV	Au	-	N15W, 70E	N35E, 15E	12-24"	10 ft.	1.0 oz/ton	1475	Chaplin, 1914, p. 345; Hill, 1933, p. 154.	
112.	Bunker Hill Prospect	IV	Au	-	-	N70E vt	50'	-	<0.1 oz/ton	1375	Hill, 1933, p. 153-154.	
113.	Janiaketa	?	Sn (?)	-	-	N55E, 50S	-	-	-	-	-	Hill, 1933, p. 154.
114.	White Association	III	W	N75E, 75N	-	-	-	-	-	1325	Mertie, 1918, p. 421.	
115.	Perrault & Murphy	IV	Au, W	-	N50E, 60N	-	18-48"	5 ft.	1.0 oz/ton	1575	Smith, 1913b, p. 166; Chaplin, 1914, p. 329-330; Hill, 1933, p. 154.	
116.	Stepovich	?	-	-	N70E, 70N	N70W, 15S	-	-	-	1575	Smith, 1913b, p. 166; Chaplin, 1914, p. 330.	
117a.	Yellow Pup #1	III	W	-	-	N75W, 30N	-	-	-	1575	Byers, 1957, p. 200-201.	
b.	Yellow Pup #2	-	-	-	-	N75W, 30N	-	-	-	-	-	Chapman & Foster, 1969, p. D-15.
118.	Edward Vogt, Monte Cristo & Melba Creek	II	Au, Te, Bi, W	E-W vt N5W, 80W	-	N45E, 70N	3-5"	5000 ft.	0.05 oz/ton	1675	Chaplin, 1914, p. 330-331; Mertie, 1918, p. 412; Hill, 1933, p. 71.	
119a.	Tungsten	III	W	N60E, 25N N70E, 20-40N	-	N70E, 33N N70E, 20-40N	12-18'	35 ft.	-	2475	Mertie, 1918, p. 419-421; Chaplin, 1919, p. 325-326.	
119b.	Schalke	III	W	-	-	N70E, 40N	10'	60 ft.	-	-	-	Hill, 1933, p. 157-158; Chaplin, 1919, p. 325-326.

Map No	Mine or Prospect	Mineral Type	Metals	Veins	Altitude Faults or Crushed Zones	Rotation of County Rock	Dimensions (Ave)			Au Grade	Surface Elev.	References
							Depth (dip)	Length	Width			
c.	Stepovich		Sb, Be, Sn, W, Mo, Mn	N70E, 35N	N40-60W, 60N (dike) NW, N #	N70E, 35N	-	-	-	-	Byers, 1957, p. 189-198.	
d.	Colbert		Sb, Sn, W, Mo, Mn	NE, 35-45N	-	N70E, 40N	-	-	-	-	Byers, 1957, p. 199-200.	
120a.	Shubert		W	-	-	-	-	-	-	-	Byers, 1957, p. 201.	
b.	Zimmerman		W	N40E, N	-	-	15-20	-	-	-	Chapin, 1919, p. 327.	
121.	Nugget Creek		Au	-	-	-	-	-	-	-	Saunders, 1967, p. 39.	
122.	Steele Creek		Au	-	-	N40E, 25N	-	-	-	-	Smith, 1913b, p. 210.	
123.	Rose Creek		Sb	N30E70N	-	-	6-8'	5 ft.	15 ft.	-	Chapin, 1914, p. 346.	
124.	William Brown		-	-	-	-	-	-	-	-	Chapin, 1914, p. 345.	
125a.	Green Mountain		Au	-	-	-	-	-	-	-	Chapin, 1914, p. 345-346.	
b.	Woodpecker		Au	-	-	-	-	-	-	-	Chapin, 1914, p. 346.	
126.	Spruce Hen		W, Mo	N50E, 45N	N50E, 45N N60E, N33E, 40N	N50E, 50N	3-4'	8 ft.	-	-	Mertie, 1918, p. 423; Chapin, 1919, p. 326-327; Smith, 1942b, p. 196; Byers, 1957, p. 201-203.	
127.	Columbia		W	-	N20W, 30E	-	-	80 ft.	-	-	Chapin, 1919, p. 326; Byers, 1957, p. 205-206.	
128.	Tanza		Au, W	N8W60E N50E, NW	-	N30E, 35N	4'	-	40 ft.	-	Byers, 1957, p. 204-205.	
129a.	Tungsten Hill		Au, W	-	-	-	-	-	-	-	Byers, 1957, p. 205.	
129b.	Anderson		W	N50E55N	-	W60E20N	-	-	-	-	Mertie, 1918, p. 424.	
130.	Blossom		W	-	-	-	-	-	-	-	Chapin, 1919, p. 327; Byers, 1957, p. 203-204.	
131.	Peterson		-	-	-	-	-	-	-	-	Hill, 1933, p. 153.	
132.	Ridge		Au	N50E; S	-	N60E, 26N	14"	-	15 ft.	0.5 oz/ton	Do	
133.	Columbia Creek		Au	-	-	-	-	-	-	-	Smith, 1913b, p. 210.	
134.	Engleer Creek		Au, Sb	N70E	-	-	-	-	-	-	Hill, 1933, p. 153.	

Table A1 (Continued)

Table A1 (Continued)

Map No	Mine or Prospect	Mineral Deposit Type	Metals	Veins	Altitudes		Dimensions (Ave)			Surface Elev.	References
					Faults or Crushed Zones	Position of Country Rock	Width	Length	Depth (dia)		
135.	McCrath	?	Au	-	-	-	-	-	-	-	Saunders, 1967, p. 37.
136.	Grant	IV	Au	N45E50S	N75W	N65E 25S	5-6'	2500 ft.	200 ft.	800'	Hill, 1933, p. 150-151; Sandvik & Henshey, 1951.
137.	Fishman	IV	Au	N30E, 70S	-	N65E, 25S	-	-	-	875'	Smith, 1933, p. 16; Smith, 1939a, p. 25; Burchett and Klins, 1981.
138.	Elmer, Nicholas & Happy Creek	IV	Au	N2530E75S; N15E78-82W	-	-	-	200 ft.	150 ft.	1250'	Hill, 1933, p. 150; McCombe & Augstine, 1931; Reed, 1939, p. 13; Smith, 1942a, p. 23.
139.	Maccomb	?	-	NE, 60S	-	-	-	-	-	900	Hill, 1933, p. 152.
140.	Mohawk	IV	Au, Sb, Pb, Zn	N40E, 30N N20E, 40N N30E, 40-70S	-	N55E, 20S	11' 6' 50'	70 ft. 500 ft. 1400 ft.	20 ft. 145 ft. 230 ft.	900	Chapin, 1914, p. 354-355; Mertle, 1918, p. 413-414; McCombe & Augstine, 1931, Smith, 1926, p. 8; Hill, 1933, p. 142-147; Joesting, 1943, p. 11.
141.	Ryan	IV	Au, Sb, Ag	N20E62-65S N20E, 40N N10E, 60N	N30W; N10W, 45W N35W 40-50N, W20E 40W, N15W 30S, NS 35E, NS50E N, 15E N5E47E N58E58W N45W	-	2-6"	220 ft. 370 ft.	75 ft.	-	Brooks, 1912, p. 33; Smith, 1913b, p. 207; Mertle, 1918, p. 413; Hill, 1933, p. 135-138; Smith, 1939b, p. 26; Reed, 1939, p. 12; Davis, 1922, p. 106-107;
142a.	McDonald & Blue Bird #1	IV	Au, Sb	N30E, 61	-	N55W, 30S	16" 15-20" 9-20" 18' 4' 20' 42'	300 ft. 90 ft. 48 ft.	90 ft. 35 ft. 200 ft. 200 ft. 30 ft. 50 ft. 65 ft.	1325 1275 1180	Chapin, 191, p. 323; Moffit, 1927, p. 12; Hill, 1933, p. 133-135; Smith, 1939a, p. 25; McCombe & Augstine, 1931; Reed, 1939, p. 9-10; Joesting, 1942, p. 11; Stewart, 1933, p. 193-140.
142b.	Crown Point	IV	Au	N40W, 65S	-	-	8-48" 36" 8-12"	10 ft. 5 ft. 5 ft.	80 ft. 100 ft. 50 ft.	1060	Chapin, 1914, p. 353.

Table A1 (Continued)

Map No	Mine or Prospect	Mineral Deposit Type	Metals	Altitudes		Dimensions (Ave)			Surface Elev.	References			
				Faults or Crushed Zones	Country Rock	Width	Length	Depth (dip)					
143.	Little Eva	IV	Au, Sb	N27W, vt N50W, 60N N65W, 50N N50W, 50N N15W, 60-70E (dike)	N10-51E, 30-70N	N25W, 22S	6-18" 4-6" 36"	570 ft. 40 ft. 15 ft.	60 ft. 60 ft. 40 ft.	1.0 oz/ton 2.0 oz/ton 2.7 oz/ton <0.1 oz/ton	750 - - -	Hill, 1933, p. 129-133; Reed, 1939, p. 9; Saxevik, 1964, p. 119-120, 127-128.	
144.	Billy Sunday	IV	Au, Sb, Pb, Zn	N45E, 55S, N5-10W 45-60E N10E, 80E N25E 70S-vt	N45E, 17S	-	3-11' 36"	150 ft.	95' 200'	-	1325 -	Mertie, 1918, p. 412-413; Hill, 1933, p. 139-142;	
145a.	Fair Chance	IV	Au	N45E, 30N	N20E, 60W	N55E, 25S	11'	70 ft.	20 ft. 75 ft.	-	1350 -	Chapin, 1914, p. 354; Hill, 1933, p. 139.	
b.	Blue Bird	?	-	-	-	N55E, 25S	-	40 ft.	-	-	-	Hill, 1933, p. 139.	
146.	Seattle Fraction	?	-	-	-	-	-	-	-	-	1000	Reed, 1939, p. 10.	
147.	Little Flower	IV	Au	N70E	-	-	-	-	-	-	1000	Reed, 1939, p. 11-12.	
148.	St. Paul	IV	Au, Sb	N40E, 38N N30E 45-70W	Horizontal	N60E, 16N	36" 36-48"	227 ft. 250 ft.	30 ft. 70 ft.	-	1475 -	Mertie, 1918, p. 409-410. Hill, 1933, p. 128-129; Reed, 1939, p. 11.	
149.	Camp Bird	?	-	NNE, 85W	-	-	-	-	-	-	1150	Reed, 1939, p. 10-11.	
150.	Clipper	IV	Au, Sb	N20W, 85W N4E, 80E	-	N65W, 10-15N	1-8"	237 ft.	-	0.6 oz/ton	1100	Hill, 1933, p. 152; Reed, 1939, p. 8-9; Killen & Mertie, 1951, p. 12, 14, 16; Stewart, 1933, p. 140; Bundzen and Kline, 1982.	
151.	Stibnite	V	Sb	N17W, 70-89S	-	-	-	-	-	-	1300	Brooks, 1916a, p. 38-39; Killen & Mertie, 1951, p. 15.	
152.	Wandering Jew	IV	Au	NS, 75-80E	EW, 37N N30W, 35-40N	N80E, 25S	4-18"	50 ft.	50 ft.	1.1 oz/ton	1325	Hill, 1933, p. 147; Reed, 1939, p. 12-13.	
153.	Killbuck	IV	Au	N5E, 75W	-	-	-	-	-	-	1350	Stewart, 1933, p. 140-141.	
154.	Last Chance	IV	Au, Sb	N45E, N st	-	-	-	-	-	-	-	-	Davis, 1922, p. 108.
155.	First Chance	IV	Au	N10E44W	-	NS, 16-20E	6-48"	70 ft.	120 ft.	1.0 oz/ton	1325	Hill, 1933, p. 147-148.	
156.	Bondholder	IV	Au, Sb	N24E45N	-	N5W, 15E	5'	150 ft.	50 ft.	0.5 oz/ton	1250	Chapin, 1914, p. 345-355; Hill, 1933, p. 146-147.	

Table A1 (Continued)

Map No	Mine or Prospect	Mineral Deposit Type	Metals	Attitudes			Dimensions (Ave)			Au Grade	Surface Elev.	References
				Veins	Faults or Crushed Zones	Foliation of Country Rock	Width	Length	Depth (dip)			
157.	Promethens	IV	Au, Sb, bb, Az, Cu	N40E, N40E70W	-	N5W, 15E	8'	-	60 ft.	0.5 oz/ton	1500	Smith, 1913b, p. 208; Chapin, 1914, p. 354-355; Hill, 1933, p. 148; McCombe & Augustine, 1931.
158.	Big Blue	?	-	N27E	-	N5W, 15E	-	-	-	-	1550	Hill, 1933, p. 148.
159.	Lincoln	IV	Au	-	-	N5W, 15E	-	-	-	-	1350	Reed, 1939, p. 15.
160.	Dorothy & Dorice; Happy Creek	V	Sb	N40E	-	-	-	-	-	-	1200	Chapin, 1914, p. 354; Joesting, 1942, p. 11.
161.	Royal Flush & Alder	IV	Au	N42E, 70W	-	-	36"	-	-	2.2 oz/ton	1200	Smith, 1939a, p. 25; Reed, 1939, p. 14.
162.	Sanford	IV	Au	N40E, 45S N20E, vi	-	N25E, 30E	10-12"	65 ft.	105 ft.	2.5 oz/ton	1550	Hill, 1933, p. 149; McCombe & Augustine, 1931; Reed, 1939.
163.	Grant #2	IV	Au, Sb	N10W, 65E	-	N30E, 20W	5-6"	40 ft.	60 ft.	0.4 oz/ton	1725	Hill, 1933, p. 121-122.
164.	Lepso Prospect	?	-	N40W	-	N70E, 20N	-	-	-	-	1600	Hill, 1933, p. 152.
165.	Mother & Murphy	IV	Au	-	-	N45E, 33S	20'	-	-	<0.1 oz/ton	1175	Hill, 1933, p. 120-122.
166.	Rogach	I	-	NS, 25W	-	NS, 25W	-	-	-	-	-	Reed, 1935, p. 5.
167a.	Blue Bonanza	IV	Au, Sb, Pb, Ag, Cu	-	-	N15E, 15W	-	-	-	-	1950	Smith, 1913b, p. 196-197; Chapin, 1914, p. 353.
b.	Parker	IV	Au	N15E, 55W	-	N15E, 15W	-	-	-	-	-	Stewart, 1933, p. 145.
168.	Flagler	IV	Au	NS, 45E	-	N40W, 30S	-	-	-	-	2325	Smith, 1913b, p. 197-198, 204; Chapin, 1914, p. 352.
169.	Mitchley	IV	Au	N4W, 60E NS, vi	-	Horizontal	2-12"	200 ft.	-	0.5 oz/ton	1500	Hill, 1933, p. 149.
170.	Farmer	IV	Au	N25E, 52W	-	N50W 15S	24"	-	-	0.4 oz/ton	1925	Hill, 1933, p. 122-123; Reed, 1939, p. 7.
171.	Farmer Lode	V	Au, Sb	NS, 40E	-	N85E, 12S	-	-	15 ft.	-	2425	Smith, 1913b, p. 198.
172.	Prospect (?)	V	Sb	N60E	-	N-S, 30W	-	-	-	-	2250	Brooks, 1916a, p. 41.

Table A1 (Continued)

Map No.	Mine or Prospect	Mineral Deposit Type	Metals	Veins	Altitudes		Dimensions (Ave)			Surface Elev.	References
					Fracture or Crashed Zones	Foliation of Country Rock	Width	Length	Depth (dip)		
173.	McQueen, Jenny C. & Black Diamond	V	Sb	N45W/51E N30E, E N40W, 75N	-	-	18-24"	-	-	2325	Brooks, 1916a, p. 40-41; Chapin, 1919, p. 323; Hill, 1933, p. 157; McCombe & Augustines, 1931; Killien & Mertle, 1951, p. 19-20.
174.	Barker & McQueen	?	Au	EW, N	-	40-45 ft.	48"	100 ft.	-	2100	Smith, 1913b, p. 209; Chapin, 1914, p. 352-353.
175.	St. Jude & Cotton Blossom	I(?)	Au, Sb	N35W, 30N	-	75 ft.	-	-	-	1750	Smith, 1913b, p. 208-209; Chapin, 1914, p. 352; Hill, 1933, p. 123; Killien & Mertle, 1951, p. 20.
176.	Vuyovich #1	IV	Au	N50E	-	60 ft.	6"	-	-	1250	Hill, 1933, p. 128.
177.	Ready Bullion Creek	?	Au	-	-	-	-	-	-	1650	Reed, 1939, p. 5-6.
178.	Silver Dollar	IV	Au	N30E, 68S	-	30 ft.	5'	5 ft.	0.9 oz/ton	1300	Hill, 1933, p. 127-128; Reed, 1939, p. 6-7.
179.	Hess & Thomas	?	-	-	-	-	-	-	-	1325	Smith, 1913b, p. 208; Hess, 1933, p. 152.
180.	Tyndall & Flynn	?	Au(?)	-	-	-	-	-	-	1060	Smith, 1913b, p. 208.
181.	Vuyovich #2	IV	Au, Sb	-	N20E, 85E	-	48"	100 ft.	-	975	Hill, 1933, p. 128.
182.	Ready Bullion	IV	Au, Sb	NS v1 N48W, 75N N15E, 70E NS, 80W NNW	N50E, 78S N58E, 50S N53E, 70N, 708, 45S	10 ft. 80 ft. - 300 ft.	48" 10" 36-48" 8'	100 ft. 80 ft. - 300 ft.	<0.3 oz/ton 1.0 oz/ton <0.3 oz/ton <0.1 oz/ton 0.3 oz/ton	1000 Do 1060 1000 1000	Hill, 1933, p. 123-127; Reed, 1939, p. 7
183.	Gale	?	Au	-	-	-	-	-	-	875	Smith, 1913b, p. 204 & 206.
184.	Koegly	?	Au	-	-	-	-	-	-	1075	Do
185.	Hudson	IV	Au	N20E, 45N N20E N45E, 50N	N70W, 60S	180 ft.	15' 4"	360 ft.	-	1325	Smith, 1913b, p. 203-206; Chapin, 1914, p. 350-352; Hill, 1933, p. 123; Chagnon & Foster, 1964, p. D-19.
186.	Maloney	IV(?)	Au, Sb	ENE, 8(?)	-	-	-	-	-	1250	Hill, 1933, p. 123.
187.	Social Security	?	Au	-	-	-	-	-	-	1225	Reed, 1939, p. 7-8.
188.	Lockout	IV	Au	N10E, v1 N20W	-	-	-	-	-	1075	Reed, 1939, p. 8.

**APPENDIX B1**  
**Summary of Thin Section Petrographic Reports for the**  
**Fairbanks Mining District**

Table B1  
 Summary of thin section petrographic reports for the Fairbanks mining district, Alaska  
 (reports by Metz, and Ablanes unpublished data; Blum (1983)).

Sample Number/ Description		Components (%)																
		Qtz	Kspar	Plag	W-mica	B-mica	Chlor	Amph	Pyrox	Garnet	Epidote	Calcite	Fe-Ox	Opauques	Sphene	Rutile	Zircon	Apatite
81 BC 6A	Mica schist	70	--	--	15	15	--	--	tr.	--	--	--	--	--	--	--	--	--
81 BC 12	N/A	--	--	--	--	--	--	--	--	--	--	--	--	--	--	--	--	--
81 BC 20	N/A	--	--	--	--	--	--	--	--	--	--	--	--	--	--	--	--	--
81 BC 33C	Feldspathic schist	35	15	15	--	5	--	--	--	--	--	30	--	--	--	--	--	--
81 BC 35	N/A	--	--	--	--	--	--	--	--	--	--	--	--	--	--	--	--	--
81 BC 40	N/A	--	--	--	--	--	--	--	--	--	--	--	--	--	--	--	--	--
81 BC 41	N/A	--	--	--	--	--	--	--	--	--	--	--	--	--	--	--	--	--
81 BC 43A	Amphibolite	5	--	--	--	--	tr.	90	--	--	--	--	3	2	--	--	tr.	--
81 BC 43C	Amphibolite	10	--	tr.	tr.	15	--	20	--	5	45	--	--	2	--	--	3	--
81 BT 100C	Marble	--	--	--	tr.	--	--	--	--	--	100	--	--	--	--	--	--	--
81 BT 100D	Amphibolite	10	--	tr.	--	--	--	40	--	45	--	--	5	tr.	--	--	--	--
81 BT 101A	Muscovite schist	45	--	--	45	5	--	--	tr.	--	--	--	tr.	--	--	--	--	--
81 BT 101B	Amphibolite	10	--	tr.	--	tr.	tr.	65	--	10	tr.	--	tr.	tr.	15	--	tr.	--
81 BT 139	Amphibolite	5	--	--	--	--	--	90	--	5	tr.	--	--	tr.	--	--	--	--
81 BT 140	Epidote schist	45	--	--	--	tr.	tr.	15	--	35	--	--	--	5	--	--	--	--
81 BT 142	Muscovite schist	35	--	--	55	3	--	--	7	--	--	--	--	--	--	--	--	--
81 BT 148	Muscovite schist	40	tr.	--	50	10	--	--	tr.	--	--	--	tr.	--	--	--	--	--
81 BT 151	Aplite	--	--	--	--	--	--	--	--	--	--	--	--	--	--	--	--	--
81 BT 152	Granodiorite	--	--	--	--	--	--	--	--	--	--	--	--	--	--	--	--	--
81 BT 168	N/A	--	--	--	--	--	--	--	--	--	--	--	--	--	--	--	--	--
81 BT 169	N/A	--	--	--	--	--	--	--	--	--	--	--	--	--	--	--	--	--
81 BT 240	N/A	--	--	--	--	--	--	--	--	--	--	--	--	--	--	--	--	--
81 BT 245	Mica schist	30	tr.	45	--	25	--	--	--	--	--	--	--	--	--	--	tr.	--
81 BT 249A	Qtz-Feld Schist	70	30	tr.	--	--	--	--	--	--	--	--	--	--	--	--	--	--
81 BT 249B	Qtz-Mus Schist	35	15	--	35	--	--	--	15	--	--	--	--	--	--	--	--	--
81 BT 251	N/A	--	--	--	--	--	--	--	--	--	--	--	--	--	--	--	--	--
81 BT 252	Amphibolite	--	--	--	--	10	tr.	80	--	--	--	--	7	3	--	--	tr.	--
81 DNS 18A	Mica schist	30	--	tr.	15	15	20	10	5	--	--	--	--	--	--	tr.	--	--
81 DNS 18D	Tremolite schist	60	--	--	--	--	--	35	--	--	--	--	--	5	--	--	--	--
81 GF 1	Muscovite schist	35	--	--	40	5	5	--	15	--	tr.	--	--	--	--	--	--	--
81 GF 1B	Amphibolite	tr.	--	--	--	tr.	--	45	--	10	30	15	--	--	--	--	--	--
81 GF 2	Muscovite schist	50	--	--	45	5	3	--	2	--	--	--	10	tr.	--	--	--	--
81 GF 3	Epidote schist	tr.	--	--	--	--	--	--	--	90	--	--	--	--	--	--	--	--
81 GF 4	Amphibolite	35	--	--	--	tr.	--	35	--	--	25	--	--	--	--	--	--	--
81 GF 5	Wollastonite schist (1)	30	--	--	--	5	--	--	20	--	--	--	5	--	--	--	--	--
81 GF 6	Wollastonite schist (1)	20	15	--	--	5	--	25	--	--	--	--	--	--	--	--	--	--
81 GF 7	Epidote schist	10	--	--	--	--	--	--	--	60	--	--	--	--	--	--	--	--
81 GF 8	Mica schist	10	--	--	20	5	25	--	--	--	40	--	--	--	--	--	--	--
81 GF 8B	Mica schist	--	--	--	55	5	10	--	--	5	20	--	--	--	--	--	--	--
81 GF 9	Mica schist	60	--	tr.	25	tr.	15	--	tr.	--	--	--	--	--	--	--	--	--
81 GF 10	Muscovite schist	30	--	--	60	5	5	--	tr.	tr.	--	--	--	--	--	--	--	--
81 GF 11	Amphibolite	30	--	--	tr.	--	--	65	--	5	--	--	--	tr.	--	--	--	--
81 GF 12	Amphibolite	30	--	tr.	--	tr.	--	55	--	15	--	--	--	tr.	--	--	--	--
81 JB 5A	Graphitic mica schist	40	--	--	40	10	--	--	--	--	--	--	--	--	--	--	--	--
81 JB 17A	N/A	--	--	--	--	--	--	--	--	--	--	--	--	--	--	--	--	--
81 JB 17C	N/A	--	--	--	--	--	--	--	--	--	--	--	--	--	--	--	--	--
81 JB 23B	N/A	--	--	--	--	--	--	--	--	--	--	--	--	--	--	--	--	--
81 JB 28C	N/A	--	--	--	--	--	--	--	--	--	--	--	--	--	--	--	--	--
81 JB 40A	N/A	--	--	--	--	--	--	--	--	--	--	--	--	--	--	--	--	--

Table B1 (Continued)

Sample Number/ Description		Components (%)																	
		Qtz	Kspar	Plag	W-mica	B-mica	Chlor	Amph	Pyrox	Garnet	Epidote	Calcite	Fe-Ox	Opques	Sphens	Rutile	Zircon	Apatite	Tourm
81 JB 41	N/A	--	--	--	--	--	--	--	--	--	--	--	--	--	--	--	--	--	--
81 JB 41A	N/A	--	--	--	--	--	--	--	--	--	--	--	--	--	--	--	--	--	--
81 JB 56	N/A	--	--	--	--	--	--	--	--	--	--	--	--	--	--	--	--	--	--
81 JB 66	N/A	--	--	--	--	--	--	--	--	--	--	--	--	--	--	--	--	--	--
81 JB 106	N/A	--	--	--	--	--	--	--	--	--	--	--	--	--	--	--	--	--	--
81 JB 108	N/A	23	23	48	--	2	2	1	--	--	tr.	--	--	--	--	--	--	--	--
81 JB 109A	N/A	--	--	--	--	--	--	--	--	--	--	--	--	--	--	--	--	--	--
81 JB 109B	N/A	--	--	--	--	--	--	--	--	--	--	--	--	--	--	--	--	--	--
81 JB 109C	N/A	--	--	--	--	--	--	--	--	--	--	--	--	--	--	--	--	--	--
81 JB 115	N/A	--	--	--	--	--	--	--	--	--	--	--	--	--	--	--	--	--	--
81 JB 116A	Granodiorite	24	15	52	tr.	9	tr.	--	--	--	tr.	--	--	--	tr.	--	--	--	--
81 JB 117	Quartz monzonite	23	33	35	--	8	1	--	--	--	tr.	--	--	--	tr.	--	--	--	--
81 JB 119A	Granodiorite	30	13	52	--	4	1	--	--	--	tr.	--	--	--	tr.	--	--	--	--
81 JB 119B	Aplite	24	39	36	tr.	1	tr.	--	--	--	--	--	--	--	tr.	--	--	--	--
81 JB 120	N/A	--	--	--	--	--	--	--	--	--	--	--	--	--	--	--	--	--	--
81 JB 123	N/A	--	--	--	--	--	--	--	--	--	--	--	--	--	--	--	--	--	--
81 JB 124	Quartz monzonite	34	27	38	tr.	1	tr.	--	--	--	--	--	--	--	--	--	--	--	--
81 JB 127	Granodiorite	23	15	48	tr.	13	1	--	--	--	tr.	--	--	--	tr.	--	--	--	--
81 JB 128	Granodiorite	29	11	51	tr.	9	tr.	--	--	--	--	--	--	tr.	--	--	--	--	--
81 JB 129	Granodiorite	32	14	46	tr.	7	1	--	--	--	tr.	--	--	--	tr.	--	--	--	--
81 JB 130	Granodiorite	23	15	44	tr.	17	1	--	--	--	tr.	--	--	--	tr.	--	--	--	--
81 JB 131	Quartz monzonite	28	32	32	--	3	1	3	--	--	1	--	--	--	tr.	--	--	--	--
81 JB 132	Granodiorite	21	19	54	tr.	5	1	--	--	--	tr.	--	--	--	tr.	--	--	--	--
81 JB 133	Aplite	31	36	30	2	--	--	--	--	--	--	--	1	--	--	--	--	--	--
81 JB 134	Granodiorite	28	28	34	tr.	8	1	--	--	--	tr.	--	--	--	tr.	--	--	--	--
81 JB 135	Quartz monzonite	28	29	35	tr.	8	tr.	--	--	--	tr.	--	--	--	tr.	--	--	--	--
81 JB 137	Quartz monzonite	38	24	34	tr.	4	tr.	tr.	--	--	tr.	--	--	--	--	--	--	--	--
81 JB 138A	Quartz monzonite	36	30	30	tr.	4	tr.	--	--	--	tr.	--	--	--	--	--	--	--	--
81 JB 138B	Aplite	39	30	29	tr.	--	--	--	--	2	--	--	--	--	--	--	--	--	--
81 JB 139	Aplite	27	38	34	tr.	1	tr.	--	--	tr.	--	--	--	--	--	--	--	--	--
81 JB 140	N/A	--	--	--	--	--	--	--	--	--	--	--	--	--	--	--	--	--	--
81 JB 141	Quartz monzonite	32	34	32	tr.	2	tr.	--	--	--	--	--	--	--	--	--	--	--	--
81 JB 142	Quartz monzonite	28	25	36	tr.	10	1	--	--	--	--	--	--	--	tr.	--	--	--	--
81 JB 143	Quartz monzonite	34	17	36	tr.	13	tr.	--	--	--	tr.	--	--	--	tr.	--	--	--	--
81 JB 144	Quartz monzonite	28	20	43	tr.	9	tr.	--	--	--	tr.	--	--	--	tr.	--	--	--	--
81 JB 145	Quartz monzonite	29	28	36	tr.	7	tr.	--	--	--	--	--	--	--	--	--	--	--	--
81 JB 146	Quartz monzonite	32	26	36	tr.	6	tr.	--	--	--	--	--	--	--	tr.	--	--	--	--
81 JB 147	N/A	--	--	--	--	--	--	--	--	--	--	--	--	--	--	--	--	--	--
81 JB 148	Quartz monzonite	26	27	36	tr.	11	tr.	--	--	--	--	--	--	--	--	--	--	--	--
81 JB 149	Quartz monzonite	26	34	36	tr.	4	tr.	--	--	--	tr.	--	--	--	tr.	--	--	--	--
81 JB 150	N/A	--	--	--	--	--	--	--	--	--	--	--	--	--	--	--	--	--	--
81 JB 152	Quartz monzonite	27	32	34	tr.	7	tr.	--	--	--	tr.	--	--	--	--	--	--	--	--
81 JB 155	Aplite	32	35	33	tr.	tr.	tr.	--	--	--	--	--	--	tr.	--	--	--	--	--
81 JB 157	Quartz monzonite	34	21	35	tr.	10	tr.	--	--	--	tr.	--	--	--	--	--	--	--	--
81 JB 159	N/A	--	--	--	--	--	--	--	--	--	--	--	--	--	--	--	--	--	--
81 JB 161	Quartz monzonite	34	21	37	tr.	8	tr.	--	--	--	tr.	--	--	--	tr.	--	--	--	--
81 JB 162	N/A	--	--	--	--	--	--	--	--	--	--	--	--	--	--	--	--	--	--
81 JB 164	N/A	--	--	--	--	--	--	--	--	--	--	--	--	--	--	--	--	--	--
81 JB 165	Quartz monzonite	30	25	39	tr.	6	--	tr.	--	--	tr.	--	--	--	tr.	--	--	--	--
81 JB 166A	N/A	--	--	--	--	--	--	--	--	--	--	--	--	--	--	--	--	--	--
81 JB 166B	N/A	--	--	--	--	--	--	--	--	--	--	--	--	--	--	--	--	--	--

Table B1 (Continued)

Sample Number/ Description	Components (%)																	
	Qtz	Kspar	Plag	W-mica	B-mica	Chlor	Amph	Pyrox	Garnet	Epidote	Calcite	Fe-Ox	Opagues	Sphene	Rutile	Zircon	Apatite	Tourm
81 JB 167	31	26	34	tr.	9	tr.	tr.	tr.	tr.	tr.	tr.	tr.	tr.	tr.	tr.	tr.	tr.	tr.
81 JB 169	N/A	tr.	tr.	tr.	tr.	tr.	tr.	tr.	tr.	tr.	tr.	tr.	tr.	tr.	tr.	tr.	tr.	tr.
81 JB 170	22	31	38	tr.	9	tr.	tr.	tr.	tr.	tr.	tr.	tr.	tr.	tr.	tr.	tr.	tr.	tr.
81 JB 171	N/A	tr.	tr.	tr.	tr.	tr.	tr.	tr.	tr.	tr.	tr.	tr.	tr.	tr.	tr.	tr.	tr.	tr.
81 JB 172	N/A	tr.	tr.	tr.	tr.	tr.	tr.	tr.	tr.	tr.	tr.	tr.	tr.	tr.	tr.	tr.	tr.	tr.
81 JB 173	25	30	38	tr.	7	tr.	tr.	tr.	tr.	tr.	tr.	tr.	tr.	tr.	tr.	tr.	tr.	tr.
81 JB 175	33	28	31	tr.	8	tr.	tr.	tr.	tr.	tr.	tr.	tr.	tr.	tr.	tr.	tr.	tr.	tr.
81 JB 177	27	30	38	tr.	5	tr.	tr.	tr.	tr.	tr.	tr.	tr.	tr.	tr.	tr.	tr.	tr.	tr.
81 JB 178	27	33	35	tr.	5	tr.	tr.	tr.	tr.	tr.	tr.	tr.	tr.	tr.	tr.	tr.	tr.	tr.
81 JB 179	32	29	34	tr.	5	tr.	tr.	tr.	tr.	tr.	tr.	tr.	tr.	tr.	tr.	tr.	tr.	tr.
81 JB 180	tr.	tr.	tr.	tr.	tr.	tr.	tr.	tr.	tr.	tr.	tr.	tr.	tr.	tr.	tr.	tr.	tr.	tr.
81 JB 182	33	30	32	1	4	tr.	tr.	tr.	tr.	tr.	tr.	tr.	tr.	tr.	tr.	tr.	tr.	tr.
81 JB 183A	tr.	tr.	tr.	tr.	tr.	tr.	tr.	tr.	tr.	tr.	tr.	tr.	tr.	tr.	tr.	tr.	tr.	tr.
81 JB 183B	tr.	tr.	tr.	tr.	tr.	tr.	tr.	tr.	tr.	tr.	tr.	tr.	tr.	tr.	tr.	tr.	tr.	tr.
81 JB 185	tr.	tr.	tr.	tr.	tr.	tr.	tr.	tr.	tr.	tr.	tr.	tr.	tr.	tr.	tr.	tr.	tr.	tr.
81 JB 186	tr.	tr.	tr.	tr.	tr.	tr.	tr.	tr.	tr.	tr.	tr.	tr.	tr.	tr.	tr.	tr.	tr.	tr.
81 JB 187	32	23	35	tr.	9	1	tr.	tr.	tr.	tr.	tr.	tr.	tr.	tr.	tr.	tr.	tr.	tr.
81 JB 188	20	48	30	1	tr.	tr.	tr.	tr.	tr.	tr.	tr.	tr.	tr.	tr.	tr.	tr.	tr.	tr.
81 JB 189	25	26	36	tr.	13	tr.	tr.	tr.	tr.	tr.	tr.	tr.	tr.	tr.	tr.	tr.	tr.	tr.
81 JB 190	38	22	31	tr.	9	tr.	tr.	tr.	tr.	tr.	tr.	tr.	tr.	tr.	tr.	tr.	tr.	tr.
81 JB 191	N/A	tr.	tr.	tr.	tr.	tr.	tr.	tr.	tr.	tr.	tr.	tr.	tr.	tr.	tr.	tr.	tr.	tr.
81 JB 192	29	26	37	tr.	8	tr.	tr.	tr.	tr.	tr.	tr.	tr.	tr.	tr.	tr.	tr.	tr.	tr.
81 JB 194	26	40	30	tr.	4	tr.	tr.	tr.	tr.	tr.	tr.	tr.	tr.	tr.	tr.	tr.	tr.	tr.
81 JB 195	30	19	41	tr.	10	tr.	tr.	tr.	tr.	tr.	tr.	tr.	tr.	tr.	tr.	tr.	tr.	tr.
81 JB 201	19	10	45	tr.	10	5	10	tr.	tr.	tr.	tr.	tr.	tr.	tr.	tr.	tr.	tr.	tr.
81 JB 202	22	10	47	tr.	10	3	8	tr.	tr.	tr.	tr.	tr.	tr.	tr.	tr.	tr.	tr.	tr.
81 JB 203	14	8	51	tr.	16	1	10	tr.	tr.	tr.	tr.	tr.	tr.	tr.	tr.	tr.	tr.	tr.
81 JB 204	21	7	43	tr.	13	1	7	tr.	tr.	tr.	tr.	tr.	tr.	tr.	tr.	tr.	tr.	tr.
81 JB 205	20	6	48	tr.	14	1	11	tr.	tr.	tr.	tr.	tr.	tr.	tr.	tr.	tr.	tr.	tr.
81 JB 206	N/A	tr.	tr.	tr.	tr.	tr.	tr.	tr.	tr.	tr.	tr.	tr.	tr.	tr.	tr.	tr.	tr.	tr.
81 JB 207	21	3	39	tr.	21	tr.	16	tr.	tr.	tr.	tr.	tr.	tr.	tr.	tr.	tr.	tr.	tr.
81 JB 208	21	2	41	tr.	16	tr.	20	tr.	tr.	tr.	tr.	tr.	tr.	tr.	tr.	tr.	tr.	tr.
81 JB 209	25	6	43	tr.	15	tr.	11	tr.	tr.	tr.	tr.	tr.	tr.	tr.	tr.	tr.	tr.	tr.
81 JB 211	29	8	46	tr.	9	2	6	tr.	tr.	tr.	tr.	tr.	tr.	tr.	tr.	tr.	tr.	tr.
81 JB 212	22	40	36	tr.	1	tr.	1	tr.	tr.	tr.	tr.	tr.	tr.	tr.	tr.	tr.	tr.	tr.
81 JB 213	29	10	53	tr.	8	1	tr.	tr.	tr.	tr.	tr.	tr.	tr.	tr.	tr.	tr.	tr.	tr.
81 JB 214	26	35	36	tr.	3	tr.	tr.	tr.	tr.	tr.	tr.	tr.	tr.	tr.	tr.	tr.	tr.	tr.
81 JB 215	19	14	53	tr.	7	2	4	tr.	tr.	tr.	tr.	tr.	tr.	tr.	tr.	tr.	tr.	tr.
81 JB 216	25	9	45	tr.	11	tr.	10	tr.	tr.	tr.	tr.	tr.	tr.	tr.	tr.	tr.	tr.	tr.
81 JB 217	21	11	49	tr.	8	1	10	tr.	tr.	tr.	tr.	tr.	tr.	tr.	tr.	tr.	tr.	tr.
81 JB 218	23	9	47	tr.	11	1	9	tr.	tr.	tr.	tr.	tr.	tr.	tr.	tr.	tr.	tr.	tr.
81 JB 250	N/A	tr.	tr.	tr.	tr.	tr.	tr.	tr.	tr.	tr.	tr.	tr.	tr.	tr.	tr.	tr.	tr.	tr.
81 JB 251	N/A	tr.	tr.	tr.	tr.	tr.	tr.	tr.	tr.	tr.	tr.	tr.	tr.	tr.	tr.	tr.	tr.	tr.
81 JB 252	N/A	tr.	tr.	tr.	tr.	tr.	tr.	tr.	tr.	tr.	tr.	tr.	tr.	tr.	tr.	tr.	tr.	tr.
81 JB 253	N/A	tr.	tr.	tr.	tr.	tr.	tr.	tr.	tr.	tr.	tr.	tr.	tr.	tr.	tr.	tr.	tr.	tr.
81 JB 254	N/A	tr.	tr.	tr.	tr.	tr.	tr.	tr.	tr.	tr.	tr.	tr.	tr.	tr.	tr.	tr.	tr.	tr.
81 JB 255A	N/A	tr.	tr.	tr.	tr.	tr.	tr.	tr.	tr.	tr.	tr.	tr.	tr.	tr.	tr.	tr.	tr.	tr.
81 JB 255B	N/A	tr.	tr.	tr.	tr.	tr.	tr.	tr.	tr.	tr.	tr.	tr.	tr.	tr.	tr.	tr.	tr.	tr.
81 JB 256	N/A	tr.	tr.	tr.	tr.	tr.	tr.	tr.	tr.	tr.	tr.	tr.	tr.	tr.	tr.	tr.	tr.	tr.
81 JB 257	N/A	tr.	tr.	tr.	tr.	tr.	tr.	tr.	tr.	tr.	tr.	tr.	tr.	tr.	tr.	tr.	tr.	tr.
81 JC 6	80	tr.	5	4	10	tr.	tr.	tr.	tr.	tr.	tr.	tr.	tr.	tr.	tr.	tr.	tr.	tr.

Table B1 (Continued)

Sample Number/ Description	Qtz	Kspar	Plag	W-mica	B-mica	Chlor	Components (%)			Epidote	Calcite	Fe-Ox	Opaxite	Sphene	Rutile	Zircon	Apatite	Tourmal
							Amph	Pyrox	Garnet									
B1 JT 34B	80	18	--	2	--	--	--	--	--	--	tr.	--	--	--	--	--	--	
B1 MA 1A	5	--	tr.	10	5	--	--	--	--	80	--	--	--	--	--	--	--	
B1 MA 1B	15	--	60	30	5	5	15	10	--	45	--	tr.	--	--	--	--	--	
B1 MA 4C	tr.	--	35	20	5	5	40	--	--	5	--	tr.	--	--	tr.	1	--	
B1 MA 24	40	--	40	10	10	tr.	40	--	--	5	--	15	2	--	tr.	--	--	
B1 MA 25	45	--	25	15	--	--	--	--	--	--	--	60	5	--	--	--	tr.	
B1 MA 27	40	--	--	tr.	--	2	45	5	10	--	--	--	--	--	--	--	--	
B1 MA 43	25	10	15	--	tr.	tr.	30	--	--	--	--	--	--	--	--	--	--	
B1 MA 43C	35	10	15	--	5	30	60	--	--	--	--	--	--	--	--	--	--	
B1 MA 51	10	10	15	--	5	15	60	--	--	--	--	--	--	--	--	--	--	
B1 MA 54	65	--	25	10	--	10	10	--	5	5	--	--	--	--	--	--	--	
B1 MA 79A	45	--	30	7	3	10	30	tr.	--	--	--	--	--	--	--	--	--	
B1 MA 83	60	tr.	30	7	3	10	30	tr.	--	--	--	--	--	--	--	--	--	
B1 MH 01	--	--	--	--	--	--	--	--	--	--	--	--	--	--	--	--	--	
B1 MH 02B	--	--	--	--	--	--	--	--	--	--	--	--	--	--	--	--	--	
B1 MH 06	--	--	--	--	--	--	--	--	--	--	--	--	--	--	--	--	--	
B1 MH 06A	--	--	--	--	--	--	--	--	--	--	--	--	--	--	--	--	--	
B1 MH 06B	--	--	--	--	--	--	--	--	--	--	--	--	--	--	--	--	--	
B1 MH 06H	--	--	--	--	--	--	--	--	--	--	--	--	--	--	--	--	--	
B1 MH 07	--	--	--	--	--	--	--	--	--	--	--	--	--	--	--	--	--	
B1 MH 09	--	--	--	--	--	--	--	--	--	--	--	--	--	--	--	--	--	
B1 MH 09A	--	--	--	--	--	--	--	--	--	--	--	--	--	--	--	--	--	
B1 MH 010C	--	--	--	--	--	--	--	--	--	--	--	--	--	--	--	--	--	
B1 MH 11B	--	--	--	--	--	--	--	--	--	--	--	--	--	--	--	--	--	
B1 MH 11C	--	--	--	--	--	--	--	--	--	--	--	--	--	--	--	--	--	
B1 MH 11D	--	--	--	--	--	--	--	--	--	--	--	--	--	--	--	--	--	
B1 MH 11E	--	--	--	--	--	--	--	--	--	--	--	--	--	--	--	--	--	
B1 MH 11B	--	--	--	--	--	--	--	--	--	--	--	--	--	--	--	--	--	
B1 MH 15	--	--	--	--	--	--	--	--	--	--	--	--	--	--	--	--	--	
B1 MH 17B	--	--	--	--	--	--	--	--	--	--	--	--	--	--	--	--	--	
B1 MH 17C	--	--	--	--	--	--	--	--	--	--	--	--	--	--	--	--	--	
B1 MH 19	--	--	--	--	--	--	--	--	--	--	--	--	--	--	--	--	--	
B1 MR 12	30	--	20	--	20	30	30	tr.	--	--	--	--	--	--	tr.	--	--	
B1 MR 14	20	5	5	40	--	15	15	10	tr.	--	--	5	--	--	--	--	--	
B1 MR 22	45	--	45	45	--	45	45	tr.	--	--	10	--	--	--	--	--	--	
B1 MR 26	15	5	25	40	5	5	5	--	--	--	--	5	--	--	--	--	tr.	
B1 MR 46	85	5	5	5	--	--	90	--	--	--	--	--	--	--	--	--	tr.	
B1 MR 97	--	--	--	--	--	--	50	--	--	--	--	--	--	--	--	--	--	
B1 MR 98B	--	--	30	--	15	tr.	50	--	--	--	--	tr.	--	--	--	--	--	
B1 MR 132A	5	--	--	--	--	--	--	--	--	--	--	--	--	--	--	--	--	
B1 MR 135	30	5	tr.	40	20	5	5	--	--	--	--	--	--	--	--	--	tr.	
B1 MR 165	60	2	8	30	--	--	90	--	--	--	--	--	3	--	tr.	--	tr.	
B1 MR 169	5	10	15	--	2	5	5	tr.	2	3.5	--	--	5	--	tr.	--	tr.	
B1 MR 172A	25	10	40	5	5	5	5	3	2	--	--	--	--	--	tr.	--	tr.	
B1 MR 181	50	--	40	5	5	5	5	--	--	--	--	--	--	--	tr.	--	tr.	
B1 MR 181A	80	--	10	10	10	10	10	--	--	--	--	--	--	--	tr.	--	tr.	
B1 MR 194	75	--	--	10	10	10	10	--	--	--	--	--	--	--	tr.	--	tr.	
B1 MR 195	99	--	--	10	10	10	10	--	--	--	--	--	--	--	tr.	--	tr.	
B1 MR 196A	60	60	5	35	--	--	--	--	--	--	--	tr.	--	--	--	--	--	
B1 MR 205	40	15	30	15	15	15	15	--	--	--	tr.	--	--	--	--	--	--	
B1 MR 208A	40	15	30	15	15	15	15	--	--	--	tr.	--	--	--	--	--	--	

Table B1 (Continued)

Sample Number/ Description		Qtz	Ksp	Plag	W-mica	B-mica	Chlor	Components (%)							Fe-Ox	Opacues	Sphene	Rutile	Zircon	Apatite	Tourm
								Amph	Pyrox	Garnet	Epidote	Calcite									
81 MR 209	N/A	--	--	--	--	--	--	--	--	--	--	--	--	--	--	--	--	--	--	--	
81 MR 219	Muscovite schist	50	5	10	35	--	--	--	--	--	tr.	--	--	--	--	--	--	--	--	--	
81 MR 234	Micaceous quartzite	70	--	10	5	--	--	--	--	--	--	--	15	--	--	--	--	--	--	--	
81 MR 235	Micaceous quartzite	95	--	--	5	--	tr.	--	--	--	--	--	--	--	--	--	--	--	--	--	
81 MR 240B	N/A	--	--	--	--	--	--	--	--	--	--	--	--	--	--	--	--	--	--	--	
81 MR CR 1	Muscovite schist	45	--	15	25	5	--	--	--	10	--	--	--	--	--	--	--	--	--	--	
81 MR CR 2	Marble	5	--	5	--	--	tr.	--	--	--	--	90	--	--	--	--	--	--	--	--	
81 MR CR 3	Amphibolite	tr.	--	20	tr.	5	--	25	--	5	45	tr.	tr.	--	--	--	--	--	--	--	
81 MR CR 4	Mica schist	20	--	10	55	5	5	--	15	--	--	--	--	--	--	--	--	--	--	tr.	
81 MR CR 5	Amphibolite	--	--	5	--	5	tr.	80	--	5	--	--	5	--	--	tr.	--	--	--	tr.	
81 MR CR 6	Muscovite schist	30	--	5	40	tr.	10	--	tr.	--	--	--	--	15	--	tr.	--	--	tr.	--	
81 MR GST 1	Mica schist	30	--	5	30	15	--	--	--	--	--	--	20	--	--	--	--	--	--	--	
81 MR GST 2	Hornfels	25	tr.	--	--	--	--	45	--	--	30	--	--	--	--	--	--	--	--	--	
81 MR GST 2A	Vesuvianite skarn (1)	20	5	15	--	10	5	15	15	--	10	--	--	--	tr.	--	--	--	--	--	
81 MR GST 2B	Hornfels	40	--	5	--	5	--	25	--	--	25	tr.	--	--	tr.	--	--	--	--	--	
81 MR GST 2C	Hornfels	10	--	tr.	--	5	5	30	--	--	25	25	--	--	--	--	--	--	--	--	
81 MR GST 3	Muscovite schist	20	tr.	5	45	10	10	--	--	10	--	--	tr.	--	--	--	--	--	--	tr.	
81 MR GST 4	Biotite feldspar schist	20	5	20	--	35	5	10	--	tr.	--	--	--	--	5	--	--	--	--	--	
81 MR GST 5	Vesuvianite skarn (1)	10	--	10	--	--	--	70	--	--	5	--	--	--	2	--	--	--	--	--	
81 MR GST 6	Hornfels	5	--	--	--	tr.	5	40	--	--	40	--	--	--	10	--	--	--	--	--	
81 MR GST 6	Amphibolite	5	--	--	--	3	2	40	--	--	40	--	--	--	10	--	--	--	--	--	
81 MR MDR 1	Amphibolite	30	tr.	10	--	tr.	5	30	--	--	2	5	--	10	--	3	--	--	--	--	
81 MR MDR 2	Amphibolite	25	5	15	--	10	5	25	--	--	10	5	--	tr.	tr.	--	--	--	--	--	
81 MR MDR 3	Mica schist	40	5	10	30	5	5	--	--	5	--	--	--	tr.	--	--	--	--	--	--	
81 MR MDR 4	Muscovite schist	20	5	10	50	10	5	--	tr.	--	--	--	--	--	--	--	--	--	--	tr.	
81 MR MDR 6	Garnet amphibolite	--	--	5	10	5	5	45	25	tr.	--	--	--	--	--	5	--	--	--	--	
81 MR MDR 7	Marble	tr.	--	tr.	tr.	--	--	tr.	tr.	--	--	99	--	--	--	--	--	--	--	--	
81 MR MDR 8	Garnet mica schist	30	5	10	30	--	3	--	5	--	5	--	--	10	--	--	--	--	--	2	
81 MR MDR 9	Amphibolite	5	--	10	--	tr.	15	60	--	--	--	5	--	--	5	--	--	--	--	--	
81 PM 02	N/A	--	--	--	--	--	--	--	--	--	--	--	--	--	--	--	--	--	--	--	
81 PM 03	N/A	--	--	--	--	--	--	--	--	--	--	--	--	--	--	--	--	--	--	--	
81 PM 04	N/A	--	--	--	--	--	--	--	--	--	--	--	--	--	--	--	--	--	--	--	
81 PM 04A	N/A	--	--	--	--	--	--	--	--	--	--	--	--	--	--	--	--	--	--	--	
81 PM 04B	N/A	--	--	--	--	--	--	--	--	--	--	--	--	--	--	--	--	--	--	--	
81 PM 05B	N/A	--	--	--	--	--	--	--	--	--	--	--	--	--	--	--	--	--	--	--	
81 PM 08	N/A	--	--	--	--	--	--	--	--	--	--	--	--	--	--	--	--	--	--	--	
81 PM 09	N/A	--	--	--	--	--	--	--	--	--	--	--	--	--	--	--	--	--	--	--	
81 PM 010	N/A	--	--	--	--	--	--	--	--	--	--	--	--	--	--	--	--	--	--	--	
81 PM 014	N/A	--	--	--	--	--	--	--	--	--	--	--	--	--	--	--	--	--	--	--	
81 PM 014B	N/A	--	--	--	--	--	--	--	--	--	--	--	--	--	--	--	--	--	--	--	
81 PM 016C	N/A	--	--	--	--	--	--	--	--	--	--	--	--	--	--	--	--	--	--	--	
81 PM 16A	Mica schist	75	5	3	3	2	10	--	tr.	--	--	--	--	--	--	--	--	--	--	--	
81 PM 21	N/A	--	--	--	--	--	--	--	--	--	--	--	--	--	--	--	--	--	--	--	
81 PM 21B	Amphibolite	--	--	35	--	10	--	25	25	--	--	3	--	--	1	--	--	--	1	--	
81 PM 21C	N/A	--	--	--	--	--	--	--	--	--	--	--	--	--	--	--	--	--	--	--	
81 PM 26	N/A	--	--	--	--	--	--	--	--	--	--	--	--	--	--	--	--	--	--	--	
81 PM 28	N/A	--	--	--	--	--	--	--	--	--	--	--	--	--	--	--	--	--	--	--	
81 PM 32A	N/A	--	--	--	--	--	--	--	--	--	--	--	--	--	--	--	--	--	--	--	
81 PM 34	Calc schist	15	--	--	10	10	--	--	--	--	--	75	--	--	--	--	--	--	--	--	
81 PM 37A	Graphitic quartzite	95	--	--	1	--	--	--	--	--	--	--	--	--	--	--	--	--	--	--	
81 PM 37B	Graphitic quartzite	99	--	--	tr.	--	--	--	--	--	--	--	--	--	--	--	--	--	--	--	

Table B1 (Continued)

Sample Number/ Description	Qtz	Kspgr	Plag	W-rckca	B-mica	Chlor	Amph	Components (%)		Grtst	Epidote	Calcite	Fe-Ox	Opaque	Sphens	Rutile	Zircon	Apatite	Tourm			
								Pyrox	Amph													
81 PM 37C																						
81 PM 41																						
81 PM 58B																						
81 PM 58 C																						
81 PM 58D	40	tr.										60										
81 PM 61	55		25	5	3	10			tr.	2												
81 PM 63B/14																						
81 PM 63B/15																						
81 PM 65																						
81 PM 86																						
81 PM 91																						
81 PM 98																						
81 PM 103																						
81 PM 105																						
81 PM 106A																						
81 PM 106B																						
81 PM 106C																						
81 PM 114																						
81 PM 140B																						
81 PM 142	85	5	7			3	80		tr.											tr.		
81 PM 144A			20																			
81 PM 144B	tr.																					
81 PM 146																						
81 PM 151																						
81 PM 156	80	tr.	10	5	5																	
81 PM 212C																						
81 PM 213A																						
81 PM 213C																						
81 TS 30	30	tr.	40	tr.	15	15			tr.												tr.	
81 TS 43																						
81 TS 45B																						
81 TS 47																						
81 TS 50																						
81 TS 51A	98		35		3	3	55					2										
81 TS 53	75											2										
81 TS 54	35	5	10	10									3	3							tr.	
81 TS 55A	90	5	25	30									5	5								
81 TS 73	80		5	15																		
81 TS 75	80		5	15																		
81 TS 52A	90		5	5																		
81 TS 82A																						
81 TS 103	5	5		85						5												
81 TS 104	45	5	10	35																	5	
81 TS 106	90	5	5	tr.																	tr.	
81 TS 109	70			15	10					5											tr.	
81 TS 111							95				5										tr.	
105																						
175	15	5	15			15	15				25										5	
182																					tr.	
186	tr.		10			5	80														2	
187																					tr.	
189																						3

Table B1 (Continued)

Sample Number/ Description	Components (%)											Zircon	Apatite	Tourmaline		
	Qtz	K-fspar	Plag	W-mica	B-mica	Chlor	Amph	Pyrox	Garnet	Epitaxial	Calcite				Fe-Ox	Opaque
190	5	--	10	--	--	--	5	5	10	25	15	--	--	--	--	--
192	25	--	25	tr.	5	45	--	--	--	tr.	--	--	tr.	--	--	--
193	N/A	--	--	--	--	--	--	--	--	--	--	--	--	--	--	--
194	N/A	--	--	--	--	--	--	--	--	--	--	--	--	--	--	--
195A	N/A	--	--	--	--	--	--	--	--	--	--	--	--	--	--	--
195B	N/A	--	--	--	--	--	--	--	--	--	--	--	--	--	--	--
196	N/A	--	--	--	--	--	--	--	--	--	--	--	--	--	--	--
197	N/A	--	--	--	--	--	--	--	--	--	--	--	--	--	--	--
198	75	--	10	8	--	2	--	30	tr.	--	--	5	--	--	--	--
200	--	--	--	--	--	10	--	20	20	--	--	40	--	--	--	--
822	20	--	--	10	--	--	--	--	tr.	--	70	tr.	--	--	--	--
823	--	--	--	--	--	--	--	--	--	--	--	--	--	--	--	--
824	--	--	--	--	--	--	75	--	3	--	20	tr.	2	tr.	--	--
825	60	20	15	4	1	--	--	--	--	--	--	--	--	--	--	tr.
1216	N/A	--	--	--	--	--	--	--	--	--	--	--	--	--	--	--
3202A	N/A	--	--	--	--	--	--	--	--	--	--	--	--	--	--	--
3202B	N/A	--	--	--	--	--	--	--	--	--	--	--	--	--	--	--
32-2C	N/A	--	--	--	--	--	--	--	--	--	--	--	--	--	--	--
3916/4	N/A	--	--	--	--	--	--	--	--	--	--	--	--	--	--	--
3916/5	N/A	--	--	--	--	--	--	--	--	--	--	--	--	--	--	--
3916/6	N/A	--	--	--	--	--	--	--	--	--	--	--	--	--	--	--
3916/7	N/A	--	--	--	--	--	--	--	--	--	--	--	--	--	--	--
82 MO 01	N/A	--	--	--	--	--	--	--	--	--	--	--	--	--	--	--
20700	N/A	--	--	--	--	--	--	--	--	--	--	--	--	--	--	--
21142A	N/A	--	--	--	--	--	--	--	--	--	--	--	--	--	--	--
21142B	Quartzite	65	--	20	5	5	tr.	--	tr.	5	--	tr.	--	--	--	--
21142C	N/A	--	--	--	--	--	--	--	--	--	--	--	--	--	--	--
21142D	N/A	--	--	--	--	--	--	--	--	10	10	tr.	--	--	--	--
21149A	Calc-silicate (1)	50	--	20	--	5	tr.	--	5	--	--	--	--	--	--	--
21149B	N/A	--	--	--	--	--	--	--	--	--	--	--	--	--	--	--
21149C	N/A	--	--	--	--	--	--	--	--	--	--	--	--	--	--	--
21149D	N/A	--	--	--	--	--	--	--	--	--	--	--	--	--	--	--
21149E	N/A	--	--	--	--	--	--	--	--	--	--	--	--	--	--	--
21150	N/A	--	--	--	--	--	--	--	--	--	--	--	--	--	--	--
21152	Chlorite-talc schist (2)	45	--	25	10	15	--	--	5	--	--	tr.	--	--	--	--
21153	N/A	--	--	--	--	--	--	--	--	--	--	--	--	--	--	--
21154	Mica schist	35	--	15	5	15	--	--	--	--	--	5	5	3	2	--
21155	Ortho-amphibolite	tr.	--	15	tr.	tr.	75	--	5	--	tr.	--	--	--	--	--
21320	Muscovite quartzite	50	5	25	10	tr.	--	--	5	--	--	--	--	tr.	--	--
21321	N/A	--	--	--	--	--	--	--	--	--	--	--	--	--	--	--
21331	Feld-mos. quartzite	30	10	15	15	10	--	--	5	--	5	--	--	--	--	tr.
21333	N/A	--	--	--	--	--	--	--	--	--	--	--	--	--	--	tr.
21334	Feld-Bio-Gar schist	50	5	15	15	5	5	--	5	--	--	--	--	--	--	tr.
21335	Banded mos. quartzite	60	--	15	10	--	15	--	--	--	--	--	--	--	--	tr.
21338	N/A	--	--	--	--	--	--	--	--	--	--	--	--	--	--	--
21344	Granulite metabasalt (2)	60	--	--	--	--	--	--	--	--	--	--	--	--	--	--
21346	Banded mica quartzite	70	5	15	tr.	tr.	tr.	--	5	--	5	tr.	--	--	--	tr.
21347	Fb-Gar schist	25	--	10	--	5	40	--	5	--	5	--	--	--	--	--
81 MTRL 02A1	N/A	--	--	--	--	--	--	--	--	--	--	--	--	--	--	--
81 MTRL 02A2	N/A	--	--	--	--	--	--	--	--	--	--	--	--	--	--	--
81 MTRL 02A3	N/A	--	--	--	--	--	--	--	--	--	--	--	--	--	--	--

Table B1 (Continued)

Sample Number/ Description		Qtz	Kspar	Plag	W-mica	B-mica	Chlor	Components (%)							Fe-Ox	Opaquest	Sphene	Rutile	Zircon	Apatite	Tourm
								Amph	Pyrox	Garnet	Epidote	Calcite									
81 M1RL 03A/20	N/A	--	--	--	--	--	--	--	--	--	--	--	--	--	--	--	--	--	--	--	
81 M1RL 03A/21	N/A	--	--	--	--	--	--	--	--	--	--	--	--	--	--	--	--	--	--	--	
81 M1RL 03A	N/A	--	--	--	--	--	--	--	--	--	--	--	--	--	--	--	--	--	--	--	
81 M1RL 03B	N/A	--	--	--	--	--	--	--	--	--	--	--	--	--	--	--	--	--	--	--	
81 M1RL 04A	N/A	--	--	--	--	--	--	--	--	--	--	--	--	--	--	--	--	--	--	--	
81 M1RL 04B	N/A	--	--	--	--	--	--	--	--	--	--	--	--	--	--	--	--	--	--	--	
81 M1RL 07A	N/A	--	--	--	--	--	--	--	--	--	--	--	--	--	--	--	--	--	--	--	
81 M1RL 09	N/A	--	--	--	--	--	--	--	--	--	--	--	--	--	--	--	--	--	--	--	
81 M1RL 10	N/A	--	--	--	--	--	--	--	--	--	--	--	--	--	--	--	--	--	--	--	
81 M1RL 15	N/A	--	--	--	--	--	--	--	--	--	--	--	--	--	--	--	--	--	--	--	
81 M1RL 20A	N/A	--	--	--	--	--	--	--	--	--	--	--	--	--	--	--	--	--	--	--	
81 M1RL 20B	N/A	--	--	--	--	--	--	--	--	--	--	--	--	--	--	--	--	--	--	--	
81 M1RL 20C	N/A	--	--	--	--	--	--	--	--	--	--	--	--	--	--	--	--	--	--	--	
81 M1RL 27	N/A	--	--	--	--	--	--	--	--	--	--	--	--	--	--	--	--	--	--	--	
80 ECC 01	N/A	--	--	--	--	--	--	--	--	--	--	--	--	--	--	--	--	--	--	--	
80 ECC 02	N/A	--	--	--	--	--	--	--	--	--	--	--	--	--	--	--	--	--	--	--	
80 ECC 03	N/A	--	--	--	--	--	--	--	--	--	--	--	--	--	--	--	--	--	--	--	
80 ECC 04	N/A	--	--	--	--	--	--	--	--	--	--	--	--	--	--	--	--	--	--	--	
80 ECC 05	N/A	--	--	--	--	--	--	--	--	--	--	--	--	--	--	--	--	--	--	--	
80 ECC 06	N/A	--	--	--	--	--	--	--	--	--	--	--	--	--	--	--	--	--	--	--	
80 ECC 07	N/A	--	--	--	--	--	--	--	--	--	--	--	--	--	--	--	--	--	--	--	
80 ECC 08	N/A	--	--	--	--	--	--	--	--	--	--	--	--	--	--	--	--	--	--	--	
79 CH 01	N/A	--	--	--	--	--	--	--	--	--	--	--	--	--	--	--	--	--	--	--	
HE-Yu Lev 1	N/A	--	--	--	--	--	--	--	--	--	--	--	--	--	--	--	--	--	--	--	
HE-Yu Lev 2	N/A	--	--	--	--	--	--	--	--	--	--	--	--	--	--	--	--	--	--	--	
79 CWS 01C	N/A	--	--	--	--	--	--	--	--	--	--	--	--	--	--	--	--	--	--	--	
79 CWS 02	N/A	--	--	--	--	--	--	--	--	--	--	--	--	--	--	--	--	--	--	--	
79 CWS COM	N/A	--	--	--	--	--	--	--	--	--	--	--	--	--	--	--	--	--	--	--	
79 CSW GRE	N/A	--	--	--	--	--	--	--	--	--	--	--	--	--	--	--	--	--	--	--	
79 CSW 147	N/A	--	--	--	--	--	--	--	--	--	--	--	--	--	--	--	--	--	--	--	
79 CSW BRO	N/A	--	--	--	--	--	--	--	--	--	--	--	--	--	--	--	--	--	--	--	
79 CSW MUS	N/A	--	--	--	--	--	--	--	--	--	--	--	--	--	--	--	--	--	--	--	
80 TPA 01	N/A	--	--	--	--	--	--	--	--	--	--	--	--	--	--	--	--	--	--	--	
80 TPA 02	N/A	--	--	--	--	--	--	--	--	--	--	--	--	--	--	--	--	--	--	--	
80 TPB 01	N/A	--	--	--	--	--	--	--	--	--	--	--	--	--	--	--	--	--	--	--	

Note: N/A - Thin section not available  
 (1) Balance-either wollastonite and/or vesuvianite  
 (2) Balance-tak  
 (3) Balance-graphite

**APPENDIX B2**  
**Summary of Polished Section Petrographic Reports for**  
**the Fairbanks Mining District**

Table B2  
Summary of polished section petrographic reports for the  
Fairbanks mining district, Alaska

[Note: Ar (arsenopyrite), Au (gold), Bn (bornite), Bo (Boulangerite), Bu (bourmonite), Ca (calcite), Ch (chlorite), Cp (chalcopyrite), Co (covelite), Ga (galena), Gr (graphite), He (hematite), Ja (jamesonite), Mo (molybdenite), Mu (muscovite), Po (polybasite), Py (pyrite), Pyr (pyrrhotite), Qt (quartz), Ru (rutile), Sc (scheelite), Se (semseyite), Sp (sphalerite), St (stibnite), Te (tetrahedrite)]

Sample No.	Deposit Type	Location	Mineralogy
81 MIRL 01A	I	Sec.19; T3N, R2E	Py - Qt - Py = Ar - Sp = Cp
81 MIRL 01B	I	Sec.19; T3N, R2E	Qt - Sp = Cp - St
81 MIRL 01C	I	Sec.19; T3N, R2E	Py = Ar - Sp = Cp - Ja
81 MIRL 01D	I	Sec.19; T3N, R2E	Py - Sp = Cp - St
81 MIRL 01E	I	Sec.19; T3N, R2E	Qt = Py - Sp = Cp - St
81 MIRL 01F	I	Sec.19; T3N, R2E	Qt = Ca = Py - Sp = Cp - St
81 MIRL 01G	I	Sec.19; T3N, R2E	Qt = Ca = Py - Ar - Sp = Cp - St
Chatham Cr 21	I	Sec.19; T3N, R2E	Qt = Py = Ar - Qt - Sp
81 MIRL 02A	I	Sec.19; T3N, R2E	Qt = Py = Ar - St
81 MIRL 02B	I	Sec.19; T3N, R2E	Py = Ar - Sp = Cp - St
81 MIRL 02C	I	Sec.19; T3N, R2E	Qt = Ca = Gr = Py = Ap = Sc - St - Qt - Py
81 MIRL 02D	I	Sec.19; T3N, R2E	Qt - Ar - Au - Sp - Ja
81 MIRL 02E	I	Sec.19; T3N, R2E	Qt - Ar - Au - Sc - Py - Sp - St
81 MIRL 02F	I	Sec.19; T3N, R2E	Py - Qt - Ar - Qt - St
81 MIRL 02G	I	Sec.19; T3N, R2E	Py - Qt - Ar - Qt - St - Qt
81 MIRL 02H	I	Sec.19; T3N, R2E	Py = Ar - St
81 MIRL 02I	IV	Sec.19; T3N, R2E	Py - Ar - Sp - Te = Ja - Qt
Cleary Hill 18A	IV	Sec.19; T3N, R2E	As - St = Sc = Co
Cleary Hill 18B	IV	Sec.19; T3N, R2E	Py = Ar - St = Co = Qt
82 CH 01A	I	Sec.19; T3N, R2E	Py = Ar = Sp = Ja = Qt
82 CH 01B	I	Sec.19; T3N, R2E	Py = Ar = Sp = Ja - Qt
82 CH 01C	I	Sec.19; T3N, R2E	As - Au = Bo - Qt
82 CH 01D	I	Sec.19; T3N, R2E	Qt = Py = As = Sp = Cp = Te = Ja - Qt
82 CH 01E	I	Sec.19; T3N, R2E	Qt = Py = As = Sp = Cp = Te = Ja - Qt
82 CH 01F	I	Sec.19; T3N, R2E	Qt = Py = As = Sp = Cp = Te = Ja - Qt
81 MIRL 04A	I	Sec. 7; T3N, R2E	Pyr - Py - Sp = Cp - Ga
81 MIRL 04B	I	Sec. 7; T3N, R2E	Pyr - Sp = Cp - Ga
81 MIRL 05A	V	Sec. 25; T1N, R3W	Ar - Cp - St - Qt
81 MIRL 05B	V	Sec. 25; T1N, R3W	Py = Ar - St - Co = He - Qt
81 MIRL 07A	IV	Sec. 28; T1N, R2W	Ar - Au - Qt
81 MIRL 07B	IV	Sec. 28; T1N, R2W	Qt - Py = Ar - Au = Sp - Qt
Grant Mine 70	IV	Sec. 28; T1N, R2W	Qt - St - He
Grant Mine 77	IV	Sec. 28; T1N, R2W	Qt - He
Grant Mine 79	IV	Sec. 28; T1N, R2W	Qt - He - St - He
Grant Mine 80	IV	Sec. 28; T1N, R2W	Qt - He - St
Grant Mine 82	IV	Sec. 28; T1N, R2W	Qt - Ar - Qt
Grant Mine 83	IV	Sec. 28; T1N, R2W	Qt - Ar - Sp - He - Qt
82 HY 01A	IV	Sec. 23; T3N, R2E	Qt - Ar - Qt - Te - Ja = Cp - Au
82 HY 01B	IV	Sec. 23; T3N, R2E	Qt - Ar = Au - Ja - Qt
82 HY 01C	I	Sec. 23; T3N, R2E	Qt - Py - Ar - Qt
82 HY 01D	IV	Sec. 23; T3N, R2E	Qt - Py = Ar - Sp - Te = Ja - Qt
82 HY 01E	IV	Sec. 23; T3N, R2E	Qt - Ar - Ja - Qt
82 HY 01F	IV	Sec. 23; T3N, R2E	Qt - Ar - Py = Au - Qt - Au = Ja - Qt
82 HY 01G	I	Sec. 23; T3N, R2E	Ar = Py - Cp
82 HY 01H	IV	Sec. 23; T3N, R2E	Qt - Ar = Au - Te - Ja - Qt = Au - Qt

Table B2 (Continued)

Sample No.	Deposit Type	Location	Mineralogy
82 HY 01I	IV	Sec. 23; T3N, R2E	Qt - Ar = Py - Te = Ja - Au - Qt - Te - Qt
82 HY 01J	I	Sec. 23; T3N, R2E	Qt - Pyr = Py = Ar - Sp = Cp = Au
82 HY 01K	IV	Sec. 23; T3N, R2E	Qt - Py = Ar - Te - Ja - Qt
82 HY 01L	IV	Sec. 23; T3N, R2E	Qt - Ar = Au - Qt
82 HY 01M	I	Sec. 23; T3N, R2E	Qt - Pyr - Sp - Cp
82 HY 01N	IV	Sec. 23; T3N, R2E	Qt - Py = Ar - Sp - Te = Ja = Au - Qt
82 HY 01O	I	Sec. 23; T3N, R2E	Qt - Pyr - Ar - Sp - Cp = Te = Ja - Ca - Qt
82 HY 01P	IV	Sec. 23; T3N, R2E	Ca - Sp - Cp - Te - Ja - Ga - Ca
82 HY 01Q	I	Sec. 23; T3N, R2E	Qt - Pyr - Py - Ar - Sp
82 HY 01R	I	Sec. 23; T3N, R2E	Qt - Pyr - Py - Ar = Au
82 HY 01S	I	Sec. 23; T3N, R2E	Qt - Pyr - Ar = Te
82 HY 01T	I	Sec. 23; T3N, R2E	Qt - Pyr - Ar
82 HY 01U	I	Sec. 23; T3N, R2E	Qt - Pyr - Ar
82 HY 01V	I	Sec. 23; T3N, R2E	Ca - Pyr - Ar - Sp = Cp - Te = Ja
75 Z 003	IV	Sec. 23; T3N, R2E	Qt - Py - Sp = Cp - Ga - Qt - Ca
75 Z 004	V	Sec. 23; T3N, R2E	Qt - Ar - St - Au - Qt
75 Z 005	V	Sec. 23; T3N, R2E	Qt - St - Cp = He = Ar - Qt
75 Z 006A	IV	Sec. 23; T3N, R2E	Qt - Py - Ar - Sp = Cp - Te = Ja = Co - Qt
75 Z 006B	IV	Sec. 23; T3N, R2E	Qt - Py - Ar - Sp = Cp - Te - Qt
Hi-Yu 54	IV	Sec. 23; T3N, R2E	Qt - Py - Ar - Sp - Cp = Te = Ja - Au - Qt
Hi-Yu 55	IV	Sec. 23; T3N, R2E	Qt - Py - Ar - Sp - Cp = Te - Au - Qt
Hi-Yu 56	I	Sec. 23; T3N, R2E	Qt - Py - Ar - Ja - Qt
Hi-Yu 57	IV	Sec. 23; T3N, R2E	Qt - Py - Ar - Sp - Cp - Te - Ja - Au - Qt
Hi-Yu 58	IV	Sec. 23; T3N, R2E	Qt - Py - Ar - Sp - Cp - Te - Ja - Au - Qt
Hi-Yu 59	IV	Sec. 23; T3N, R2E	Qt - Py - Ar - Sp - Cp - Bo - Qt
Hi-Yu 60	IV	Sec. 23; T3N, R2E	Qt - Py - Ar - Sp - Cp - Te - Ja - St - Qt
Hi-Yu 61	IV	Sec. 23; T3N, R2E	Qt - Py - Ar - Sp - Cp - Te - Bo - Cp - Co - Qt
Hi-Yu 62	IV	Sec. 23; T3N, R2E	Qt - Py - Ar - Sp - Cp - Te - Bo - Co - Qt
Hi-Yu 63	IV	Sec. 23; T3N, R2E	Qt - Py - Ar - Sp - Cp - Ja - Te - Au - Py - Qt
Hi-Yu 64	I	Sec. 23; T3N, R2E	Qt - Py - Ar - Sp - Cp - Te
Hi-Yu 69	V	Sec. 23; T3N, R2E	Qt - Ar - St - Qt
81 MIRL 09A	V	Sec. 25; T3N, R1E	Qt - Ar - St - Py - Qt
81 MIRL 09B	V	Sec. 25; T3N, R1E	Qt - Ar - Py - St - Qt
81 MIRL 09C	V	Sec. 25; T3N, R1E	Qt - Ar - Sp - Cp - St - Qt
Johnson Pros 15A	I	Sec. 25; T3N, R1E	Qt - Py - Ar - St - Sc - Qt - Mu = Ch
Johnson Pros 15B	I	Sec. 25; T3N, R1E	Qt - Py - Ar - St - Sc - Qt - Mu = Ch
81 MIRL 10A	I	Sec. 28; T3N, R2E	Qt - Py - Qt
81 MIRL 10B	I	Sec. 28; T3N, R2E	Qt - Py - Qt
81 MIRL 10C	I	Sec. 28; T3N, R2E	Qt - Py - Qt
81 MIRL 10D	I	Sec. 28; T3N, R2E	Qt - Py - Ar - Qt
82 McM 01A	V	Sec. 28; T3N, R2E	Qt - St - Qt
82 McM 01B	IV	Sec. 28; T3N, R2E	Qt - Py - Ar - Sp - St - Co - Qt
82 McM 01C	IV	Sec. 28; T3N, R2E	Qt - Ja - Au - St - Qt
82 McM 01D	IV	Sec. 28; T3N, R2E	Qt - Py - Ar - Ja - Qt
82 McM 01E	I	Sec. 28; T3N, R2E	Qt - Pyr - Py - Ar - Au - Ja - Qt
82 McM 01F	I	Sec. 28; T3N, R2E	Qt - Ar - Ja - Qt
82 McM 01G	IV	Sec. 28; T3N, R2E	Qt - Ar - Ja - Au - Qt
82 McM 01H	IV	Sec. 28; T3N, R2E	Qt - Ar - Ja - Au - Qt
82 McM 01I	IV	Sec. 28; T3N, R2E	Qt - Ar - Ja - Au - Qt
82 McM 01J	I	Sec. 28; T3N, R2E	Qt - Pyr - Py - Ar - Au - St - Qt
82 McM 01K	I	Sec. 28; T3N, R2E	Qt - Pyr - Py - Ar - St - Qt

Table B2 (Continued)

Sample No.	Deposit Type	Location	Mineralogy
82 McM 01L	IV	Sec. 28; T3N, R2E	Qt - Pyr - Py - Ar - Te - An - Qt
82 McM 01M	I	Sec. 28; T3N, R2E	Qt = Mu - Py - Ar - Ja = Qt
82 McM 01N	I	Sec. 28; T3N, R2E	Qt = Mu - Py - Ar - Qt
82 McM 01O	I	Sec. 28; T3N, R2E	Qt = Mu - Py - Ar - Qt
81 MIRL 11A	I	Sec. 32; T1N, R2W	Qt = Mu - Py - Ar - Sp - Cp - Sc - Qt
81 MIRL 11B	I	Sec. 32; T1N, R2W	Qt = Mu - Py - Ar - Sp - Cp - Sc - Qt
81 MIRL 11C	I	Sec. 32; T1N, R2W	Qt = Mu - Pyr - Py - Ar - Sp - Cp - Qt
82 M-1A	I	Sec. 32; T1N, R2W	Qt - Py - Ar - Qt
82 M-1B	I	Sec. 32; T1N, R2W	Qt - Py - Ar - Qt
82 M-2C	I	Sec. 32; T1N, R2W	Qt - Py - Ar - Qt
82 M-3B	I	Sec. 32; T1N, R2W	Qt - Py - Ar - Qt
82 M-3C	I	Sec. 32; T1N, R2W	Qt - Py - Ar - Qt
82 M-4B	I	Sec. 32; T1N, R2W	Qt - Py - Ar - Qt
82 M-5B	I	Sec. 32; T1N, R2W	Qt - Py - Ar - Qt
*Newsboy 12A	I	Sec. 25; T3N, R1E	Qt - Py - Sp - Cp - Ga - Ca
*Newsboy 12B	I	Sec. 25; T3N, R1E	Qt - Py - Ar - Sp - Cp - Ca
*Newsboy 12C	I	Sec. 25; T3N, R1E	Qt - Pyr - Py - Ar - Sp - Cp - He - Ca
*Newsboy 12D	I	Sec. 25; T3N, R1E	Qt - Pyr - Py - Ar - Sp - Cp - Ca
TPB 44	I	Sec. 25; T3N, R1E	Qt - Py - Ar - Sp - Cp - Ja - Co - Ca
TPB 45	I	Sec. 25; T3N, R1E	Qt - Py - Ar - Sp - Cp - Ja - Ga - Co - Ca
TPB 46	I	Sec. 25; T3N, R1E	Qt - Py - Ar - Sp - Cp - Te - Ja - Ga - Ca
TPB 47	I	Sec. 25; T3N, R1E	Qt - Py - Ar - Sp - Ja - Ga - Ca
TPB 48	I	Sec. 25; T3N, R1E	Qt - Py - Ar - Sp - Cp - Ja - Ga - Co - Qt - Ca
81 MIRL 13	IV	Sec. 26; T1N, R3W	Qt - Ar - Au - Ga - Qt
81 MIRL 15A	IV	Sec. 32; T1N, R2W	Qt - Ar - Qt
81 MIRL 15B	IV	Sec. 32; T1N, R2W	Qt - Ar - Qt
Ryan Lode 71	IV	Sec. 32; T1N, R2W	Qt - Ar - Qt
Ryan Lode 73	IV	Sec. 32; T1N, R2W	Qt - Ar - Au - Qt
Ryan Lode 74	IV	Sec. 32; T1N, R2W	Qt - Ar - He - Qt
75 Z 009	IV	Sec. 32; T1N, R2W	Qt - Ar - He - Co - Qt
82 RL-C-380A	I	Sec. 32; T1N, R2W	Qt - Ch - Ar - Qt
82 RL-C-380B	I	Sec. 32; T1N, R2W	Qt - Ch - Ar - Qt
82 RL-D-338	I	Sec. 32; T1N, R2W	Qt - Ch - Ar - Qt
82 RL-G-1	I	Sec. 32; T1N, R2W	Qt - Ch - Ar - Qt
82 RL-H-3	I	Sec. 32; T1N, R2W	Qt - Ch - Ar - Qt
82 RL-I-3	I	Sec. 32; T1N, R2W	Qt - Ch - Ar - Qt
RLO-3A	IV	Sec. 32; T1N, R2W	Qt - Py - Ar - Sp - Ja - Sc - St - Qt
RLO-B	I	Sec. 32; T1N, R2W	Qt - Ch - Ar - Qt
81 MIRL 16A	V	Sec. 16; T2N, R1W	Qt - Py - Ar - St - Qt
81 MIRL 16B	V	Sec. 16; T2N, R1W	Qt - Py - Ar - St - Qt
Silver Fox 13A	II	Sec. 8; T3N, R1E	Qt - Py - Ar - Sp - Te - Ga - Qt
Silver Fox 13B	II	Sec. 8; T3N, R1E	Qt - Py - Sp - Cp - Ga - Qt
75 Z 010	II	Sec. 8; T3N, R1E	Qt - Py - Ar - Sp - Cp - Te - Ga - Po
81 MIRL 18A	IV	Sec. 17; T1N, R1E	Qt - Ar - Qt
81 MIRL 18B	IV	Sec. 17; T1N, R1E	Qt - Ar - Co - Qt
Tolo Mine 2	V	Sec. 25; T3N, R1E	Qt - Py - Ar - St - Qt
Tolo Mine 3	IV	Sec. 25; T3N, R1E	Qt - Py - Ar - Sp - Bo - St - Ca
Tolo Mine 4	V	Sec. 25; T3N, R1E	Qt - Py - Ar - St - Ca = Qt
Tolo Mine 5	V	Sec. 25; T3N, R1E	Qt - Py - Ar - St - Ca = Qt
Tolo Mine 6	V	Sec. 25; T3N, R1E	Qt - Py - Ar - St - Ca = Qt
Tolo Mine 7	V	Sec. 25; T3N, R1E	Qt - Py - Ar - St - Ca = Qt

Table B2 (Continued)

Sample No.	Deposit Type	Location	Mineralogy
Tolo Mine 8	V	Sec. 25; T3N, R1E	Qt - St - Ca = Qt
81 MIRL 19A	V	Sec. 25; T3N, R1E	Qt - Py - Ar - St - Ca = Qt
81 MIRL 19B	V	Sec. 25; T3N, R1E	Qt - Py - Ar - St - Ca = Qt
Tolo Mine 19A	V	Sec. 25; T3N, R1E	Qt - Py - Ar - St - Ca = Qt
Tolo Mine 19B	V	Sec. 25; T3N, R1E	Qt - Py - Ar - St - Ca = Qt
81 MIRL 19C	V	Sec. 25; T3N, R1E	Qt - Py - Ar - St - Qt
81 MIRL 19D	V	Sec. 25; T3N, R1E	Qt - Py - Ar - St - Qt
81 MIRL 19E	V	Sec. 25; T3N, R1E	Qt - Py - Ar - St - Ca = Qt
81 MIRL 19F	V	Sec. 25; T3N, R1E	Qt - Py - Ar - Au - St - Qt
81 MIRL 19G	V	Sec. 25; T3N, R1E	Qt - Py - Ar - St - Ca = Qt
81 MIRL 19H	V	Sec. 25; T3N, R1E	Qt - Py - Ar - St - Ca = Qt
81 MIRL 19I	V	Sec. 25; T3N, R1E	Qt - Py - Ar - St - Ca = Qt
81 MIRL 19J	V	Sec. 25; T3N, R1E	Qt - Py - Ar - St - Ca = Qt
81 MIRL 19K	V	Sec. 25; T3N, R1E	Qt - Ar - St = Qt
81 MIRL 19L	V	Sec. 25; T3N, R1E	Qt - Py - Ar - St - Ca = Qt
81 MIRL 19M		Sec. 25; T3N, R1E	Qt - Py - Ar - St - Ca = Qt
81 MIRL 19N	V	Sec. 25; T3N, R1E	Qt - Py - Ar - St - Ca = Qt
81 MIRL 19O	V	Sec. 25; T3N, R1E	Qt - St - Ca = Qt
81 MIRL 19P	V	Sec. 25; T3N, R1E	Qt - Ar - St - Ca = Qt
81 MIRL 19Q	V	Sec. 25; T3N, R1E	Qt - Py - Ar - St - Ca = Qt
81 MIRL 19R	V	Sec. 25; T3N, R1E	Qt - Py - Ar - St - Ca = Qt
81 MIRL 19S	V	Sec. 25; T3N, R1E	Qt - Py - Ar - St - Ca = Qt
81 MIRL 19T	V	Sec. 25; T3N, R1E	Qt - Py - Ar - St - Ca = Qt
81 MIRL 19U	V	Sec. 25; T3N, R1E	Qt - Py - Ar - Au - St - Co - Qt
81 MIRL 19V	V	Sec. 25; T3N, R1E	Qt - Py - Ar - St - Ca = Qt
81 MIRL 19W	V	Sec. 25; T3N, R1E	Qt - Py - Ar - St - Ca = Qt
81 MIRL 19X	V	Sec. 25; T3N, R1E	Qt - Py - Ar - St - Ca = Qt
81 MIRL 19Y	V	Sec. 25; T3N, R1E	Qt - Py - Ar - St - Ca = Qt
81 MIRL 19Z	V	Sec. 25; T3N, R1E	Qt - Py - Ar - St - Ca = Qt
82 TV 04A	IV	Sec. 25; T3N, R1E	Qt - Ar - Au = Sc - Co - Qt
82 TV 04B	IV	Sec. 25; T3N, R1E	Qt - Ar - Au - Sp - Bu = Te - Co - Qt
82 TV 05	I	Sec. 25; T3N, R1E	Qt - Ar - Au - Te - Se = Ja - Qt
21156	I	Sec. 25; T3N, R1E	Qt - Mu - Py - Ar
81 MIRL 21A	IV	Sec. 20; T3N, R2E	Qt - Py - Ar - Ga = Ja = Bm - Co - Qt
75 Z 007A	IV	Sec. 20; T3N, R2E	Qt - Py - Ar - Bn - Te - Bo - St - Co - Qt
75 Z 007B	IV	Sec. 20; T3N, R2E	Qt - Py - Ar - Au - St - Qt
75 Z 007C	IV	Sec. 20; T3N, R2E	Qt - Pyr - Py - Ar - Au - St - Qt
75 Z 008	IV	Sec. 20; T3N, R2E	Qt - Ar - Au - Sp - Qt
Vetter 10A	IV	Sec. 20; T3N, R2E	Qt - Ar - Au - St - Co - Qt
Vetter 10B	IV	Sec. 20; T3N, R2E	Qt - Ar - Au - Ga - Co - Qt
Vetter 10C	IV	Sec. 20; T3N, R2E	Qt - Ar - St - Co - Qt
Vetter 10D	IV	Sec. 20; T3N, R2E	Qt - Ar - St - Co - Qt
Keystone 72	IV	Sec. 20; T3N, R2E	Qt - Ar - St - Qt
Wack 14A	I	Sec. 36; T3N, R1E	Qt - Mu - Py - Ar - Ga = Ja - Co - Qt
Wack 14B	I	Sec. 36; T3N, R1E	Qt - Mu - Py - Ar - Ga = Bo = Bn - Qt
Wack 22	I	Sec. 36; T3N, R1E	Qt - Mu - Py - Ar - Ga = Ja - Co - Qt
Wack 23	I	Sec. 36; T3N, R1E	Qt - Mu - Py - Ar - Ja - Qt
Wack 24	I	Sec. 36; T3N, R1E	Qt - Mu - Py - Ar - Ja - Co - Qt
Wack 25	I	Sec. 36; T3N, R1E	Qt - Mu - Py - Ar - Ja - Qt
Wack 26	I	Sec. 36; T3N, R1E	Qt - Mu - Py - Ar - Te = Ja - Co - Qt
Wack 27	I	Sec. 36; T3N, R1E	Qt - Mu - Py - Ar - Ja - Co - Qt

Table B2 (Continued)

Sample No.	Deposit Type	Location	Mineralogy
Wack 28	I	Sec. 36; T3N, R1E	Qt - Mu - Ga = Te = Ja = Au - Co - Qt
Wack 29	I	Sec. 36; T3N, R1E	Qt - Mu - Ar - Ja - St - Qt
Wack 30	I	Sec. 36; T3N, R1E	Qt - Mu - Ar - Ja - St - Qt
Wack 31	I	Sec. 36; T3N, R1E	Qt - Py - Ar - Ga = Ja - Co - Qt
Wack 32	I	Sec. 36; T3N, R1E	Qt - Py - Ar - Ja = Bn - Qt
Wack 33	I	Sec. 36; T3N, R1E	Qt - Py - Ar - Ja - Qt
Wack 34	I	Sec. 36; T3N, R1E	Qt - Py - Ar - Ga = Ja = Bn - Co - Qt
81 MURL 22A	I	Sec. 36; T3N, R1E	Qt - Py - Ar - Ja = Bn - Co - Qt
81 MURL 22B	I	Sec. 36; T3N, R1E	Qt - Py - Ar - Ja - Co - Qt
81 MURL 22C	I	Sec. 36; T3N, R1E	Qt - Py - Ar - Ja - Co - Qt
81 MURL 22D	I	Sec. 36; T3N, R1E	Qt - Py - Ja = Bn - Qt
81 MURL 22E	I	Sec. 36; T3N, R1E	Qt - Py - Ar - Ga = Ja = Bn - Qt
81 MURL 22F	I	Sec. 36; T3N, R1E	Qt - Py - Ar - Ja = Bn - Qt
81 MURL 22G	I	Sec. 36; T3N, R1E	Qt - Py - Ar - Ja - Bn - Qt
81 MURL 22H	I	Sec. 36; T3N, R1E	Qt - Py - Ar - Ja - Qt
81 MURL 22I	I	Sec. 36; T3N, R1E	Qt - Py - Ar - Ja - Qt
81 MURL 22J	I	Sec. 36; T3N, R1E	Qt - Py - Ar - Ja - Qt
81 MURL 22K	I	Sec. 36; T3N, R1E	Qt - Py - Ar - Sp - Cp - Te = Ja - Qt
81 MURL 22L	I	Sec. 36; T3N, R1E	Qt - Py - Ar - Ga = Ja - Co - Qt
81 MURL 22M	I	Sec. 36; T3N, R1E	Qt - Py - Ar - Ga = Ja - Co - Qt
81 MURL 22N	I	Sec. 36; T3N, R1E	Qt - Py - Ar - Ga = Ja - Co - Qt
75 Z/001	I	Sec. 36; T3N, R1E	Qt - Py - Ar - Bn = Po - Au - Qt
81 MURL 23A	I	Sec. 24; T3N, R1E	Qt - Py - Ar - Sp - Cp - St - Ca
81 MURL 23B	I	Sec. 24; T3N, R1E	Qt - Py - Ar - Sp - Cp - Bn = Te - St - Qt
81 MURL 23C	I	Sec. 24; T3N, R1E	Qt - Py - Ar - Sp - Cp - St - Ca - Qt
81 MURL 23D	I	Sec. 24; T3N, R1E	Qt - Py - Ar - St - Ca - Qt
81 MURL 23E	I	Sec. 24; T3N, R1E	Qt - Py - Ar - Sp - Cp - Ca - Qt
81 MURL 23F	I	Sec. 24; T3N, R1E	Qt - Py - Ar - Sp - Cp - Bn - St - Qt
81 MURL 23G	I	Sec. 24; T3N, R1E	Qt - Py - Ar - Sp - Cp - Te - Qt
80 TPA 35	I	Sec. 24; T3N, R1E	Qt - Py - Ar - Sp - Cp - Qt
80 TPA 36	I	Sec. 24; T3N, R1E	Qt - Py - Ar - Sp - Cp - St - Ca - Qt
80 TPA 37	I	Sec. 24; T3N, R1E	Qt - Py - Ar - Sp - Cp - Bn - St - Ca
80 TPA 38	I	Sec. 24; T3N, R1E	Qt - Py - Ar - Sp - Cp - Te - St - Ca - Qt
80 TPA 39	I	Sec. 24; T3N, R1E	Qt - Py - Ar - Sp - Cp - Bn - St - Co - Ca - Qt
80 TPA 40	I	Sec. 24; T3N, R1E	Qt - Py - Ar - Sp - Cp - Bn - St - Ca - Qt
80 TPA 41	I	Sec. 24; T3N, R1E	Qt - Py - Ar - Sp - Cp - Bn = Ja - Ca - Qt
80 TPA 42	I	Sec. 24; T3N, R1E	Qt - Py - Ar - Sp - Cp - Te = Ja - Co - Ca - Qt
80 TPA 43	I	Sec. 24; T3N, R1E	Qt - Py - Ar - Sp - Cp - Bn - St - Ca - Qt
80 TPA 44	I	Sec. 24; T3N, R1E	Qt - Py - Ar - Sp - Cp - Bn - St - Ca - Qt
80 TPA 45	I	Sec. 24; T3N, R1E	Qt - Py - Ar - Sp - Cp - Bn - St - Ca - Qt
80 TPA 66	I	Sec. 24; T3N, R1E	Qt - Py - Ar - Cp - Sc - Au - Ca - Qt
81 MURL 24A	I	Sec. 33; T3N, R1E	Qt - Mu - Py - Cp - Sc - St - Qt
81 MURL 24B	I	Sec. 33; T3N, R1E	Qt - Mu - Py - Ar - St - Qt
81 MURL 24C	I	Sec. 33; T3N, R1E	Qt - Mu - Py - Ar - St - Qt
81 MURL 24D	V	Sec. 33; T3N, R1E	Qt - Mu - Py - Ar - St - Qt
81 MURL 24E	V	Sec. 33; T3N, R1E	Qt - St - Qt
Woods 49	IV	Sec. 33; T3N, R1E	Qt - St - Qt
Woods 50	IV	Sec. 33; T3N, R1E	Qt - Py - Ar - Au - Sc - St - He - Qt
Woods 51	V	Sec. 33; T3N, R1E	Qt - Py - Ar - Au - Sc - St - He - Qt
Woods 52	V	Sec. 33; T3N, R1E	Qt - St - Qt
Woods 53	V	Sec. 33; T3N, R1E	Qt - Py - Ar - St - Co - Qt
81 MURL 25A	IV	Sec. 30; T3N, R2E	Qt - Py - Ar - Au - Sp - St - Qt

Table B2 (Continued)

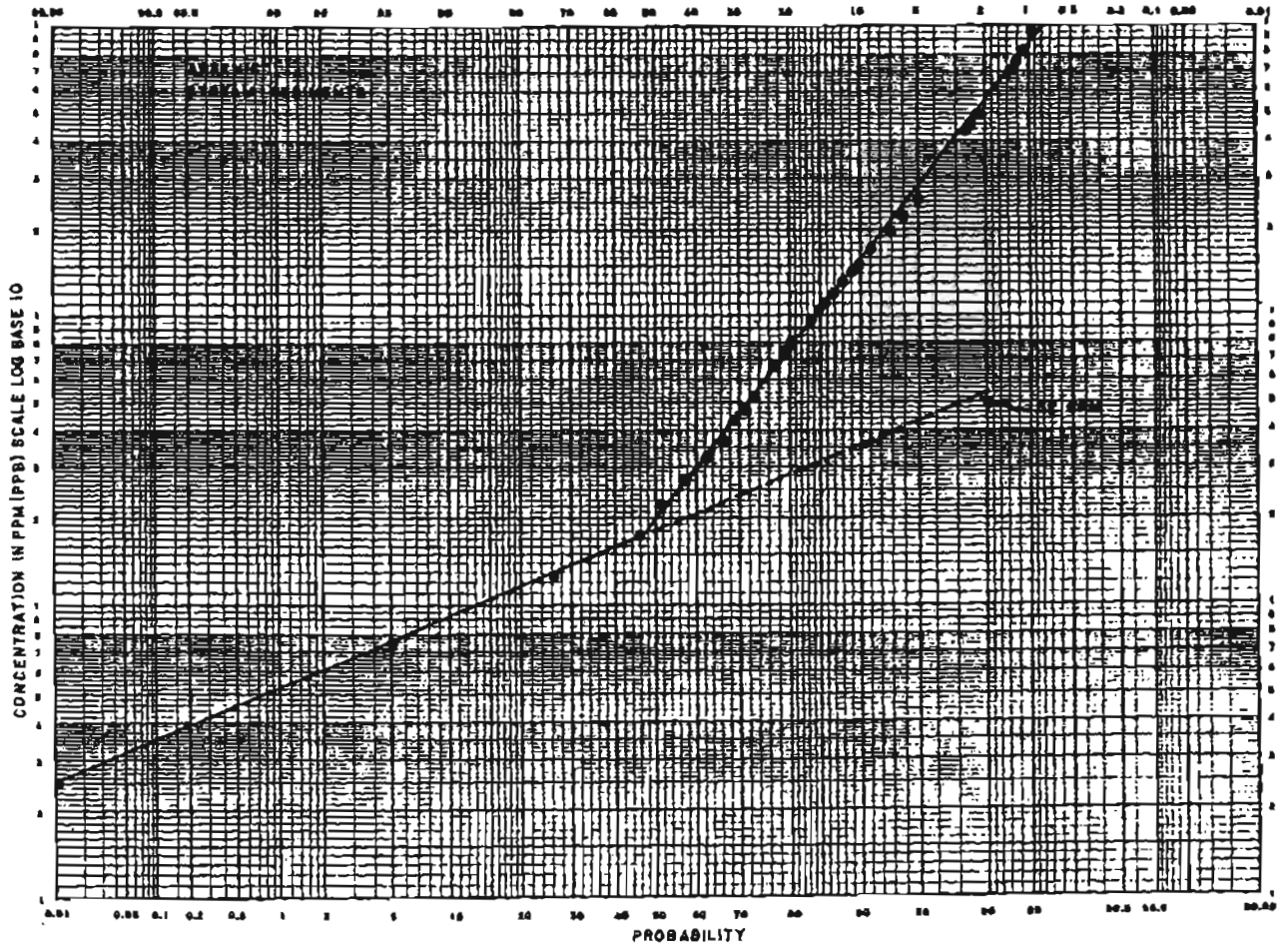
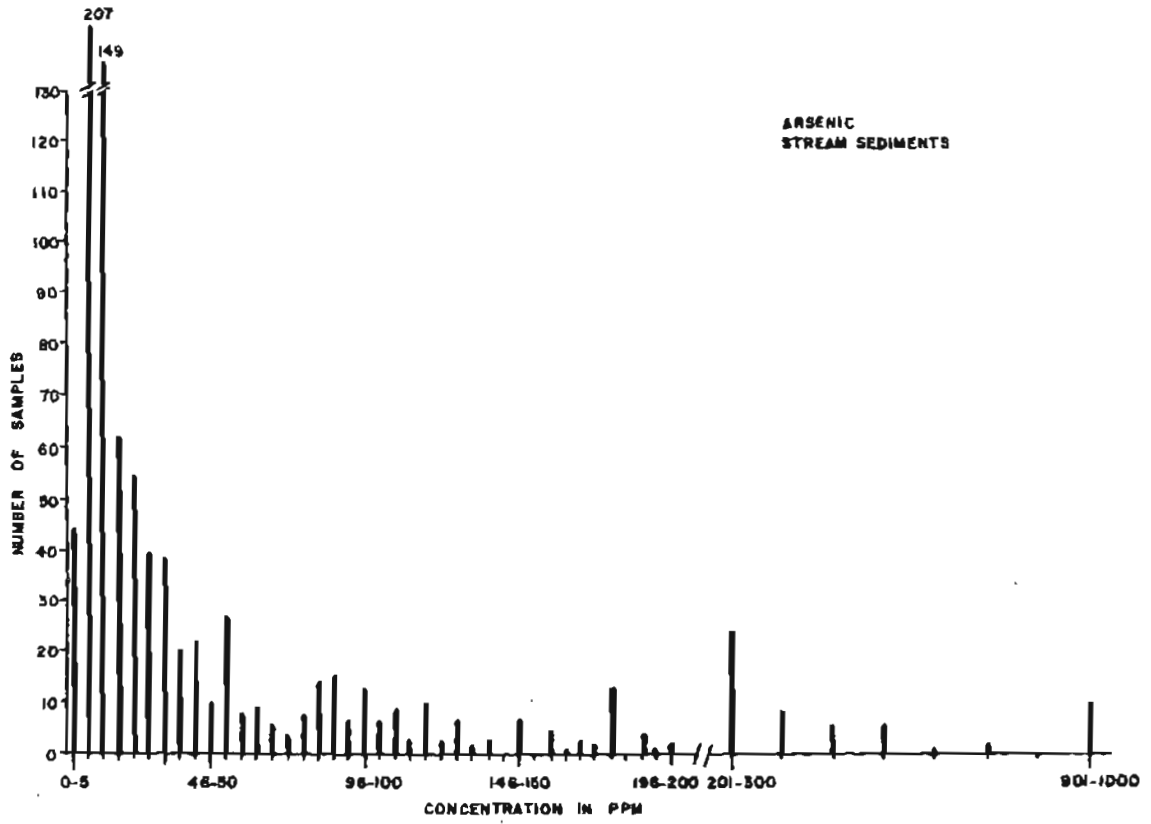
Sample No.	Deposit Type	Location	Mineralogy
81 MIRL 25B	IV	Sec. 33; T3N, R1E	Qt - Py - Ar - Au - Sp - Cp - St - Qt
81 MIRL 25C	IV	Sec. 33; T3N, R1E	Qt - Py - Ar - Au - Sp - Cp - Qt
81 MIRL 25D	IV	Sec. 33; T3N, R1E	Qt - Ar - Au - Te - St - Co - Qt
81 MIRL 25E	IV	Sec. 33; T3N, R1E	Qt - Ar - Au - St - Qt
81 MIRL 25F	IV	Sec. 33; T3N, R1E	Qt - Ar - Sp - Cp - Au - St - Qt
81 MIRL 25G	IV	Sec. 33; T3N, R1E	Qt - Ar - Au - St - Au - Qt
81 MIRL 27A	I	Sec. 24; T3N, R1E	Qt - Pyr - Ar - Cp - Sc - Ca
81 MIRL 27B	I	Sec. 24; T3N, R1E	Qt - Pyr - Py - Ca
81 PM 106	I	Sec. 26; T3N, R1E	Pyr - Cp - Ca
3202C	I	Sec. 26; T3N, R1E	Qt - Mu - Pyr - Cp - Sp - Sc - Au - St - Qt
82 FM 01A	I	Sec. 26; T3N, R1E	Pyr - Sp - Cp - Sc - St - Qt
82 FM 01B	I	Sec. 26; T3N, R1E	Pyr - Py - Cp - Qt
81 PM 63B	I	Sec. 26; T3N, R1E	Pyr - Py - Sp - Cp - St
81 PM 213A	I	Sec. 26; T3N, R1E	Pyr - Cp
81 PM 213B	I	Sec. 26; T3N, R1E	Pyr - Cp
82 YP 03	III	Sec. 22; T2N, R2E	Qt - Py - Ar - Qt
21147A	I	Sec. 16; T2N, R2E	Qt - Mu - Pyr - Py - Ar - Cp - Qt
75 Z 002	IV	Sec. 26; T3N, R1E	Qt - Py - Ar - Cp - St - Qt
82 NB 01A	IV	Sec. 26; T3N, R1E	Qt - Py - Ar - Qt
82 NB 02B	V	Sec. 26; T3N, R1E	Qt - Py - Ar - St - Qt
193	III	Sec. 24; T2N, R1E	Qt - Sc - Qt
194A	III	Sec. 26; T3N, R1E	Qt - Sc - Qt
194B	III	Sec. 26; T3N, R1E	Qt - Sc - Qt
21187A	III	Sec. 26; T3N, R1E	Qt - Pyr - Cp - Sc - Qt
21187B	III	Sec. 26; T3N, R1E	Qt - Pyr - Cp - Sc - Mo - Qt
21187C	III	Sec. 26; T3N, R1E	Qt - Sc - Qt
21187D	III	Sec. 26; T3N, R1E	Qt - Py - Sc - Qt
20509A	II	Sec. 8; T1N, R1E	Qt - Py - Qt
20509B	II	Sec. 8; T1N, R1E	Qt - Py - Qt
21142A	II	Sec. 16; T2N, R2E	Qt - Pyr - Cp - Qt - Ru
21142B	II	Sec. 16; T2N, R2E	Qt - Pyr - Qt = Ru
21142C	II	Sec. 16; T2N, R2E	Qt - Pyr - Cp - Qt = Ru
21149A	II	Sec. 16; T2N, R2E	Qt - Pyr - Cp - Qt = Ru
21149B	II	Sec. 16; T2N, R2E	Qt - Pyr - Cp - Qt = Ru
21149C	II	Sec. 16; T2N, R2E	Qt - Pyr - Cp - Qt = Ru
21149D	II	Sec. 16; T2N, R2E	Qt - Pyr - Cp - Qt = Ru
21149E	II	Sec. 16; T2N, R2E	Qt - Pyr - Cp - Qt = Ru
21149F	II	Sec. 16; T2N, R2E	Qt - Pyr - Cp - Qt = Ru
21149G	II	Sec. 16; T2N, R2E	Qt - Pyr - Py - Cp - Qt = Ru
21149H	II	Sec. 16; T2N, R2E	Qt - Pyr - Cp - Qt = Ru
21149I	II	Sec. 16; T2N, R2E	Qt - Pyr - Py - Cp - Qt = Ru
21333A	V	Sec. 16; T2N, R1W	Qt - Py - Ar - St - Co - Qt
21333B	V	Sec. 16; T2N, R1W	Qt - Py - Ar - St - Qt
Nord Adit MSZ	I	Sec. 21; T3N, R2E	Qt - Ar - Au - Sp - Qt
Nord Adit A	I	Sec. 21; T3N, R2E	Qt - Mu - Py - Ar - St
Nord Adit B	I	Sec. 21; T3N, R2E	Qt - Mn - Py - Ar - Ru
21150A	IV	Sec. 21; T3N, R2E	Qt - Py - Ar - St - Qt
21150B	IV	Sec. 21; T3N, R2E	Qt - Py - Ar - Se - Qt
21150C	I	Sec. 21; T3N, R2E	Qt - Mu - Py - Sp - Gr - Ru
21150D	I	Sec. 21; T3N, R2E	Qt - Mu - Pyr - Py - Ar - Ca
21152A	I	Sec. 21; T3N, R2E	Qt - Mu - Pyr - Ru

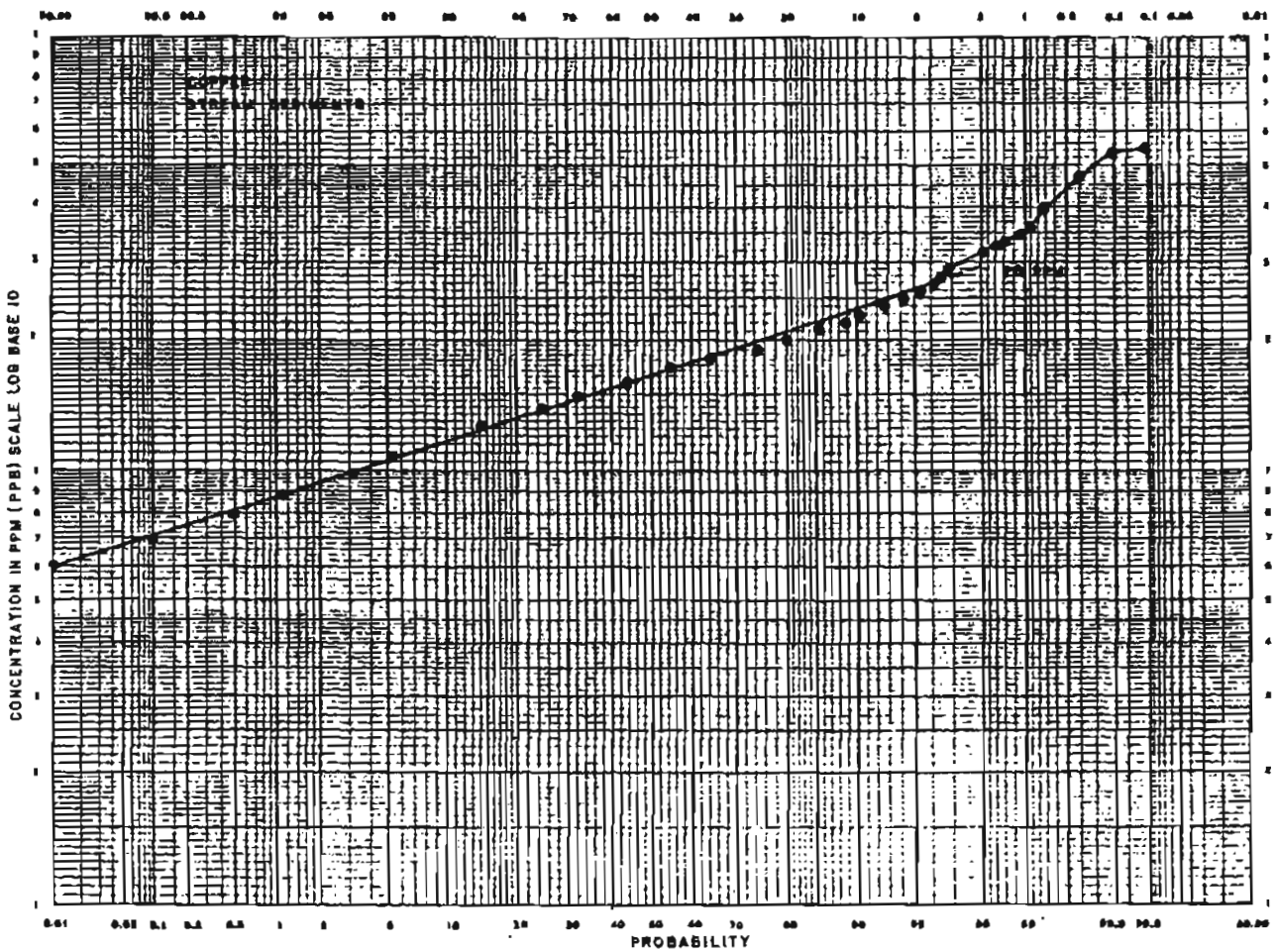
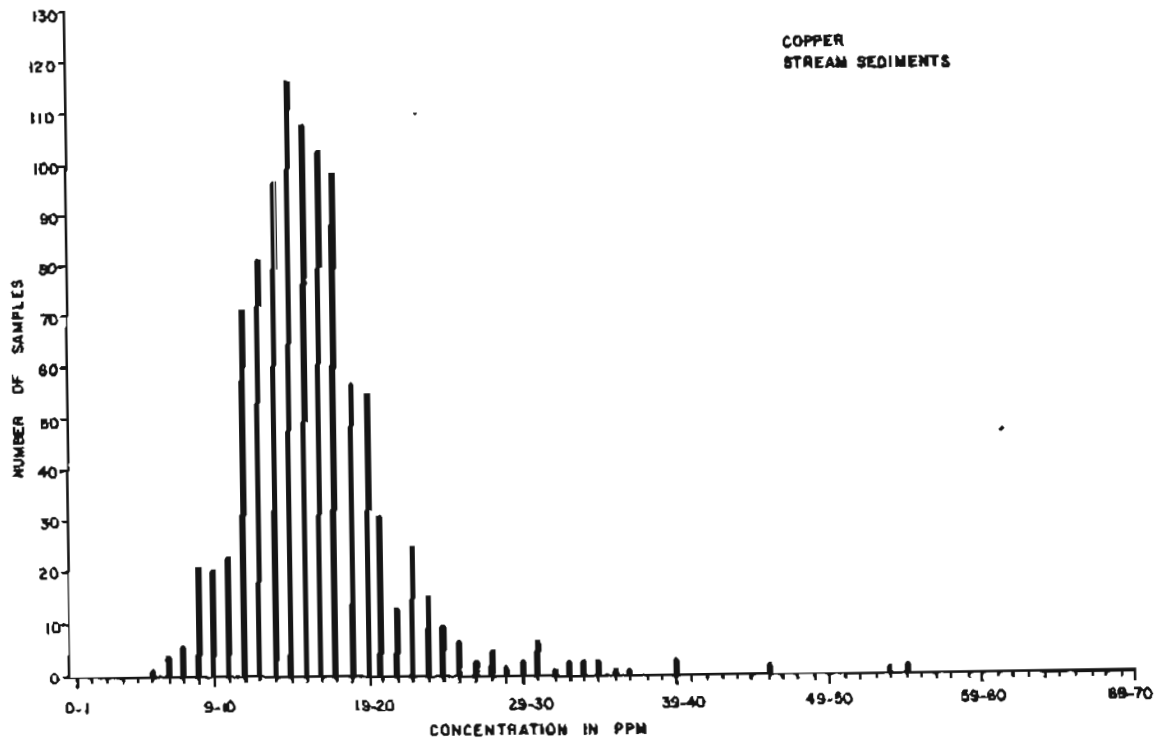
Table B2 (Continued)

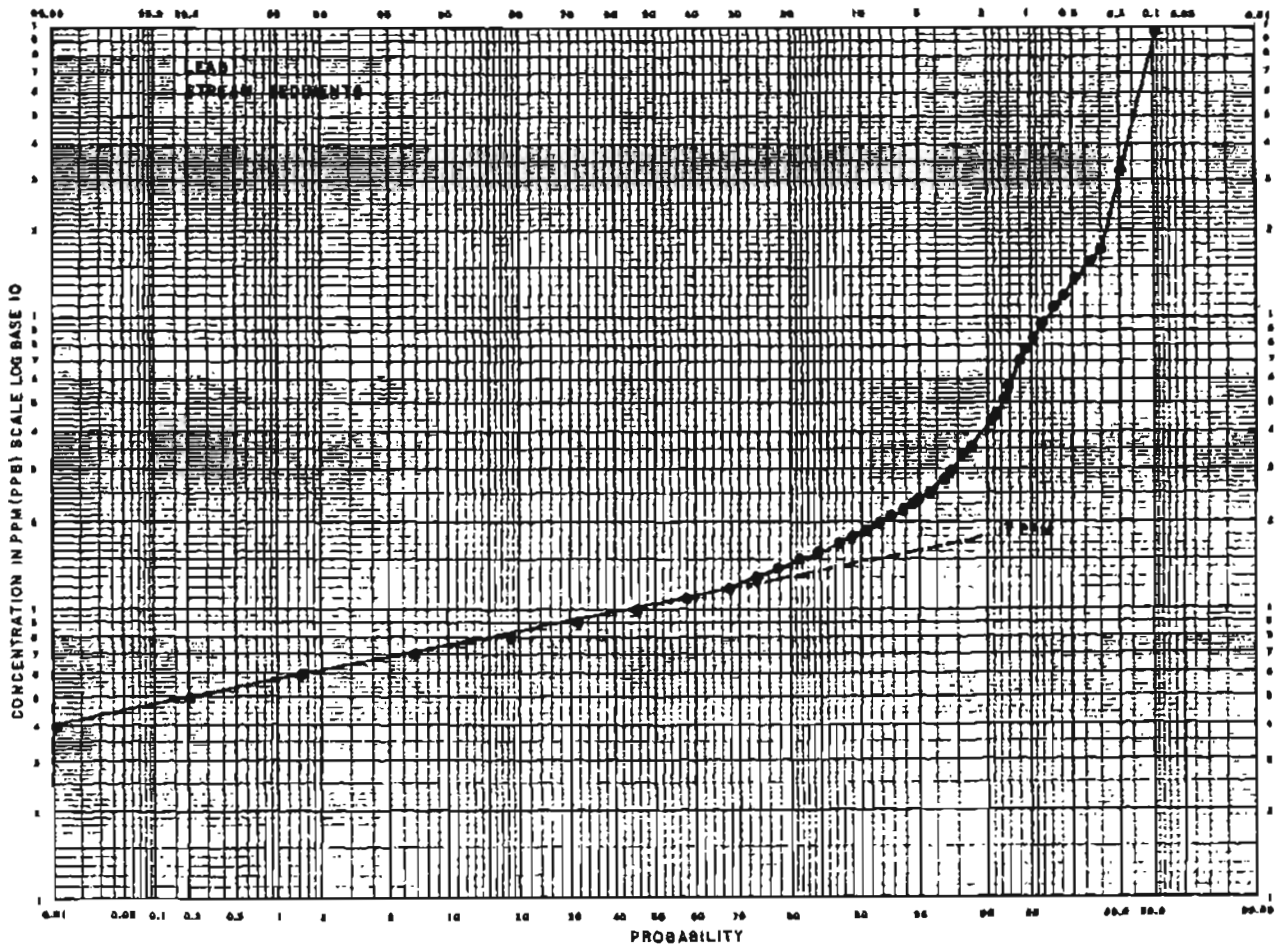
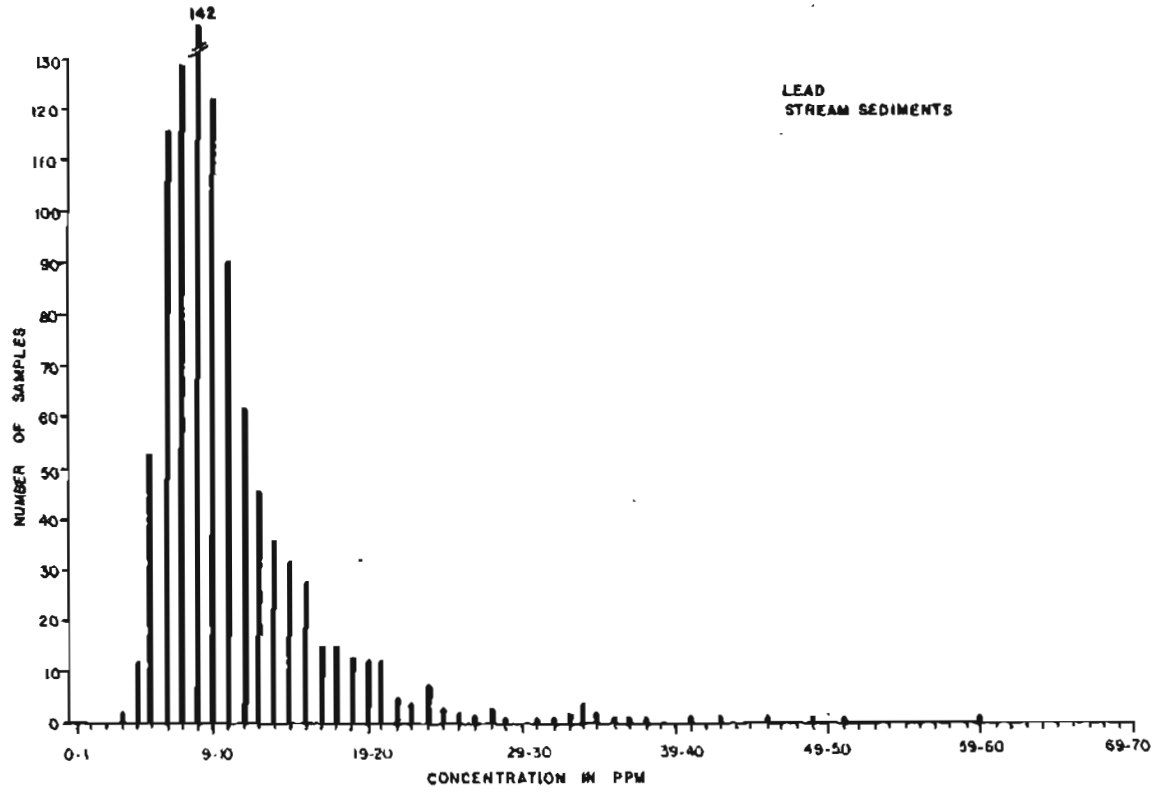
Sample No.	Deposit Type	Location	Mineralogy
21152B	I	Sec. 21; T3N, R2E	Qt - Mu - Pyr - Py - Ar
21152C	I	Sec. 21; T3N, R2E	Qt - Mu - Pyr - Ar - Ru
21153A	I	Sec. 21; T3N, R2E	Qt - Mu - Pyr - Py - Cp - Ga
Christina 600	V	Sec. 20; T3N, T2E	Qt - Py - Ar - St - Au - Qt
Christina 800	V	Sec. 20; T3N, T2E	Qt - Py - Ar - St - Qt
Christina 1100A	I	Sec. 20; T3N, T2E	Qt - Mu - Py - Ar - Au - Sp - Ru
Christina 1100B	I	Sec. 20; T3N, T2E	Qt - Mu - Py - Ar
82 CA 04	I	Sec. 20; T3N, T2E	Qt - Mu - Py - Ar - Sp - St - Qt

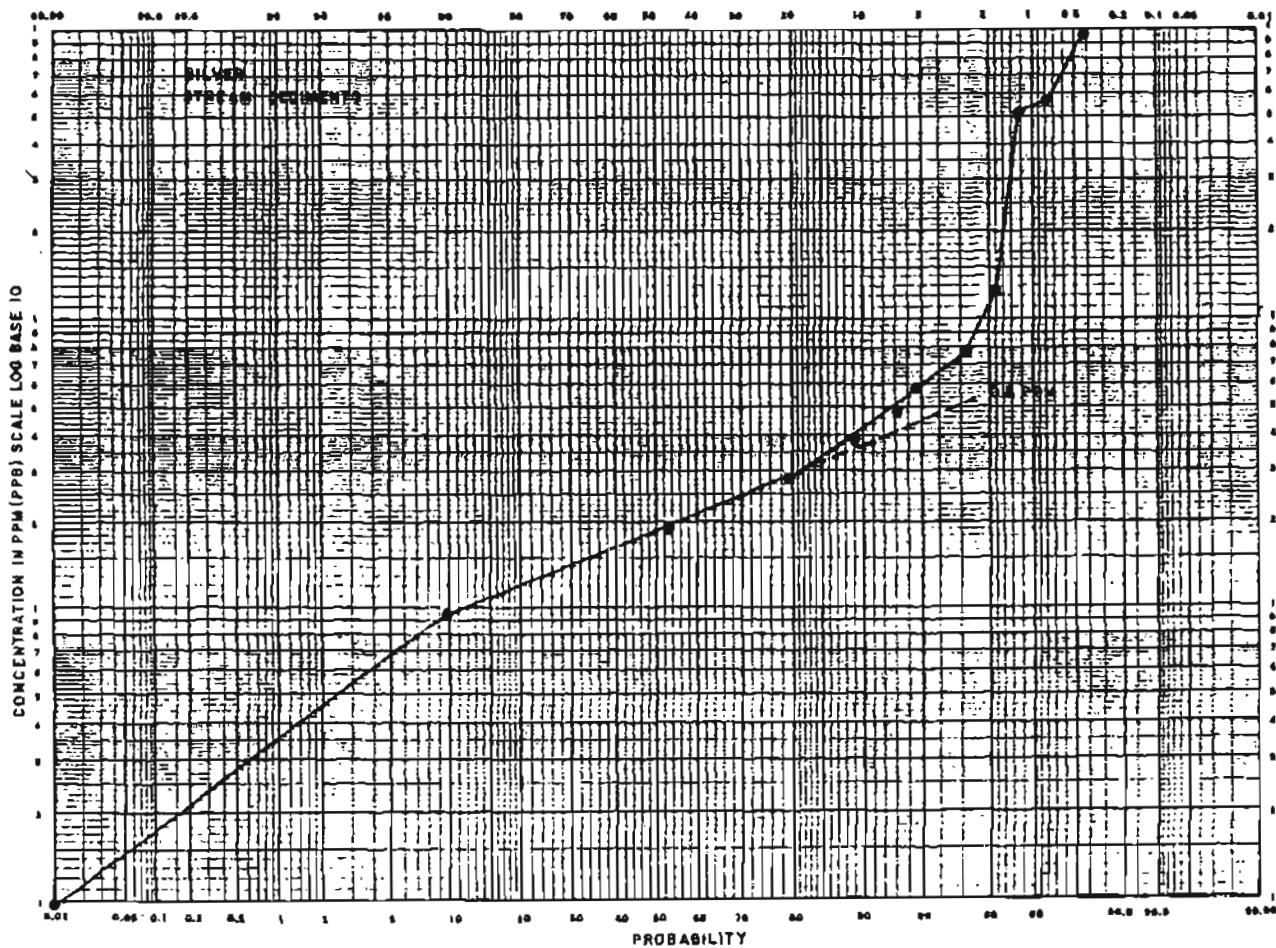
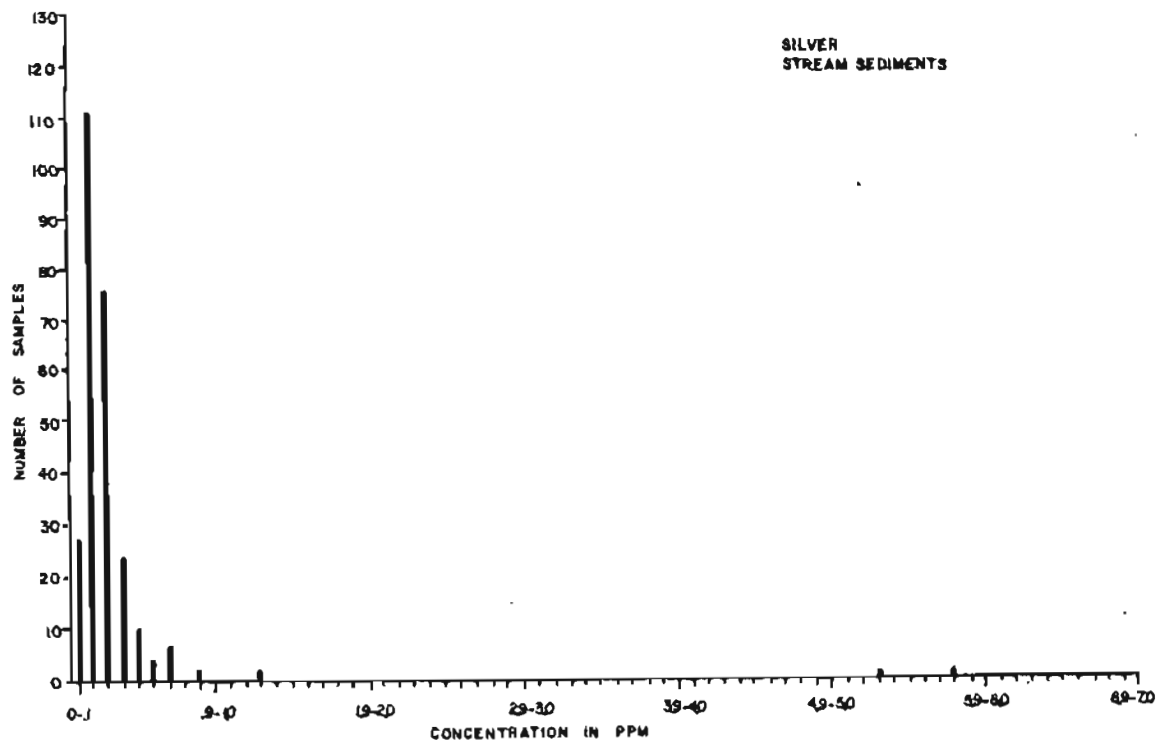
\*Note: Newsboy samples actually from Cheechako Prospect

**APPENDIX C1**  
**Histograms and Log Concentration-Probability Plots of**  
**Stream Sediment, Pan Concentrate, and Rock Geochemical Data**  
**from the Fairbanks Mining District**

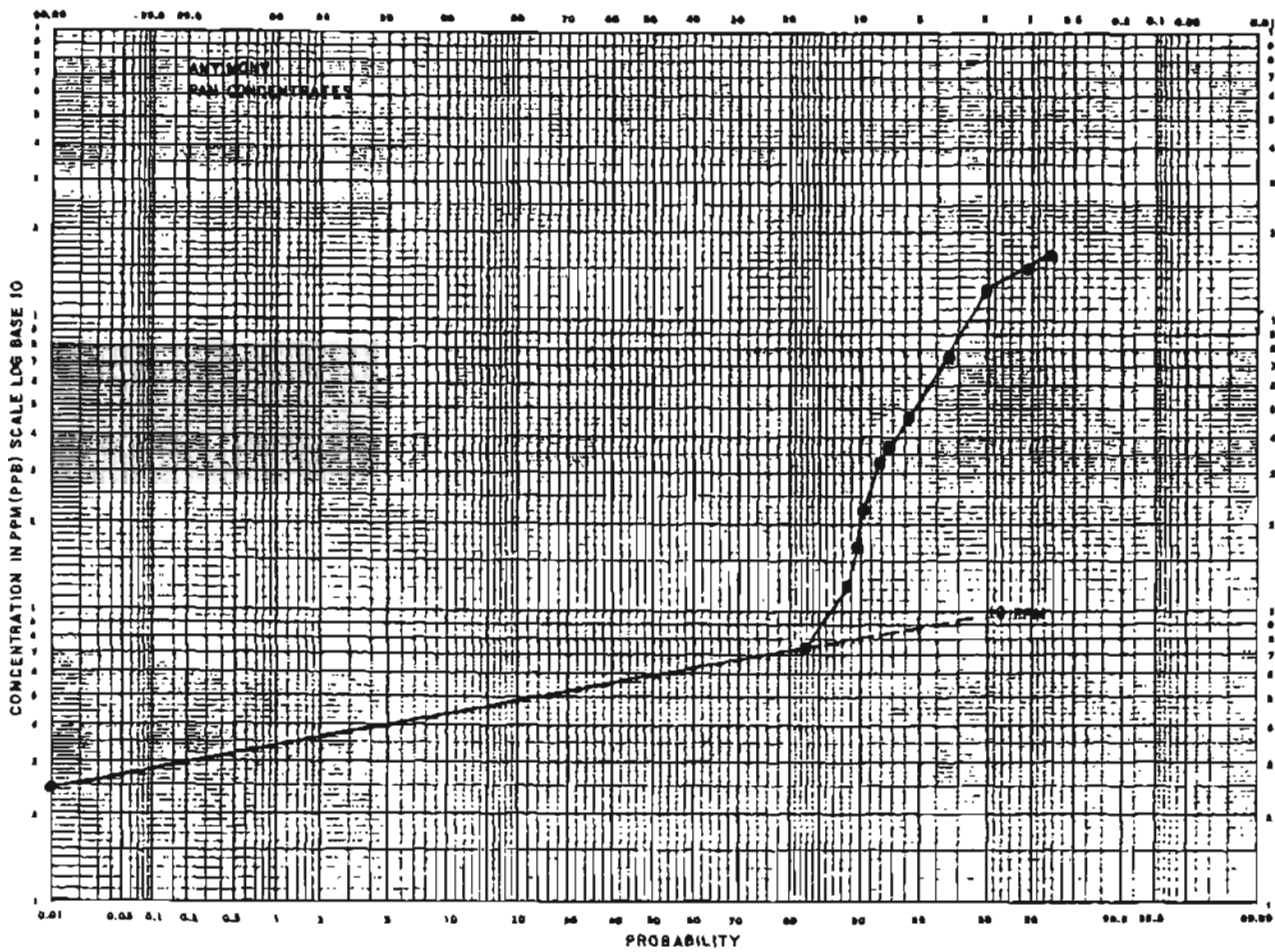
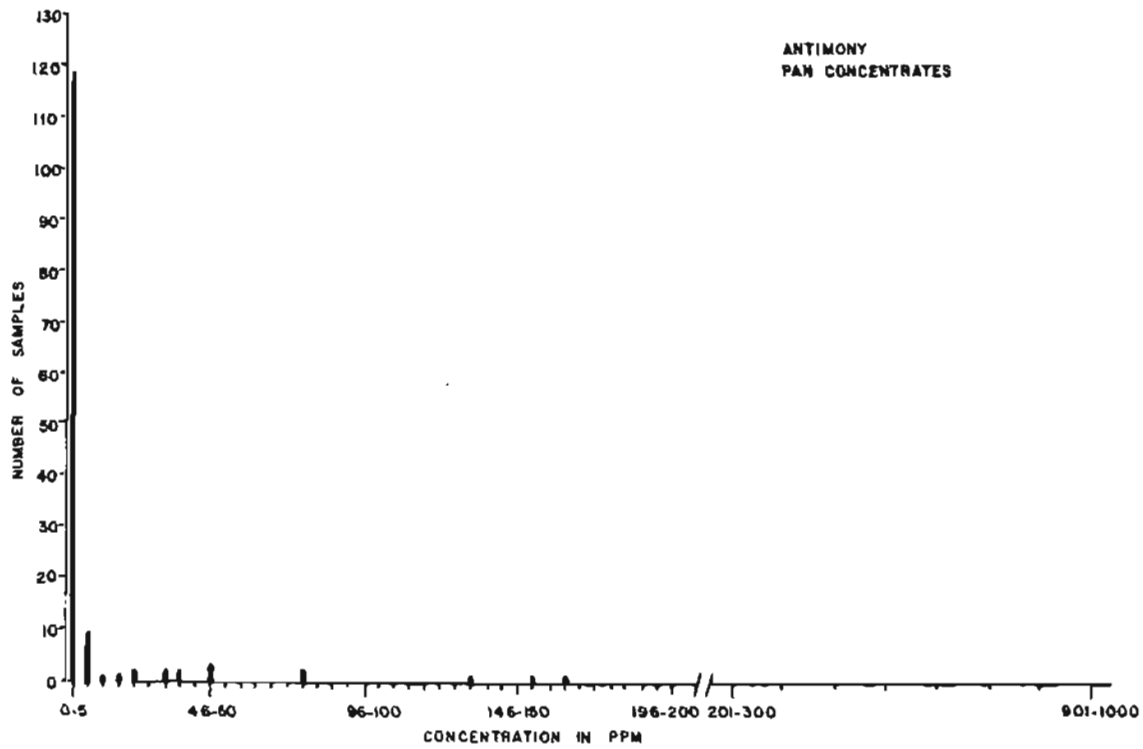


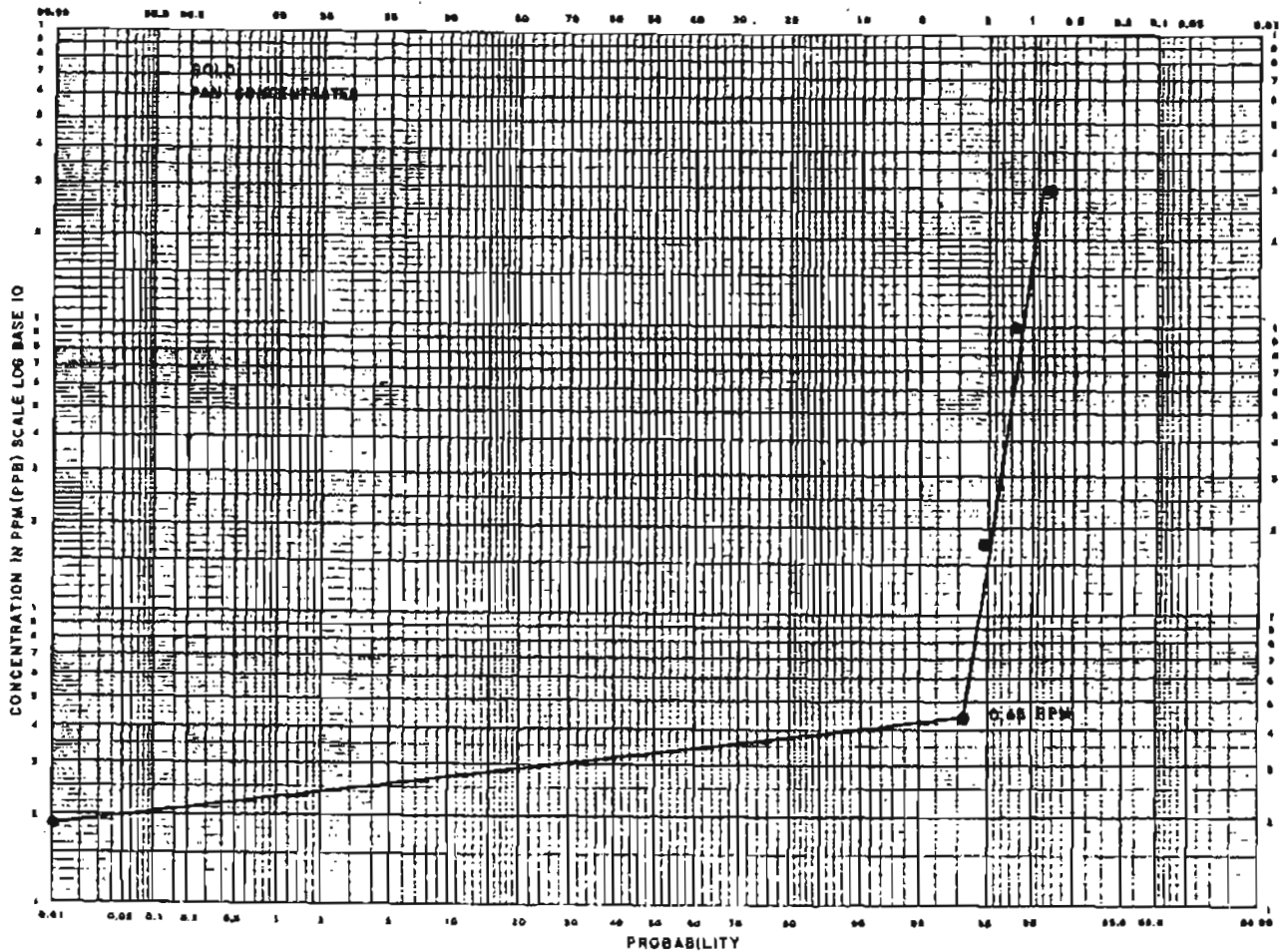
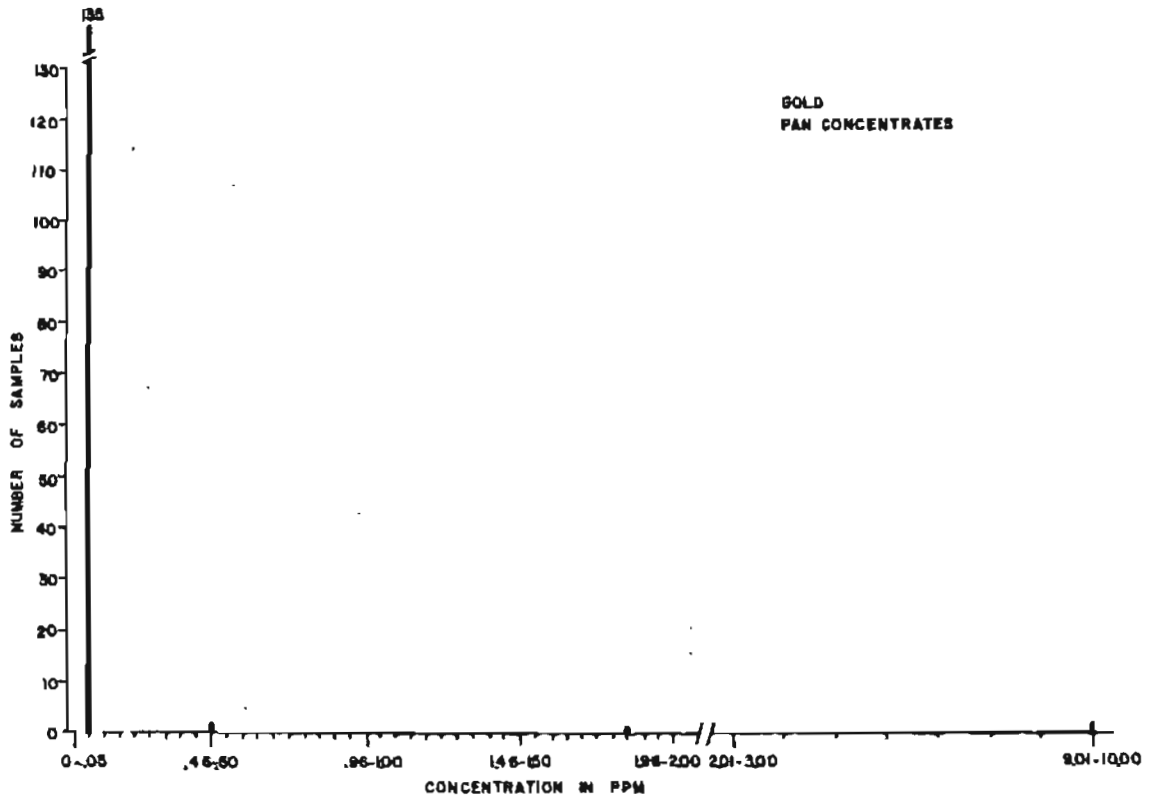






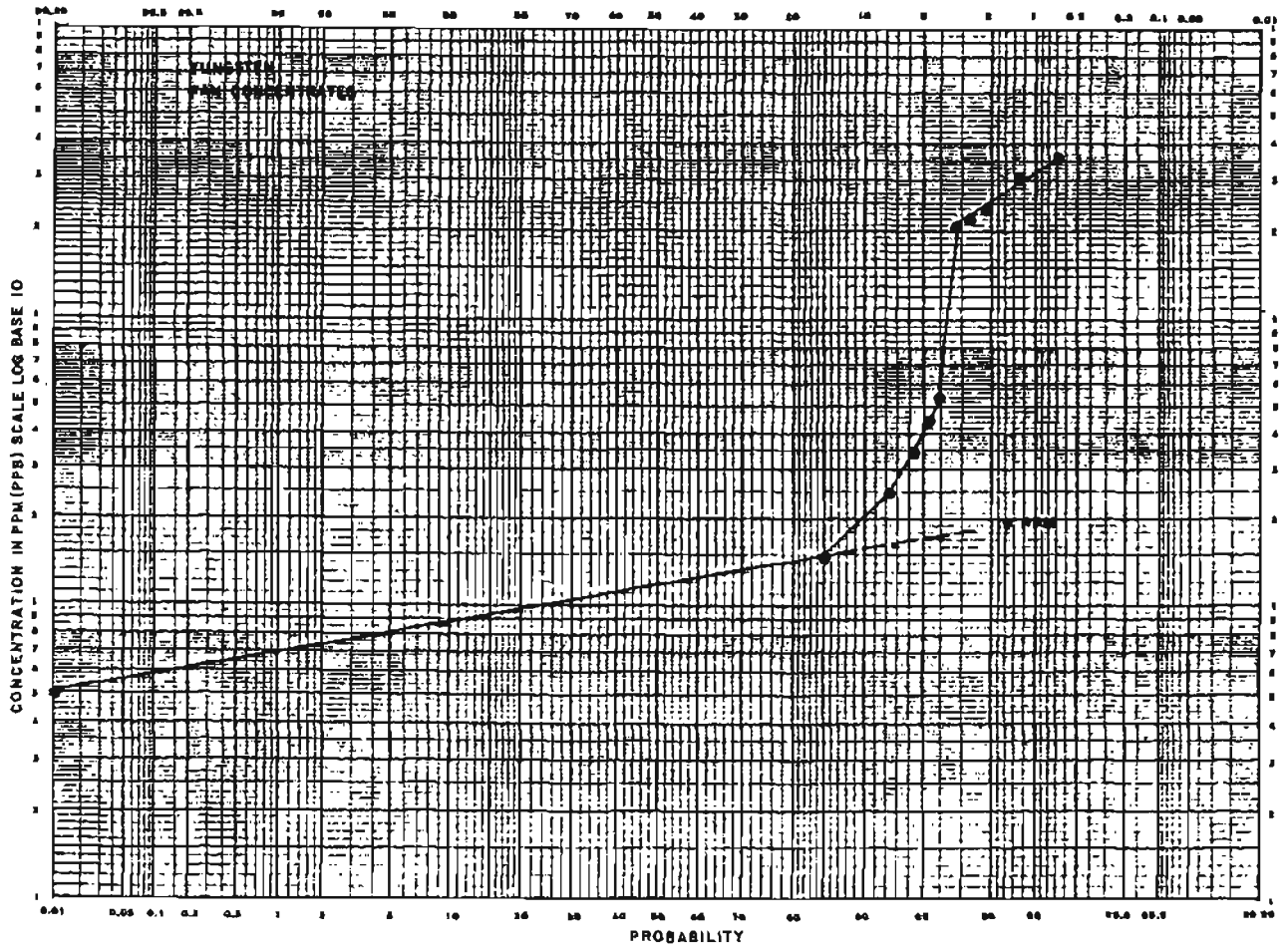
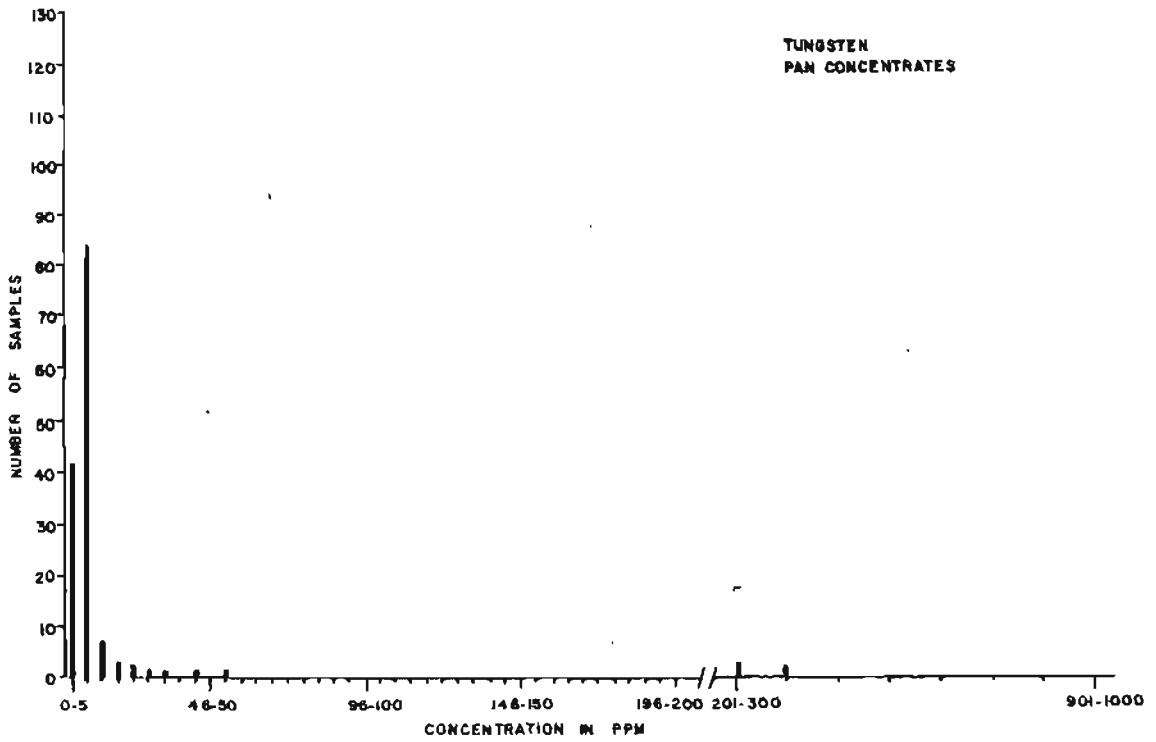


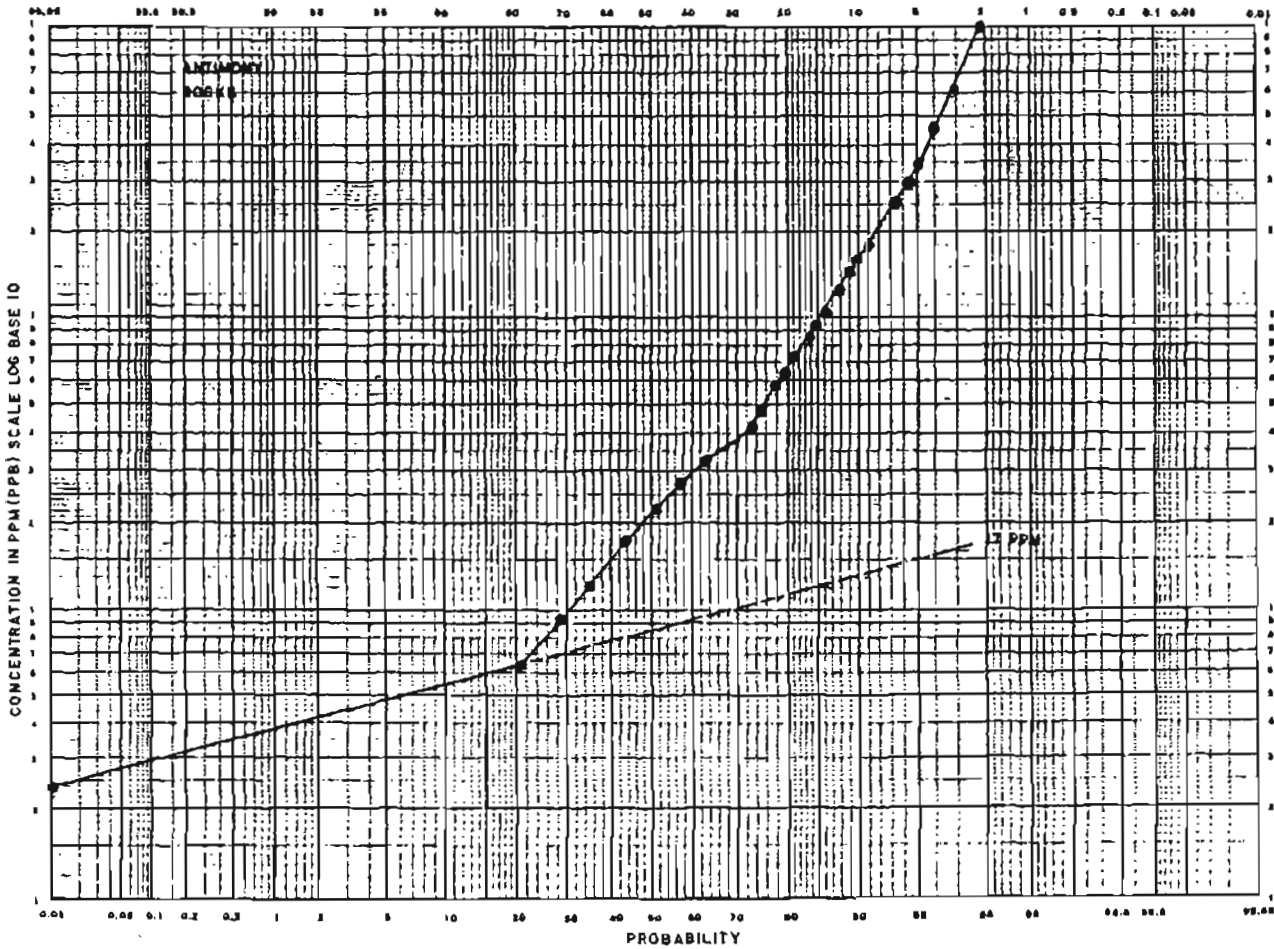
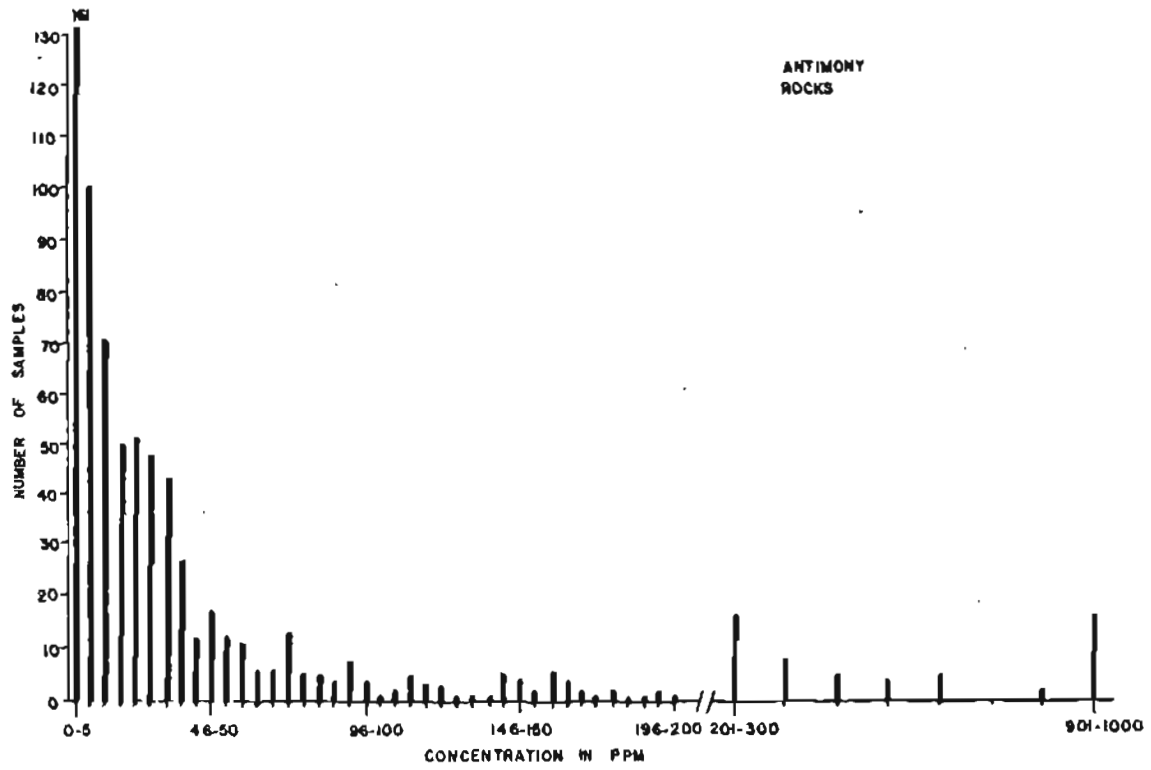


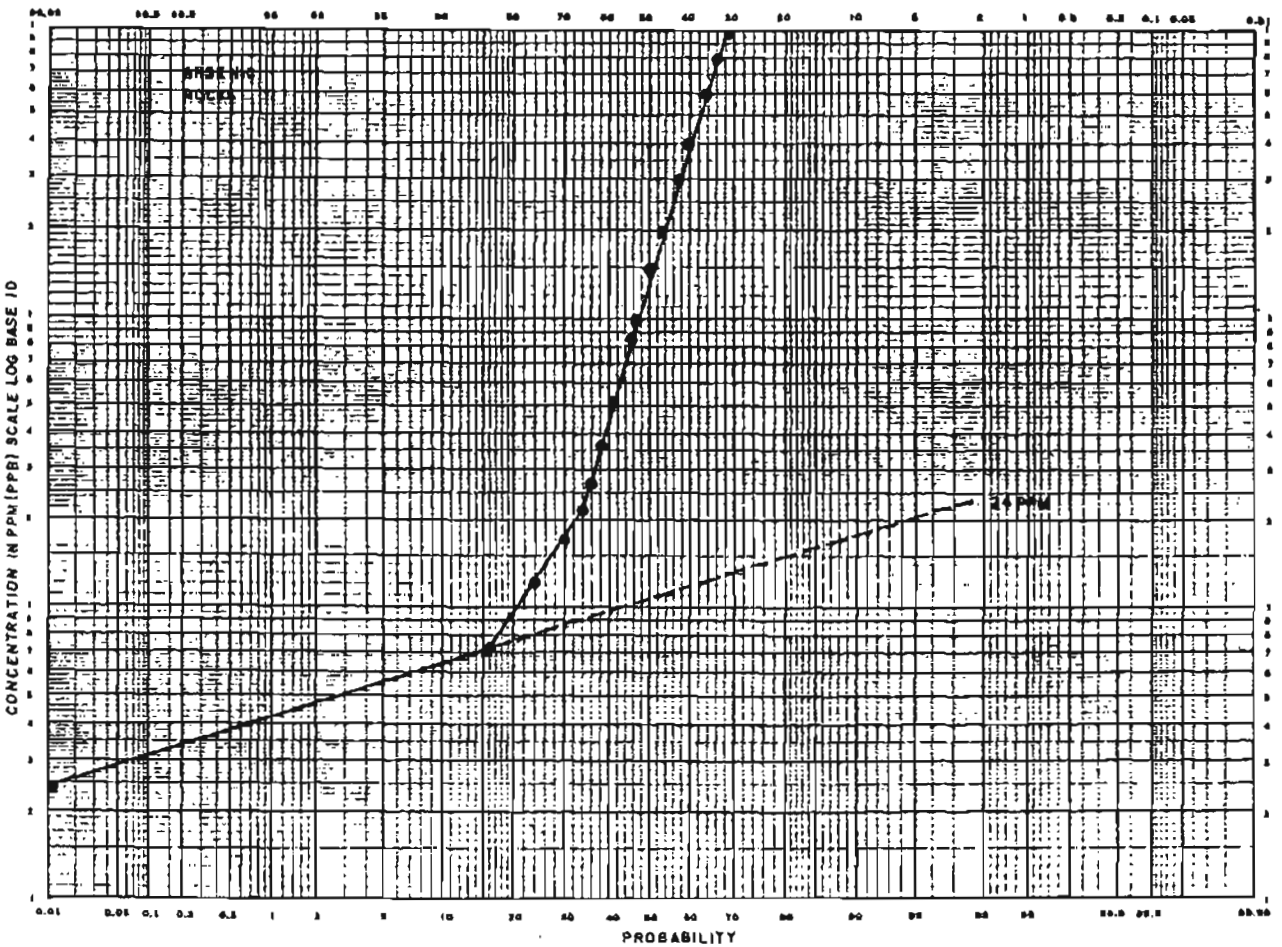
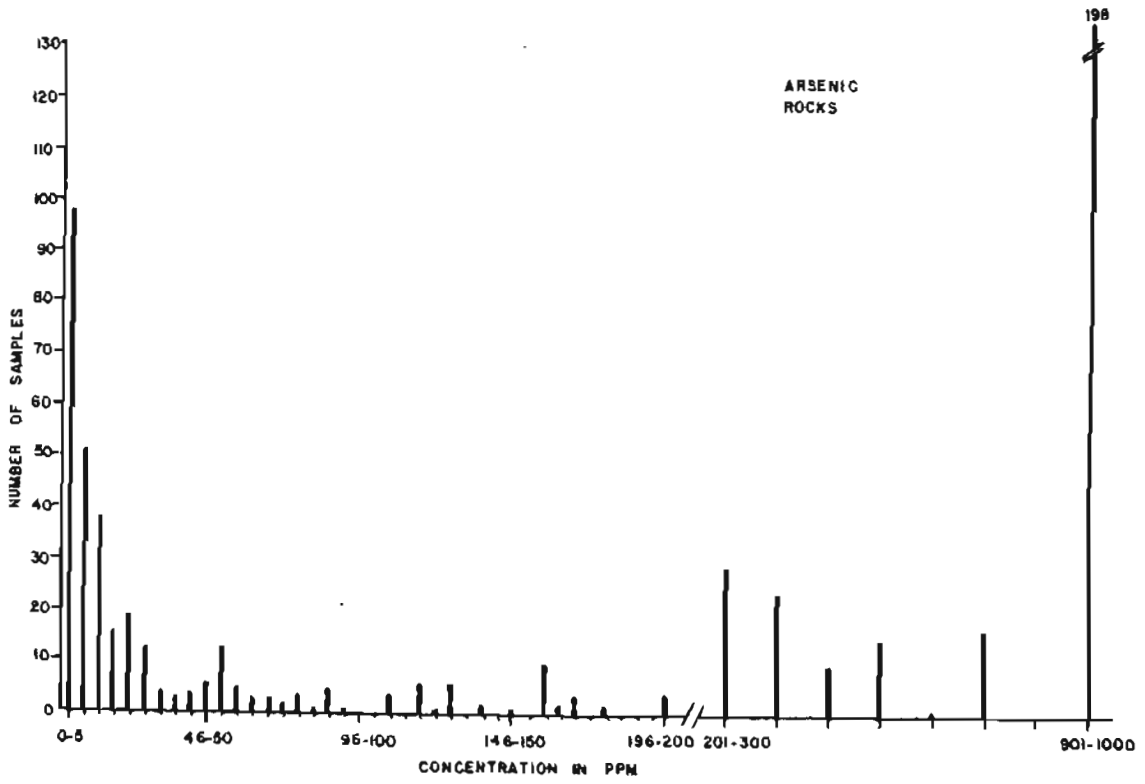


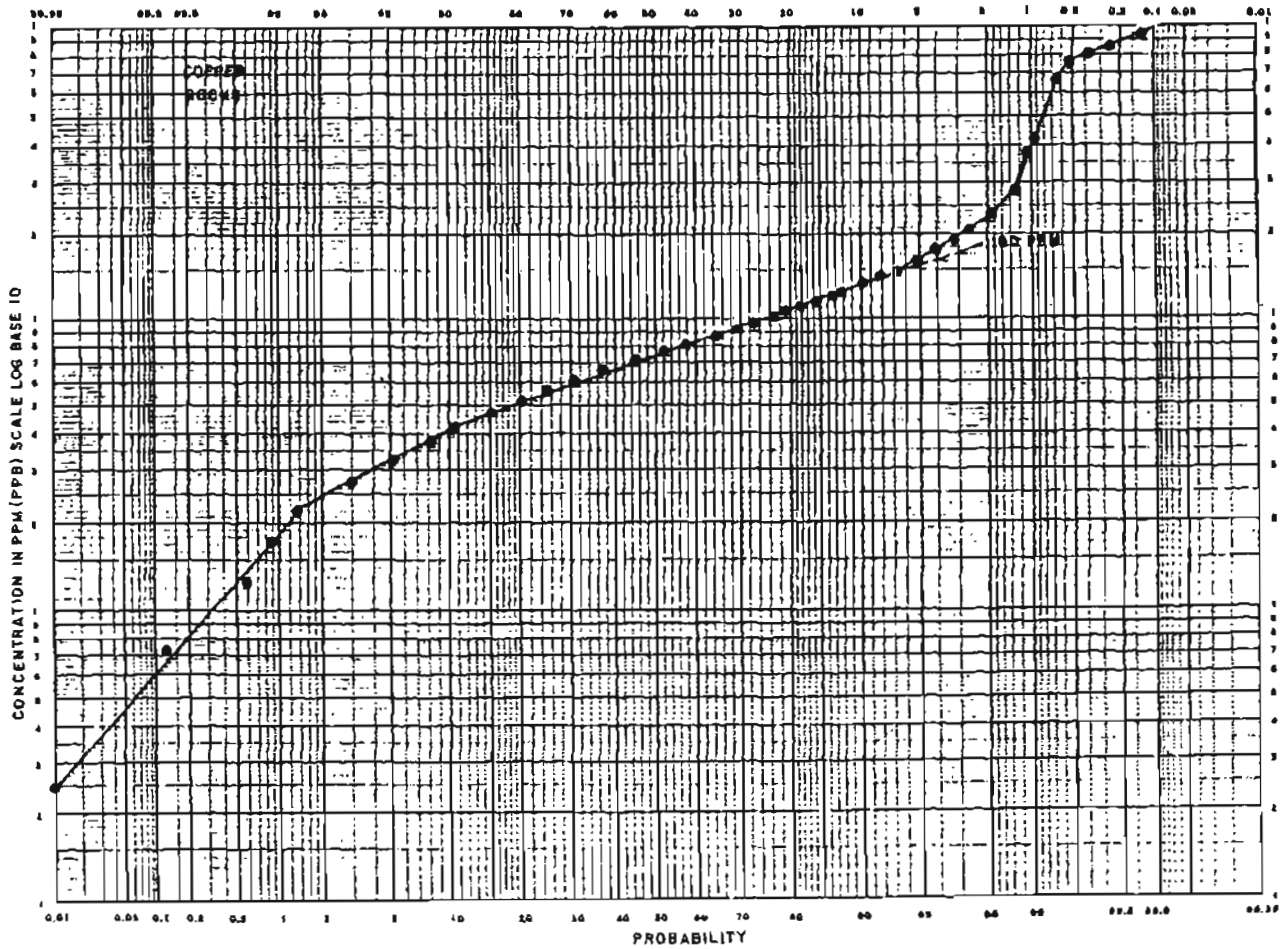
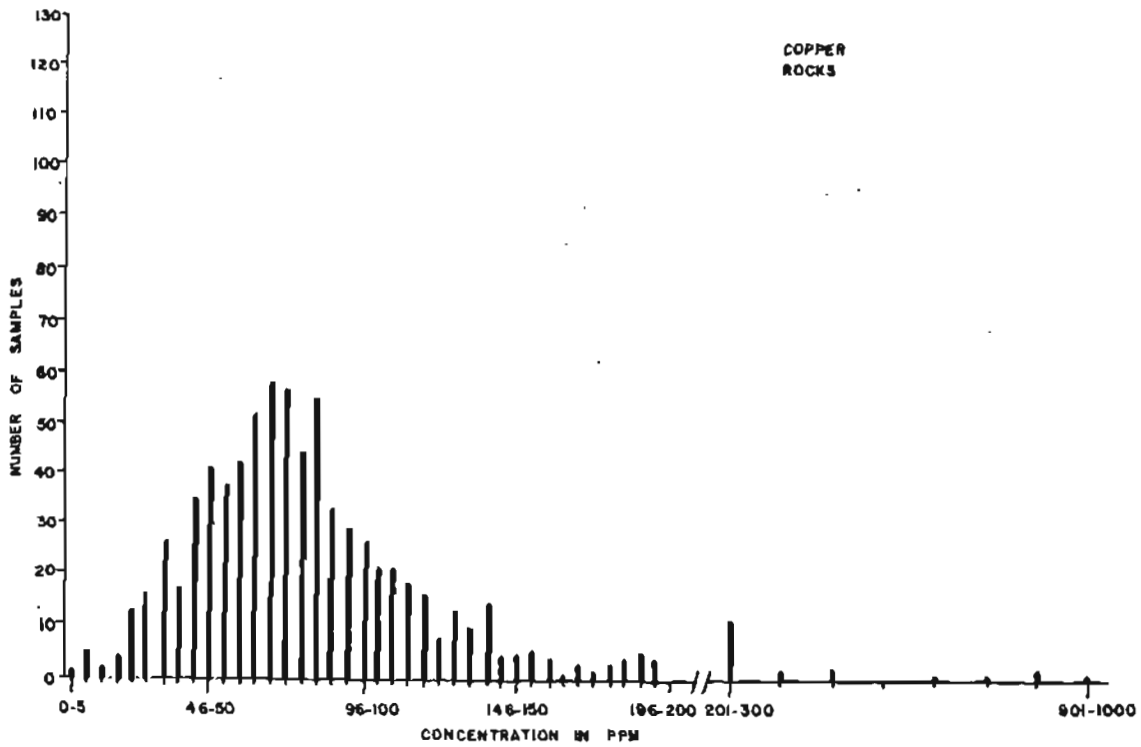


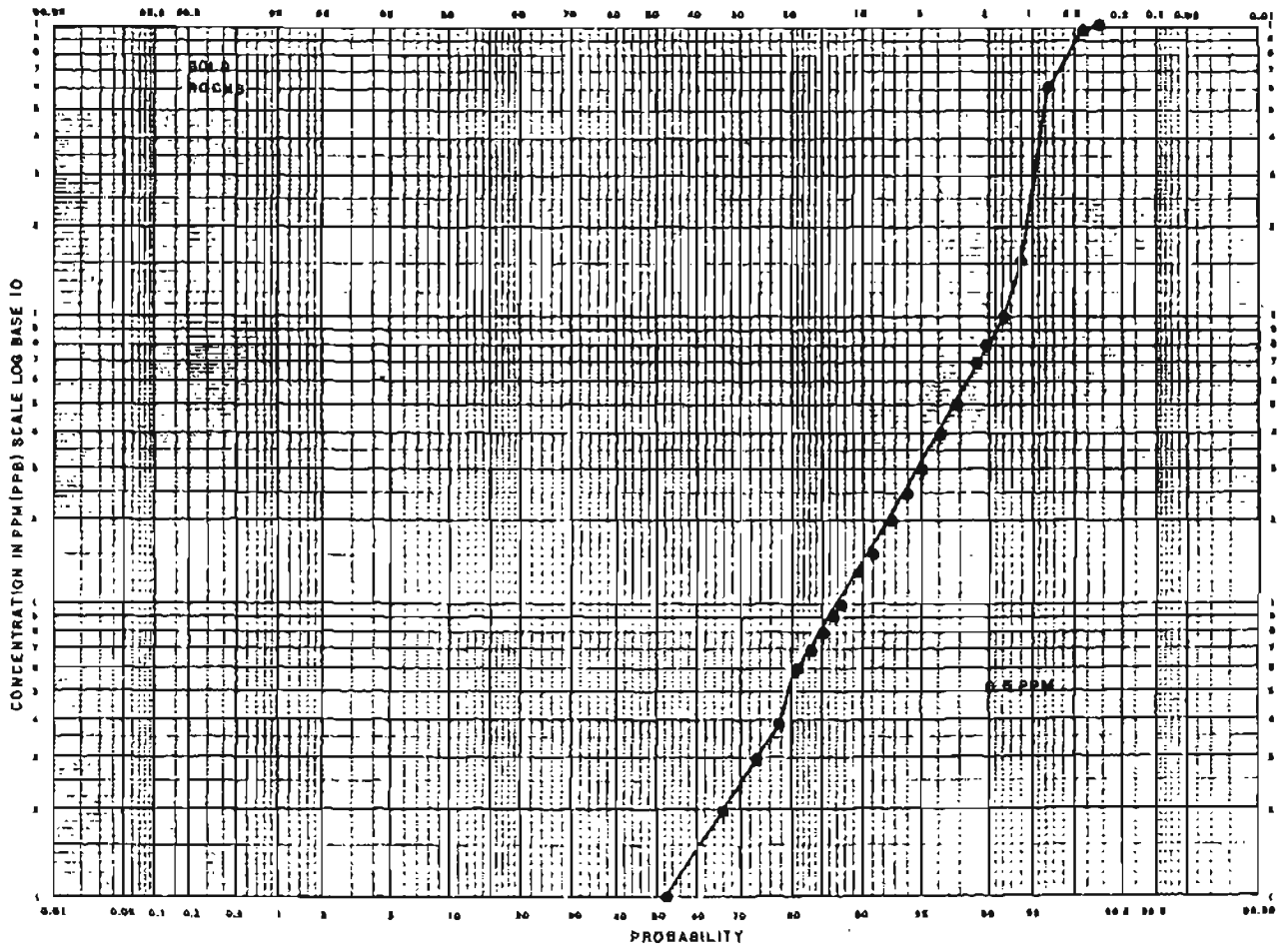
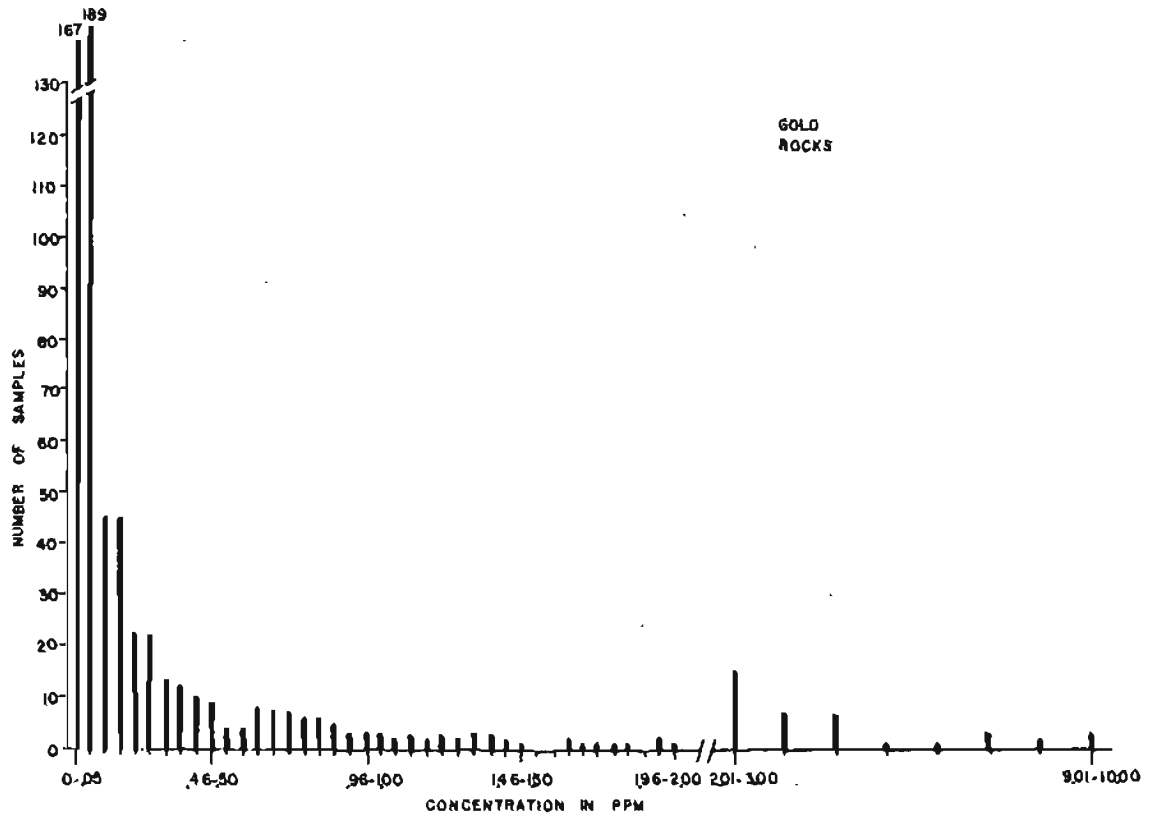
TUNGSTEN  
PAN CONCENTRATES

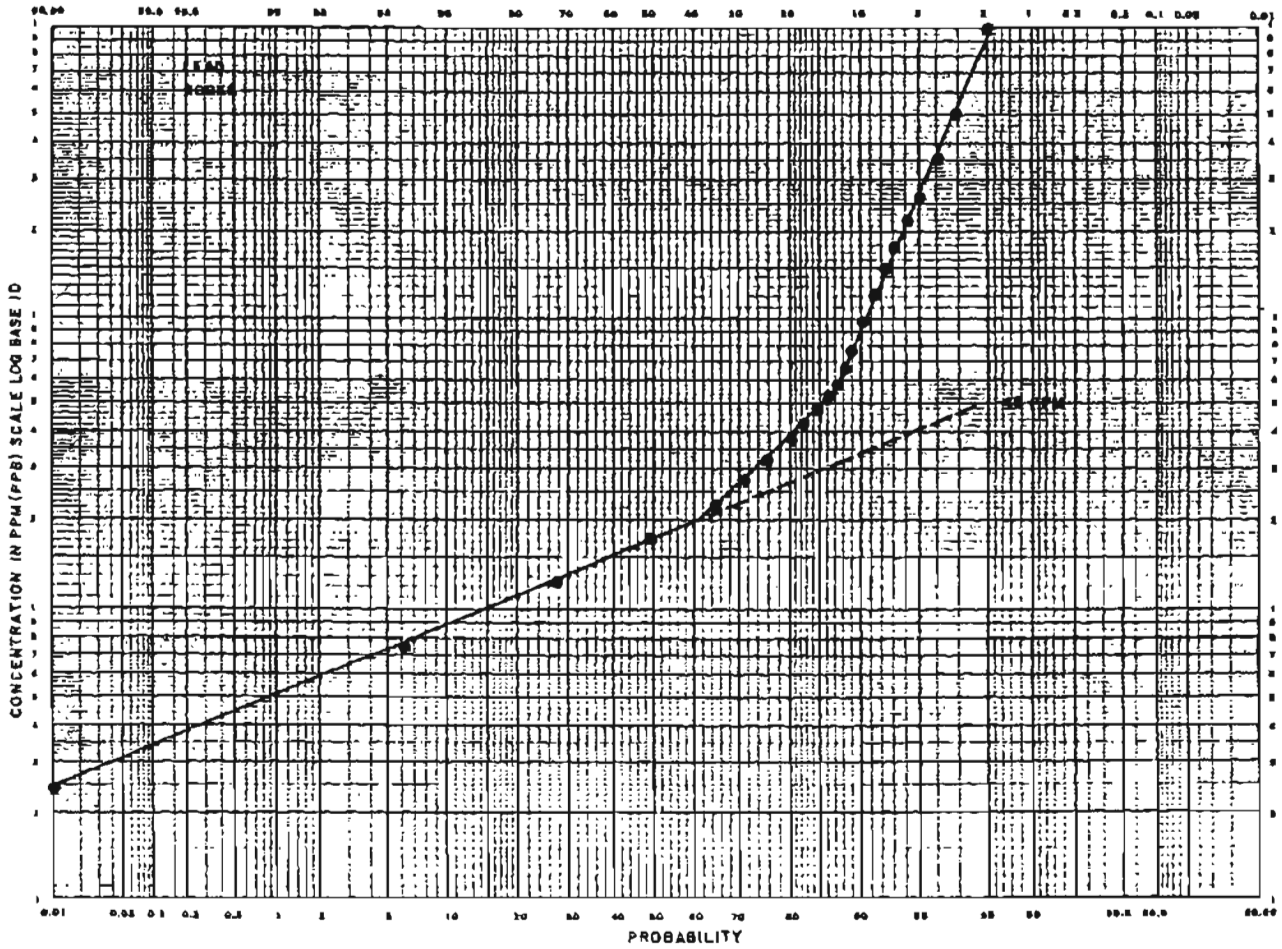
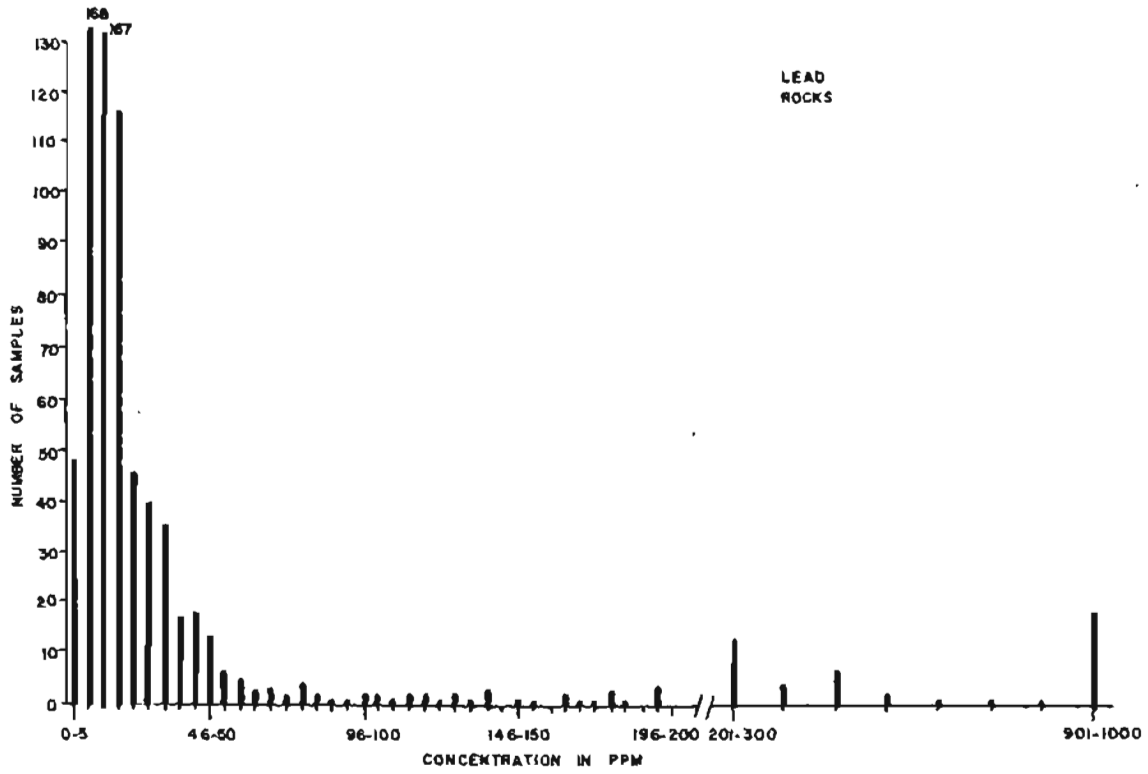


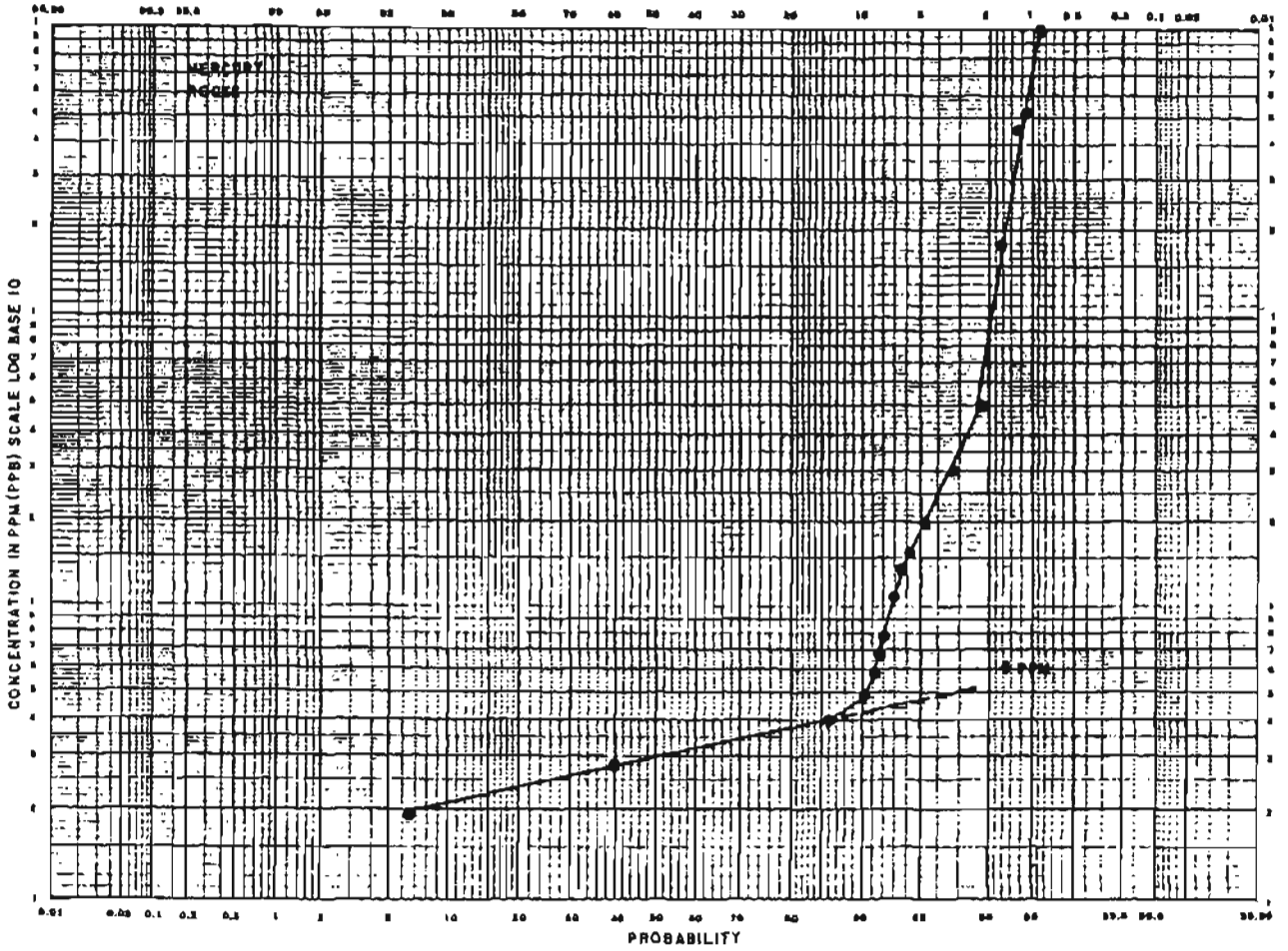
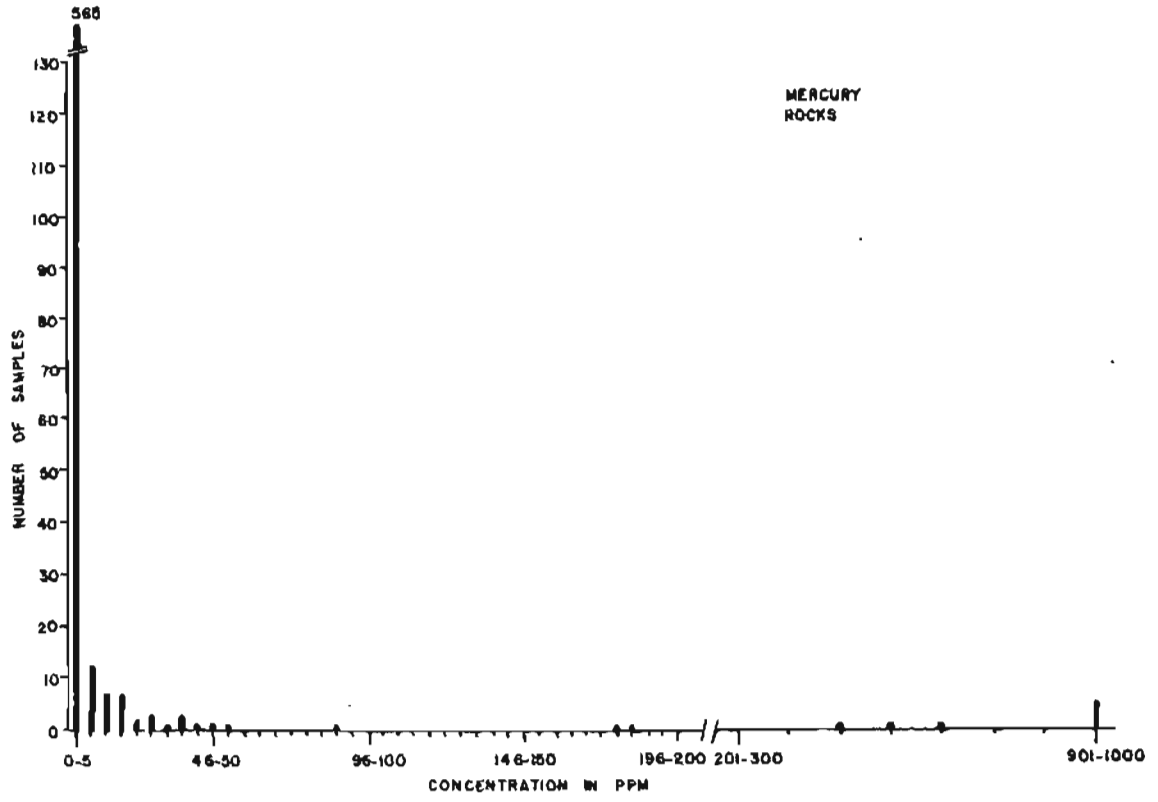


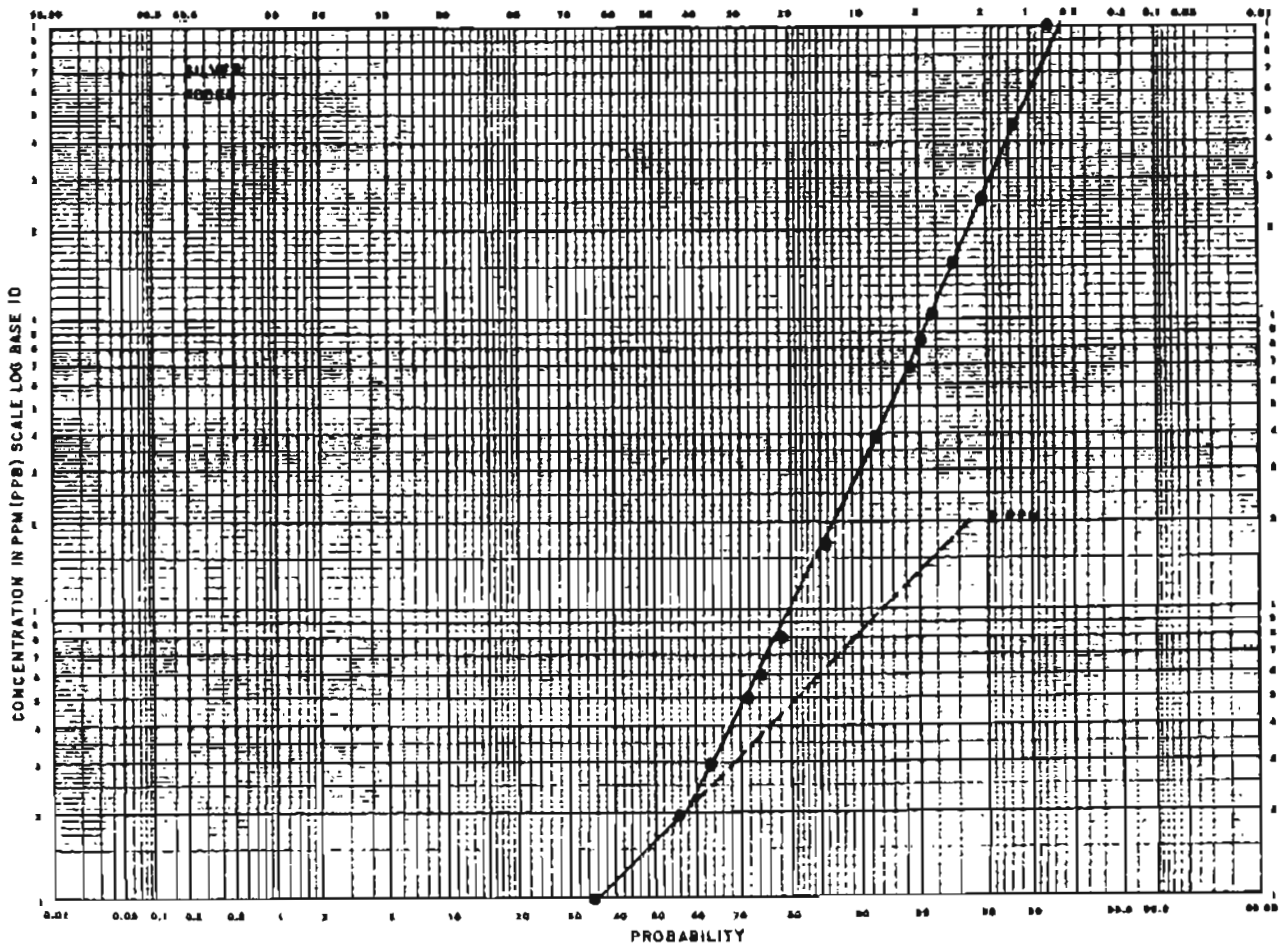
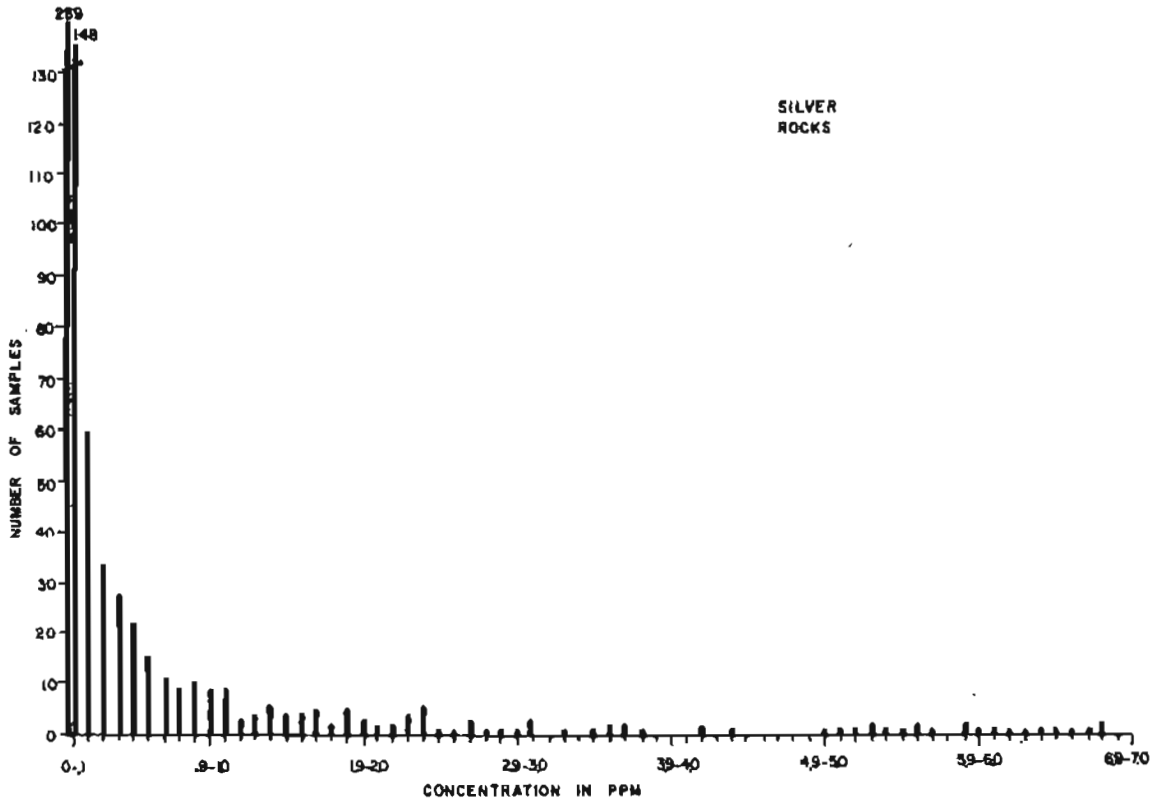


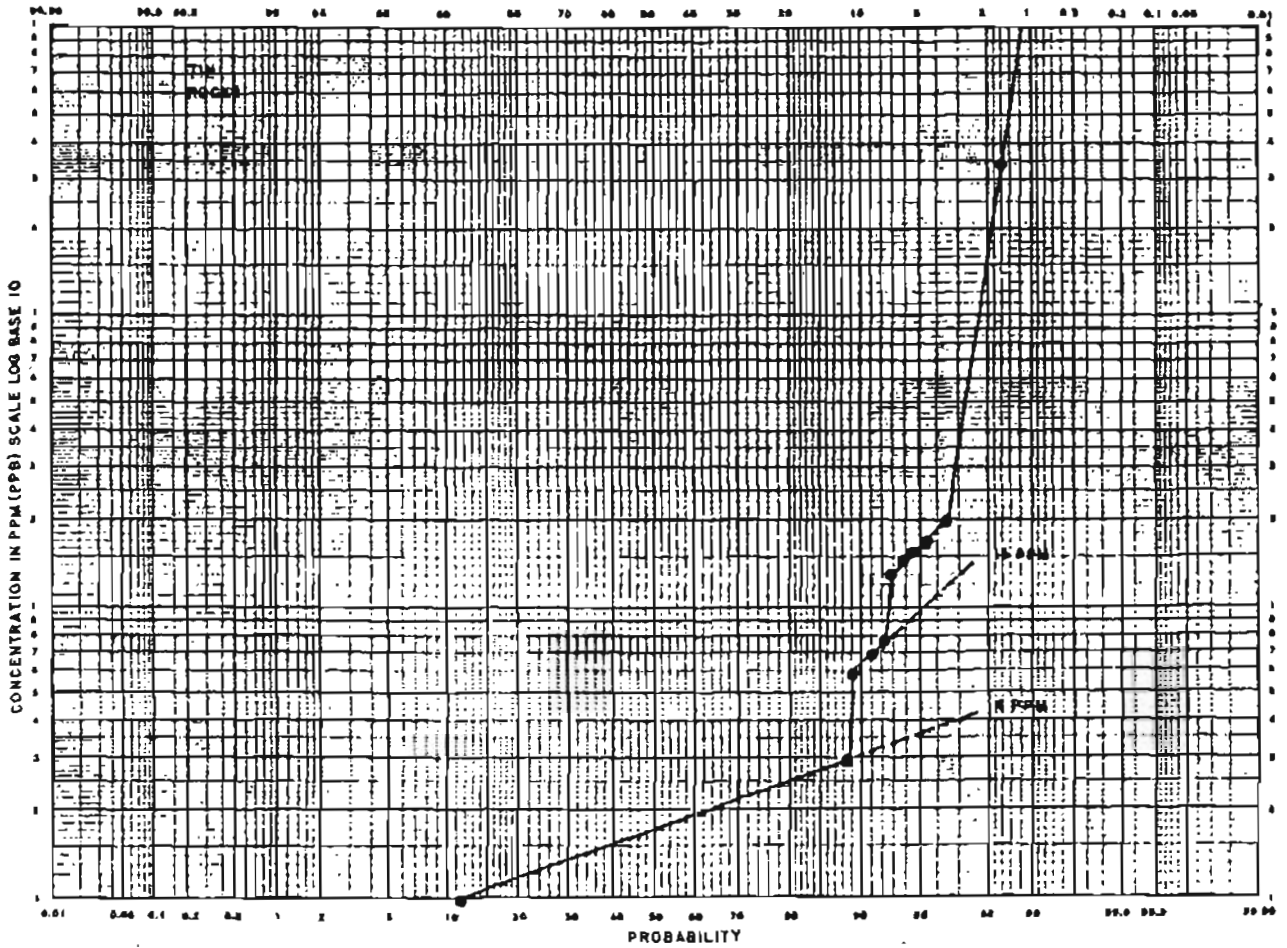
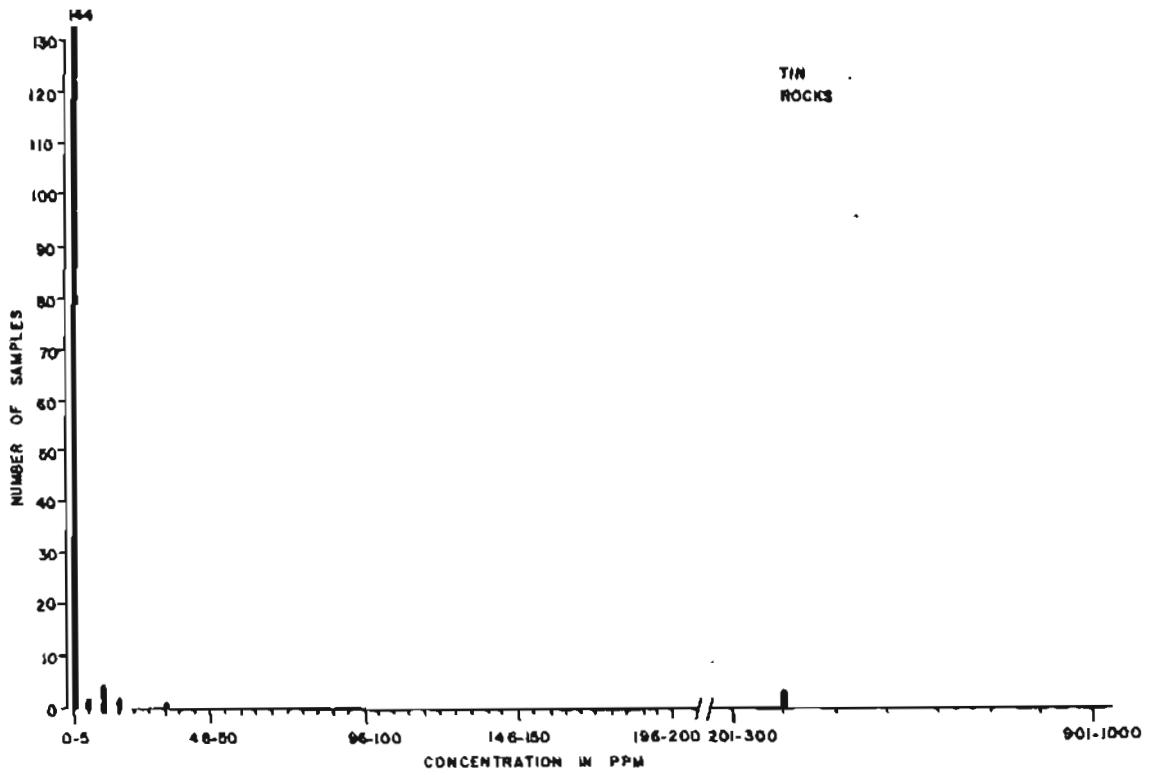


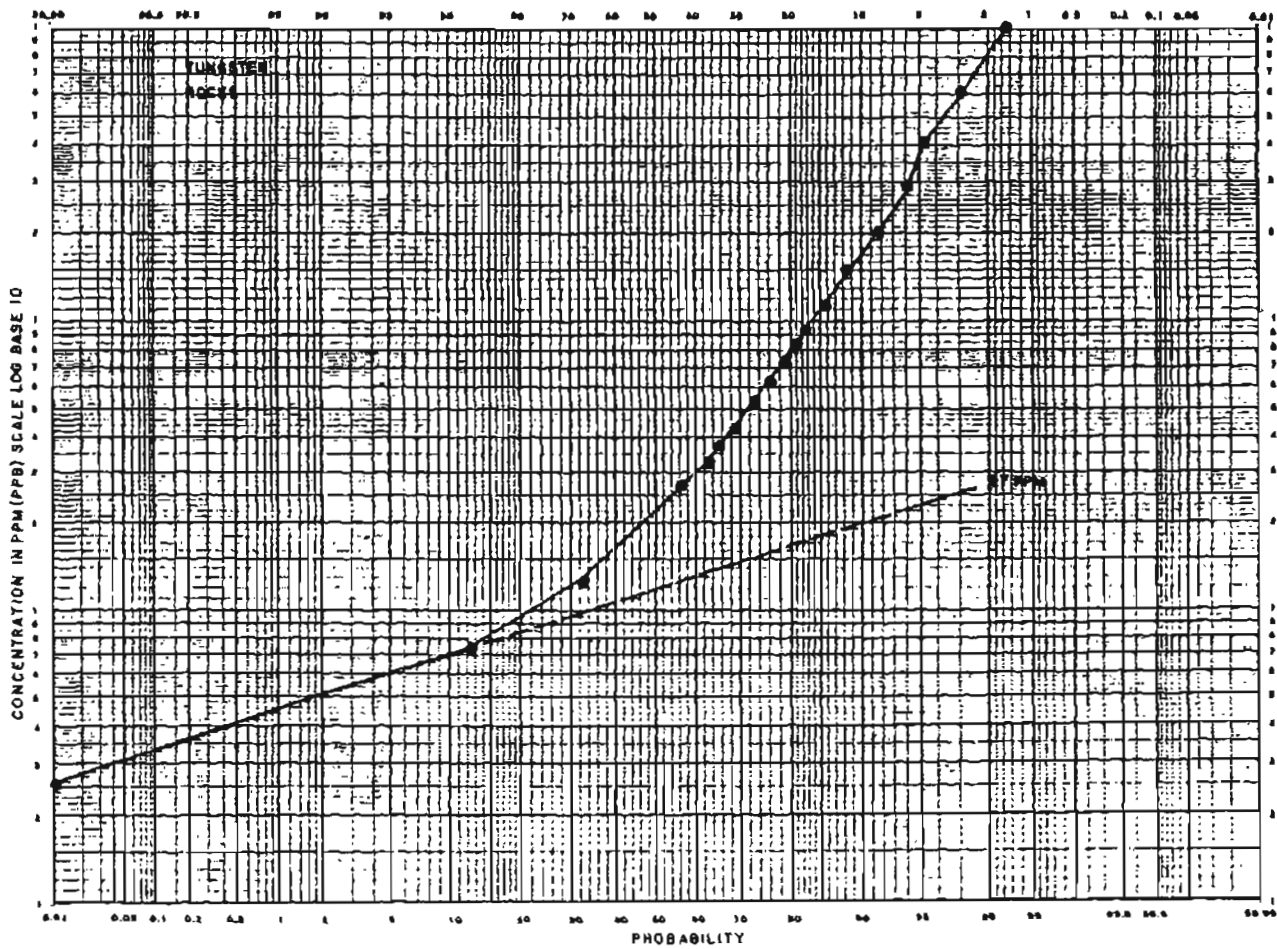
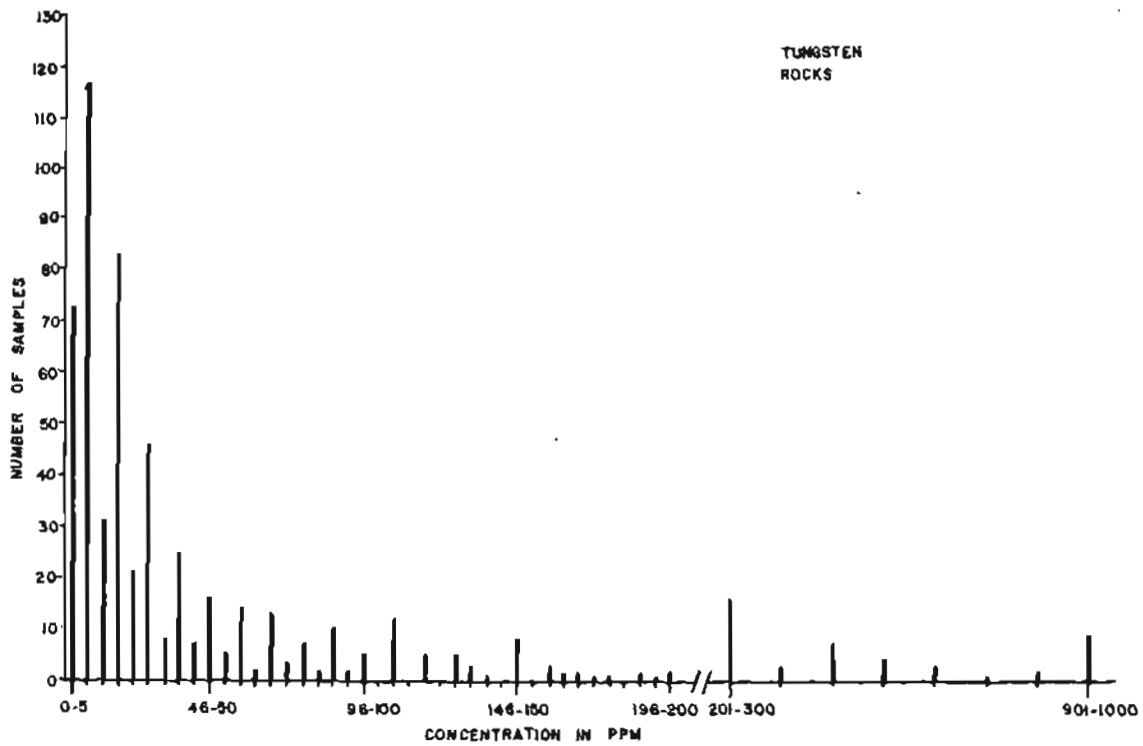


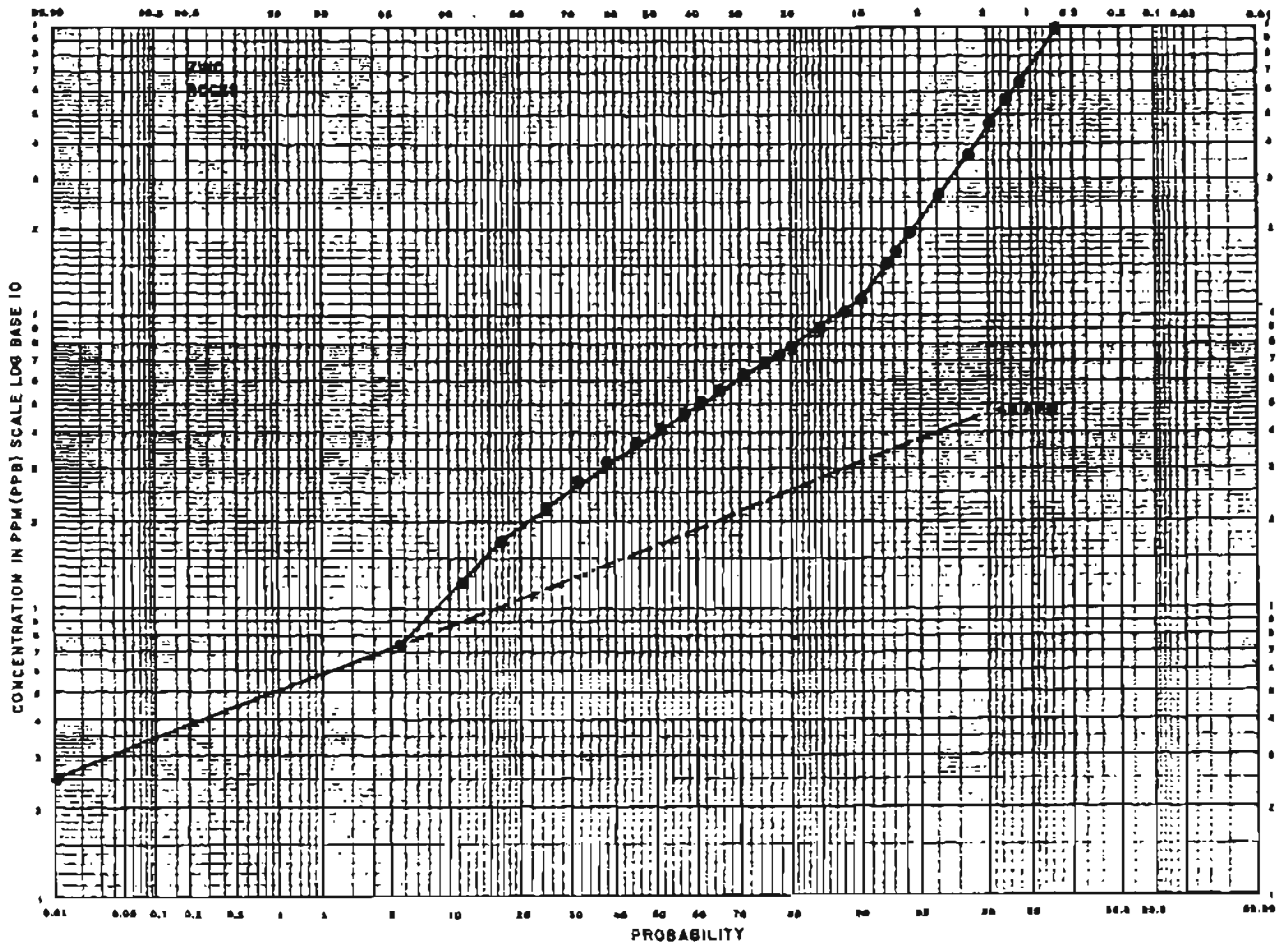
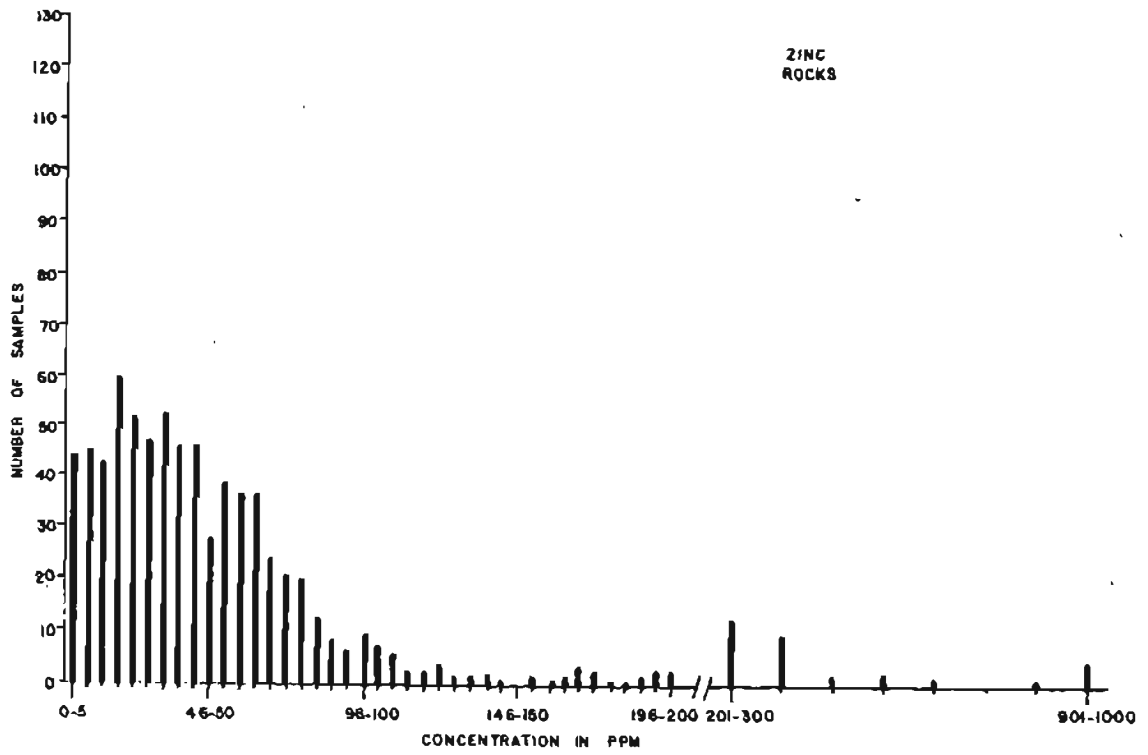




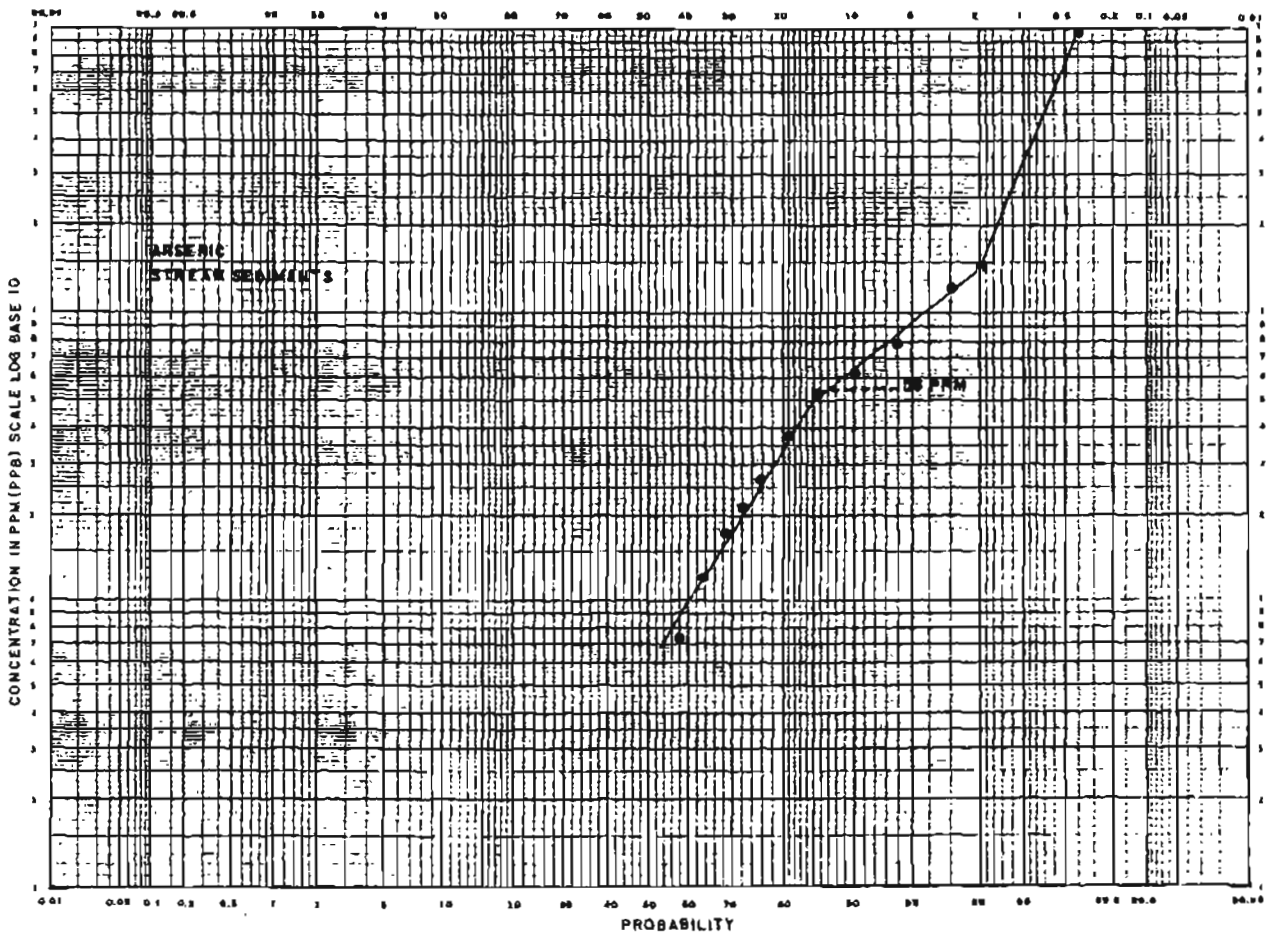
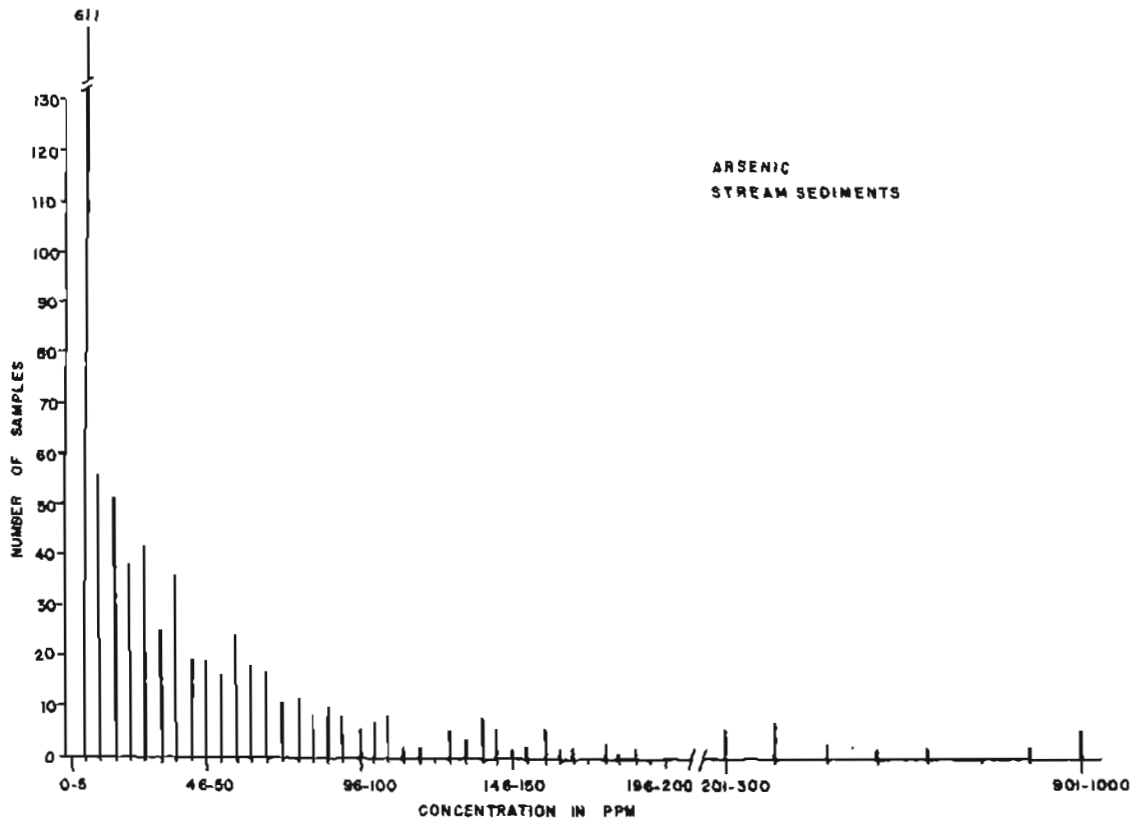


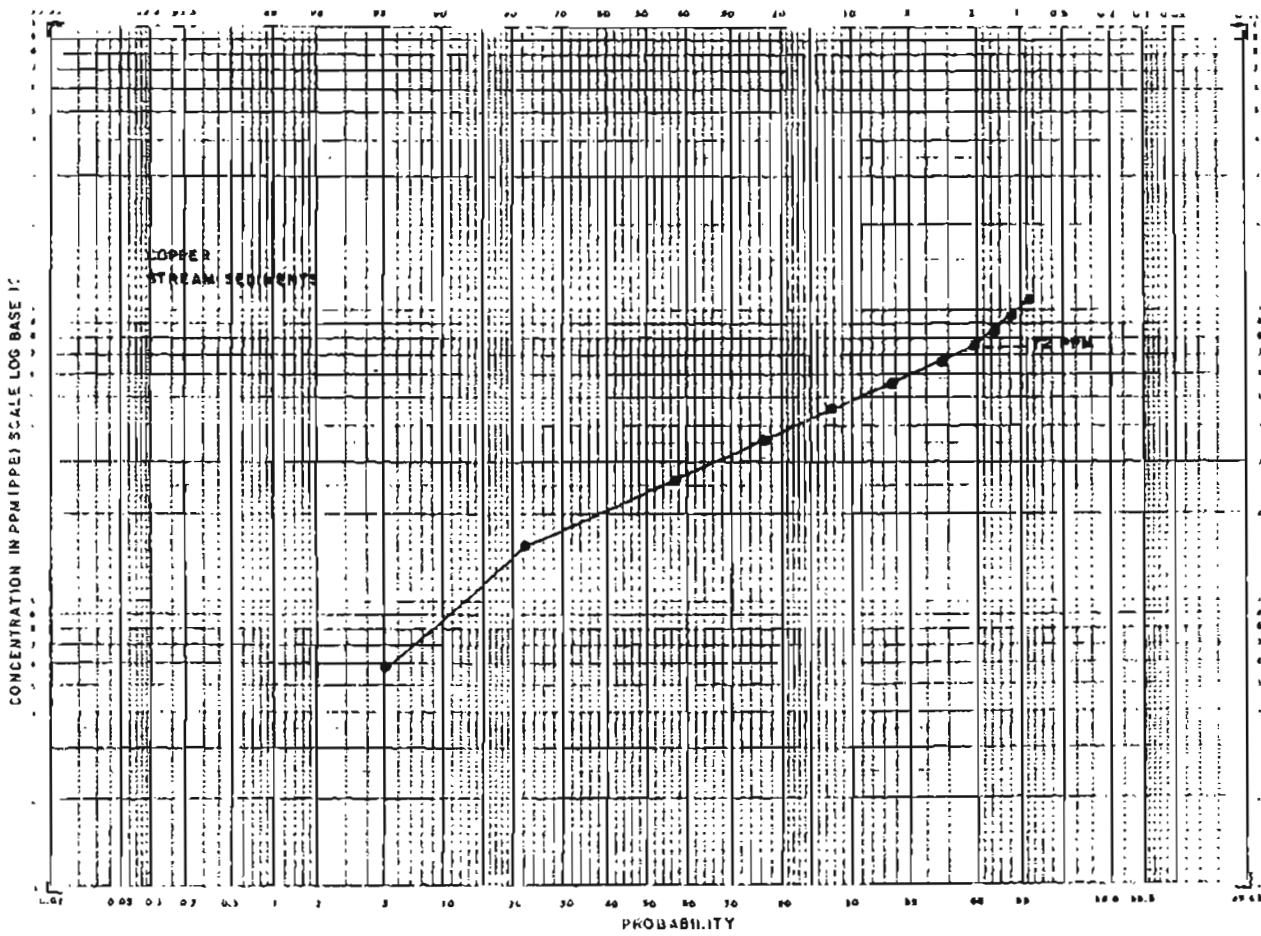
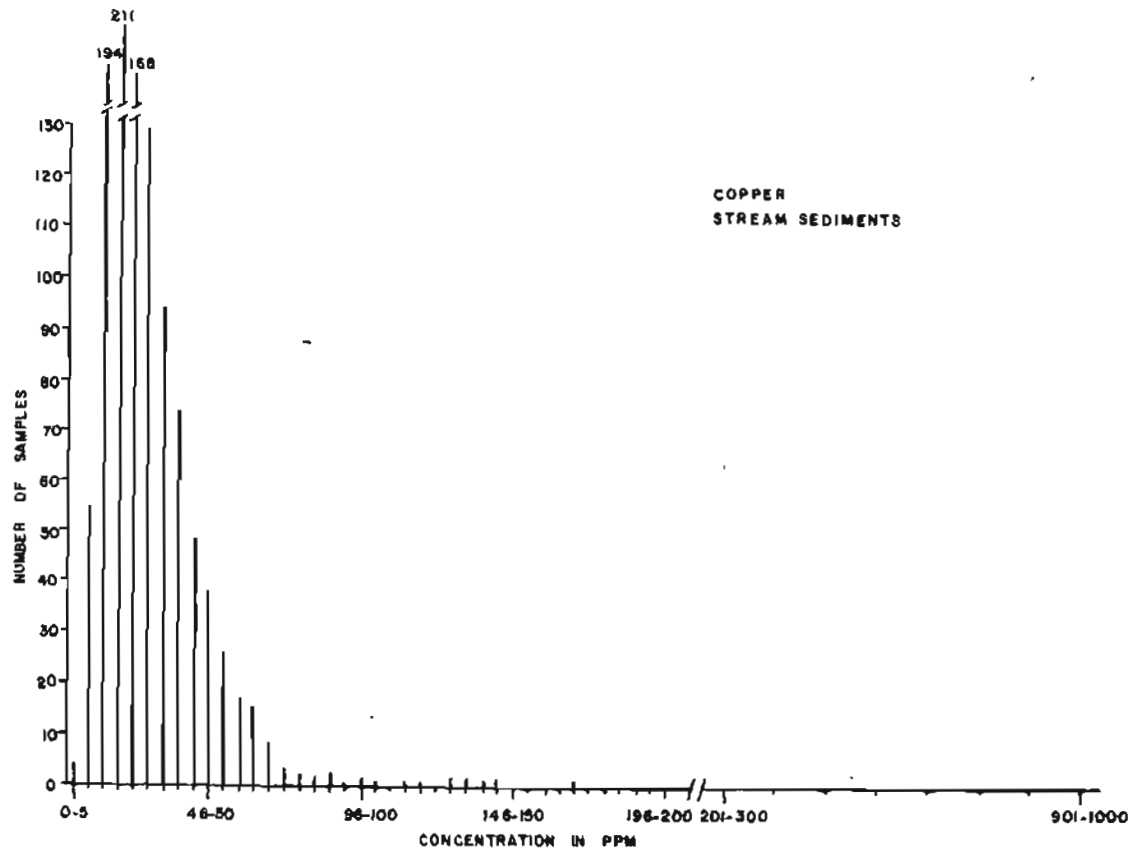


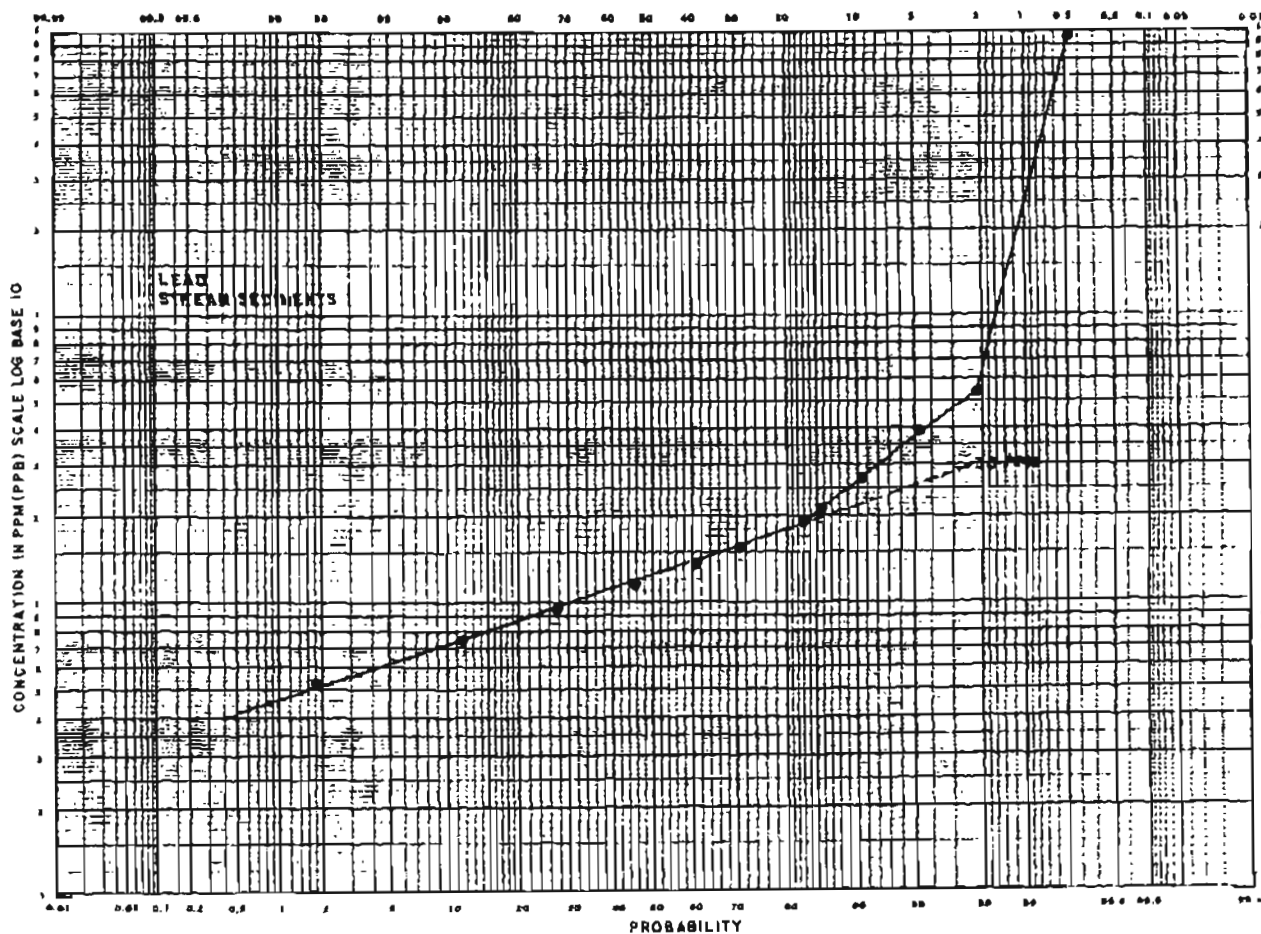
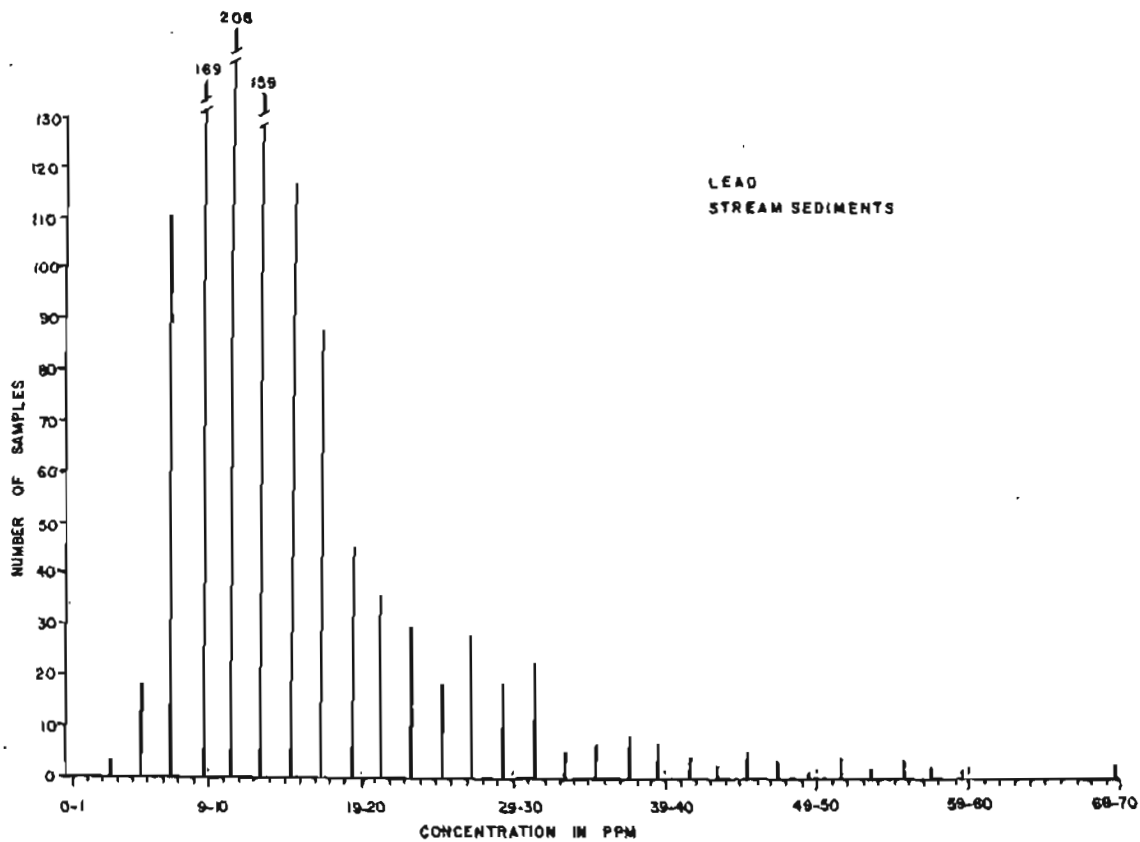




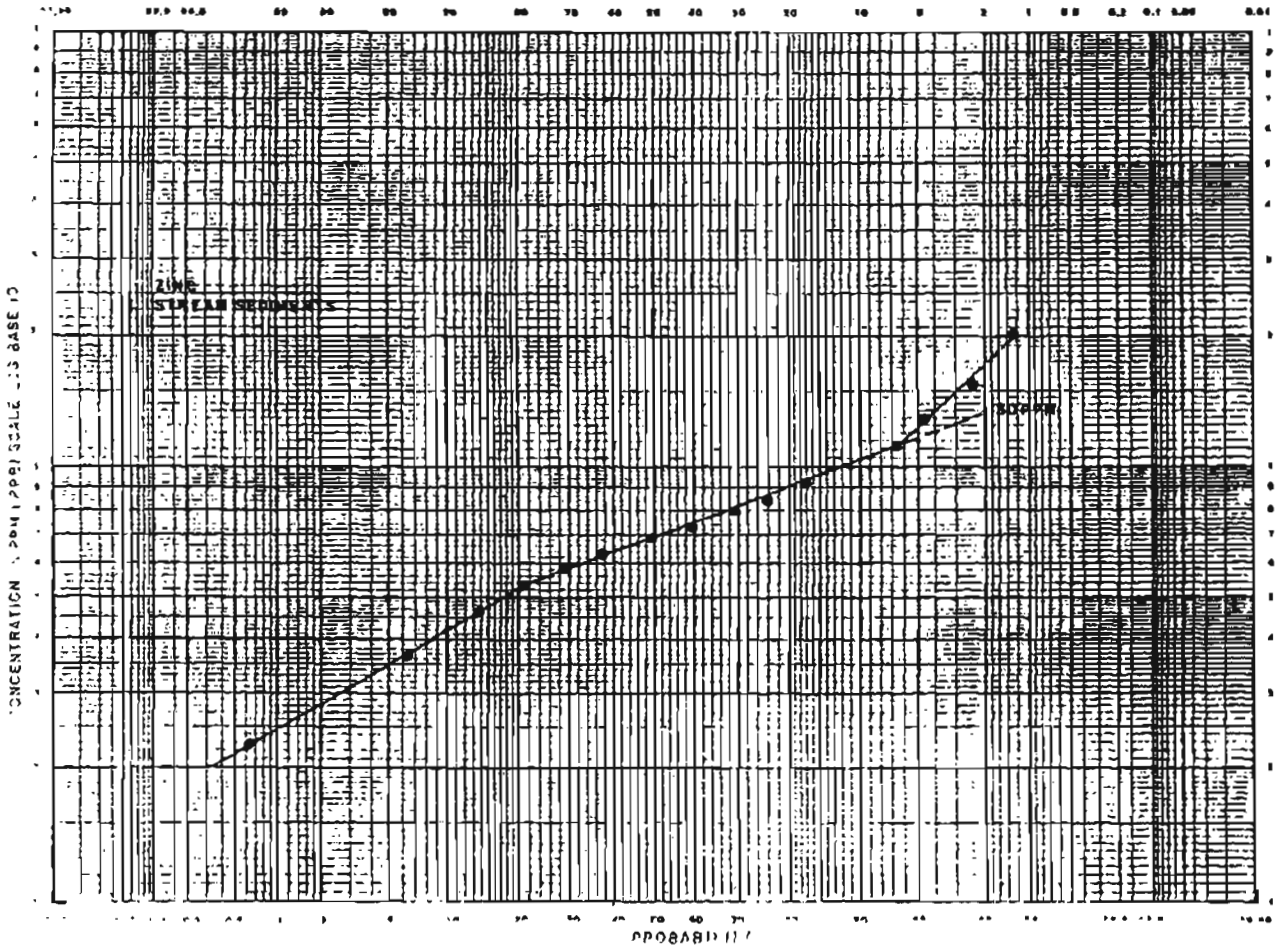
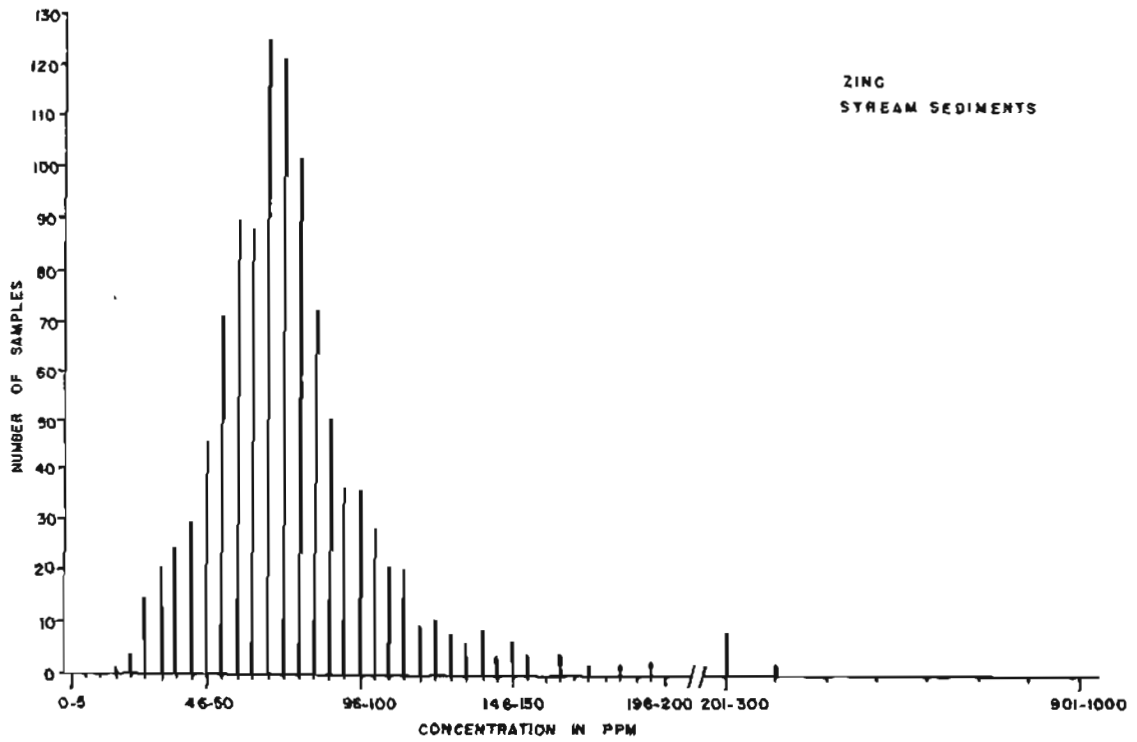
APPENDIX C2  
Histograms and Log Concentration-Probability Plots of  
Stream Sediment Data from the Circle Mining District



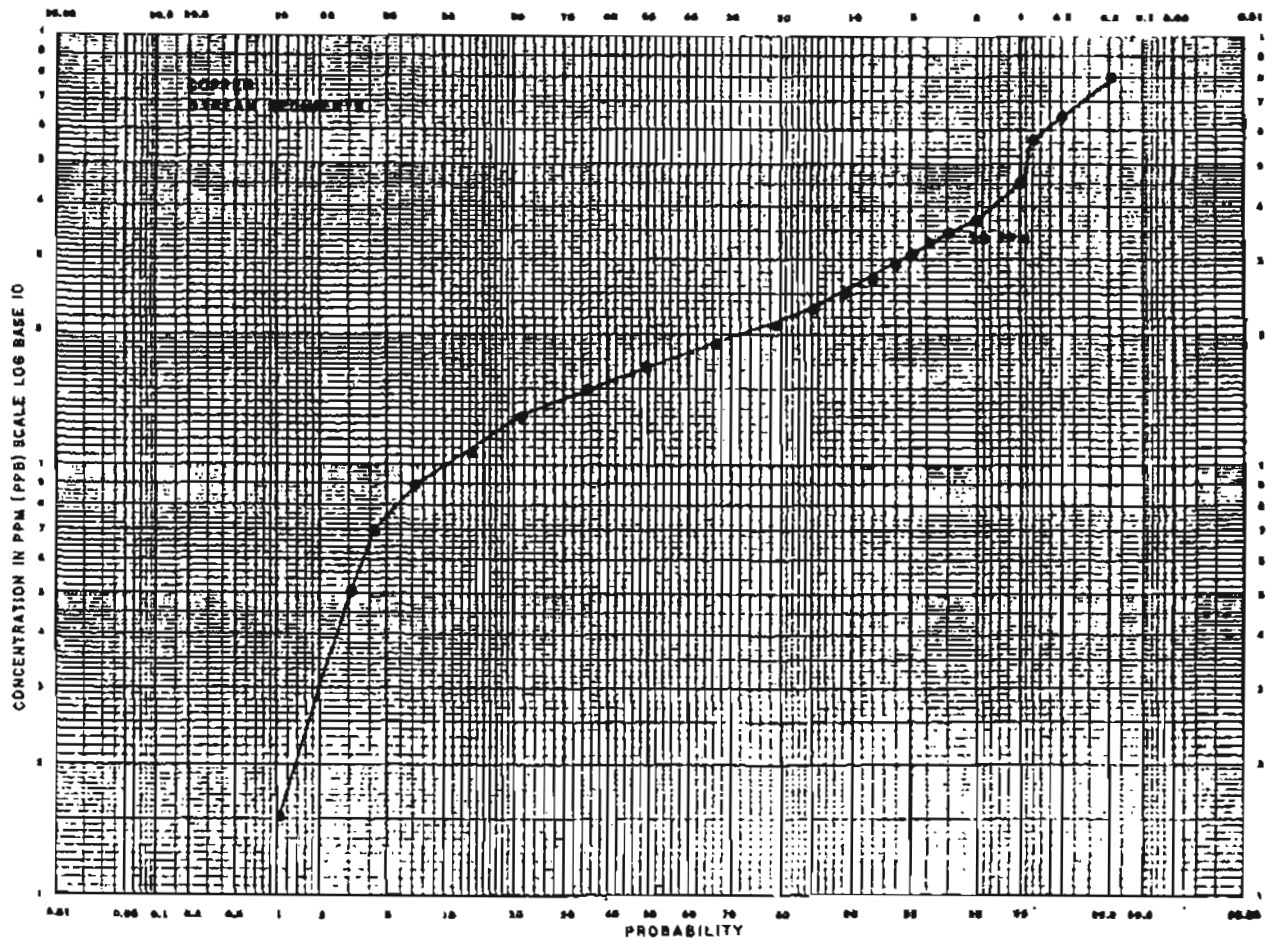
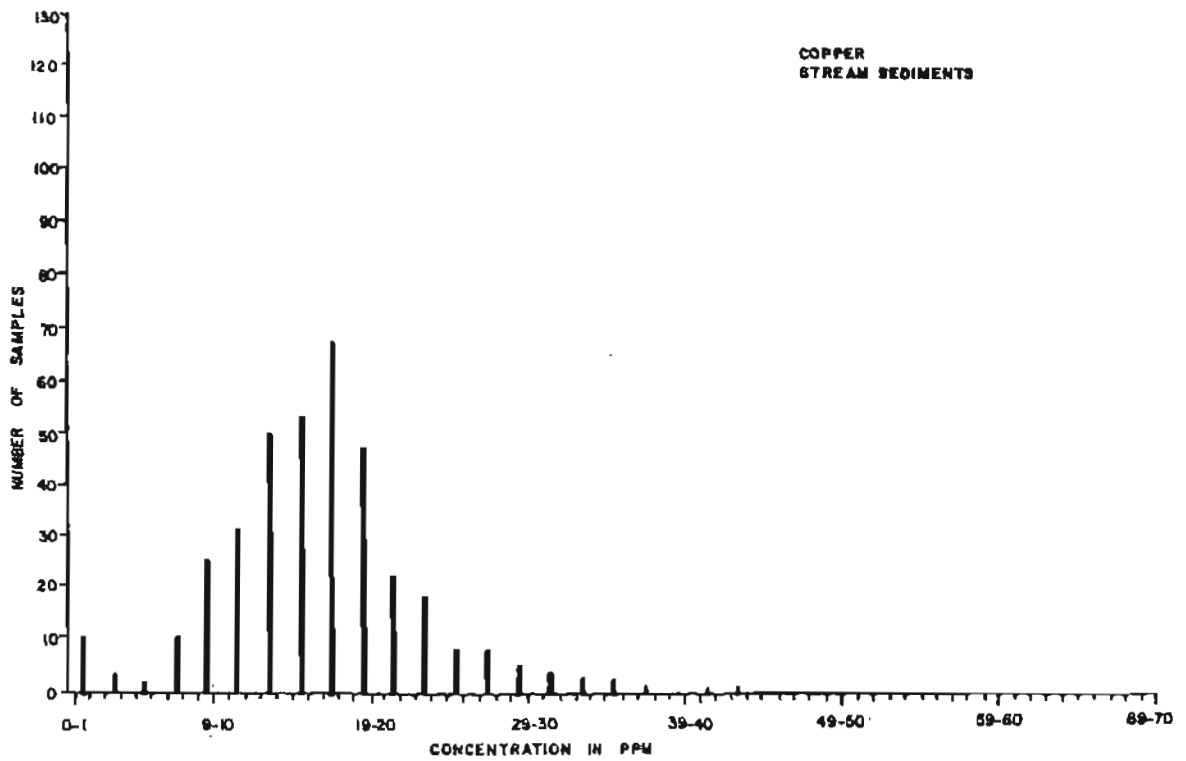


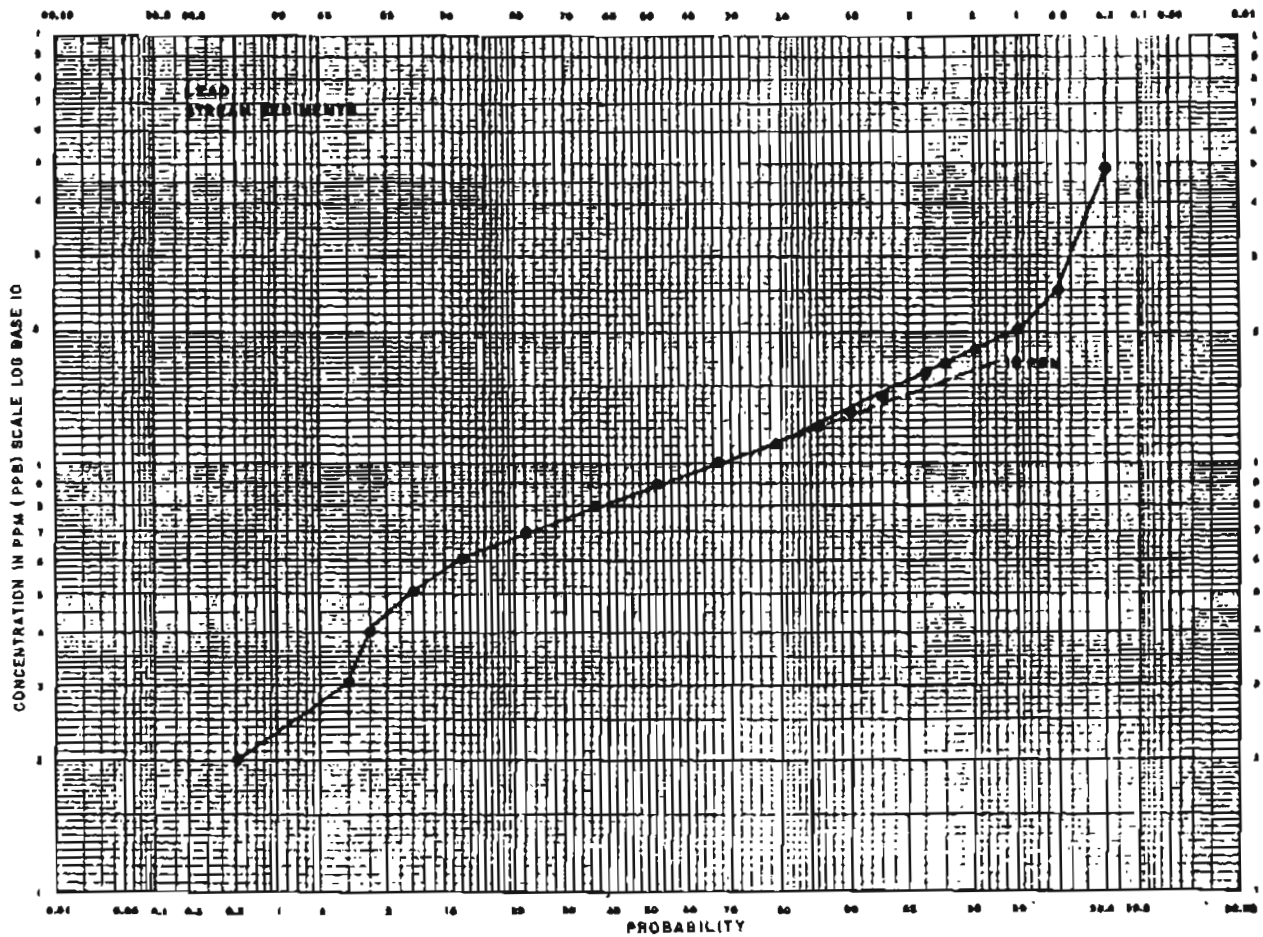
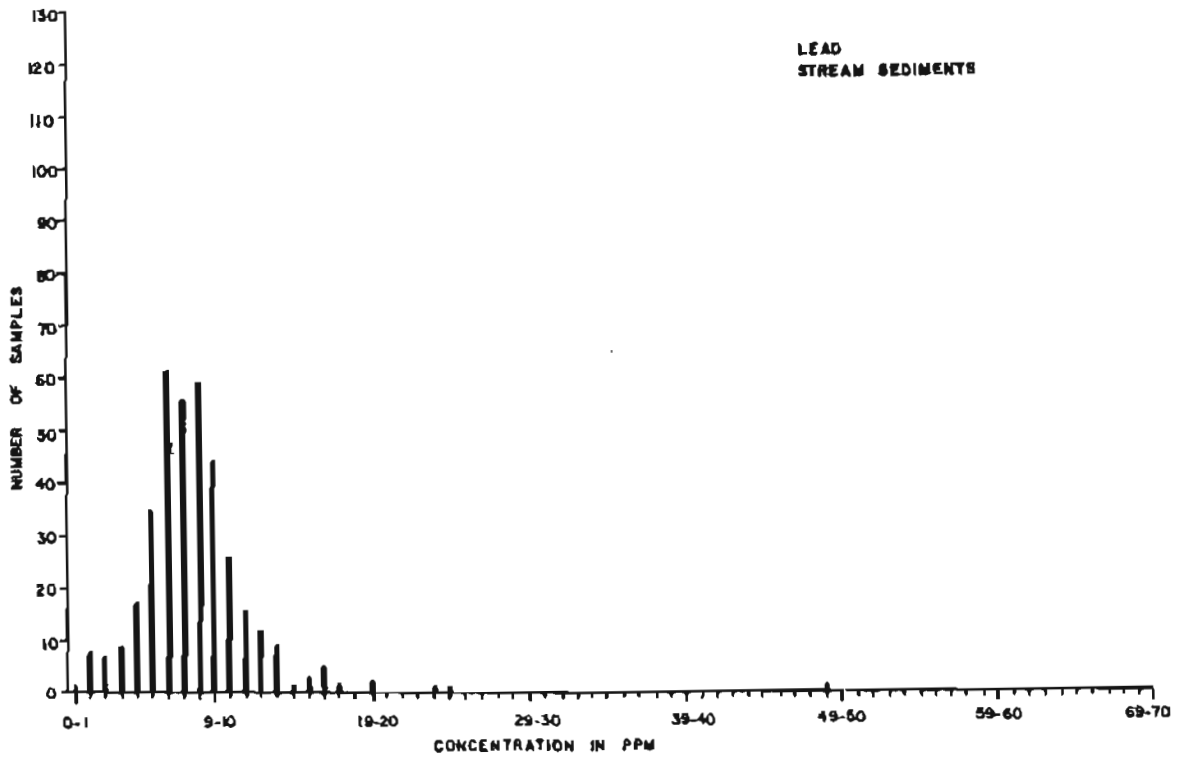




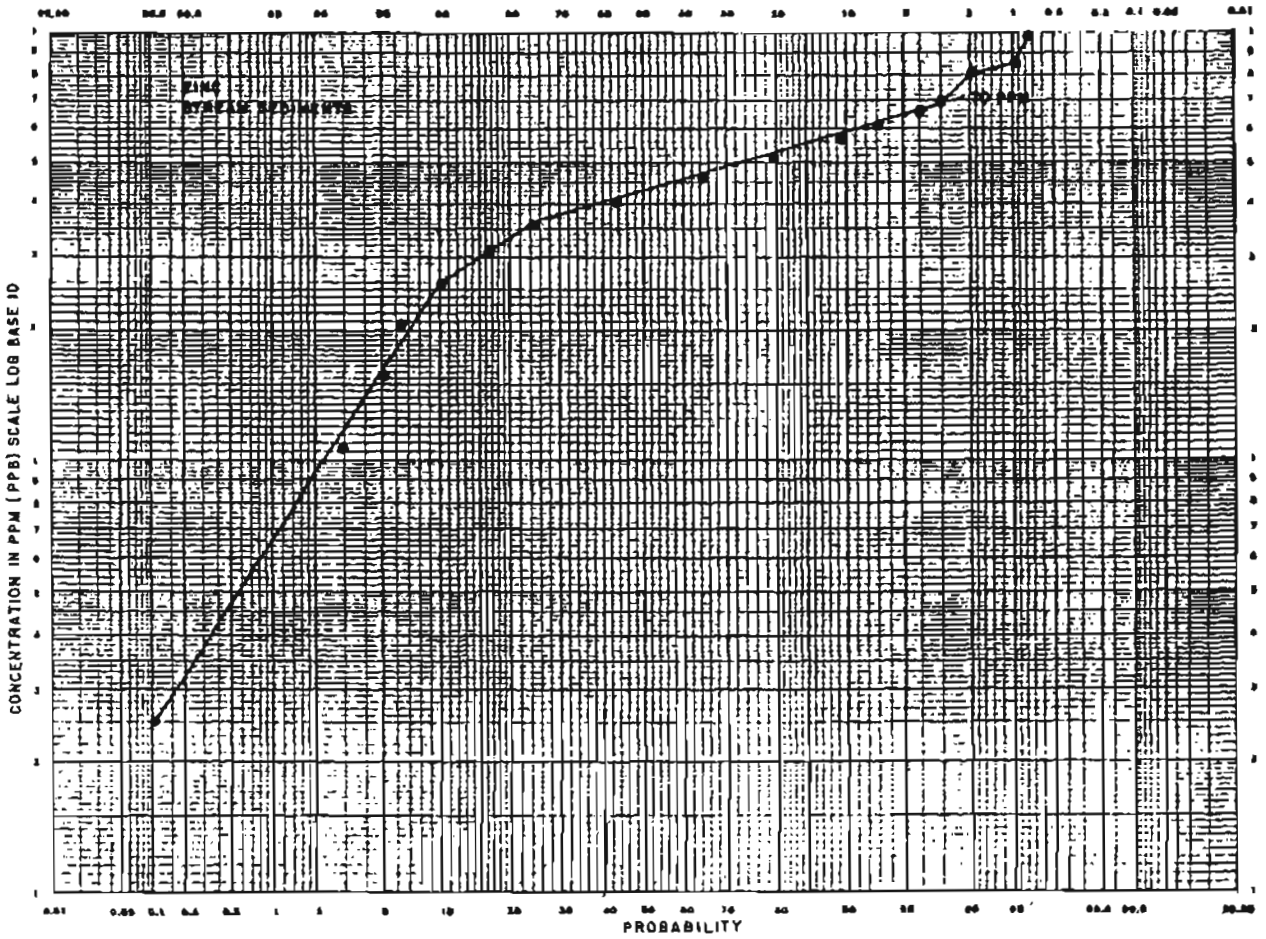
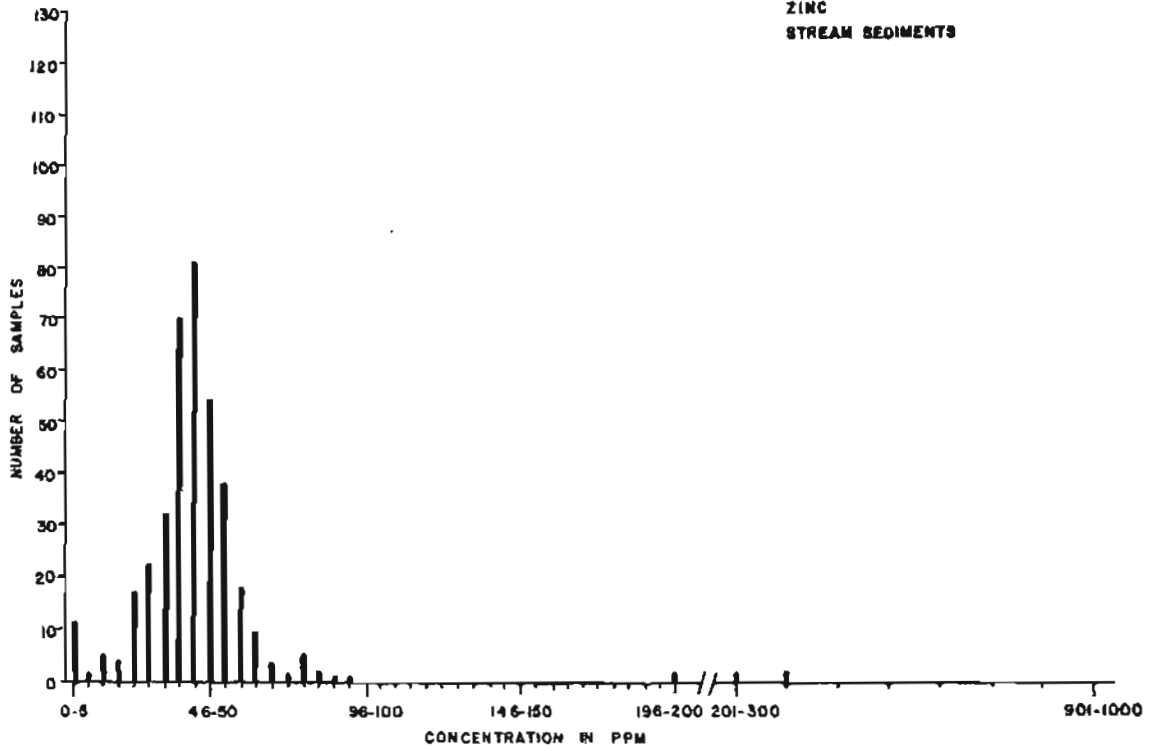


APPENDIX C3  
Histograms and Log Concentration-Probability Plots of  
Stream Sediment and Pan Concentrate Data  
from the Richardson Mining District

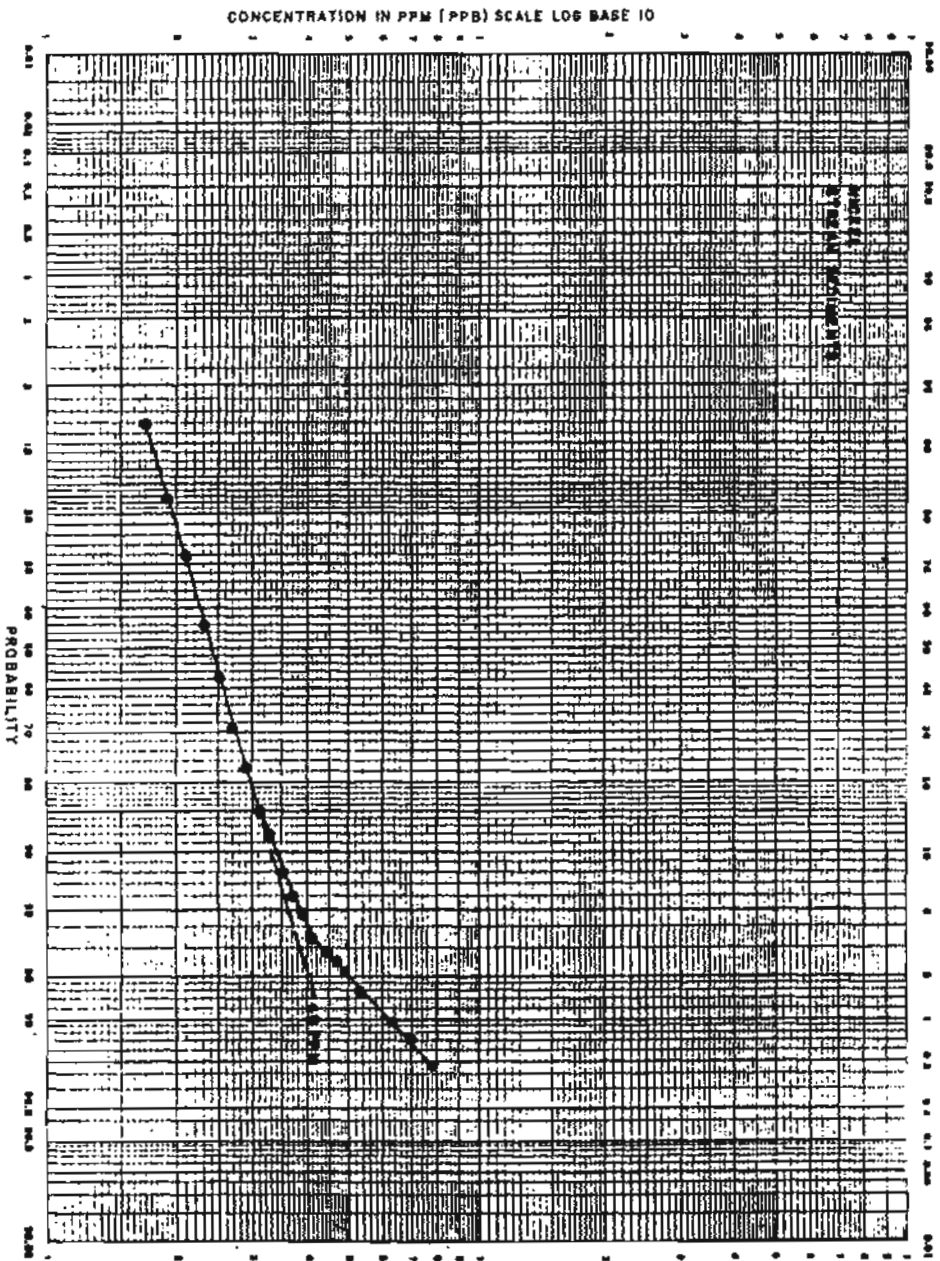
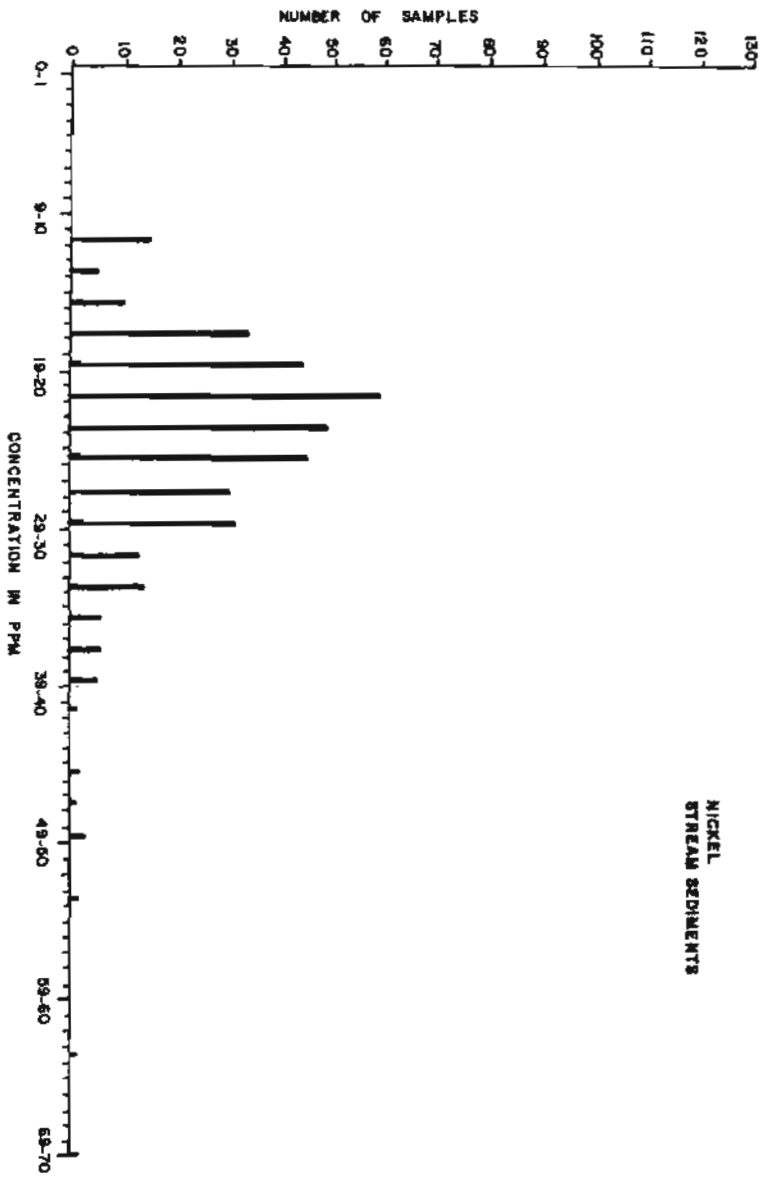




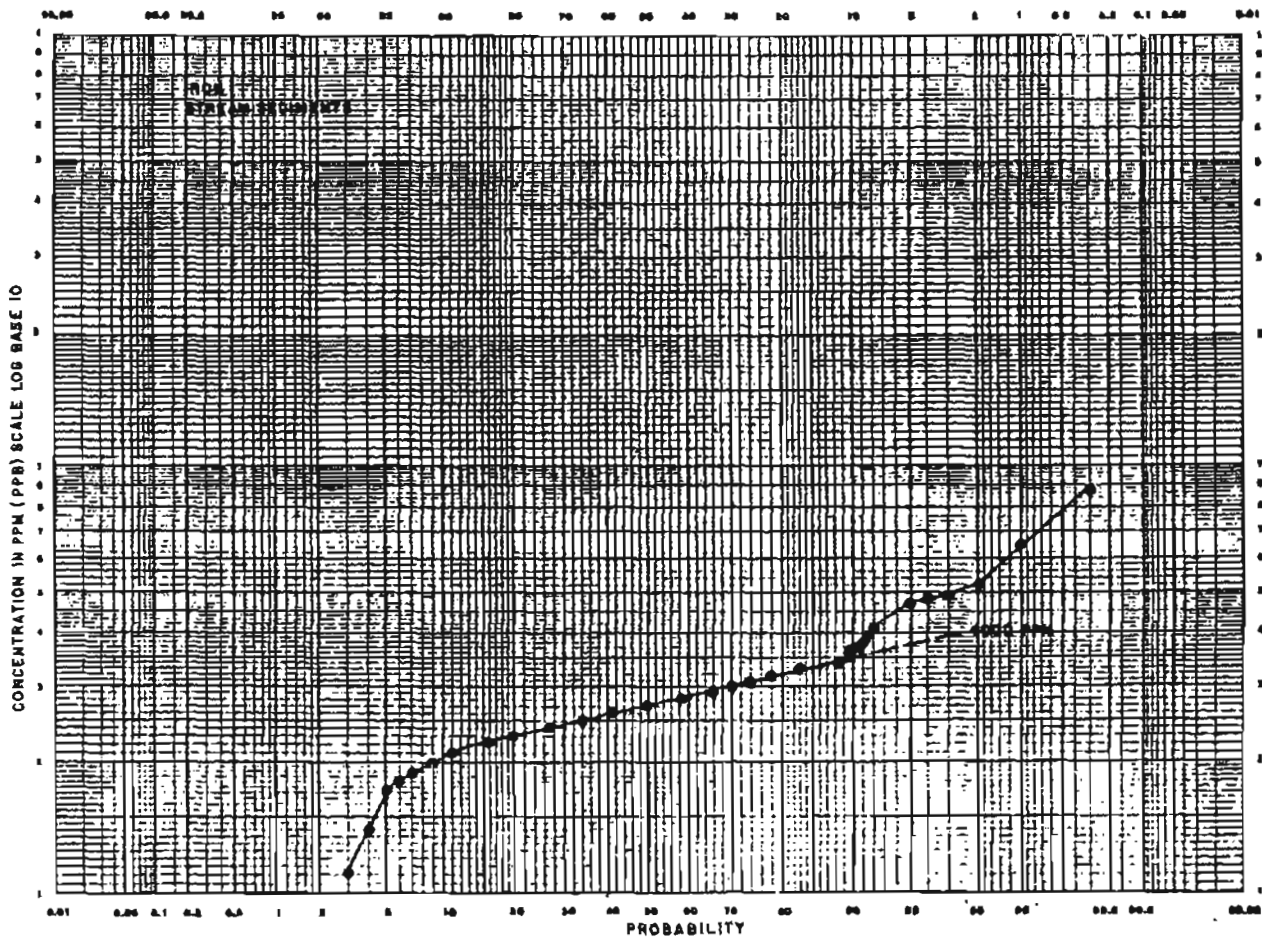
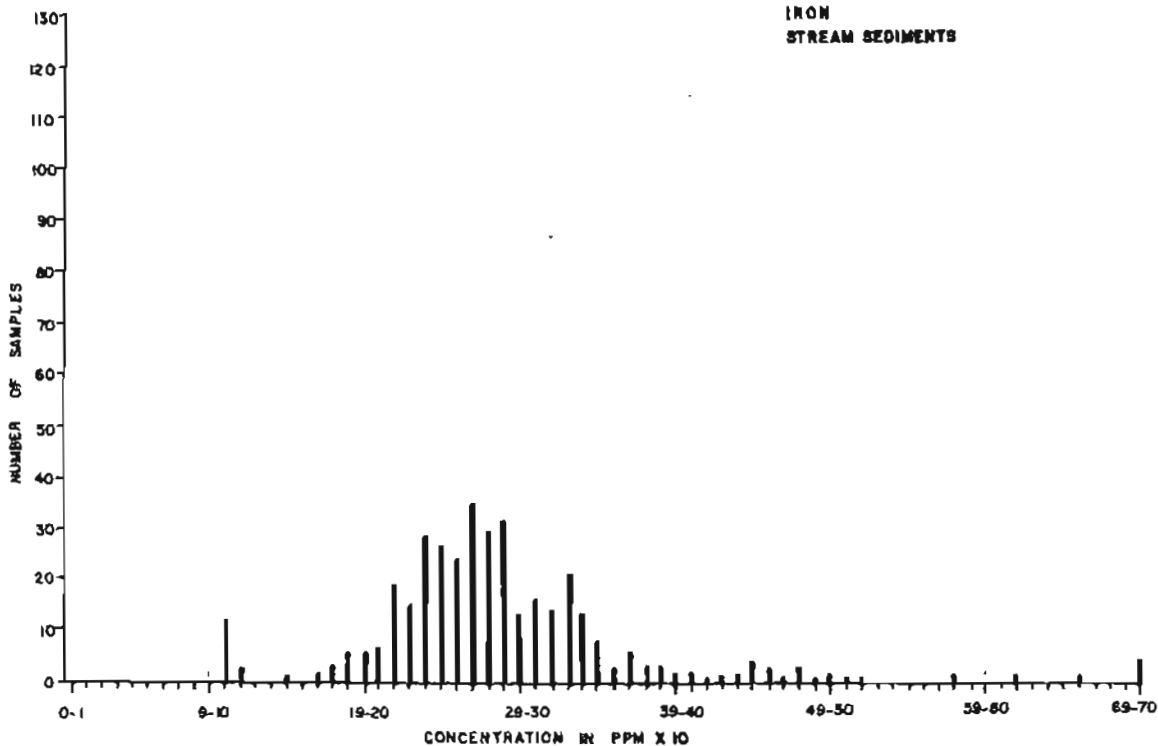
ZINC  
STREAM SEDIMENTS



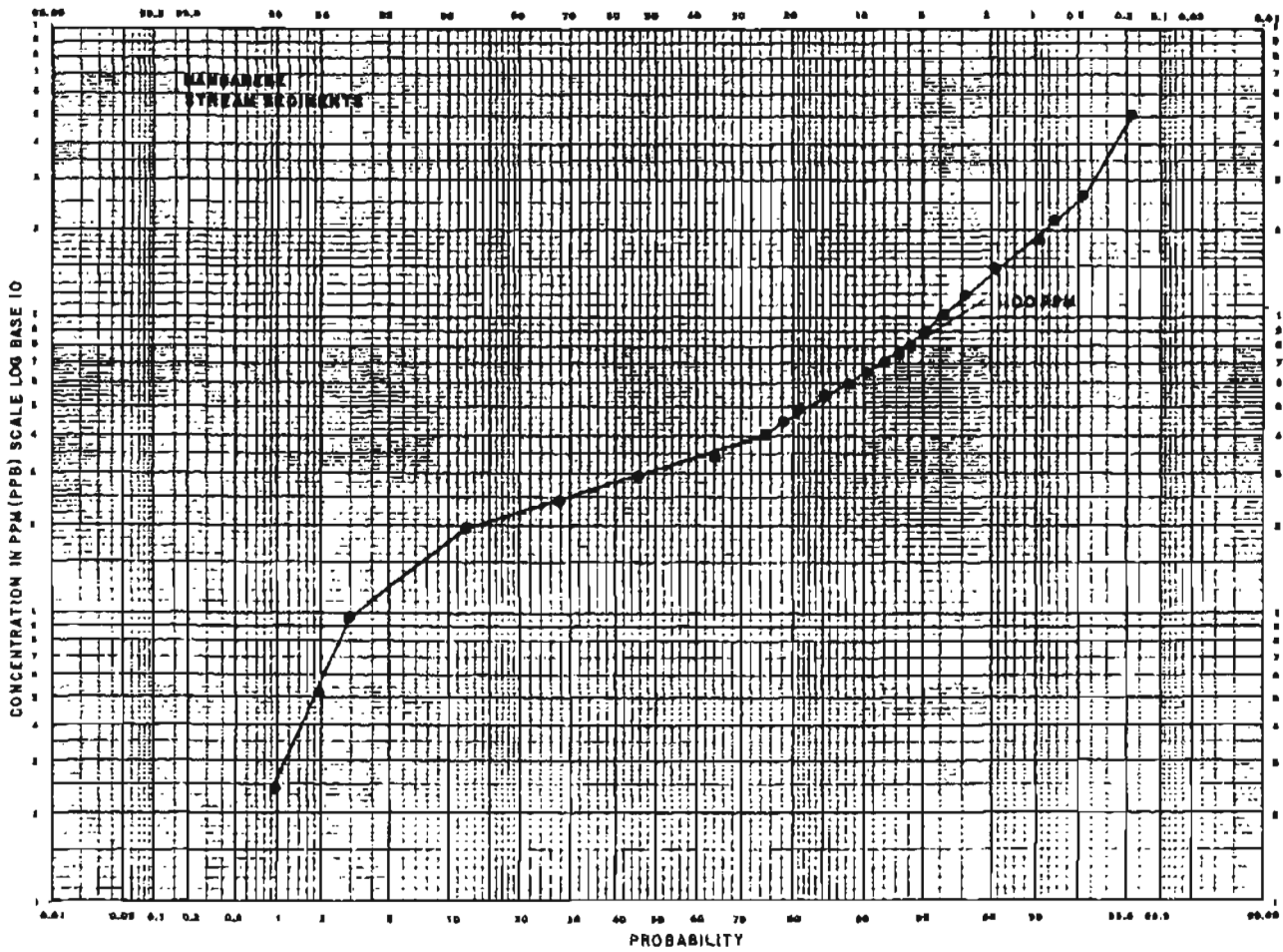
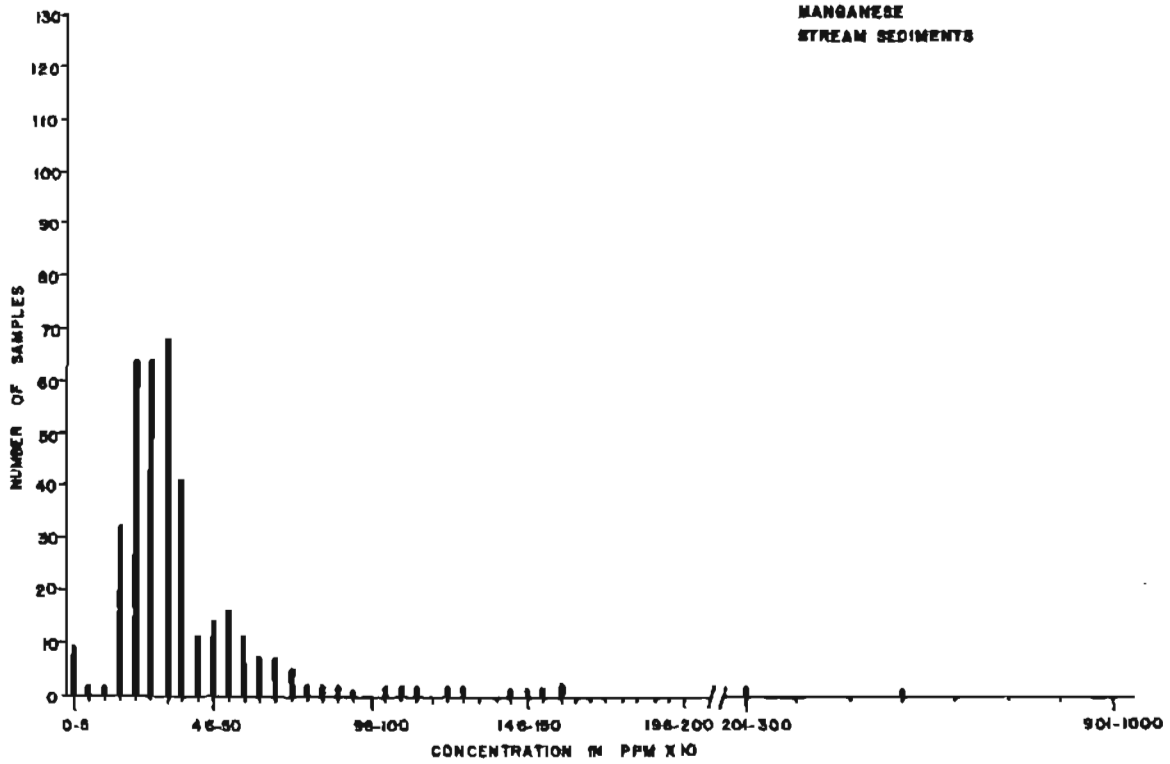
NICKEL  
STREAM SEDIMENTS

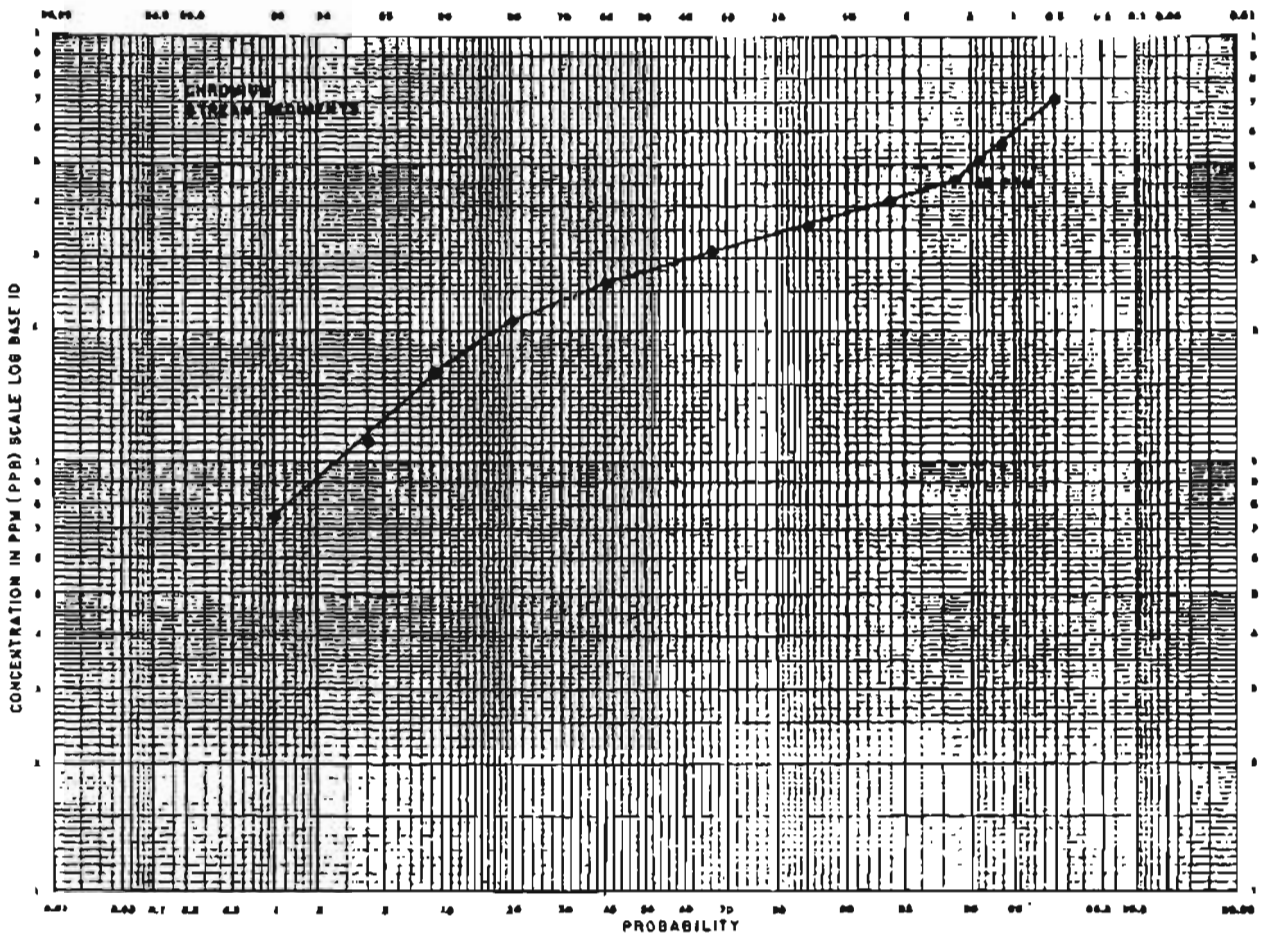
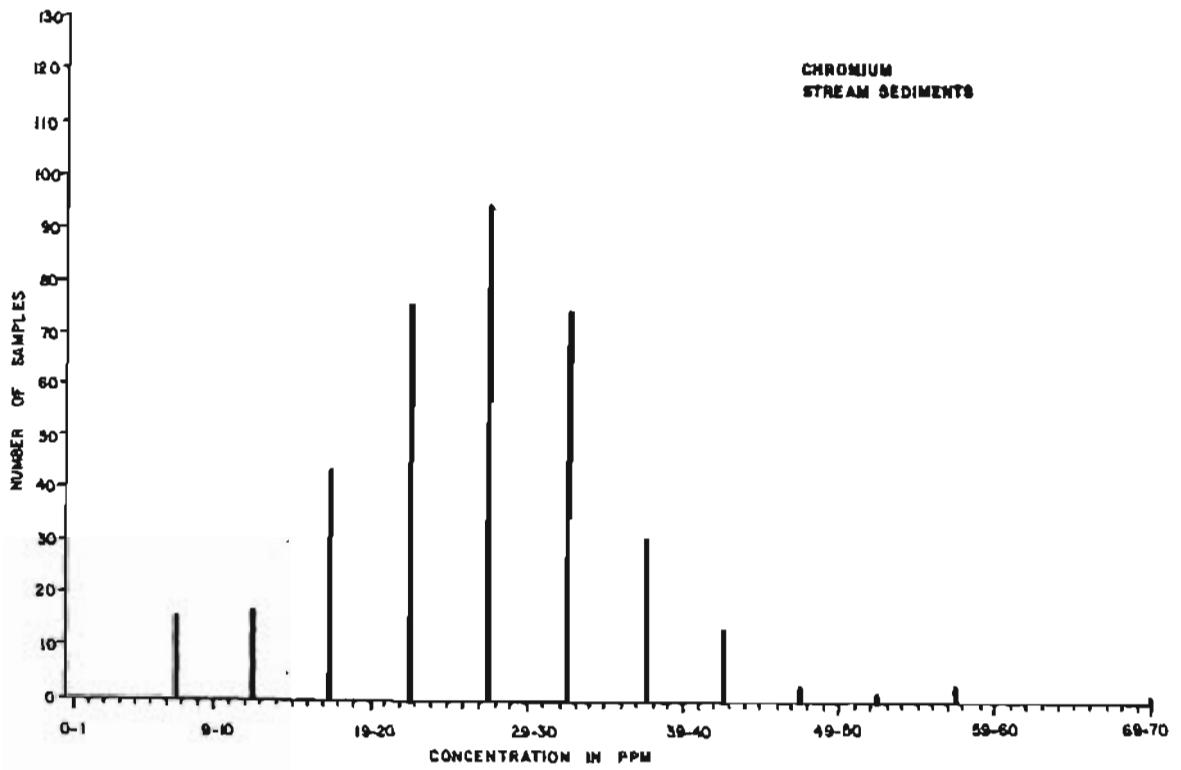


IRON  
STREAM SEDIMENTS

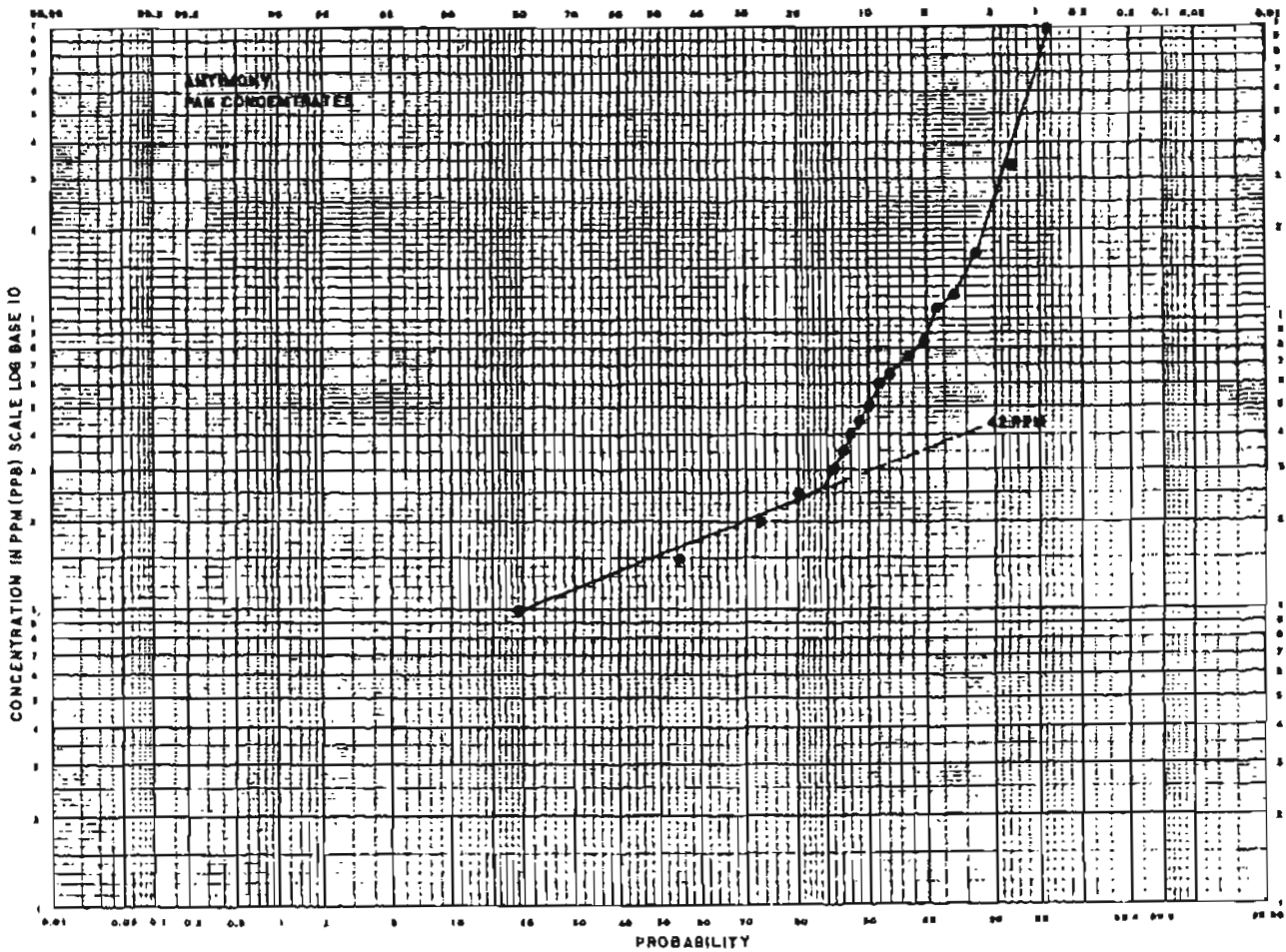
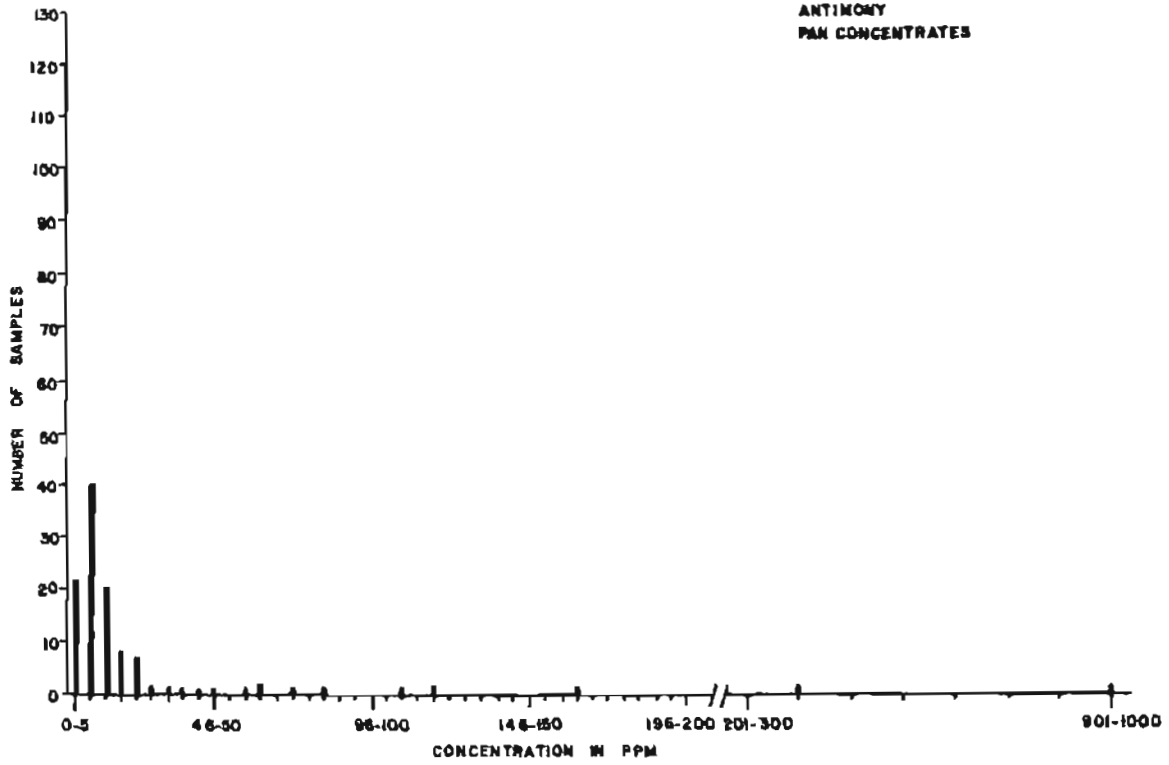


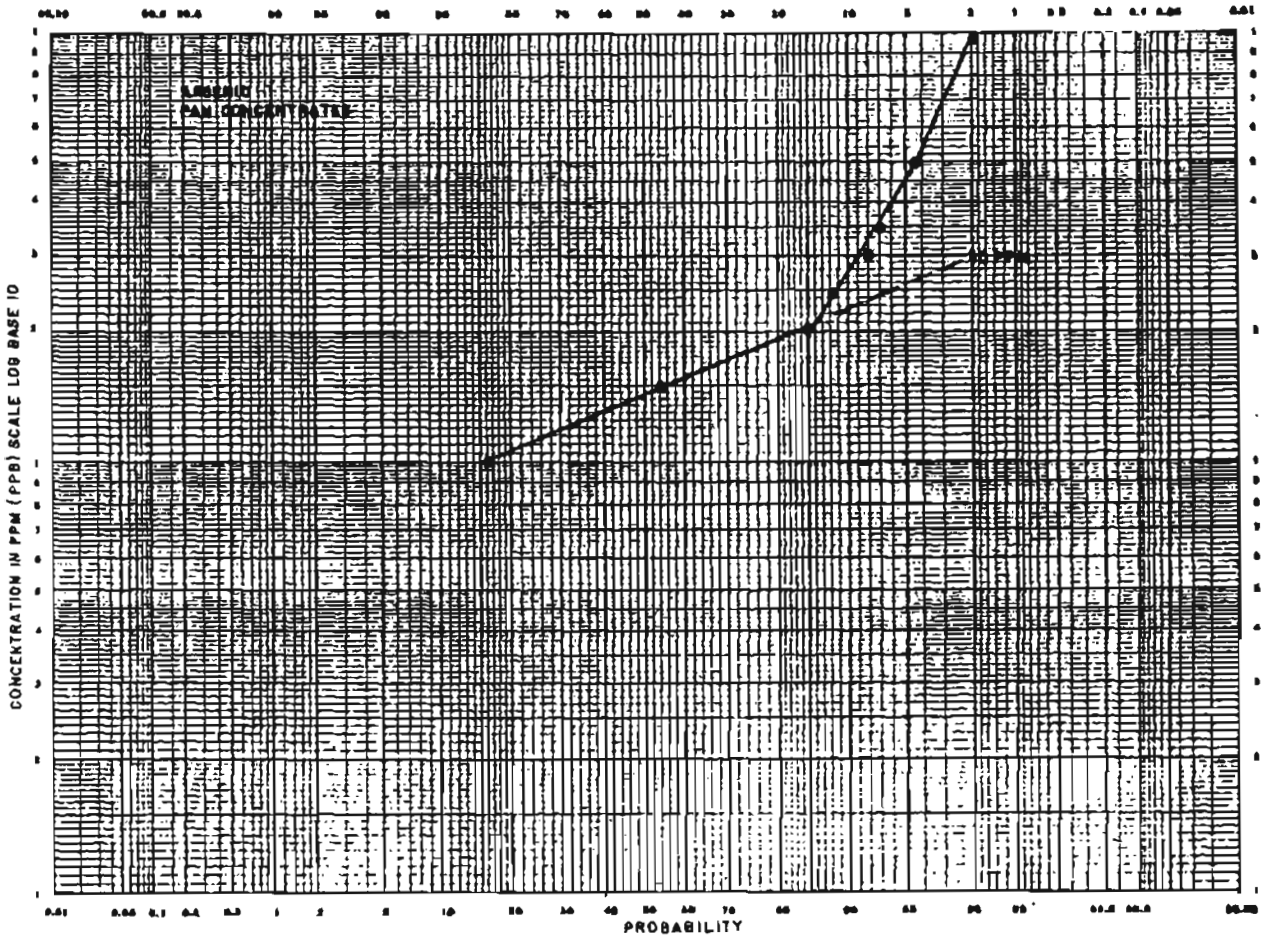
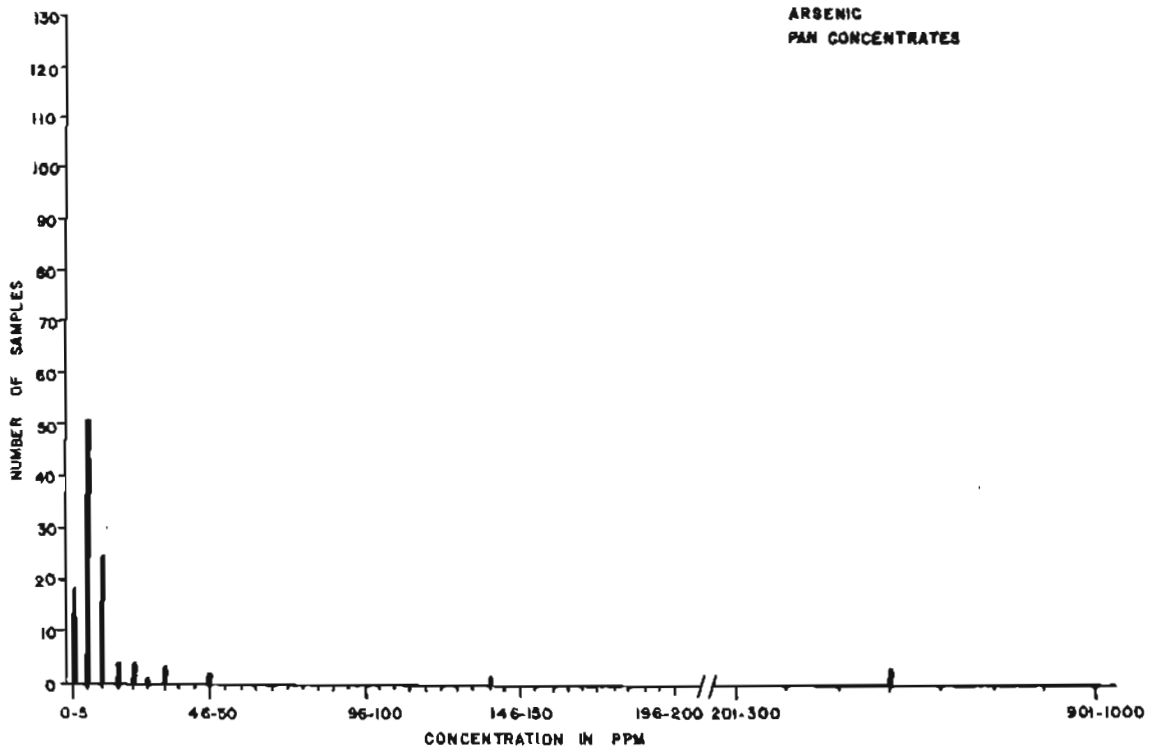
**MANGANESE  
STREAM SEDIMENTS**

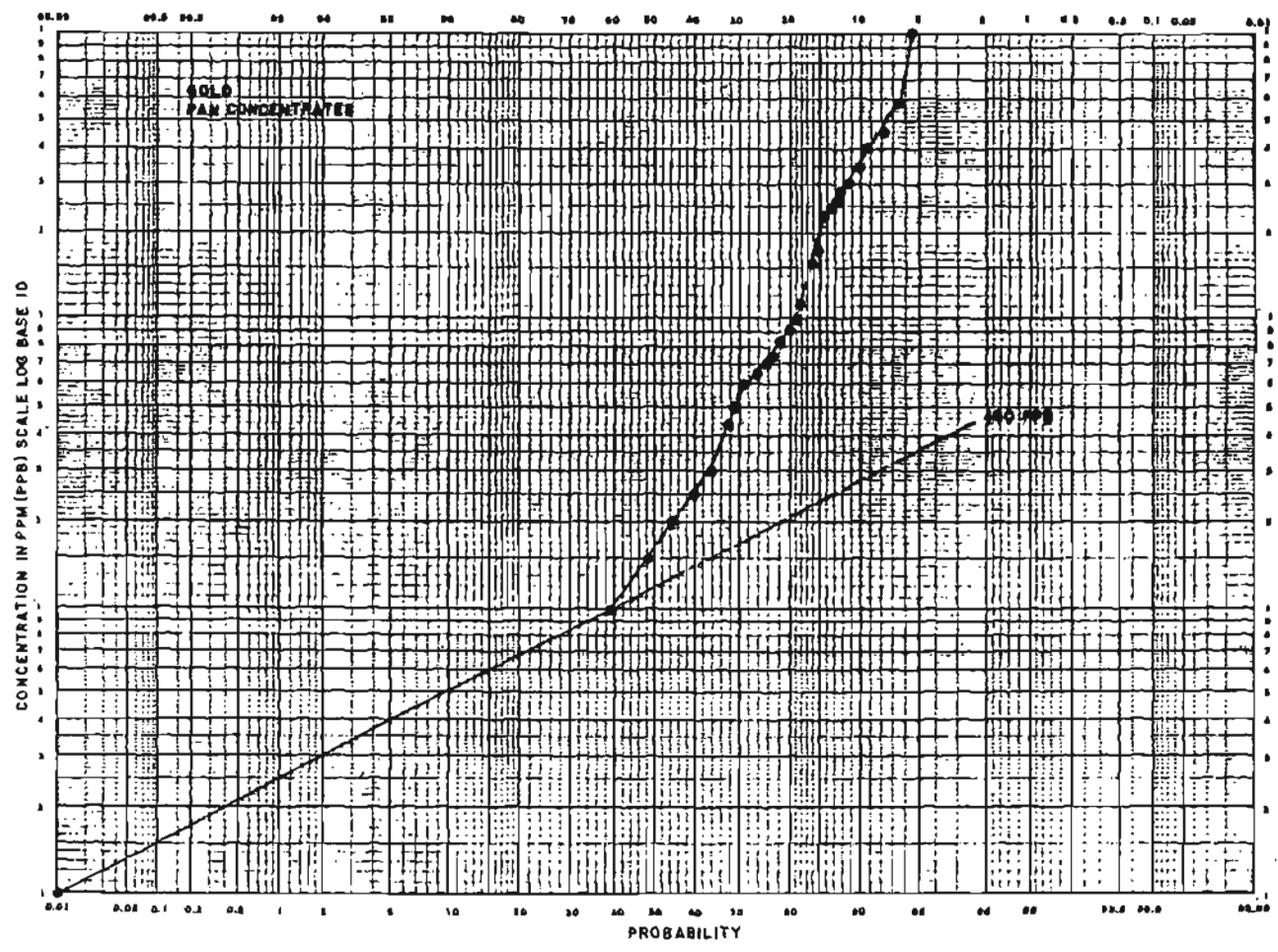
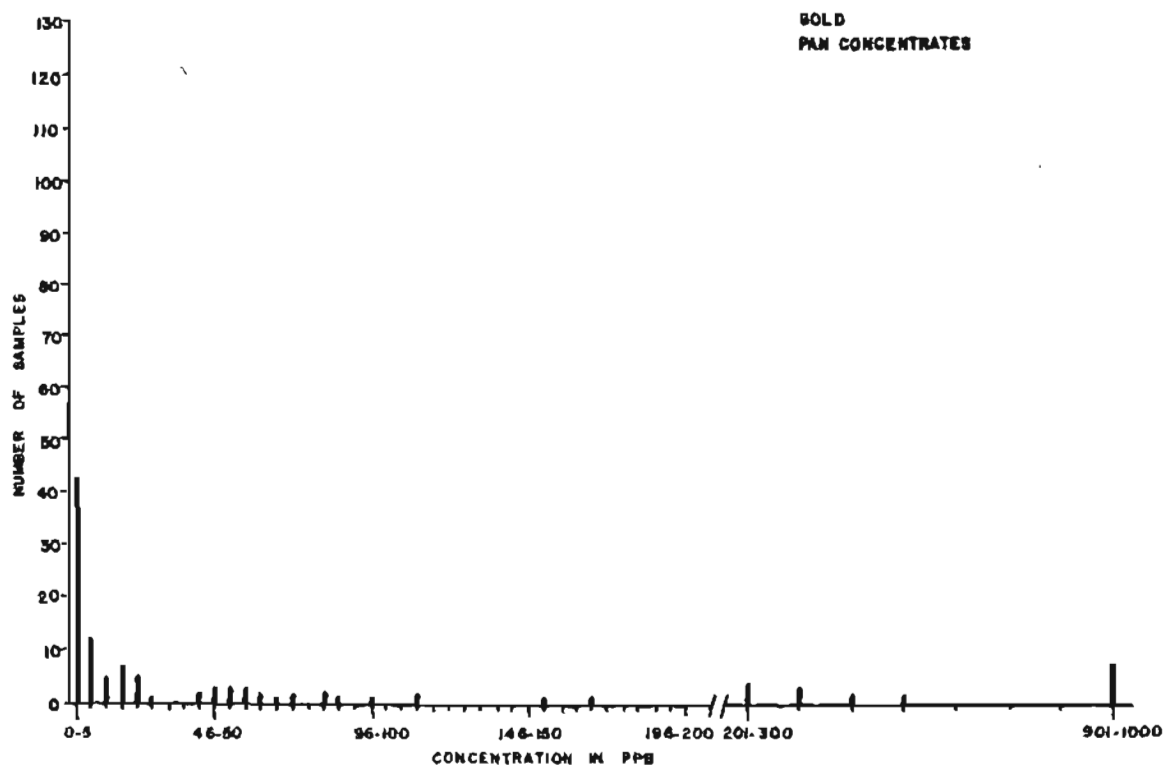


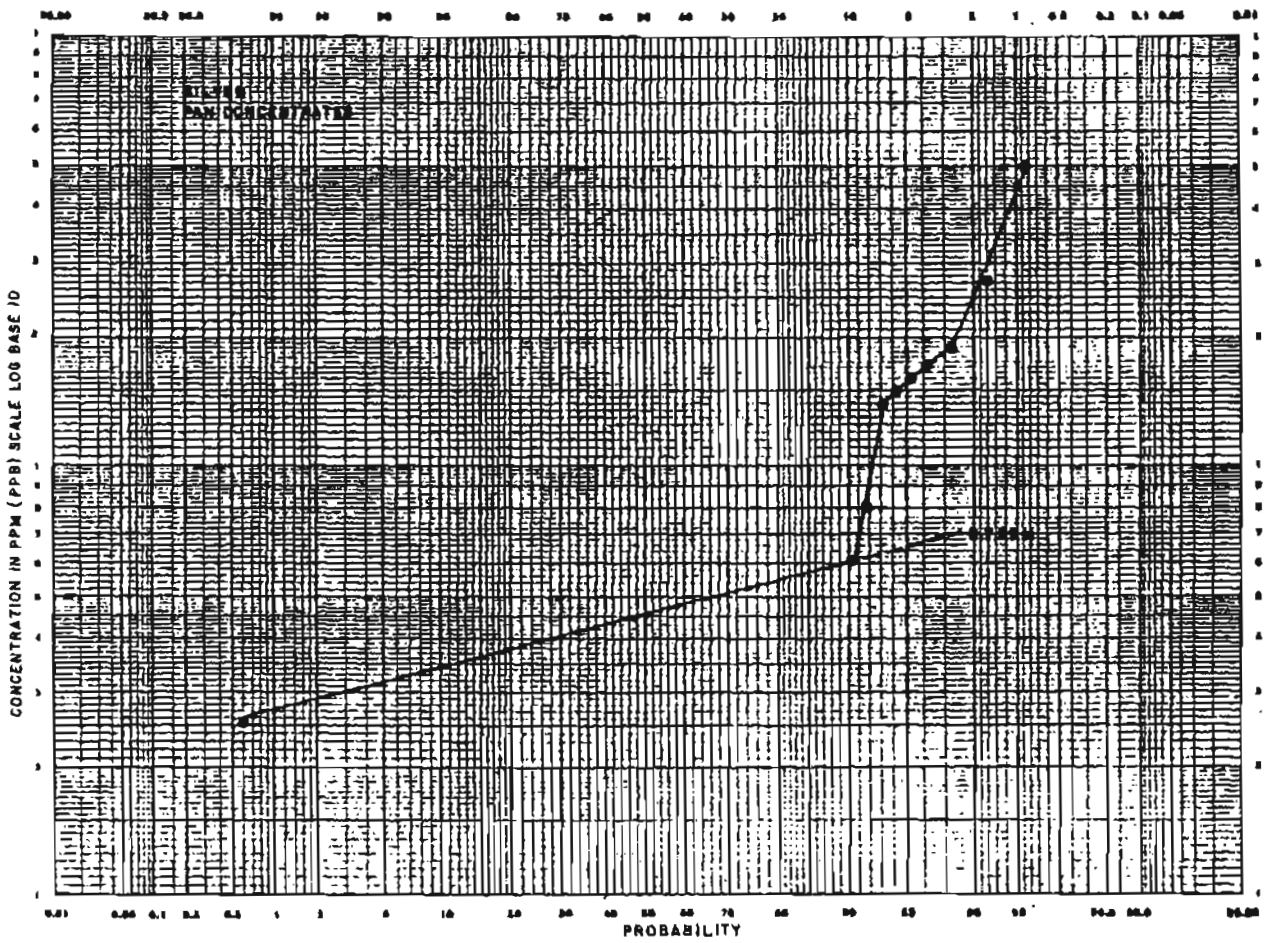
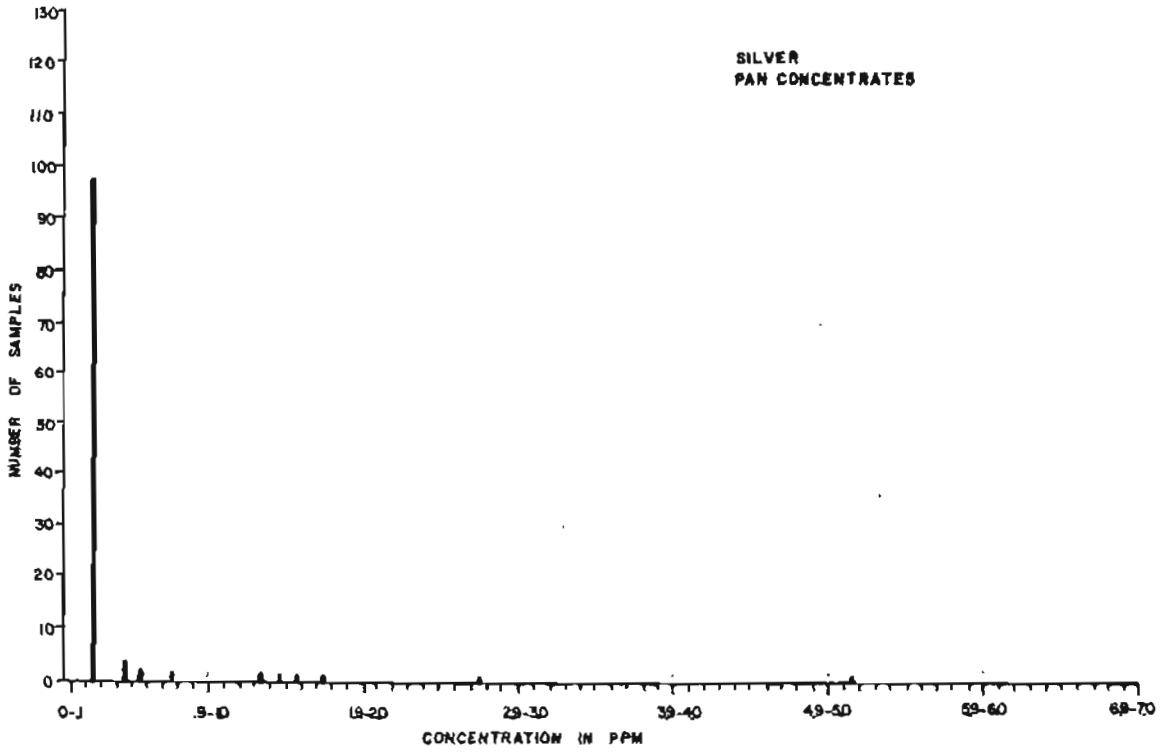


ANTIMONY  
PAN CONCENTRATES

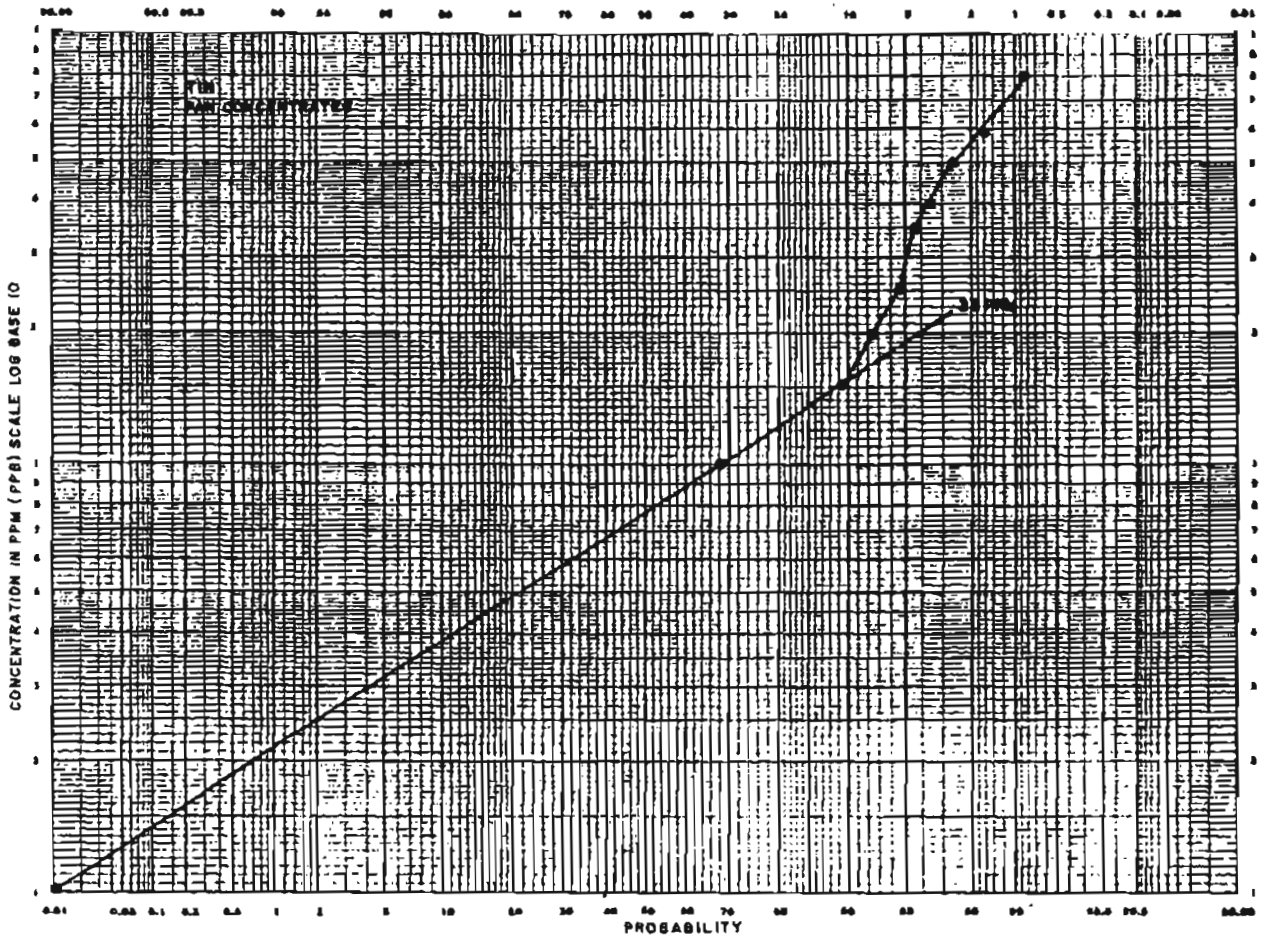
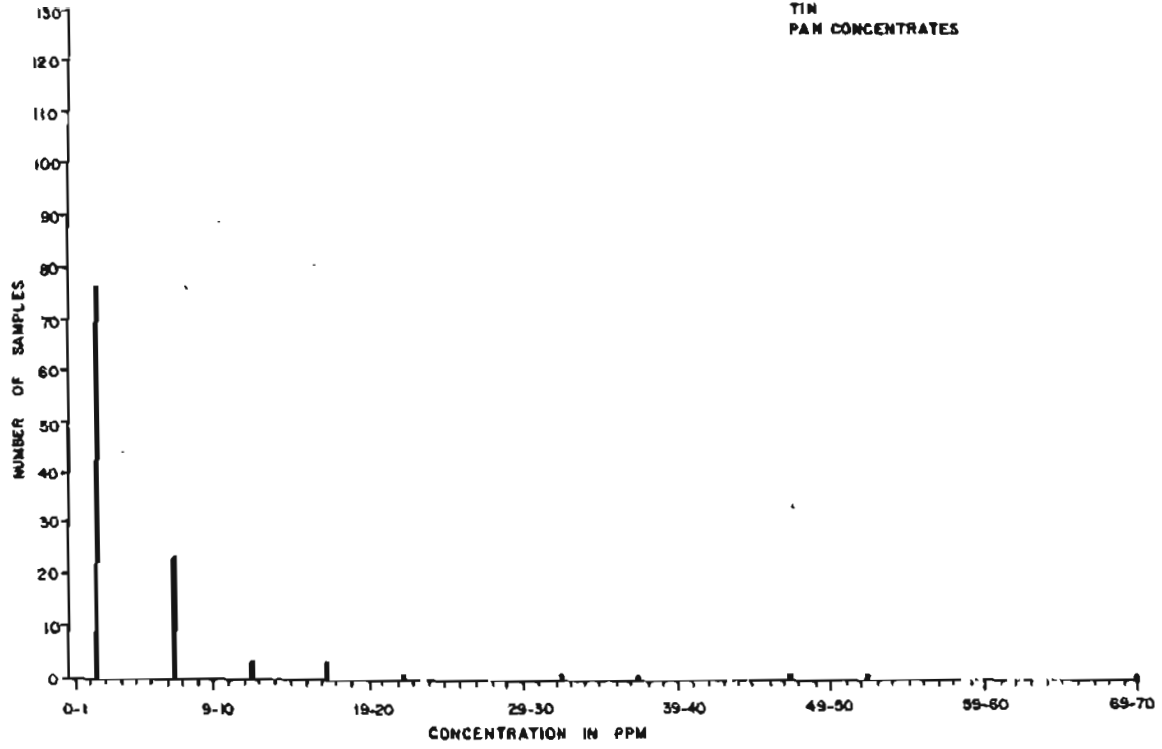




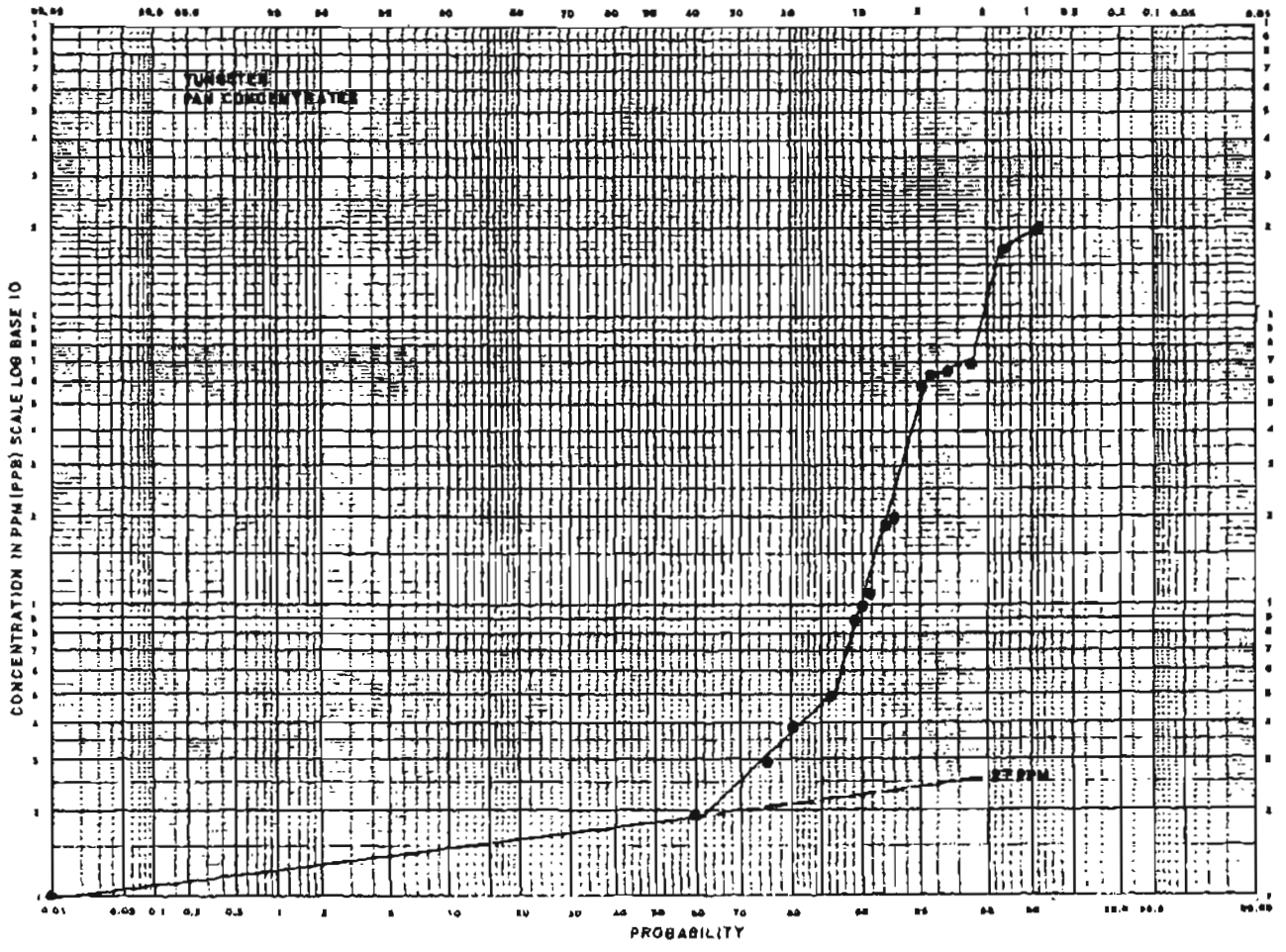
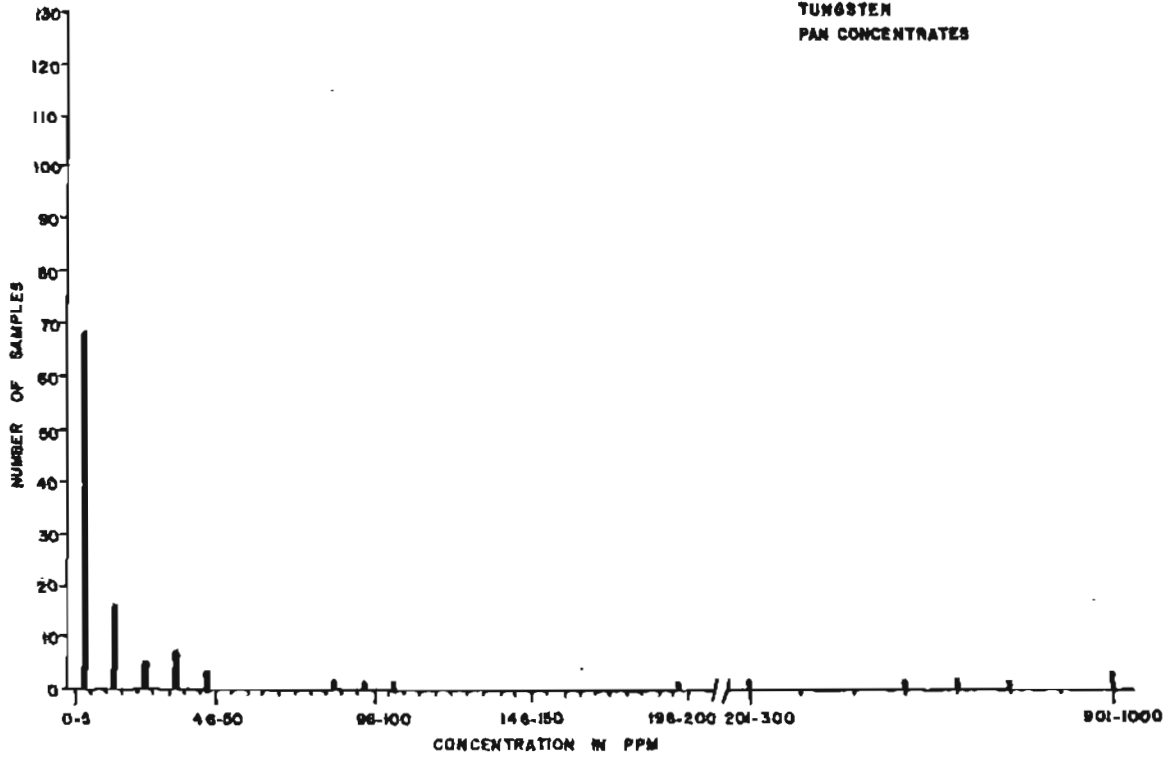




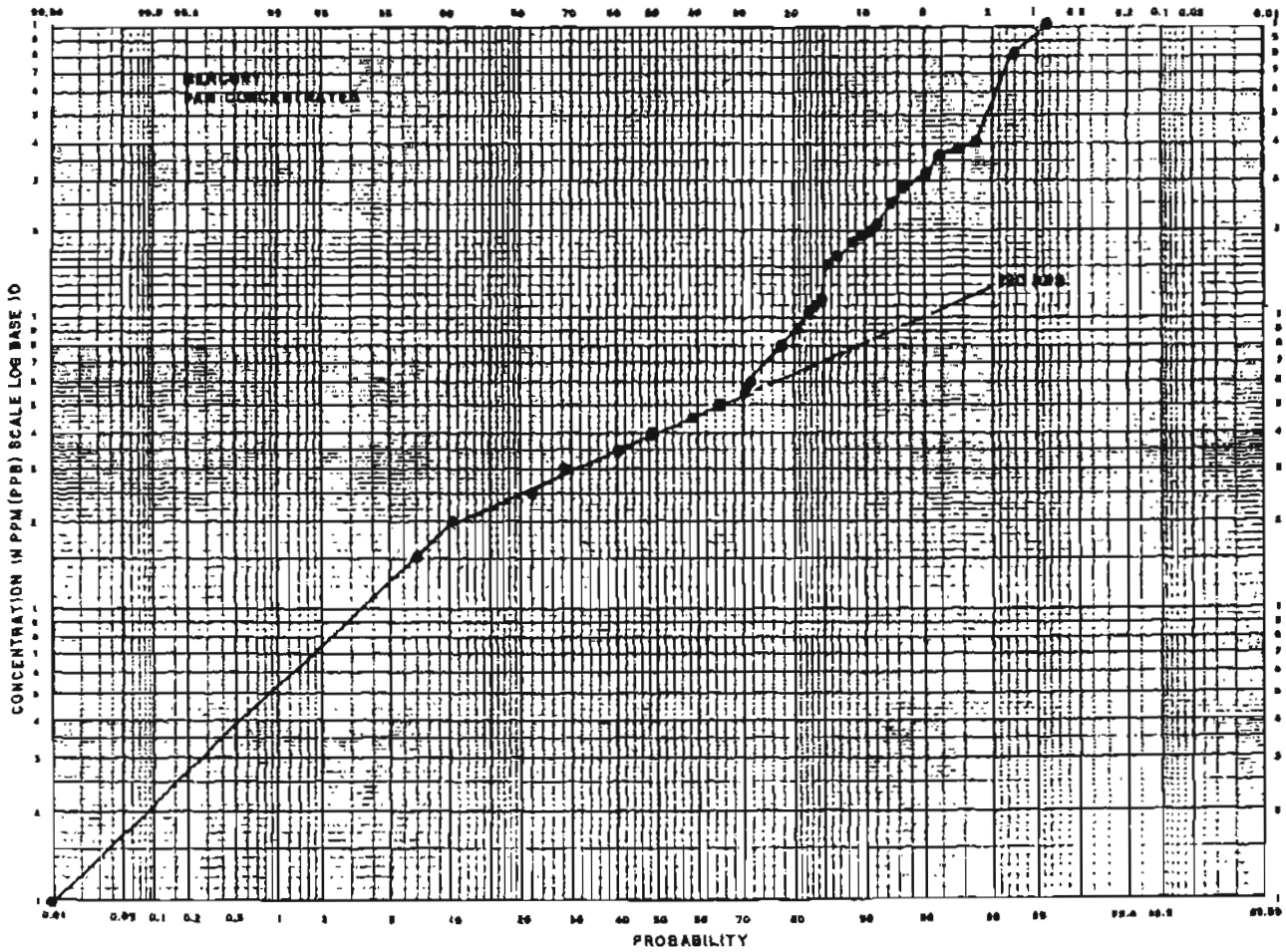
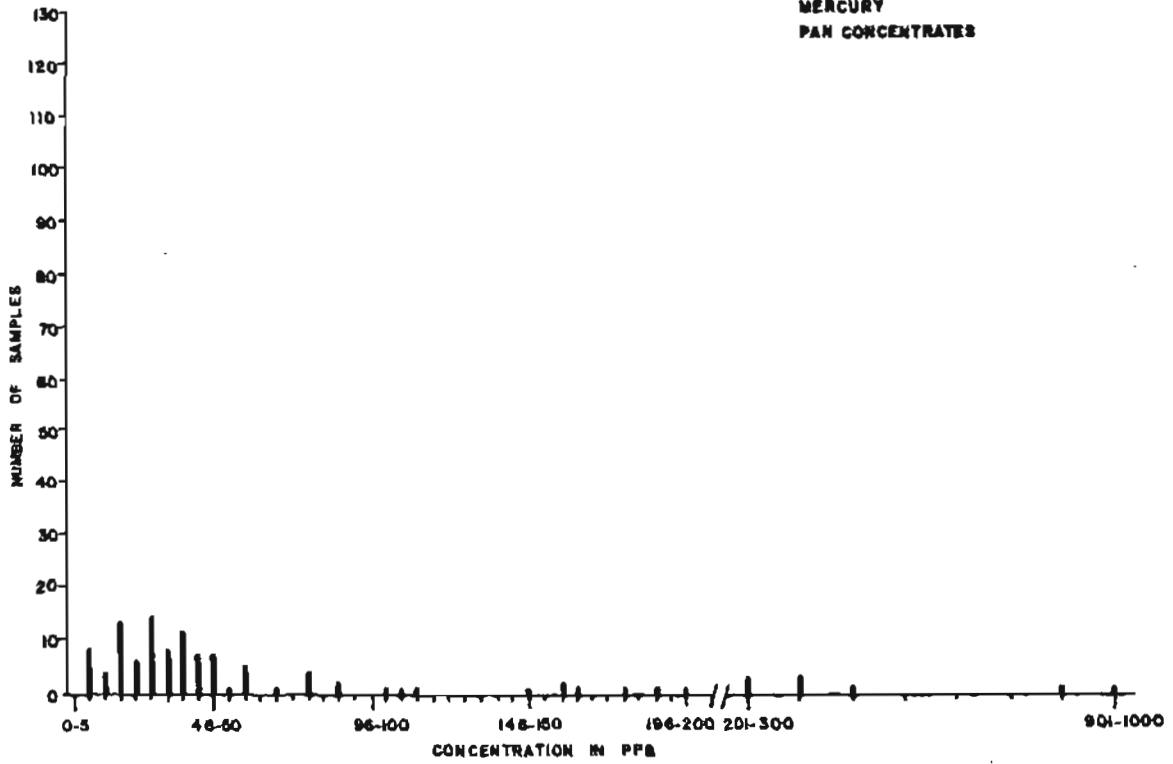
TIN  
PAM CONCENTRATES



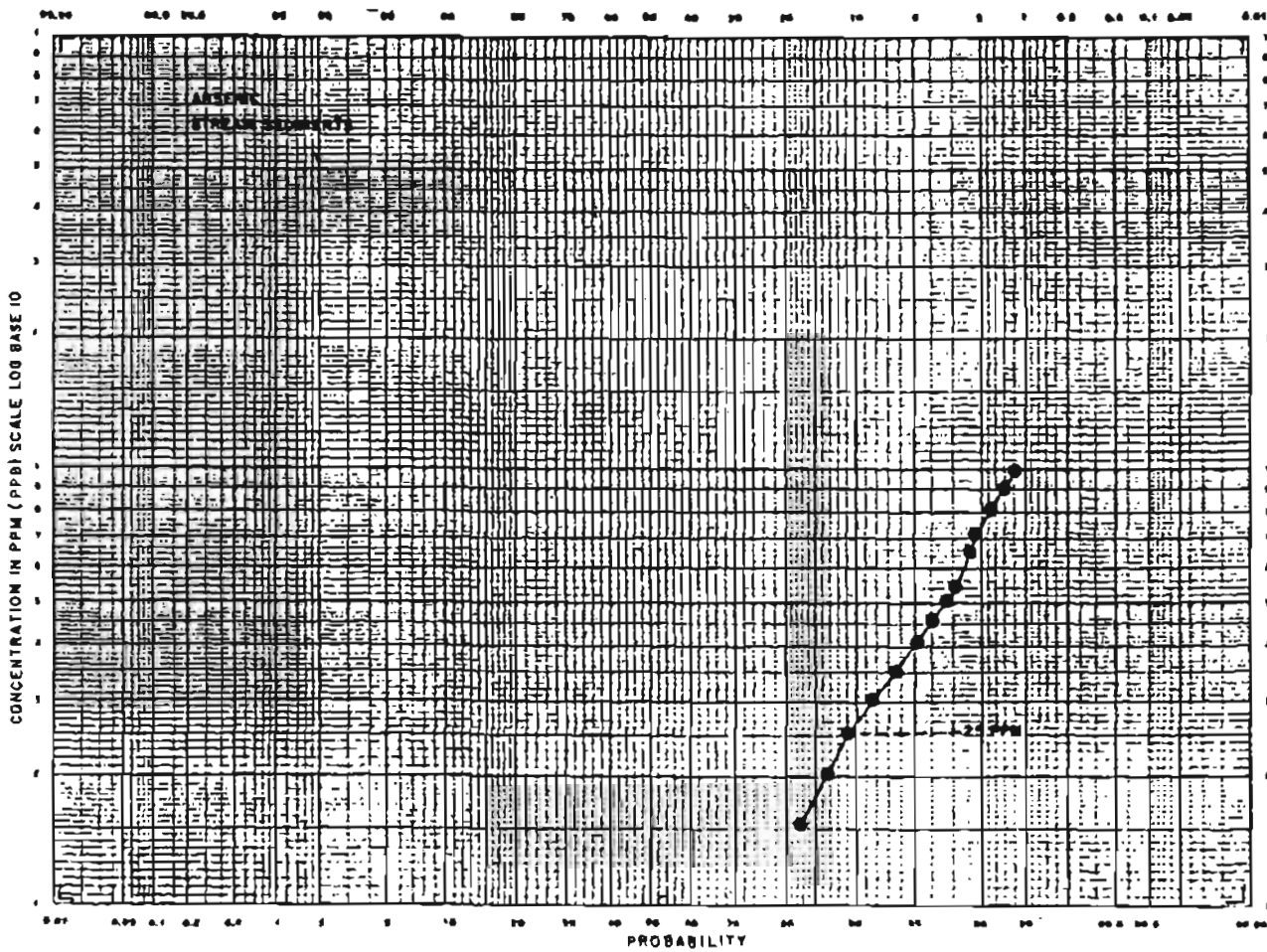
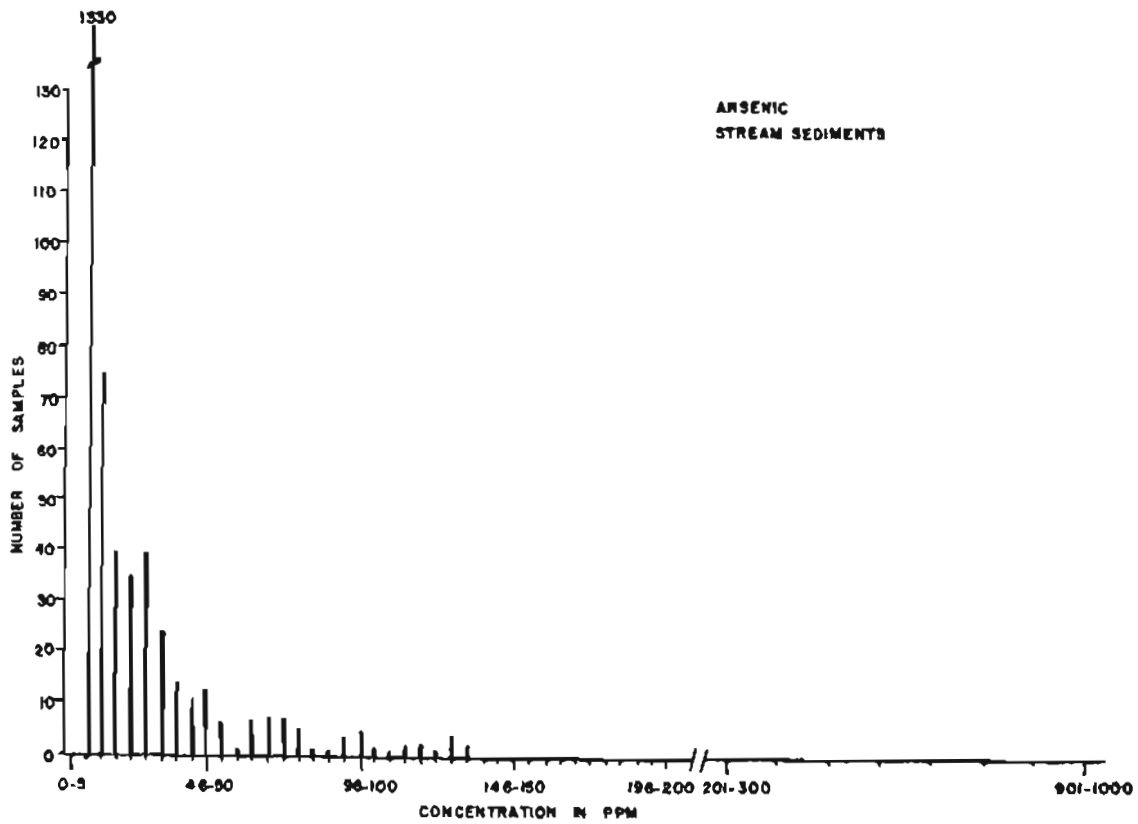
**TUNGSTEN  
PAN CONCENTRATES**

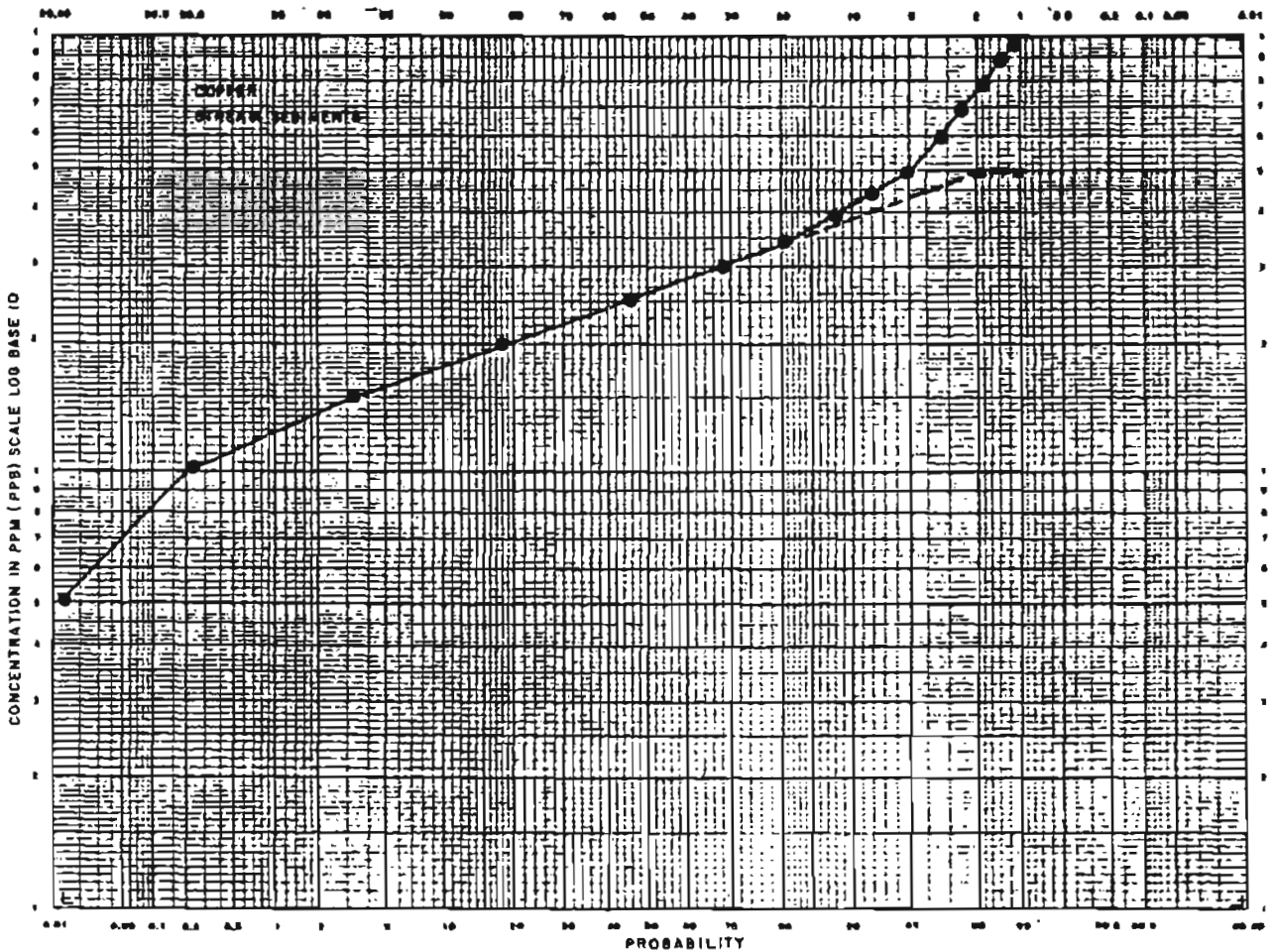
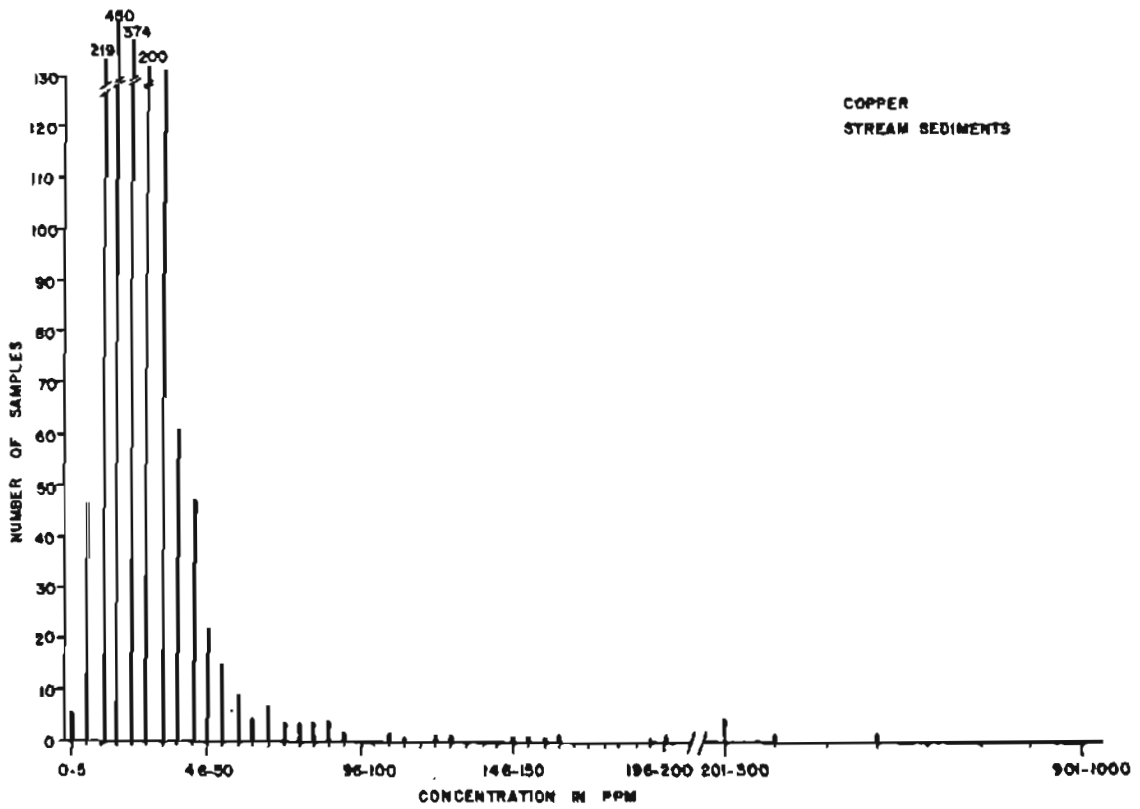


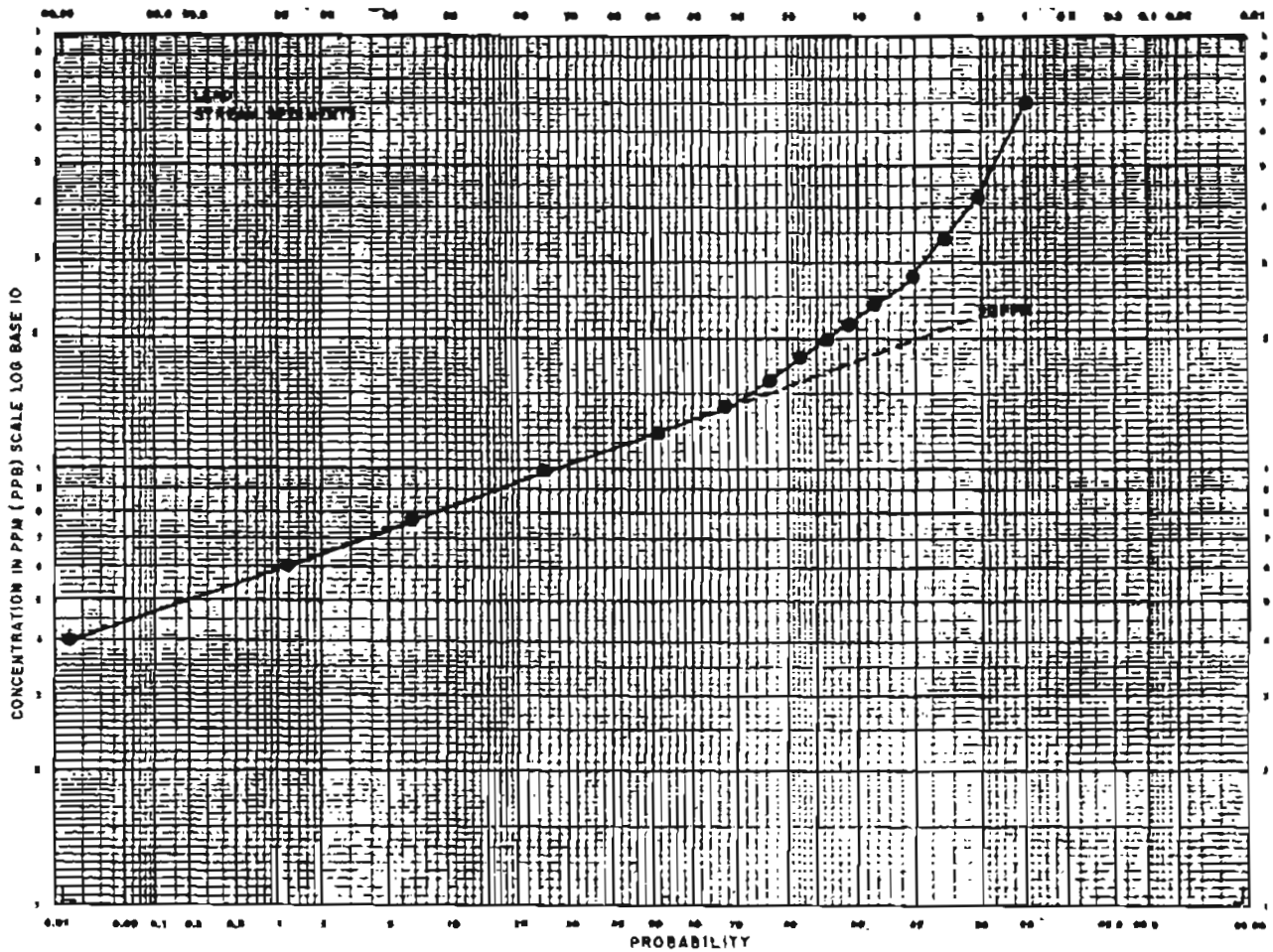
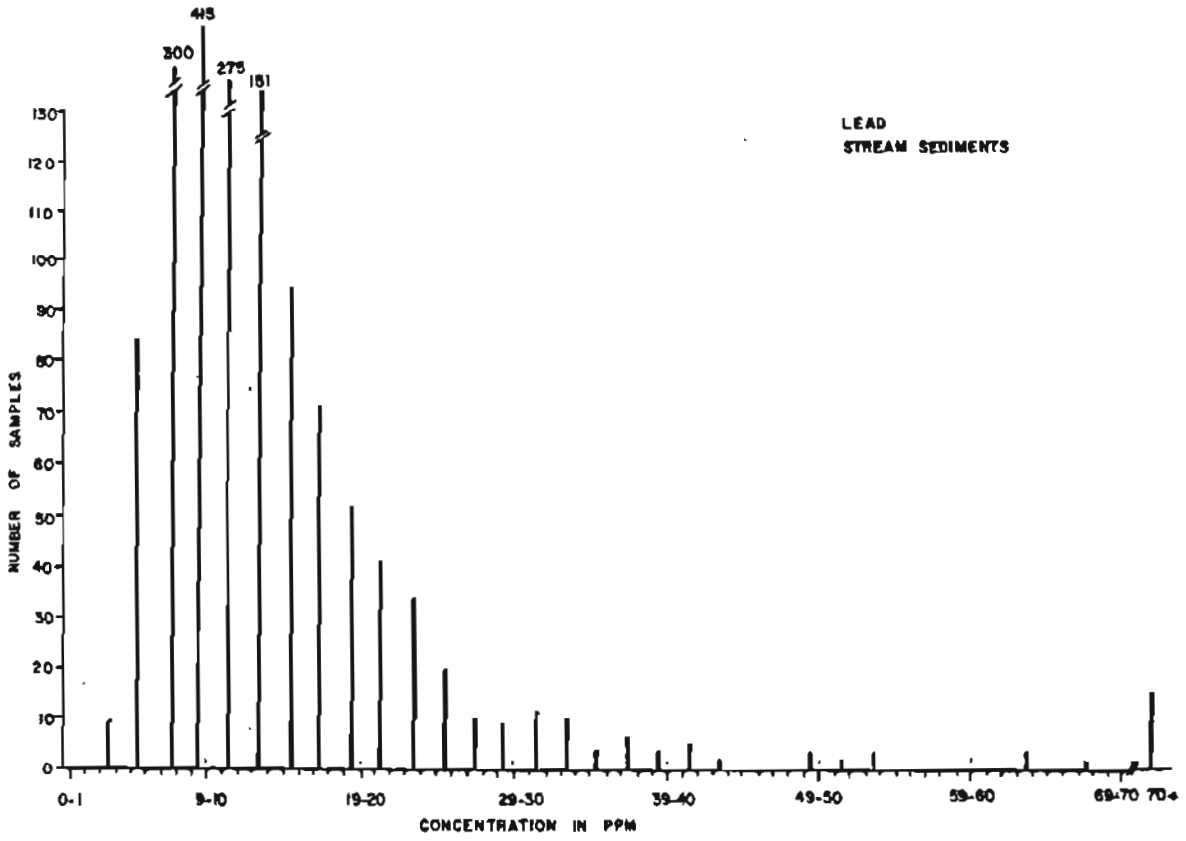
MERCURY  
PAN CONCENTRATES

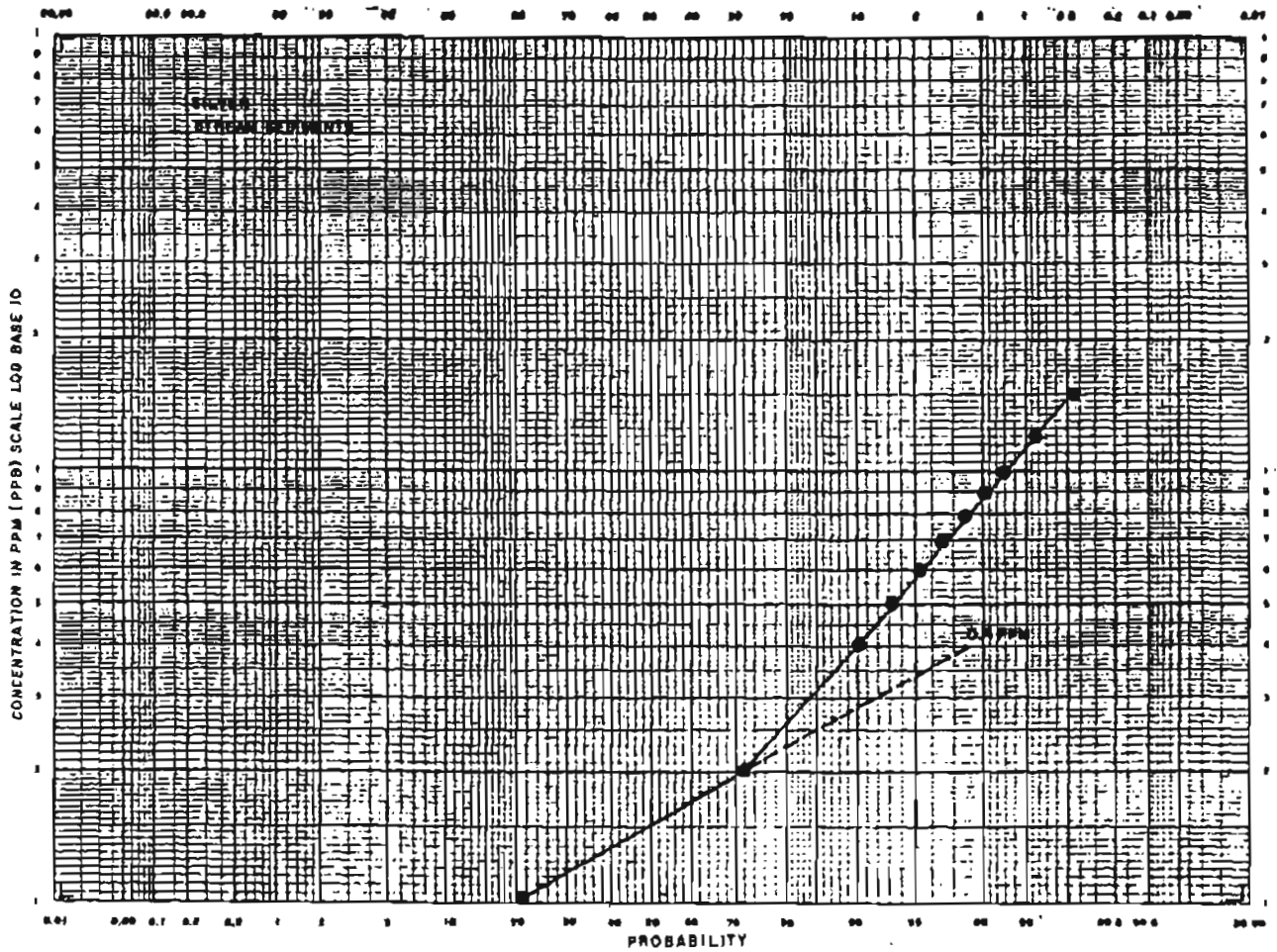
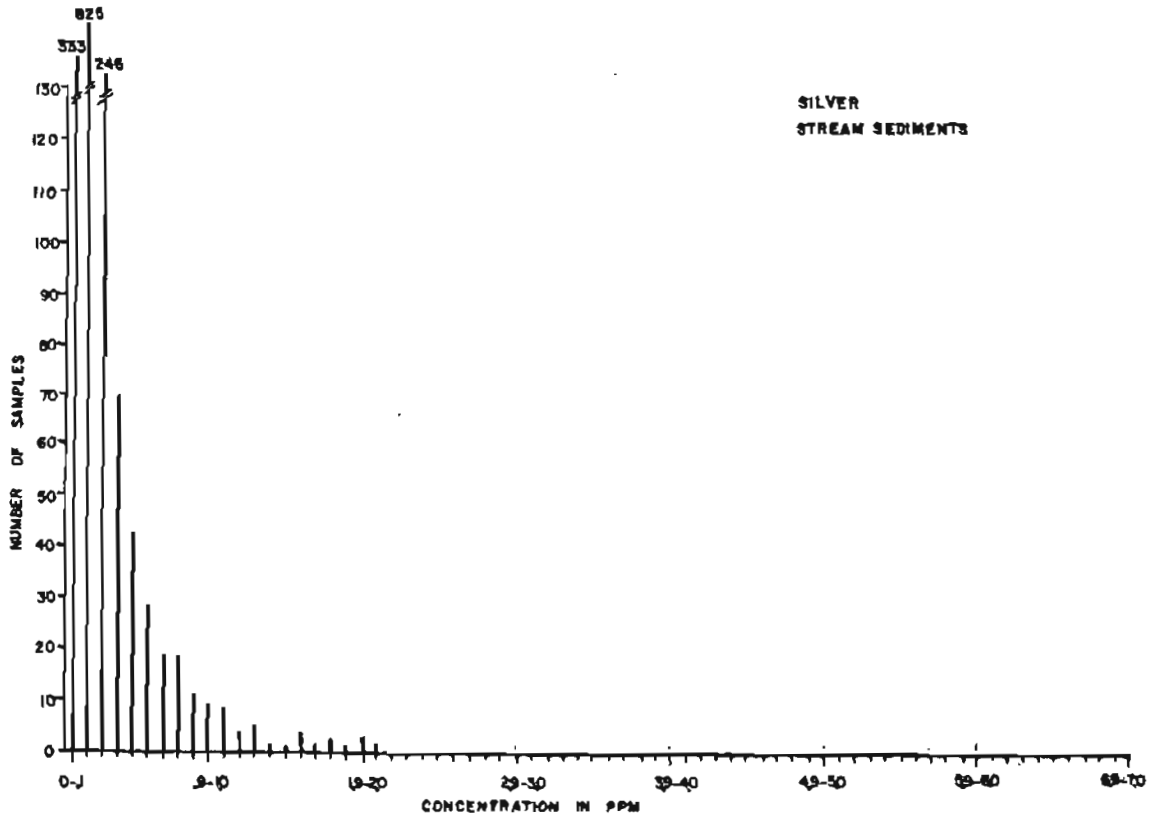


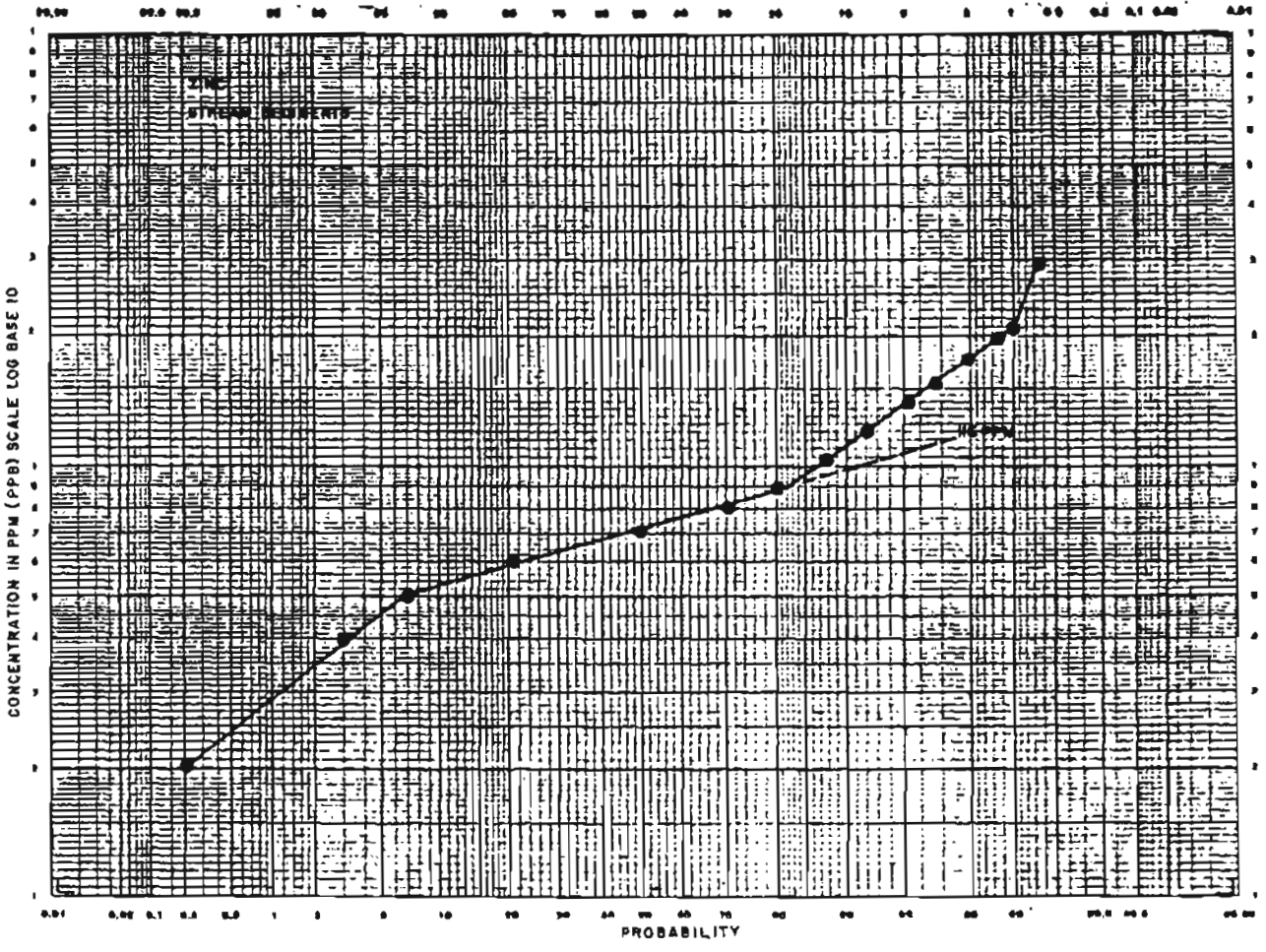
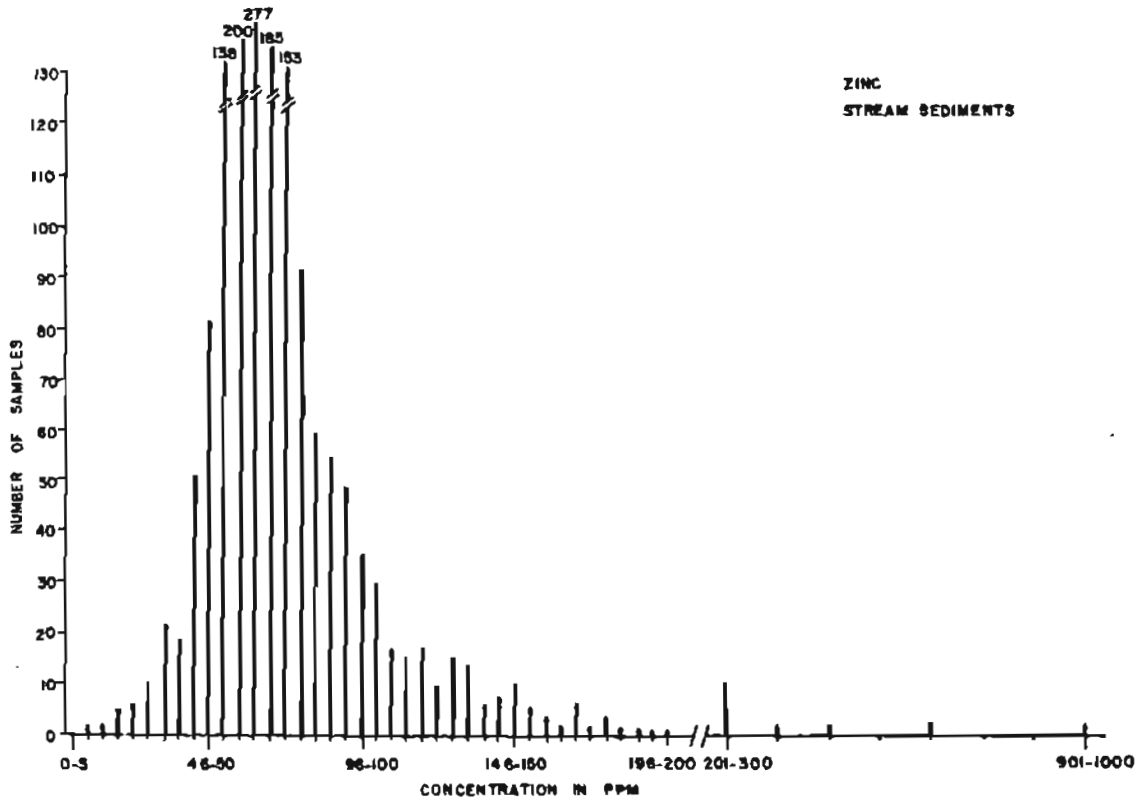
**APPENDIX C4**  
**Histograms and Log Concentration-Probability Plots of**  
**Stream Sedimen, Pan Concentrate, and Rock Geochemical Data**  
**from the Tolovana Mining District**

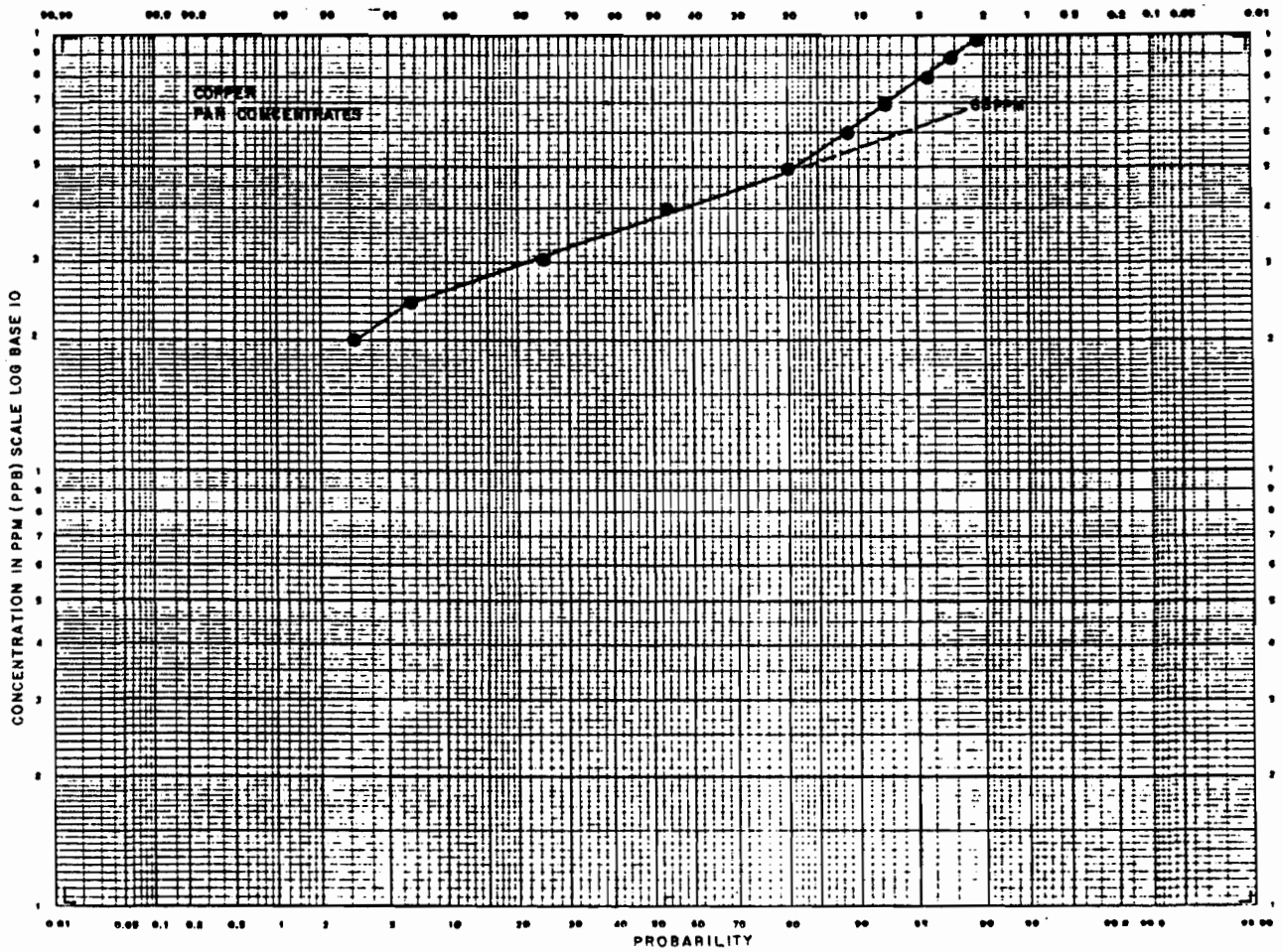
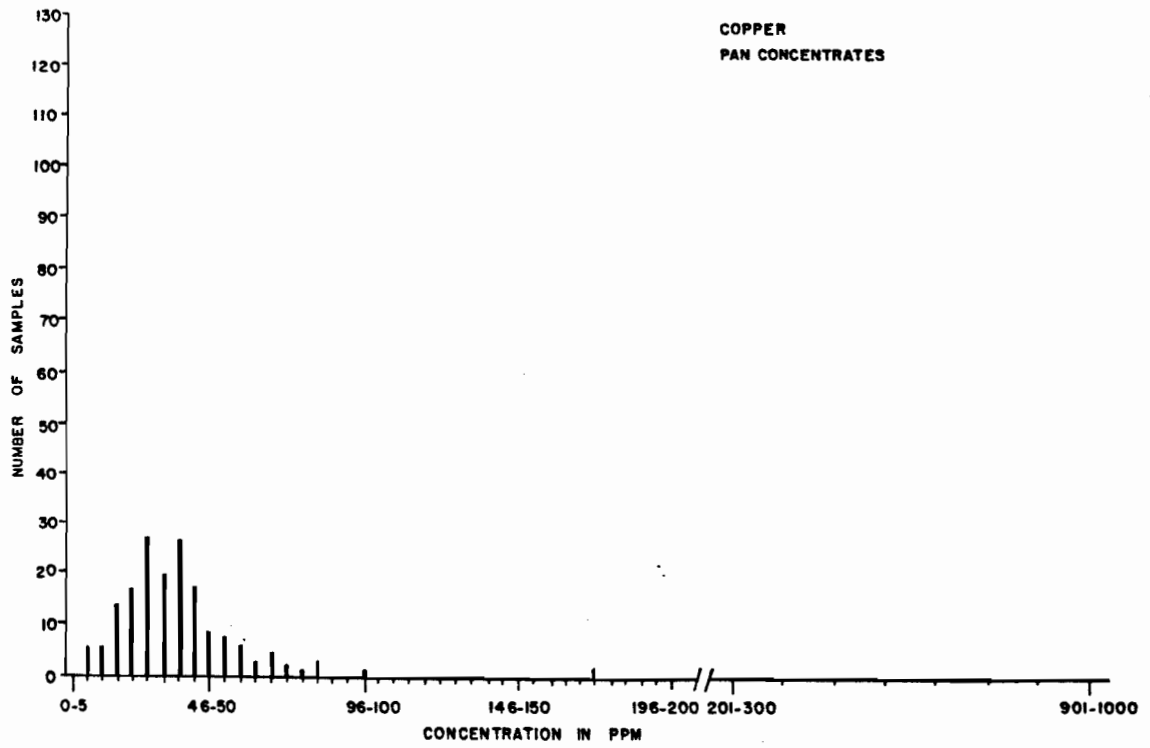


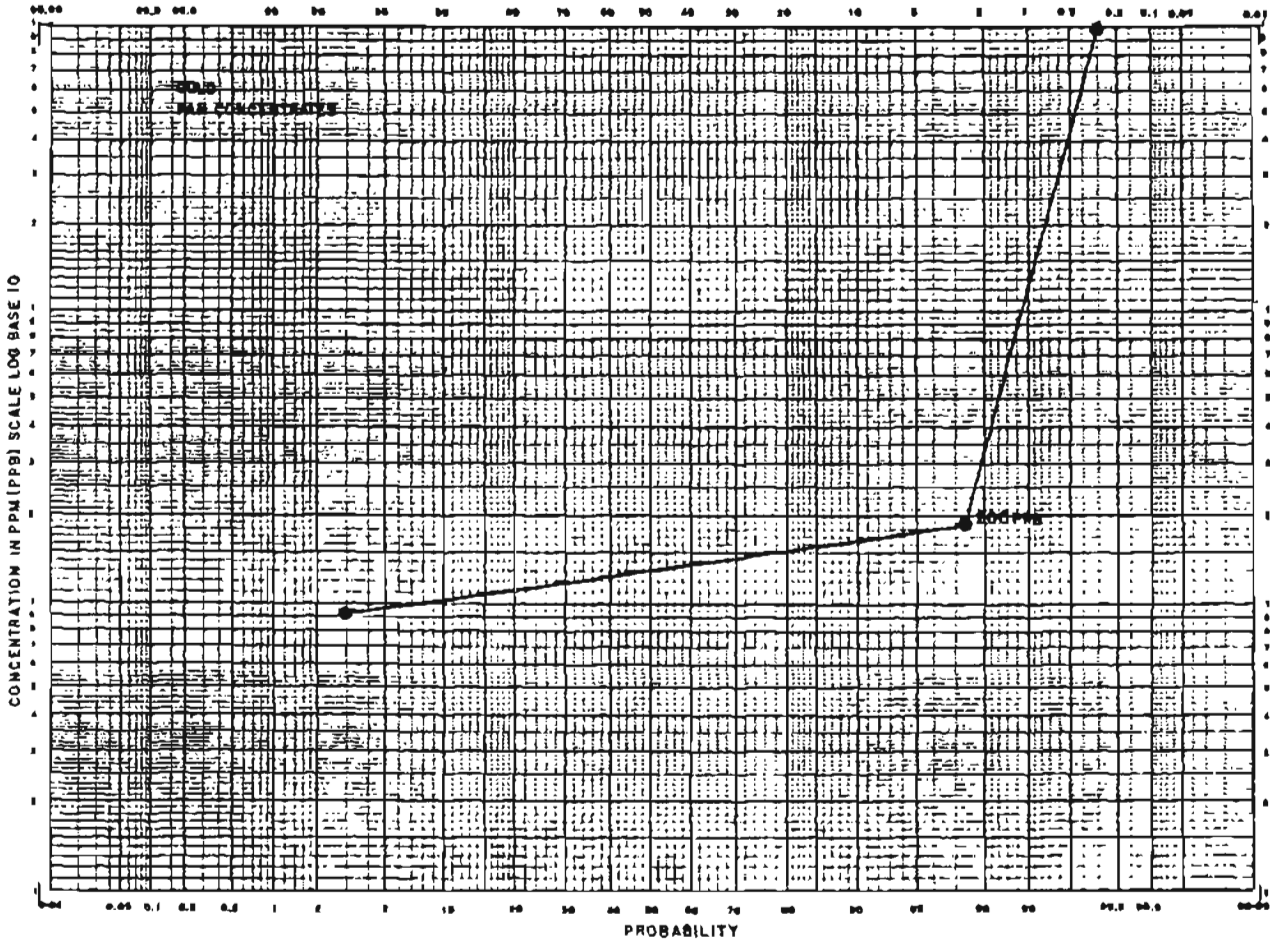
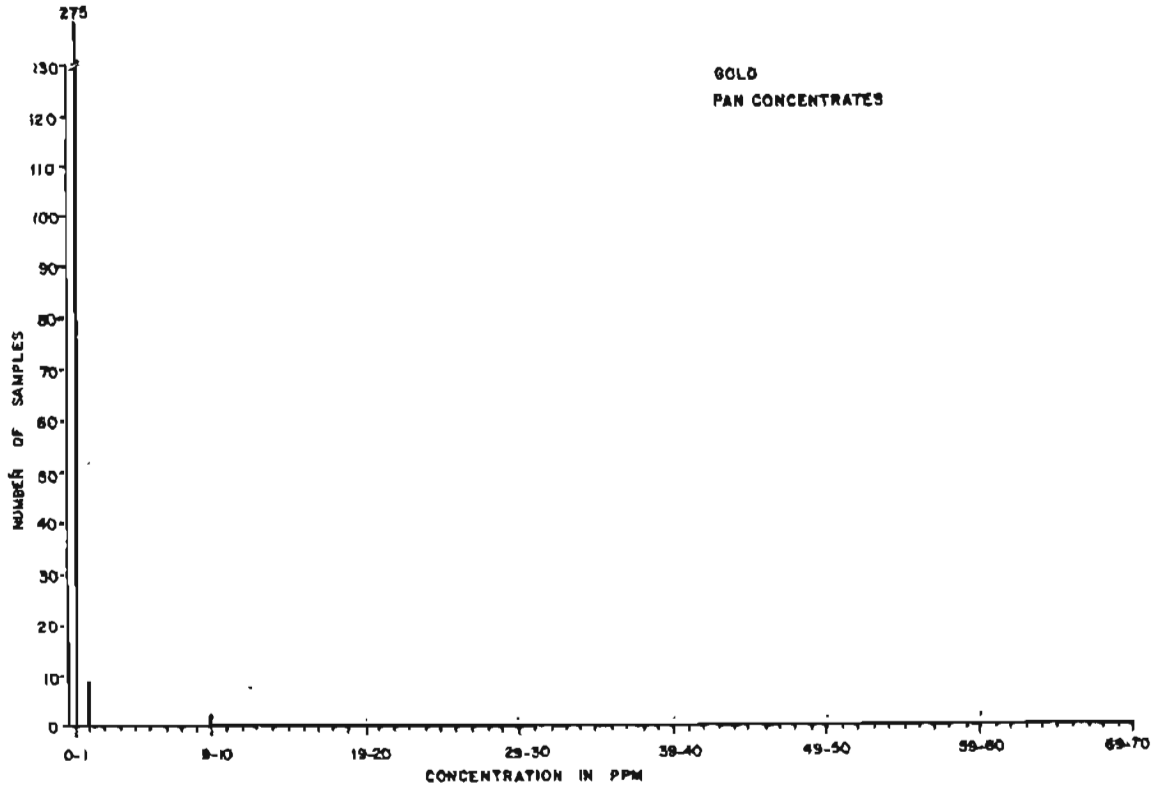




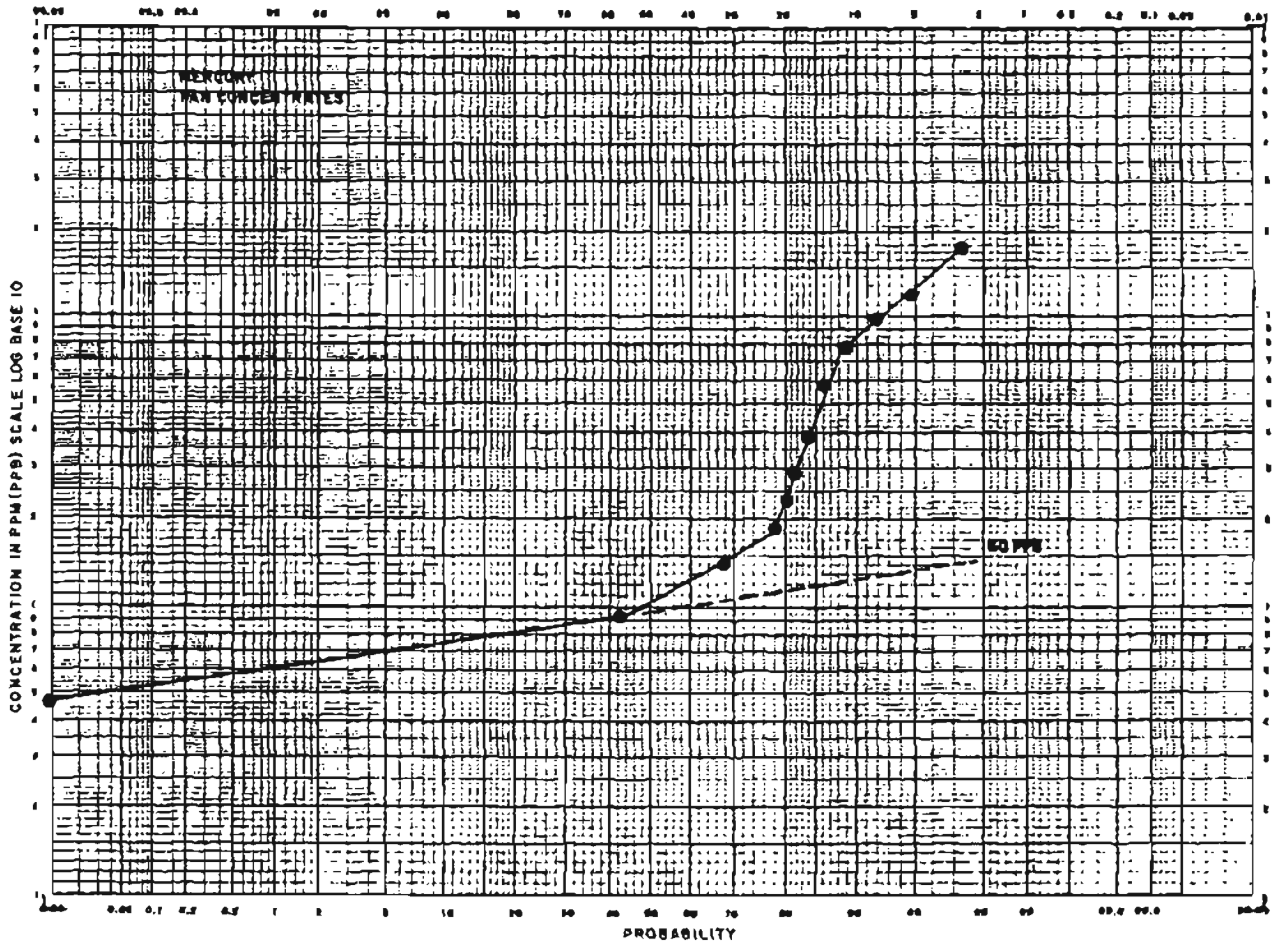
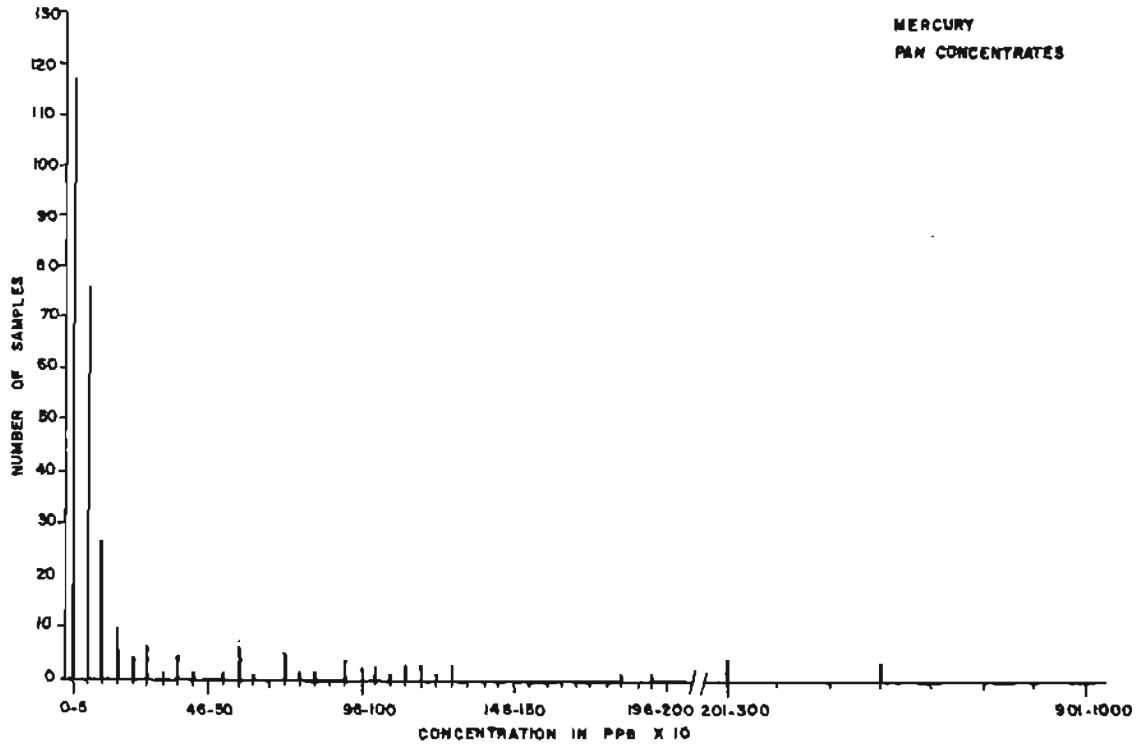


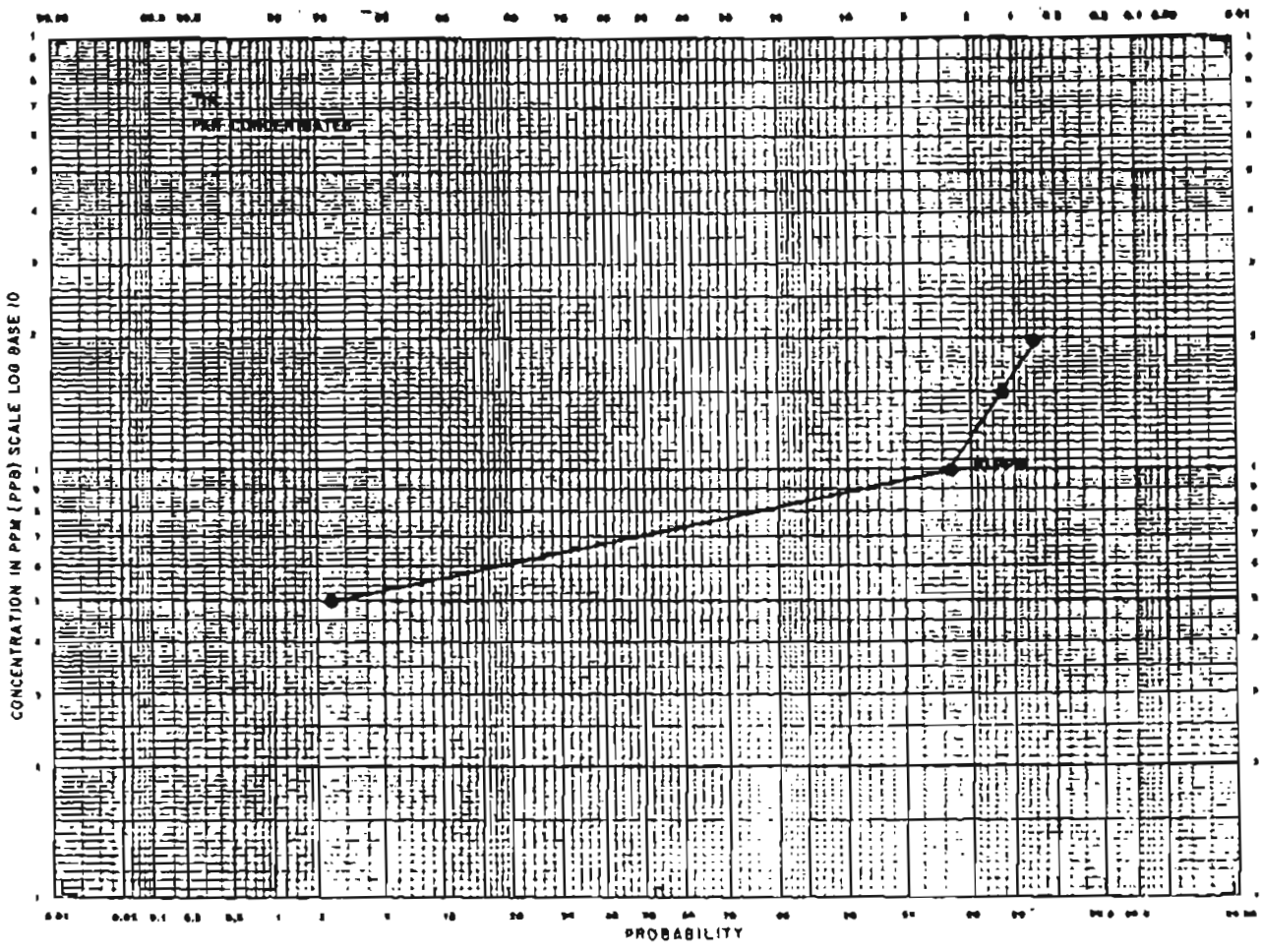
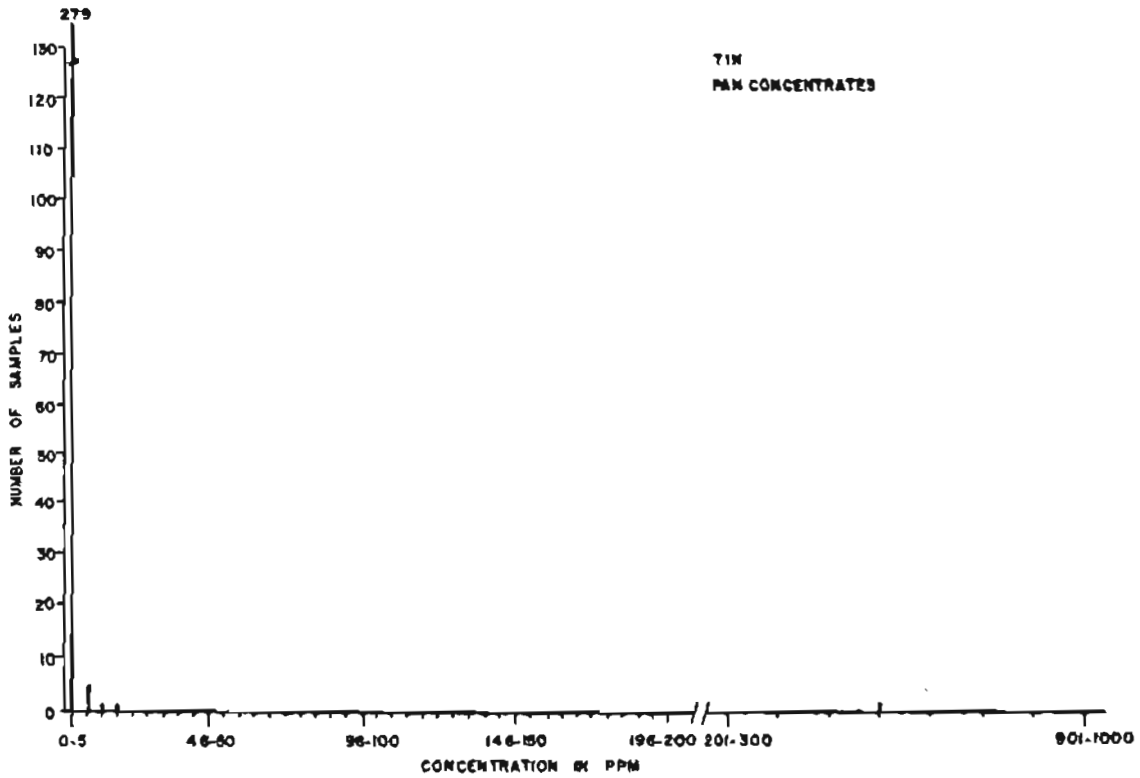


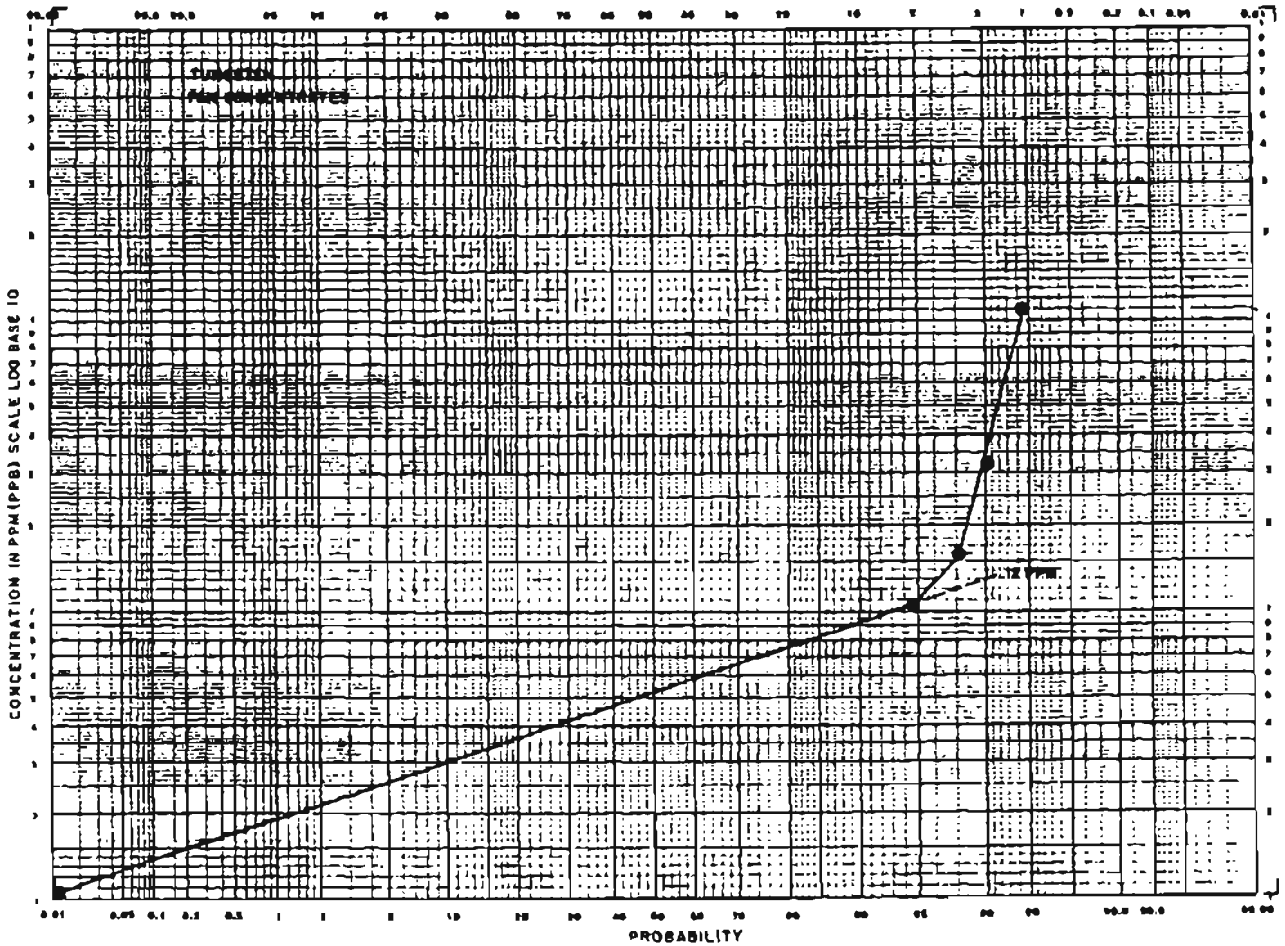
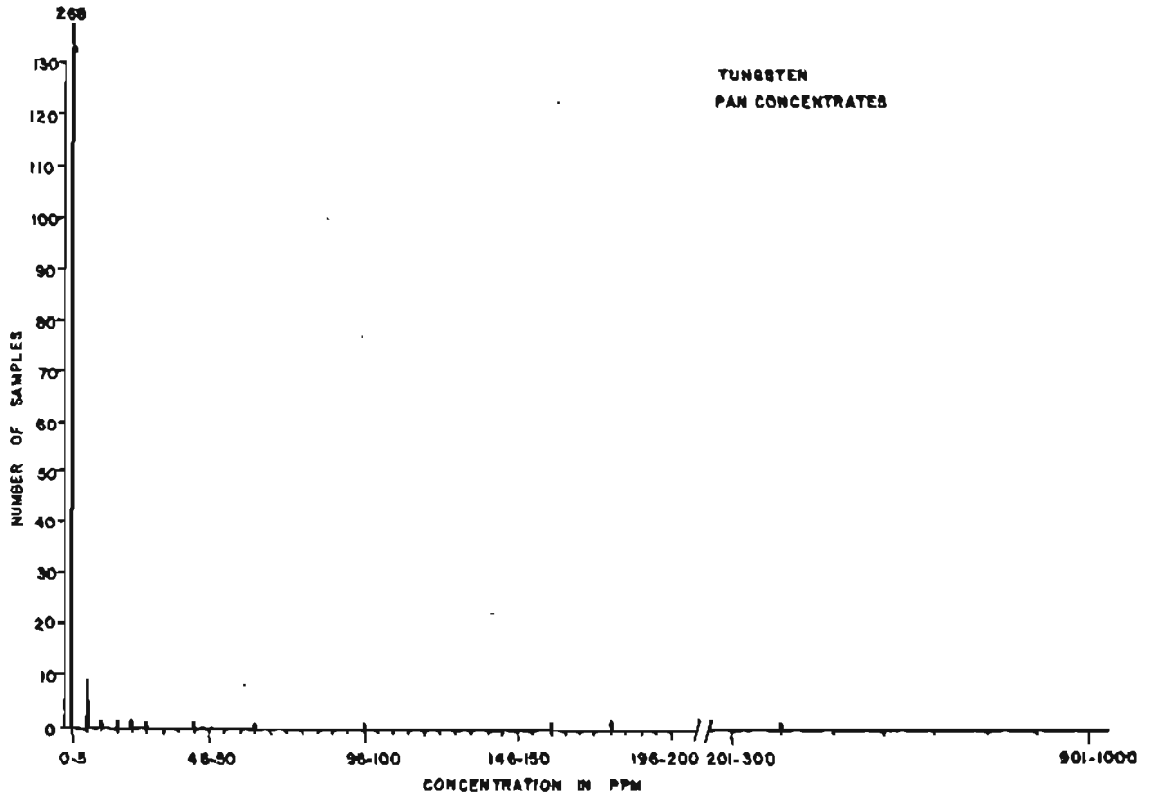




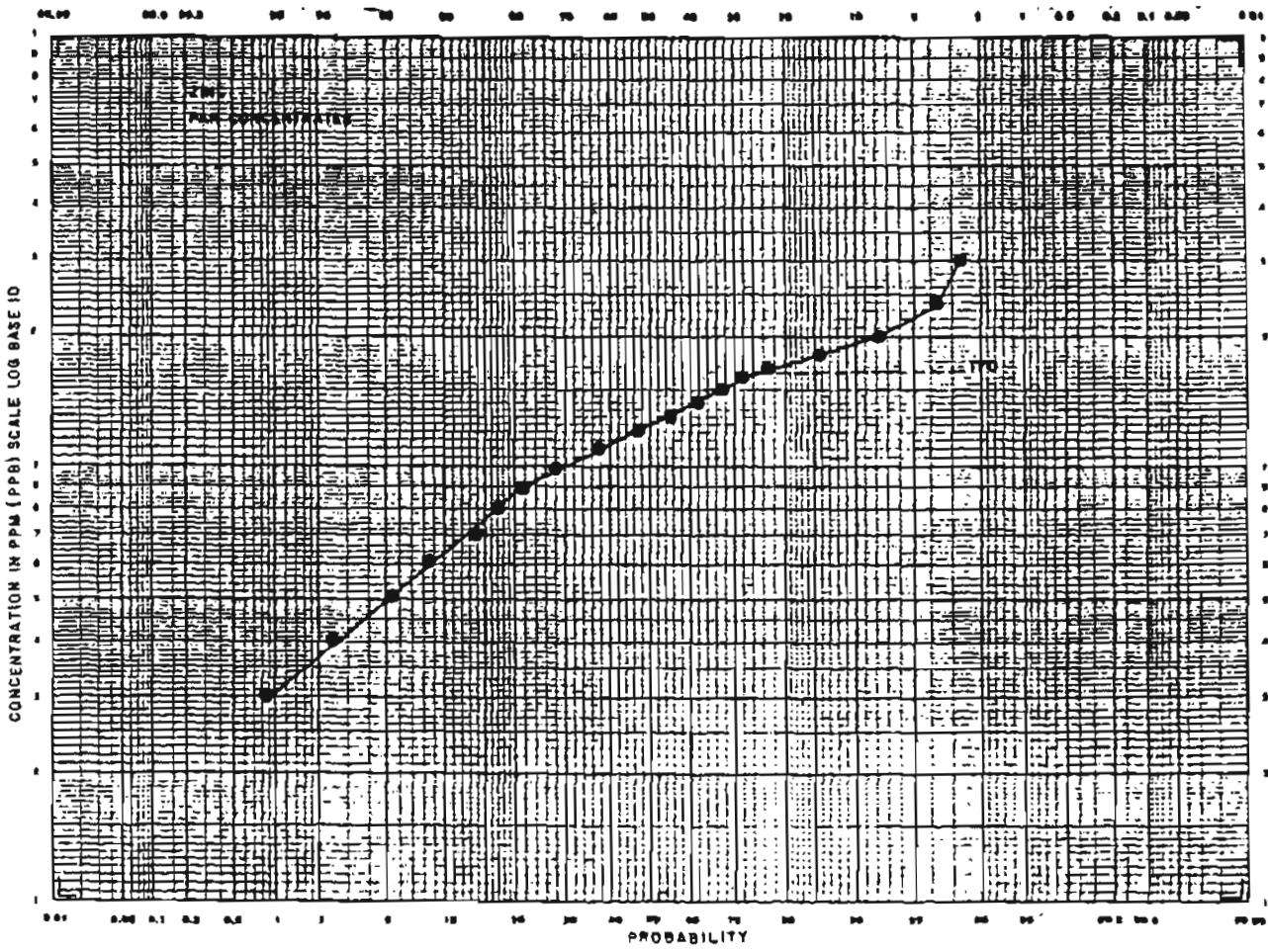
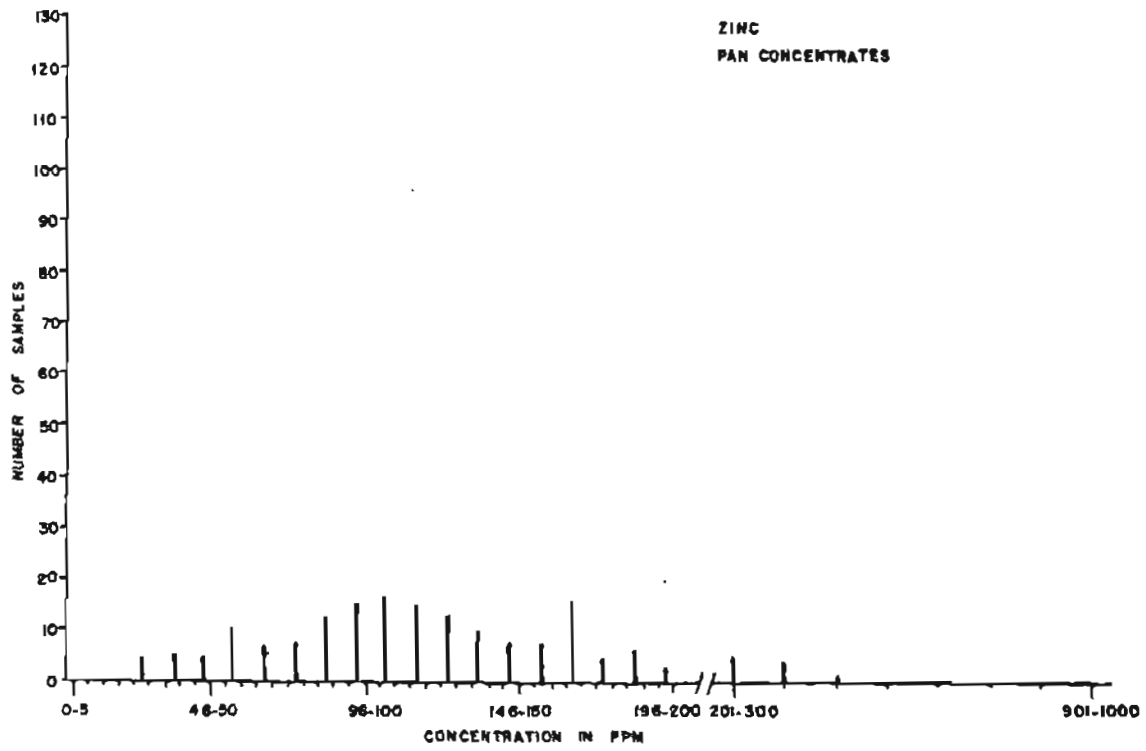
MERCURY  
PAN CONCENTRATES

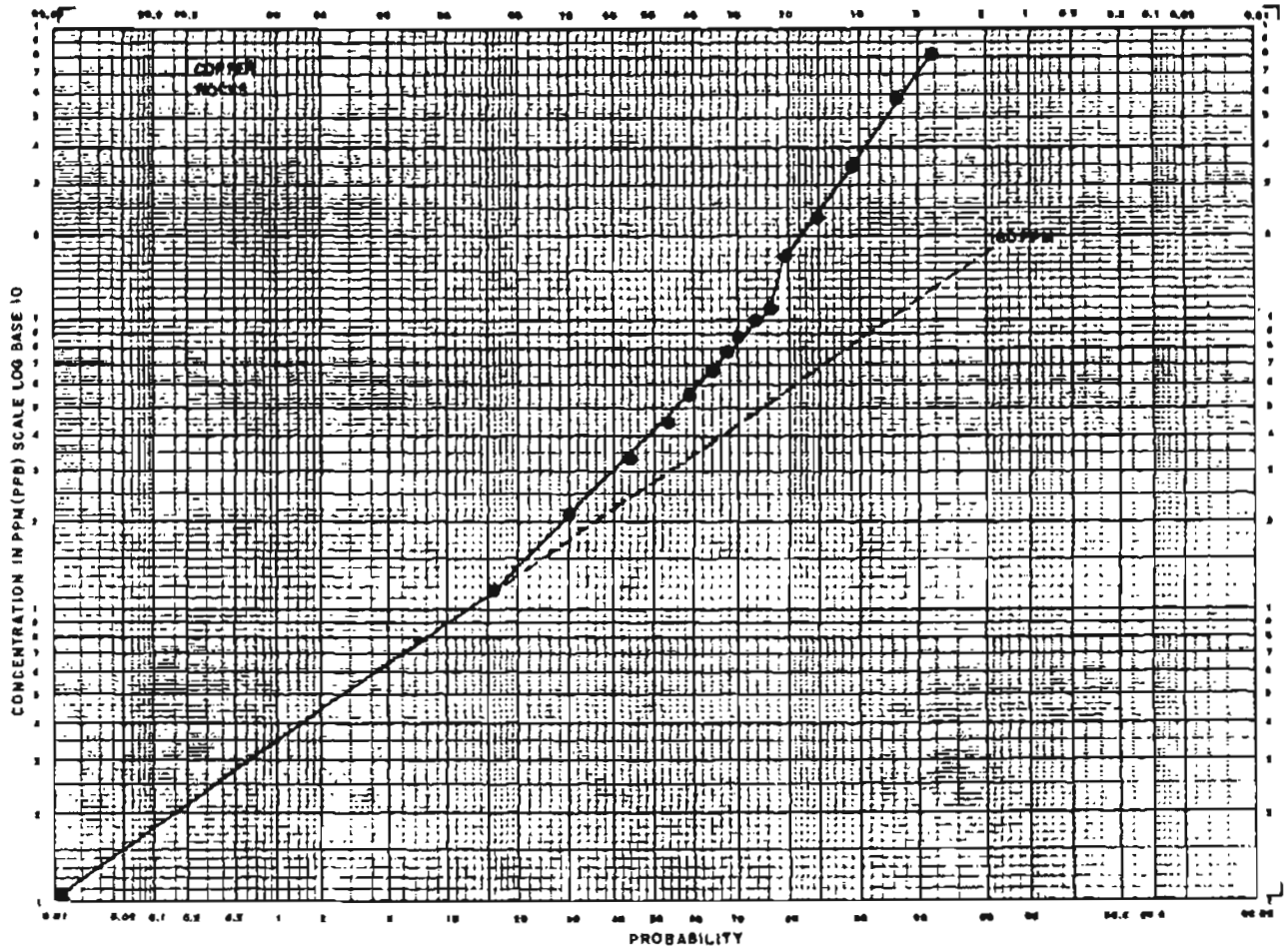
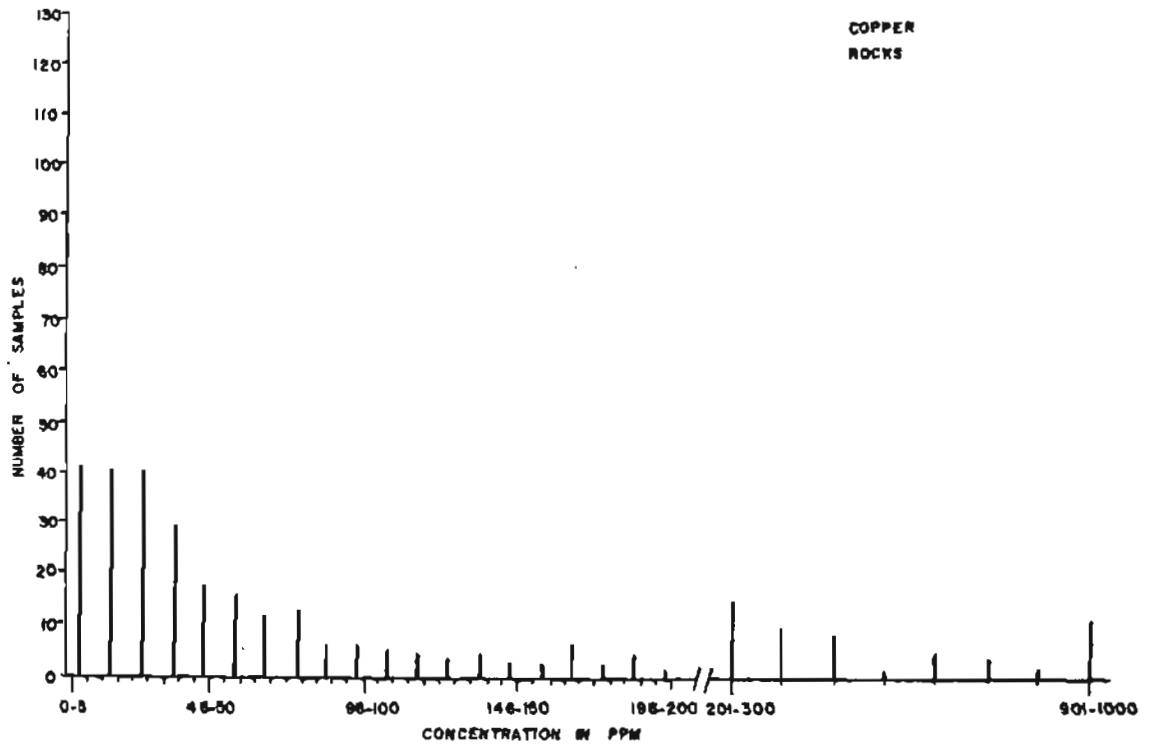


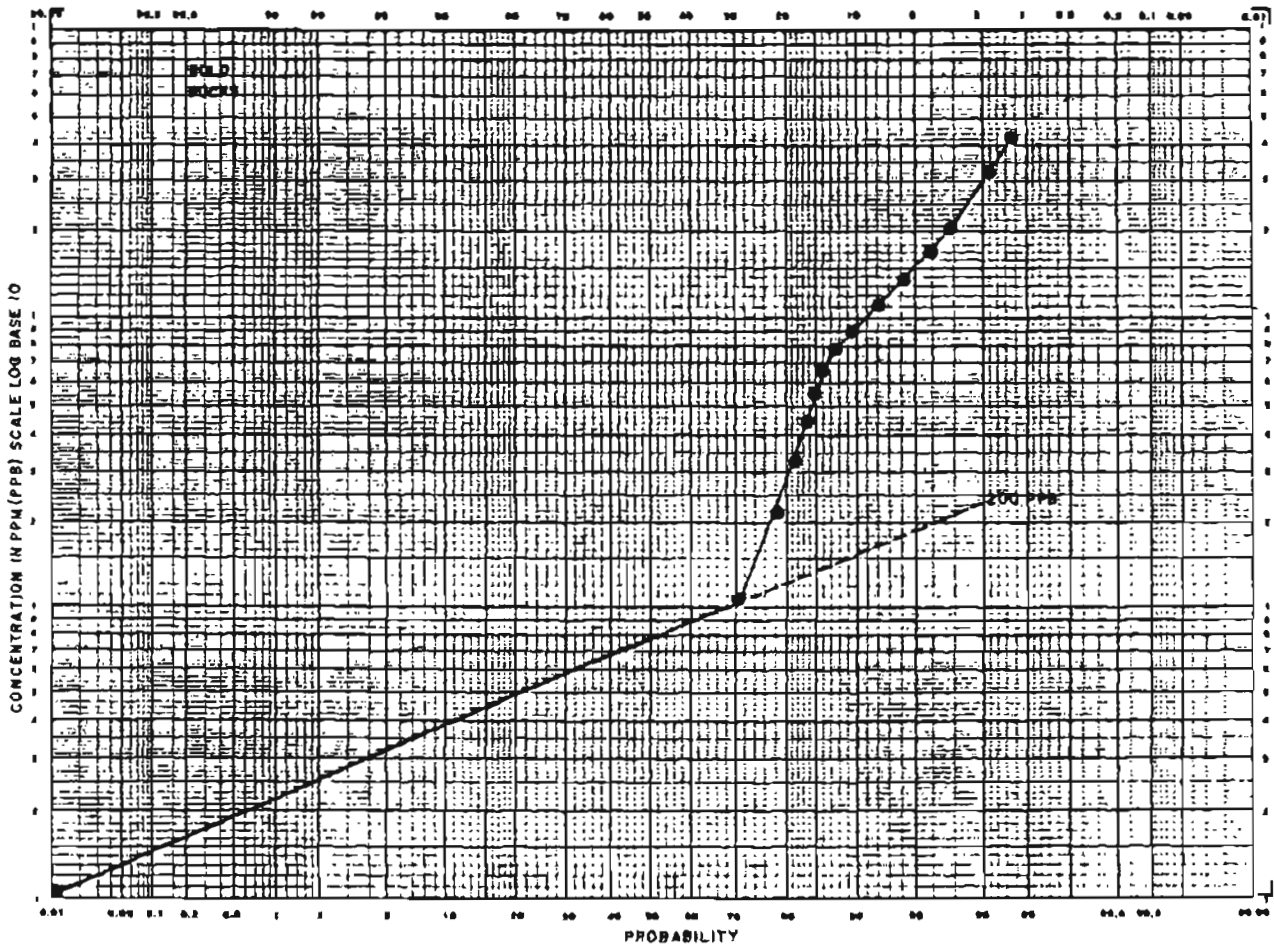
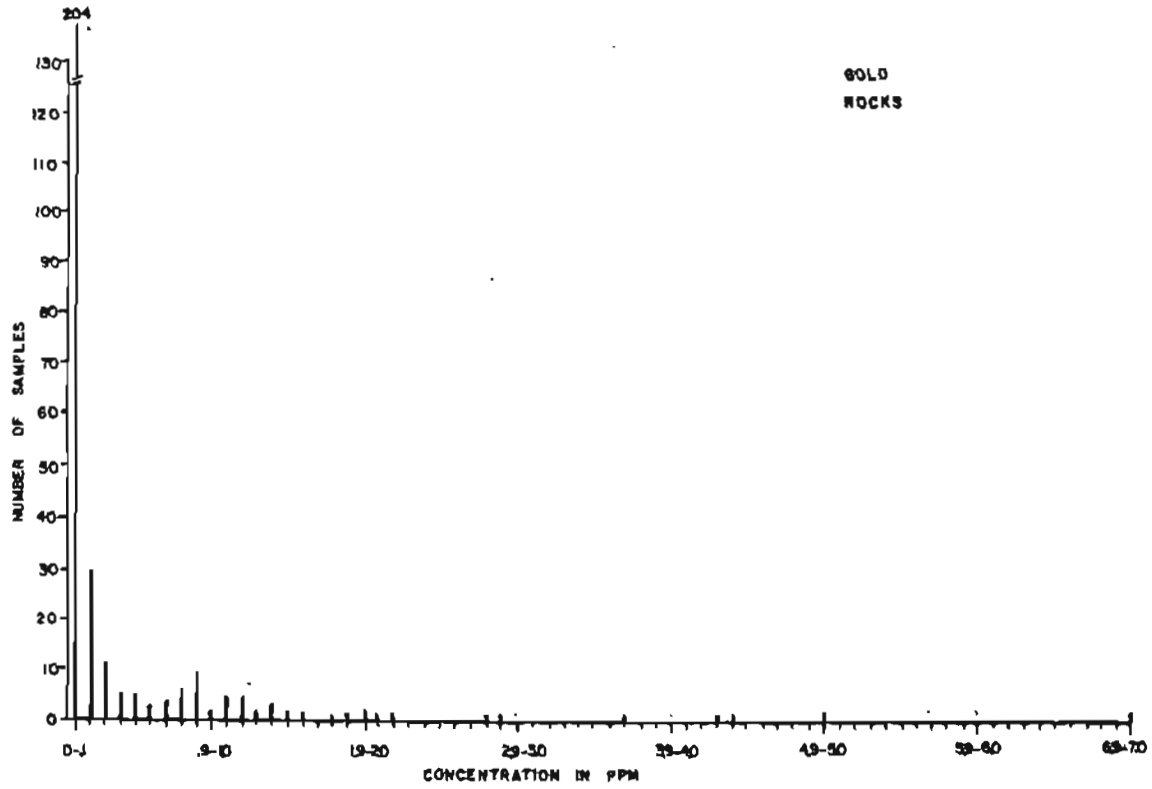


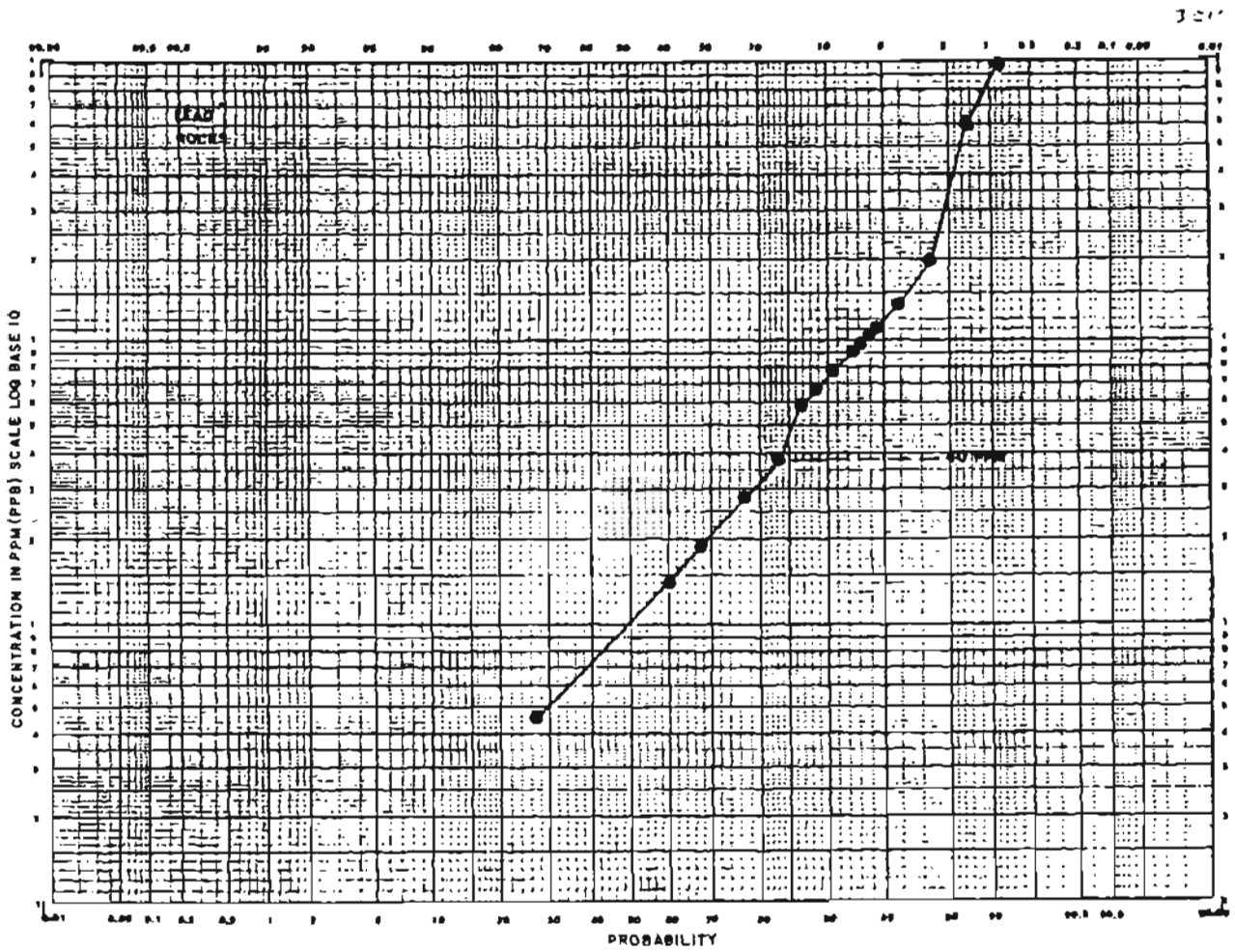
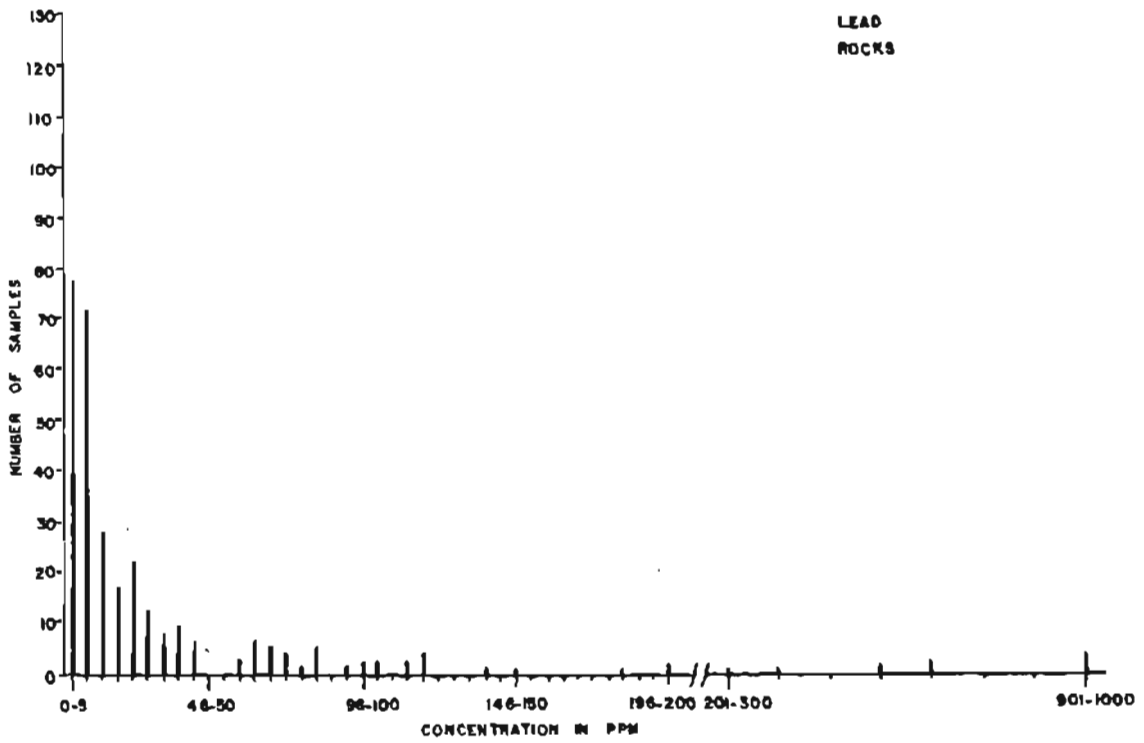


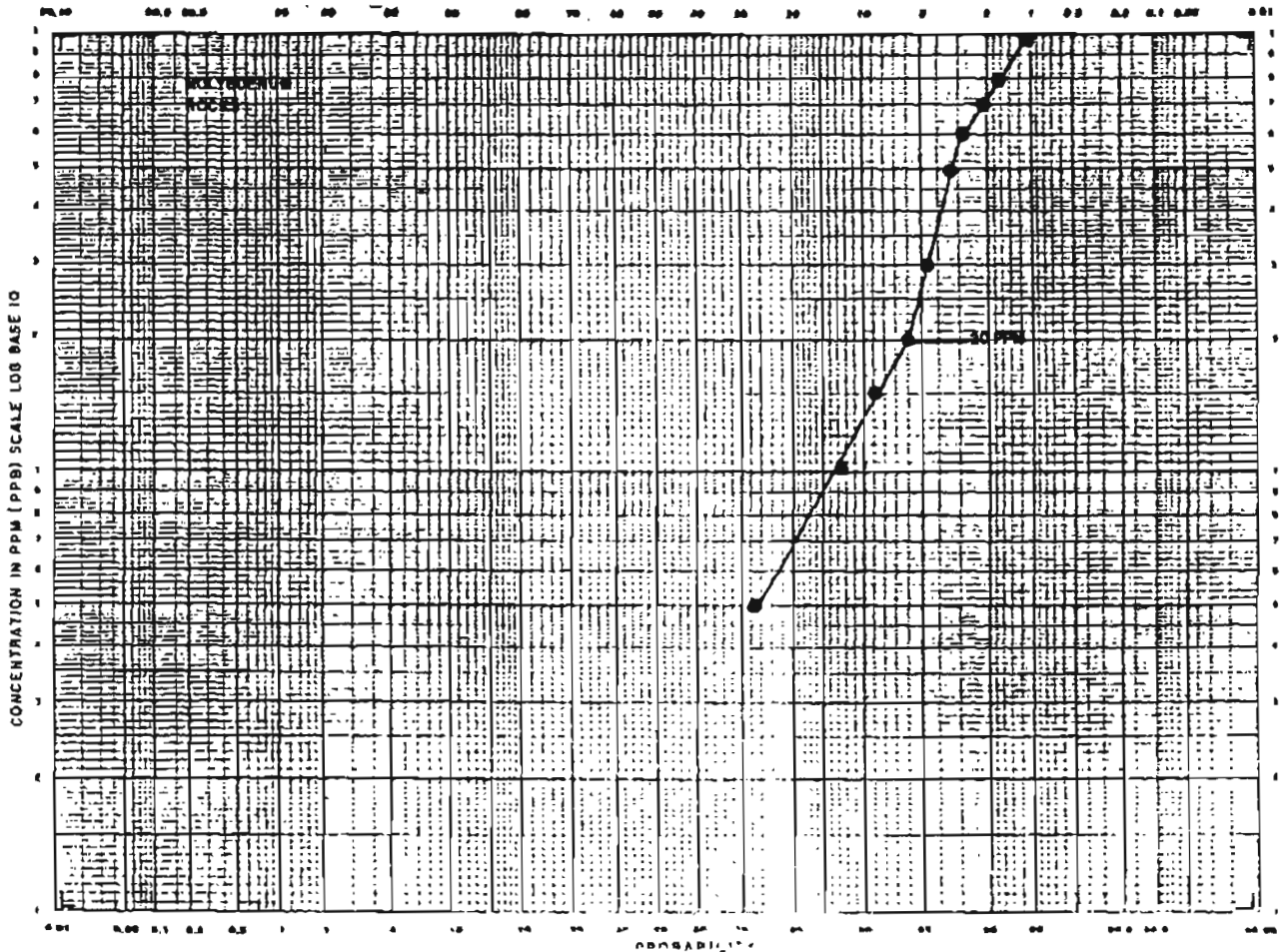
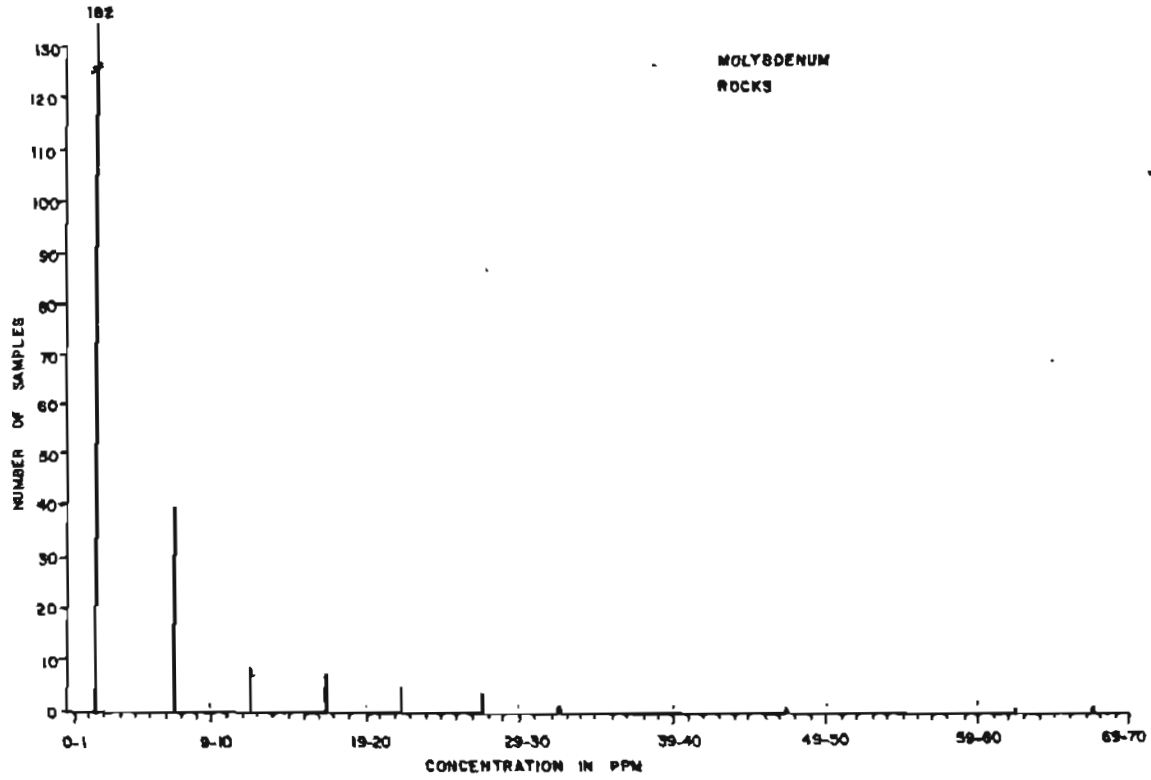
ZINC  
PAN CONCENTRATES

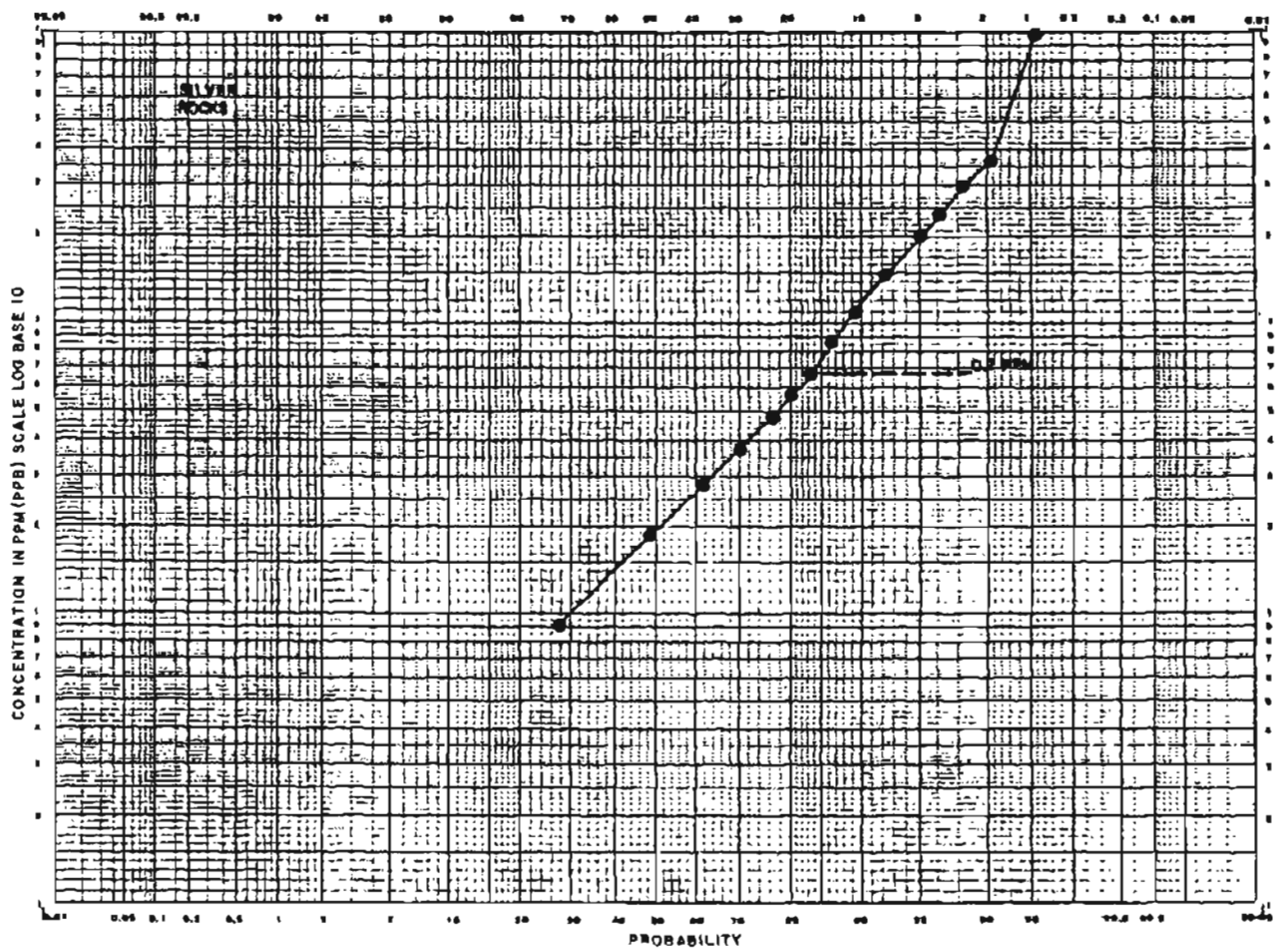
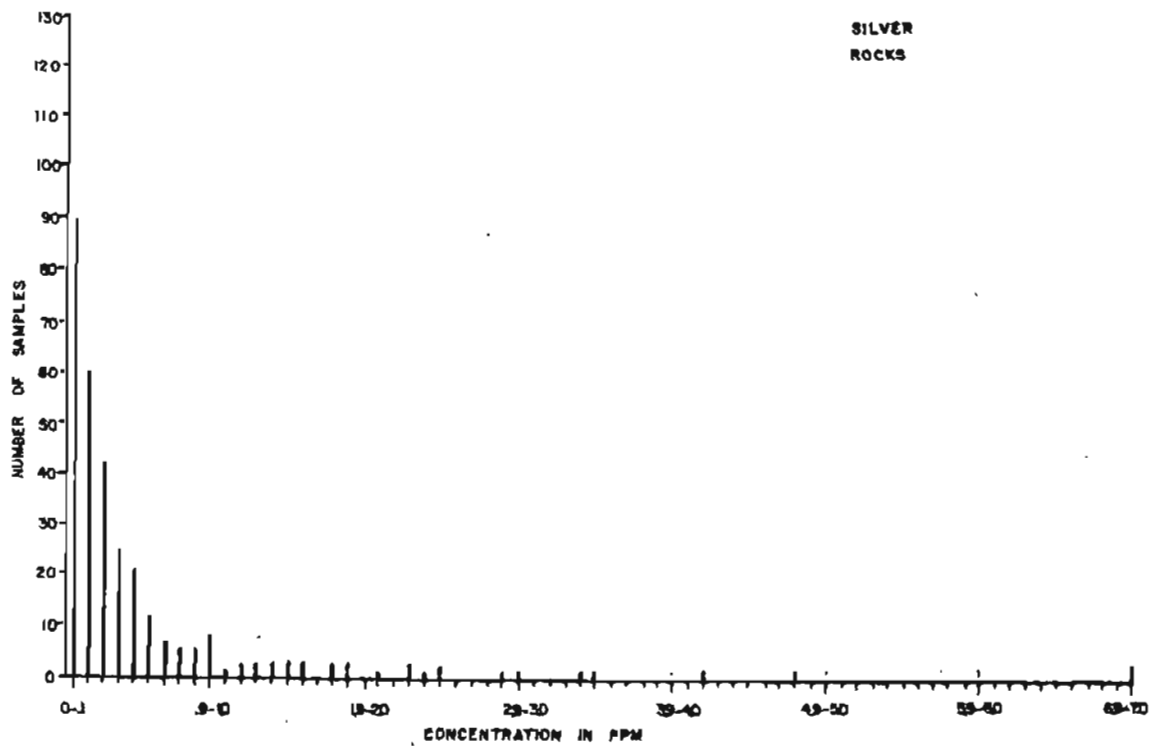


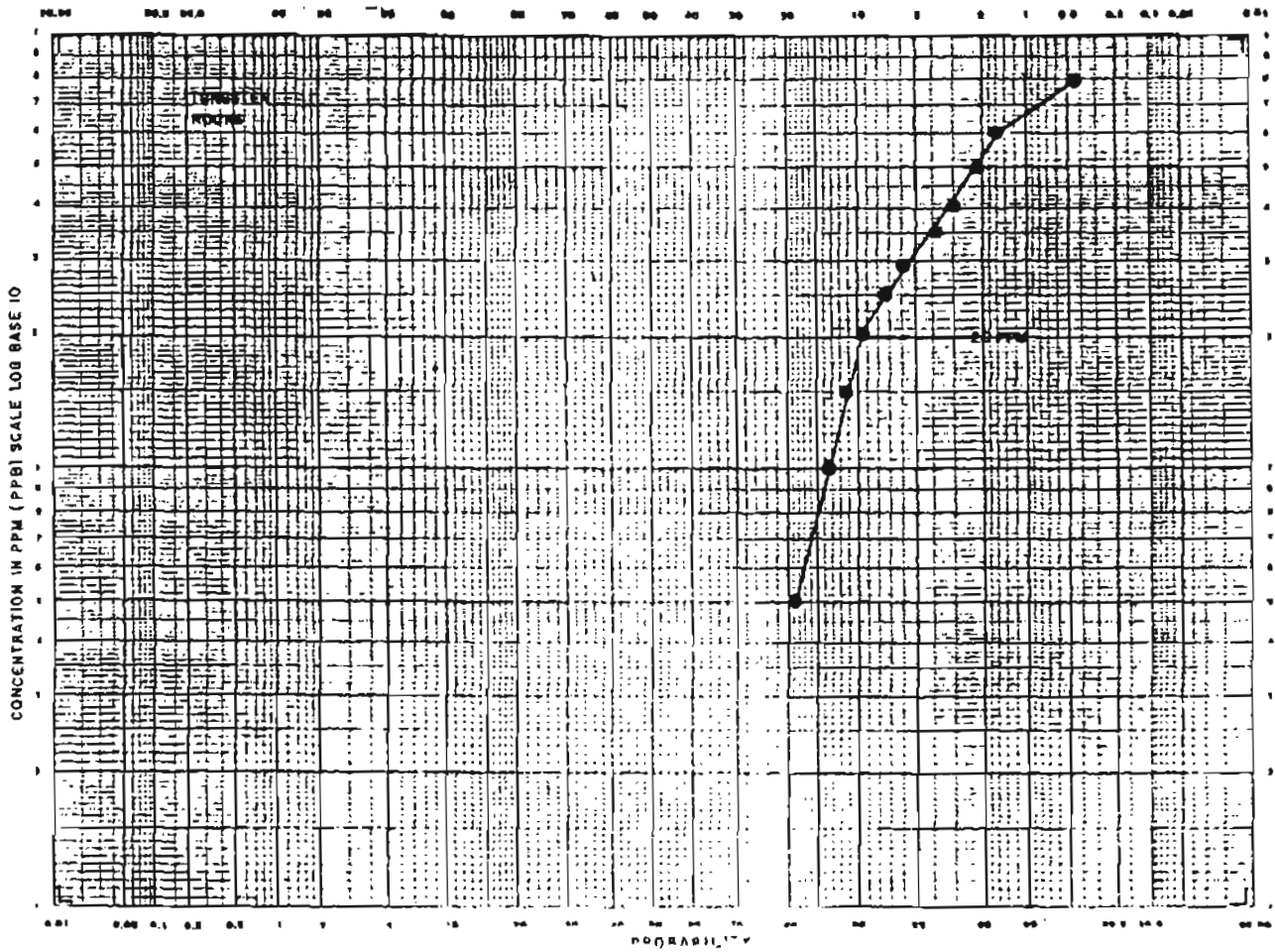
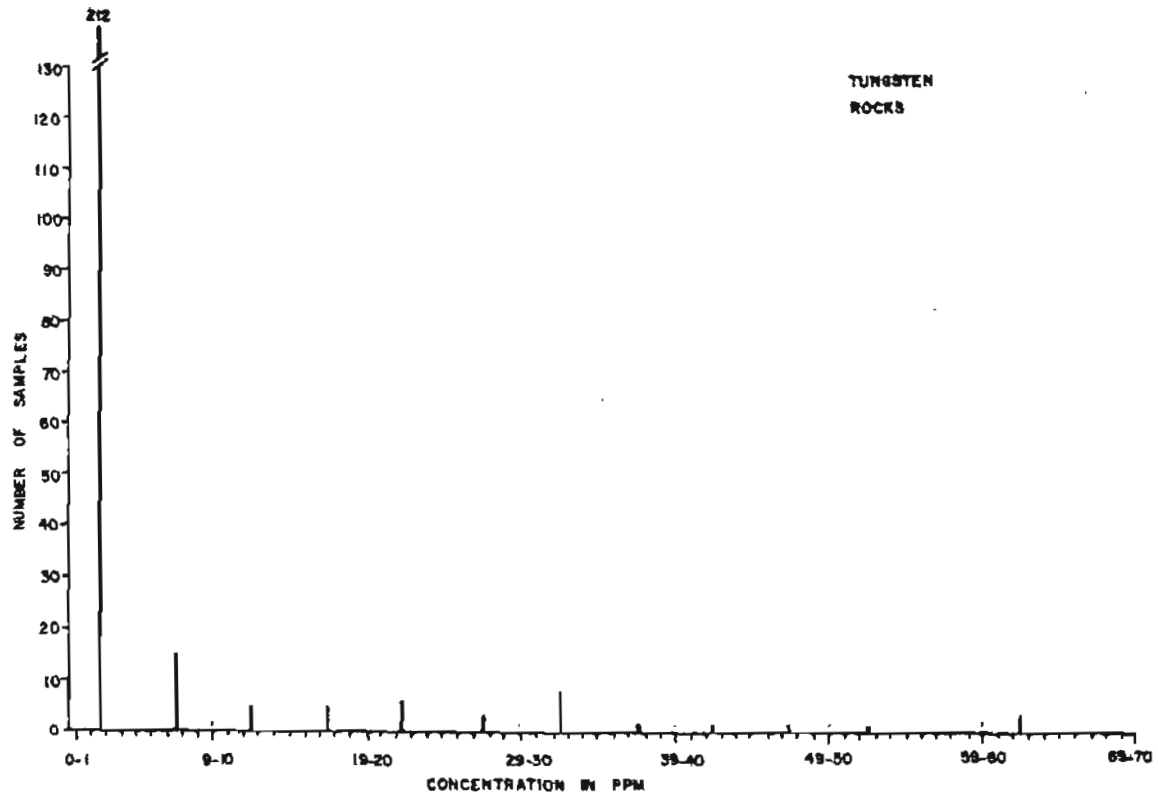


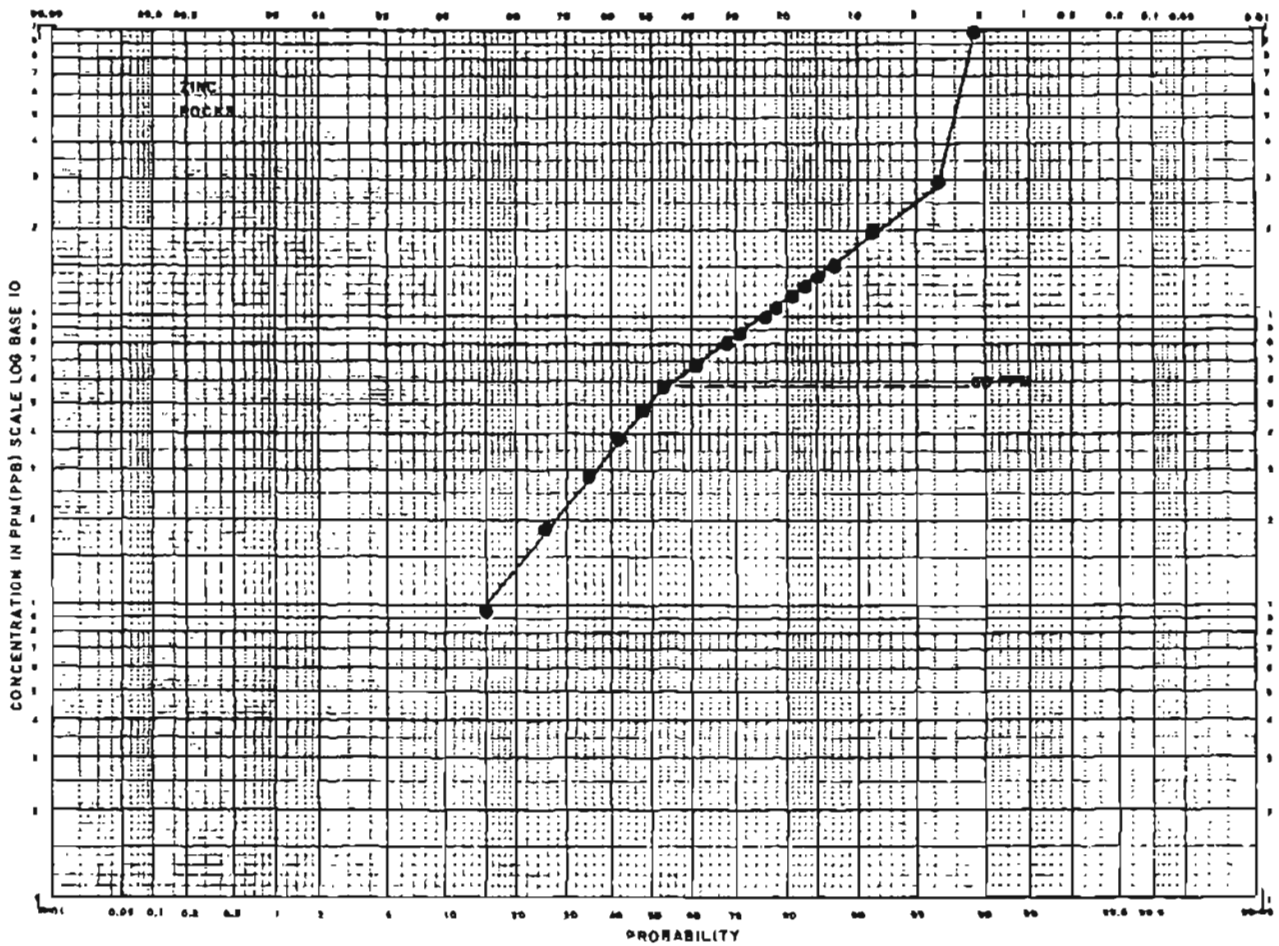
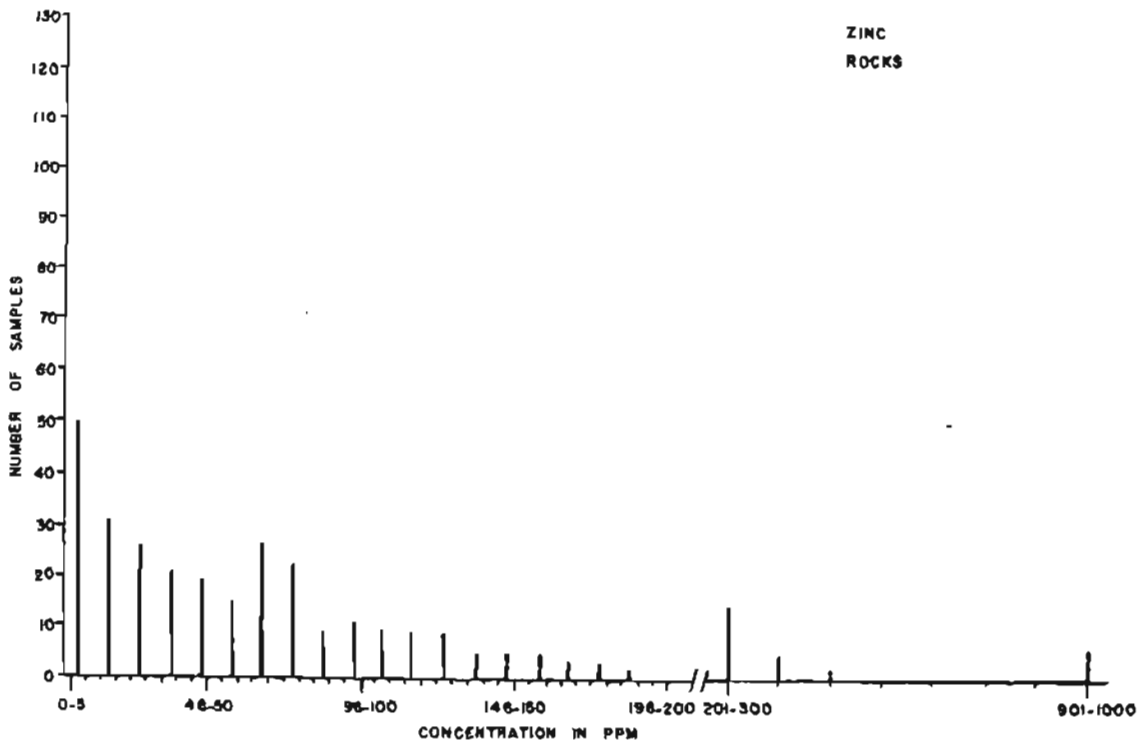












**APPENDIX D1**  
**Summary of Placer Mines and Prospects in**  
**the Fairbanks Mining District, Alaska**

Table D1  
Placer mines and prospects in the Fairbanks mining district, Alaska.

Name	Township and Range	Average Gold Fineness (after Metz and Hawkins, 1980)	Commodity	Description (after Menzie and others, 1983)	Reference
1. Alder Creek	T3N,R3E	867	Au(?)	Possibly auriferous gravels were prospected in 1907. No definite report of mining. Location on creek not given.	Brooks, 1908; Prindle, 1908; Ellsworth and Parker, 1911
2. Bear Creek	T3N,R2E		Au(?)	Has been prospecting.	Ellsworth, 1910
3. Bedrock Creek	T3N,R1E	829	Au,Sn,W	Cassiterite and scheelite in concentrates. Bedrock has been mined from an open-cut on Discovery and milled. Gold (certainly placer and probably lode) were mined.	Brooks, 1923; Joesting, 1942; Byers, 1957
4. Big Eldorado Creek	T2N,R1W	--	Au	Stream flows in asymmetrical valley. Thick mass of terrace deposits on gentle slope. In upper part of valley gold is in gravel 50 ft deep. Has been minor production of gold. Includes reference (Prindle and Katz, 1913 (B 525), p. 106) to Eldorado Creek.	Brooks, 1908, 1916; Prindle, 1908; Prindle and Katz, 1909, 1913; Smith, 1917
5. Chatanika River	T3N,R1E	894	Au	Placers are deep; about 200 ft at mouths of Dome and Vault Creeks. From 1911 to 1927 all mining was from drift mines; dredging began near mouth of Cleary Creek in 1928 and continued until World War II; drift mining was reported as recently as 1938. See also: (Cleary Creek, near Fairbanks), (Dome Creek), (Vault Creek).	Prindle and Katz, 1909, 1913; Ellsworth and Parker, 1911; Brooks, 1914; Smith, 1917, 1930, 1932, 1933, 1934, 1936, 1937, 1938, 1939, 1941, 1942; Koschmann and Bergendahl, 1968; Mulligan, 1974
6. Chatham Creek	T3N,R1E	875	Sb,Au, Sn,W	Bedrock schist; granitic rock near head. Mining, largely by open-cut methods, in most years from 1903 to 1915. Production through 1910 was worth about \$300,000. Dredge operated from 1926 or 1927 to 1934. Stibnite has been found in veins in schist and was common on piles of dredge tailings. Concentrates contain scheelite and cassiterite as well as gold and stibnite.	Prindle, 1904, 1906, 1908, 1910; Brooks, 1905, 1907, 1916; Purington, 1905; Ellsworth, 1910, 1912; Ellsworth and Davenport, 1913; Prindle and Katz, 1913; Chapin, 1914; Eakin, 1915; Smith, 1929, 1930, 1932, 1933, 1934, 1936, 1937; Joesting, 1942, 1943; Kilhean and Merue, 1951; Byers, 1957
7. Cleary Creek, near Fairbanks	T3N,R2E	904	Sb,Au, Sn,W	Bedrock schist. Creek and its major tributaries head in mineralized zone that extends from Last Chance Creek to Fairbanks Creek. With tributaries, was most productive placer-gold stream in Fairbanks district; from 1903	Prindle, 1904, 1905, 1906, 1908; Brooks, 1905, 1907, 1908, 1911, 1914, 1915, 1916, 1918,

Table D1 (Continued)

Name	Township and Range	Average Gold Fineness (after Metz and Hawkins, 1980)	Commodity	Description (after Menzie and others, 1983)	Reference
				through 1924 production was about 1,129,650 fine oz worth \$23,349,900. Most was from drift mines working a pay streak 150 ft wide and with an average thickness of 5 ft. Beginning in 1924 and until as recently as 1940 dredges also operated. Concentrates contained gold, stibnite, cassiterite, scheelite, pyrite, garnet, and rutile. A lens of stibnite 75 ft long was uncovered by placer mining near mouth of Willow Creek. See also (Chatanika River).	1922, 1923, 1925; Collier, 1925; Hess and Graon, 1905; Purington, 1905; Prindle and Katz, 1909, 1913; Ellsworth, 1910, 1912; Johnson, 1910; Ellsworth and Parker, 1911; Hess, 1912; Ellsworth and Davenport, 1913; Chapin, 1914; Eakin, 1915; Smith, 1917, 1926, 1929, 1932, 1933, 1934, 1936, 1937, 1938, 1939, 1941, 1942; Martin, 1919, 1920; Brooks and Martin, 1921; Brooks and Capps, 1924; Capps, 1924; Moffit, 1927; Hill, 1933; Joesting, 1942, 1943; Thorne and others, 1948; Killeen and Murtle, 1951; Wedow, Killeen, and others, 1954; Byers, 1957; Burand, 1968; Koschmann and Bergendahl, 1968; Cobb, 1973
8. Crane Creek (Gulch)	T3N,R2E	908	Au	About 1,765 oz of gold (as mined) produced in 1908.	Prindle and Katz, 1913
9. Cripple Creek	T1S,R2W	865	Au, Sn	Bedrock mainly mica schist. In early days (1908-1913) most (if not all) production was from benches. Some of ground as much as 100 ft deep. Preparations for large-scale dredging began 1936; dredge began operating in 1940. Rare cassiterite has been reported from placers.	Brooks, 1907, 1908; Prindle, 1908; Ellsworth, 1910, 1912; Ellsworth and Davenport, 1913; Prindle and Katz, 1913; Chapin, 1914; Smith, 1938, 1939, 1941, 1942; Joesting, 1942
10. Deep Creek	T3N,R3E	886	Au	Gold discovered, 1913. More recent data probably included with that on Fairbanks Creek.	Chapin, 1914
11. Dome Creek	T2N,R1E	930	Au,Sn,W	Ground 30 to 200 ft deep. Pay streak 130-165 ft wide and about 5 ft thick. Production, including that from tributaries, from 1903 through 1920 was about 394,245 fine oz worth \$8,149,000. Mining	Prindle, 1906, 1908; Brooks, 1907, 1908, 1914, 1915, 1918, 1922, 1923; Prindle

Table D1 (Continued)

Name	Township and Range	Average Gold Fineness (after Metz and Hawkins, 1980)	Commodity	Description (after Mezzie and others, 1983)	Reference
				continued until as recently as 1940. Concentrates contained gold, scheelite, and a little cassiterite. See also (Chatanika River).	and Katz, 1909, 1913; Ellsworth, 1910, 1912; Ellsworth and Parker, 1911; Ellsworth and Davenport, 1913; Chapin, 1914; Eakin, 1915; Smith, 1917, 1930, 1932, 1934, 1936, 1937, 1938, 1939, 1941, 1942; Martin, 1919, 1920; Brooks and Martin, 1921; Capps, 1924; Moffit, 1927; Joesting, 1942, 1943; Thorne and others, 1948; Byers, 1957; Koschmann and Bergendahl, 1968; Mulligan, 1974
12. Emma Creek	T1S,R3W	--	Au(?)	May have been a little mining in 1910.	Ellsworth and Parker, 1911
13. Engineer Creek	T1N,R1E	901	Au	Depth to bedrock from about 50 ft to more than 100 ft. Gold in basal 4-7 ft of gravel, much of which was derived from granite. Placer mining reported in most years from 1907 to 1916. Later mining (mainly dredging) was probably with that on Goldstream.	Prindle, 1908; Prindle and Katz, 1909, 1913; Ellsworth, 1910, 1912; Ellsworth and Parker, 1911; Ellsworth and Davenport, 1913; Brooks, 1914; Chapin, 1914; Eakin, 1915; Smith, 1917, 1933
14. Ester Creek	T1S,R2W	896	Sb,Au,W	Placer deposits (both stream and bench) deeply buried; bedrock floor between Ester and Cripple Creeks nearly flat. Mined from 1905 to 1963; dredged from 1937 on. Stibnite and scheelite in concentrates. Includes references to (Esther Creek); see also (Cripple Creek).	Prindle, 1906, 1908; Brooks, 1907, 1908, 1911, 1914, 1915, 1916, 1918, 1922, 1923, 1925; Prindle and Katz, 1909, 1913; Ellsworth, 1910, 1912; Ellsworth and Parker, 1911; Ellsworth and Davenport, 1913; Chapin, 1914; Eakin, 1915; Smith, 1917, 1926, 1929, 1930, 1932, 1933, 1934, 1936, 1937, 1938, 1939, 1941, 1942; Martin, 1919,

Table D1 (Continued)

Name	Township and Range	Average Gold Fineness (after Metz and Hawkins, 1980)	Commodity	Description (after Menzie and others, 1983)	Reference
					1920; Brooks and Martin, 1921; Brooks and Capps, 1924; Capps, 1924; Moffit, 1927; Joesting, 1924; Killeen and Merlie, 1951; Wedow, Killeen, and others, 1954; Byers, 1957; Burand, 1966; Koschmann and Bergendahl, 1968, Cobb, 1973
15. Eva Creek	T1S,R2W	824	Au	Placer gold mining or prospecting, 1911-15. No data on total production; about 24,000 fine oz recovered in 1912. Mining near mouth may have been reported for Ester Creek. Many lode prospects on ridge east of Eva Creek.	Ellsworth, 1912; Ellsworth and Davenport, 1913; Chapin, 1914; Eakin, 1915; Brooks, 1916
16. Fairbanks Creek	T3N,R3E	896	Sb,Au, Ag,Sn,W	Bedrock mainly schist; from 15 to 110 or more ft deep. Placer mining from 1903 to as recently as 1940. Dredging began in 1911, but drift and other mining also continued. Production, including that from tributaries, from 1903 through 1920 was about 380,115 fine oz worth \$7,857,000. Minerals in concentrates included gold, wolframite, cassiterite, rutile, stibnite, and scheelite. Mineralized schist, opened by a short tunnel, carries 60 oz silver per ton and \$4 in gold (gold at \$20.67 an oz) per ton. Quartz stringers carry the same amount of gold, but no silver.	Prindle, 1904, 1905, 1906, 1908; Brooks, 1905, 1907, 1908, 1911, 1914, 1915, 1916, 1918, 1922, 1923, 1925; Purington, 1905; Prindle and Katz, 1909, 1913; Ellsworth, 1910, 1912; Johnson, 1910; Ellsworth and Parker, 1911; Hess, 1912; Ellsworth and Davenport, 1913; Smith, 1913, 1917, 1926, 1929, 1930, 1932, 1933, 1934, 1936, 1937, 1938, 1939, 1941, 1942; Chapin, 1914; Eakin, 1915; Martin, 1919, 1920; Brooks and Martin, 1921; Brooks and Capps, 1924; Capps, 1924; Moffit, 1927; Joesting, 1942; Wedow, Killeen, and others, 1954; Byers, 1957; Chapman and Foster, 1969; Cobb, 1973

Table D1 (Continued)

Name	Township and Range	Average Gold Fineness (after Metz and Hawkins, 1980)	Commodity	Description (after Menzie and others, 1983)	Reference
17. First Chance Creek (tributary of Goldstream Creek)	T2N,R1E	915	Au,Sn,W	Gold reported as early as 1908 and as recently as 1940. Some of ground mined was as much as 42 ft deep. Abundant placer scheelite derived from lodes at head of creek; clogged some sluice-box riffles. Cassiterite rare in concentrates.	Prindle and Katz, 1909, 1913; Ellsworth, 1912; Ellsworth and Davenport, 1913; Chapin, 1914; Eakin, 1915; Smith, 1917, 1939, 1941, 1942; Joesting, 1942; Byers, 1957
18. Fish Creek	T2N,R2E	902	Sb,Bi,Au, Sn,W	Stream into which Fairbanks Creek flows. Mining, probably mainly drifting, began about 1909 where depth to bedrock was about 25 ft; continued until about 1916. Dredging began in 1926, continued through 1935, and was resumed in 1940; other types of mining also reported, 1927-40. Stibnite, auriferous bismuth nuggets, cassiterite, and scheelite in concentrates. No data on total gold production. See also Vogt (Fairbanks quadrangle).	Prindle and Katz, 1909, 1913; Ellsworth, 1910, 1912; Ellsworth and Parker, 1911; Ellsworth and Davenport, 1913; Brooks, 1914; Smith, 1917, 1929, 1930, 1932, 1933, 1934, 1936, 1937, 1938, 1939, 1941, 1942; Eakin, 1915; Joesting, 1942; Wedow, Killen, and others, 1954; Wedow, White, and others, 1954; Byers, 1957; Hasler and others, 1973
19. Flume Creek	T2N,R1E	903	Au	Has been placer mining. Probably was normally reported with that on Pedro Creek.	Brooks, 1916; Chapman and Foster, 1969
20. Fox Creek	T2N,R1E	897	Au, W	Placer gold mined sporadically from as early as 1908 to as recently as 1926; gravels 6-19 ft deep; hand methods only. Much scheelite (estimated 90% of concentrates) near head of creek. Granite at head of creek. Lode near mouth has been prospected for gold.	Prindle, 1908; Prindle and Katz, 1909, 1913; Ellsworth, 1910; Smith, 1913, 1929; Joesting, 1943; Thorne and others, 1948; Byers, 1957; Mulligan, 1974
21. Gilmore Creek	T2N,R1E	933	Bi,Au,W	Granitic rocks and area with lode scheelite occurrences in contact-metamorphosed limestone and gold-bearing quartz veins near head. Gravels (stream and bench) as much as 60 ft deep. Mined from 1905 to as recently as 1940. Dredge tailings now in lower valley. Concentrates contained bismuth, some intergrown with gold, and scheelite.	Prindle, 1906, 1908; Prindle and Katz, 1909, 1913; Ellsworth, 1910, 1912; Ellsworth and Parker, 1911; Ellsworth and Davenport, 1913; Chapin, 1914; Eakin, 1915; Brooks, 1916, 1918; Smith, 1917, 1938, 1939, 1941, 1942; Joesting, 1942; Wedow,

Table D1 (Continued)

Name	Township and Range	Average Gold Fineness (after Metz and Hawkins, 1980)	Commodity	Description (after Menzie and others, 1983)	Reference
					Killeen and others, 1954; Wedow, White and others, 1954; Byers, 1957
22. Happy Creek	T1N,R2W	961	Au	Gold placer mining, 1913--16, 1938-40. Some ground as deep as 140 ft. (See also Dorothy and Dorice)	Brooks, 1914, 1916; Chapin, 1914; Eakin, 1915; Smith, 1917, 1939, 1941, 1942
23. Hill Creek	T2N,R2E	931	Au	Eluvial placer developed on and in weathered granite of a stock; gold derived from a mineralized zone near the contact between granite and schist.	Prindle, 1908; Brooks, 1911, 1925
24. Iowa Creek	T1N,R3E		Au	One report of gold worth \$19.00 per oz (old price).	Prindle and Katz, 1913
25. Last Chance Creek	T2N,R3E		Au	Placer mining, 1911-14. Includes reference to (First Chance Creek, tributary Fish Creek).	Ellsworth, 1912; Ellsworth and Davenport, 1913; Chapin, 1914; Eakin, 1915
26. Little Eldorado Creek	T3N,R1E	891	Au,Sn,W	Bedrock mainly schist; heads in quartz diorite of Pedro Dome. Concentrates contain gold, cassiterite, scheelite, and wolframite. Mining 1907-27, 1930-31, 1938-40 or later. Production through 1926 was worth \$2,414,000 (about 116,800 fine oz). No dredging. Includes references to (Eldorado Creek).	Brooks, 1908, 1914, 1915, 1916, 1918, 1922, 1923, 1925; Prindle, 1908; Prindle and Katz, 1909, 1913; Ellsworth, 1910, 1912; Johnson, 1910; Ellsworth and Parker, 1911; Ellsworth and Davenport, 1913; Smith, 1913, 1917, 1926, 1929, 1930, 1933, 1939, 1941, 1942; Chapin, 1914; Eakin, 1915; Martin, 1919, 1920; Brooks and Martin, 1921; Capps, 1924; Moffit, 1927; Joesting, 1942; Byers, 1957
27. Little Nugget Creek	T2N,R2E		Au	Has been placer mining.	Chapman and Foster, 1969
28. Melba Creek	T2N,R2E		Au	Has been placer mining. See also Vogt.	Chapman and Foster, 1969
29. Monte Cristo Pup	T2N,R2E		Au	Placer mining in 1914.	Eakin, 1915
30. Moose Creek, tributary of Estez Creek	T1S,R3W		Sb,Au	Stibnite makes up cobbles as much as 6 in. in diameter in old placer workings. No further data on placer activity on this creek	Killeen and Mertie, 1951

Table D1 (Continued)

Name	Township and Range	Average Gold Fineness (after Metz and Hawkins, 1980)	Commodity	Description (after Menzie and others, 1983)	Reference
				in this or any other reference to mining in the Fairbanks district, but it is safe to assume that the placer miners were looking for and found some gold.	
31. Nugget Creek, tributary of Goldstream Creek	T1N,R3W	853	Au	Placer gold mining, 1938-40.	Smith, 1939, 1941, 1942
32. Nugget Creek, tributary of Smallwood Creek	T2N,R2E		Au	Has been placer mining.	Chapman and Foster, 1969
33. O'Connor Creek	T2N,R2W		Au	Stream flows in an asymmetrical valley similar to that of Big Eldorado Creek. Ground 100-130 ft deep. About 55 oz of gold worth \$18.00 per oz mined in 1907.	Prindle, 1908; Prindle and Katz, 1913
34. Our Creek	T2N,R2W	908	Au	Very little mining; probably less than 250 oz gold produced. Production reported in 1908 only. Where mined depth to bedrock was 75 ft.	Brooks, 1908; Prindle, 1908; Prindle and Katz, 1909, 1913
35. Pearl Creek	T2N,R2E	908	Bi,Au,W	Placer gold mined 1911-14, 1938-40. Concentrates contain native bismuth, wolframite, and much scheelite. Creek heads in area with occurrences of lode scheelite. Includes references to (Yellow Pup Creek); see also White Association.	Ellsworth, 1912; Ellsworth and Davenport, 1913; Chapin, 1914; Eakin, 1915; Mertie, 1918; Hill, 1933; Smith, 1939, 1941, 1942; Joesting, 1942, 1943; Wedow, White and others, 1954; Byers, 1957
36. Pedro Creek (Fairbanks quadrangle)	T2N,R1E	913	Au,Sn	Site of first gold discovery in district. Headwater branch of Goldstream Creek. Placers mainly deep and frozen. Mined, 1902 to as recently as 1940; dredge from 1930 on. Cassiterite is a rare constituent of concentrates. Production usually reported as part of Goldstream basin. See also (Pedro Creek) Livengood quadrangle.	Prindle, 1905, 1906, 1908; Purington, 1905; Brooks, 1907, 1914, 1916, 1918; Prindle and Katz, 1909; Ellsworth, 1910, 1912; Ellsworth and Parker, 1911; Ellsworth and Davenport, 1913; Chapin, 1914; Eakin, 1915; Smith, 1917, 1929, 1930, 1932, 1933, 1934, 1936, 1937, 1938, 1939, 1941, 1942; Joesting, 1942; Wedow, Killeen and others, 1954; Koschmann and Bergendahl, 1968; Cobb, 1973

Table D1 (Continued)

Name	Township and Range	Average Gold Fineness (after Metz and Hawkins, 1980)	Commodity	Description (after Menzie and others, 1983)	Reference
37. Pedro Creek (Livengood quadrangle)	T2N,R1E		Au,Sn	Site of original discovery of placer gold in district, 1902. Depth to bedrock 8-40 ft. Concentrates contain gold, magnetite, garnet, rutile, pyrite, and cassiterite. Mining was by drifting, open cuts, dredges; from 1903 to as recently as 1940. No mining reported 1917-25. Data on mining frequently combined with that for Goldstream, Fairbanks quadrangle. See also (Pedro Creek) Fairbanks quadrangle.	Prindle, 1904, 1905, 1906, 1908; Purington, 1905; Brooks, 1905, 1907, 1914, 1916, 1918; Prindle and Katz, 1909, 1913; Ellsworth, 1910, 1912; Ellsworth and Parker, 1911; Ellsworth and Davenport, 1913; Chapin, 1914; Eakin, 1915; Smith, 1917, 1929, 1930, 1932, 1933, 1934, 1936, 1937, 1938, 1939, 1941, 1942; Joesting, 1942; Wedow, Killeen and others, 1954; Cobb, 1973
38. Ready Bullion Creek	T1S,R2W	871	Au	Placer gravels as much as 80 ft below surface. Mined from 1907 to 1914. Production well over 25,000 fine oz. Several hundred tons of ore said to have been mined from broken veins and masses of quartz in schist on ridge SW of creek.	Ellsworth, 1910, 1912; Ellsworth and Parker, 1911; Ellsworth and Davenport, 1913; Prindle and Katz, 1913; Chapin, 1914; Eakin, 1915; Chapman and Foster, 1969
39. Rose Creek, placer	T2N,R1E	885	Au,W	Has been placer gold mining. Scheelite in concentrates. Includes reference to (New Years Pup).	Prindle and Katz, 1913; Chapin, 1914; Byers, 1957
40. St. Patrick Creek	T1N,R2W	878	Au	Placer mining or prospecting between 1909 and 1916. No good data on amount produced, but it was undoubtedly small by Fairbanks district standards. Many lode mines and prospects in drainage basin.	Ellsworth, 1910, 1912; Ellsworth Parker, 1911; Prindle and Katz, 1913; Eakin, 1915; Smith, 1917
41. Sheep Creek	T1N,R2W		Au	Has been placer mining.	Chapman and Foster, 1969
42. Smallwood Creek	T1N,R2E	948	Au	Bedrock is schist with granite at head of creek. Placer ground is deep (40 ft near head of creek increasing downstream to more than 300 ft); gold in 3-4 ft of gravel and upper part of bedrock. Mining reported from 1907 to 1916 and in 1927. No data on total production or composition of concentrates.	Brooks, 1908, 1914; Prindle, 1908; Prindle and Katz, 1909, 1913; Ellsworth, 1912; Ellsworth and Davenport, 1913; Chapin, 1914; Smith, 1917, 1930
43. Steamboat Pup (Creek)			Au	Has been placer mining. Data on activity and production were probably included with those for Pedro Creek in most years.	Prindle and Katz, 1918; Brooks, 1916; Chapman and Foster, 1969

Table D1 (Continued)

Name	Township and Range	Average Gold Fineness (after Metz and Hawkins, 1980)	Commodity	Description (after Menzie and others, 1983)	Reference
44. Steel Creek, placer	T1N,R1E	901	Au	Has not been particularly profitable drift mining of deeply buried frozen gold placer.	Mulligan, 1974
45. Treasure Creek	T2N,R1W	919	Au	Gold discovered, 1906, and drift mined until about 1913. Deposit permanently frozen, deep (200 ft), about 7 ft thick, and as much as 225 ft wide. Production more than \$250,000; possibly as much as \$500,000. Lode gold (no other data given) near mouth of a tributary.	Brooks, 1907, 1914; Prindle, 1908; Prindle and Katz, 1909, 1913; Ellsworth, 1910, 1912; Ellsworth and Davenport, 1913; Smith, 1913; Chapin, 1914; Mulligan, 1974
46. Twin Creek	T2N,R1E	898	Au, Sn	Bedrock is quartzite schist and porphyritic granite. Most of placer ground was shallow (12 ft is deepest mentioned). Cassiterite in concentrates. Mined sporadically from 1903 to 1927.	Prindle, 1904, 1905; Brooks, 1905, 1916; Purington, 1905; Prindle and Katz, 1909, 1913; Johnson, 1910; Ellsworth and Davenport, 1913; Chapin, 1914; Eakin, 1915; Smith, 1917, 1930; Joesting, 1942
47. Vault Creek	T3N,R1W	900	Au	Bedrock probably all schist. Placers up to about 200 ft deep. Near mouth in Chatanika Flats alluvium is 319 ft thick; gold on false bedrock at 160 ft. Gold on upper creek coarse; one-third of pieces worth \$1 or more (gold at \$20.67 per fine oz). Most of mining before World War II was drift mining. Mining from 1906 to as recently as 1940. Gold production, including that from tributaries, through 1924 was about 133,000 fine oz worth \$2,749,000. No data on composition of concentrates. See also (Chatanika River).	Brooks, 1907, 1908, 1914, 1915, 1916, 1918, 1922, 1923, 1925; Prindle, 1908; Prindle and Katz, 1909, 1913; Ellsworth, 1910, 1912; Ellsworth and Parker, 1911; Ellsworth and Davenport, 1913; Chapin, 1914; Eakin, 1915; Smith, 1917, 1926, 1929, 1933, 1934, 1936, 1937, 1938, 1939, 1941, 1942; Martin, 1919, 1920; Brooks and Martin, 1921; Brooks and Capps, 1924; Capps, 1924; Moffit, 1927; Koschmann and Bergendahl, 1968; Mulligan, 1974
48. Walnut Creek	T3N,R3W		Au	Coarse gold recovered from shallow ground, 1906-08, 1912. Any more recent production probably included with that from Fairbanks Creek.	Ellsworth and Parker, 1911; Prindle and Katz, 1913; Ellsworth and Davenport, 1913

Table D1 (Continued)

Name	Township and Range	Average Gold Fineness (after Metz and Hawkins, 1980)	Commodity	Description (after Menzie and others, 1983)	Reference
49. Wildcat Creek	T2N,R1W	899	Au	Gold-bearing gravels for about half a mile above mouth. A little mining reported 1908-15.	Prindle and Katz, 1913; Ellsworth and Davenport, 1913; Brooks, 1914, 1916; Chapin, 1914
50. Wolf Creek	T3N,R2E	858	Au	Gold is bright and some very rough. Ground as much as 60 ft deep; gold in base of gravel and top 2 ft of bedrock. Sporadic mining from 1903 to 1915 and 1937-40.	Prindle, 1904, 1905, 1906, 1908; Ellsworth, 1910; Ellsworth and Parker, 1911; Ellsworth and Davenport, 1913; Prindle and Katz, 1913; Chapin, 1914; Eakin, 1915; Brooks, 1916; Smith, 1917, 1939, 1941, 1942

**APPENDIX D2**  
**Summary of Placer Mines and Prospects in**  
**the Circle Mining District, Alaska**

Table D2  
Placer mines and prospects in the Circle mining district, Alaska.

Name	Township and Range	Average Gold Fineness (after Metz and Hawkins, 1980)	Commodity	Description (after Menzie and others, 1983)	Reference
1. Bear Creek	T7N,R10E			Years of known activity: 1972-1983.	ADGS
2. Bedrock Creek	T8N,R13E		Au,Cu,W,Th	Granitic intrusion into mica schist. Sample of granite when concentrated contained 10 percent monazite and a small amount of scheelite. Also present: pyrrhotite, garnet, ilmenite, zircon, biotite, topaz, and malachite. Fluorometric tests indicated the presence of uranium in several minerals but not in amounts to be of economic interest. Concentrates from gravel on upper Bedrock Creek contain tin and tungsten.	Eberlein and others, 1977, p. 18; Barker, 1979, p. 10; Nelson, West, and Matzko, 1954, p. 13
3. Birch Creek	T5N,R11E	874	Au	Gold was discovered somewhere on Birch Creek in 1893, and was the initial discovery in the Circle district. Production began the following year. Placer production has been largely from major tributaries such as Harrison Creek (see Harrison Creek) but there has been minor production from Birch Creek proper, largely river bars, of which Buckley Bar was probably the most productive.	Koschmann and Bergendahl, 1968, p. 23; Brooks, 1907, p. 192; Eberlein and others, 1977, p. 18
4. Birch Creek, South Fork	T5N,R16E		Au	Years of known activity: 1977 and 1980.	ADGS
5. Bonanza Creek	T8N,R12E	850	Au(Pb)	Placer gold known to be present in valley of Bonanza Creek since early days of the Circle camp (1895-1896), but serious mining apparently was not undertaken until 1927. Mining reported most years from 1929 to 1937. Work on upper part of creek in 1980. Pay streak in lower valley 75-150 ft wide. Locally derived gravel is well rounded, of moderate size, 3-6 ft thick, and overlain by 2-8 ft of muck. Most of mining on lower part of creek, where bedrock is mostly blocky quartzite and quartz-mica schist, chlorite schist, and graphitic schist (Bonanza Creek sequence). Gold rather coarse with considerable intergrown quartz. Nuggets reported as large as 10 1/2 oz. Little variation in fineness of the gold over a 10 yr mining period (mean = 850 gold, 140 silver). Gold, zircon, garnet, ilmenite, pyrrhotite, pyrite, and galena present in heavy concentrate. On upper part of the creek 6 ft of gravel lies on weathered bedrock; pay streak is 150 ft to 200 ft wide. Some tin and zinc recovered with the gold. Largest nugget reported was 1 oz.	Eberlein and others, 1977, p. 18

Table D2 (Continued)

Name	Township and Range	Average Gold Fineness (after Metz and Hawkins, 1980)	Commodity	Description (after Menzie and others, 1983)	Reference
6. Bottom Dollar Creek (tributary of Harrison Creek)	T7N,R14E	714	Au	Placer gold discovered in winter 1909-1910. Prospecting or small-scale mining reported 1909-1910, 1912, 1936, 1938-1939. Sluicing 1975. Some small operations in 1984. Pay streak narrow and gold distribution spotty. Most all gravels in narrow creek bed have been processed for gold at least once. Fineness reportedly ranged from 702-797 gold, 195-285 silver. (See also Half Dollar Creek and Two Bit Gulch)	Eberlein and others, 1977, p. 18
7. Boulder Creek (tributary of Crooked Creek)	T8N,R13E		Au,Sn,(Cu, RE's,U)	Good placer gold prospects reported in benches, 1916. Mining 1929 and possibly at other times. Mining operations were suspended in 1975 due to the difficulty of operating a sluice box in gravels with heavy concentrations of cassiterite. It was estimated by the miner that the pay gravels were yielding in excess of 2 lbs of cassiterite per yard at the mine. Gold occurred primarily as thin irregular flakes. Hematite, magnetite, and scheelite also occurred in the concentrate. Depths to bedrock about 8 ft with most of the gold localized in lower 3 1/2 ft of the gravel. Bedrock is schist intruded by granitic rocks. Concentrate from sample of granite contained 45 percent allanite and 15 percent chalcopyrite (by volume) and several other minerals which gave positive fluorimetric tests for the presence of uranium. Granitic bedrock also contains vugs of fluorite.	Eberlein and others, 1977, p. 18; Barker, 1979, p. 8
8. Butte Creek (tributary to Birch Creek southwest of Gold Dust Creek)	T7N,R11E	915	Au	Placer mining reported in 1916, 1937, perhaps 1932, and 1983. A hydraulic plant was installed in 1916 but operated only a short time because of scarcity of water. No production data but weighted mean of all gold mined through 1937 was 900 parts gold and 88 parts silver per thousand. Stream drains bedrock area of quartz-mica schist and chlorite schist with abundant arsenopyrite and pyrite (Bonanza Creek sequence). Gravel deposits in the stream bed are 250 ft wide and consist of large rounded boulders of quartz and quartzite up to 1/2 m in diameter.	Eberlein and others, 1977, p. 19; Brooks, 1918, p. 56
9. Crooked Creek	T9N,R13E	828		Gold known in the valley of Crooked Creek near mouth of Deadwood Creek since early 1900's but was too disseminated for profitable exploitation by the crude hand methods of that time. Placer mining in 1952 assumed to be near the mouth of Mammoth Creek. Mining activity from 1973-1984 near mouth of Mammoth Creek and eastward for	Brooks, 1907, p. 192; Cobb, 1976, p. 15; Brown, Luong, and Forshang, 1982, p. 419

Table D2 (Continued)

Name	Township and Range	Average Gold Fineness (after Metz and Hawkins, 1980)	Commodity	Description (after Menzie and others, 1983)	Reference
10. Deadwood Creek	T8N,R14E	824	Au,Sn,W, (Hg)	<p>several km. At least 2 units of gravel present; an upper gray gravel and an underlying, weathered, orange-colored gravel; both carry gold. Gold flakes very flattened, commonly 1-3 mm in largest dimension. Lower gravel unit is probably Tertiary in age.</p> <p>Placer gold discovered 1894 and mining has continued with few interruptions until the present time. Dredge operated in 1937-1938, but most of the production has been by other methods. Some claims worked in 1896 yielded 2 to 3 oz gold per man per day. One source (Prindle, 1905) reports total production through 1903 was about 72,570 oz; another (Brooks, 1907) indicates about 33,850 oz 1894-1906. Gold at that time had been found in commercial quantities from a point about a mile above the mouth throughout the length of the creek, a distance of nearly 9 mi. Gold placers in gravels of present creek and in benches along northwest side of valley. Principal bedrock is massive quartzite schist and quartz-mica schist with subordinate carbonaceous and chloritic schist (Bonanza Creek sequence) intruded in places by granitic rocks and their fine-grained equivalents. Mafic dikes also present. Alluvial deposits of valley floor range from 5-20 ft. Schist cut by numerous quartz veins, some of which contain metallic minerals. Gravel (3-14 ft thick) derived mostly from local bedrock; overlain by a few inches to 8 ft or more of muck. Gold occurs both in the gravels and in crevices in bedrock. Near the mountain front 6-9 ft of gray gravel overlies an orange brown silty-clayey pebble gravel with weathered clasts; both units contain fine gold. Creek gold is generally flattened and in places rather flaky; nuggets to 6 oz. Bench gold is rougher and more lumpy. Mean fineness on basis of seven assays from 1934 through 1936 production is 796 gold, 198 silver. Fineness remains constant downstream from Switch Creek, but increases upstream. Minerals in placer concentrates include gold, cassiterite, wolframite (all three of which were recovered during mining), scheelite, cinnabar, arsenopyrite, galena, pyrite, tourmaline and garnet. Several of these heavy minerals contain small amounts of uranium. Fluorite is present in granite. Gravels below Discovery Gulch contain wolframite and gold with pieces of quartz attached. Wolframite not known to occur in placers above this gulch. (See also Switch Creek)</p>	Eberlein and others, 1977, p.19; Brooks, 1907, p. 188-193; Prindle, 1905, p. 56-61; Cobb, 1976, p. 16

Table D2 (Continued)

Name	Township and Range	Average Gold Fineness (after Metz and Hawkins, 1980)	Commodity	Description (after Menzie and others, 1983)	Reference
11. Discovery Gulch	T7N,R14E			(Also see Deadwood Creek)	ADGS
12. Eagle Creek	T7N,R11E	883	Au	Gold discovered in 1895. Since 1901 much profitable mining has been done on this stream from the mouth to near the heads of Mastodon and Miller forks. Mining reported nearly every year through 1984. Production through 1906 about 29,000 fine oz. Bedrock mainly quartzitic schist cut by numerous quartz veins. Schistosity strikes N 60°E; dips 30°-40°NW. Pay streak 150-200 ft wide extended down Mastodon Fork and Eagle Creek in present stream gravels 5-20 ft thick and overlain by 2-15 ft of muck. Gold in gravel and upper few feet of bedrock; coarse-grained and intergrown with considerable quartz. Most of the gravels in the main creek have been mined. Bar gravels bordering Eagle Creek carry coarse gold and were being prospected in 1980. Fineness about 883 gold, 108 silver, with overall general increase downstream. Grade is about highest reported for Marmoth and Deadwood Creeks area.	Brooks, 1907, p. 197; Spurr, 1898, p. 293, 354-355; Eberlein and others, 1977, p. 20; ADGS
13. Eastley Creek	T8N,R14E			Bedrock is syngranite which weathers to tors. Years of known activity: 1979 and 1980.	ADGS
14. East Great Unknown Creek	T6N,R12E			Years of known activity: 1974 and 1976-1983.	ADGS
15. Fish Creek	T7N,R11E			Years of known activity: 1972-1983.	ADGS
16. Fryingpan Creek	T6N,R11E		Au	Good values reported by prospectors during winter 1909-1910 in hole about 20 ft deep. More recent activity in 1974-1984. Schist bedrock; 4-5 ft of pay gravel beneath 15 ft of overburden. No record of any production.	Eberlein and others, 1977, p. 20; ADGS
17. Gold Dust Creek	T7N,R11E		Au	Gravel of Gold Dust Creek prospected during 1936. Two active placer operations during 1975 and active mining in 1980 to present. Stream heads south of Mastodon Dome and drains area underlain by quartz-mica schist, graphitic schist (Bonanza Creek sequence), and mafic schist. Gold also reported in a fracture zone on this creek. Average thickness of gravel 4 m, average gold value \$3.50-\$5.00/yd <sup>3</sup> at \$500./oz. Concentrates include ilmenite granules up to 1/2 cm. Hematite nodules up to 2 cm, pyrite and scheelite. Gold fragments up to .75 cm across.	Eberlein and others, 1977, p. 20; ADGS

Table D2 (Continued)

Name	Township and Range	Average Gold Fineness (after Metz and Hawkins, 1980)	Commodity	Description (after Menzie and others, 1983)	Reference
18. Graveyard Creek	T8N,R14E			Activity unknown: 1977-1983.	ADGS
19. Greenhorn Creek (Greenhorn Gulch)	T7N,R14E		Au(Ag)	Mined as early as 1896. Intermittent activity to present. Gravels about 4 ft thick on bedrock of schist. Fragments of vein quartz contain disseminated free gold and weathered sulfide minerals. One such fragment assayed 24 oz silver per ton.	Eberlein and others, 1977, p. 20
20. Half Dollar Creek	T7N,R14E	721	Au(Sn,W)	Placer gold discovered winter 1909-1910. Prospecting and (or) mining 1909-1914, 1935, 1938-1942 and probably 1976-1983. Pay streak narrow and gold distribution spotty. Cassiterite abundant and scheelite common in placer concentrates but no indication that either was recovered during mining. Granitic rocks exposed in drainage basin contain allanite, garnet, hematite, limonite, pyrrhotite, sphene and zircon. Fluorimetric tests indicate the presence of uranium in several of these minerals. (See also Bouzon Dollar Creek and Two Bit Gulch)	Eberlein and others, 1977, p. 20; ADGS
21. Harrison Creek	T6N,R13E	837	Au,(Sn)	Gold discovered at Pitka Bar (at mouth of North Fork) in 1893. Intermittent mining until 1929. Mining reported annually except one year, 1929-1984. The most productive placers are located on the North Fork. Bedrock mainly weathered mafic schist, quartz-mica and mica schist cut by numerous quartz veins. Fragment of one such vein contained grains of gold as much as 3/16 in diameter. Gravel, mostly unfrozen, of moderate size, and 4-12 ft thick, with little or no overlying muck. Gravel composed mostly of pebbles and cobbles of locally derived schist and subordinate granitic rocks. Gold in lower 3 ft of gravel and upper foot or two of bedrock. Gold in the gravel tends to be fine grained, flaky and bright; that on and near bedrock is fairly coarse. Mean fineness, based on 13 North Fork assays, is 837 gold, 154 silver. Distribution of gold values and occurrence of attached quartz suggest derivation from diverse local sources. Concentrates contain a little cassiterite and considerable garnet and pyrite. This creek has been extensively mined. (See also Harrison Creek, North Fork, and South Fork)	Eberlein and others, 1977, p. 21; Cobb, 1976, p. 30; ADGS
22. Harrison Creek, North Fork	T7N,R12E	861	Au	Before the middle of 1896 the whole of the North Fork of Harrison Creek was staked. Prospecting and (or) mining	Spurr, 1898, p. 351; Brooks, 1907, p. 188; Ellis-

Table D2 (Continued)

Name	Township and Range	Average Gold Fineness (after Metz and Hawkins, 1980)	Commodity	Description (after Menzie and others, 1983)	Reference
				1905, 1924, 1953-1981. Most of the creek has been mined. Gravels are about 4 m thick and the pay streak 30-40 m wide. Gold has worked its way into the fractures in the bedrock as far as 1 m. Three varieties of gold are present: an orange gold, a yellow gold, and silver-colored gold. Bedrock is tightly folded and fractured mafic schist. (See also Harrison Creek)	worth, 1910, p. 238; ADGS
23. Harrison Creek, South Fork	T6N,R12E		Au	Years of known activity: 1977, 1979-1983	Eakins and Daniels, 1980, p. 19; ADGS
24. Holdem Creek	T8N,R14E		Au	Gold discovered in 1932. Mined 1933-1934. Bedrock is porphyritic granite which weathers to tors. (See also Ketchem Creek)	Eberlein and others, 1977, p. 21
25. Hot Springs Creek	T8N,R15E		Au	Scheelite, allanite, sphene and zircon present; last 3 minerals indicated as uranium and (or) thorium bearing, but no analytical data available. Bedrock is syenogranite.	Cobb, 1976, p. 35
26. Independence Creek	T8N,R12E	810	Au(Pb,Sr, RE's,U,W)	Gold placers have been worked since 1894 or 1895. Creek has been a steady large producer to present time, although its pay streak is not as rich as the best part of the Mastodon Creek pay streak. The gold is very "flat." Bedrock is mica schist, quartz-mica schist, chlorite schist, and graphitic schist (Bonanza Creek sequence) cut by numerous quartz veins. Pay gravel as much as 425 ft but generally no more than 325 ft wide, 4-8 ft thick, and overlain by 0-10 ft of muck. The gold is fine-grained and lies mainly within 3 ft of the gravel-bedrock contact. In one part of creek weighted mean fineness (eight assays) was 787 gold, 201 silver; in another it was 810 gold, 175 silver (five assays representing 1500 oz of gold). Gold fineness increases progressively downstream. Source of gold believed by miners to be localized in area of Mastodon Dome. Heavy minerals in placer concentrates; wolframite, xenotime, zircon, garnet, and hematite, some of which are slightly uraniferous. (See also Mammoth, Mastodon, and Miller Creek)	Eberlein and others, 1977, p. 21
27. Ketchem Creek	T8N,R15E	783	Au(Sr,RE's, U,W)	Placer gold mined 1933-1940 and more recently including 1975 and 1989. Creek drains contact zone between quartz-mica schist and granitic intrusive. 4-17 ft of moderate sized gravel overlain by 3-7 ft of sand and muck.	Eberlein and others, 1977, p. 22

Table D2 (Continued)

Name	Township and Range	Average Gold Fineness (after Metz and Hawkins, 1980)	Commodity	Description (after Menzie and others, 1983)	Reference
28. Loper Creek	T8-9N, R10E	900	Au	Granite boulders 3-4 ft diameter were a serious problem in the area just below Holden Creek. Gold in lower part of gravel, in the upper part of the bedrock, and in a fine-grained arkosic sand that locally covers the bedrock surface. Gold is fine-grained, but pieces weighing 7-10 grains have been found. Some of the gold has considerable quartz attached. Fineness reported 783 parts gold and 207 parts silver per thousand. Heavy concentrates also contain scheelite, cassiterite, allanite, garnet, sphene, and zircon, some of which contain small amounts of uranium. (See also Holden Creek)	Eberlein and others, 1977, p. 22; ADGS
29. Mammoth Creek	T8N,R12E	831	Au (Cu,Pb, RE's,U,Mo,W)	Gold discovered 1894. Production through 1906 almost 100,000 oz. Mined mostly by hydraulic methods before 1915. Dredging in 1915-1916 and 1936-1940. Bedrock mainly quartzitic micaceous schist, chlorite schist, and graphitic schist (Bonanza Creek sequence) cut by granitic bodies. About 12 ft of locally derived gravel overlain by 3 ft overburden. Gold in upper valley fairly coarse and light colored. Fineness about 831, increasing downstream. Source of gold believed to be quartz veins and mineralized zones in the bedrock. Sample of granite talus contained allanite, galena, molybdenite, scheelite, iron sulfide minerals and hematitic, copper carbonate minerals, garnet and topaz. Presence of uranium detected by fluorimetric tests. (See also Independence, Mastodon, and Miller Creeks)	Eberlein and others, 1977, p. 21; Cobb, 1976, p. 41
30. Mastodon Creek	T8N,R12E	840	Au (Sn)	Mined 1894 to as recently as 1989. Dredges operated 1912-1913 and 1918-1926. Total gold production well over 150,000 oz (one of the largest producing creeks in Circle district). Bedrock mainly chlorite schist, quartzite and graphitic schist (Bonanza Creek sequence) cut by numerous quartz veins and locally by granitic rocks. Closely folded impure limestone near mouth. Depth to bedrock 10-15 ft. Pay streak in lower valley about 200 ft wide and 7-10 ft thick in mostly unfrozen gravels. Gold coarsest near head of stream and contains much quartz. Downstream the gold becomes more flaky, carries less quartz and shows an increase in	Eberlein and others, 1977, p. 22; ADGS

Table D2 (Continued)

Name	Township and Range	Average Gold Fineness (after Metz and Hawkins, 1980)	Commodity	Description (after Menzle and others, 1983)	Reference
31. Miller Creek	T8N,R12E	832	Au	<p>fineness (820-854). Cassiterite reported in concentrates. (See also Mammoth, Independence, and Miller Creeks)</p> <p>Placer gold mined intermittently from 1894-1984, but apparently has not been a large producer. Bedrock mainly chlorite schist, graphitic schist, quartzite and quartzitic schist (Bonanza Creek sequence) veined with quartz. Granitic dikes occur on divide between Miller and Eagle Creeks. Gravel 4-16 ft thick including about 4 ft of overlying admixed muck. Locally, up to 3 ft of clay between bedrock and gravel which contains most of the gold; at most places gold found in lower few feet of gravel and upper part of decomposed bedrock. Pay streak has maximum width of about 50 ft. Weighted mean, based on seven assays of production in 1919, 1920, 1923, 1924, and 1928, representing 965 oz of gold, had a fineness 832 gold, 162 silver. (See also Independence, Mastodon, and Mammoth Creeks)</p>	Spurr, 1898, p. 349-350; ADGS; Eberlein and others, 1977, p. 23
32. Porcupine Creek	T9N,R11E	820	Au (Ag)	<p>Placer gold discovered in 1890's but mining was intermittent and on small scale until 1930's. Some mining in late 1950's and (or) early 1960's. Two operators active in 1975, and activity in 1980-1989. Placers mined in 1936 consisted of about 13 ft of gravel overlain by about 2 ft of muck with mining over about 1000 ft of creek bed. Bedrock is chlorite schist, graphitic schist, and marble (Bonanza Creek sequence), quartzitic schist and quartz mica schist with vertical foliation, locally. Gravel composed mostly of bedrock material. Most pebbles do not exceed a foot in diameter and average size is much less. Some boulders as large as 3 ft in diameter have been uncovered in mining operations. Gold mainly on and in bedrock and is coarse, ragged and shotty. Numerous nuggets; some to 2-3 oz, all with considerable quartz attached. Weighted mean of gold mined 1934 and 1935 shows a fineness of 822 gold, 168 silver. An assay of gold produced in 1936 shows a fineness of 818 gold and 172 silver. Gravel being mined in 1980 was 3-8 m thick, pay streak 30-70 m wide, and there are 2 layers of "pay." Along with the gold, cassiterite and scheelite occur. A four-ounce nugget was recently recovered, although an 8 1/2 oz nugget was reportedly recovered and is the largest nugget known</p>	Eberlein and others, 1977, p. 23; Bakins, and Daniels, 1980, p. 21

Table D2 (Continued)

Name	Township and Range	Average Gold Fineness (after Metz and Hawkins, 1980)	Commodity	Description (after Menzie and others, 1983)	Reference
				from the area. A little cassiterite occurs in the concentrates. A mineralized zone has been prospected near the head of Dome Creek, a small tributary of Porcupine Creek and may be a source of some gold and (or) tin in the placers. (See also Porcupine Dome and Yankee Creek)	
33. Portage Creek (flows into Medicine Lake)	T7N,R15E	806	Au(W,RE's, Sn)	Gold discovered in early 1900's. About 10 oz said to have been recovered from one claim in 1906. Sustained mining began about 1933. Mining hampered by many large boulders. Two operators active 1975 and other work has been done more recently. Values of \$17.00/yd <sup>3</sup> at \$500/oz gold reported. Bedrock is syenogranite. Cassiterite a common constituent of placer concentrates. No data on production or occurrence of the gold. Heavy concentrates also include allanite, arsenopyrite, hematite, ilmenite, magnetite, monazite, uranothorite, zircon, apatite, sphalerite, sphene, garnet, scheelite, cassiterite, bismuthinite, wolframite, and topaz. Fluorite occurs in vugs in granite.	Eberlein and others, 1977, p. 24
34. Portage Creek (tributary to Birch Creek)	T6N,R15B			Years of known activity: 1976, and 1979-1984.	ADGS
35. Parmigan Creek (heads below Porcupine Dome)	T7N,R11E			Years of known activity are 1925, 1953, 1954 and 1969-1982. Bedrock is chlorite schist, and quartzite (Bonanza Creek sequence).	Burand, 1965, p. 28; ADGS
36. Sawpit Creek	T8N,R13E			Years of known activity include 1958 with various years up to 1983.	ADGS
37. Squaw Creek (Squaw Gulch)	T7N,R14E	891	Au	Gold discovered as early as 1894. Prospected and mined on small scale through 1896 and some activity known from 1953-1984. The channel is narrow with little gravel but good color can be obtained by panning. In 1981 coarse gold with values of \$5-15/yd <sup>3</sup> at \$500/oz gold were recovered from coarse gravel.	Eberlein and others, 1977, p. 24; ADGS
38. Switch Creek	T7N,R14E	760	Au (Pb,W7)	Important source of placer gold from 1906 intermittently until World War II and 1942-1956. Some activity from 1963-1983. Both drift and hydraulic mining. Bedrock is mainly quartzitic schist and quartz-mica schist cut by numerous quartz-feldspar veins and intruded by granitic plutons. Some of the quartz-feldspar veins carry arsenopyrite. Schist gar-	Eberlein and others, 1977, p. 24

Table D2 (Continued)

Name	Township and Range	Average Gold Fineness (after Metz and Hawkins, 1980)	Commodity	Description (after Menzie and others, 1983)	Reference
				netiferous near contacts with granitic rocks. Both present creek and bench gravels carry gold. Gold coarse; large nuggets have quartz attached. Weighted mean of eight assays showed fineness of 760 gold, 231 silver (somewhat lower than that from Deadwood Creek). Concentrates contain gold, arsenopyrite, pyrite, galena, magnetite, ilmenite, garnet, tourmaline, and limonite. Wolframite reported on lower Switch Creek.	
39. Thomas Creek	T6N,R13E			Years of known activity: 1974-1981. Bedrock is calc schist and minor graphitic schist.	ADGS
40. Two Bit Gulch	T7N,R14E		Au	Good placer gold prospects found and profitable mining during winter 1909-1910. Pay streak is narrow and irregular. Any other activity in this gulch probably was reported under Half Dollar Creek. Bedrock is granodiorite. (See also Half Dollar Creek)	Eberlein and others, 1977, p. 25
41. Willow Creek (between Bear Creek and Fish Creek)	T7N,R10E		Au	Years of known activity: 1958 and 1972 and various other years up through 1983.	ADGS
42. Willow Creek (east of Loper Creek)	T9N,R10E		Au	Years of known activity: 1977-1978, and 1980-1983.	ADGS
43. Yankee Creek	T8N,R11E		Au (Sn)	Small camp established in 1932 near junction with Porcupine Creek. Mined intermittently through 1984. Bedrock is chlorite schist, quartzite, graphitic schist, and marble (Bonanza Creek sequence). Cassiterite associated with the placer gold. Source of both believed by miners to be mineralized zone on Porcupine Dome. (See also Porcupine Creek and Porcupine Dome)	Eberlein and others, 1977, p. 25; ADGS

APPENDIX D3  
Summary of Placer Mines and Prospects in  
the Steese Mining District, Alaska

Table D3  
Placer mines and prospects in the Steese mining district, Alaska.

Name	Township and Range	Average Gold Fineness (after Metz and Hawkins, 1980)	Commodity	Description (after Menzie and others, 1983)	Reference
1. American Creek	T8N,R7E	905	Au	Years of known activity: 1954, 1974, and 1975.	ADGS
2. Bachelor Creek (tributary to Preacher Creek)	T8N,R8E	—	Au	Placer gold discovered 1908. Considerable mining activity during the summer of 1909. In 1910 small-scale mining of bench gravel. Present stream gravels are unfrozen, average 7 to 8 ft thick, and consist mainly of schist with considerable proportion of vein quartz and some granite porphyry. Only reported production was from low bench gravels 20 ft thick on east side of creek. Bedrock principally quartz-mica, quartzitic, and carbonaceous schist (Paleozoic and/or) Precambrian cut by sill-like body of granite porphyry 75 ft thick parallel to schistosity (N 60° E)	Ellsworth, 1910, p. 238; Prindle, 1910, p. 208; Eberlein and others, 1977, p. 18; Cobb, 1976, p. 5
3. Champion Creek	T7N,R4E	941	Au	Staked for placer gold in 1976.	Barker and Clautice, 1977, p. 4
4. Charity Creek	T7N,R7E	—	Au	Placer gold discovered in early 1900's or earlier. Development work that had been underway for several years was not continued in 1909. Mining in 1979. Creek drains area of schist intruded by granitic rocks. Gravel thickness 6-8 ft with little muck cover. Pay streak from top of gravel to 2 ft into bedrock. Richest values \$10/yd at \$300/oz gold. A sample panned in 1980 produced 1 color. (See also Homestake Creek)	Eberlein and others, 1977, p. 19
5. Convert Creek	T8N,R7E	—		Years of known activity: 1974-1977.	ADGS
6. Deep Creek	T6N,R7E	902	Au	Small placer mine operated in 1946 with possible activity in 1968. No information on production, but probably small as indicated from workings. Creek drains schist bedrock (Paleozoic and/or) Precambrian cut by bodies of granitic rocks (Late Cretaceous-early Tertiary). (See also Faith Creek)	Eberlein and others, 1977, p. 19; ADGS
7. Homestake Creek	T7N,R7E		Au	Placer gold mined in early 1900's. No mining reported in literature after 1912. Gravel 8 ft thick. Gold said to have been found in place along intrusive contact between schist (Paleozoic and/or) Precambrian and granite porphyry (Late Cretaceous-early Tertiary). (See also Charity Creek)	Eberlein and others, 1977, p. 21

Table D3 (Continued)

Name	Township and Range	Average Gold Fineness (after Metz and Hawkins, 1980)	Commodity	Description (after Menzie and others, 1983)	Reference
8. Hope Creek	T7N,R7E		Au	Placer gold discovered early 1900's, but apparently never mined extensively. Bedrock is quartzite and quartzitic schists intruded by granitic rocks. Samples of granite from near head of creek contained trace to small amounts of allanite(?), fluorite, galena, malachite, molybdenite, pyrite, pyrrhotite, rutile, scheelite, stibnite, and other heavy minerals. Stibnite, reported to have been found in bedrock in 1926, apparently buried.	Cobb, 1976, p. 34
9. Idaho Creek	T6N,R8E			Scheelite, allanite, sphene and zircon present; last 3 minerals indicated as uranium and/or thorium bearing, but no analytical data available.	Cobb, 1976, p. 35
10. Little Champion Creek	T7N,R5E		Au(U)	Staked for placer gold in 1976. Anomalous amounts of uranium (as much as 570 ppm) were detected in sediment samples from springs localized along contact of the Mount Prindle granitic pluton (early Tertiary) with quartzite schist, micaceous quartzite and lesser amounts of quartz-mica, phyllitic and calcareous schist (Paleozoic and/or Precambrian). Stream sediments in area were found to contain up to 400 ppm uranium.	Barker and Clautice, 1977, p. 4; Eberlein and others, 1977, p. 22
11. McManus Creek	T6N,R8E			Years of known activity: 1980 and 1981.	ADGS
12. McKinley Creek	T8N,R9E			Years of known activity: 1974-1977.	ADGS
13. Moose Creek (east of Table Top Mountain)	T6N,R5E			Years of known activity: 1974-1981.	ADGS
14. Nome Creek	T6N,R5E	901	Au(Sn,Th)	Placer gold discovered 1910. Dredging 1926-1931, 1939-1940, 1946 and probably later. Mining in progress several seasons between 1960 and 1982. Most of the mining has been from about 1 km above the junction with Summer Creek to the junction with Moose Creek, a distance of about 10 km. Some work was also done on Sumner Creek just above its junction with Nome Creek. Creek heads in Mt. Prindle area where a small early Tertiary pluton intruded Paleozoic and/or Precambrian schist. Ground about 15 ft deep with 2-4 ft of pay gravel. No data on production, but workings suggest total is substantial. Concentrates also contain cassiterite, monazite, topaz, and tourmaline. Heavy fraction reportedly contained eU of 0.012 percent.	Eberlein and others, 1977, p. 23; Cobb, 1976, p. 50; ADGS

Table D3 (Continued)

Name	Township and Range	Average Gold Fineness (after Metz and Hawkins, 1980)	Commodity	Description (after Menzie and others, 1983)	Reference
15. Preacher Creek	T8-12N, R8-11E		Au	Gold strike reported in 1913, but may have been a strike on Bachelor Creek or Loper Creek. Numerous claims have been staked at various localities on Preacher Creek and minor tributaries in 1928 and 1976-1981. Claims near localities 92a, e, and g on the main stream were active 1978-1981; claims near locality 92c were active in 1928 and 1979-1981. Claims on small, unnamed tributaries near localities 92b, f, and h were active 1978-1981 and claims near 92d were active 1976-1981. No indication of any significant production from Preacher Creek.	Cobb, 1976, p. 56; ADGS
16. Sourdough Creek	T6N,R6E	928	Au (Sn,W,Sb)	Placer gold mined 1932-1940 and intermittently 1946-1959. Prospecting and maintenance work, 1966. Activity in various years through 1981. Total production not known, but about 2850 oz gold reportedly produced 1937-1941. 200 oz cleanup reported from single 300 ft by 150 ft cut on discovery claim. Little if any ground prospected ahead of mining. Creek has been largely mined. Gravel 10-11 ft thick. Gold reported to be mostly fine, 3/16 in. to flour size. Largest nugget 1/4 in. by 3/4 in. and flat. Bedrock is quartzite and quartzitic schist of Paleozoic and/or Precambrian age with a small granitic pluton of probable Late Cretaceous or early Tertiary near head of creek. Placer concentrates contain gold, stibnite, and sparse cassiterite. Stibnite and scheelite identified in samples of granitic rocks (talus). (See also Dempsey Pup)	Eberlein and others, 1977, p. 24
17. Twelve-mile Creek	T7N,R9E			Years of known activity: 1980-1982.	ADGS

**APPENDIX D4**  
**Summary of Placer Mines and Prospects in**  
**the Richardson Mining District, Alaska**

Table D4  
Placer mines and prospects in the Richardson mining district, Alaska.

Name	Township and Range	Average Gold Fineness (after Metz and Hawkins, 1980)	Commodity	Description (after Menzie and others, 1983)	Reference
1. Democrat	T7S,R7E	928	Au,Ag	Residual placer on Cretaceous rhyolite porphyry.	Brooks, 1909, 1923; Ellsworth, 1910; Ellsworth and Parker, 1911; Ellsworth and Davenport, 1913; Prindle and Katz, 1913; Chapin, 1914; Eakin, 1915; Smith, 1914, 1926, 1929, 1930, 1932, 1933; Saunders, 1965; Koschmann and Bergendahl, 1968; Cobb, 1972, 1977; Mulligan, 1974; Bundtzen and Reger, 1977; Eberlein and others, 1977; MacKevett and Holloway, 1977; Menzie and Foster, 1979
2. Buckeye Creek	T7S,R7E	693	Au,Ag, Pb,Sn,W	Residual placer on Cretaceous rhyolite porphyry.	Prindle and Katz, 1913; Smith, 1917, 1930, 1932; Brooks, 1918; Wedow and others, 1954; Saunders, 1965; Koschmann and Bergendahl, 1968; Cobb, 1972, 1977; Mulligan, 1974; Bundtzen and Reger, 1977; Eberlein and others, 1977; MacKevett and Holloway, 1977; Menzie and Foster, 1979
3. Hinkley Gulch	T7S,R7E		Au,Ag, Sn	Residual placer on Cretaceous rhyolite porphyry.	Smith, 1933; Saunders, 1965; Cobb, 1972, 1977; Bundtzen and Reger, 1977; Eberlein and others, 1977; MacKevett and Holloway, 1977; Menzie and Foster, 1979
4. Banner Creek	T7S,R7E	737	Au,Ag, Sn	Residual placer on Cretaceous rhyolite porphyry.	Brooks, 1908, 1909, 1918; Ellsworth, 1910; Ellsworth and Parker, 1911; Prindle and Katz, 1913; Chapin, 1914; Smith, 1917; Wedow and others, 1954; Saunders, 1965; Cobb, 1972, 1977; Bundtzen and Reger, 1977; Eberlein and others,

Table D4 (Continued)

Name	Township and Range	Average Gold Fineness (after Metz and Hawkins, 1980)	Commodity	Description (after Menzie and others, 1983)	Reference
5. Tenderfoot	T7S,R8E	901	Au,Ag, Pb	Evidence for stream capture. Schist and gneiss bedrock. Alluvium and loess near head of creek 30 ft thick; more than 155 ft thick near mouth. Creek was worked mainly by drifting, during which gold-bearing galena float was found. Stream was major producing creek in old Richardson gold district, the total production of which was about 95,000 oz of gold and 24,000 oz of silver before 1930 and an unknown amount since then. As of 1978 there has been recent prospecting, claim staking, and possibly a little mining.	1977; MacKevett and Holloway, 1977; Foster and others, 1979; Menzie and Foster, 1979  Prindle, 1906, 1908; Brooks, 1907; 1908, 1916, 1918, 1923; Ellsworth, 1910; Ellsworth and Parker, 1911; Ellsworth and Davenport, 1913; Prindle and Katz, 1913; Chapin, 1914; Smith, 1929, 1930, 1932, 1933; Wedow and others, 1954; Saunders, 1965; Koachmann and Bergendahl, 1968; Cobb, 1972, 1977; Mulligan, 1974; Bundtzen and Reger, 1977; Eberlein and others, 1977; MacKevett and Holloway, 1977; Eberlein and Menzie, 1978; Foster and others, 1979; Menzie and Foster, 1979

**APPENDIX D5**  
**Summary of Placer Mines and Prospects in**  
**the Tolovana Mining District, Alaska**

Table D5  
Placer mines and prospects in the Tolovana mining district, Alaska.

Name	Township and Range	Average Gold Fineness (after Metz and Hawkins, 1980)	Commodity	Description (after Menzie and others, 1983)	Reference
1. Amy Creek	T8N,R4W	918	Sb,Cr,Au	Bedrock mainly chert, some granite, basalt porphyry, limestone, and argillite. Some of ground as much as 100 ft deep. Concentrates contain gold, magnetite, limonite, chromite, pyromorphite, stibnite, and chrome spinel. Mining from 1918 to as recently as 1968.	Smith, 1917, 1926, 1929, 1930, 1932, 1933, 1934, 1936, 1937, 1938, 1939, 1941, 1942; Mertie, 1918; Martin, 1920; Overbeck, 1920; Brooks and Capps, 1924; Joesting, 1942; Foster, 1968; Cobb, 1973
2. Ester Creek	T8N,R4W		Au,Hg	Bedrock 20 ft deep where being mined in 1916; 90 ft deep farther downstream. Concentrates contain gold, magnetite, ilmenite, picotite, cinnabar, limonite, and zircon. Prospecting or mining, 1915-16, 1928-34. Includes references to (Lucky Gulch) if not definitely to (Goodluck Creek).	Brooks, 1916; Mertie, 1918; Smith, 1930, 1932, 1933, 1934, 1936; Malone, 1965
3. Franklin Creek (Gulch)	T8N,R5W		Au	Shallow placer mined, probably in 1915.	Brooks, 1916
4. Gertrude Creek	T8N,R5W	920	Au	Bedrock near mouth is chert. Bench and creek placers. Concentrates contain gold, magnetite, ilmenite, picotite, and zircon. Placer mining, 1915-18, and 1930 to as recently as 1940. A lode prospect is in silica-carbonate rock that contains minor amounts of gold. See also (Glen Gulch).	Brooks, 1916, 1918; Mertie, 1918; Martin, 1920; Overbeck, 1920; Smith, 1933, 1934, 1936, 1937, 1938, 1939, 1941, 1942; Foster, 1968; Koschmann and Bergendahl, 1968
5. Glen Gulch	T8N,R5W		Au	Fine, angular gold (a few pieces worth \$1, old price) in 204 ft of gravel on silicified limestone bedrock. Mining in 1916, 1931-34. See also (Gertrude Creek).	Mertie, 1918; Smith, 1933, 1934, 1936
6. Goodluck Creek	T8N,R4W	911	Cr,FM,Au, Hg,RE,Sn	Chert and silicified limestone apparently separated by a small body of diorite or greenstone. In 1916 or earlier a shaft sunk 60 ft to bedrock found some gold just above bedrock. Mining reported in 1918, 1934, and 1939. Concentrates contain gold, chromite, chrome spinel, limonite, hematite, magnetite, ilmenite, cinnabar, cassiterite, and a niobium-titanium-uranium-rare earth mineral of the euxenite-poly-crase series. Includes references to (Lucky Creek) (Gulch) if obviously to this stream.	Mertie, 1918; Martin, 1920; Smith, 1936, 1941; Joesting, 1942; Wedow, Killeen, and others, 1954; Wedow, White, and others, 1954; Cobb, 1973

Table D5 (Continued)

Name	Township and Range	Average Gold Fineness (after Metz and Hawkins, 1980)	Commodity	Description (after Meuzic and others, 1983)	Reference
7. Lillian Creek	T8N,R5W	926	Sb,Cr,Au Hg,Ni,Ag, W	Stream and bench placers; bedrock (sandstone, shale, and slate) surface beneath benches is irregular and slopes steeply toward the creek. Concentrates contain angular coarse gold, magnetite, ilmenite, picotite, chromite, limonite, cinnabar, scheelite, zircon, pyrite, stibnite, barite, arsenopyrite. A vein of stibnite is reported to have been uncovered during placer mining. A mineralized zone in a cut-bank contains stibnite and traces of cinnabar and gold. A sample of serpentine contained small amounts of nickel sulfides and silicates. Cinnabar in decomposed granitic material. Auriferous arsenopyrite-quartz-scorodite veins contain as much as 48 ppm gold and 2 ppm silver. Mining began in 1915 and was being carried on as recently as 1974.	Brooks, 1916, 1918; Smith, 1926, 1929, 1930, 1932, 1933, 1934, 1936, 1937, 1938, 1939, 1941, 1942; Mertie, 1918, 1923; Martin, 1920; Overbeck, 1920; Moffit, 1927; Joesting, 1942; Malone, 1965; Burand, 1966; Berg and Cobb, 1967; Foster and Chapman, 1967; Foster, 1968; Koschmann and Bergendahl, 1968; Cobb, 1973; Mulligan, 1974
8. Livengood Creek	T8N,R5W	934	Sb,Cr,Au, Sn,W	Gold discovered, 1914. Most of gold in old channel under bench parallel to and northwest of creek; traced for about 4 miles. Average depth to bedrock is 80 ft; average width of channel is about 125 ft. Bedrock mainly chert; some greenstone and limestone. Gold in basal gravel and weathered bedrock. Concentrates contain gold, magnetite, ilmenite, picotite, hematite, pyrite, barite, chromite, arsenopyrite, zircon, cassiterite, scheelite, monazite. Stibnite vein uncovered by placer drift mining; some said to have been shipped out by parcel post during World War I. Placer mining, 1914-1970. Dredge operated near town of Livengood in 1940, 1946, and probably other years. Plans for resuming large-scale mining, 1974. Complex geomorphic history; divided between Livengood and Hess Creeks shifted back and forth as a result of successive stream piracy.	Brooks, 1915, 1916, 1918, 1922, 1923, 1925; Smith, 1917, 1929, 1930, 1932, 1933, 1934, 1936, 1937, 1938, 1939, 1941, 1942; Mertie, 1918; Martin, 1920; Overbeck, 1920; Brooks and Martin, 1921; Brooks and Capps, 1924; Moffit, 1927; Joesting, 1942; Wedow, Killeen, and others, 1954; Berg and Cobb, 1967; Foster and Chapman, 1967; Foster, 1968; Koschmann and Bergendahl, 1968; Cobb, 1973; Eakins, 1974
9. Lucille Creek (Gulch)	T8N,R4W		Cr,Au	Considerable prospecting, but no record of mining, though there probably was some, as chromite and chrome spinels are reported to occur in the placers.	Mertie, 1918; Smith, 1936; Joesting, 1942; Foster, 1968
10. Myrtle Creek	T8N,R5W	933	Au	Gold reported to have been mined in 1916 probably was reconcentrated from bench deposit of Livengood Creek. See also (Livengood Creek).	Brooks, 1918; Cobb, 1973

Table D5 (Continued)

Name	Township and Range	Average Gold Fineness (after Metz and Hawkins, 1980)	Commodity	Description (after Menzie and others, 1983)	Reference
11. Olive Creek	T8N,R5W	907	Cr,Au,Hg, Ag,W	Bedrock is slate and sandstone intruded by now highly altered granitic rock. Cinnabar in altered rock; explored by about 270 ft of adits and tunnels; some material reported to run 20-30 lbs mercury per ton. Some mercury probably was recovered (Hudson property). Nearby an altered and brecciated felsic rock in chert and argillite contains gold and a little silver; pyrite and arsenopyrite present. Creek was a major placer-gold producer, 1914 to as recently as 1967. Some gold on sandstone bedrock and some on false bedrock 80 ft above true bedrock. Concentrates contained gold, magnetite, ilmenite, plentiful cinnabar, picotite, limonite, scheelite, chromite, pyrite, arsenopyrite, zircon. Includes references to: Hudson, Sunshine No. 2.	Brooks, 1915, 1916, 1918; Smith, 1917, 1929, 1930, 1932, 1933, 1934, 1936, 1938, 1939, 1941, 1942; Mertie, 1918; Martin, 1920; Overbeck, 1920; Brooks and Capps, 1924; Moffit, 1927; Joesting, 1942; Malone, 1962, 1965; Burand, 1966; Berg and Cobb, 1967; Foster and Chapman, 1967; Foster, 1968; Koschmann and Bergendahl, 1968; Cobb, 1973
12. Ruth Creek	T8N,R5W	866	Sb,Cr,Au, Hg,Ag, W	One of major gold-producing streams in Livengood area. Bedrock is a mixture of many types of Devonian sedimentary rocks (including much black crystalline limestone) and a variety of intrusive rocks. On spur west of creek quartz veinlets carry pyrite, arsenopyrite, and gold; some samples show as much as \$12 a ton in gold and \$2 a ton in silver (1916 prices). Many grains of chromite scattered through mineralized rock; some exposed by excavation about 1916. Stibnite vein exposed and reburied in placer cut. Some slightly auriferous breccia found at a lode prospect, late 1960's. Concentrates contain gold, scheelite, magnetite, cinnabar, chromite, pyrite, arsenopyrite, zircon, monazite, chrome spinels, stibnite.	Smith, 1917, 1926, 1929, 1930, 1932, 1933, 1934, 1936, 1937, 1938, 1939, 1941, 1942; Brooks, 1918; Mertie, 1918; Martin, 1920; Overbeck, 1920; Moffit, 1927; Joesting, 1941, 1942; Bates and Wedow, 1953; Wedow, Killeen, and others, 1954; Burand, 1966; Berg and Cobb, 1967; Foster and Chapman, 1967; Overstreet, 1967; Foster, 1968; Koschmann and Bergendahl, 1968; Cobb, 1973
13. Steel Creek	T7N,R4W		W	Wolframite in concentrate samples.	Joesting, 1943; Cobb, 1973
14. Wilbur Creek	T7N,R4W	818	Au	One of very few productive streams in area that do not drain Army Dome or Money Knob; source of gold not known. Gold had been found in either 1915 or 1921. Mining 1926 to as recently as 1940. No good data on geometry of deposit, composition of concentrates, or amount of production.	Brooks, 1916, 1923; Brooks and Capps, 1924; Smith, 1929, 1930, 1932, 1933, 1934, 1936, 1937, 1938, 1939, 1941, 1942; Cobb, 1973

**APPENDIX D6**  
**Classification of and Structural Data for Lode Mines and Prospects**  
**in the Kantishna Mining District, Alaska**

Table D6  
Classification of and structural data for lode mines and prospects in the  
Kantishna mining district, Alaska (after Bundtzen, 1981)

Map No.	Mine or Prospect	Mineral Deposit Type	Metals	Attitudes		Dimensions (Ave)					References
				Veins, Faults or Crushed Zones	Foliation of Country Rock	Width	Length	Depth (dip)	Grade	Surface Elev. (Ft.)	
1.	"Antimony Mine" or Slate Creek deposit Taylor Mine	V	Sb	N50E, 82SE	NS, 25W	6 m	120 m	?	45% Sb	2700	Wells, 1933; Capps, 1919, p. 107
2.	Brooker Mountain prospect	V	Sb	N75E	NS, 35W	?	20 m	?		3500	Bundtzen, 1981
3.	Upper Bunnell prospect	II	Sb,Pb,Ag	N50-55E, SE	N45W, 15S	0.5 m	?	?		2100	Bundtzen, 1981
4.	Bunnell prospect or Neversweat	II	Sb,Cu,Pb, Ag,W	E-W N70E, 50-75SE	N45W, 15S	?	?	?	0.34 OPT Au; 13.5 OPT Ag	2200	Wells, 1933
5.	Arizona claims	?	?	N20-50E	N45E, 25S	?	?	?		2800	Bundtzen, 1981
6.	Eagles Den or "Don Antimony"	V	Sb	N30W, 35NE	N60E, 15S	6 m	25 m	?		2100	Hawley, 1978
7.	Busia Mountain prospect (Lucky Tuesday)	V	Sb	E-W S30W	N75W, 10S	?	?	?		2500	Bundtzen, 1981
8.	Unnamed (75Ast3040)	?	?	N30E, 20NW	N15E, 20W	?	?	?		3400	Bundtzen, 1981
9.	Alpha mine (Virginia City claims)	IV	Sb,Cu,Pb, Ag	N70E	N40W, 35S	3 m	100 m	?		3000	Bundtzen, 1981

Table D6 (Continued)

Map No.	Mine or Prospect	Mineral Deposit Type	Metals	Attitudes		Dimensions (Ave)				References
				Veins, Faults or Crushed Zones	Foliation of Country Rock	Width	Length	Depth (dip)	Grade	
10.	Alpha Ridge claim	IV	?	N55E, 50SE	N80W, 20S	?	?	?	3000	Bundtzen, 1981
11.	Whistler	IV	Sb,Cu,Pb, Ag	NE	N20W, 40S	?	150 m	?	3000	Bundtzen, 1981
12.	Bright Light	IV	Pb,Ag,Zn	N-NE	N20W, 40W	?	?	?	2300	Bundtzen, 1981
13.	Eldorado No. 3	V	Sb	N75E	N50E, 15S	2 m	45 m	?	2000	Bundtzen, 1981
14.	Unnamed (75Ast2003)	I	Zn	N70E, 10SE	N70E, 10S	?	?	?	2000	Bundtzen, 1981
15.	Unnamed (75Ast2003)	IV	Pb	N35E, 80SE	N75E, 10S	0.8 m	?	?	1900	Bundtzen, 1981
16.	Iron Dome skarn	III	?	?	N5W, 20W	?	?	?	2200	Bundtzen, 1981
17.	Eureka-stibnite part of 'Pick' claim block	V	Sb	?	N50E, 40S	1.0 m	?	?	2000	Bundtzen, 1981
18.	Friday Rim (75Ast1998)	IV	?	?	N45E, 15W	?	?	?	2700	Bundtzen, 1981
19.	Red Top (includes Silver King extension)	IV	Sb,Cu,Au,Pb, Ag	N70E	N45E, 75W	3 m	?	?	2000	Bundtzen, 1981
20.	Galena	IV	Cu,Au,Pb,Ag	N45E, 65SE	N80E, 20N	2 m	?	?	2000	Bundtzen, 1981

Table D6 (Continued)

Map No.	Mine or Prospect	Mineral Deposit Type	Metals	Attitudes		Dimensions (Ave)				References	
				Veins, Faults or Crushed Zones	Foliation of Country Rock	Width	Length	Depth (dip)	Grade		Surface Elev. (Ft.)
21.	Lucky Strike	IV	Cu,Au,Pb,Ag	N55E, 84SE	N50E, 40S	2 m	65 m	?		2000	Bundtzen, 1981
22.	a) Star b) Friday c) Martha Q  d) Polly Wonder (Dalton Group)	IV	Cu,Au,Pb,Ag Cu,Au,Pb,Ag Cu,Au,Pb,Ag  Cu,Au,Pb,Ag	a) NW b) NE c) N15W, 56E d) EW, 65-70S	N45E, 75W	0.1 m	200 m	?		2000	Davis, 1922 Bundtzen, 1981 Bundtzen, 1981  Bundtzen, 1981
23.	a) Francis b) Little Maud	IV	Cu,Au,Pb,Ag,Zn Cu,Au,Pb,Ag,Zn	a) N75E b) N55E, 60-70SE	Horizontal	?	?	?		2500	Bundtzen, 1981 Davis, 1922; Wells, 1933
24.	Silver Pick (includes Darling Extension)	IV	As,Cu,Au,Pb, Ag,Zn	N88E, 63NW; N65SE, 67SE	Horizontal	?	500 m	?		2500	Seraphim, 1961
25.	Gold Eagle	IV	As,Cu,Au,Pb, Ag,Zn	N65E, 75SE	N70E, 45N	3 m	100 m	?		2500	Bundtzen, 1981
26.	Gold Dollar	IV	As,Cu,Au,Pb, Ag,Zn	N65E, 75SE	N70E, 45N	?	?	?		2500	Bundtzen, 1981
27.	Little Annie (includes Little Annie 2)	IV	As,Sb,Cu,An, Pb,Ag,Zn	N58E, SE	N70E, 45N	?	?	?		2700	Bundtzen, 1981
28.	Gold King	IV	As,Sb,Cu,An, Pb,Ag,Zn	N80E	Horizontal	2 m	?	?		2800	Bundtzen, 1981

Table D6 (Continued)

Map No.	Mine or Prospect	Mineral Deposit Type	Metals	Attitudes		Dimensions (Ave)				References
				Veins, Faults or Crushed Zones	Foliation of Country Rock	Width	Length	Depth (dip)	Grade	
29.	East Gold King Pittsburgh veins	?	?	?	Horizontal	2 m	?	?	2900	Davis, 1922
30.	Pennsylvania Keystone (includes William Julian Prospect and Perseverance Group)	IV	As,Sb,Cu,An, Pb,Ag,W,Zn	N30E; N65E, 85SE	Horizontal	3 m	450 m	?	2500	Bundtzen, 1981
31.	White Hawk	IV	As,Sb,Cu,An, Pb,Ag,Zn	NE	N10E, 50W	?	150 m	?	2000	Bundtzen, 1981
32.	Water Level claim	IV	As,Sb,Cu,Pb, Ag,Zn	N70E, 65NW	N45W, 50S	2 m	15 m	?	2000	Bundtzen, 1981
33.	Sulphide claim	IV	As,Pb,Ag	?	N45W, 50S	?	50 m	?	2200	Davis, 1922
34.	Silver King <sup>a</sup> and Merry Widow	IV	Cu,Pb,Ag,Zn	N70E, 65NW	?	2 m	15 m	?	2400	Bundtzen, 1981
35.	Banjo	IV	As,Sb,Cu,Au, Pb,Ag,W,Zn	NE	N15E, 25W	3 m	?	? 0.46 OPT Au, 0.52 OPT Ag	3000	Bundtzen, 1981
36.	Jupitar-Mars	IV	As,Sb,Cu,Au, Pb,Ag,W,Zn	N65-70E	N65E, 35N	3 m			3000	Bundtzen, 1981
37.	Chlorine prospect	IV	As,Pb,Ag,Zn	NE	N65E, 35N				3200	Bundtzen, 1981
38.	Unnamed (75Ast1941, 1942)	IV	?	N15E	N65E, 35N	?	?	?	3000	Bundtzen, 1981

Table D6 (Continued)

Map No.	Mine or Prospect	Mineral Deposit Type	Metals	Veins, Faults or Crushed Zones	Attitudes		Dimensions (Ave)			References	
					Foliation of Country Rock	Foliation of Country Rock	Width	Length	Depth (dip)		Grade
39.	Flourence Lode	IV	As,Sb,Cu,Pb Ag,Zn	N10E	N70E, 25N		1 m	11 m	?	3500	Bundtzen, 1981
40.	Unnamed (75As1949)			N40E	N70E, 25N		?	25 m	?	3400	Bundtzen, 1981
41.	Upper-Bosart vein	IV	Cu,Pb,Ag,Zn	N40-60E, SE	N20E, 30W		1.5 m	?	?	3000	Bundtzen, 1981
42.	Bosart prospect	IV	Sb,Cu,Pb,Ag,Zn	N50E	N20E, 30W		?	45 m	?	2800	Bundtzen, 1981
43a.	Unnamed (75As12960)	IV	As	N30W	N30W, 10S		?	?	?	3300	Bundtzen, 1981
43b.	Unnamed (75As12964)	IV	As,Pb	NW	N20W, 25S		?	?	?	3500	Bundtzen, 1981
44.	Waterloo (75As11955)	IV	Pb,Zn	N10W	N20E, 25W		0.6 m	?	?	3300	Bundtzen, 1981
45a.	Weiler or Parkey prospect	IV	Cu,Pb,Ag,Zn	N40E, 60-70SW	N50E, 10S		1.0 m	15 m	?	3300	Searphim, 1961
45b.	Eureka or Griess prospect	IV	Cu,Pb,Ag	N45E, 60NW	N50E, 10S		1.2 m	?	?	3300	Well, 1933; Capps, 1918
46.	Unnamed (75As11959)	IV	As	N-S	N45E, 35N		3 m	?	?	3500	Bundtzen, 1981
47.	Saddle prospect; (75As11960)	IV	As	N10E	N45E, 35N		3 m	?	?	3600	Bundtzen, 1981

Table D6 (Continued)

Map No.	Mine or Prospect	Mineral Deposit Type	Metals	Attitudes		Dimensions (Ave)				References
				Veins, Faults or Crushed Zones	Foliation of Country Rock	Width	Length	Depth (dip)	Grade	
48.	Unnamed (75Ast1964)	IV	As	N50E, 30NW	N50E, 30N	1.2 m	?	?	3100	Bundtzen, 1981
49.	Unnamed (75Ast1974)	IV	As	N20-40W	N40W, 40S	2 m	?	?	3300	Bundtzen, 1981
50.	Unnamed	IV	Pb	NE	NS, 35W	?	?	?	3500	Bundtzen, 1981
51.	McConnigill	IV	As,Pb,Ag,Zn	N58E, 34NW	N45E, 40W	3 m	100 m	? 1.45 OPT Au	3300	Davis, 1922, p. 131
52.	Glenn	IV	As,Pb,Ag,Zn	N80-85E	NS, 50W	3 m	250 m	?	4000	Capps, 1919; Wells, 1933
53.	Glenn Ridge 1 or Skookona prospect	IV	As,W	N20-40W, 65SW	NS, 25W	10 m	300 m	?	4000	Wells, 1931; Capps, 1919
54.	Pension(?) claim (75Ast 1973)	IV	As,Pb	NW	Horizontal	?	?	?	3500	Bundtzen, 1981
55.	Arkansas claim	IV	As,Pb,Ag	N70E	N40E, 40S	1.2 m	50 m	?	3500	Bundtzen, 1981
56.	Lloyd prospect	I	Cu,Zn	N30E	N30E, 25S	3 m	?	?	2800	Bundtzen, 1981
57.	Unnamed (75Ast2018-2019)	IV	Pb	N25-45E	N50E, 45N	1 m	?	?	4000	Bundtzen, 1981
58.	Unnamed	IV	As,Pb	?	N80E, 15N	?	?	?	3000	Bundtzen, 1981
59a.	Rainy Creek Ridge 1	IV	As,Sb,Pb	N75-85E	N80E, 55S	5 m	800 m	?	3800	Bundtzen, 1981

Table D6 (Continued)

Map No.	Mine or Prospect	Mineral Deposit Type	Metals	Attitudes		Dimensions (Ave)				References	
				Veins, Faults or Crushed Zones	Foliation of Country Rock	Width	Length	Depth (dip)	Grade		Surface Elev. (Ft.)
59b.	Rainy Creek Ridge 2	IV	As	N60-75E	N80E, 55S	5 m	?	?		3800	Bundtzen, 1981
60.	Lena and Silver Wire	IV	Cu,Pb,Ag	N60-70E, 80SE	N45E, 45N	1.5 m	?	?		4000	Bundtzen, 1981
61.	Humbolt	IV	As,Pb,Zn	N55E	N70E, 30N	1.0 m	?	?		3500	Capps, 1919, p. 99
62.	Ridge-Top claim or Spruce Creek #1	IV	Cu,Pb,Zn	N65E, 22NW	N65E, 42N	2.5 m	?	?		4300	Davis, 1927, p. 133; Wells, 1931, p. 374
63a.	Home Lode	V	Sb	?	N20W, 30S	?	?	?		2700	Wells, 1931
63b.	Caribou Lode or Last Chance	IV	As,Sb,Au,Ag	N15-20E, 50NW	N30E, 25W	2.0 m	180 m	?		2000	Hawley, 1978
64.	Unnamed (75Ast1861)	IV	?	N20-50E	N20E, 20W	?	?	?		3700	Bundtzen, 1981
65.	Mammoth Claim Lucky Jim(?)	IV	Cu,Pb	N40E	N70E, 25N	?	?	?		4200	Capps, 1919, p. 99; Davis, 1922, p. 132
66a,b.	Unnamed (75Ast1881)	I	As	N30E	N30E, 50S	2.0 m	80 m	?		3800	Bundtzen, 1981
66c.	Unnamed (75Ast1882, 1884)	I	As	N50-60E	N50E, 30S	?	?	?		4000	Bundtzen, 1981

Table D6 (Continued)

Map No.	Mine or Prospect	Mineral Deposit Type	Metals	Attitudes		Dimensions (Ave)				References
				Veins, Faults or Crushed Zones	Foliation of Country Rock	Width	Length	Depth (dip)	Grade	
67.	Unnamed (75Ast3061)	I	Sb,Pb,Zn	N15E	N15E, 30S	0.6 m	?	?	3500	Bundtzen, 1981
68.	Unnamed (75Ast2922)	I	Cu	N45E	N45E, 20S	2.0 m	?	?	4500	Bundtzen, 1981
69.	Unnamed (75Ast1914)	IV	Pb	NE	N55E, 40S	10 m	110 m	?	4700	Bundtzen, 1981
70a.	Moonlight-stibnite (Tosdal antimony)	IV	Sb	N30E, 20NW	N30E, 20W	0.25 m	2 m	?	3100	Bundtzen, 1981
70b.	Unnamed (75Ast2824)	IV	Pb	N10E, 20SE	N75E, 30S	?	?	?	3700	Bundtzen, 1981
71.	Unnamed; Canyon Creek occurrence	II	Sb	NE	N25E, 12W	?	?	?	2300	Bundtzen, 1981
72a.	Unnamed (75Ast1558)	IV	Cu	NE	N10E, 10W	0.3 m	?	?	2700	Bundtzen, 1981
72b.	Unnamed (75Ast1540)	IV	?	N35E, 45SE	Horizontal	?	?	?	3000	Bundtzen, 1981
73.	Stampede Mine (includes Glory, Surface, Hole, Emil Winze, and Mooney ore bodies)	V	Sb	NE	N35E, 25S	10 m	300 m	56% Sb	2300	Hawley, 1978
74.	Kobuk Lode	V	Sb	N74E	N40E, 20W	0.4 m	?	?	2200	Bundtzen, 1981

Table D6 (Continued)

Map No.	Mine or Prospect	Mineral Deposit Type	Metals	Attitudes		Dimensions (Ave)				References	
				Veins, Faults or Crushed Zones	Foliation of Country Rock	Width	Length	Depth (dip)	Grade		Surface Elev. (Ft.)
75.	'Clearwater Barite' (75Ast2548)	?	Ba	N5W, 40SW	N50E, 45N	1.0 m	?	?		1700	Bundtzen, 1981
76a.	Upper-Ridge claims	V	Sb	N10-35W	N10W, 80E	?	?	?		2800	Bundtzen, 1981
76b.	Nessie deposit	I	Sb	N65E, 20NW	N65E, 20W	?	?	?		3200	Bundtzen, 1981
77a.	Little Caribou prospect	III	Cu,Zn	?	N20E, 25W	1.5 m	?	?		2600	Bundtzen, 1981
77b.	Unnamed; 'Stibnite Caribou'	I	Sb	N20E	N20E, 25W	?	?	?		2900	Bundtzen, 1981
78.	Unnamed	III	Pb,Zn	?	NS, 30E	?	?	?		2100	Bundtzen, 1981
79.	'Crooked Creek prospect'	I	Ba	N20E	N20E, 50S	?	?	?		2000	Bundtzen, 1981
80a.	Gossan 1	I	Zn	N45E	N45E, 40W	?	?	?		2000	Bundtzen, 1981
80b.	Gossan 2	I	Zn	N45E	N45E, 40W	?	?	?		2000	Bundtzen, 1981
81.	Gossan 3	I	Zn	N45E	N45E, 40W	?	?	?		2000	Bundtzen, 1981
82.	Quartz Lode 1 (75Ast1754)	IV	Cu,Pb	N40W, 70SW	N50E, 40W	1.0 m	?	?		1700	Bundtzen, 1981
83.	Unnamed (75Ast1714)	IV	Pb,Zn	N20-40W	N50E, 20N	1.0 m	?	?		2000	Bundtzen, 1981
84.	Chitsia zone (75Ast1735)	I	Bz,Pb,Zn	N45E	N45E, 40N	5 m	?	?		3200	Bundtzen, 1981

Table D6 (Continued)

Map No.	Mine or Prospect	Mineral Deposit Type	Metals	Attitudes		Dimensions (Ave)				References
				Veins, Faults or Crushed Zones	Foliation of Country Rock	Width	Length	Depth (dip)	Grade	
85a.	Unnamed (75Ast2765)	I	Cu	N45E	N45E, 30S	?	?	?	3000	Bundtzen, 1981
85b.	Unnamed (75Ast2771)	IV	Cu	N20-50W	N45E, 30N	?	?	?	3000	Bundtzen, 1981
86.	Unnamed (75Ast2794)	I	Pb,Ag,Zn	N70E	N70E, 30N	?	?	?	2900	Bundtzen, 1981
87.	Unnamed (75Ast1785)	IV	Pb	N55E, 55SE	N55E, 50N	?	?	?	2200	Bundtzen, 1981

**APPENDIX D7**  
**Summary of Placer Mines and Prospects in**  
**the Kantishna Mining District, Alaska**

Table D7  
Placer mines and prospects in the Kantishna mining district, Alaska.

Name	Township and Range	Average Gold Fineness (after Metz and Hawkins, 1980)	Commodity	Description (after Menzie and others, 1983)	Reference
1. Bearpaw River (Creek)	T14S,R18W		Au	Placer mining reported was probably on tributaries. See also: (Caribou Creek), (Crevice Creek), (Friday Creek), (Eureka Creek), (Glacier Creek), (Last Chance Creek), (Twenty-two Gulch), (Yellow Creek).	Prindle, 1906; Brooks, 1912; Bundtzen and others, 1976; Hawley, C.C. and Associates, Inc., 1978
2. Caribou Creek	T15S,R17W	677	Sb,Au,W	In upper Caribou Creek (MF-366, loc. 48) creek gravel is 2 1/2 to 7 ft thick; contains gold (some coarse; nugget weighing about half an ounce recovered), stibnite, and scheelite. Bench gravel on lower Caribou Creek (MF-366, loc. 47) leaner; gold finer. Mined intermittently from about 1906 to as recently as 1975. One of the major placer producers of district, especially 1939-41 when dragline operations recovered up to 300 oz of gold per week.	Prindle, 1907; Brooks, 1911, 1916, 1923; Capps, 1918, 1919, 1924; Davis, 1923; Brooks and Capps, 1924; Smith, 1929, 1934, 1937, 1939, 1941, 1942; Reed, 1961; Cobb, 1973; Bundtzen and others, 1976; Cobb, 1977; MacKevett and Holloway, 1977
3. Chitisa Creek	T11S,R14W		Au	Placer gold discovered in 1903 during Wickersham expedition to climb (unsuccessfully) Mt. McKinley.	Reed, 1961; Cobb, 1973, 1977; Bundtzen and others, 1976; MacKevett and Holloway, 1977
4. Crevice Creek	T15S,R17W		Au	Coarse gold, probably less than 1,000 fine oz, mined in early 1906. Largest nugget about 4.35 fine oz.	Prindle, 1907; Brooks, 1911; Cobb, 1977; MacKevett and Holloway, 1977
5. Crooked Creek	T13S,R15W	881	Au	Has been placer gold mining since about 1926; total produced is probably considerably less than 1,000 oz.	Smith, 1929, 1934, 1938, 1939, 1942; Cobb, 1973, 1977; Bundtzen and others, 1976; MacKevett and Holloway, 1977; Hawley, C.C. and Assoc., Inc., 1978
6. Eldorado Creek	T16S,R18W		Sb,Au	Has been placer mining as recently as 1975. In early days gold was considered to be too unevenly distributed for successful mining; recent mining has been from above silt false bedrock. Production probably less than 1,000 fine oz. Abundant stibnite float.	Capps, 1918, 1919; Brooks and Capps, 1924; Wells, 1933; Bundtzen and others, 1976; Cobb, 1977; MacKevett and Holloway, 1977
7. Eureka Creek	T16S,R17W	906	Sb,Au,Pb	Placer gold discovered in 1905; mining as recently as 1975; total production more than 1,000 and probably less than 10,000 fine oz. Concentrates contain considerable stibnite, some galena, and a little	Brooks, 1907, 1911, 1912, 1916, 1922; Prindle, 1907; Capps, 1918, 1919, 1924;

Table D7 (Continued)

Name	Township and Range	Average Gold Fineness (after Metz and Hawkins, 1980)	Commodity	Description (after Menzie and others, 1983)	Reference
				black sand. Sketchy report of about 50 tons of antimony ore being mined in about 1915 from stibnite-quartz vein. Some of placer gold very coarse; nuggets with as much as 32.8 fine oz gold reported. Bench and stream gravels being mined in 1975. Most of previous production probably from creek gravels.	Davis, 1923; Brooks and Capps, 1924; Smith, 1929, 1930, 1932, 1933, 1934, 1936, 1937, 1938, 1939, 1941, 1942; Moffit, 1933; Wells, 1933; Cobb, 1973, 1977; Bundtzen and others, 1976; MacKevett and Holloway, 1977
8. Friday Creek	T16S,R18W	806	Sb,Au,Pb,Ag	Mining from early 1900's to as recently as 1975. Gold near and in top few feet of schist bedrock; gravels 3-6 ft thick; in places partially buried by frozen slide material from valley walls. Gold both fine and in nuggets, some of which weigh more than an ounce; some of gold exhibits crystal faces. Stibnite, argentiferous galena, and black sand in concentrates. Total production probably less than 1,000 fine oz of gold.	Brooks, 1907, 1911, 1916; Prindle, 1907; Capps, 1918, 1919, 1924; Davis, 1923; Capps, 1924; Cobb, 1973, 1977; Bundtzen and others, 1976; MacKevett and Holloway, 1977
9. Glacier Creek	T15S,R17W	773	Au,Pb	Creek gravels coarse, 2-5 ft thick, and as wide as 250 ft. Some of gold coarse (nugget valued at \$365 (gold at \$20.67) reported). Bench gravels also auriferous. Both creek and bench gravels have been mined. Total production probably more than 1,000 and less than 10,000 fine oz. Considerable galena, some black sand, and garnet in concentrated. Gold discovered in 1904 or 1905; mining as recently as 1975.	Prindle, 1907; Brooks, 1911, 1923; Capps, 1918, 1919, 1924; Davis, 1923; Brooks and Capps, 1924; Smith, 1929, 1930, 1936, 1939; Moffit, 1933; Wells, 1933; Reed, 1961; Cobb, 1973, 1977; Bundtzen and others, 1976; MacKevett and Holloway, 1977
10. Glen(n) Creek	T16S,R16W	896	Sb,Au,Pb, Sn(?),Rh	Gravels as much as 3 ft thick; gold concentrated at or in top of bedrock in some places; in others gold distributed through 2 ft of gravel; pay gravels 30-150 ft wide. Some of gold very coarse; many nuggets from 1 1/2 to 7 oz. Concentrates contain black sand, garnets, galena, stibnite, and pyrite; large boulders of rhodonite (some gem quality) present. Cassiterite crystals seen by F.G. Wells (USGS) said to have come from this creek. Mining from early 1900's to as recently as 1975. Total production probably between 1,000 and 10,000 fine oz of gold.	Prindle, 1907; Brooks, 1911, 1912, 1922; Capps, 1918, 1919, 1924; Davis, 1923; Brooks and Capps, 1924; Smith, 1929, 1930, 1932, 1933, 1934, 1936, 1939; Moffit, 1933; Wells, 1933; Bundtzen and others, 1976; Cobb, 1977; MacKevett and Holloway, 1977

Table D7 (Continued)

Name	Township and Range	Average Gold Fineness (after Metz and Hawkins, 1980)	Commodity	Description (after Menzie and others, 1983)	Reference
11. Little Moose Creek	T13S,R15W	584	Au,Ag,W	Short, steep, narrow valley with unstable walls; gravels 8-10 ft thick. Mining as recently as 1941. Gold shot-like and low grade (old assays said to have been about \$12 per oz when gold was \$20.67). Small nuggets of native silver recovered with the gold. Scheelite common in concentrates. Total production less than 1,000 oz.	Capps, 1918, 1919; Brooks, 1922, 1923; Davis, 1923; Brooks and Capps, 1924; Smith, 1929, 1930, 1932, 1933, 1934; Moffit, 1933; Joesting, 1942; White, 1942; Cobb, 1973, 1977; Bundtzen and others, 1976; MacKevett and Holloway, 1977; Hawley, C.C., and Assoc. Inc., 1978
12. Marten Creek	T13S,R15W		Au	Small-scale placer mining in 1929 and 1937 reported. Includes reference to (Martin Creek).	Smith, 1932, 1939
13. Moose Creek	T16S,R18W	812	Au	At site of most mining (MF-366, loc. 44) gold in creek and low-bench gravels on false bedrock; some concentrated on false bedrock; no gold below false bedrock, but true bedrock not reached; pay streak 400-600 ft wide; attempt at large-scale hydraulicking in 1920's not successful. In 1906 small-scale mining in canyon further downstream (MF-366, loc. 42). Placers at lower elevations than terraces of glacial material. Gold production reported intermittently from 1906 to as recently as 1939; total probably less than 1,000 fine oz.	Prindle, 1906, 1907; Brooks, 1911, 1912, 1922, 1923; Capps, 1918, 1919, 1924; Davis, 1923; Brooks and Capps, 1924; Smith, 1929, 1939, 1941; Moffit, 1933; Reed, 1961; Bundtzen and others, 1976; Cobb, 1977; MacKevett and Holloway, 1977
14. Rainy Creek	T16S,R17W		Au	Was placer mining in 1922 and possibly other years. No data on deposit or amount of production.	Davis, 1923; Bundtzen and others, 1976
15. Spruce Creek	T16S,R16W		Au	Bedrock several kinds of "Birch Creek" schists and some limestone; gold coarse, some pieces with quartz attached. Placer mining as recently as 1975, when a considerable amount of gravel was moved.	Prindle, 1907; Brooks, 1911; Davis, 1923; Brooks and Capps, 1924; Bundtzen and others, 1976; Cobb, 1977; MacKevett and Holloway, 1977
16. Stampede Creek	T13S,R15W	567	Au,W	Placer mining in 1940's and possibly at other times. Production less than 1,000 oz of gold. Scheelite common in concentrates. See also Stampede.	Joesting, 1942; White, 1942; Cobb, 1973, 1977; Bundtzen and others, 1976; MacKevett and Holloway, 1977; Hawley, C.C., and Assoc. Inc., 1978

Table D7 (Continued)

Name	Township and Range	Average Gold Fineness (after Metz and Hawkins, 1980)	Commodity	Description (after Menzie and others, 1983)	Reference
17. Willow Creek	T16S,R16W		Au	Mining or prospecting reported, 1934. Production, if any, must have been considerably less than 1,000 oz gold.	Smith, 1936; Cobb, 1980a
18. Yellow Creek	T16S,R17W	898	Au,Pb	Headwater tributary of Glacier Creek. Mining or prospecting from about 1906 to as recently as 1975; total production probably less than 1,000 oz of gold. Concentrates contain considerable galena.	Prindle, 1907; Brooks, 1911; Capps, 1918, 1919; Smith, 1929, 1933, 1934, 1937, 1938, 1939; Wells, 1933; Bundtzen and others, 1976; Cobb, 1980a; MacKevett and Holloway, 1977